MESOZOIC TECTONIC EVOLUTION OF THE PAMIR: AN ANALYSIS OF THE STRUCTURAL STYLE, MAGNITUDE, AND TIMING OF CRUSTAL SHORTENING AND TERRANE ACCRETION

by

Dustin Patrick Villarreal

A dissertation submitted to the Department of Earth and Atmospheric Sciences,

College of Natural Sciences and Mathematics

in partial fulfillment of the requirements for the degree of

Doctor of Philosophy

in Geology

Chair of Committee: Alexander Robinson

Committee Member: Thomas Lapen

Committee Member: Michael Murphy

Committee Member: Daniel Imrecke

University of Houston
December 2019

Copyright 2019, Dustin Patrick Villarreal

DEDICATION

This work is dedicated to Nicole, my wife.

EPIGRAPH

"Most geologist now map regions, not to put color on previously blank maps, but rather to solve specific problems that require better geologic maps than currently exist."

Peter Molnar, "Continental tectonics in the aftermath of plate tectonics", 1988

ACKNOWLEDGMENTS

This dissertation could not have been completed without the help of many people. First, I would like to express my sincere gratitude to my advisor, Alex Robinson, for both giving me the opportunity to further my education and to have worked on such an incredible project. Alex is an outstanding advisor that has an incredible passion and enthusiasm for geology. He continued to push me in my understanding of geology and quality of work, and I will forever be grateful for all he taught me.

I would to thank Mike Murphy and Tom Lapen for taking the time to answer my questions the numerous times I walked into their office without any notice. I had invaluable discussions with each of them about my research and geology as a whole. They continually tested my knowledge and always had many good comments.

Last, but foremost, I would like to thank my family. My wife, Nicole, has provided me emotional support and been more understanding throughout the last seven years than I could have ever hoped for. Nicole was not only there for support but also made me realize that I had more potential than I ever thought. My mother in-law, Maria, sacrificed an incredible amount of her time ensuring that I had the time I needed to complete my research. Maria consistently gave me encouragement and support over the years. Most importantly, Nicole and Maria put up with an incredibly busy father and were always there to reassure me that I was doing the right thing for our family. I would also like to think my grandparents and mother who have given me encouragement and support throughout my entire education.

ABSTRACT

The timing for suturing of Gondwanan crustal fragments and the magnitude and timing of subsequent upper crustal deformation in the Pamir Mountains are not well resolved. To investigate these issues, I conducted three studies. First, to address the timing of terrane accretion, a provenance analysis of clastic deposits within the Southern Pamir was done. The clastic deposits are the Late Triassic Rhaetian Lokzun Group Flysch and the Early Jurassic Darbasatash Group that have well-constrained stratigraphic ages and lie directly below and above the angular unconformity, respectively. Petrographic results and U-Pb analysis for both successions suggest sediment was sourced from the Northern Pamir's Permian–Triassic Karakul-Mazar accretionary arc complex, which indicates accretion occurred by the end of the Triassic.

Second, it has commonly been suggested that the Tanymas fault accommodated Cenozoic convergence between India and Asia. However, this interpretation is due in large part to uncertainty of ages associated with the Tanymas fault. Mapping of deposits in the footwall of the Tanymas thrust fault and ages from detrital zircon U-Pb analysis, Muscovite $^{40}Ar/^{39}Ar$ ages, and zircon fission track analysis show that the deposits are related to shortening (syn-orogenic) and are Early-mid Cretaceous. This age for displacement along the Tanymas fault is similar to what has been documented along the Rushan-Pshart suture and in the fold and thrust belt of the Southern Pamir.

Third, the Southern Pamir Fold and Thrust Belt has been suggested to have accommodated ~50 km of upper crustal shortening and has recently been interpreted to be Cretaceous in age. Through geologic mapping and forward modeling of the fold and thrust belt, we suggest that only ~4.25 km (~7.5%) of upper crustal shortening has been accommodated within the fold and

thrust belt, significantly lowering the amount of upper crustal shortening in the Southern Pamir. The modeling results also suggests that the fold and thrust belt is both propagating and verging to the south. These results imply that the Northern Pamir was elevated and thickened prior to accretion of the Gondwana terranes and that upper crustal shortening within the Central Pamir and Southern Pamir was the result of Cretaceous retroarc deformation.

TABLE OF CONTENTS

DEDICATION ..... *iii*

EPIGRAPH ..... *iv*

ACKNOWLEDGMENTS ..... *v*

ABSTRACT ..... *vi*

LIST OF TABLES ..... *xi*

List of Figures ..... *xii*

I. Evidence for Late Triassic crustal suturing of the Central and Southern Pamir *1*

1.0 Introduction **1**

2.0 Regional Geology **2**

3.0 Geology of the Southern Pamir **6**

4.0 Petrographic description **9**

4.1.0 Results 12

5.0 Detrital Zircon Analysis **12**

5.1.0 Methods 12

5.2.0 Triassic Lokzun Group 14

5.2.1. Sample DV 8-08-16-1 14

5.2.2. Sample DV 7-25-15-1 14

5.3.0 Jurassic Darbasatash Group 16

5.3.1. Sample DV 7-09-15-4 16

5.3.2. Sample DV 7-12-15-4 16

5.3.3. Sample DV 8-08-16-3 16

5.3.4. Sample 13P99 17

5.3.5. Sample DV 7-25-15-2 17

5.4.0 Results 18

5.5.0 Statistical Analysis 19

6.0 Discussion **20**

6.1.0 Timing of Suturing 20

6.2.0 Implications for the Cimmerian Orogeny 24

6.3.0 Implications for Paleogeography 24

6.4.0 Possible post-orogenic Extension? 26

7.0 Conclusion **27**

II. Timing for displacment along the Tanymas fault *28*

1.0 Introduction **28**

2.0 Geologic Background **31**

2.1.0 Cimmerian Orogeny....33
2.2.0 Post-Cimmerian Deformation....34
2.3.0 Post-Jurassic Terrigenous Clastic Deposits....36

3.0 Lithologic Descriptions and Field Observations....38
3.1.0 Northern Pamir Terrane....38
3.2.0 Central Pamir....42

4.0 Geochronology and Thermochronology Methods....43
4.1.0 Methods....43
4.2.0 Detrital Zircon....44
4.3.0 Muscovite $^{40}Ar/^{39}Ar$....46
4.4.0 Zircon Fission Track....46

5.0 Results....48
5.1.0 Muskol Range....48
5.1.1 DV 7-5-15_f1....48
5.1.2 DV 7-7-15_2....48
5.1.3 DV 7-7-15_4....49
5.1.4 15_006....49
5.1.5 15_020....51
5.2.0 Vanch Valley....51
5.2.1LY725171....51
5.3.0 Summary of U-P Detrital Zircon Results....51
5.3.0 Thermochronology Results....52
5.3.1 Muscovite $^{40}Ar/^{39}Ar$....52
5.3.2 Zircon Fission Track....53

6.0 Discussion....55
6.1.0 Provenance of Tanymas Footwall Deposits....55
6.2.0 Age of Clastic Deposits and Timing of Tanymas Fault Displacement....57
6.3.0 Timing of Deformation in the Pamir....58
6.4.0 Broader Implications....59

7.0 Conclusion....62

III. Magnitude and structural style of upper crustal shortening in the souther Pamir...64

1.0 Introduction....64

2.0 Geologic Background....66

3.0 Geologic Mapping and Field Observations....69
3.1 Stratigraphic Observations....72
3.1.1 Permian–Triassic....72
3.1.2 Jurassic–Cretaceous....73
3.2 Structural Geology....75

4.0 Forward Modelling the Southern Pamir Fold and Thrust Belt....79
4.1 Location of Cross Sections....79

4.2 Stratigraphic Constraints....81
4.3 Forward Modeling Assumptions....81
4.3.1 Prior to activation of the Southern Pamir Fold and Thrust Belt....82
4.3.2 During Activation of the Fold and Thrust Belt....82
4.3.3 Following Cessation of the Fold and Thrust Belt....83

5.0 Results of Models....84
5.1 Model 1....84
5.2 Model 2....89
5.3 Preferred Model and Structural Style....92

6.0 Discussion....94
6.1.0 Minimal Upper Crustal Shortening in the Pamir and Implication for Crustal thickness....94
6.2.0 Alternative Methods to Crustal Thickening....94
6.3.0 Broader implication....95

7.0 Conclusion....96

IV. Bibliography....98

V. Appendices....105

A. Appendix 1: U-P Zircon Analysis....105

B. Appendix 2: U-Pb Zircon Analysis....150

C. Appendix 3: Muscovite $^{40}Ar/^{39}Ar$ Analysis....189

D. Appendix 4: Zircon Fission Track....193

LIST OF TABLES

TABLE I-1 LOCATION AND MAXIMUM DEPOSITIONAL AGE FOR EACH SAMPLE 13
TABLE I-2 CROSSPLOT STATISTICAL ANALYSIS OF DETRITAL ZIRCONS 19
TABLE II-1 LOCATION AND MAXIMUM DEPOSITIONAL AGE FOR EACH SAMPLE 46

LIST OF FIGURES

FIG. I.1 REGIONAL GEOLOGIC MAP OF THE PAMIR 3
FIG. I.2 GEOLOGIC MAP OF THE EASTERN SOUTHERN PAMIR 7
FIG. I.3 STRATIGRAPHIC COLUMN AND FIELD PHOTOS FROM THE SOUTHERN PAMIR 8
FIG. I.4 PETROGRAPHIC ANALYSIS OF THE LOKZUN GROUP AND DARBASATASH GROUP 11
FIG. I.5 DETRITAL ZIRCON PROBABILITY DIAGRAMS 15
FIG. I.6 TRIASSIC-JURASSIC TECTONIC MODEL OF THE PAMIR 23
FIG. I.7 LIMITED EXPOSURE OF THE DARBASATASH GROUP 25
FIG. I.8 DARBASATASH GROWTH STRATA 26
FIG. II.1 TECTONIC MAP OF THE PAMIR 29
FIG. II.2 GEOLOGIC MAP OF CLASTIC DEPOSITS 30
FIG. II.3 GEOLOGIC MAP OF STUDY AREA 32
FIG. II.4 FIELD PHOTOS 40
FIG. II.5 CROSS SECTION ALONG MAPPING TRANSECT AND CORRELATIVE THIN SECTIONS 41
FIG. II.6 SUBREGIONAL MAP OF THE PAMIR 45
FIG. II.7 PROBABILITY DENSITY PLOT FOR U-PB 50
FIG. II.8 ZFT AND AR/AR AGES FOR SAMPLES 15_006 AND 15_020 54
FIG. II.9 CRETACEOUS SCHEMATIC CROSS SECTION OF THE PAMIR 60
FIG. II.10 LATE JURASSIC–CRETACEOUS TECTONIC MODEL 61
FIG. III.1 REGIONAL TECTONIC MAP OF THE PAMIR 68
FIG. III.2 GEOLOGIC MAP OF THE EASTERN PAMIR 70
FIG. III.3 FIELD PHOTOS FROM THE SOUTHERN PAMIR 71
FIG. III.4 STEREONETS FROM THE SOUTHERN PAMIR 76
FIG. III.5 STRUCTURE MAP OF THE EASTERN PAMIR 77
FIG. III.6 PRESENT DAY CROSS SECTION 80
FIG. III.7 MODEL 1-TRISHEAR 85
FIG. III.8 MODEL 2 – RAMP 90

I. EVIDENCE FOR LATE TRIASSIC CRUSTAL SUTURING OF THE CENTRAL AND SOUTHERN PAMIR

1.0 Introduction

The Pamir lie at the western end of the Tibetan orogen and shares a broadly similar history of ocean basin closure, terrane accretion, and subsequent deformation as the Tibetan Plateau (Burtman and Molnar, 1993; Yin and Harrison, 2000; Robinson, 2015). Despite broad similarities, the timing of terrane accretion in the Pamir region remains less well constrained, raising questions of along-strike variability in the timing and nature of terrane accretion, correlation of geologic terranes across the orogen, and the nature of subsequent tectonic activity. One of the key outstanding questions in the Pamir is the timing of accretion of Gondwana terranes (Central and Southern Pamir terranes) to the Northern Pamir terrane, which closed the Paleotethys and Rushan ocean basins and resulted in the Pamir Cimmerian Orogeny. Although closure of the Paleotethys ocean and collision of the Central Pamir with the southern margin of Asia is generally interpreted to have occurred in the Latest Triassic (Burtman and Molnar, 1993; Robinson et al., 2004; Schwab et al., 2004; Angiolini et al., 2013), the timing of collision between the Southern Pamir and Central Pamir terranes is less clear and is suggested to have occurred either during the Late Jurassic to Early Cretaceous (Schwab et al., 2004; He et al., 2018) or during the Late Triassic to Early Jurassic (Angiolini et al., 2013). These disparate interpretations have significant implications for the correlation of terranes between the Pamir and Tibetan Plateau, and possible along-strike variations in the tectonic evolution of the Tibetan orogen. Here we address this debate through petrographic and detrital zircon provenance analysis of detrital sediments located above and below a regional unconformity developed after the

Cimmerian Orogeny. Our results provide new insight into the timing of regional ocean basin closure and terrane accretion, as well as the nature of the Cimmerian orogeny in the Pamir.

2.0 Regional Geology

The western portion of the Himalayan-Tibetan orogen consists of the Pamir-Karakoram mountain ranges. The Pamir mountains form a broad salient that has been displaced northward over the Tarim-Tajik basins along the north-vergent Main Pamir thrust system (MPT), which is kinematically linked with the left-lateral Darvaz Fault (DF) (Burtman and Molnar, 1993; Robinson, 2015) and right-lateral Kashgar Yecheng Transfer System (KYTS) (Cowgill, 2010; Sobel et al., 2011) to the west and east, respectively (Fig. I.1). Northward displacement on the MPT has been suggested to be up to ~300 km as a result of the Cenozoic India-Asia collision (Burtman and Molnar, 1993), although several recent studies suggest significantly less Cenozoic displacement (Chapman et al., 2017a; Chen et al., 2018).

The Pamir-Karakoram salient has traditionally been divided into three tectonic terranes: The Northern Pamir, Central Pamir, and Southern Pamir-Karakoram, which are separated by the Tanymas and Rushan-Pshart thrust, respectively (Fig. I.1). The Northern Pamir can be divided into two separate geologic terranes: 1) a northern portion which is the western continuation of the Paleozoic Kunlun terrane of Northern Tibet and 2) a southern portion, the Karakul-Mazar accretionary arc-complex, which is equivalent to the Triassic Hoh-Xil-Songpan-Ganzi terrane of Tibet (Schwab et al., 2004; Robinson et al., 2012). The Northern Pamir terranes were part of a cordilleran-style margin that developed along the southern margin of Asia through the late Paleozoic to Triassic during northward subduction of the Paleotethys oceanic lithosphere. Following closure of the Paleotethys ocean, Gondwana terranes of the Central and Southern

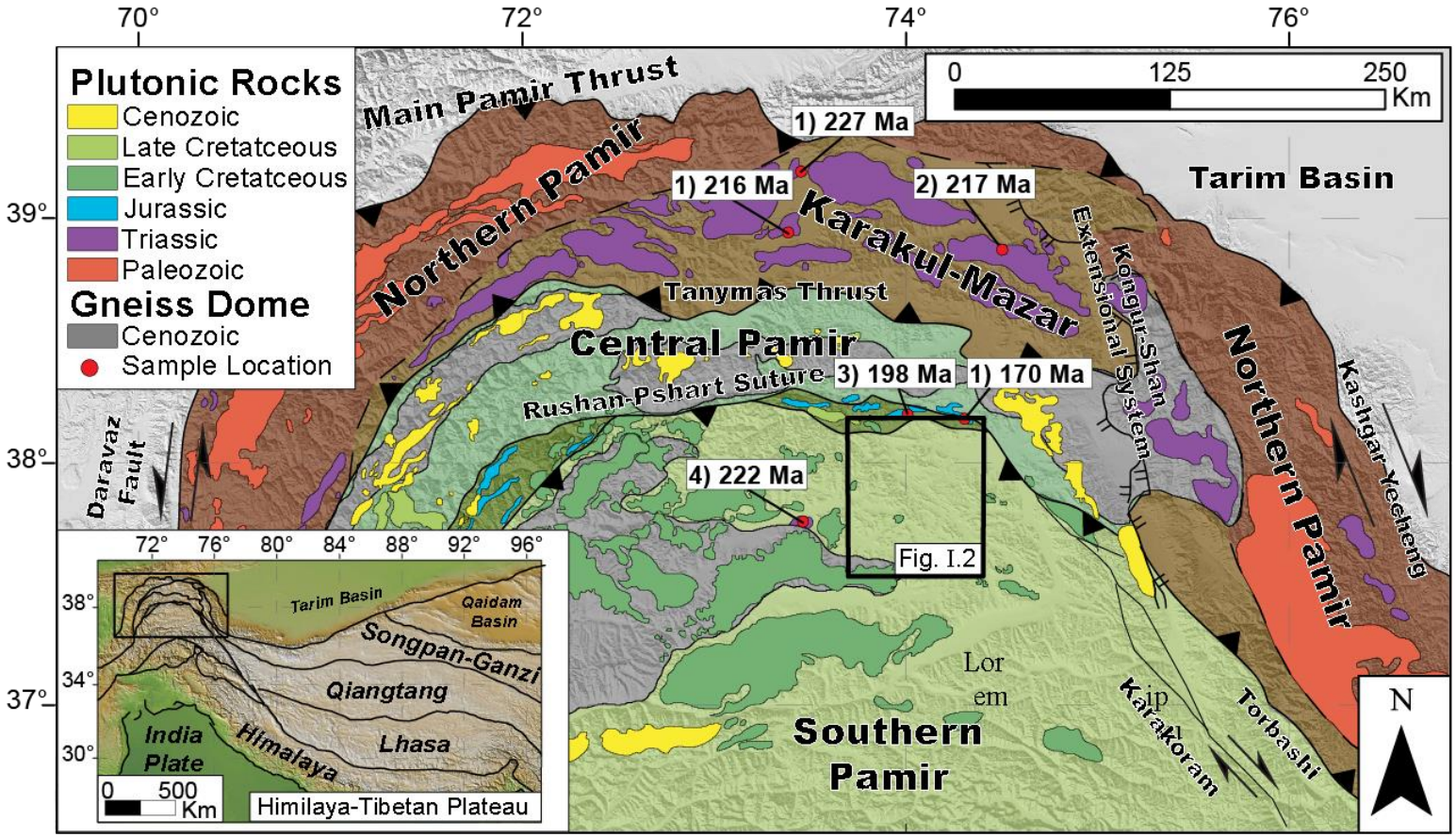

Fig. I.1 Regional Geologic map of the Pamir

Inset map shows tectonic terranes of Tibet and location of the geologic map of the Pamir. Larger map shows the tectonic terranes, sutures, and the distribution of plutons and gneiss domes within the Pamir. Red circles represent sample locations and sources of data come from 1) Schwab et al., (2004); 2) Robinson et al., (2007); and 3) Chapman et al., (2017); 4) Zanchetta et al. (2018). (modified from Schwab et al., (2004); Schmidt et al., (2011); Robinson (2014); Chapman et al., (2017))

Pamir were accreted to the southern margin of Asia, resulting in the Pamir Cimmerian orogeny (Schwab et al., 2004; Burtman, 2010; Robinson, 2015). In Tajikistan, this boundary separating Gondwanan crustal fragments from the Northern Pamir is defined by the northward-dipping Tanymas thrust (Burtman and Molnar, 1993) and in western China by the northward-dipping Torbashi thrust (Robinson et al., 2012; Imrecke et al., 2019).

The Central Pamir, Southern Pamir, and Karakoram terranes originated as part of the Gondwana supercontinent before separating in the late Carboniferous (Angiolini et al., 2013, 2015; Metcalfe, 2013). Evidence for rifting is recorded by clastic deposits that are directly overlain by Lower Permian deposits with cold water fauna. During rifting, the Rushan ocean basin opened between the Central and Southern Pamir during the Permian to Middle Triassic (Leven, 1995; Burtman, 2010), with possible rifting between the Southern Pamir and Karakoram terrane (Zanchi and Gaetani, 2011; Angiolini et al., 2013). After rifting, the Gondwana terranes drifted northward from their southern latitudes as the Paleotethys oceanic basin subducted below Asia. Conformably above the Lower Permian strata are Upper Permian clastic marine deposits that contain paleoequatorial fauna which are overlain by a regionally extensive Triassic carbonate platform in both the Southern Pamir and Karakoram terranes (Zanchi and Gaetani, 2011; Angiolini et al., 2013; Gaetani et al., 2013).

The Central Pamir, Southern Pamir, and Karakoram terranes have generally been interpreted to be the western equivalent of the Qiangtang terrane and part of the broad Cimmerian continent (Metcalfe, 2013). This correlation is based on similar histories of rifting and subsequent movement across the Paleotethys ocean that have been documented in the Qiangtang terrane (Dewey et al., 1988; Metcalfe, 2002), limited dextral-slip along the

Karakoram fault (Phillips et al., 2004; Upadhyay et al., 2005; Searle and Phillips, 2007; Robinson, 2009), and stratigraphic similarities (Angiolini et al., 2013).

Timing of closure of the Paleotethys ocean and collision between the Central Pamir and Northern Pamir is interpreted to be Late Triassic in age, indicated by a cessation of igneous activity at the end of the Triassic in the Karakul-Mazar arc-complex and Early Jurassic zircon metamorphic ages from both sides of the Tanymas suture zone (Xiao et al., 2002a; Schwab et al., 2004; Robinson et al., 2012; Robinson, 2015). However, timing of closure of the Rushan ocean and collision between the Central and Southern Pamir are less well constrained. Schwab et al., (2004) suggested that collision between the Southern Pamir and the Central Pamir was Late Triassic to Early Jurassic, based on the presence of Jurassic intrusive bodies in the Rushan-Pshart Zone (RPZ) and their interpretation that the Southern Pamir represents the western extent of the Lhasa terrane of Tibet. However, Angiolini et al. (2013) suggested that the timing of collision was Late Triassic to Early Jurassic in age due to petrographic analysis of a post-Cimmerian orogeny Early Jurassic terrigenous red bed from the Southern Pamir, along with limited displacement along the dextral Karakoram fault (Phillips et al., 2004; Robinson et al., 2004; Upadhyay et al., 2005; Searle and Phillips, 2007). Further evidence for Late Triassic to Early Jurassic closure of the RPZ is the Triassic ophiolitic Bashgumbaz Complex (BSC) within the Southern Pamir which has been suggested to have been derived from the Rushan ocean basin (Shvol'man, 1978; Pashkov and Shvol'man, 1979; Shvol'man, 1980). Recent work suggest that the BSC formed in a suprasubduction zone environment in the Late Triassic and was subsequently obducted onto the Southern Pamir during northward subduction of the Rushan ocean below the Central Pamir (Zanchetta et al., 2018).

The Southern Pamir and the Karakoram terrane are separated by the Wakhan-Tirich boundary Suture Zone (TBZ). Due to the lack of an ophiolite sequence or marine deposits, it is unclear whether an oceanic basin fully developed or whether it represents a region of attenuated continental crust (Zanchi et al., 2000; Zanchi and Gaetani, 2011; Zanchetta et al., 2018). Regardless of the nature of the boundary, the Karakoram was adjacent to the Southern Pamir by the Late Triassic to Early Jurassic (Zanchi and Gaetani, 2011).

3.0 Geology of the Southern Pamir

The Southern Pamir can be divided into a Southwestern (SW) and Southeastern (SE) Pamir that is separated by a Cenozoic extensional system (Schwab et al., 2004; Schmidt et al., 2011; Stübner et al., 2013b). The SW Pamir is dominated by the Miocene Shakdhara gneiss dome which exposes mid- to lower-crustal rocks in the footwall of a regionally extensive detachment system (Schmidt et al., 2011; Stübner et al., 2013b). The SE Pamir is composed of a dominantly Permian to Cretaceous sedimentary sequence that has experienced periodic contractional deformation from the Late Triassic to Late Cretaceous (Fig. I.2) (Burtman and Molnar, 1993; Schwab et al., 2004; Angiolini et al., 2013; Robinson, 2015; Chapman et al., 2018)

Our field observations and geologic mapping (Fig. I.2 and I.3) within the Southeast Pamir are consistent with those documented by Angiolini et al. (2013, 2015). The lower portion of the sedimentary sequence consists of Permian through Triassic non-marine and marine sedimentary deposits, which Angiolini et al. (2013, 2015) classified as developing during a syn-rift to drift succession. The upper portions of this sequence consist of a Triassic carbonate platform (Korchagin, 2008, 2009) that is capped by the Lokzun group flysch deposit that is

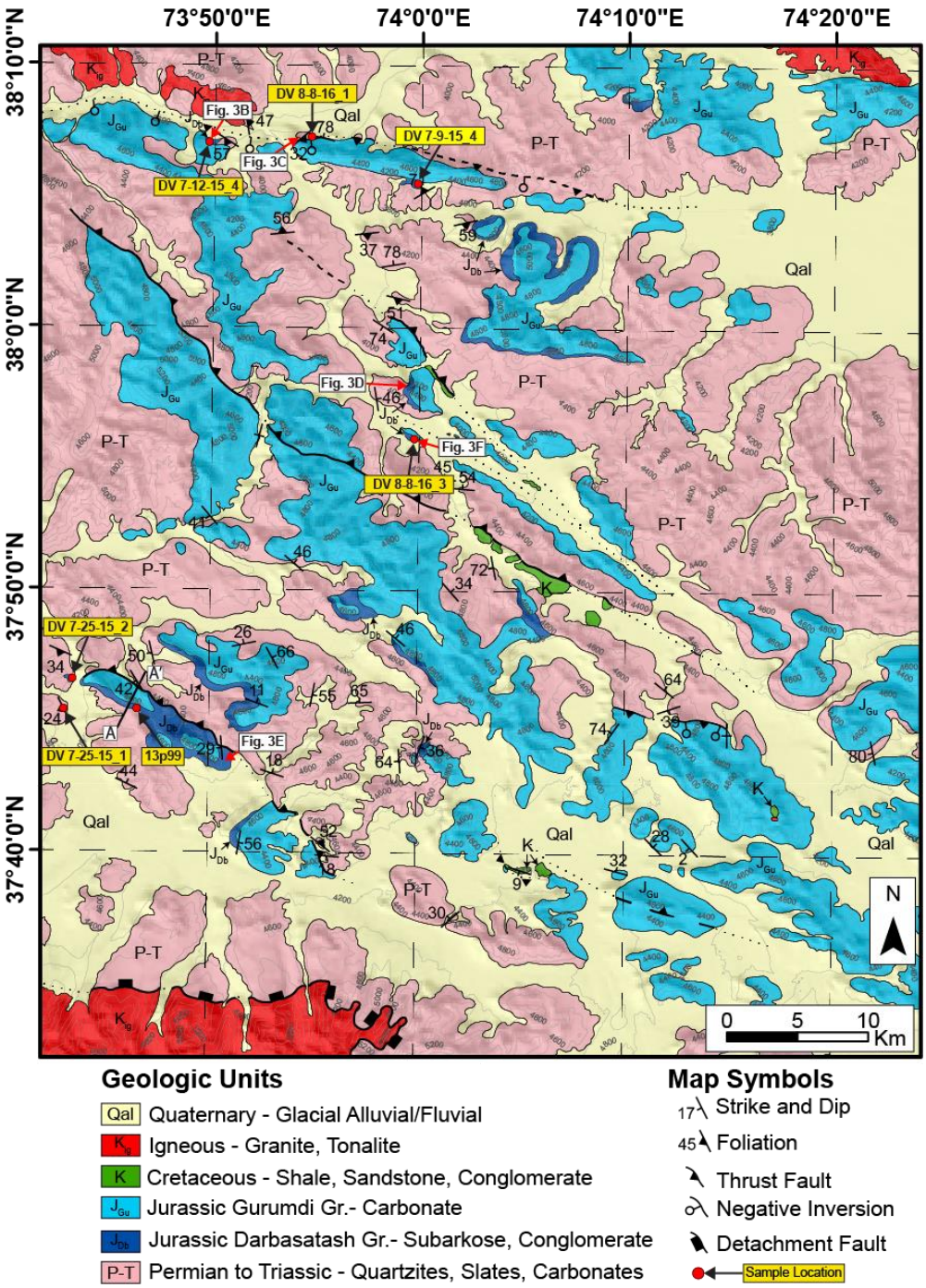

Fig. I.2 Geologic map of the eastern Southern Pamir

Map of the eastern Southern Pamir to show the local geology, along with the location of samples and field photos from Fig. 3. Red arrows for field photos indicate the direction in which the pictures were taken. Location of map is shown in Figure 1.

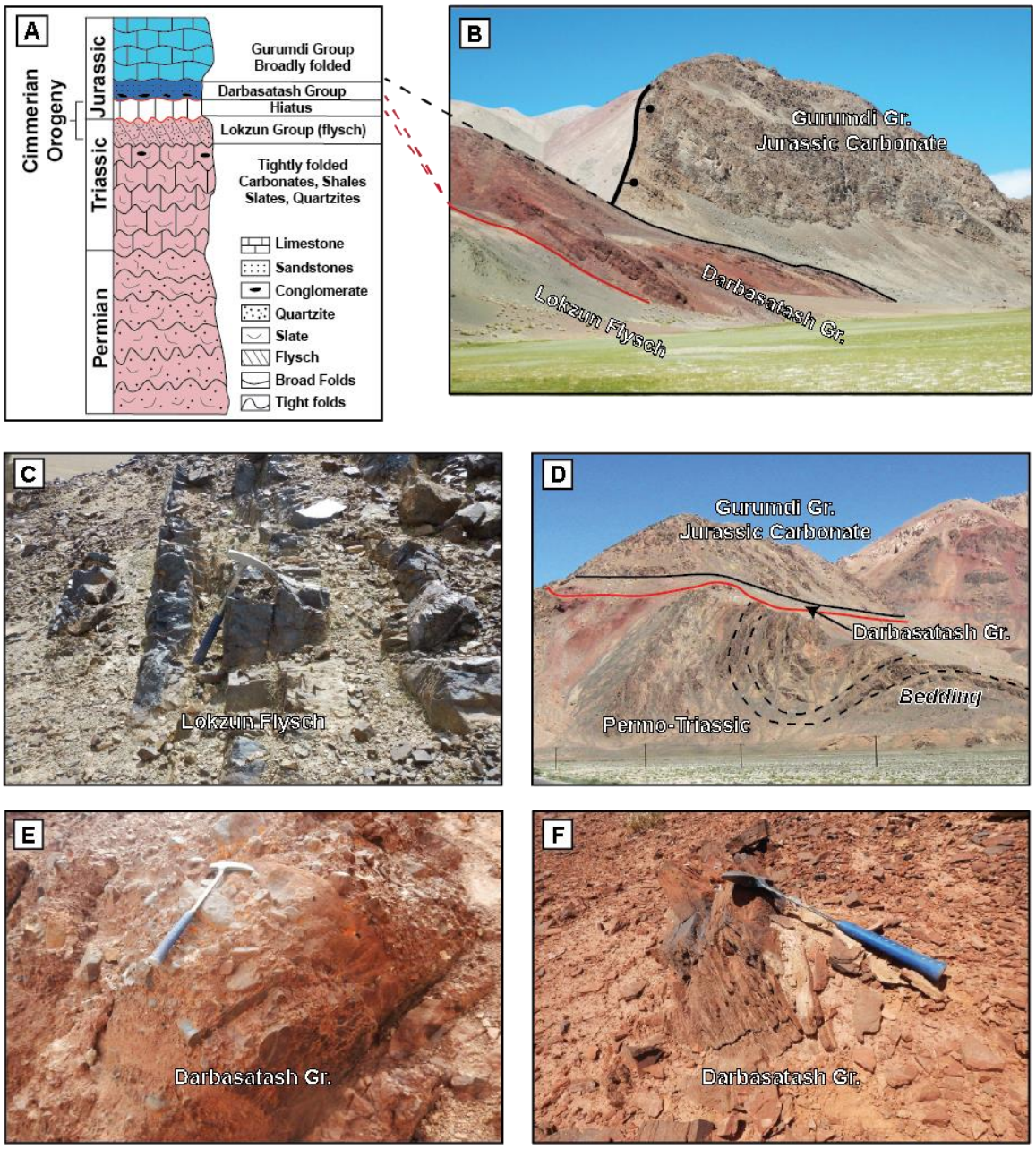

Fig. I.3 Stratigraphic column and field photos from the Southern Pamir
(A) Simplified stratigraphic column of the Southeast Pamir showing prominent lithology and tightness of folded structures (modified from Angiolini et al., 2013). (B) Representative geology correlated to stratigraphic column in Fig. A (ridge location: 37.73N, 73.98E) (Landscape in the background is in the footwall of a small normal fault). (C) Lokzun Group Triassic flysch (location: 38.121N, 73.915N). (D) Post-Cimmerian unconformity (in red) separating the folded Permo-Triassic strata from the overlying sub-horizontal Darbasatash Group and Gurumdi Group (location: 37.95N, 74.00N). (E) Basal conglomerate of the Darbasatash Group (location: 37.732N, 73.845N). (F) Darbasatash Group sandstone (location: 37.929N 73.992E).

Rhaetian in age (Dronov et al., 2006). This Upper Paleozoic–Triassic sequence experienced very low grade metamorphism and significant deformation characterized by tight isoclinal folds, which are often overturned and heavily faulted, which is interpreted to have occurred during the Cimmerian Orogeny and closure of the Paleotethys and Rushan oceans (Angiolini et al., 2013). This sequence is capped by a regionally extensive angular unconformity (hereafter referred to as the post-Cimmerian unconformity).

Overlying the Late Paleozoic–Triassic, above the angular unconformity, is a Jurassic sequence. This sequence begins with the sparsely exposed Early Jurassic Darbasatash Group which is composed of shales, sandstones, and conglomerates. Conformably overlying the Darbasatash Group are the regionally extensive platform carbonates of the Gurumdi Group which are Hettangian in age (Dronov et al., 2006). The Jurassic sequence has experienced minor deformation interpreted to be Cretaceous in age consisting of broad open folds and local thrust faults (Chapman et al., 2018).

In this paper, we focus on the formations immediately below and above the post-Cimmerian unconformity, the Lukzon and Darbasatash groups respectively, addressing their provenance through petrographic and detrital zircon (DZ) analysis. These results yield critical constraints into the timing of ocean closure and terrane accretion within the Pamir.

4.0 Petrographic description

Petrographic analysis of detrital framework grains in sandstones has been shown to provide important insight into provenance type driven by tectonic processes (Dickinson and Suczek, 1979). For this study, petrographic thin sections were made for two samples from the Lokzun group and four samples from the Darbasatash Group. Four-hundred detrital framework grains (quartz, feldspar, and lithic rock fragments) were then counted for each sample following the

Gazzi-Dickenson point counting method. Grain types identified are monocrystalline quartz (Qm), Feldspar (F), sedimentary (Ls) (excluding chert), chert (Lch), and metamorphic (Lm). For this study, feldspar lithic grains were not differentiated. Sedimentary lithic fragments consisted of siltstone, limestone, mudstone, and ooids. Chert lithic fragments (Lch) were separated into their own category due to their significance in convergent zones with most having undergone low grade metamorphism and recrystallization. Metamorphic lithic grains (Lm) consisted of polycrystalline quartz where there was the presence of grain boundary migration and grain suturing had occurred. The modal abundance was then calculated for each sample and plotted on the QmFLt Provenance Plot (Dickinson et al., 1983; Dickinson, 1985).

The Lokzun Group Flysch is the youngest Triassic strata and lies directedly below the post-Cimmerian unconformity (Fig. I.3). The Lokzun Group has a well-developed slaty cleavage and experienced very low-grade metamorphism, slightly recrystallizing chert grains and precipitating authigenic quartz within depositional pore space. Petrographic analysis shows the two samples contain an abundance of monocrystalline quartz (65–74%), unaltered feldspar (<5%), and lithic rock fragments (20–32%) (Fig. I.4).

The Lower Jurassic Darbasatash Group is the oldest formation above the post-Cimmerian unconformity (Fig. I.3). The sandstones from the Darbasatash Group contain an abundance of monocrystalline quartz (67–84%), feldspar (<5%), and lithic rock fragments (15–30%). However, the feldspar in the Darbasatash Group has been heavily altered from diagenesis and, in many places, replaced by calcite (Fig. I.4).

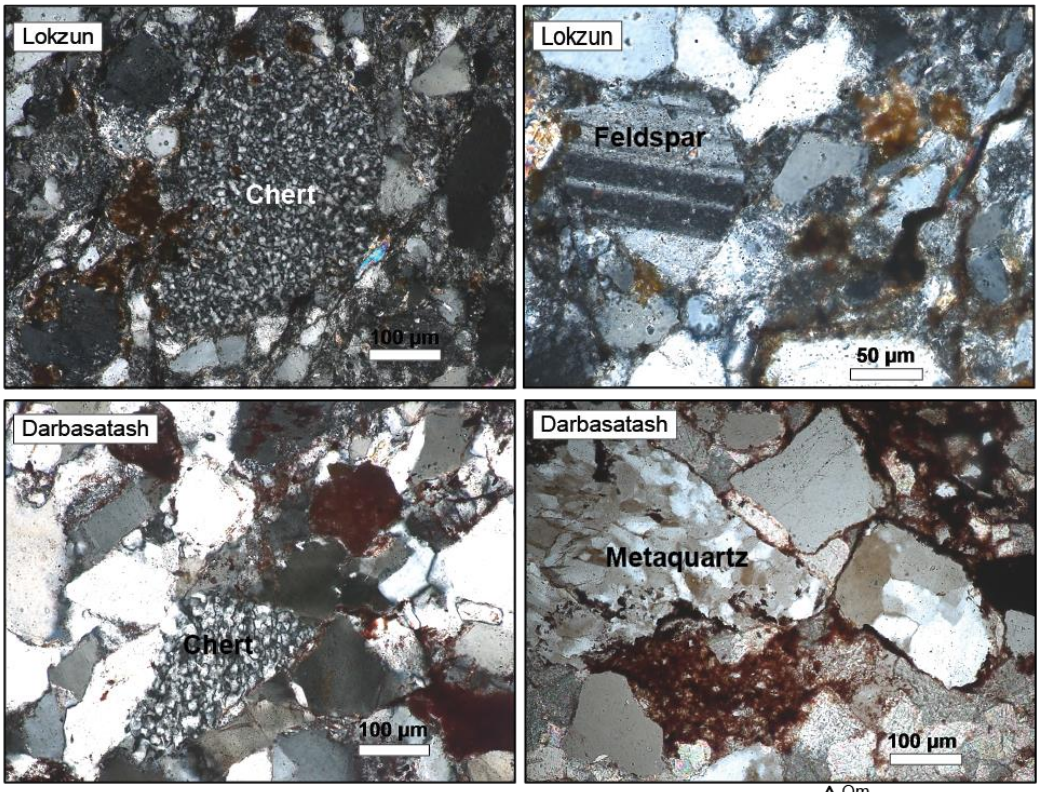

								Modal percentage		
Formation	Sample	Qm	F	Lt	Ls	Lch	Lm	Qm	F	Lt
Lokzun	DV 8-08-16_1	259	14	127	0	77	50	64.75	3.50	31.75
Lokzun	DV 7-25-15_1	304	15	81	0	55	26	76.00	3.75	20.25
Darbasatash	DV_7-9-15_4	303	23	74	0	14	60	75.75	5.75	18.50
Darbasatash	DV_7-12-15_4	337	5	57.6	0	32	26	84.33	1.25	14.41
Darbasatash	DV_8-08-16_3	302	3	95	46	18	31	75.50	0.75	23.75
Darbasatash	13P99	Not Counted						Not Counted		
Darbasatash	DV7-25-15_2	270	11	119	0	91	28	67.5	2.75	29.75

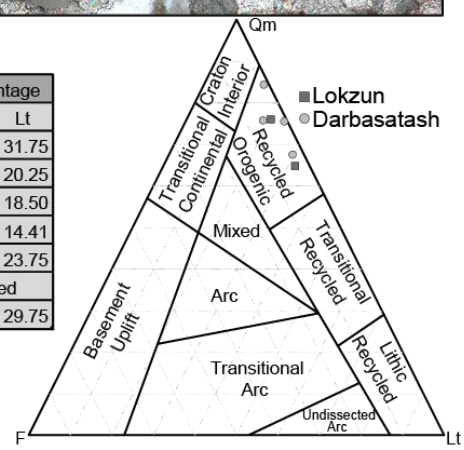

Fig. I.4 Petrographic analysis of the Lokzun Group and Darbasatash Group
Petrography of the Upper Triassic Lokzun Group flysch and Lower Jurassic Darbasatash Group terrigenous deposit. Lokzun Group and Darbasatash Group are dominated by monocrystalline quartz, minor chert, and polycrystalline quartz. Both contain rare feldspar; however, the feldspar is relatively unaltered in the Lokzun Group and heavily altered to replaced in the Darbasatash Group. 400 points were counted for each sample and modal percent was calculated and plotted on the QmFLt Provenance Plot (Dickinson, 1985). Qm = monocrystalline quartz; F = Feldspar; Lt = total lithics; Ls = sedimentary grains; Lch = chert grains; Lm = metamorphic grains.

4.1.0 Results

Average sandstone framework compositions from the Lokzun Group and Darbasatash Group plot within the recycled orogen field on the QmFLt Provenance Plot (Dickinson, 1985) (Fig. I.4). These results are consistent with previous analyses of the Jurassic Darbasatash group (Angiolini et al., 2013). However, although both samples share similarities in grain composition, grains in the Darbasatash Group are generally coarser than those in the Lukzon Group, indicating the Jurassic sandstones are not simply reworked Triassic flysch.

5.0 Detrital Zircon Analysis

5.1.0 Methods

Two slate samples from the Lokzun Group and five sandstone samples from the Darbasatash Group were processed for detrital zircons by conventional mineral separation methods of jaw crushing and disc milling, followed by water table and heavy liquid density separation, and final magnetic separation. Separated zircons grains were then mounted in epoxy and polished to expose the grain interiors. Zircon U-Th-Pb analyses were conducted via LA-ICP-MS at the University of Houston and at the University of Arizona Laserchon Center (laserchon.org). At the University of Houston, analyses were conducted using a Photon Machines Analyte.193 excimer laser attached to a Varian 810 Quadrupole mass spectrometer. Laser ablation consisted of a 25 μm spot and a fluence of 2.99 J/cm^2 at 10 Hz for 300 bursts resulting in an ablate time of ~30 seconds (proceeded with a background analysis of ~20 seconds). The data collected was then reduced using "U-Pb Reduction," an in-house software program written in MATLAB (Sundell, 2017). Laser ablation at the University of Arizona was performed with an ablate spot size of 20 μm using a Teledyne Photon Machines G2™ solid state NeF excimer system coupled to a Thermo Fisher Scientific ELEMENT 2™ single collector

inductively coupled plasma mass spectrometer (ICP-MS). Detailed information on data collection and reduction can be found in Gehrels et al. (2008). For each sample, 150 – 315 detrital zircons were analyzed and a minimum of 127 analyses were used to create individual probability diagrams using "isoplot" (Ludwig, 2003). Maximum depositional ages were calculated from the 3 youngest grains that overlapped within error and are within 2σ (Dickinson and Gehrels, 2009) (Table I-1).

Table I-1 Location and maximum depositional age for each sample

Sample	Latitude	Longitude	Maximum Depositional Age (U/Pb)
Darbasatash sublitharenite (Lower Jurassic)			Ma
DV 7-09-15_4	38.092	73.996	229 ± 10
DV 7-12-15_4	38.119	73.829	229.8 ± 9.9
DV 7-25-15_2	37.774	73.722	216.2 ± 7.7
DV 8-08-16_3	37.930	73.993	226.1 ± 7.9
13P99	37.758	73.774	225.0 ± 9.8
Lokzun Group Flysch (Triassic)			
DV 7-25-15_1	37.757	73.717	227.1 ± 8.1
DV 8-08-16_1	38.121	73.915	229.4 ± 9.0

5.2.0 Triassic Lokzun Group

5.2.1. Sample DV 8-08-16-1

Sample DV 8-08-16-1 is a slate from the footwall of the Aksu Thrust fault (Fig. I.2). 200 zircon grains were analyzed with 183 being within 10 percent of error and having less than 25% discordance. The age distribution shows several key populations: two small Precambrian peaks and two prominent Phanerozoic peaks. The oldest Precambrian population is centered ~1860 Ma and the younger, broader population from ~1100–700 Ma. The older Phanerozoic population is Early Cambrian to Late Devonian with a peak at ~411Ma. The youngest and most prominent population is middle Mississippian to Late Triassic (340–220 Ma) with two peaks at 300 and 265 Ma (Fig. I.5). The youngest detrital zircon grain is 225 Ma, and the sample yields a maximum depositional age of 229±9 Ma.

5.2.2. Sample DV 7-25-15-1

Sample DV 7-25-15-1 is a quartzite. 150 individual detrital zircon grains from the sample were analyzed with 125 having less than 10% error and having less than 25% discordance. The age distribution shows three minor Precambrian age populations and two prominent Phanerozoic populations. The Precambrian ages yield a small population between ~2600–2400 Ma, a medium population centered at ~1840 Ma (~2100–1600 Ma), and a small broad population between ~900 – 700 Ma. Phanerozoic ages yield an early Paleozoic population (~500–360 Ma) with a Silurian to Devonian peak and a younger and more prominent middle Mississippian to Late Triassic population (~340–200 Ma) with a prominent Triassic peak (~233 Ma) (Fig. I.5). The youngest detrital zircon from the sample is 220 Ma and the sample yields a maximum deposition age of 227±8 Ma.

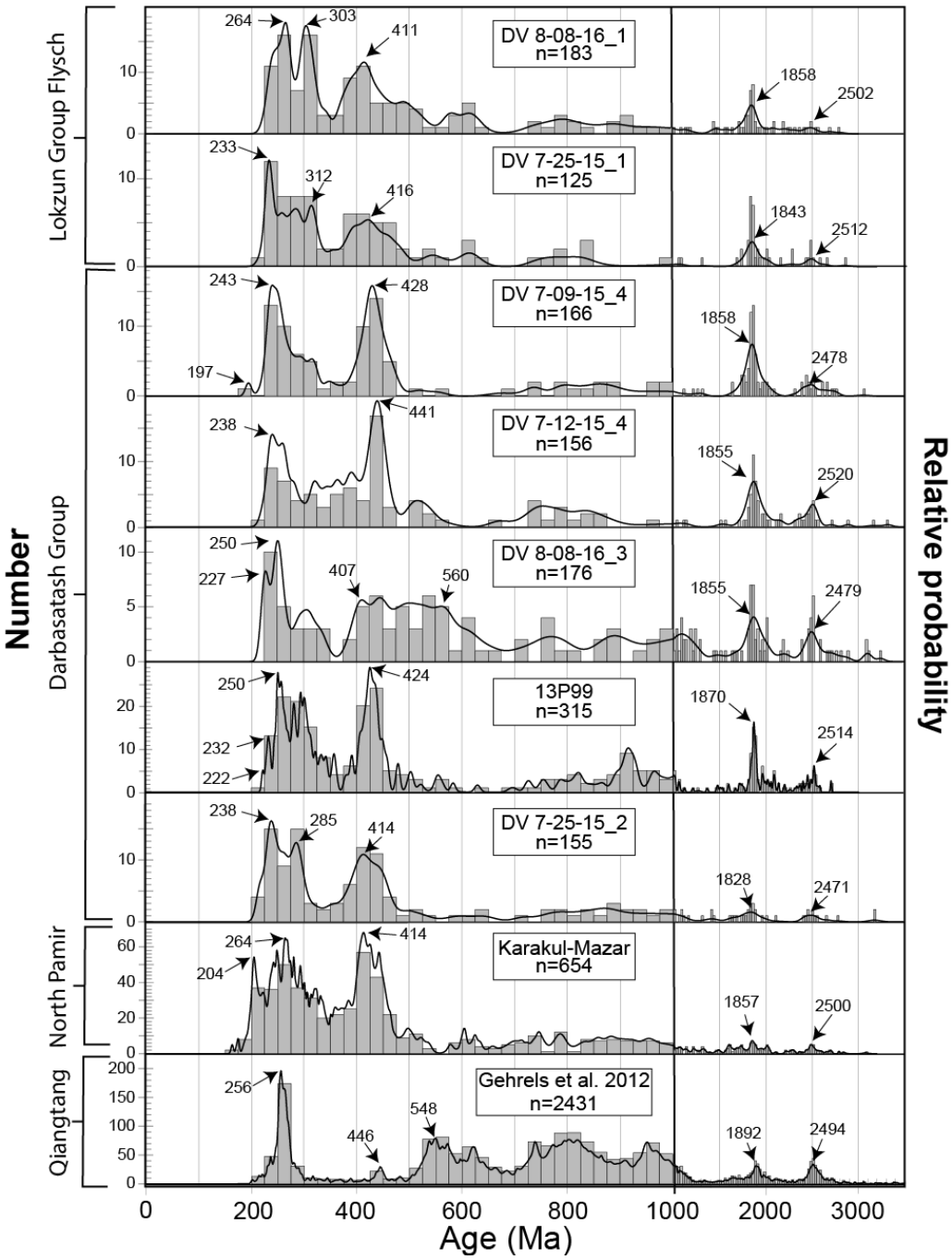

Fig. I.5 Detrital zircon probability diagrams

Relative probability plots (black lines) and 25 Ma histograms (grey bars) for detrital zircon U-Pb geochronology from the Pamir and Qiangtang. Significant peaks are annotated by ages in Ma. The Lokzun Group flysch and Darbasatash Group is from this study and results are discussed herein. The Karakul Mazar is a combination of Robinson et al., (2012) and Imrecke et al., (2019). Qiangtang is an integration of the Northern and Southern Qiangtang from Gehrels et al., (2011).

5.3.0 Jurassic Darbasatash Group

5.3.1. Sample DV 7-09-15-4

For sample DV 7-09-15-4, 200 individual grains were analyzed with 156 meeting requirements for plotting and interpretation. The age distribution shows one prominent Precambrian population at ~1860 Ma, with minor scattered ages between ~2600–2400 Ma and a small broad population between ~900–700 Ma. There are two prominent Phanerozoic populations: an early Paleozoic population with a strong Silurian peak at ~430 Ma and a Carboniferous to Late Triassic population (~340–220 Ma) with a strong Early Triassic peak (240 Ma) (Fig. I.5). The youngest detrital zircon from the sample is an outlier at 195 Ma with the sample yielding a maximum deposition age of 229±10 Ma.

5.3.2. Sample DV 7-12-15-4

For sample DV 7-12-15-4, 156 of the 200 individual zircon analyses met requirements for plotting and interpretation. The age distribution shows two prominent Precambrian peaks: a small one centered at ~2520 Ma (~2600–2400 Ma), a larger peak centered at ~1855 Ma (~2100–1600 Ma), as well as a small broad population between ~900–700 Ma. Phanerozoic ages yield a broad population of Paleozoic through Triassic ages with two prominent peaks in the Silurian (~440 Ma) and Late Permian to Triassic (~240 Ma) (Fig. I.5). The youngest age is 220 Ma and the sample yields a maximum deposition age is 230±10 Ma.

5.3.3. Sample DV 8-08-16-3

For sample DV 8-08-16-3, 176 of the 200 detrital zircon analyses met requirements for plotting and interpretation. The age distribution yields two small Precambrian peaks and two prominent Phanerozoic peaks. The older Precambrian peak is ~2500 Ma (~2700–2400 Ma), with a younger more prominent peak at ~1855 Ma (~2100–1600 Ma), as well as a broad population

from ~1300–700 Ma. The sample yields a broad prominent peak that is late Proterozoic–Devonian (~650–400 Ma) and a younger more prominent Permian to Triassic population (~270–220 Ma) (Fig. I.5). The youngest detrital zircon grain is 225 Ma and the sample yields a maximum depositional age of 226±8 Ma.

5.3.4. Sample 13P99

Sample 13P99 was analyzed at the University of Arizona Laserchron Center and yielded 315 ages meeting the previously-stated criteria. The age distribution for this sample has three minor Precambrian peaks and two prominent Phanerozoic peaks. The Precambrian peaks are at ~2500 Ma (~2600–2400 Ma), ~1870 Ma (~1900–1800 Ma) and a broad distribution of ages from ~950–875 Ma. Phanerozoic ages yield two main populations: a strong Silurian through Early Devonian population and a Late Carboniferous to Late Triassic population (Fig. I.5). The youngest detrital zircon grain is 220 Ma, and the sample yields a maximum depositional age is 225±10 Ma.

5.3.5. Sample DV 7-25-15-2

For Sample DV 7-25-15-2, 155 of the 200 individual zircon analyses met requirements for plotting and interpretation. The age distribution shows three small Precambrian peaks and two prominent Phanerozoic peaks. The Precambrian peaks are a narrow population centered at ~2470 Ma (2600–2400 Ma), ~1830 Ma (2000–1600 Ma), and a broad population from ~1100–700 Ma. Phanerozoic ages yield a strong Early Ordovician to Late Devonian population and a strong bimodal Permian to Late Triassic population with peaks at ~285 and 240 Ma (Fig. I.5). The youngest detrital zircon grain is 215 Ma and the sample yields a maximum depositional age of 216±8 Ma.

5.4.0 Results

The Lokzun Group and Darbasatash samples from this study yield similar DZ age populations that have three minor Precambrian age groups and two prominent Phanerozoic age groups (Fig. I.5). The two oldest Precambrian age populations of ~2600–2400 Ma and ~2000–1600 Ma are prominent in all samples analyzed, as well as being present in both Asian and Gondwanan terranes, and are not significant for the scope of this study. The youngest Precambrian age population in all samples is broad and generally ranges from ~1100–700 Ma. Although the Late Proterozoic age population is broad and varies between samples, there are no peaks statistically significant enough to affect comparison between the age distributions.

Phanerozoic detrital zircon ages for all seven samples are broadly similar, with all samples yielding two prominent age peaks: an Early Paleozoic peak that is generally Silurian to early Devonian (~440–410 Ma) and a younger peak that is generally Late Carboniferous to Triassic (320–200 Ma). We interpret this strong similarity to show that the samples were all sourced from the same terrane. One notable exception is sample DV 8-08-16_3 which has a broad late Neoproterozoic to Devonian age population (~560 Ma) (rather than the strong Silurian–Devonian population), although the sample has the same strong Carboniferous–Triassic population as the others. In comparing our results to previously-published detrital zircon populations from terranes in the Tibetan orogen, the two prominent Phanerozoic peaks are most similar to detrital ages from the Karakul Mazar Terrane of the Northern Pamir (Robinson et al., 2012; Imrecke et al., 2019) and Songpan-Ganzi terrane of northern Tibet (e.g. Ding et al., 2013; Weislogel et al., 2010, 2006). Further, the Phanerozoic populations are notably different than those obtained from the Gondwanan Qiangtang terrane of northern Tibet and Central Pamir (Gehrels et al., 2011; He et al., 2018). In particular, the strong Silurian–Devonian peak in most of

the samples is absent in Gondwanan terranes, as are the strong Late Carboniferous to Triassic age populations (Fig. I.5). For a complete list of U-Pb results see Appendix 1.

5.5.0 Statistical Analysis

Literature reveals that previous quantitative comparison of DZ data sets has proven challenging, with various tests potentially yielding incorrect results (Vermeesch, 2005; Saylor and Sundell, 2016). In particular, the Kolmogorov-Simirnov (K-S) and Kuiper test p values have been shown to be problematic in comparing detrital zircon age populations. To address this concern, we conducted statistical comparisons between the samples using R2 crossplot values calculated using Saylor and Sundell's (2016) DZstats. For a sample that has 50 age groups and n = ~150, an R^2 crossplot value greater than 0.70±0.10 suggest the samples are related and have a common source. All but a few comparison values produced from quantitative analyses of the Lokzun Group, Darbasatash Group, and Karakul Mazar terrane fall within this range or are higher. R^2 crossplot values that lie below this range are associated with sample DV 8-08-16_3, which has a distinct late Proterozoic-early Paleozoic population, as discussed in the previous section (Table I.2). Although this statistical analysis supports our interpretation that the samples were all sourced from the same terrane, visual comparison of stacked probability diagrams may still be most reliable for this particular data set.

Table I-2 crossplot statistical analysis of detrital zircons

	DV 8-08-15_1	DV 7-25-15_1	DV 7-09-15_4	DV 7-12-15_4	DV 8-08-16_3	13P99	DV 7-25-15_2	North Pamir
DV 8-08-15_1	1	0.9308	0.76	0.7989	0.6667	0.7376	0.8684	0.8174
DV 7-25-15_1	0.9308	1	0.8437	0.8395	0.6806	0.6897	0.8993	0.8044
DV 7-09-15_4	0.76	0.8437	1	0.9005	0.6492	0.7343	0.7778	0.6979
DV 7-12-15_4	0.7989	0.8395	0.9005	1	0.673	0.7067	0.769	0.7487
DV 8-08-16_3	0.6667	0.6806	0.6492	0.673	1	0.5105	0.6289	0.5432
13P99	0.7376	0.6897	0.7343	0.7067	0.5105	1	0.6756	0.6949
DV 7-25-15_2	0.8684	0.8993	0.7778	0.769	0.6289	0.6756	1	0.8956
North Pamir	0.8174	0.8044	0.6979	0.7487	0.5432	0.6949	0.8956	1

6.0 Discussion

Sediment provenance analyses of the Upper Triassic Lokzun Group and Lower Jurassic Darbasatash Group provide important new insights into the timing of suturing between the Southern and Central Pamir with the southern margin of Asia, the nature of the Cimmerian Orogeny in the Pamir, and the Mesozoic paleogeography of the Pamir.

6.1.0 Timing of Suturing

Petrographic analyses of the Lokzun Group and Darbasatash Group samples show both formations are comprised of an abundance of monocrystalline quartz and lithic rock fragments (metamorphic quartz, chert, and siltstone) – typical of recycled orogenic deposits derived from continental convergence orogens, subduction zones, and foreland uplifts (Dickinson and Suczek, 1979). Furthermore, the formations plot in the recycled orogen field of the QmFLt Provenance Plot (Fig. I.4) (Dickinson and Suczek, 1979), as has been shown previously for the Darbasatash group (Angiolini et al., 2013). Due to the nature of the contact between the Lokzun flysch and the Darbasatash (i.e., an angular unconformity), it is likely that the Darbasatash was partly sourced from the Lokzun Group. However, the monocrystalline quartz in the Darbasatash samples are slightly coarser than in the Lokzun Group, suggesting that the source of sediment for the formations was similar but that the Darbasatash was not primarily sourced from the Lokzun Group.

Based on the strong Late Carboniferous to Triassic signature, as well as the strong Silurian–Devonian population (Fig. I.5) within our detrital zircon analyses, we interpret both the Lokzun Group and Darbasatash Group to have been largely sourced from the Karakul Mazar Terrane of the Northern Pamir. Furthermore, although Carboniferous through Triassic magmatism is well documented in the Northern Pamir and Western Kunlun Shan, the only

Triassic magmatism documented in the Central and Southern Pamir is the Bashgumbaz Complex within the Southern Pamir which has yielded an igneous age of ~220 Ma (Zanchetta et al., 2018) (Fig. I.1). Although the Bashgumbaz Complex may be a partial source for Triassic ages, it does not account for the strong Permian–Triassic or Silurian–Devonian age populations present in the Lokzun Group or Darbasatash Group. Carboniferous–Triassic ages are also not present in detrital zircon results from pre-Jurassic sediments from Gondwanan terranes (Gehrels et al., 2011; Schwab et al., 2004; Robinson et al., 2007; Chapman et al., 2017). Comparison of age populations from the Lokzun Group and the Darbasatash Group to Gondwanan Tibetan terranes suggest that the samples have limited local (i.e., Gondwanan) sources based on the lack of a strong late Proterozoic–Cambrian age population (Gehrels et al., 2011). As noted above, however, sample DV 8-08-16_3 appears to have had a more prominent local source due to a strong late Proterozoic to Early Devonian (~600–400 Ma) age population (Fig. I.5).

Based on our evidence that both the Lokzun Flysch and Darbasatash formations were sourced from the Karakul-Mazar terrane, initial closure of both the Paleotethys and Rushan oceans must have occurred in the Late Triassic, with sediment from the Karakul-Mazar accretionary arc terrane being shed across the Central Pamir and onto the Southern Pamir immediately prior to deformation related to the Cimmerian orogeny (Fig. I.6). Our results also suggest closure of the two oceans was broadly coeval. Initial collision between the southern margin of Asia and both the Central and Southern Pamir by the end of the Triassic is coeval with (or slightly pre-dates) closure of the Paleotethys ocean along the northern margin of the Qiangtang terrane to the east (Kapp and DeCelles, 2019 and references thererin), clearly documenting that the Central Pamir and Southern Pamir were part of the larger Cimmerian terrane of Metcalf (2013).

The timing of the Wakhan suture, which separates the Southern Pamir from the Karakoram, is not as well defined and may post-date the collision of the Southern Pamir and Central Pamir with the Northern Pamir. In the Karakoram deposition of the Aghil formation, carbonates continued through the Norian (later than Triassic carbonates in the Southern Pamir) and are then capped by the Lower Jurassic quartz-lithic sandstones of the Ashtigar Formation. Although the Ashtigar Formation has been suggested to be of similar age as the Darbasatash Group, its age is not well defined (Gaetani et al., 1993, 2013; Angiolini et al., 2013). Unlike the Gurumdi Group-Darbasatash Group angular unconformity, the Ashtigar Formation is conformable with the Aghil Formation. Instead, the Ashtigar Formation is unconformably overlain by the Lower Jurassic Yashkuk Formation, which has a Pliensbachian base (Gaetani et al., 1993, 2013) and is a molassic red sandstone that contains sedimentary and metasedimentary clasts. As the unconformity separating the Ashtigar and Yashkuk Formations is younger then the post-Cimmerian unconformity in the Southern Pamir, it suggests the collision of the Karakoram with the Southern Pamir occurred after accretion of the Central Pamir and Southern Pamir with the Northern Pamir. Further studies of the Ashtigar and Yashkuk formations may shed new light onto possible sediment sources (e.g. from the Karakul-Mazar terrane, Rushan-Pshart Suture zone, or another source) and whether closure of the Paleotethys, Rushan Ocean, and Tirich Mir oceans were coeval or if closure of the Tirich Mir ocean occurred later (Fig. I.6).

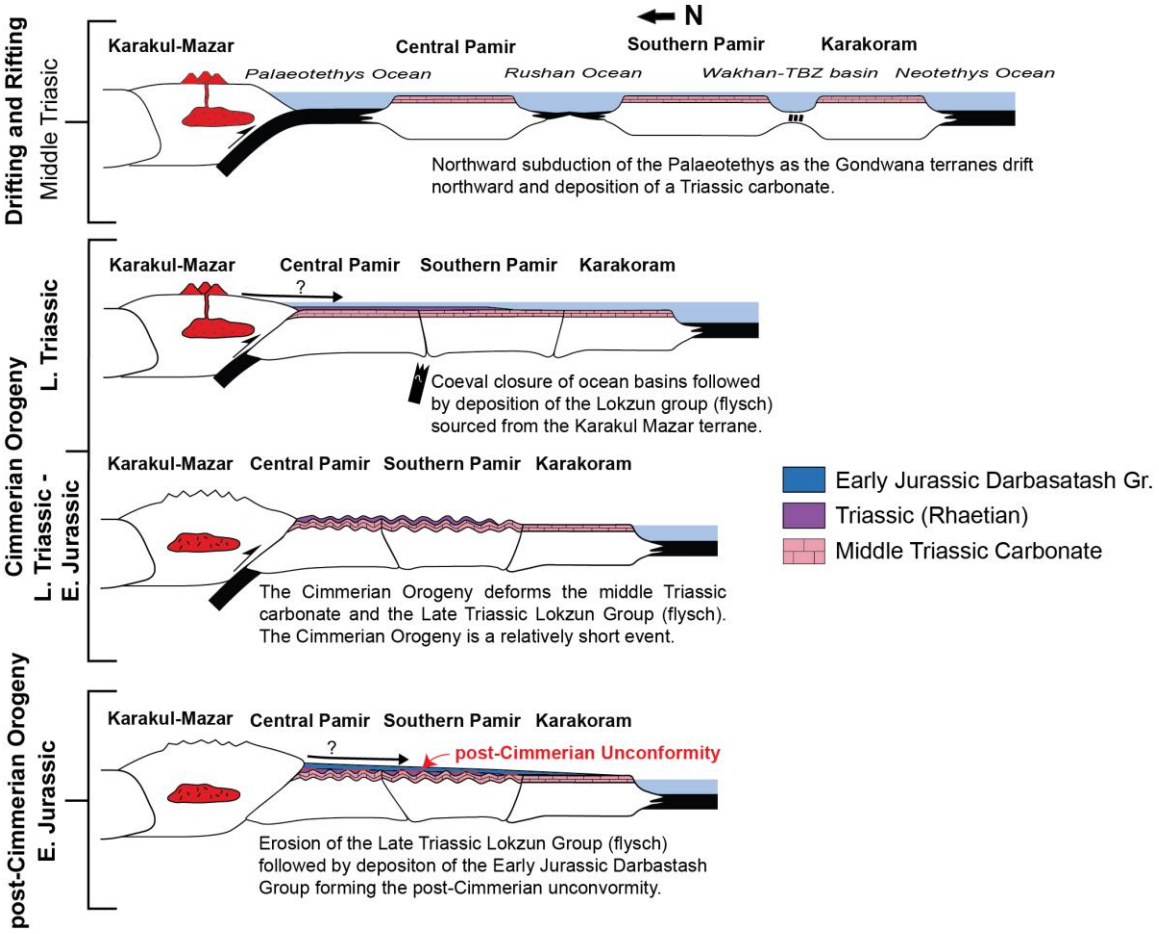

Fig. I.6 Triassic-Jurassic tectonic model of the Pamir

Permian to Early Jurassic tectonic history of the Pamir showing rifting of the Gondwana terranes, implications of the Cimmerian Orogeny, and source and deposition of Late Triassic to Early Jurassic clastic rocks. (modified from Angiolini et al., (2013) and Robinson, (2015))

6.2.0 Implications for the Cimmerian Orogeny

Within the Pamir, the Cimmerian Orogeny is a regionally-developed deformation event that resulted from the accretion of the Central Pamir and Southern Pamir to the Paleozoic southern Margin of Asia. The Upper Triassic (Rhaetian) Lokzun Flysch, which records the initial collision of the Central and Southern Pamir with Asia, is the youngest formation deformed by the Cimmerian orogeny (Fig. I.3 and I.6). The regional unconformity that developed after Cimmerian deformation is overlain by the Lower Jurassic Darbasatash Group, the stratigraphic age of which is constrained by the overlying Hettangian age Gurumdi Group carbonate platform (Fig. I.3) (Dronov et al., 2006; Angiolini et al., 2013). These constraints leave a narrow time period of several million years during which the Cimmerian Orogeny (and subsequent erosion) could have occurred, showing that the orogeny was a short-lived event within the Pamir. Further, both the very low grade of metamorphism of the rocks below the unconformity and the presence of a carbonate platform overlying the region immediately after indicate that crustal thickening related to the Cimmerian orogeny was limited, all of which indicate a “soft” collision between the Central and Southern Pamir and southern margin of Asia.

6.3.0 Implications for Paleogeography

One of the interesting implications of the results of our study is that the Karakul-Mazar terrane of the Northern Pamir was a sediment source for clastic deposits in the Southern Pamir both before and after Cimmerian orogeny deformation. As the late Paleozoic–Triassic southern margin of Asia was a cordilleran-style margin prior to the Cimmerian Orogeny – with associated magmatism, crustal thickening, and high-grade metamorphism (Robinson et al., 2004; Schwab et al., 2004; Schmidt et al., 2011) – the Northern Pamir was likely a region of elevated topography (Fig. I.6). More importantly, the Northern Pamir appears to have been a region of elevated

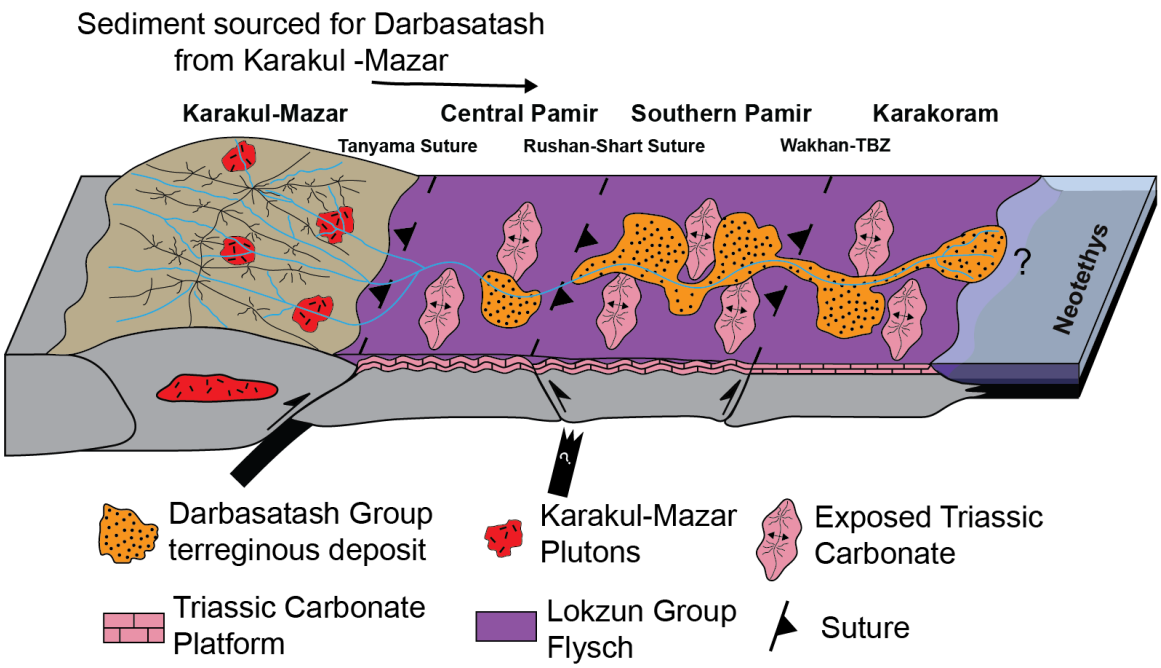

Fig. I.7 Limited exposure of the Darbasatash Group
Block model of the Pamir during the Early Jurassic. Note the Early Jurassic Darbasatash Group is sourced from the topographically elevated Karakul-Mazar Terrane and is deposited in paleo-lows along fluvial systems resulting in limited geographic exposure.

topography relative to surrounding regions throughout the Mesozoic as 1) there are no post-Triassic sedimentary deposits in the Northern Pamir (and Western Kunlun), unlike the Tarim-Tajik basins and Central and Southern Pamir, 2) the Northern Pamir continued to be a source of sediment for the Tarim basin to the north throughout the Mesozoic and Cenozoic (Sobel, 1999; Bershaw et al., 2012; Cao et al., 2015; Blayney et al., 2016) as well as the Southern Pamir (i.e. the Darbasatash Group) in the Jurassic, and 3) cooling ages in the Northern Pamir record continued exhumation through the Jurassic and Cretaceous (Robinson et al., 2004). Finally, the discontinuous nature of exposures of the Darbasatash Group within the Southern Pamir support the interpretation that the Darbasatash Group filled paleo-lows and previously-incised valleys as suggested by Angiolini et al. (2013) (Fig. I.7).

6.4.0 Possible post-orogenic Extension?

In the Southwest portion of the field area an uncharacteristically thick section of the Darbasatash group is exposed. Within this succession the Darbasatash lying conformably above Triassic slates is sub-vertical, and progressively transitions to shallowly dips up section directly below the Jurassic carbonates of the Gurumdi Group that lie conformably over the Darbasatash (Fig. I.8). We interpret this change in orientation to represent growth strata that we suggest was deposited in a small half graben as a result of minor extension immediately after the Cimmerian orogeny. However, this growth strata is the only evidence for extension, as there have been no Jurassic normal faults (or other evidence of extension) documented in the region.

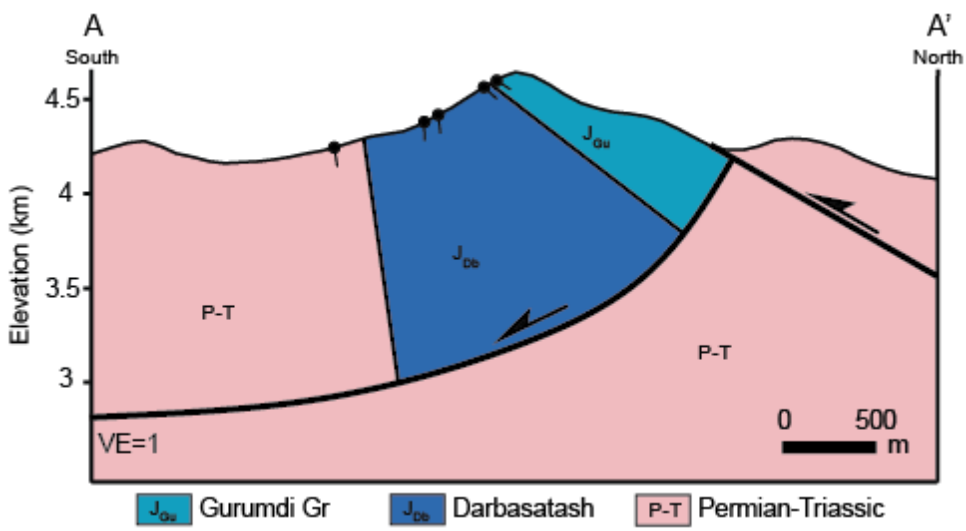

Fig. I.8 Darbasatash growth strata
Schematic cross section displaying Darbasatash growth strata as a result of a listric fault. Location of cross section is shown in southeast corner of map in Fig. I.2.

7.0 Conclusion

Our U-Pb detrital zircon and petrographic analyses from the Lokzun Group and Darbasatash Group, in combination with previous studies and geologic mapping of the Southeast Pamir, indicate the following:

1. Closure of the Paleotethys and Rushan Ocean was broadly coeval, with the Southern Pamir and Central Pamir accreting to the Northern Pamir (Paleozoic margin of Asia) by the end of the Triassic (Rhaetian) – resulting in the Cimmerian Orogeny.
2. The Karakul-Mazar detrital zircon signature is recorded in both the low-grade Upper Triassic (Rhaetian) Lokzun Group flysch, marking the timing of initial collision of the Central and Southern Pamir to the southern margin of Asia, and the post-Cimmerian Lower Jurassic Darbasatash Group that is overlain by the Hettangian age Gurumdi Group carbonate platform. This stratigraphic succession suggests that the Cimmerian orogeny was a short-lived event within the Pamir that resulted in minimal crustal thickening and that docking of the Gondwanan terranes resulted in a “soft” collision.
3. Sourcing of both the Lukzon group and Darbasatash formation from the Karakul-Mazar terrane indicate that the Northern Pamir was topographically elevated relative to surrounding regions both prior to and after the accretion of the Central and Southern Pamir and may have represented a region of elevated topography throughout the Mesozoic.
4. Closure of the oceanic basins in the Pamir is coeval with the closure of the Paleotethys in Tibet, supporting interpretations that the Central Pamir and Southern Pamir are the western extension of the Qiangtang terrane of Tibet.

II. TIMING FOR DISPLACMENT ALONG THE TANYMAS FAULT

1.0 Introduction

The Central Pamir has a present-day thickness of ~70 km, which is commonly thought to be the result of crustal stacking of thrust sheets caused by the convergence of the Indian and Asian continental collision (Burtman and Molnar, 1993; Rutte et al., 2017a). As such, observations within the region have been interpreted in the framework of supporting the idea of significant Cenozoic crustal shortening. An example of such is related to the widespread terrigenous clastic deposits found within the footwall of thrusts in the Central Pamir, most notably along the Tanymas and Rushan-Pshart suture zones which separate the Northern and Central Pamir and the Central and Southern Pamir, respectively (Figs. II.1). These deposits are generally described as Paleogene in age and have been interpreted to be syntectonic and related to subsequent shortening that accommodated the ongoing Cenozoic collision between India and Asia. However, recent work (e.g., Chapman et al., 2018; Robinson, 2015) shows that the age of these deposits are likely Cretaceous (Fig. II.2), and upper crustal deformation is suggested to be the result of a cordilleran style margin as the Neotethys Oceanic basin subducted northward below the Pamir (Stübner et al., 2013b; Chapman et al., 2018).

Analyses of detrital zircons using U-Pb and zircon fission track dating on terrigenous deposits within the footwall of the Rushan-Pshart fault and throughout the Southern Pamir have shown that they are, in fact, middle-Late Cretaceous in age (Fig. II.2) (Chapman et al., 2018). Our work shows that the terrigenous deposits along the Tanymas fault are syntectonic and date the timing of displacement along the Tanymas fault rather than being a component of Cenozoic

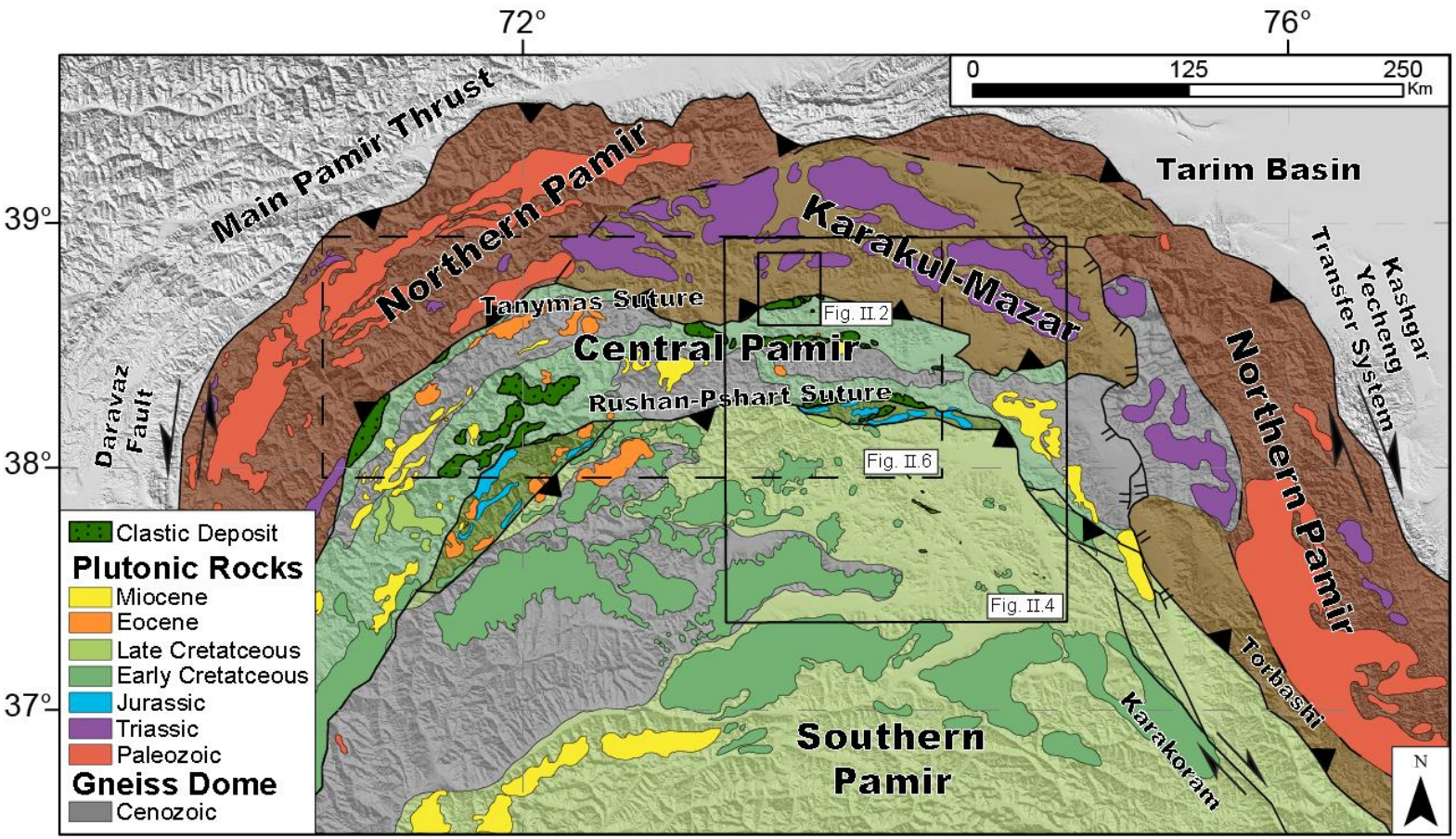

Fig. II.1 Tectonic Map of the Pamir

Regional map of the Pamir showing the different tectonic terranes, plutons and associated ages, Cenozoic gneiss domes, and clastic deposit of interest for this study. Location for Fig. II.2 and II.4 are outlined. Map modified from Schwab et al. (2004); Robinson (2015); Chapman et al. (2018)

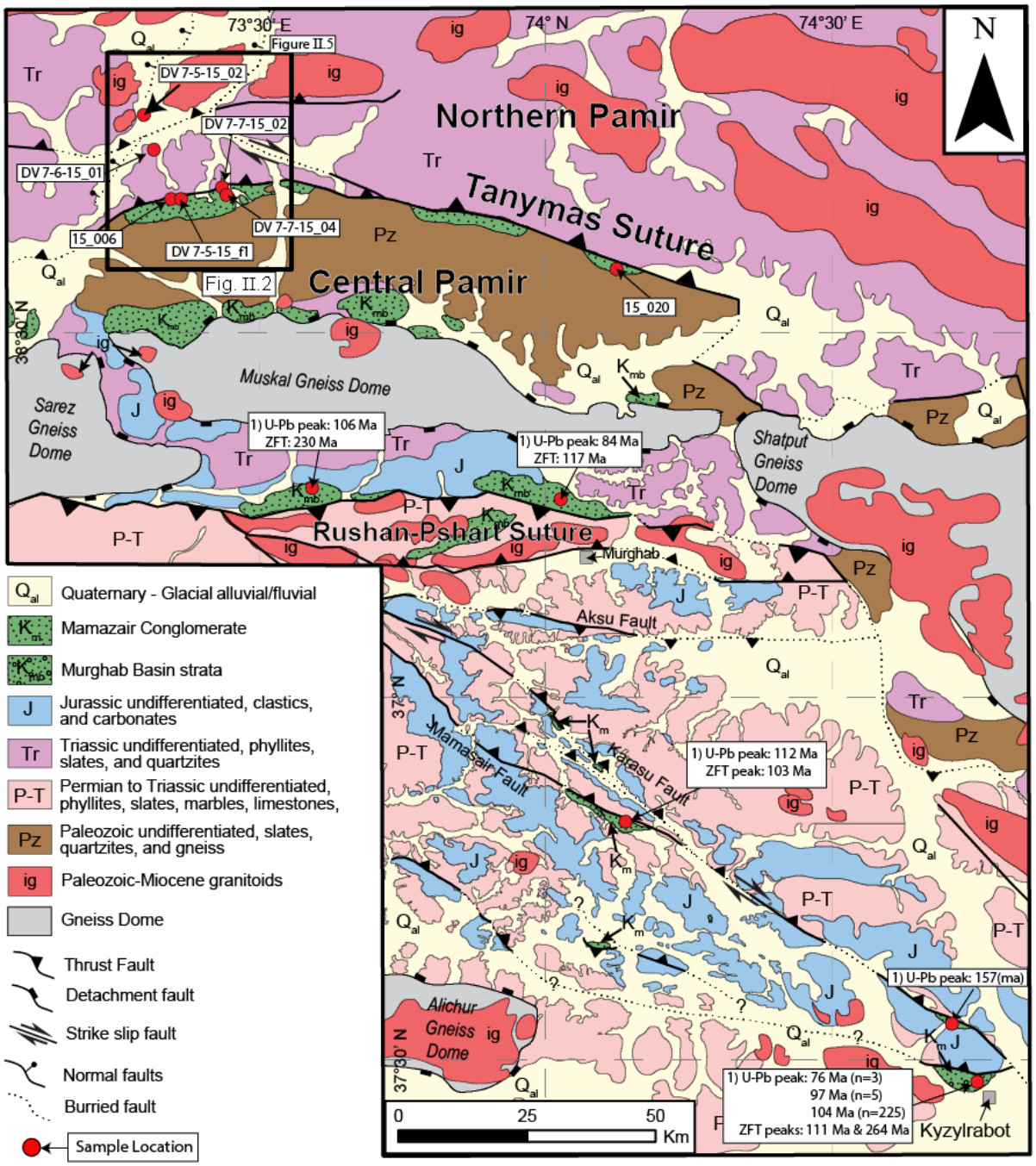

Fig. II.2 Geologic Map of Clastic Deposits

Regional geologic Map of the of the eastern Pamir. Map location is in Figure II.1. The geologic map is compiled from this study, Vlasov et al. (1991), Robinson et al. (2015), Chapman et al. (2018), He et al. (2018). Sample from syntectonic deposits are represented by red circles. Samples with ages are from Chapman et al. (2018) and samples with labels are from this study. Location of Fig. II.3 is represented by the outline.

crustal stacking (e.g., Burtman and Molnar, 1993; Rutte et al., 2017a). In order to better understand the age of the terrigenous deposits and their related structures throughout the region, we conducted geologic field mapping along the north dipping Tanymas fault and collected samples from clastic deposits within its footwall (Fig. II.3). The age and provenance of the deposits were then determined from U-Pb detrital zircon U-Pb analysis, zircon fission tracking, and muscovite Ar-Ar ages. In this study, we determine the depositional age of the red beds and suggest that the Tanymas fault has not been active since the Early Cretaceous, and, as such, cannot be a result of the Cenozoic collision between India and Asia.

2.0 Geologic Background

The Pamir region of Central Asia lies at the western end of the greater Himalayan-Tibetan orogenic system and consists of the Northern Pamir, Central Pamir, and Southern Pamir (Fig. II.1). The Northern Pamir is commonly divided into two separate regions: a Paleozoic portion that is the western extent of the Kunlun terrane of Tibet, and the Karakul-Mazar accretionary arc complex that is correlative to the Hoh-Xil-Songpan-Ganzi terrane of Tibet and has an abundance of Permian to Triassic aged granitoids (Xiao et al., 2002b; Schwab et al., 2004; Robinson et al., 2012; Imrecke et al., 2019). The Central Pamir is composed of deformed Gondwana Paleozoic rocks overlain by Triassic–Jurassic metasiliciclastic and carbonate platform type rocks (Vlasov et al., 1991; Schwab et al., 2004). Additionally, approximately 1/3 of the surface geology of the Central Pamir is made up of Cenozoic gneiss domes (Fig. II.1).

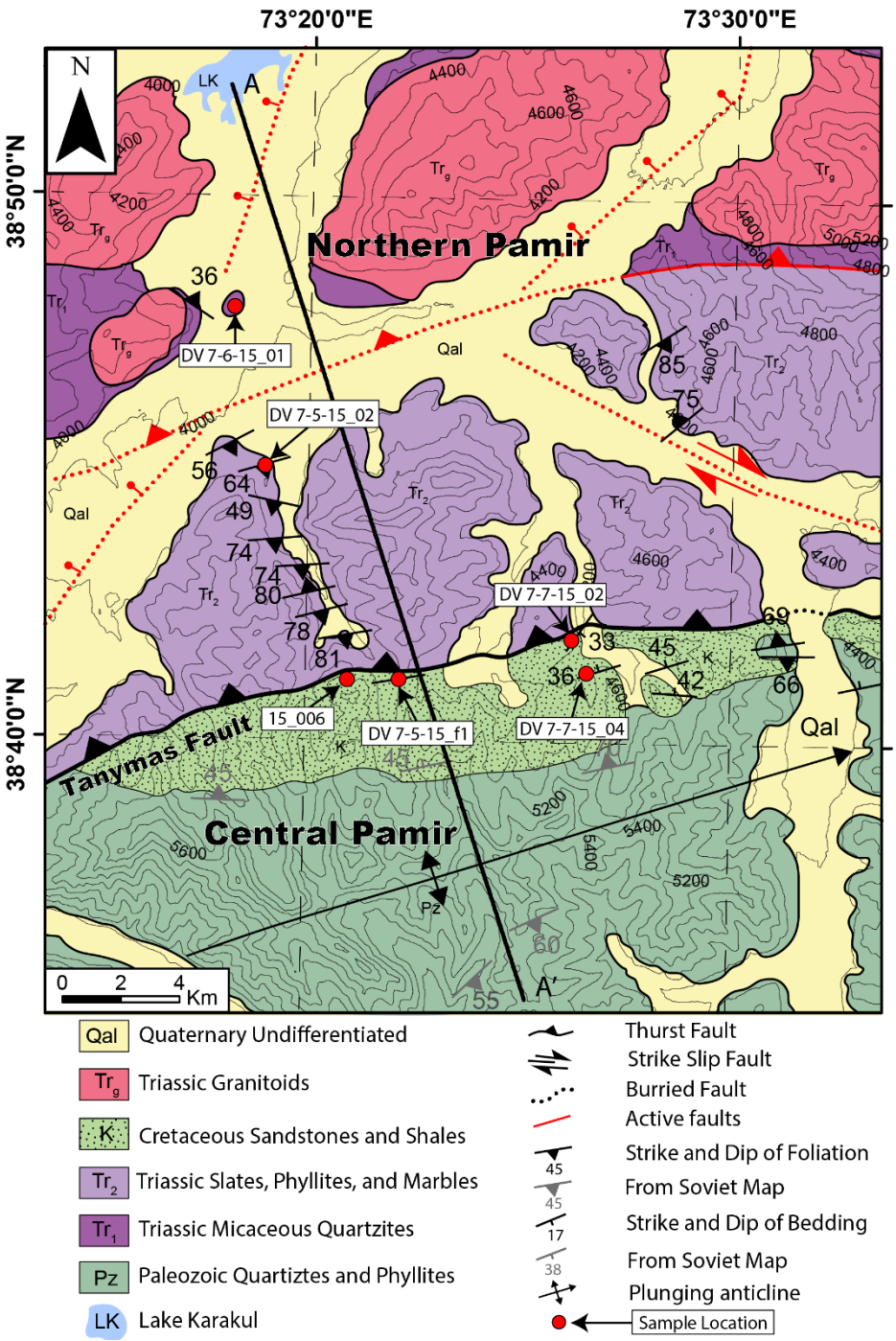

Fig. II.3 Geologic Map of Study Area

Geologic map of the study area along the Tanymas fault that separates the Northern Pamir from the Southern Pamir. Red circles show sample location for this study. Transect A-A' is location of Figure II.4

The Central and Southern Pamir collided with the Northern Pamir during the Cimmerian orogeny following consumption of the Paleotethys ocean, creating the south verging Tanymas suture (Fig. II.1). Subduction of the Rushan Ocean resulted in collision of the Central and Southern Pamir and the formation of the north verging Rushan-Pshart suture zone (Robinson, 2015). The timing for the development of the two sutures has been controversial. However, recent work has shown that they likely formed coevally during the latest Triassic (Chapter 1).

2.1.0 Cimmerian Orogeny

The collision of accretionary arc-complexes and Gondwana crustal fragments with the Paleozoic southern margin of Asia is referred to as the Cimmerian orogeny (Şengör, 1979, 1984; Burtman and Molnar, 1993). In the Pamir-Tibetan Orogen, the boundary separating Gondwana crustal fragments from the Paleozoic southern margin of Asia can be traced along the Tanymas fault in the Tajik Pamir, the Torbashi thrust in the Chinese Pamir (Schwab et al., 2004; Robinson et al., 2012), and the Jinsha suture in Tibet (Dewey et al., 1988; Yin and Harrison, 2000). The Gondwana crustal fragments in the Pamir are the Central Pamir and Southern Pamir, which are separated by the Rushan-Pshart suture and are interpreted to be the western extent of the Qiangtang terrane of Tibet (Robinson et al., 2012). Although the Rushan-Pshart suture is a prominent feature in the Pamir (Chapter 1; Robinson, 2015), its eastern continuation is uncertain. Angiolini et al. (2013) link the Rushan-Pshart suture with the Shuanghu suture, interpreted by some to divide the Qiangtang terrane (e.g., Zhang et al., 2006). Robinson et al. (2012), however, suggest the Rushan-Pshart suture may terminate at the Karakoram fault.

In the Central Pamir, an angular unconformity separating Paleozoic rocks from Upper Triassic–Lower Jurassic clastic rocks may be correlative to the post-Cimmerian angular unconformity found in the Southern Pamir (Leven, 1995), which separates complexly deformed

Permian–Triassic rocks from relatively undeformed Lower Jurassic clastics and carbonates (Angiolini et al., 2013). In the Southern Pamir, Angiolini et al. (2013) documented Cimmerian structures characterized by N-S to NNW-SSE trending folds, consistent with Soviet era maps (~1960s), whereas Rutte et al. (2017a) documented generally East-West striking structures that verge to the north. These two interpretations indicate that there is a large amount of variability in Cimmerian structures across the Southern Pamir, also noted by field observations detailed in Chapter 3.

Although there has been recognition of the highly-deformed nature of Cimmerian structures, the total amount of strain accommodated within the Permian-Triassic section due to the Cimmerian orogeny is unclear. In contrast to the underlying, highly-deformed Permian-Triassic section, relatively-undeformed overlying early Jurassic carbonates indicate that topography was at or below sea level at the time of their deposition. The presence of these Lower Jurassic carbonates in the Southern Pamir argue against the possibility that the crust was elevated and thickened by the Cimmerian orogeny (Robinson, 2015; Chapter 1).

2.2.0 Post-Cimmerian Deformation

A common question concerning the evolution of the Pamir is the timing of post-Cimmerian upper crustal shortening following the Late Triassic Cimmerian accretion of the Gondwana terranes. Previous studies have suggested that post-collisional convergence of the Central and Southern Pamirs with respect to the Northern Pamir occurred during either the Late Jurassic to Late Cretaceous (Shvol'man, 1978; Pashkov and Shvol'man, 1979; Pashkov and Budanov, 1990) or during the Cenozoic (Burtman and Molnar, 1993). This variability in the proposed timing of upper crustal deformation in the Pamir is due in large part to uncertainty in the age of terrigenous clastic deposits found throughout the Central and Southern Pamirs. These

beds are cited as being either Paleogene or Cretaceous in age by varying authors and even sometimes as having different ages for contiguous packages across map sheets by the same author (e.g., Vlasov et al., 1991; Yushin et al., 1964). As these clastic deposits are interpreted to be syntectonic (Burtman and Molnar, 1993; Robinson, 2015; Rutte et al., 2017a), the age and depositional nature of them is important to constraining the timing of upper crustal deformation. For example, Central Pamir syntectonic terrigenous red beds in the footwalls of the Rushan-Pshart fault (Figs. II.1, and II.2) and within the Southern Pamir Fold and Thrust Belt that were previously interpreted to be Paleogene in age (Yushin et al., 1964; Vlasov et al., 1991) have recently been dated via U-Pb detrital zircon and zircon fission tracking as being Cretaceous in age, which shows that upper crustal deformation occurred prior to India colliding with Asia (Chapman et al., 2018).

In addition to timing, the magnitude of upper crustal shortening within the Central and Southern Pamirs is also in question. Burtman and Molnar (1993) suggested that 340 km of post-collisional convergence between the Northern Pamir and the Southern and Central Pamirs was accommodated in 4 primary zones: nappe structures interpreted to root into the Tanymas suture (> 20 km), displacement of thrust sheet within the Central Pamir (~80 km), along the Rushan-Pshart suture (80 km), and in the Southern Pamir by upper crustal shortening (>50 km) and a basement-involved thrust nappe (>100 km) (Burtman and Molnar, 1993; Rutte et al., 2017a). However, recent studies indicate there has perhaps been less than 200 km of internal shortening within the Central and Southern Pamirs (Stübner et al., 2013b; Chapman et al., 2018). For instance, in the Southern Pamir, a structural boundary between basement and cover rocks previously interpreted as a nappe structure has been shown to be extensional in origin –shear zones bounding the exhumed Shakhdara-Alichur gneiss dome (Stübner et al., 2013b) –removing

100 km of interpreted shortening. Additionally, retrodeformable cross sections within the Southern Pamir's thrust belt suggest less than 4.5 km of upper crustal internal shortening (Chapter 3), greatly reducing the previously-mentioned estimate of >50 km. These studies show that the widely cited previous estimates of Burtman and Molnar (1993) are likely incorrect.

These new revelations for the timing of upper crustal shortening in the Central Pamir and in the timing and magnitude of upper crustal shortening in the Southern Pamir raise the question of whether syntectonic terrigenous red beds in the footwall of the Tanymas fault are Cretaceous or Cenozoic (Paleogene) in age as they are similar to those analyzed by Chapman et al. (2018). If the terrigenous red beds in the footwall of the Tanymas fault are also Cretaceous in age, it would imply that displacement along the Tanymas ceased in the Cretaceous and did not accommodate any convergence between India and Asia. Thus, the magnitude of overall shortening of Asian crust in response to India colliding that has been accommodated in the Pamir would be further reduced.

2.3.0 Post-Jurassic Terrigenous Clastic Deposits

Terrigenous clastic deposits lie unconformably on Paleozoic–Cretaceous rocks throughout the Central and Southern Pamir (Figs. II.2 and II.3) (Burtman and Molnar, 1993; Robinson, 2015; Chapman et al., 2018). Within the footwall of the Rushan Suture of the Central Pamir, these deposits are referred to as the Murghab Basin strata (Rutte et al., 2017a; Chapman et al., 2018). Chapman et al. (2018) described the Murghab Basin strata as having a base composed of thinly-bedded (<50 cm) shale, fine-grained, rippled sandstone, and dolostone that is overlain by a cobble conglomerate and basalt flows. Attempts to date the basalt flows via radiometric and thermochronologic data have been unsuccessful (Rutte et al., 2017b). The

conglomerate is generally massive, clast-supported, and red. Interbedded sandstone, granule-pebble conglomerate, and siltstone overlay the basalt (Chapman et al., 2018).

Within the Southern Pamir, the clastic deposits are composed of numerous, disparate red beds that are referred to as the Mamazair conglomerate (Fig. II.2) (Chapman et al., 2018). The conglomerates are composed of discontinuous lenses of sandstone interspersed among distinct conglomeratic bedding planes that range from one meter to 10s of meters thick. The Mamazair conglomerate is primarily clast-supported, with subangular to subrounded, pebble to cobble sized clasts and rare boulders. Clasts are predominantly carbonate (~85–95%), but also consist of sandstone, chert, and quartzite.

As mentioned earlier, the stated depositional age of these clastic rock packages has varied from Cretaceous to Cenozoic (Paleogene) (e.g., Vlasov et al., 1991; Yushin et al., 1964). However, the clastic deposits have consistently been interpreted as being syntectonic in nature, as they are found within the cores of synclines and footwalls of thrust (Burtman and Molnar, 1993; Robinson, 2015; Rutte et al., 2017a; Chapman et al., 2018). Thus, understanding the proper age of these beds is critical, as they will reveal a maximum age of deformation synonymous with their time of deposition.

Paleontological data suggest that the Murghab Basin strata of the Central Pamir were deposited during the Maastrichtian (Yushin et al., 1964), and U-Pb zircon geochronological data support this age (Chapman et al., 2018). Recent U-Pb detrital zircon geochronological analysis coupled with zircon fission track analysis from the Mamazair conglomerate of the Southern Pamir, indicate that the Mamazair is also likely Late Cretaceous in age (Chapman et al., 2018). Late Cretaceous deposition of these two syntectonic rocks packages is significant, because it indicates that most of the post-Cimmerian shortening occurred prior to India colliding with Asia

in the Cenozoic. Similar to the Murghab Basin strata and the Mamazair conglomerate, terrigenous clastic deposits within the footwall of the Tanymas suture, which has been reactivated into a south verging thrust fault, have previously been defined as both Cretaceous and Paleogene in age (Yushin et al., 1964; Vlasov et al., 1991). We believe that these beds are also syntectonic and that their age is coeval with displacement along the Tanymas fault. If the terrigenous deposits in the footwall of the Tanymas fault are Cretaceous in age, then they support the idea that post-Cimmerian deformation is the result of a Cretaceous cordilleran margin and not the result of India colliding with Asia.

3.0 Lithologic Descriptions and Field Observations

Geologic field mapping was conducted in two valleys of the Muskol Range directly south of Lake Karakul (Fig. II.3) on 1:100,000 scale maps. Lithologic contacts were then extended using satellite imagery and previously published maps. In the following sections, we describe the structural architecture and lithologic characteristics in a north-to-south transect from Lake Karakul to the clastic deposits within the footwall of the Tanymas fault (Fig. II.3).

3.1.0 Northern Pamir Terrane

The northernmost section of the north-to-south transect consists of foliated micaceous quartzites that have been intruded by granites (Tr_1 Figs. II.3 and II.4). Metamorphic foliation strikes to the northwest and moderately dips to the northeast. The foliations stike planes contain stretching lineations that trend 074°, 32° (Fig. II.4A). Thin section analysis of the quartzite (Fig II.6 Tr_1) indicates 75–85° polycrystalline quartz with irregular grain boundaries, 5-10% well-formed mica, and rare (<1%) potassium feldspar. Rare garnets that are <1 mm in diameter were seen in the field, however, none were seen in the thin section analysis. The polycrystalline quartz

shows dynamic recrystallization (Fig. II.5 Tr_1) suggesting high temperature alteration, characterized as regime 3 by Hirth and Tullis (1992).

Farther to the south, within the Northern Pamir, metamorphic grade decreases over a short distance. Lithologies consist of dark grey to black slates and phyllites interbedded with quartzites and occasional marbles (Tr_2 Figs. II.3, II.4B, and II.5). Phyllites contain occasional pyrite porphyroblasts and white mica. Foliation is subvertical and strikes to the WSW–ENE. Additionally, there is internal small-scale folding with similar axial plane orientation as the larger structures (Fig. II.4C). Within the foliated marble are asymmetrical carbonate clasts that indicate a top to the southeast sense of shear (Fig. II4B). Thin section analysis of a quartzite sample (Figs II.5 Tr_2) shows monocrystalline quartz 125-300 µm in diameter, ~50% of which contain undulatory extinction. The monocrystalline quartz shows very little (<1%) bulging recrystallization, indicating that the rocks have undergone no dynamic recrystallization. We interpret this decrease in metamorphic grade, from north to south, to indicate that there is a south-verging thrust fault placing higher grade rocks onto lower grade rocks (Figs. II.3 and II.5).

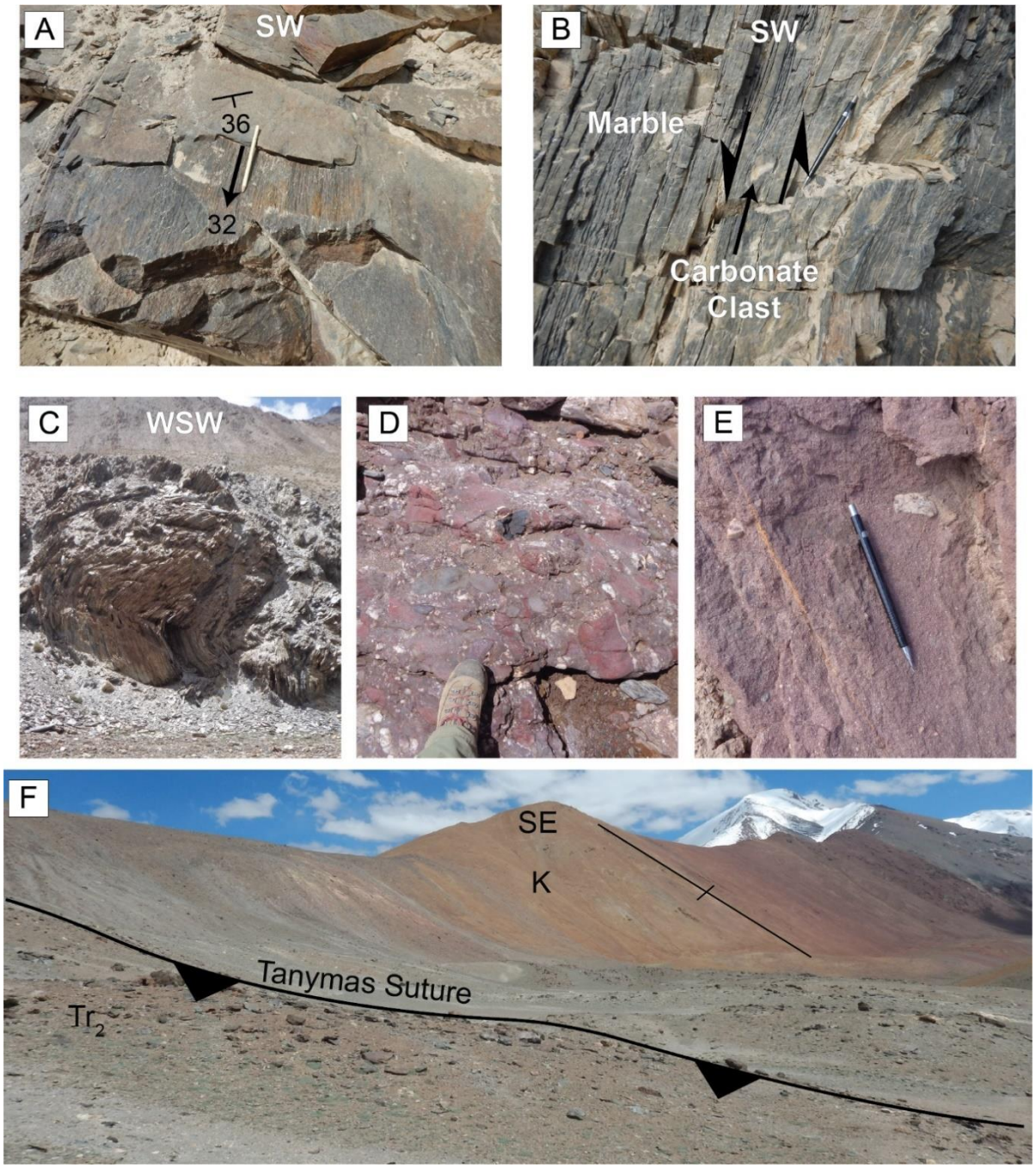

Fig. II.4 Field Photos

Field Photos from map area (A) Foliation and stretching lineation in Tr_1 (location: 38.8N, 73.29E). (B) Foliation in a marble from Tr_2 and a rotated clast with a top to the north sense of shear (location: 38.74N, 73.32E). (C) Internal folding within Tr_2 (location: 38.7N, 73.35E). (D) Cobble conglomerate within the terrigenous clastic deposit (location: 38.67N, 73.44E). (E) A sandstone from the terrigenous clastic deposit with a floating clast (location: 38.69N, 73.44E) (F) Field photo of the terrigenous clastic deposit. Beds are subvertical to SE dipping (Ridge location: 38.69N, 73.37E).

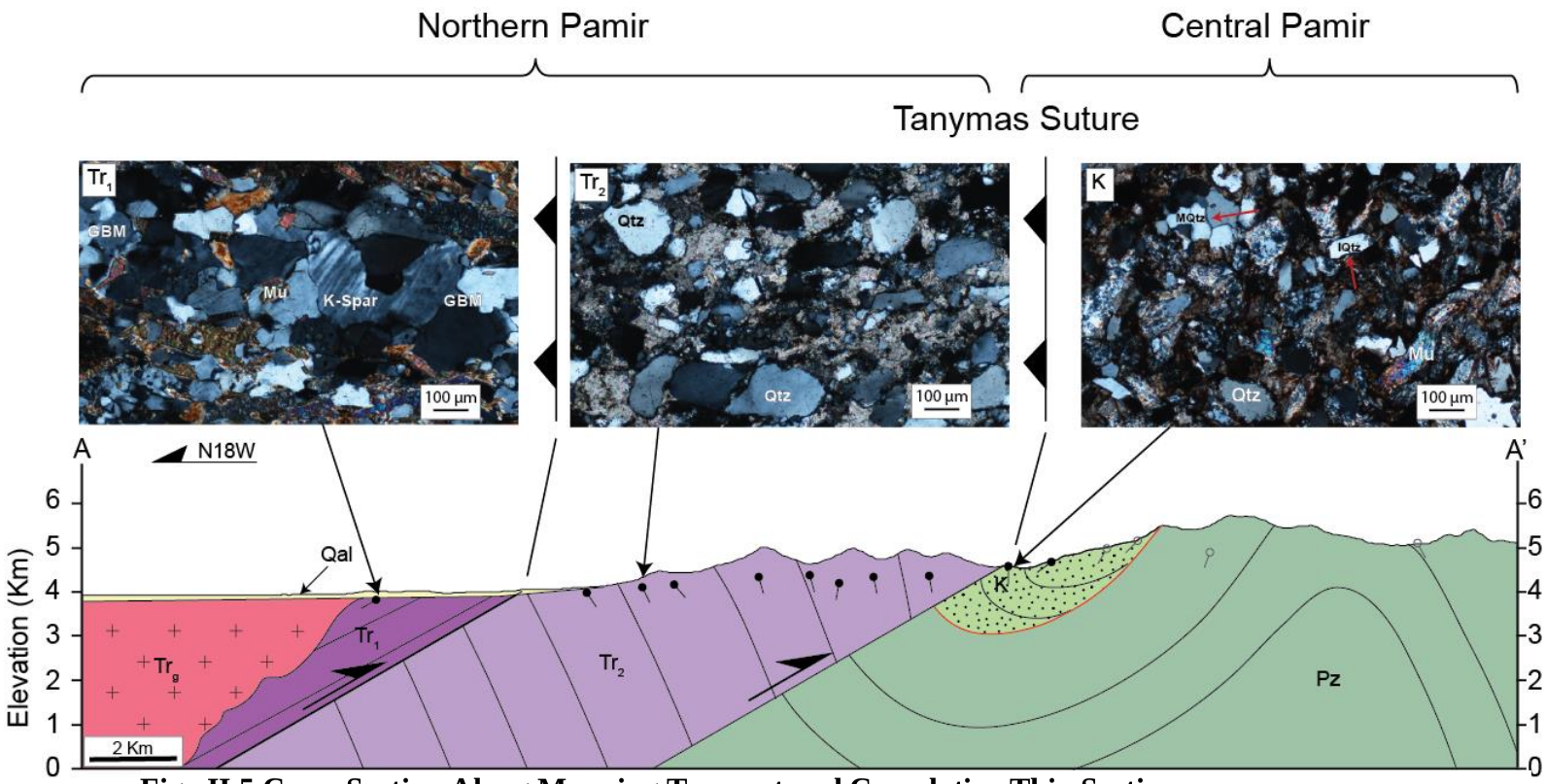

Fig. II.5 Cross Section Along Mapping Transect and Correlative Thin Sections
Geologic cross section along A-A'. Photomicrographs above cross section show representative examples of different units. Geologic unit Tr_1 preserves Grain Boundary Migration (GBM) associated with Regime 3 of Hirth and Tullis (1992). Tr_2 underwent low-grade metamorphism and no dynamic recrystallization. K is the synorogenic clastic deposit of interest for this study and petrographically it contains polycrystalline quartz that has GBM and monocrystalline grains with irregular grain boundaries, similar to the polycrystalline quartz and indicative of GBM, and undulatory extinction. GBM=Grain Boundary Migration, K-Spar=potassium feldspar, Mu=Muscovite, Qtz=quartz, MQtz-metamorphic quartz, IQtz=Quartz with irregular grain boundaries

3.2.0 Central Pamir

Continuing south, crossing the Tanymas fault into the Central Pamir, lithologies change from metamorphic rocks to terrigenous clastic deposits (as previously-mentioned in Section 2.3) found in the footwall of the Tanymas fault. Structurally, the beds initially strike generally E-W and dip to the southeast subvertically to 60° with local internal folding present (Fig. II.4C). Further to the south, the beds begin to dip up to 45° to the NW (Fig. II.2). Overall, we interpret this structure to be an asymmetrical syncline that occurred during the same deformation event that resulted in displacement along the Tanymas fault.

Lithologically, the clastic deposits are composed of pebble-to-cobble size conglomerates, sandstones, and shales. The conglomerates contain rounded clasts of red sandstones, limestones, quartzites, and phyllites (Fig. II.4D). The sandstones and shales are interbedded, and individual beds range from centimeter to ~1 meter in thickness. The sandstones are red to light brown, poorly-sorted, fine to coarse, and subangular to subrounded with rare floating metamorphic clasts (Fig. II4D) (i.e., quartzite, phyllite). The sandstone is composed of predominantly quartz grains with moderate amounts of feldspar, and mica that are visible in hand sample.

In the thin sections of the sandstones from the Central Pamir (Fig. II.5 K), we see detrital mica that has been compacted along contiguous grains. We interpret the mica to be detrital due its appearance (i.e., compaction deformation and distinct grain boundaries). The quartz morphology is composed of fine polycrystalline sand grains (220 µm) with internal grain boundary migration that contain individual, interlocking medium silt-fine sand (20-100 µm) quartz grains (Fig. II.3K MQtz). Numerous medium-silt to fine-sand (20-100 µm) quartz clasts are angular–subangular with irregular grain boundaries (Fig. II.5 K IQtz) that are reminiscent of the individual component boundaries within the fine polycrstalline sand grains (MQtz) (red

arrows in Fig. II.5 K). Due to the similarities in their appearance and the tendency for larger, interlocking grains to break up along grain boundaries, we believe that these smaller, medium silt-fine sand quartz clasts are individual components of disaggregated polycrystalline metamorphic clasts. Due to grain morphology, we believe that the polycrystalline metamorphic quartz and the individual monocrystalline medium silt-fine sand quartz grains are derived from the higher-grade, hanging-wall metamorphic rocks and plutonic rocks within the Northern Pamir (Tr_1). There are also larger, very fine-medium sized (100-200 µm) monocrystalline quartz grains with undulatory extinction that are subangular-subrounded. These appear to have been sourced from the lower-grade footwall metamorphic rocks within the Northern Pamir (Tr_2).

4.0 Geochronology and Thermochronology Methods

4.1.0 Methods

To understand the timing of displacement along the Tanymas thrust, six samples from the footwall were collected and processed for detrital zircon U-Pb analysis. Four samples (DV 7-5-15_f1, DV 7-7-15_2, DV 7-7-15_4, and 15_006) were gathered from the Muskol Range south of Lake Karakul, one (15_020) from the eastern footwall of the Tanymas fault, and one (LY725171) was obtained from the Vanch Vally (Sample location Table II.1, Fig. II.2 and II.6). Two of the six samples (15_006 and 15_020) were also analyzed for detrital muscovite $^{40}Ar/^{39}Ar$ and detrital zircon fission track dating. U-Pb analysis of detrital zircons from samples DV 7-6-15_01 and DV 7-5-15_02 were attempted, but fewer than 10 zircons were obtained for each. All samples were separated for analysis via jaw crusher, disk milling, water table density separation, heavy liquid density separation, and magnetic separation then mounted with epoxy or Teflon.

4.2.0 Detrital Zircon

Geochronological ages were determined from U-Th-Pb ratios in detrital zircons that were collected via LA-ICP-MS at the University of Houston and at the University of Arizona Laserchron Center (laserchron.org). At the university of Houston, detrital zircons were analyzed by a Photon Machine Analyte.193 excimer laser ablation system coupled to a Varian 810 Quadrupole mass spectrometer. The laser ablation settings consisted of ~ 20 seconds of background analysis followed by 30 seconds of ablation time that consisted of 300 bursts at 10 Hz with a spot size of 25 µm and a fluence of 2.99 J/cm^2. Data was then reduced using an in-house program "U-Pb Data Reduction" (Sundell, 2017). At the University of Arizona, laser ablation was conducted with a spot size of 20 µm using a Teledyne Photon Machine G2™ solid state NeF excimer attached to a single collector Thermo Fischer Scientific Element 2™ inductively coupled plasma mass spectrometer. For more details concerning the analytical techniques and for data reduction procedures refer to Gehrels et al. (2008). For visual observation of the age spectrum, probability density plots were created of concordant ages from each sample using isoplot (Ludwig, 2003). For each sample, the three youngest grains that overlapped in error were then used to calculate a maximum depositional age (Dickinson and Gehrels, 2009).

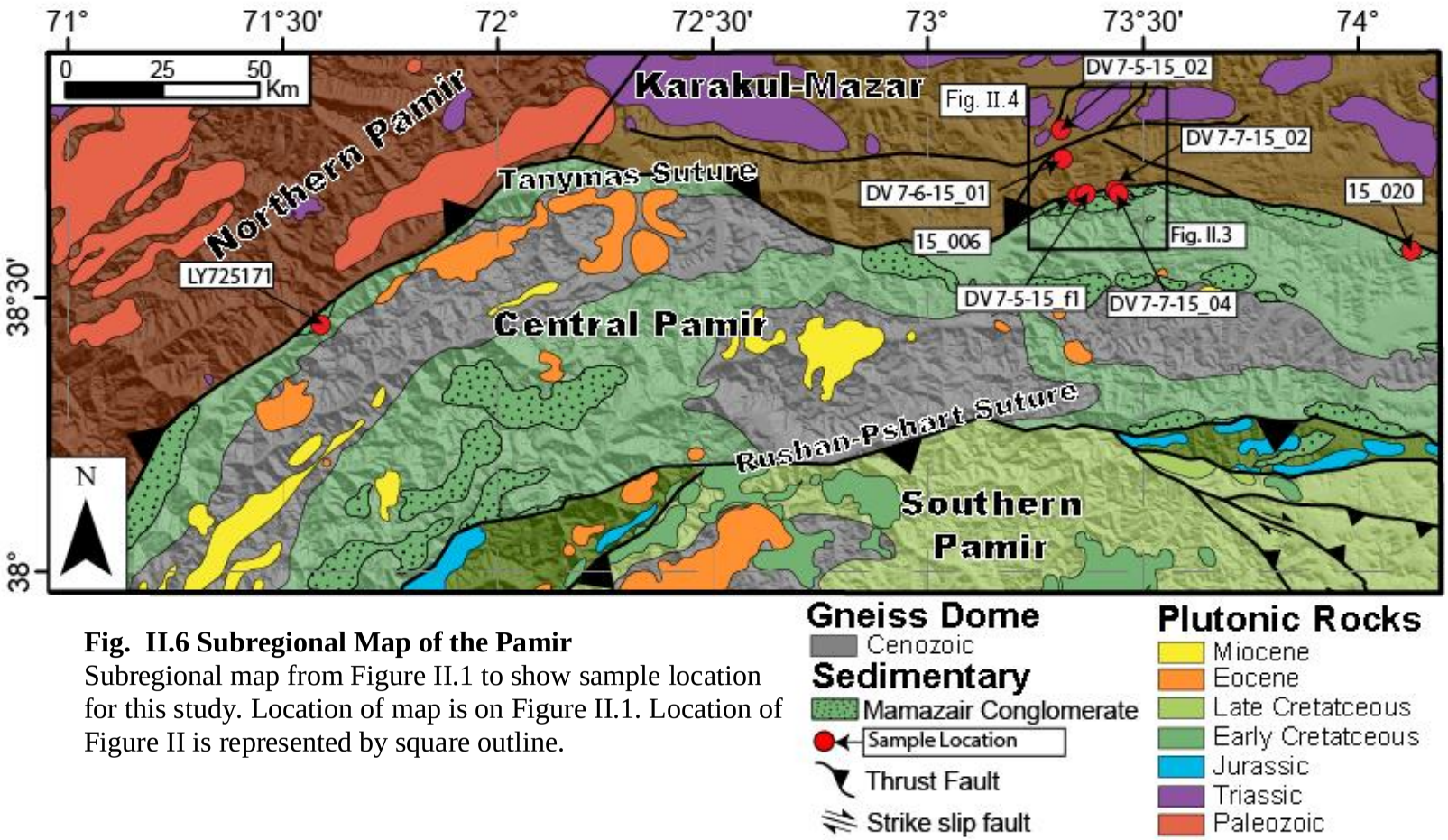

Fig. II.6 Subregional Map of the Pamir
Subregional map from Figure II.1 to show sample location for this study. Location of map is on Figure II.1. Location of Figure II is represented by square outline.

Table II-1 Location and Maximum Depositional Age for Each Sample

Sample	Latitude	Longitude	Maximum Depositional Age (Ma)		
			U-Pb	ZFT	Ar/Ar
Tanymas Footwall					
DV 7-5-15_f1	38.688	73.369	242 ± 8.7		
DV 7-7-15_2	38.699	73.438	203± 6.6		
DV 7-7-15_4	38.689	73.444	161± 5.2		
15_006	38.688	73.349	258± 4.7	130	128± 2.7
15_020	38.587	74.123	208± 3.2	139	117± 6.3
LY25171	38.453	71.590	219± 2.8		
Northern Pamir					
DV 7-06-15_1	38.7995	73.3037	No Zircons.		
DV 7-05-15_2	38.7506	73.3164	No Zircons		

4.3.0 Muscovite $^{40}Ar/^{39}Ar$

Samples 15_006 and 15_020 were also analyzed for $^{40}Ar/^{39}Ar$ analysis. The micas collected form the sample were 62-500 microns in diameter and separated from the clastic deposits via Wilfley table, magnetic separation, and heavy liquids. The micas where handpicked for analyses, then ultrasonically cleaned in distilled water and packed. The samples were then analyzed at the U.S. Geological Survey Laboratory in Denver Colorado. At the USGS the samples were irradiated in the TRIGA reactor and the neutron flux was monitored using 28.2 ± 0.8 Ma Fish Canyon Tuff sanidine (Kuiper et al., 2008) . The Muscovite samples were then analyzed for $^{40}Ar/^{39}Ar$ at the USGS laboratory on a Mass Analyzer Products 215-50 Mass spectrometer with heating conducted by an infrared (CO_2) laser.

4.4.0 Zircon Fission Track

A subset of detrital zircon grains (~100) from samples 15-006 and 15-020 were analyzed for Zircon fission track (ZFT) thermochronology and U-Th-Pb of the same detrital zircon grains for “double dating”. ZFT analysis was conducted at the University of Arizona Laserchron center

using the LA-ICP-MS fission track method and a modified zeta calibration (Hurford and Green, 1983; Hasebe et al., 2004; Donelick, 2005).

Detrital zircon grains were mounted in a Teflon mount and the interior of the grains were exposed through polishing. The zircons were than etched in a eutectic melt of NaOH-KOH at ~220 ºC for 9 to 12 hours followed by sonication for 5 minutes in 1% solution nitric acid for cleaning. The mounts were then carbon coated and imaged using the backscatter electron (BSE) signal from a Hitachi 3400N scanning electron microscope (SEM) at the University of Arizona Laserchron SEM facility. ZFTs were then counted on the BSE images within an area of 100 to 400 μm^2 that was free from any alterations or impurities (i.e. heavy scratching, cracks, dislocations, inclusions, and U domain boundaries such as rim/core zonation).

The concentration of U from detrital zircon unknowns was determined via LA-ICP-MS using an ablation spot size of 15 μm positioned in the same area fission tracks were calculated. The detrital zircon unknows were interspersed with a subset of Sri Lanka zircon standards (SL-F) and R33 zircon standards. The U concentration of the SL-F zircon standards were determined to be 518 ppm, consistent with isotope dilution thermal ionization mass spectrometry (ID-TIMS) of SL-F zircons (Bernet and Garver, 2005). For each sample group, the ratio of U concentration of the SL-F zircons and the average U intensity for SL-F standards was then used to determine the U concentration in detrital zircon unknowns. The uncertainty (1σ) in U concentration was measured from repeated analysis of U intensity in SL-F standards and calculated to be 10% - 13%. The uncertainty includes variability in SF-L U concentration and instrument uncertainty. Uncertainty was then incorporated into the calculation for ZFT age determination. R33 zircon standard U concentration was determined to be 107 ± 14 ppm (n=66) (Data Repository 2), within error determined by ID-TIMS (132 ± 51 ppm, n=14) (Black et al., 2004).

Zeta calibration was conducted from 431 Fish Canyon Tuff (FCT) zircon standards that were analyzed during ablation of detrital zircon unknowns. The FCT zircon standards were then divided into 21 sets that contained $\geq$ 20 grains each and a compiled zeta factor of 2729 ± 107 (analyst = J. Chapman) was calculated. The average single-grain uncertainty (1σ) for ZFT of detrital zircon unknowns is 26.1% (Data Repository 2). Age distribution of ZFT single-grain ages are displayed as kernel density estimation (KDE) plots using DensityPlotter (Vermeesch, 2012).

5.0 Results

5.1.0 Muskol Range

5.1.1 DV 7-5-15_f1

For sample DV 7-5-15_f1, 176 individual zircon analyses met requirements for plotting and interpretation. The age distribution of the sample shows two prominent peaks: an Ordovician to Middle Devonian (485–380 Ma) and a Permian to Middle Triassic (300–240 Ma) age population. There is also a minor Late Triassic and Late Jurassic peak, but these peaks are only composed of 2 and 1 individual zircon analyses, respectively. Therefore, a maximum depositional age of 242±8.7 Ma was calculated.

5.1.2 DV 7-7-15_2

For sample DV 7-7-15_2, 200 individual zircons were analyzed and 130 met the requirements for plotting and interpretation (Fig. II.7). Analyses of the sample yielded two minor broad age populations and one larger age population that are Phanerozoic in age. The two broad populations are Cambrian to Late Devonian (540–360 Ma) and Permian to Middle Triassic (300–240 Ma) in age. The larger more prominent age population is Late Triassic (230–200 Ma). The

youngest detrital zircon analysis from the sample is an outlier at 175 Ma, and a maximum depositional age of 203±6.6 Ma was calculated (Table II.1).

5.1.3 DV 7-7-15_4

For sample DV 7-7-15_4, 150 individual detrital zircon analyses were conducted and 138 met the requirements for plotting and interpretation (Fig. II.7). There are two minor age population that fall within the Silurian to Permian (430–250 Ma). However, the vast majority (~66%) of the detrital zircon analyses fall within the Middle to Late Triassic (235–200 Ma). There is a minor age population that is Late Jurassic in age that is composed of three individual zircon analyses that overlap in error. Therefore, a maximum depositional age of 161±5.2 Ma was calculated (Table II.1).

5.1.4 15_006

Sample 15_006 was analyzed at the University of Arizona Laserchron Center, and 89 individual detrital zircons met the requirement for plotting and interpretation (Fig. II.7). Analyses of the sample yielded detrital zircon ages populations that spanned from the Proterozoic to the Phanerozoic. Half of the of the detrital zircon ages are within the Phanerozoic and generate two major age populations: a Cambrian to Late Devonian (540–360 Ma) and a Permian to Middle Triassic (300–240 Ma). The youngest detrital zircon age from the sample is considered an outlier and is 210 Ma. Thus, a maximum depositional age of 258±4.7 Ma was calculated (Table II.1).

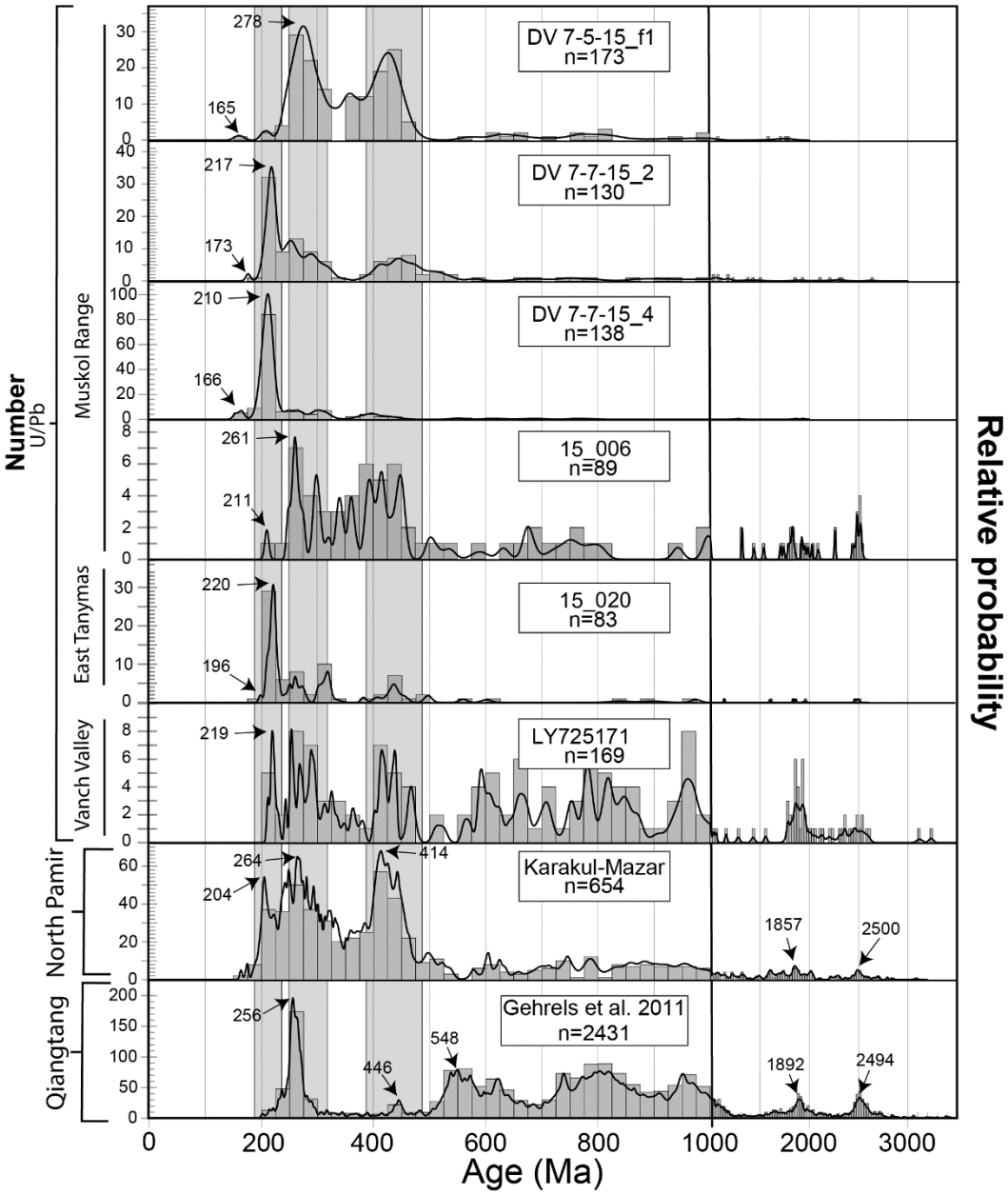

Fig. II.7 Probability Density Plot for U-Pb

Relative probability plots (black lines) and 25 Ma histograms (grey bars) for detrital zircon U-Pb geochronology from the clastic samples, Karakul-Mazar, and Qiangtang. Significant peaks are annotated by ages in Ma. Three age groups are highlighted by grey vertical bars. The Vanch Valley and Muskol Range are from this study and results are discussed herein. The Karakul Mazar is a combination of Robinson et al., (2012) and Imrecke et al., (2019). Qiangtang is a combination of the Northern and Southern Qiangtang from Gehrels et al., (2011).

5.1.5 15_020

Sample 15_020 was analyzed at the University of Arizona Laserchron Center, and 83 detrital zircon ages met the requirements for plotting and interpretation (Fig. II.7). The age distribution for this sample has two minor and one prominent Phanerozoic age populations. The minor age populations are Cambrian to Early Devonian (540–400 Ma) and Permian to Middle Triassic (300–240 Ma). The larger, more prominent age population is Triassic (252–200 Ma) in age and contains ~40% of the analyses. The youngest detrital zircon from the sample is 197.8 Ma, and a maximum depositional age of 208±3.2 Ma was calculated (Table II.1).

5.2.0 Vanch Valley

5.2.1LY725171

For sample LY725171, 169 of 200 detrital zircon analyses met requirements for plotting and interpretation (Fig. II.7). Analysis of the sample yielded age populations within the Precambrian and Phanerozoic. The age distribution for the Precambrian has one minor age population that is ~2,500–~1900 Ma and three prominent age populations that are ~2,100–1,750 Ma, ~1,000–900 Ma, and ~880–~560 Ma. The Phanerozoic age distribution yields three prominent age populations: a Cambrian to Early Devonian (540–400 Ma), Permian to Middle Triassic (300–240 Ma), and Late Triassic (230–200 Ma). The youngest detrital zircon age from the sample is 211 Ma, and a maximum depositional age of 219±2.8 Ma was calculated (Table II.1).

5.3.0 Summary of U-P Detrital Zircon Results

All samples yield abundant Phanerozoic age populations, with three significant age populations: an Early Paleozoic (500–380 Ma), Late Carboniferous to Permian (320–250 Ma), and Triassic (240–200 Ma) (Fig. II.7). Samples DV 7-7-15_f1, 15-006 and LY25171 have a

broad distribution of Early Paleozoic ages that are from ~500-380 Ma. Samples DV-7-15-f1, DV 7-7-15_2, 15_006 and LY725171 contain a prominent age population that falls within the Late Carboniferous to Late Permian age group. The Triassic age population is prominent in all samples, excepting DV 7-5-15_f1, and 15_006. One important variance is the strong Late Proterozoic age distribution that is only present in sample LY725171, which suggests an additional source. For a complete list of the data refer to Appendix 2.

The maximum depositional ages (MDA) for the samples can be split into three age populations (Table II.1): a late Permian to Middle Triassic, Late Triassic, and Late Jurassic. The late Permian–Middle Triassic MDA is represented by samples DV 7-5-15_f1, and 15_006, with an age of 242 ± 8.7 and 258 ± 4.7 Ma, respectively. The Late Triassic MDA is represented by sample DV 7-7-15_2 with an MDA of 203 ± 6.6 Ma, sample 15_020 with an MDA of 208 ± 3.2 Ma, and sample LY25171 with an MDA of 219±2.8 Ma. A Late Jurassic MDA is only found in sample DV 7-7-15_4 and is 161± 5.2 MA. Although a Late Jurassic age is only calculated in one sample, a single Early Jurassic age is present in DV 7-5-15_f1 and 2 detrital zircons in sample DV 7-7-15_2.

5.3.0 Thermochronology Results

5.3.1 Muscovite $^{40}Ar/^{39}Ar$

samples 15_006 and 15_020 were analyzed for detrital muscovite $^{40}Ar/^{39}Ar$ and the results plotted as probability density plots (PDP) and kernel density plots (KDE) (Fig. 4). Refer to Appendix 3 for a complete list of data. For sample 15_006, ages range from 228±3 to 125±7 Ma and fall within three age groups: Late Triassic, Early–Middle Jurassic, and Early Cretaceous. The most prominent age group (n=22) is the Early–Middle Jurassic. The Late Triassic peak has an n=14 and the Early Cretaceous age group has an n=10. Sample 15_020 contains $^{40}Ar/^{39}Ar$ ages

that range from 227±4 to 114±9 Ma with similar Late Triassic, Early–Middle Jurassic, or Early Cretaceous age populations. The Late Triassic (n=18) and Early–Middle Jurassic (n=17) are similar in abundance, whereas the Early Cretaceous (n=5) is the least prominent age group. For both samples, the Late Triassic age group corresponds well with the detrital zircon ZFT and U-Pb Late Triassic age population. Although the Early to Middle Jurassic $^{40}Ar/^{39}Ar$ age group is quite significant in both samples, it is of minor importance in both the ZFT and U-Pb data. The Early Cretaceous age group is the least significant in both samples, correlates with a similar ZFT age population in both samples.

5.3.2 Zircon Fission Track

For samples 15_006 and 15_020, a subgroup of the detrital zircons that were analyzed for U-Pb geochronology were also analyzed for Zircon fission tracks (ZFT) (Double Dating). The purpose of the double dating is to obtain cooling ages and assist with provenance determination. The ZFT data is displayed as kernel density estimate (KDE) plots using DensityPlotter (Vermeesch, 2012) (Fig. 2) and ZFT vs. U-Pb ages. For a complete list of the data refer to Appendix 4.

For sample 15_006, 89 detrital zircons were analyzed for ZFTs. Ages range from 507±115 Ma to 97±26 Ma. The age distribution shows three age populations with peaks at ~310 Ma, ~210 Ma, and ~130 Ma. The youngest detrital ZFT age population (~130 Ma) is composed of detrital zircons that have U-Pb ages that span from the Triassic to the Precambrian (Fig. II.8). As ZFT ages record a low-temperature cooling age and U-Pb ages record crystallization age, ZFT ages should be the same age or younger than those determined by U-Pb. ZFT ages older than their U-Pb age (indicated by the black line in the ZFT vs. U-Pb plot in Fig. II.8) are within error of their U-Pb age.

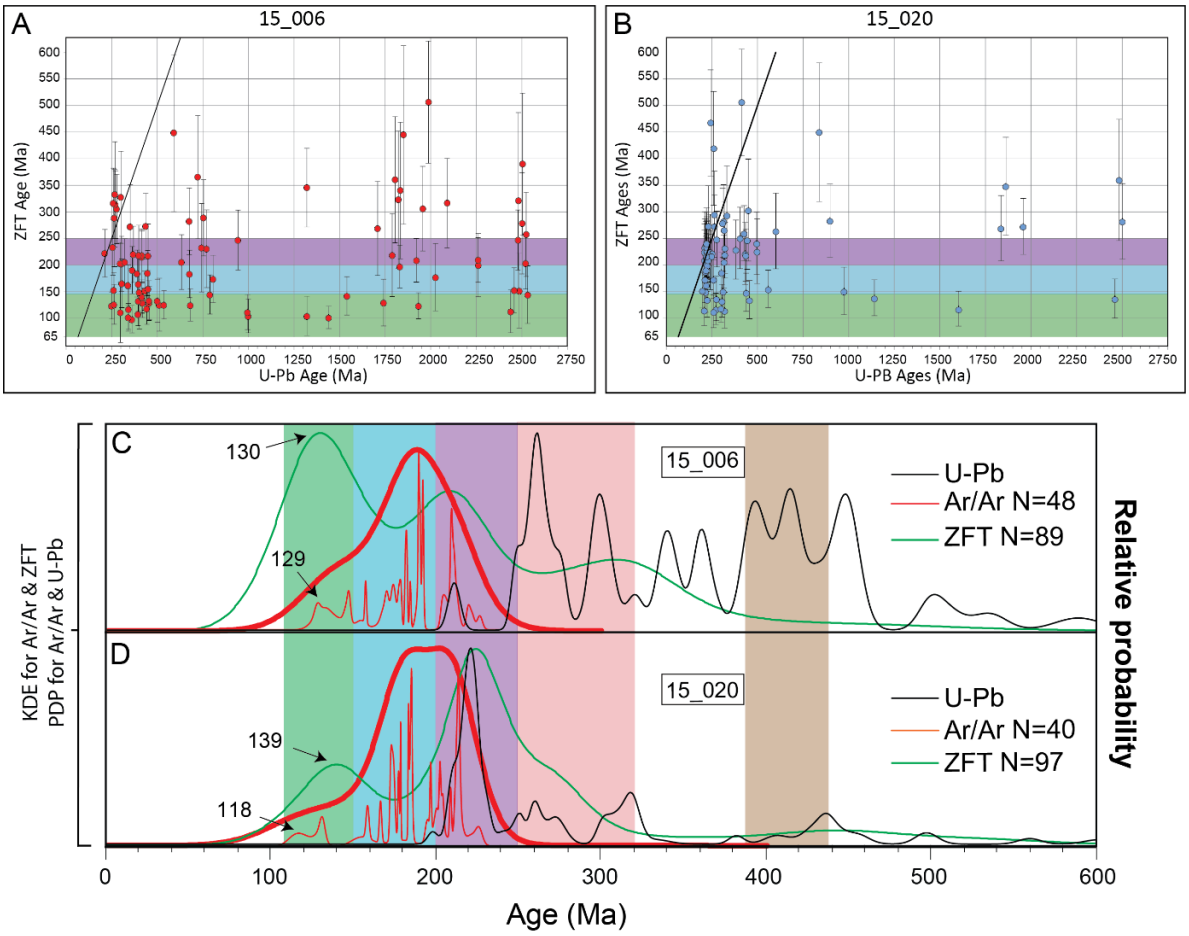

Fig. II.8 ZFT and Ar/Ar ages for Samples 15_006 and 15_020
Figures (A) and (B) are ZFT vs. U-Pb ages. Ages are represented by red dots and vertical bars are ZFT errors for each sample. Ages that lie to the left of the black lines have U-Pb ages younger than there corresponding ZFT age, however, most are still within error. Horizontal color bars represent the following ZFT ages: Green = Cretaceous, Blue = Jurassic, Purple = Triassic. (C) and (D) are kernel density estimates for Ar/Ar and ZFT, and probability density plots for Ar/Ar and U-Pb. Thick red line is KDE for Ar/Ar and thin red line is PDP for Ar/Ar. Prominent peaks are labeled with ages in Ma. Vertical bars represent the following thermochronological ages: Green Cretaceous, Blue=Jurassic, Purple=Triassic, Pink=Middle Carboniferous–Triassic, Brown=Silurian–Devonian

For sample 15_020, 97 detrital zircons were analyzed for ZFTs, and ages range from 507±115 Ma to 97±26 Ma. When plotted on a KDE, there are two prominent age populations that have peaks at ~224 Ma and ~139 Ma (Fig. II.8). The Cretaceous age peak is composed of detrital ZFT ages that are 110 Ma to 161 Ma and correlate to individual U-Pb detrital zircon ages that are Triassic to Precambrian.

6.0 Discussion

6.1.0 Provenance of Tanymas Footwall Deposits

For the samples from this study, terrigenous clastic deposits of the footwall of the Tanymas thrust within the Central Pamir have a strong U-Pb detrital zircon Phanerozoic age distribution with a Permian–Triassic age signature as the most prominent, youngest age population (Fig. II.7). This strong similarity in age populations indicates that they are derived from a similar source (provenance). A synthesis of magmatism throughout the Pamir composed by Chapman et al. (2018) shows that igneous rocks within the Central Pamir are primarily Early Cretaceous-Miocene aged, within the Rushan-Pshart suture zone are Jurassic-Eocene aged, and within the Southern Pamir are Cretaceous-Eocene. Of note, Jurassic ages only appear with the Rushan-Pshart suture (Fig. II.1). The only Permian-Triassic age distribution shown by magmatic age dating is within the Northern Pamir, suggesting a likely source (Robinson et al., 2004; Schwab et al., 2004).

Published detrital zircon data from the Karakul Mazar accretionary arc complex of the Northern Pamir (Fig. II.7) (Robinson et al., 2012; Imrecke et al., 2019) also indicate a strong Permian-Triassic population that is not present in the Gondwana Terranes of Tibet (Fig. II.7) (Gehrels et al., 2011) – the along-strike equivalent of the Central and Southern Pamirs. This

Permian-Triassic age population, along with the general character of age distributions for the six samples of this study, suggests that they were sourced from the Karakul-Mazar accretionary arc complex rather than Gondwana terranes of the Central and Southern Pamir.

Lithological analyses, (i.e., field observations and hand sample/thin section descriptions) further corroborate this match due to pronounced similarities in mineralogy. Thin section results reveal that the clastic deposits contain an abundance of polycrystalline quartz with internal dynamic recrystallization and monocrystalline quartz. Polycrystalline quartz from the clastic deposits resembles the metamorphic quartz from the northern Pamir. Monocrystalline quartz from the clastic deposits has two distinct morphology characteristics: fine (200-100 µm) grain quartz grains with irregular grain boundaries and coarse (125-300 µm) monocrystalline quartz (Fig. II.5). The individual quartz grains with irregular grain boundaries are similar in morphology and size to the individual grains from the polycrystalline quartz of the Northern Pamir. The larger, monocrystalline quartz is similar in size and morphology to two possible sources within the Northern Pamir: monocrystalline quartz of the northern Pamir metamorphic terrane or plutonic quartz related to the Triassic arc magmatism.

One exception of note is sample LY25171. Proterozoic age populations within this sample indicate that it is not only sourced from the Karakul Mazar terrane. A potential source for these additional ages is the Northern Pamir's Kunlun equivalent terrane (Burtman and Molnar, 1993; Xiao et al., 2002b; Schwab et al., 2004). This addition of a prominent Proterozoic age population suggests that the Karakul Mazar terrane may pinch out to the west (Fig. 1 and 3) and that this area received sediment input from the Karakul-Mazar and Kunlun equivalent terrane.

Detrital thermochronology results for samples 15_006 and 15_020 indicate prominent Mesozoic cooling ages in both samples (Fig. II.8). The most prominent being an $^{40}Ar/^{39}Ar$ age

population in each sample that is Late Triassic to Early Jurassic (Fig. II.8). A younger less prominent Early Cretaceous age is present in the ZFT and $^{40}Ar/^{39}Ar$ data for both samples (Fig. II.8). These Late Triassic to Early Cretaceous ages have been documented in biotite and muscovite $^{40}Ar/^{39}Ar$ cooling ages within the Karakul-Mazar arc complex of the Northern Pamir (Robinson et al., 2004; Schwab et al., 2004). This correlation of $^{40}Ar/^{39}Ar$ and ZFT cooling ages serves as further evidence that these two samples were sourced from the Northern Pamir.

6.2.0 Age of Clastic Deposits and Timing of Tanymas Fault Displacement

Historically, the age of terrigenous clastic deposits within the Central and Southern Pamirs has been variable and interpreted as being Jurassic, Cretaceous, or Cenozoic (Paleogene) (Yushin et al., 1964; Liu, 1988; Vlasov et al., 1991; Burtman and Molnar, 1993). Samples from the terrigenous deposits in the footwall of the Tanymas fault dated with both detrital ZFT and muscovite $^{40}Ar/^{39}Ar$ indicate a minimum cooling age of 117–130 Ma for 15_006 and 15_020, indicating their maximum depositional age (Table II.1 and Fig. II.8). Detrital zircon U-Pb geochronology and muscovite $^{40}Ar/^{39}Ar$ ages from modern river drainages within the Northern, Central, and Southern Pamir show strong 110 Ma and 45 Ma peaks (Lukens et al., 2012). As these ages are not present in any of the samples, the age of these deposits is likely older than 110 Ma, and thus must fall between 110 Ma and 130 Ma – or Early-mid Cretaceous. Due to the $^{40}Ar/^{39}Ar$ cooling ages from these two samples and the strong similarity in analysis among all the samples (previous section), we suggest that the clastic deposits along the footwall of the Tanymas thrust within the Central Pamir were sourced from the Northern Pamir and are Early-mid Cretaceous (125-112 Ma). Integrated with our geologic field mapping indicating that the terrigenous clastic deposits are syntectonic suggests that displacement along the Tanymas fault was Early Cretaceous (~130Ma–112 Ma).

6.3.0 Timing of Deformation in the Pamir

Recent work in the Pamir region has shown that much of the upper crustal deformation is Cretaceous. Within the Northern Pamir, amphibolite-facies schists record metamorphic ages of 130–110 My and have been interpreted to record evidence for crustal thickening at that time (Robinson et al., 2004). The event that created these rocks was then followed by the emplacement of the Amphibolite-facies schists onto lower grade metamorphic rocks along the Shala-tala-thrust in the eastern Northern Pamir no later than 100 Ma (Robinson et al., 2004). Emplacement of higher-grade rocks onto lower grade rocks is also seen in the eastern Northern Pamir, along the Torbashi thrust (Imrecke et al., 2019).

As discussed in section 2.3, recent work from post-Cimmerian syntectonic terrigenous deposits within both the Southern Pamir Fold and Thrust Belt and along the footwall of the Rushan-Pshart suture within the Central Pamir suggest that the age of those clastic deposits are likely Late Cretaceous in age (Fig. II.2) (Chapman et al., 2018), thus placing a significant period of deformation within the mid-Late Cretaceous. Our work in combination with previous studies (i.e., Chapman et al., 2018; Imrecke et al., 2019; Robinson et al., 2004) suggest Early-mid Cretaceous shortening within the Northern Pamir and northern portion of the Central Pamir with southward migration of deformation through the Central and subsequently Southern Pamirs from mid-Late Cretaceous (Fig. II.9). Interestingly, this Early-mid Cretaceous age coincides with the docking of the Lhasa Terrane to Qiangtang that occurred by ~118 Ma (Kapp and DeCelles, 2019 and references therein), suggesting that the deformation may be related with this event. Subsequent mid-Late Cretaceous deformation interpreted to be related to a retroarc deformational event, as the Neotethys subducted below the Gondwana terranes (Robinson, 2015; Chapman et al., 2018).

6.4.0 Broader Implications

The Tanymas-Jinsha suture is a significant boundary across the Pamir-Tibetan Orogen that separates the Late Paleozoic southern margin of Asia from Gondwana crustal fragments. This study coupled with other studies (Robinson et al., 2012; Chapman et al., 2018; Imrecke et al., 2019; Kapp and DeCelles, 2019) suggest that post-collisional upper crustal shortening across the orogenic system occurred both earlier and further north in the Pamir than it did in Tibet (Fig. II.10). In the Pamir, Early-mid Cretaceous shortening occurred within the Northern Pamir and along the Tanymas fault (Fig. II.9) (This study; Robinson et al., 2004, 2007). However, in Tibet, the Northern Pamir equivalent Hoh-Xil-Songpan-Ganzi terrane and Jinsha suture experienced no Cretaceous deformation (Kapp and DeCelles, 2019). Early Cretaceous shortening then ceased along the Tanymas fault and swept southward from the Rushan-Pshart suture, which bounds the Central Pamir to the Southern Pamir, and into the Southern Pamir during the mid-Late Cretaceous (100-80 Ma) (Chapman et al., 2018). This mid–Late Cretaceous shortening coincides with the timing of Cretaceous shortening along the southern margin of Qiangtang, along the Bangong suture, and in Lhasa (Kapp et al., 2007a, 2007b; Volkmer et al., 2007, 2014; Kapp and DeCelles, 2019)

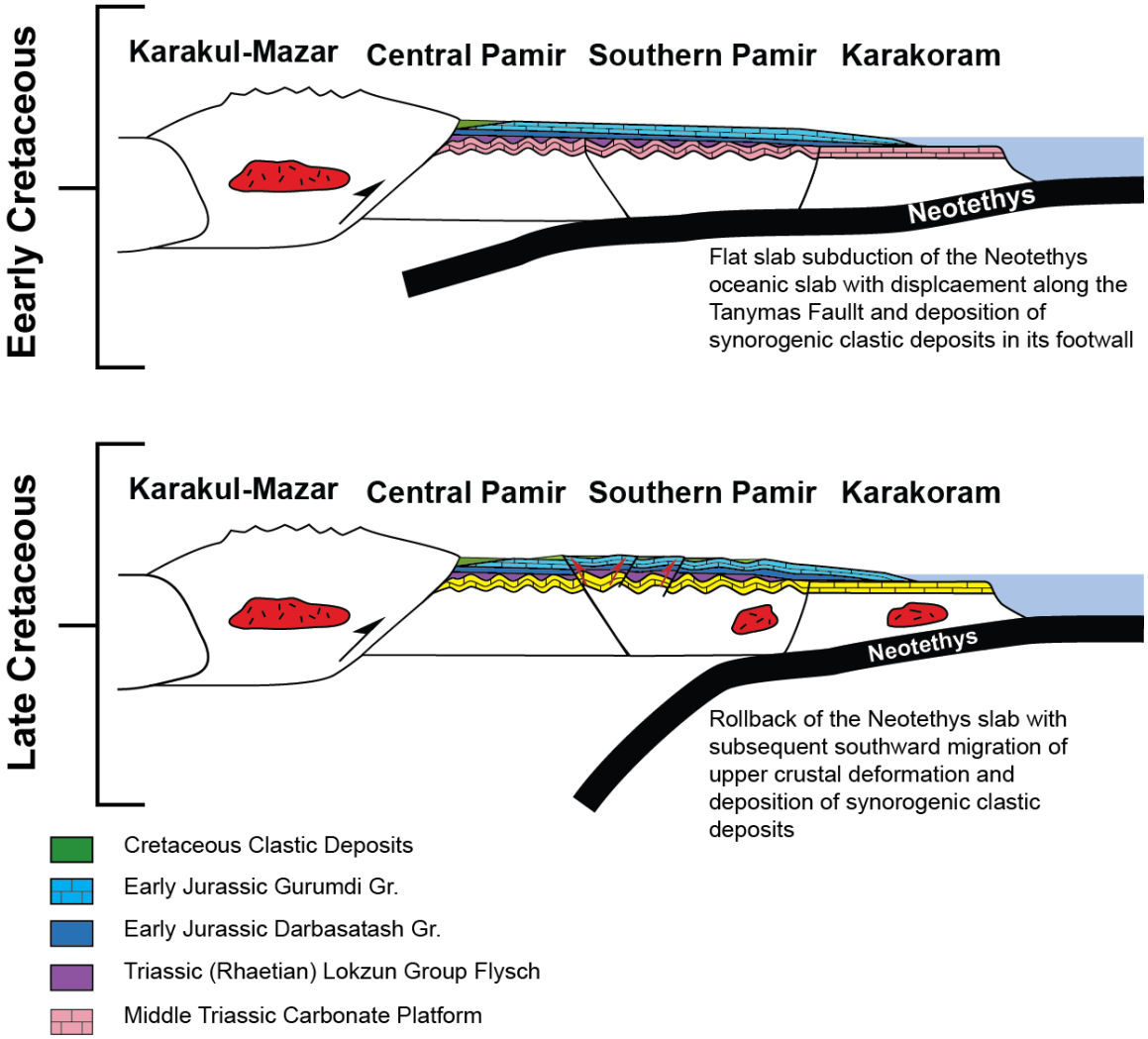

Fig. II.9 Cretaceous Schematic Cross Section of the Pamir
Early Cretaceous flat slab subduction of the Neotethys resulted in displacement along the Tanymas fault and deposition of synorogenic clastic deposits. Late Cretaceous slab rollback resulted in southward migration of upper crustal deformation and deposition of clastic deposits in the footwalls of thrust and cores of synclines.

.

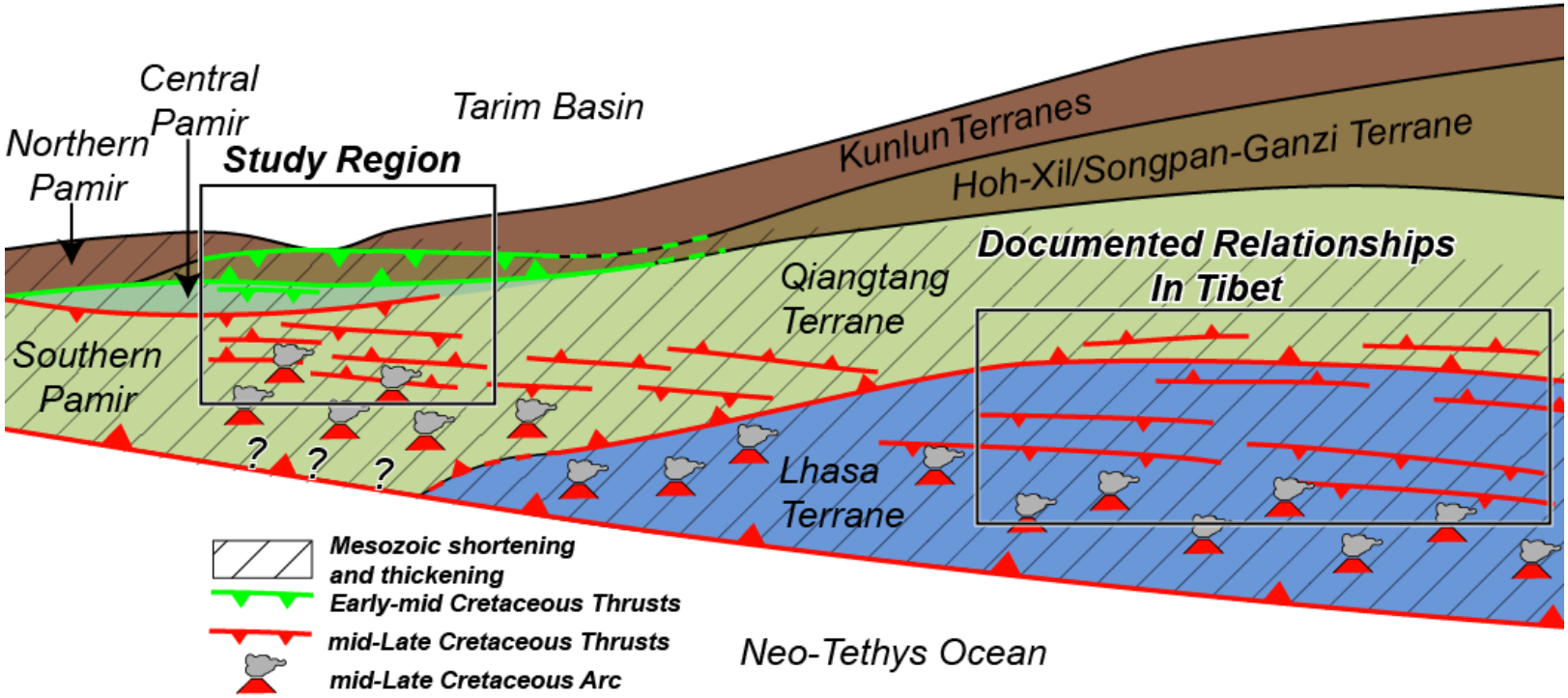

Fig. II.10 Late Jurassic–Cretaceous Tectonic Model
Tectonic model of the Himalayan-Tibetan orogen sowing Early-mid Cretaceous shortening and mid-Late Cretaceous shortening. Cretaceous shortening occured bother earlier and further to the north in the Pamir than it did in Tibet. This early shortening in Pamir may be related to Lhasa accreting to Tibet. Mid-Late Cretaceous shortening and magmatism is due to the Neotethys being subducted below the Pamir and Tibet.

7.0 Conclusion

Our geologic field mapping integrated with detrital zircon U-Pb geochronology, zircon fission track analysis, and muscovite $^{40}Ar/^{39}Ar$ ages from clastic deposits along the footwall of the Tanymas fault suggest the following relationships:

1) Sediment for the terrigenous clastic deposits along the Tanymas fault was sourced from the Northern Pamir, indicating that the Northern Pamir was topographically elevated relative to the Central Pamir allowing for sediment to be shed southward from the Northern Pamir to the Central Pamir.
2) Zircon fission track and $^{40}Ar/^{39}Ar$ thermochronology coincide with Cretaceous exhumation ages of the northern Pamir (Robinson et al., 2004), suggesting that the Northern Pamir was a source through an extended period of time.
3) The lack of mid-Late Cretaceous U-Pb ages – which are found in the Murghab Basin strata and Mamazair Conglomerate to the South– indicate that displacement along the Tanymas fault ceased in the Early Cretaceous (125-112 Ma).
4) The youngest population of detrital ZFT and $^{40}Ar/^{39}Ar$ thermochronology ages from our work suggests that these terrigenous red beds are Early-Middle Cretaceous (130–120 Ma) in age and date the timing of motion along the Tanymas fault.
5) This work coupled with previous studies (Chapman et al., 2018) suggest that deformation occurred in the Northern Pamir and along the Tanymas fault in the Early Cretaceous (~140–112 Ma) and then migrated south into the Southern Pamir during the mid–Late Cretaceous (~112-76 Ma).
6) Cretaceous deformation is expressed early and further to the north in the Pamir then it is in Tibet. In Tibet, only mid–Late Cretaceous and was located within the southern margin

of the Qiangtang terrane, along the Bangong suture, and within the Lhasa terrane (Fig. II.9) (Kapp and DeCelles, 2019). Interestingly, this Early Cretaceous deformation in the Pamir may coincide with the suturing of Lhasa to Qiangtang.

III. MAGNITUDE AND STRUCTURAL STYLE OF UPPER CRUSTAL SHORTENING IN THE SOUTHER PAMIR

1.0 Introduction

The Pamir Mountains are the western continuation of Tibet and have a present day topographic elevation above 4,000 m and a crustal thickness of ~70 km (Mechie et al., 2012; Schneider et al., 2013). Early models suggest that the Indo-Asian collision drove the development of the high topography and present-day crustal thickness in both regions due to northward migrating deformation derived from and originating within the collision zone. Assuming that continental crust was 35-40 km thick in the Pamir prior to collision, this model requires approximately 400-600 km of north-south plane-strain shortening likely resulting in significant crustal deformation (i.e., duplexing and crustal stacking) to account for the current crustal thickness (Schmidt et al., 2011; Chapman et al., 2018). However, extensive field work, mapping, and geochronological data has shown that much of the shortening is Cretaceous in age (Chapman et al., 2018), much less than previously thought (Chapman et al., 2018; This study) and may be largely offset by Cenozoic extension (Stübner et al., 2013a, 2013b; Chapman et al., 2018).

Although few works have focused on the Pamir, much research has been conducted within Tibet, thus the region is often utilized as an analogue for understanding the tectonic evolution of the Pamir. The idea that deformation began prior to the India and Asia collision has been widely-accepted in Tibet, as research has shown that the Mesozoic southern margin of Asia experienced major upper crustal shortening prior to India colliding with Asia (Murphy et al., 1997; Yin and Harrison, 2000; Ding and Lai, 2003; Ding et al., 2003; Kapp et al., 2005, 2007b, 2007a; Kapp and DeCelles, 2019). Past works have demonstrated that there were two main

periods of deformation predating Indo-Asian collision within Tibet: a period of Gondwana terrane accretion, taking place in the early Jurassic (Qiantang collision) and early Creatceous (Lhasa accretion), followed by retroarc deformation caused by the northward-directed subduction of the Neotethys below the Gondwana terranes in the Early-Late Cretaceous, (Murphy et al., 1997; Yin and Harrison, 2000; Ding and Lai, 2003; Kapp et al., 2007a, 2007b; Volkmer et al., 2007, 2014; Kapp and DeCelles, 2019).

Early models of the Pamir suggested that India colliding with Asia during the Cenozoic resulted in more than 340 km of upper crustal deformation within the Central Pamir and Southern Pamir Gondwana terranes (Burtman and Molnar, 1993). However, recent work has shown that both the magnitude and timing of shortening in the Gondwana terranes may be incorrect. For instance, the basal thrust fault of a previously-interpreted thrust nappe in the Southern Pamir, which was suggested to have accommodated more than 100 km of the upper crustal internal shortening, has been shown to, in fact, be a detachment fault forming a gneiss dome that was exhumed during Cenozoic north–south extension (Stübner et al., 2013b). Further, studies within the eastern Southern Pamir fold and thrust belt suggest that upper crustal deformation occurred in the Cretaceous and preliminary results have shown that shortening may be <10 km (Chapman et al., 2018), as opposed to ~50 km previously suggested by Burtman and Molnar (1993).

This paper addresses the magnitude of shortening through detailed field mapping and forward modeling of the Southern Pamir Fold and Thrust Belt. We utilized our geologic field mapping in combination with published maps (Yushin et al., 1964; Vlasov et al., 1991) in order to generate retrodeformable cross sections across the fold and thrust belt to understand the magnitude and structural style of upper crustal shortening. Our results imply that the Pamir

plateau did not thicken as a result of plane-strain shortening and that there must be one or several additional drivers within the mid-lower crust that also have an effect, as first suggested by Robinson et al. (2007).

2.0 Geologic Background

The Southern Pamir terrane is juxtaposed against the Central Pamir terrane to the north and against the Karakoram terrane to the south via the Rushan-Pshart suture and Wakhan-Tirich suture, respectively (Fig. III.1) (Burtman and Molnar, 1993; Schwab et al., 2004; Angiolini et al., 2013; Robinson, 2015). The three terranes rifted from Gondwana during the Carboniferous and drifted northward as the Paleotethys subducted below the southern margin of Asia (Burtman and Molnar, 1993). The Permian–Triassic rocks consist of thick clastic successions and carbonate rocks that record the rift to drift phase of the Gondwana terranes (Gaetani et al., 2004; Zanchi and Gaetani, 2011; Angiolini et al., 2015). The presence of a Triassic accretionary arc complex within the Karakul Mazar Terrane of the Northern Pamir (Fig. III.1) documents the northward subduction of the Paleotethys below the southern margin of Asia (Xiao et al., 2002a; Schwab et al., 2004).

Once the Paleotethys was fully consumed, the three Gondwana terranes collided with the Southern margin of Asia in the Late Triassic, resulting in the Cimmerian orogenic event (Angiolini et al., 2013; Chapter 1). In the Southern Pamir, Angiolini et al. (2013) characterized Cimmerian deformation as N-S to NNW-SSE trending folds and high angle reverse faults, whereas Rutte et al. (2017a) suggested that Cimmerian deformation is characterized by north verging folds. This discrepancy in structural architecture suggest that the kinematics of the Cimmerian event may vary within the Pamir. However, the presence of a regionally widespread Jurassic carbonate within the Central and Southern Pamir (Fig. III.2) suggest that the topography

remained at or just below sea level, indicating minimal crustal thickening associated with the Cimmerian orogeny. The Carbonate is the post-collisional Early Jurassic Gurumdi Group, which is separated from Permian–Triassic rocks below by the post-Cimmerian angular unconformity (Angiolini et al., 2013). Due to the Gurumdi Group being widespread throughout the Southern Pamir (Fig. III.2), it is an ideal strain marker for understanding the magnitude and structural style of post accretional deformation.

Following deposition of the Early Jurassic Gurumdi Group carbonate, deformation of the Central and Southern Pamir was the result of a Mesozoic cordilleran style margin followed by Cenozoic India-Asia collision. The modern thickness of the Pamir has commonly been associated with the Indian-Asian collision. In the Central Pamir, thrust sheets and internal shortening, which have accommodated ~100 km of shortening, have been used to explain the current thickness of the crust, as well as the Oligocene–Miocene prograde metamorphism of exhumed Cenozoic gneiss domes (Rutte et al., 2017a). Although it would be ideal to use this same explanation for the thickness and prograde metamorphism of gneiss domes in the Southern Pamir, there is no evidence for large imbricated thrust sheets or large magnitudes of internal shortening in the Southern Pamir (Chapman et al., 2018; This study). Additionally, upper crustal shortening in the Southern Pamir has been shown to be Cretaceous in age rather than Cenozoic (Chapman et al., 2018). Furthermore, the exhumed gneiss domes in the Southern Pamir (e.g., Shakhdara- Alichur) are associated with ~90 km of North-South directed extension (Stübner et al., 2013b). Presently within the Southern Pamir, there are active right-lateral strike-slip faults that overprint the Southern Pamir Fold and Thrust Belt and, collectively, they are referred to as the Murghab-Aksu-Southeast Pamir thrust-wrench belt (Rutte et al., 2017a).

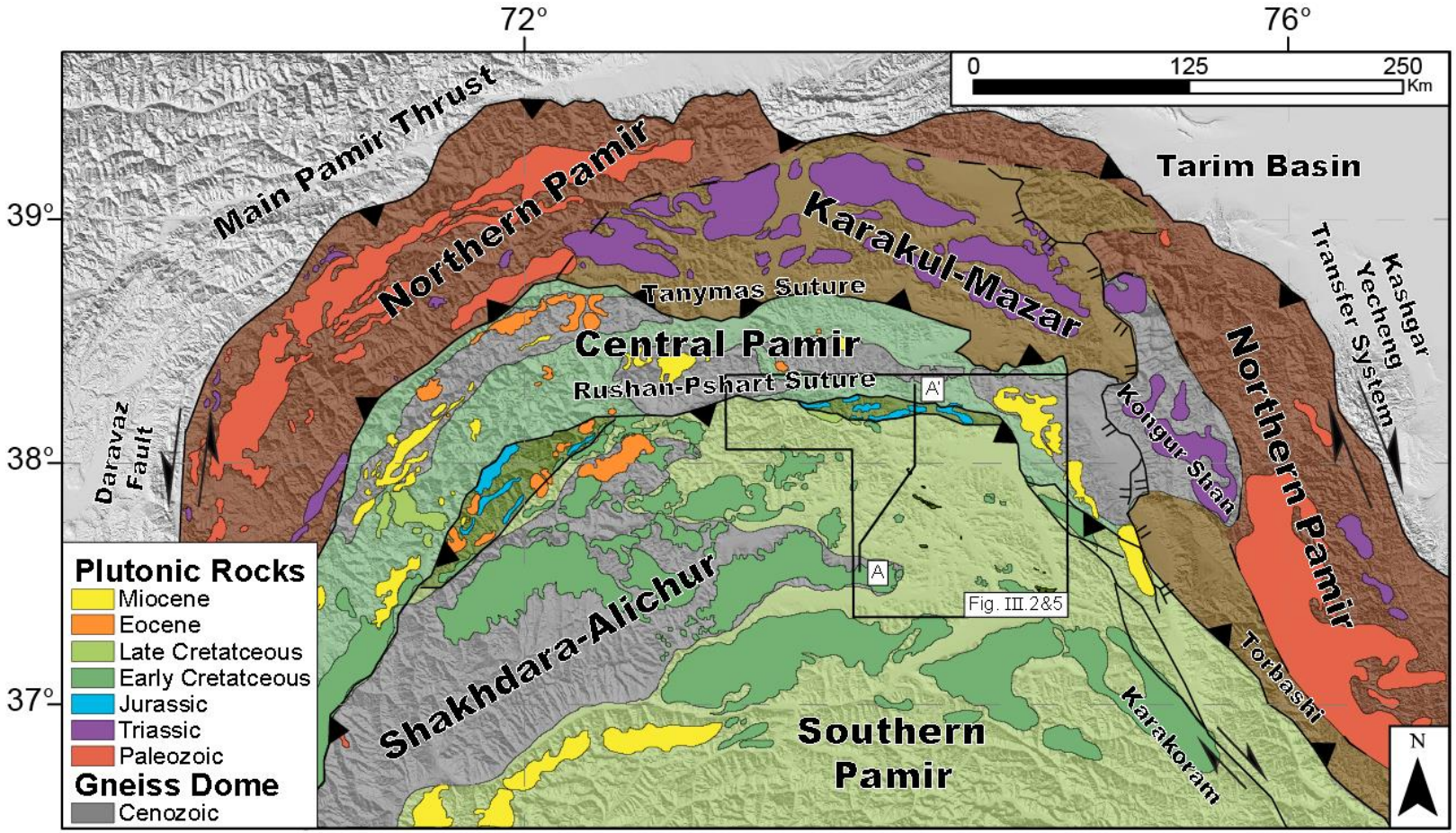

Fig. III.1 Regional tectonic map of the Pamir

Tectonic map of the Pamir shows terranes, pluton ages, Cenozoic gneiss domes, location of figure 2 and 5, and location of cross sections A-A'. Modified from Robinson et al. (2015) and Chapman et al. (2018)

3.0 Geologic Mapping and Field Observations

The primary focus of this study is the post-accretionary upper crustal deformation of the Southern Pamir, in particular, the magnitude and style of shortening in the Southern Pamir fold and Thrust belt. In order to evaluate the magnitude of shortening, extensive geologic field mapping of the Early Jurassic Gurumdi Group carbonates that lie above the post-Cimmerian unconformity was undertaken (Fig. III.3A). This succession is an ideal strain marker, allowing for evaluation of the magnitude of post-accretionary upper crustal shortening. A portion of geologic mapping was focused on the deformed Permian–Triassic section beneath the angular unconformity in order to understand the structural style below and above the post-Cimmerian unconformity, largely in order to resolve the effect of the underlying beds and the differences in structure.

Geologic field mapping of the eastern Southern Pamir terrane was conducted during the summers of 2015 and 2016 on 1:100,000 scale topographic maps and aerial imagery. To evaluate upper crustal deformation, mapping was focused along a N–S transect from the town of Murghab to just north of the Shakhdara-Alichur dome (A–A' Fig. III.2). This area was chosen due to fairly continues exposure of the Gurumdi Group. Along with our field mapping, Google Earth and ASTER images were used to fill gaps not accessible during fieldwork, check the accuracy and geometry of contacts, and to resolve differences between our mapping and previous published maps (Yushin et al., 1964; Vlasov et al., 1991).

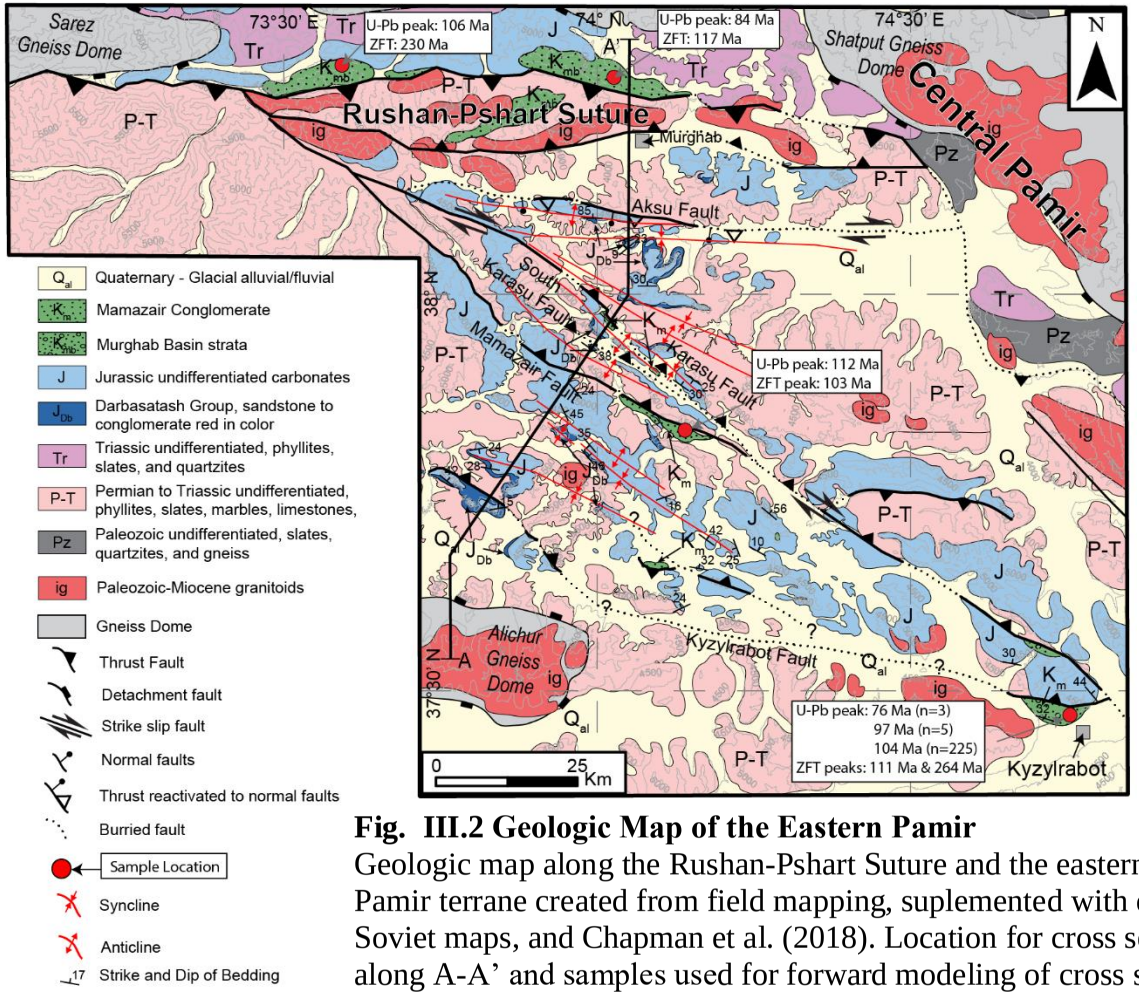

Fig. III.2 Geologic Map of the Eastern Pamir

Geologic map along the Rushan-Pshart Suture and the eastern Southern Pamir terrane created from field mapping, suplemented with data from Soviet maps, and Chapman et al. (2018). Location for cross sections is along A-A' and samples used for forward modeling of cross sections are highlighted by red circles and were obtained from Chapman et al. (2018). Location of map is shown in Fig. III.1.

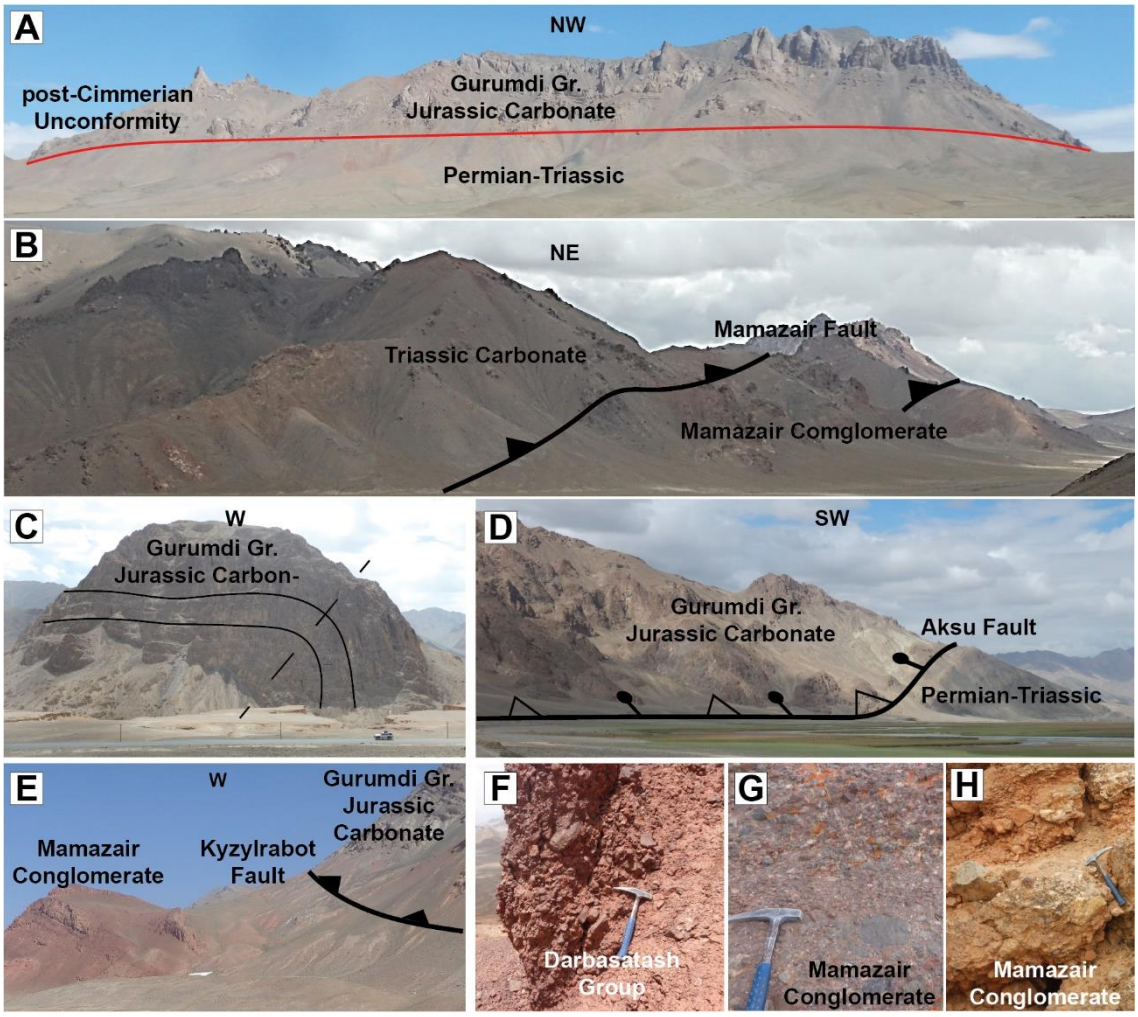

Fig. III.3 Field Photos from the Southern Pamir

Photographs from the eastern Southern Pamir Terrane (A) Subhorizontal post-Cimmerian angular unconformity beneath the Early Jurassic Gurumdi Group Carbonate (ridge location: 37.72N, 73.84E) (B) Mamazair thrust fault placing Triassic Carbonates onto the Mamazair Conglomerate (Fault location: 37.85N, 74.1E,) (C) Hanging wall deformation of the Gurumdi Group carbonate due to Aksu Fault trishear faulting reactivated to a normal fault (location: 38.11N, 73.88E) (D) Thrust reactivated into a normal sense of shear along the Aksu fault places the Gurumdi Group carbonate (hanging wall) above the Permain to Triassic section (footwall) (fault location: 38.12N, 73.91E) (E) The Kyzylrabot Fault places the Gurumdi Group carbonate onto the Mamazair Conglomerate (fault location: 37.48N, 75.77E) (F) The Darbasatash Group contains shales to cobble size clast and is often difficult to sample and collect structural measurements (photo location: 38.1N, 74.0E) (G) and (H) The Mamazair Conglomerates may be either well lithified or easily friable, but generally contains an abundance of subangular to subrounded, pebble to conglomerate clast with rare boulders. The lithology of the clast is mostly carbonate (>85%) with sandstone, chert, and quartzite also present. (location of photos G: 37.83N, 74.15E and H: 37.66N,

The eastern Southern Pamir is composed of Permian to Cretaceous rocks that can be largely divided into two separate groups that are separated by a regional angular unconformity: 1) those deposited from the Permian to the Triassic before the Cimmerian orogeny 2) and those deposited after, from the Jurassic to the Cretaceous on top of the angular unconformity. The Permian-Triassic rocks are indicative of rift-to-drift and subsequent collision (i.e., below the post-Cimmerian angular unconformity), whereas the Jurassic-Cretaceous rocks are characterized by massively bedded carbonates with broad open folds and syntectonic clastic deposits (i.e., above the post-Cimmerian angular unconformity).

3.1 Stratigraphic Observations

3.1.1 Permian–Triassic

The oldest rocks observed in the Southern Pamir are Permian–Triassic and differentiation of the units was not done due to the complexly deformed nature of the rocks making comprehensive mapping of the Cimmerian structures difficult. The Permian–Triassic section is composed of low-grade metasedimentary rock (sub-greenschist facies). Permian rocks consist of interbedded dark grey to black phyllites, slates, and quartzites, and light to dark grey carbonates. Bedding thickness often ranges from millimeter to 0.5 meters in scale.

The majority of the Triassic section (>95%) is composed of light grey/tan to dark grey carbonates that have a bedding thickness of millimeter to more than 1 meter. The carbonate is largely micrite to very fine spar, and macrofossils are rare to absent. At the top of the Triassic section is the Lokzun Group flysch deposit (Angiolini et al., 2013) that is composed of interbedded fine-grained to medium-grained sandstones and has a well-defined Late Triassic stratigraphic age (Angiolini et al., 2013).

3.1.2 Jurassic–Cretaceous

Overlying the Permian-Triassic succession via an angular unconformity is the Lower Jurassic Darbasatash Group, which has a thickness that varies from 0–200 meters. Due to its distinctive nature, the Darbasatash Group can be used to help distinguish between Jurassic carbonates above it from Triassic carbonates below it, however it is not present everywhere. Composed of terrigenous shales, sandstones and conglomerates, the dominant lithology of the Darbasatash Group is a sandstone that is dark red and composed of beds that are ~1 cm to 0.5 meters in thickness throughout the region. Although the Darbasatash Group is a significant marker bed in the region, mapping revealed largely discontinuous packages that indicate likely deposition within paleo topographic lows. In some areas, talus on slopes completely covered any likely Darbasatash outcrops.

The conglomerates of the Darbasatash Group can be divided into two main types. The first are clast-supported basal conglomeratess that contains sub-rounded to rounded, pebble to cobble sized metamorphic clasts (typically quartzite and slate) with a thickness of up to 10 meters. The second is present higher in the section and contains rounded sedimentary clast that are red to tan in color and matrix to clast supported (Fig. II.3F). Previous analysis of the Darbasatash Group suggests that it was largely sourced from a volcanic arc (Angiolini et al., 2013), with sediment likely derived from the Northern Pamir's Karakul-Mazar accretionary arc complex (Chapter 1).

Lying conformably above the Darbasatash Group is the Hettangian aged limestone of the Gurumdi Group (Fig. III.3A) (Dronov et al., 2006). Where the Darbasatash Group is absent, the Gurumdi Group directly overlies the Triassic and Permian rocks via an angular unconformity. The Gurumdi Group consists of a lower and upper unit that are conformable (Dronov et al.,

2006; Angiolini et al., 2013; Chapman et al., 2018). The lower unit of the Gurumdi Group is composed of tan to dark grey carbonates that contains bed thicknesses that range from a quarter meter to several meters thick and is interbedded with claystone. The upper unit of the Gurumdi Group is a light grey carbonate with bed thickness ranging from ~1 meter to massive. In many places the massive beds contain no distinct layering, making it difficult to obtain structural measurements.

The youngest sedimentary rock in the eastern Southern Pamir is the Mamazair conglomerate (Fig. III.3G and 3H) (Chapman et al., 2018). The Mamazair conglomerate is most often found within the footwalls of thrust and the cores of synclines and lies unconformably on Jurassic or Triassic carbonates. Due to the laterally discontinuous nature of the Mamazair conglomerate its lithologic characteristics vary. The largest exposure of the Cretaceous red bed is within the footwall of the north dipping Mamazair Fault (Fig. III.3B). At this locale, the Mamazair conglomerate is a clast supported, subangular to subrounded, pebble to cobble conglomerate that contains rare boulders. The clasts are mostly carbonates (~85–95%), with subordinate clasts of sandstone, chert, and quartzite. The conglomerate contains individual beds that range from meter to 10s of meters thick. Discontinuous lenses of sandstone are present within the Cretaceous red beds. Roughly 20 km to the south the Mamazair conglomerate is present within the footwall of a south dipping thrust. Here, the Mamazair conglomerate contains 90–95% carbonate clasts with the remaining being quartzite. Detrital zircon U-Pb analyses, and zircon fission track analyses suggest that the Mamazair conglomerate is mid-Late Cretaceous and syntectonic (Chapman et al., 2018).

3.2 Structural Geology

The geology of the Southern Pamir can be broadly divided into two characteristic deformation styles: tightly-folded Permian-Triassic rocks deformed during the Cimmerian orogeny and younger rocks deformed by broad open folds. Angiolini et al. (2013) documented N-S to NNW-SSE trending folds in the Permian-Triassic rocks of the eastern Southern Pamir that were deformed during the Cimmerian orogeny, consistent with the previously published maps (Yushin et al., 1964; Vlasov et al., 1991) of the western portion of the eastern Southern Pamir. An analysis of reviously published maps (Yushin et al., 1964; Vlasov et al., 1991) by Bunge (2014) and this study (Fig. III.4) show that the eastern Southern Pamir has E-W to NW-SE trending folds. This variability, i.e., between Angiolini et al. (2013) and earlier maps and our observations, documents lateral variation in Cimmerian deformation in different parts of the Southern Pamir.

The boundary between these more tightly-folded rocks and the broadly-folded overlying strata is the post-Cimmerian angular unconformity (Fig. III.3A). The primary unit above the post-Cimmerian angular unconformity is the Jurassic Gurumdi group carbonate. The base of the Gurumdi Group lies at ~4100-4400 m in elevation thoughout the region. Deformation of the Gurumdi Group carbonate is characterized by generally broad, open folds that have wavelengths of >2 km and trend toward tge WNW-ESE with dips rarely exceeding 40° (Fig. III.5). However, there is evidence for internal folding and the most structurally complex areas are within the hanging wall directly above associated thrust faults, most notably along the Aksu Fault (Fig. III.3C). Shortening of the Early Jurassic Gurumdi group deposition occurred during the Cretaceous as the Neotethys subducted northwards below it, forming the Southern Pamir Fold and Thrust belt (Chapman et al., 2018). Our mapping indicates that the Southern Pamir Fold and

Trust belt incorporates Permian–Cretaceous rocks and is characterized by northwest to southeast striking, north dipping thrusts that have a southward sense of vergence (Fig. III.5). However, along the northern boundary of the fold and thrust belt, the Aksu Fault that strikes East-West and has been interpreted as being north-dipping (Chapman et al., 2018) or south dipping (Rutte et al., 2017a) with purely a reverse sense of shear. Our field observations show that the Aksu fault dips southward (Fig. III.2, 3D, and III.5) and juxtaposes the Gurumdi Group carbonate in the hanging wall onto the low-grade metamorphic Late Triassic Lokzun Group flysch deposit. This juxtaposition indicates a normal sense of shear (Fig. III.3E). From south to north, the Aksu fault hanging wall is subhorizontal then steepens to sub-vertical at the fault cut off (Fig. III.3C and III.5). This fold has an axial plane that strikes E-W and dips ~50 to the south.

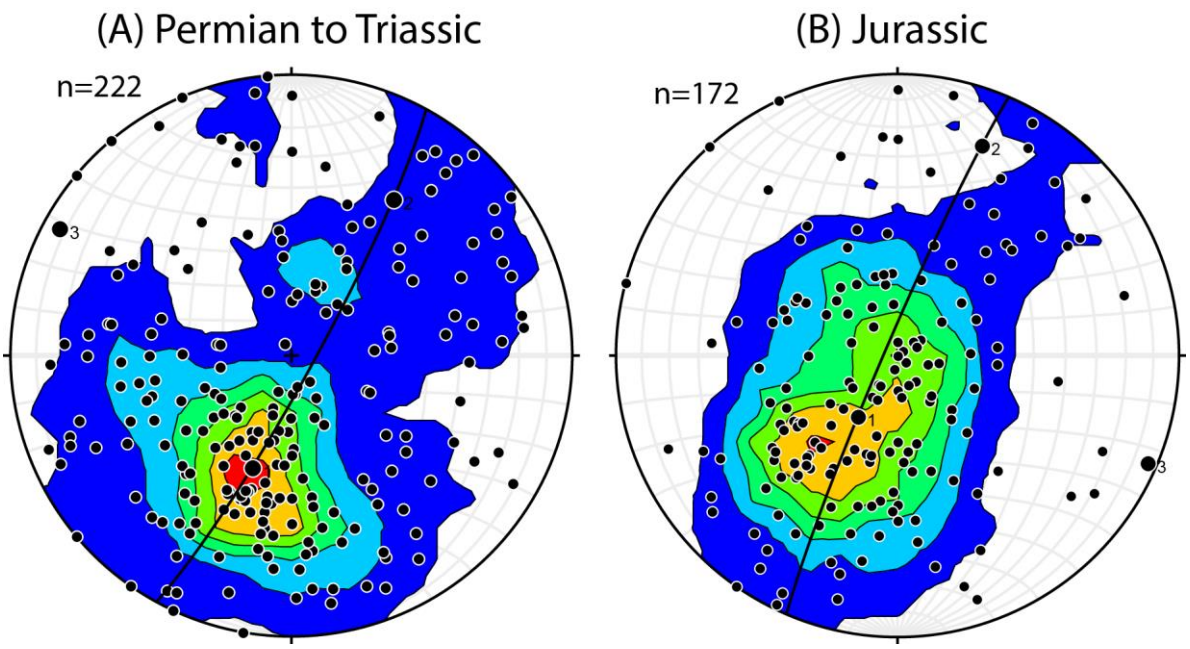

Fig. III.4 Stereonets from the Southern Pamir
Poles to planes of bedding from the eastern Southern Pamir. A) Permian–Triassic data indicates a NW-SE trend of folds with steeply dipping beds. B) Darbasatash and Gurumdi Group data indicate broad open folds with WNW-ESE trending folds.

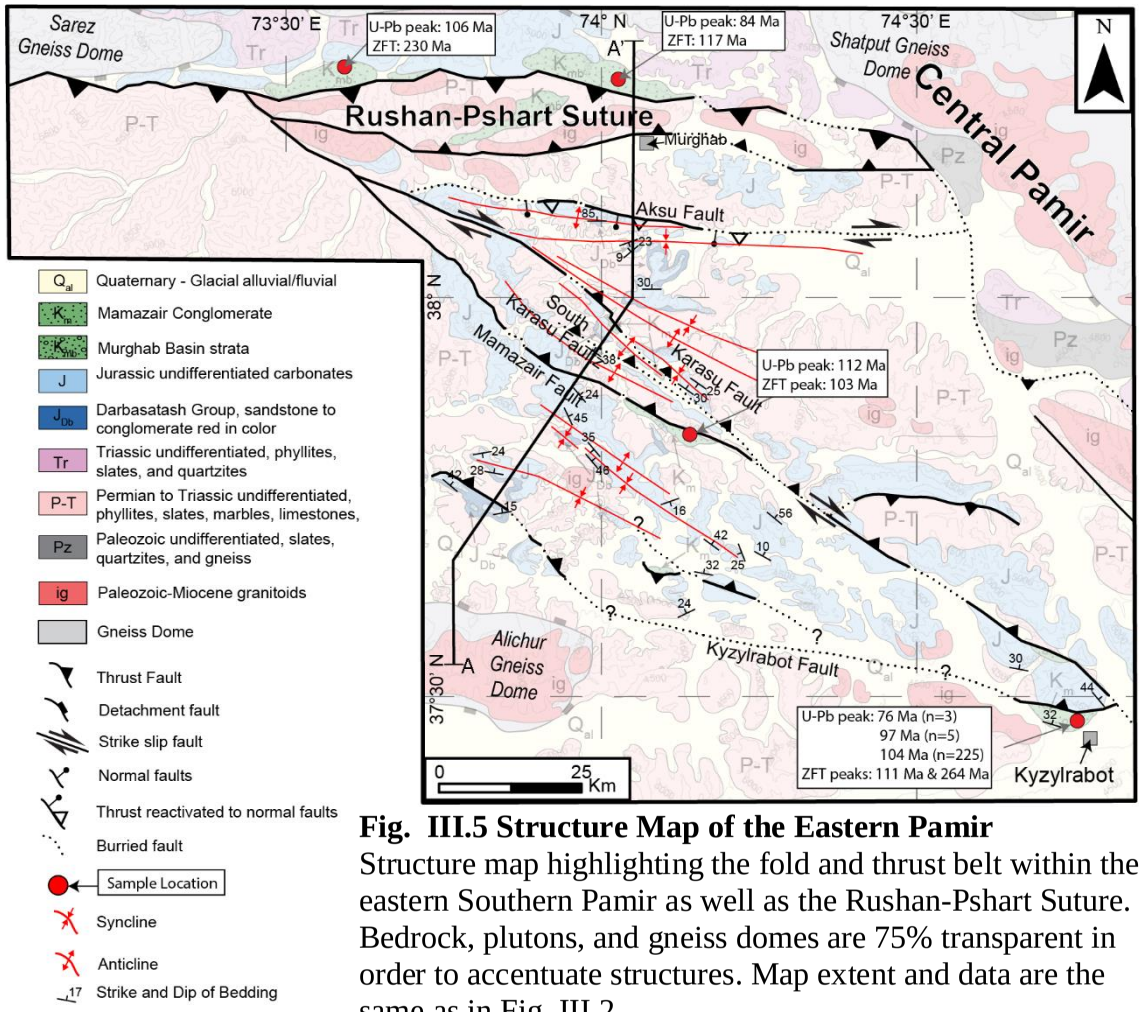

Fig. III.5 Structure Map of the Eastern Pamir
Structure map highlighting the fold and thrust belt within the eastern Southern Pamir as well as the Rushan-Pshart Suture. Bedrock, plutons, and gneiss domes are 75% transparent in order to accentuate structures. Map extent and data are the same as in Fig. III.2.

South of the Aksu fault are the southwest verging Karasu Fault, South Karasu Fault, and Mamazair Fault. Map relations indicate these faults root into the same décollement as the Aksu Fault, as indicated by a singular branch point between all three faults (Fig. III.2 & III.5). The Karasu Fault is the most significant fault in the mapped area as it extends ~150 km across the eastern Southern Pamir from the Rushan-Pshart fault in the NW to the Karakoram fault in the SE and juxtaposes Permian–Triassic rocks against Jurassic rocks. While the Karasu fault has primarily accommodated southwest directed shortening, it is presently an active right-lateral fault (Fig III.2 and III.5). The South Karasu Fault is a minor fault in the area, extending for less than ~50 km, and is entirely buried beneath Quaternary deposits. The presence of the fault is documented by repetition of the Darbasatash Group and overlying Gurumdi Group. We interpret the fault to strike NW-SE and have a SW sense of vergence. This structural orientation is based on the structural orientation and architecture of the repeated Darbasatash Group and Gurumdi Group. To the south, the Mamazair fault branches from the Karasu fault and extends for ~75 km before it rejoins with the Karasu fault. The Mamazair fault strikes NW-SE and dips to the NE and emplaces either Permian–Triassic or Jurassic rocks onto Jurassic. The Mamazair Fault also contains the largest outcrop of the synorogenic Mamazair conglomerate within its footwall (Fig. 3B). South of the Mamazair Fault is the south-verging Kyzylrabot fault (Figs. 2 and 4) and an unnamed fault. We interpret the unnamed fault to be a continuation of the Kyzylrabot Fault and therefore use this idea in the development of our model. The Kyzylrabot Fault strikes to the NW-SE and dips to the NE. Near the town of Kyzylrabot, the Mamazair conglomerate is present within its footwall and the hanging wall is the Jurassic Gurumdi Group (Fig. III.3E). At this location, near the town Kyzylrabot, was the only place that a fault plane was exposed. The structural orientation of the fault here is N47°W,23°NE.

4.0 Forward Modelling the Southern Pamir Fold and Thrust Belt

We present two models for a retrodeformable cross section of the Southern Pamir Fold and Thrust Belt to evaluate the structural style and magnitude of Cretaceous shortening (Fig. II.6). In this work, we focus on restoring the Early Jurassic Gurumdi Group carbonate the lies directly above the post-Cimmerian angular unconformity. We focus on the Gurumdi Group as it is an ideal strain marker for post-accretional deformation within the Southern Pamir.

4.1 Location of Cross Sections

Two cross sections were constructed along line A-A' (Fig. III.6) in a N37°E to N-S transect. (Figs. III.1, III.2, and III.5) The orientation of the line trends parallel to the convergence direction of the fold and thrust belt, and the location was chosen to maximize the interaction of topography with our geologic mapping and structural measurements. A summed stereonet analysis of bedding orientation for the Darbasatash Group and Gurumdi Group suggested a convergence direction that fell within 10% of the chosen direction (Fig. III.4). The fold and thrust belt has a present-day length of ~53 km, however, the transect was extended to ~120 km to include the Alichur Gneiss dome (southward) and the Rushan-Pshart suture (northward), as we believe they both have had an impact on the evolution of the fold and thrust belt (implications to follow). The kinks in the line were essential in order to meet these requirements. As the history of the Aksu fault is unclear we have two reconstructions that model it differently and have other implications for the evolution of the rest of the fold and thrust belt.

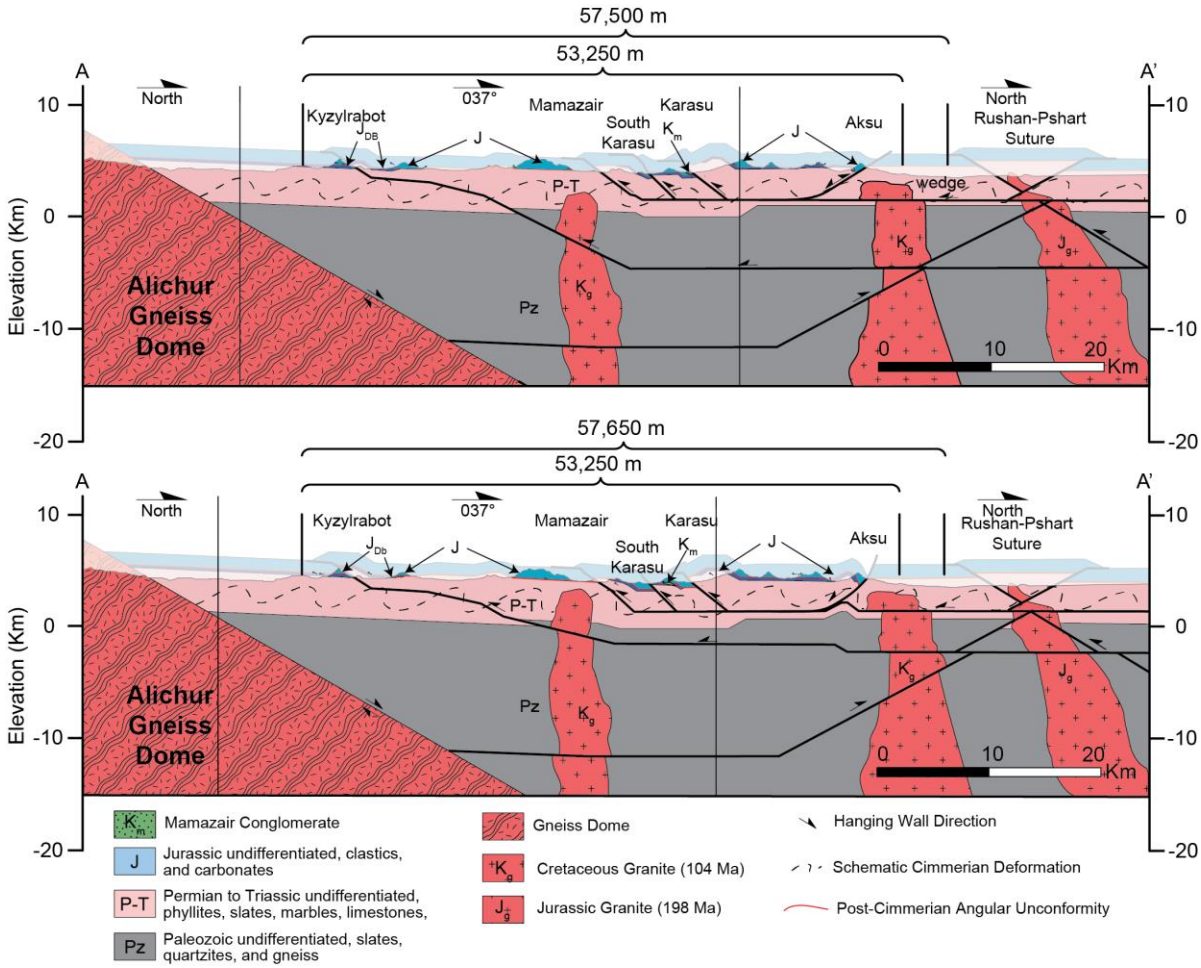

Fig. III.6 Present Day Cross Section

Two models proposed for the development of the Southern Pamir Fold and Thrust Belt along transect A-A' (Fig. III.1, III.2, and III.4) . Key differences are the development of the Aksu Fault, detachment level for Fault B, and magnitudes of displacement along faults (expanded upon in text and in Figs. III.7 and III.8) with strike and dips, plutons, the Alichur Gneiss dome and north verging tightly folded Permian to Triassic rocks. Initial length and present-day length are noted above the cross section.

4.2 Stratigraphic Constraints

For our kinematic restoration, the stratigraphic thickness of the units within the region was determined from our mapping, and previously published maps (Yushin et al., 1964; Vlasov et al., 1991; Bunge, 2014; Chapman et al., 2018). The thickness of the Permian to Triassic section was estimated from Soviet-era maps and interpreted to be ~3,500 m thick (this study in conjunction with Bunge, 2014). However, this Permian to Triassic thickness is a minimum estimate, because, other than the exhumed gneiss dome, basement rock is not exposed in the region. The stratigraphic thickness of the Early Jurassic Darbasatash Group was determined from our geologic mapping in combination with published data (e.g., Chapman et al., 2018; Angiolini et al., 2013) and its thickness ranged from 0 to 200 m. The base of the contact of the Darbasatash Group lacks concordance with underlying strata and the deposit itself is not laterally continuous, which indicates that it was likely deposited in paleo-lows and incised valleys. Therefore, structural data from the overlying Gurumdi Group was used due to its widespread exposure throughout the eastern Southern Pamir. Our field mapping of the Early Jurassic Gurumdi Group carbonate, in combination with Bunge (2014) and Chapman et al., (2018), determined that its gross thickness was ~1,000 m.

4.3 Forward Modeling Assumptions

A forward modeling approach was taken to generate balanced retrodeformable cross sections of upper crustal shortening within the Southern Pamir Thrust Belt. Midland Valley Move was utilized to generate the models. The focus of the models was to quantify the magnitude of shortening that involved Jurassic and younger formations. Several assumptions were made at three main stages during the construction of the cross sections: 1) prior to

deformation/at the time of deposition, 2) during the development of deformation, and 3) after the fold-and-thrust belt developed.

4.3.1 Prior to activation of the Southern Pamir Fold and Thrust Belt

Prior to deformation, it was assumed that the Jurassic strata were laid down in a similar, horizontal manner. Although we know that the Permian-Triassic stratigraphy was folded and faulted by the Cimmerian orogeny, it likely had little to no effect on the deposition of the Jurassic carbonate. We also assumed at the initial stage of the model that the post-Cimmerian angular unconformity was flat-lying prior to deposition of the Jurassic Gurumdi Group carbonate. Although the underlying Darbasatash Group's limited deposition and thickness variations within the region suggest that topography was not completely flat locally prior to deposition of the Gurumdi Group, it is reasonable to approximate a flat surface on a larger scale (~60 km) (Figs III.7 and III.8).

4.3.2 During activation of the Fold and Thrust Belt

The second set of assumptions for the model were during the deformation and evolution of the shortening structures. For all but the Aksu Fault, the simple shear algorithm was used in Midland Valley Move with an axial plane of 75°. The fault dips for the Rushan-Pshart suture zone was assumed to be ~30º. Fault geometry within the Southern Pamir Fold and Thrust Belt was determined from geologic mapping of the faults and observed hanging wall geometry. Our geologic mapping indicates that the Aksu Fault, Karasu Fault, South Karasu Fault, and Mamazair Fault share a common branch line. Therefore, we interpret that they all root into the same horizontal décollement within the Permian–Triassic section. We interpret the unnamed fault along the southern section of the transect to link up with the Kyzylrabot Fault.

4.3.3 Following cessation of the Fold and Thrust Belt

The final model assumptions involved subsequent extension in the region. As mentioned in section 3.2 the only evidence for extension within the fold and thrust belt is along the Aksu fault that place the Jurassic Gurumdi Group carbonate onto the Lokzun Group flysch, which has undergone low-grade metamorphism. The elliptical fault displacement algorithm in Midland Valley Move was used for extension along the Aksu fault. This algorithm allows for faults to have a maximum amount of displacement at a preferred location and eventually have no displacement at a point designated by the user.

Post-Miocene extension also resulted in one of the largest subaerially exposed gneiss domes in the world, the Shakhdara-Alichur gneiss dome, which is ~17 km south of the fold and thrust belt (Figs III.1, and III.2). We assume that the exhumation of the gneiss dome likely tilted the southern portion of the fold and thrust belt, and, in both models, we tilt the stratigraphy south of the Mamazair fault by 2.5 degrees. This tilt was necessary for forward modeling in order to match the present day architecture of the fold and thrust and belt.

Quaternary strike-slip faulting is present along the Karasu fault and possibly the Aksu Fault within the fold and thrust belt. Offset river terraces crossing the Karasu fault indicate active right-lateral strike-slip motion (Strecker et al., 1995; Rutte et al., 2017a). Field observations indicate that there has been very little to no throw in response to strike-slip motion within the fold and thrust belt. We feel that strike slip faulting had no effect on quantifying the magnitude of Cretaceous shortening along the fold and thrust belt. Therefore, we do not compensate for strike-slip motion in either model.

5.0 Results of Models

The present-day length of the Southern Pamir Fold and Thrust belt is 53.2 km from the footwall of the Aksu Fault to the footwall of the Kyzylrabot Fault. Forward modeling of the fold and thrust belt indicate that the original length of the fold and thrust belt was 57.5 km in the first model (7.4% shortening) and 57.7 km in the second model (7.63% shortening) (Fig. III.7 and III.8). Upper crustal shortening can be split into two systems for each of the models: a northern to central section rooted into a shallow detachment and a southern section rooted into a deeper detachment.

5.1 Model 1

The first two steps of the model require activation of the Rushan-Pshart Suture zone. The dip for both the north dipping fault and south dipping fault were set to ~30°. Activation of the north dipping fault occurred first based on the south dipping fault cutting it. As it is unclear how much displacement occurred along the north dipping Rushan-Pshart fault and it does not appear to directly connect to the fold and thrust belt, 1000 m of heave was used to show the structural relationship between it and the southward dipping Rushan-Pshart fault (Fig. 7B). The second step was displacement of the southward dipping Rushan-Pshart fault. For this southward dipping fault, we used a ramp that reached a depth of -12 km before transitioning into a geometrically flat detachment (Fig. III.7C). The southward dipping Rushan-Pshart fault required 1,900 m of heave in order to bring up the Permian–Triassic rocks within the footwall and hanging wall of the Aksu fault, as well as the hanging wall of the Karasu fault (Fig. III.7C). Our field mapping and forward modeling resulted in a shallow, horizontal detachment that kinematically links the Aksu fault, Karasu Fault, South Karasu Fault, and the Mamazair Fault.

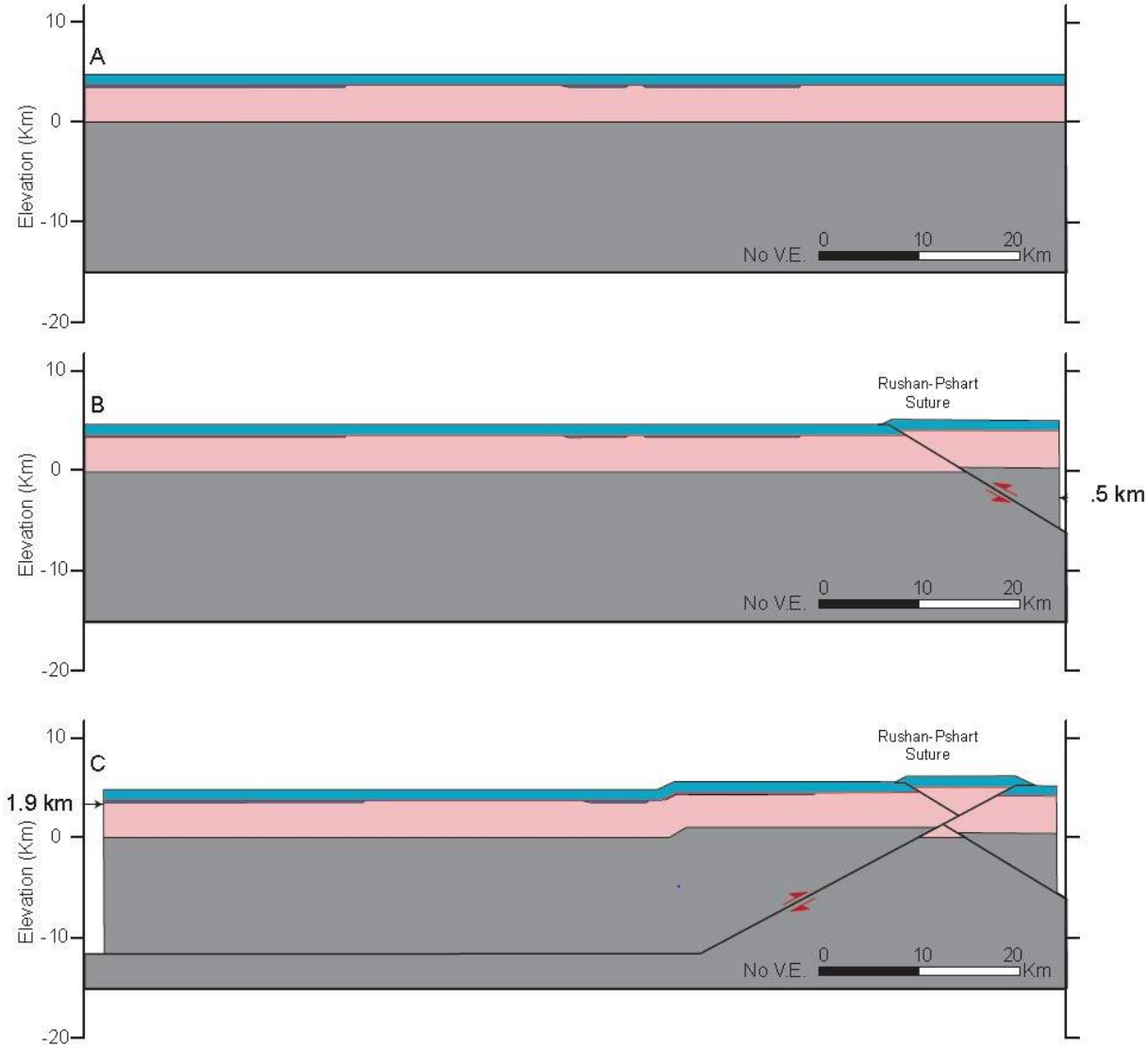

Fig. III.7 Model 1-Trishear
Forward model along A-A' red arrows show active fault and displacement direction. (A) Initial condition with layer cake stratigraphy. (B) Displacement of the north dipping Rushan-Pshart suture with 500 m of heave. (C) Displacement of South dipping Suture with 1,900 m of heave.

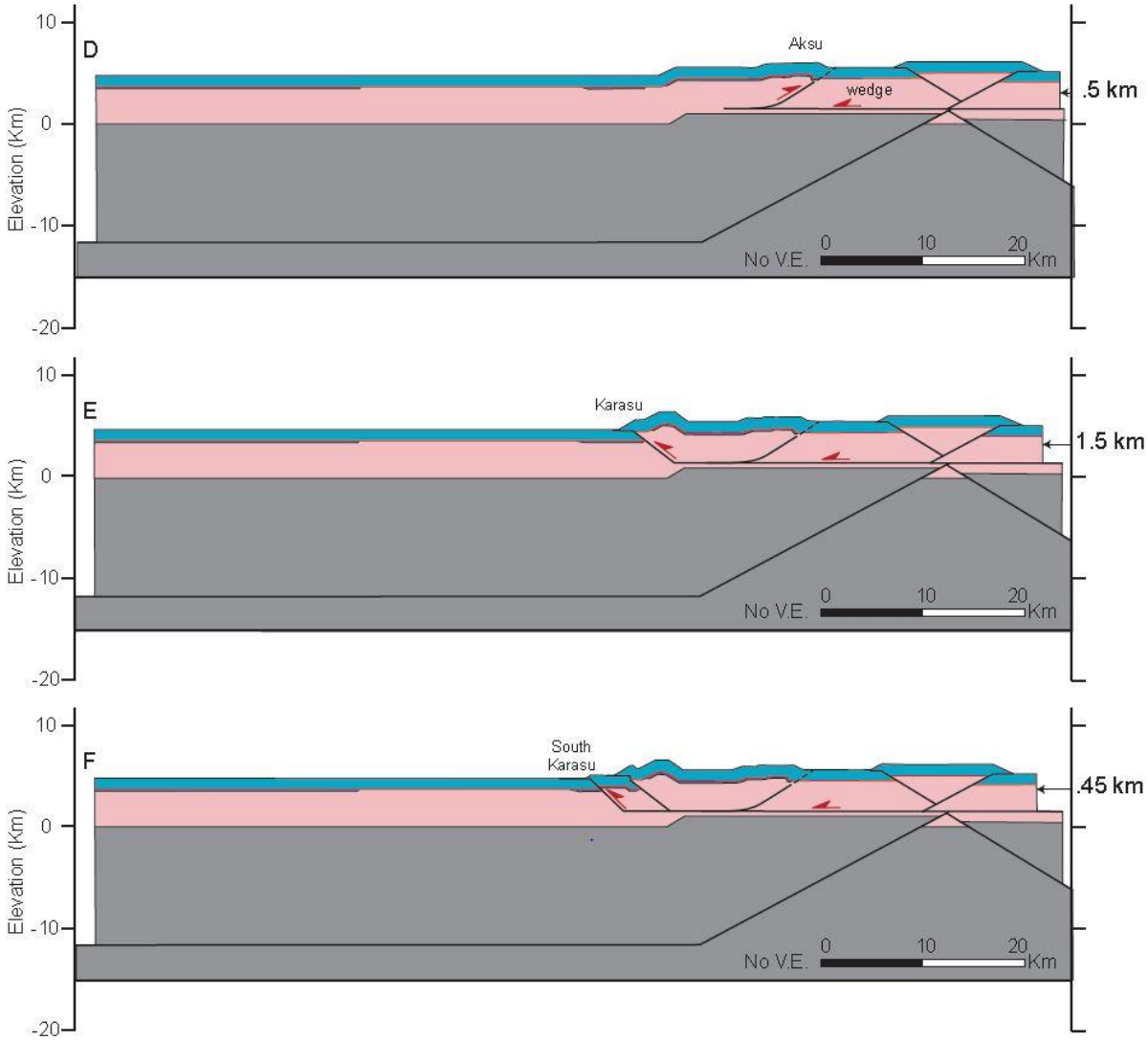

Fig. III.7 Continued Model 1- Trishear
(D) Trishear displacement along the Aksu fault accommodating 500 m of heave due to a southward directed wedge. (E) Displacement of the South verging Karasu Fault accommodating 1,500 m of heave. (F) Displacement of the south verging South Karasu Fault accommodating 450 m of heave.

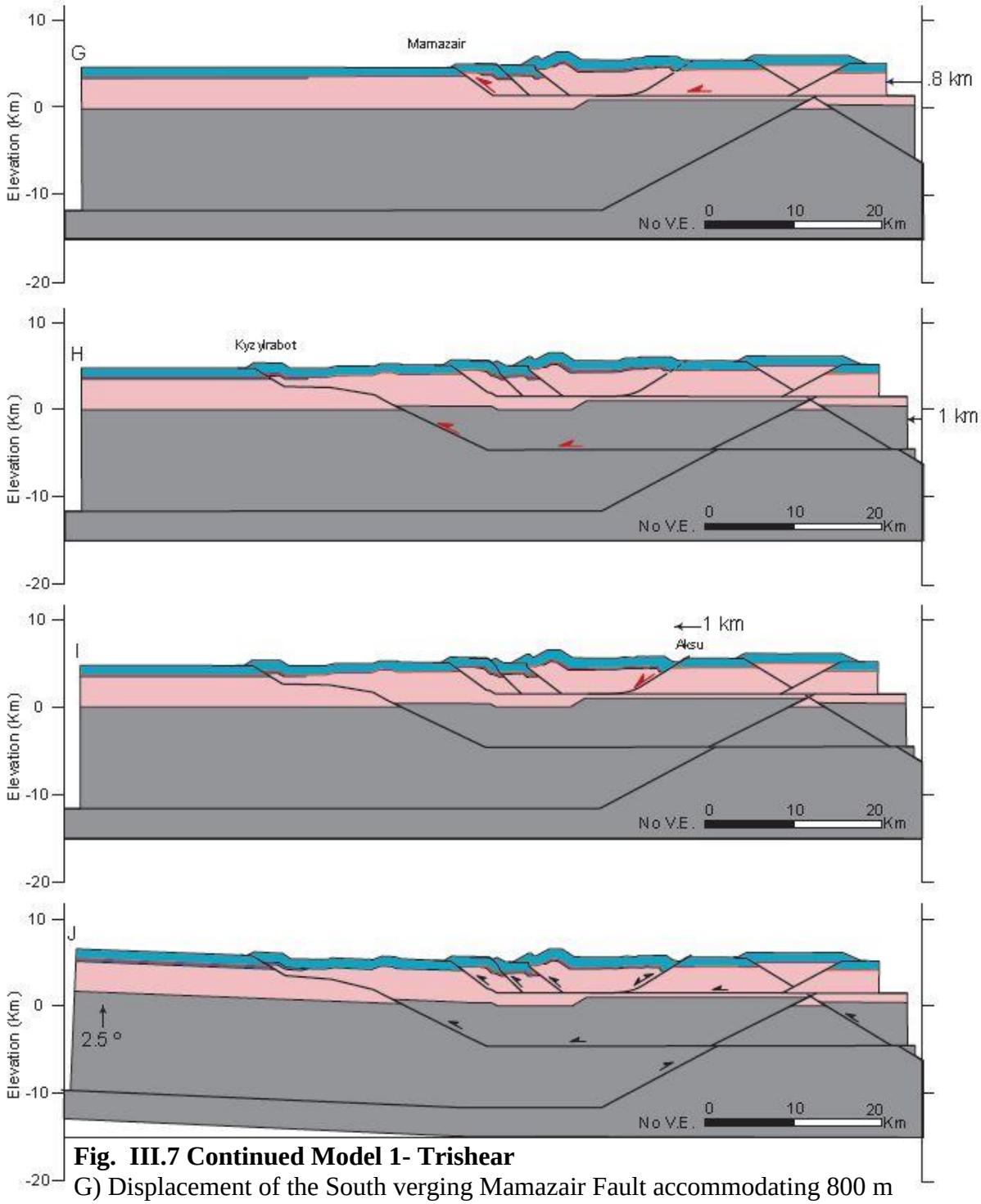

Fig. III.7 Continued Model 1- Trishear

G) Displacement of the South verging Mamazair Fault accommodating 800 m of heave. (H) Displacement along the Kyzylrabot Fault accommodating 1,000 m of heave and rooting into a deeper detachment. I) The Aksu fault reactivated into a normal fault and accommodating 1,000 m of local extension J) Tilting of the southern section of the Southern Pamir fold and thrust belt due to exhumation of the Shakadara-Alichur gneiss dome.

The Aksu Fault was modeled as a trishear fold that is controlled by a southward directed wedge (Fig. III.7D). In this trishear scenario, 500 m of reverse, horizontal displacement is required to achieve the hanging wall deformation that was observed in the field (Fig. III.3C) – relatively flat lying stratigraphy rolling over into steeper dips until terminating at the fault cutoff.

South of the Aksu fault are the Karasu Fault, South Karasu Fault, and Mamaziar Fault that accommodated 1500 m, 450 m, and 800 m, of upper crustal shortening, respectively (Fig. III.7E, III.7F, and III.7G). Our modeling suggest that these faults initiated sequentially southward from the same décollement as the thrust belt migrated southward. This southward propagation of the fold and thrust belt resulted in backward rotation (steeping) of faults and higher deformed hanging wall geometry at the surface as they were affected by younger faults. Net accommodation of upper crustal shortening in this section of the fold and thrust belt is 3,250 m (5.7%).

The final step for shortening is 1,000 m (1.74%) of horizontal displacement along the Kyzylrabot Fault (Fig. III.7H). Although a measurement of the fault was taken near the town of Kyzylrabot, our mapping and modeling suggest that along the transect the fault dips ~30 ° before transitioning into a shallow north dipping flat. The subhorizontal flat then transitions into a 30° ramp that reaches a depth of ~-9 km (-5 km elevation) (Fig. III.7H). This ramp-flat-ramp geometry was required to create the geometry of the hanging wall observed within the field and to bring up a large section of the crust (Fig. III.7H). Hanging wall geometries consist of an anticline syncline pair above where the shallow ramp transitions into a flat. At the surface, above the transition from the shallow flat to deeper ramp, there are broad open folds to subhorizontal bedding within the Jurassic Gurumdi Group. The transition from a ramp to a horizontal detachment at ~5 km back rotates (steepens) the Mamazair fault and the South Karasu Fault,

along with their associated footwall and hanging walls. This deep detachment is modeled as horizontal and likely reaches the Rushan-Pshart suture and has no structural effect on the fold and thrust belt north of the South Karasu Fault.

The final step is extension along the Aksu fault. By allowing for 1,000 m of extension along the Aksu fault, the base of the Jurassic Gurumdi Group steepened to subvertical which is what was observed in the field (Fig. III.7I). It is unclear whether this extension occurred during post-Miocene extension or at a different time. However, it is likely that it occurred after shortening was accommodated by the fold and thrust belt. Following extension along the Aksu fault the model required 2.5° of tilt to the southern section to match surficial geologic mapping. As mentioned in section 4.3.3, the Southern Pamir contains one of the largest gneiss domes in the world, the Shakhdara-Alichur gneiss dome. This gneiss dome exhumed from a depth of more than 35 km since the Miocene (Stübner et al., 2013b, 2013a; Hacker et al., 2017) and is only ~15 km south of the fold and thrust belt. Therefore, we interpret that it isostatically uplifted the southern section of the fold and thrust belt south of the Mamazair fault. We accounted for this by using a 2.5° tilt, which made it possible to retrodeform and balance the model.

5.2 Model 2

As previously mentioned, the only difference between the two models is the kinematics for the development of the Aksu Fault. Therefore, only the differences between the two models will be discussed in this section. In the second model (Fig. III.8), the Aksu fault accommodates no horizontal displacement. Instead, the anticline present in our field observation is from a ramp that is present in the deeper detachment. In this model the Karasu Fault, South Karasu Fault, and Mamazair Fault accommodated 1,500 m, 400 m, and 800 m of upper crustal shortening,

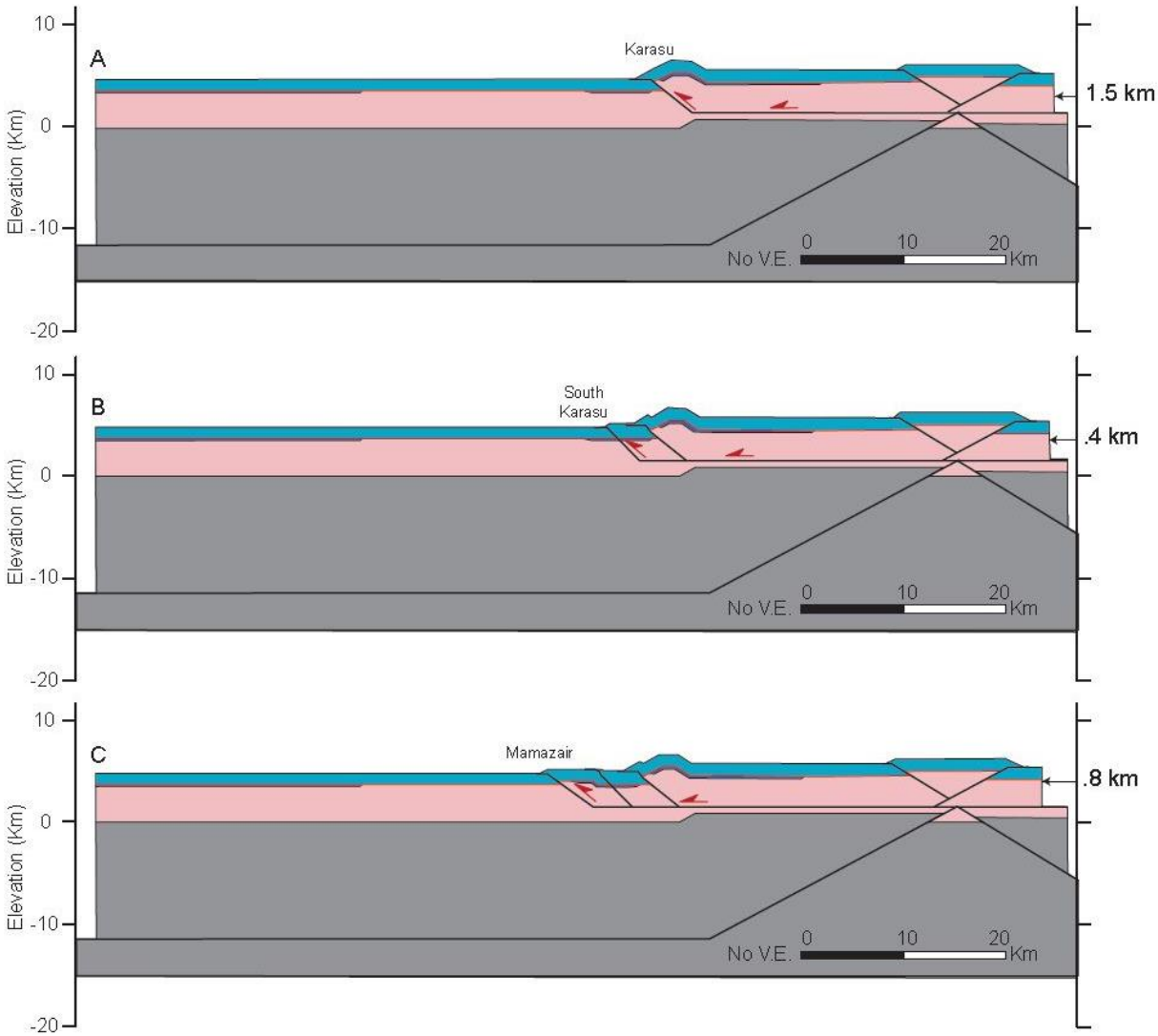

Fig. III.8 Model 2 – Ramp
(A) Displacement of the south verging Karasu Fault accommodating 1500 m of shortening. (B) Displacement of the south dipping South Karasu Fault accommodating 400 m of heave and back rotating the Karasu fault (C) Displacement of the south verging Mamazair Fault accommodating 800 m of heave and back rotating the South Karasu Fault.

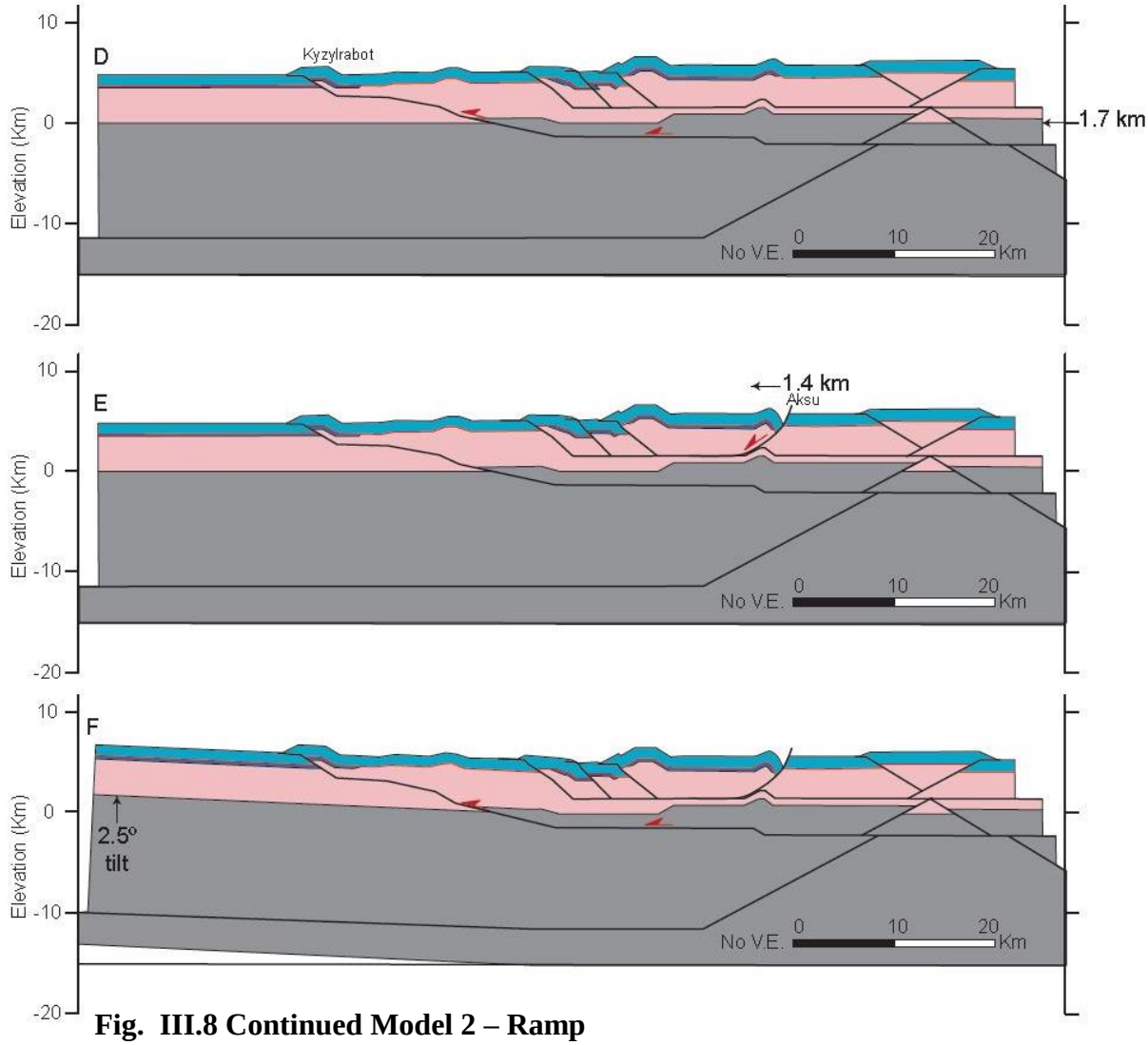

Fig. III.8 Continued Model 2 – Ramp

(D) Displacment of the south verging Kyzylrabot accommodating 1,700 m of shortening and rooting into a shallower detachment then in model 1. Antiform for Aksu fault forms at this time due to a ramp in the deeper detachment. The Mamazair fault is also slightly back rotated (E) Extension along the Aksu Fault accommodating 1,400 m of heave and hanging wall geometrically steepens due to a listric fault. (F) Sothern section of cross section tilts 2.5 degrees in response to exhumation of the Shakadara-Alichur gneiss dome.

(Figs. III.8D, III.8E, III8F). The difference in displacement along the South Karasu Fault was due to the geometric change along the Kyzylrabot Fault. However, the difference in shortening is only 50 m and has little effect on the evolution of the fold and thrust belt. Like the first model, these faults propagated southward from a common décollement that extended to the Rushan Fault. Net accommodation of upper crustal shortening in this section of the fold and thrust belt is 2,700 m (4.68%).

In the second model, a ramp along the Kyzylrabot Fault produces the anticline observed where the present day Aksu fault is (Fig. III.8G). This model requires that 1,700 m (2.95%) of displacement is accommodated along the fault in order to generate the fault bend fold geometry that is seen at the surface. However, because there is more displacement, a shallower dipping deep ramp along the Kyzylrabot fault is required so that it has little effect on vertical uplift of its hanging wall. This shallower dipping ramp thus results in a shallower décollement at a depth of ~2 km, however, the detachment is still likely to be below the Permian–Triassic section (Fig. III.8G).

As with the first model, extension along the Aksu fault post-dates shortening along the fold and thrust belt. A listric fault allowing for 1,400 m of extension along the Aksu fault is used to generate the present-day field observations of the hanging wall along the Aksu fault (Fig. III.8H). Like the first model, it is unclear of exactly when extension along the Aksu fault occurred. The southern section of the cross section was then tilted 2.5° to match the geology mapped on the surface.

5.3 Preferred Model and Structural Style

As it better matches the field data, i.e., the hanging wall geometry of the Aksu fault being subhorizontal then steeping deeply, model 1 (Fig. 5; the trishear model) is preferred. However,

the preferred model choice does not have a large effect on the outcome for the evolution of the fold and thrust belt as the difference in total shortening accommodated between the two models is only 150 m (.24%). Our conclusions from the models are as follows: The fold and thrust belt in the Southern Pamir appears to initiate along a shallow detachment from the Aksu Fault to the Mamazair fault (Fig. III.7) and feed into the Rushan suture. During this time, net shortening is minimal and results in no crustal stacking or duplexing but generates broad to open folds that are observed in the Jurassic Gurumdi Group (Fig. III.3A). A second deeper detachment then initiates the last stage of deformation. The deeper detachment is associated with the Kyzylrabot Fault that may also root into the Rushan suture.

Angiolini et al. (2013) suggested that the trend of folds in the post-Cimmerian and Cimmerian rock packages are oblique to each other, and, therefore, infered that the deformation was two different events (Angiolini et al., 2013; Bunge, 2014). The idea that the post-Cimmerian structures were at oblique angles to the Cimmerian structures suggested that post-Cimmerian deformation may be rooted into a shallow detachment, likely along the post-Cimmerian unconformity (Bunge, 2014). However, our field observations do not find a contrast in the structural trends between the Cimmerian and post-Cimmerian deformation structures; Gurumudi Group folds have axial planes that strike WNW-ESE, consistent with Chapman et al. (2018), and Permian-Triassic axial traces strike NW-SE, consistent with previously published maps (Fig. III.4) (Yushin et al., 1964; Vlasov et al., 1991). Thus, as Permian-Triassic, and possibly basement, rocks are incorporated into the fold and thrust belt, it is possible that Cimmerian structures were reactivated.

6.0 Discussion

6.1.0 Minimal Upper Crustal Shortening in the Pamir and Implication for Crustal thickness

Our forward modeling of the fold and thrust belt in this study suggest that internal shortening accommodated by the fold and thrust belt may be as little as 4.25 km (7.5%) but is certainly much less than 50 km (Figs. III.7 and III.8). U-Pb analysis coupled with zircon fission track analysis of the synorogenic Mamazair Conglomerate interpreted deformation associated with the fold and thrust belt to be mid-Late Cretaceous (112-76 Ma) (Chapman et al., 2018). The presence of the Jurassic Gurumdi Group carbonate requires that the Southern Pamir was at sea level at the end of the Jurassic, suggesting that the crust was no thicker than 30-35 km. If we assume the Southern Pamir fold and thrust belt resulted in plane strain deformation and take the upper limit for the thickness of the crust (35km) then crustal shortening resulted in only 2.3 km thickening. This thickness is substantially less than what is required in order to reach the current day crustal thickness of 70 km (Mechie et al., 2012; Schneider et al., 2013). Therefore, there must be another driving force for the development of the current crustal thickness of the Southern Pamir.

6.2.0 Alternative Methods to Crustal Thickening

The thick crust and high topography in the Pamir have commonly been associated with Cenozoic upper crustal shortening that occurred as a result of India colliding with Asia (Burtman and Molnar, 1993; Schmidt et al., 2011; Rutte et al., 2017a). However, past explanations involving Cenozoic internal shortening and crustal stacking of thrust sheets (Burtman and Molnar, 1993) are inconsistent with the data we have obtained in the field and our interpretations regarding the Southern Pamir. An alternative explanation for crustal thickening in the Southern

Pamir is underthrusting and underplating of external lithosphere in response to the complex subduction beneath the Pamir. Two possibilities for this scenario is the underthrusting of either the Indian crust (Kufner et al., 2016) or Central Pamir (Robinson et al., 2012) or possible some combination. Chapman et al (2018) suggested that Indian lower crust may be incorporated into the Pamir upperplate due to the underthrusted Indian mantle lithosphere lying beneath a large portion of the Pamir today (Schneider et al., 2013; Sippl et al., 2013; Kufner et al., 2016). This underplating scenario also supports the idea that there was decoupling of the crust along a shear zone at the mid to lower crustal levels (Robinson et al., 2007). However, crustal thickening solely due to underplating does not explain the prograde metamorphism of the Cenozoic gneiss domes present in the Southern Pamir (e.g., Shakhdara-Alichur dome), which is composed of local Gondwana material (Stübner et al., 2013b, 2013a). The burial depths of domes in the Southern Pamir have been estimated to have been 30-50 km by the Miocene (Stübner et al., 2013a; Hacker et al., 2017). If burial of the domes cannot be explained by upper crustal stacking, then there must be a decoupling shear zone above this depth separating lower crustal thickening from upper crustal extension (Chapman et al., 2018).

6.3.0 Broader implication

Geochronological analysis of the Mamazair Conglomerate (Chapman et al., 2018) and forward modeling of the Southern Pamir Fold and Thrust belt indicates that the fold and thrust belt was both verging and propagating southward towards the once northward subducting Neotethys oceanic plate. This is atypical of a standard fold and thrust belt, such as the Andes, that has a defined foreland propagating fold and thrust belt with a foreland basin system. However, the propagation direction of Cretaceous upper crustal deformation in Tibet, also propagates southward towards the subducting Neotethys Oceanic plate (Kapp and DeCelles,

2019 and references therein). The differences in the kinematics of fold and thrust belts could likely be attributed to the nature of plate collision – oceanic-continental convergence zones with a stable craton and passive margin (i.e., Andes) as compared to a region characterized by micro-continent terrane accretion to an already thickened crust followed immediately by an oceanic subduction zone as in the Northern Pamir (chapter 1 and 2) (i.e., Pamir and Tibet). One other reason could also be Early-mid Cretaceous low-angle subduction of the Neotethys that resulted in deformation along the Tanymas fault. This was then followed by rollback of the Neotethys in the mid-Late Cretaceous that resulted in subsequent southward propagation of upper crustal deformation into the Southern Pamir(Chapman et al., 2017b).

7.0 Conclusion

In this study, we constrained the magnitude of shortening and structural style within the Southern Pamir Fold and Thrust Belt. The modeling was driven by geologic mapping of the post-Cimmerian angular unconformity and the overlying Jurassic Gurumdi Group carbonate that was used as a strain marker. Our results indicate the following:

- Structural observations in the Southern Pamir indicates that the fold and thrust belt resulted in only minor offset and produced broad open folds (>2 km wavelength) within the Gurumdi Group.
- To construct and retrodeform a balanced cross section, the Southern Pamir Fold and Thrust Belt requires two separate detachment levels: a shallow one in the Permian–Triassic that the Aksu Fault, Karasu Fault, South Karasu Fault, and Mamazair Fault root into, and a deeper one possibly within basement rocks into which the Kyzylrabot Fault roots. The existence of two detachment levels suggest that the fold and thrust belt was originally thin-skinned and transitioned into thick skinned.

- This study coupled with geochronologic ages from both the Mamazair conglomerate (Chapman et al., 2018) and footwall of the Tanymas Thrust (Robinson et al., 2004) (chapter 2) indicate an overall southward migration of upper crustal Cretaceous shortening in the Pamir.
- Upper crustal deformation alone cannot produce the modern-day thickness of the Southern Pamir. It is likely underthrusting and underplating of external lithosphere has contributed to the modern thickness.

IV. BIBLIOGRAPHY

Angiolini, L. et al., 2015, From rift to drift in South Pamir (Tajikistan): Permian evolution of a Cimmerian terrane: Journal of Asian Earth Sciences, v. 102, p. 146–169.

Angiolini, L., Zanchi, A., Zanchetta, S., Nicora, A., and Vezzoli, G., 2013, The Cimmerian Geopuzzle: New data from South Pamir: Terra Nova, v. 25, p. 352–360.

Bernet, M., and Garver, J.I., 2005, Fission-track analysis of detrital zircon: Reviews in Mineralogy and Geochemistry, Mineralogical Society, p. 205–238.

Bershaw, J., Garzione, C.N., Schoenbohm, L., Gehrels, G., and Tao, L., 2012, Cenozoic evolution of the Pamir plateau based on stratigraphy, zircon provenance, and stable isotopes of foreland basin sediments at Oytag (Wuyitake) in the Tarim Basin (west China): Journal of Asian Earth Sciences, v. 44, p. 136–148.

Black, L.P. et al., 2004, Improved 206Pb/238U microprobe geochronology by the monitoring of a trace-element-related matrix effect; SHRIMP, ID-TIMS, ELA-ICP-MS and oxygen isotope documentation for a series of zircon standards: Chemical Geology, v. 205, p. 115–140.

Blayney, T. et al., 2016, Indentation of the Pamirs with respect to the northern margin of Tibet: Constraints from the Tarim basin sedimentary record: Tectonics, v. 35, p. 2345–2369.

Bunge, E.M., 2014, Forward modeling of post-Jurassic shortening in the southeast Pamir Mountains, Tajikistan: The University of Houston, 72 p.

Burtman, V.S., 2010, Tien Shan, Pamir, and Tibet: History and geodynamics of Phanerozoic oceanic basins: Geotectonics, v. 44, p. 388–404.

Burtman, V.S., and Molnar, P., 1993, Geological and geophysical evidence for deep subduction of continental crust beneath the Pamir: Geological Society of America Special Papers, v. 281, p. 1–76.

Cao, K., Wang, G.C., Bernet, M., van der Beek, P., and Zhang, K.X., 2015, Exhumation history of the West Kunlun Mountains, northwestern Tibet: Evidence for a long-lived, rejuvenated orogen: Earth and Planetary Science Letters, v. 432, p. 391–403.

Chapman, J.B., Carrapa, B., Ballato, P., DeCelles, P.G., Worthington, J., Oimahmadov, I., Gadoev, M., and Ketcham, R., 2017a, Intracontinental subduction beneath the Pamir Mountains: Constraints from thermokinematic modeling of shortening in the Tajik fold-and-thrust belt: Bulletin of the Geological Society of America, v. 129, p. 1450–1471.

Chapman, J.B., Ducea, M.N., Kapp, P., Gehrels, G.E., and DeCelles, P.G., 2017b, Spatial and temporal radiogenic isotopic trends of magmatism in Cordilleran orogens: Gondwana Research, v. 48, p. 189–204.

Chapman, J.B., Robinson, A.C., Carrapa, B., Villarreal, D., Worthington, J., Decelles, P.G., Kapp, P., Gadoev, M., Oimahmadov, I., and Gehrels, G., 2018, Cretaceous shortening and exhumation history of the South Pamir terrane: Lithosphere, v. 10, p. 494–511.

Chapman, J.B., Scoggin, S.H., Kapp, P., Carrapa, B., Ducea, M.N., Worthington, J., Oimahmadov, I., and Gadoev, M., 2017c, Mesozoic to Cenozoic magmatic history of the

Pamir: Earth and Planetary Science Letters, v. 482, p. 181–192.

Chen, X. et al., 2018, Arcuate Pamir in the Paleogene? Insights from a review of stratigraphy and sedimentology of the basin fills in the foreland of NE Chinese Pamir, western Tarim Basin: Earth-Science Reviews, v. 180, p. 1–16.

Cowgill, E., 2010, Cenozoic right-slip faulting along the eastern margin of the Pamir salient, northwestern China: Bulletin of the Geological Society of America, v. 122, p. 145–161.

Dewey, J.F., Shackleton, R.M., Chengfa, C., and Yiyin, S., 1988, The Tectonic Evolution of the Tibetan Plateau: Philosophical Transactions of the Royal Society of London . Series A , Mathematical and Physical Sciences, v. 327, p. 379–413.

Dickinson, W.R., 1985, Interpreting provenance relations from detrital modes of sandstones: Provenance of Arenites, p. 333–361.

Dickinson, W.R., Beard, L.S., Brakenridge, G. Robert Erjavec, J.L., Ferguson, R.C., Knepp, R.A., Alan, L.F., and Ryberg, P.T., 1983, Provenance of North American Phanerozoic sandstones in relation to tectonic setting: Geological Society of America Bulletin, v. 94, p. 222–235.

Dickinson, W.R., and Gehrels, G.E., 2009, Use of U-Pb ages of detrital zircons to infer maximum depositional ages of strata: A test against a Colorado Plateau Mesozoic database: Earth and Planetary Science Letters, v. 288, p. 115–125.

Dickinson, W.R., and Suczek, C.A., 1979, Plate-Tectonics and Sandstone Compositions: Aapg Bulletin, v. 63, p. 2164–2182.

Ding, L. et al., 2013, Provenance analysis of the Mesozoic Hoh-Xil-Songpan-Ganzi turbidites in northern Tibet: Implications for the tectonic evolution of the eastern Paleo-Tethys Ocean: Tectonics, v. 32, p. 34–48.

Ding, L., Kapp, P., Zhong, D., and Deng, W., 2003, Cenozoic volcanism in Tibet: evidence for a transition from oceanic to continental subduction: Journal of Petrology, v. 44, p. 1833–1865.

Ding, L., and Lai, Q., 2003, New geological evidence of crustal thickening in the Gangdese block prior to the Indo-Asian collision: Chinese Science Bulletin, v. 48, p. 1604–1610.

Donelick, R.A., 2005, Apatite Fission-Track Analysis: Reviews in Mineralogy and Geochemistry, v. 58, p. 49–94.

Dronov, V.L., Melnikova, G.K., Salibjev, G.C., Bardashev, I.A., Minajiev, V.E., and Muchabatov, N.M., 2006, Stratigraphic dictionary of the Pamir, *in* Technische Universität Bergakademie Freiberg, p. 252.

Gaetani, M., Jadoul, F., Erba, E., and Garzanti, E., 1993, Jurassic and Cretaceous Orogenic events in the North Karakoram: age constraints from sedimentary rocks: Himalayan Tectonics Geological Society Special Publications, p. 39–52.

Gaetani, M., Nicora, A., Henderson, C., Cirilli, S., Gale, L., Rettori, R., Vuolo, I., and Atudorei, V., 2013, Refinements in the Upper Permian to Lower Jurassic stratigraphy of Karakorum, Pakistan: Facies, v. 59, p. 915–948.

Gaetani, M., Zanchi, A., Angiolini, L., Olivini, G., Sciunnach, D., Brunton, H., Nicora, A., and Mawson, R., 2004, The Carboniferous of the Western Karakoram (Pakistan): Journal of Asian Earth Sciences, v. 23, p. 275–305.

Gehrels, G. et al., 2011, Detrital zircon geochronology of pre-Tertiary strata in the Tibetan-Himalayan orogen: Tectonics, v. 30.

Hacker, B.R., Ratschbacher, L., Rutte, D., Stearns, M.A., Malz, N., Stübner, K., Kylander-Clark, A.R.C., Pfänder, J.A., and Everson, A., 2017, Building the Pamir-Tibet Plateau—Crustal stacking, extensional collapse, and lateral extrusion in the Pamir: 3. Thermobarometry and petrochronology of deep Asian crust: Tectonics, v. 36, p. 1743–1766.

Hasebe, N., Barbarand, J., Jarvis, K., Carter, A., and Hurford, A.J., 2004, Apatite fission-track chronometry using laser ablation ICP-MS: v. 207, p. 135–145.

He, J., Kapp, P., Chapman, J.B., DeCelles, P.G., and Carrapa, B., 2018, Structural setting and detrital zircon U–Pb geochronology of Triassic–Cenozoic strata in the eastern Central Pamir, Tajikistan: Geological Society, London, Special Publications, v. 483, p. 605–630.

Hurford, A.J., and Green, P.F., 1983, The zeta age calibration of fission-track dating: Chemical Geology, v. 41, p. 285–317.

Imrecke, D.B., Robinson, A.C., Owen, L.A., Chen, J., Schoenbohm, L.M., Hedrick, K.A., Lapen, T.J., Li, W., and Yuan, Z., 2019, Mesozoic evolution of the eastern Pamir: Lithosphere, v. 11, p. 560–580.

Kapp, P., and DeCelles, P.G., 2019, Mesozoic–Cenozoic geological evolution of the Himalayan-Tibetan orogen and working tectonic hypotheses: American Journal of Science, v. 319, p. 159–254.

Kapp, P., DeCelles, P.G., Gehrels, G.E., Heizler, M., and Ding, L., 2007a, Geological records of the Lhasa-Qiangtang and Indo-Asian collisions in the Nima area of central Tibet: Bulletin of the Geological Society of America, v. 119, p. 917–932.

Kapp, P., DeCelles, P.G., Leier, A.L., Fabijanic, J.M., He, S., Pullen, A., Gehrels, G.E., and Ding, L., 2007b, The Gangdese retroarc thrust belt revealed: GSA Today, v. 17, p. 4–9.

Kapp, P., Yin, A., Harrison, T.M., and Ding, L., 2005, Cretaceous-Tertiary shortening, basin development, and volcanism in central Tibet: Bulletin of the Geological Society of America, v. 117, p. 865–878.

Korchagin, O.A., 2008, Foraminifers and stratigraphy of the Karatash Group (lower Triassic-Middle Anisian), the southeastern Pamir: Stratigraphy and Geological Correlation, v. 16, p. 248–256.

Korchagin, O.A., 2009, Kaeveria fluegeli (Zaninetti, Altiner, Dager et Ducret, 1982) (Foraminifera) from Upper Triassic of the south-east Pamirs: Stratigraphy and Geological Correlation, v. 17, p. 62–67.

Kufner, S.K. et al., 2016, Deep India meets deep Asia: Lithospheric indentation, delamination and break-off under Pamir and Hindu Kush (Central Asia): Earth and Planetary Science Letters, v. 435, p. 171–184.

Kuiper, K.F., Deino, A., Hilgen, F.J., Krijgsman, W., Renne, P.R., and Wijbrans, J.R., 2008, Synchronizing rock clocks of earth history: Science, v. 320, p. 500–504.

Leven, E.J., 1995, Permian and Triassic of the Rushan-Pshart zone (Pamir): Rivista Italiana di Paleontologia e Stratigrafia, v. 101, p. 3–16.

Liu, Z.Q., 1988, Geologic Map of the Qinghai-Xizang Plateau and its Neighboring Regions: Chengdu Institute of Geology and Mineral Resources, v. Geological.

Ludwig, K.R., 2003, User's manual for Isoplot 3.00: A geochronological toolkit for Microsoft Excel: Berkeley Geochronology Center Special Publication, v. 4, p. 70.

Lukens, C.E., Carrapa, B., Singer, B.S., and Gehrels, G., 2012, Miocene exhumation of the Pamir revealed by detrital geothermochronology of Tajik rivers: Tectonics, v. 31, p. 1–12.

Mechie, J. et al., 2012, Crustal and uppermost mantle velocity structure along a profile across the Pamir and southern Tien Shan as derived from project TIPAGE wide-angle seismic data: Geophysical Journal International, v. 188, p. 385–407.

Metcalfe, I., 2013, Gondwana dispersion and Asian accretion: Tectonic and palaeogeographic evolution of eastern Tethys: Journal of Asian Earth Sciences, v. 66, p. 1–33.

Metcalfe, I., 2002, Permian tectonic framework and palaeogeography of SE Asia: Journal of Asian Earth Sciences, v. 20, p. 551–566.

Murphy, M.A., An, Y., Harrison, T.M., Durr, S.B., Chen, Z., Ryerson, F.J., Kidd, W.S.F., Wang, X., and Zhou, X., 1997, Did the Indo-Asian collision along create the Tibetan plateau? Geology, v. 25, p. 719–722.

Pashkov, B.R., and Budanov, V.I., 1990, Tectonics of the SE-SW Pamir Junction: Geotectonics, v. 24, p. 246–253.

Pashkov, B.R., and Shvol'man, V.A., 1979, Rift margins of Tethys in the Pamirs: Geotectonics, v. 13, p. 447–456.

Phillips, R.J., Parrish, R.R., and Searle, M.P., 2004, Age constraints on ductile deformation and long-term slip rates along the Karakoram fault zone, Ladakh: Earth and Planetary Science Letters, v. 226, p. 305–319.

Robinson, A.C., 2009, Geologic offsets across the northern Karakorum fault: Implications for its role and terrane correlations in the western Himalayan-Tibetan orogen: Earth and Planetary Science Letters, v. 279, p. 123–130.

Robinson, A.C., 2015, Mesozoic tectonics of the Gondwanan terranes of the Pamir plateau: Journal of Asian Earth Sciences, v. 102, p. 170–179.

Robinson, A.C., Ducea, M., and Lapen, T.J., 2012, Detrital zircon and isotopic constraints on the crustal architecture and tectonic evolution of the northeastern Pamir: Tectonics, v. 31, p. 1–16.

Robinson, A.C., Yin, A., Manning, C.E., Harrison, T.M., Zhang, S.H., and Wang, X.F., 2007, Cenozoic evolution of the eastern Pamir: Implications for strain-accommodation mechanisms at the western end of the Himalayan-Tibetan orogen: Bulletin of the Geological Society of America, v. 119, p. 882–896.

Robinson, A.C., Yin, A., Manning, C.E., Harrison, T.M., Zhang, S.H., and Wang, X.F., 2004, Tectonic evolution of the northeastern Pamir: Constraints from the northern portion of the Cenozoic Kongur Shan extensional system, western China: Bulletin of the Geological Society of America, v. 116, p. 953–973.

Rutte, D., Ratschbacher, L., Schneider, S., Stübner, K., Stearns, M.A., Gulzar, M.A., and Hacker, B.R., 2017a, Building the Pamir-Tibetan Plateau—Crustal stacking, extensional collapse, and lateral extrusion in the Central Pamir: 1. Geometry and kinematics: Tectonics,.

Rutte, D., Ratschbacher, L., Schneider, S., Stübner, K., Stearns, M.A., Gulzar, M.A., and Hacker, B.R., 2017b, Building the Pamir-Tibetan Plateau—Crustal stacking, extensional collapse, and lateral extrusion in the Central Pamir: 2. Timing and rates Daniel: Tectonics, v. 36, p. 342–384.

Schmidt, J. et al., 2011, Cenozoic deep crust in the Pamir: Earth and Planetary Science Letters, v. 312, p. 411–421.

Schneider, F.M. et al., 2013, Seismic imaging of subducting continental lower crust beneath the Pamir: Earth and Planetary Science Letters, v. 375, p. 101–112.

Schwab, M. et al., 2004, Assembly of the Pamirs: Age and origin of magmatic belts from the southern Tien Shan to the southern Pamirs and their relation to Tibet: Tectonics, v. 23, p. 1–31.

Searle, M.P., and Phillips, R.J., 2007, Relationships between right-lateral shear along the Karakoram fault and metamorphism, magmatism, exhumation and uplift: evidence from the K2-Gasherbrum-Pangong ranges, north Pakistan and Ladakh: Journal of the Geological Society, v. 164, p. 439–450.

Şengör, A.M.C., 1979, Mid-Mesozoic closure of Permo-Triassic Tethys and its implications: v. 279, p. 590–593.

Şengör, A.M.C., 1984, The Cimmeride Orogenic System and the Tectonics of Eurasia: , p. 1–74.

Shvol'man, V.A., 1980, Mesozoic ophiolites in the Pamir: Geotectonics, v. 14, p. 465- 470.

Shvol'man, V.A., 1978, Relicts of The Mesotethys in the Pamirs: Himalayan Geology, v. 8, p. 369–378.

Sippl, C. et al., 2013, Geometry of the Pamir-Hindu Kush intermediate-depth earthquake zone from local seismic data: Journal of Geophysical Research: Solid Earth, v. 118, p. 1438–1457.

Sobel, E.R., 1999, Basin analysis of the Jurassic–Lower Cretaceous southwest Tarim basin, northwest China: Geological Society of America Bulletin, v. 111, p. 709–724.

Sobel, E.R., Schoenbohm, L.M., Chen, J., Thiede, R., Stockli, D.F., Sudo, M., and Strecker, M.R., 2011, Late Miocene-Pliocene deceleration of dextral slip between Pamir and Tarim: Implications for Pamir orogenesis: Earth and Planetary Science Letters, v. 304, p. 369–378.

Strecker, M.R., Frisch, W., Hamburger, M.W., Ratschbacher, L., Semiletkin, S., Zamoruyev, A., and Sturchio, N., 1995, Quaternary deformation in the Eastern Pamirs, Tadzhikistan and Kyrgyzstan: Tectonics, v. 14, p. 1061–1079.

Stübner, K. et al., 2013a, The giant Shakhdara migmatitic gneiss dome, Pamir, India-Asia collision zone: 2. Timing of dome formation: Tectonics, v. 32, p. 1404–1431.

Stübner, K., Ratschbacher, L., Rutte, D., Stanek, K., Minaev, V., Wiesinger, M., Gloaguen, R., and ProjectTIPAGEmembers, 2013b, The Giant Shakhdara migmatitic gneiss dome, Pamir, India – Asia collision zone, I : Geometry and kinematics: Tectonics, v. 32, p. 948–979.

Sundell, K.E., 2017, Cenozoic surface uplift and basin formation in the Peruvian central Andes: University of Houston.

Upadhyay, R., Rai, J., and Sinha, A.K., 2005, New record of Bathonian-Callovian calcareous nannofossils in the eastern Karakoram block: A possible clue to understanding the dextral offset along the Karakoram Fault: Terra Nova, v. 17, p. 149–157.

Vermeesch, P., 2012, On the visualisation of detrital age distributions: Chemical Geology, v. 312–313, p. 190–194.

Vlasov, N., Yu, G., Dyakov, A., and E.S., C., 1991, Geological map of the Tajik SSR and adjacent territories, 1:500,000: Vsesojuznoi Geologic Institute of Leningrad, Saint Petersburg,.

Volkmer, J.E., Kapp, P., Guynn, J.H., and Lai, Q., 2007, Cretaceous-Tertiary structural evolution of the north central Lhasa terrane, Tibet: Tectonics, v. 26, p. 1–18.

Volkmer, J.E., Kapp, P., Horton, B.K., Gehrels, G.E., Minervini, J.M., and Ding, L., 2014, Northern Lhasa thrust belt of central Tibet: Evidence of Cretaceous-early Cenozoic shortening within a passive roof thrust system? Special Paper of the Geological Society of America, v. 507, p. 59–70.

Weislogel, A.L., Graham, S.A., Chang, E.Z., Wooden, J.L., Gehrels, G.E., Survey, S.S.G., and Analysis, M., 2010, Detrital zircon provenance from three turbidite depocenters of the Middle – Upper Triassic Songpan-Ganzi complex , central China : Record of collisional tectonics , erosional exhumation , and sediment production: GSA Bulletin, v. 122, p. 2041–2062.

Weislogel, A.L., Graham, S. a, Chang, E.Z., Wooden, J.L., Gehrels, G.E., and Yang, H., 2006, Detrital zircon provenance of the Late Triassic Songpan-Ganzi complex : Sedimentary record of collision of the North and South China blocks: Geology, v. 34, p. 97–100.

Xiao, W.J., Windley, B.F., Chen, H.L., Zhang, G.C., and Li, J.L., 2002a, Carboniferous-Triassic subduction and accretion in the western Kunlun, China: Implications for the collisional and accretionary tectonics of the northern Tibetan Plateau: Geology, v. 30, p. 295–298.

Xiao, W.J., WINDLEY, B.F., Liu, D.Y., Jian, P., Liu, C.Z., Yuan, C., Sun, M., HAO, J., and LI, J., 2002b, Arc-ophiolite obduction in the Western Kunlun Range (China): implications for the Palaeozoic evolution of central Asia: The Journal of Geology, v. 159, p. 517–528.

Yin, A., and Harrison, T.M., 2000, Geologic evolution of the Himalayan-Tibetan orogen: Annual Reviews of Earth and Planetary Sciences, v. 28, p. 211–280.

Yushin, I.P., Sass, M.E., Karapetov, S.S., Altukhov, S.M., Teplov, I.C., Raeakov, C.R., Harkov, S.I., and Davidchenko, A.G., 1964, J-43-Xxi, Xxii, Xxvii, Xxviii: Russian Geological Research Institute,.

Zanchetta, S., Worthington, J., Angiolini, L., Leven, E.J., Villa, I.M., and Zanchi, A., 2018, The Bashgumbaz Complex (Tajikistan): Arc obduction in the Cimmerian orogeny of the Pamir: Gondwana Research, v. 57, p. 170–190.

Zanchi, A., and Gaetani, M., 2011, The geology of the Karakoram range, Pakistan: The new 1:100,000 geological map of Central-Western Karakoram: Italian Journal of Geosciences, v. 130, p. 161–262.

Zanchi, A., Poli, S., Fumagalli, P., and Gaetani, M., 2000, Mantle exhumation along the Tirich Mir Fault Zone, NW Pakistan: pre-mid-Cretaceous accretion of the Karakoram terrane to the Asian margin: Geological Society, London, Special Publications, v. 170, p. 237–252.

Zhang, K., Cai, J., Zhang, Y., and Zhao, T., 2006, Eclogites from central Qiangtang , northern Tibet (China) and tectonic implications: v. 245, p. 722–729.

V. APPENDICES

A. Appendix 1: U-P Zircon Analysis

LA-ICP-MS analyses conducted at the University of Arizona Laserchron Center

13P99	37.758° N; 73.774° E					Isotope ratios							Apparent ages (Ma)						
	U	^{206}Pb	U/Th	^{206}Pb*	±	^{207}Pb*	±	^{206}Pb*	±	error	^{206}Pb*	±	^{207}Pb*	±	^{206}Pb*	±	Best age	±	
Analysis	(ppm)	^{204}Pb		^{207}Pb*	(%)	^{235}U	(%)	^{238}U	(%)	corr.	^{238}U*	(Ma)	^{235}U	(Ma)	^{207}Pb*	(Ma)	(Ma)	(Ma)	Discordance
13P99-129	869	21203	8.3	14.4577	1.1	1.2428	2.5	0.1303	2.3	0.90	789.7	16.9	820.1	14.1	903.7	22.2	789.7	16.9	87.4
13P99-130	201	12783	1.3	17.8134	1.5	0.5408	2.4	0.0699	1.8	0.78	435.4	7.7	439.0	8.4	457.8	32.9	435.4	7.7	95.1
13P99-131	94	4738	1.2	20.2869	5.6	0.2691	6.0	0.0396	2.1	0.35	250.3	5.2	242.0	13.0	161.8	131.9	250.3	5.2	NA
13P99-132	213	8969	8.3	17.0363	2.5	0.5485	3.0	0.0678	1.7	0.57	422.7	7.1	444.0	11.0	555.9	54.6	422.7	7.1	76.0
13P99-133	40	5889	0.8	13.6236	2.1	1.7029	3.1	0.1683	2.3	0.75	1002.5	21.6	1009.6	19.9	1025.1	41.6	1002.5	21.6	97.8
13P99-134	388	12082	2.0	15.7972	1.5	1.0419	2.5	0.1194	2.0	0.79	727.0	13.8	724.9	13.1	718.4	32.7	727.0	13.8	101.2
13P99-135	693	12534	1.8	14.7955	0.9	1.2262	3.1	0.1316	2.9	0.96	796.9	22.0	812.6	17.2	856.0	18.8	796.9	22.0	93.1
13P99-136	153	20999	2.8	12.2576	1.2	2.3168	2.1	0.2060	1.8	0.84	1207.3	19.9	1217.5	15.2	1235.5	22.7	1207.3	19.9	97.7
13P99-137	145	5731	2.3	17.7189	1.5	0.6261	2.6	0.0805	2.1	0.82	498.8	10.1	493.6	10.0	469.6	32.9	498.8	10.1	106.2
13P99-138	1221	34610	3.0	18.9603	1.3	0.2961	2.3	0.0407	1.9	0.83	257.3	4.8	263.3	5.3	317.7	28.8	257.3	4.8	NA
13P99-139	386	45799	4.5	8.1820	0.8	6.0354	2.0	0.3582	1.8	0.91	1973.4	31.2	1981.0	17.5	1988.9	14.6	1988.9	14.6	99.2
13P99-140	317	24461	1.8	18.0288	1.4	0.5326	2.4	0.0696	2.0	0.83	434.0	8.4	433.5	8.6	431.1	30.2	434.0	8.4	100.7
13P99-141	146	23256	6.3	17.6756	1.6	0.5191	2.5	0.0666	2.0	0.77	415.3	7.9	424.6	8.8	475.0	36.0	415.3	7.9	87.4
13P99-142	596	18388	8.7	10.8503	0.9	1.5854	2.3	0.1248	2.1	0.93	757.9	15.2	964.5	14.3	1470.7	16.5	757.9	15.2	51.5
13P99-143	155	8310	1.7	14.4523	1.0	1.4771	1.9	0.1548	1.6	0.83	928.0	13.5	921.0	11.4	904.5	21.5	928.0	13.5	102.6
13P99-144	238	25782	3.8	14.2688	1.2	1.4642	2.1	0.1515	1.7	0.82	909.5	14.8	915.7	12.9	930.8	25.4	909.5	14.8	97.7
13P99-145	228	48746	2.5	6.5809	0.7	9.2643	1.7	0.4422	1.6	0.91	2360.4	31.3	2364.5	15.9	2368.0	12.1	2368.0	12.1	99.7
13P99-146	74	12242	1.3	8.9337	1.2	5.0078	2.4	0.3245	2.1	0.86	1811.5	33.1	1820.6	20.6	1831.1	22.5	1831.1	22.5	98.9
13P99-147	137	3139	2.0	18.9104	1.8	0.4881	2.7	0.0669	2.0	0.74	417.7	8.1	403.6	8.9	323.7	40.7	417.7	8.1	129.0
13P99-148	484	10601	1.8	19.5422	1.1	0.3227	2.4	0.0457	2.2	0.89	288.3	6.1	284.0	6.0	248.6	25.1	288.3	6.1	NA
13P99-149	1112	26619	9.6	8.0729	1.3	5.8116	3.4	0.3403	3.1	0.93	1888.0	51.1	1948.1	29.2	2012.7	22.5	2012.7	22.5	93.8
13P99-150	883	122948	7.2	8.1514	0.8	4.7193	6.9	0.2790	6.8	0.99	1586.3	95.8	1770.7	57.5	1995.5	14.1	1995.5	14.1	79.5
13P99-151	324	16740	2.6	14.4724	0.9	1.4727	1.9	0.1546	1.6	0.86	926.6	13.8	919.2	11.2	901.6	19.6	926.6	13.8	102.8

13P99-152	117	12426	1.9	19.1009	2.9	0.2986	3.8	0.0414	2.4	0.63	261.3	6.1	265.3	8.9	300.9	67.2	261.3	6.1	NA
13P99-153	66	9562	1.9	6.1448	1.1	10.5814	2.8	0.4716	2.6	0.93	2490.5	53.1	2487.1	25.8	2484.3	17.8	2484.3	17.8	100.2
13P99-154	2015	25970	3.2	19.0771	0.9	0.3401	2.2	0.0471	2.0	0.92	296.4	5.9	297.2	5.7	303.7	19.4	296.4	5.9	NA
13P99-155	207	5646	2.2	19.4852	1.7	0.3012	2.5	0.0426	1.9	0.76	268.7	5.1	267.3	6.0	255.3	38.2	268.7	5.1	NA
13P99-156	199	6135	84.6	18.2814	1.7	0.5434	2.5	0.0720	1.8	0.73	448.5	7.8	440.6	8.8	400.0	37.8	448.5	7.8	112.1
13P99-157	91	3670	1.7	18.6036	2.2	0.4486	3.1	0.0605	2.2	0.71	378.8	8.0	376.3	9.7	360.7	48.6	378.8	8.0	NA
13P99-158	259	23376	2.1	8.8311	0.8	5.0859	1.8	0.3257	1.6	0.88	1817.7	25.0	1833.8	15.2	1852.0	15.3	1852.0	15.3	98.1
13P99-159	116	10988	0.9	13.7825	1.4	1.6102	2.3	0.1610	1.7	0.77	962.1	15.6	974.2	14.1	1001.6	29.0	962.1	15.6	96.1
13P99-160	258	19128	1.0	15.4886	1.2	1.0148	2.8	0.1140	2.5	0.91	695.9	16.8	711.3	14.3	760.1	24.7	695.9	16.8	91.6
13P99-161	211	34426	1.1	17.6719	1.5	0.5325	2.5	0.0682	1.9	0.78	425.6	8.0	433.5	8.7	475.5	33.8	425.6	8.0	89.5
13P99-162	104	5962	1.3	18.8776	2.5	0.3101	3.6	0.0425	2.5	0.70	268.1	6.5	274.3	8.5	327.6	57.7	268.1	6.5	NA
13P99-163	209	11255	1.0	14.1211	1.0	1.5924	2.4	0.1631	2.2	0.91	973.9	20.0	967.2	15.2	952.1	20.5	973.9	20.0	102.3
13P99-164	74	4830	1.3	17.7086	1.7	0.6561	2.8	0.0843	2.2	0.79	521.6	10.9	512.2	11.1	470.9	37.5	521.6	10.9	110.8
13P99-165	512	25160	6.1	14.2804	1.1	1.4664	2.0	0.1519	1.7	0.86	911.5	14.7	916.6	12.2	929.1	21.6	911.5	14.7	98.1
13P99-166	322	5752	2.1	19.7194	3.3	0.3344	3.7	0.0478	1.7	0.46	301.1	5.1	292.9	9.5	227.7	76.2	301.1	5.1	NA
13P99-167	1851	36187	4.6	17.9964	0.9	0.5241	5.1	0.0684	5.1	0.99	426.6	20.9	427.9	18.0	435.1	19.3	426.6	20.9	98.0
13P99-168	221	21689	2.0	13.2329	1.0	1.8605	2.0	0.1786	1.7	0.87	1059.1	16.8	1067.2	13.0	1083.7	19.2	1059.1	16.8	97.7
13P99-169	138	10703	4.8	8.2553	1.0	5.4152	2.0	0.3242	1.7	0.85	1810.3	26.4	1887.3	16.8	1973.0	18.3	1973.0	18.3	91.8
13P99-170	331	66371	2.1	17.1722	1.3	0.6530	2.2	0.0813	1.7	0.79	504.0	8.4	510.3	8.8	538.6	29.3	504.0	8.4	93.6
13P99-171	319	40448	1.5	19.3019	1.5	0.2871	2.3	0.0402	1.8	0.77	254.0	4.5	256.3	5.3	277.0	34.6	254.0	4.5	NA
13P99-172	334	28874	5.8	16.4694	1.1	0.8584	2.1	0.1025	1.8	0.85	629.2	10.7	629.2	9.8	629.3	24.0	629.2	10.7	100.0
13P99-173	482	7274	0.6	19.0280	1.7	0.2610	2.6	0.0360	1.9	0.74	228.1	4.3	235.5	5.4	309.6	39.7	228.1	4.3	NA
13P99-174	3344	39334	4.3	18.2101	0.9	0.4611	2.9	0.0609	2.8	0.95	381.1	10.3	385.0	9.4	408.7	20.0	381.1	10.3	NA
13P99-175	257	25263	6.0	8.7010	1.1	6.0140	2.3	0.3795	2.0	0.87	2074.0	34.7	1977.9	19.7	1878.8	20.4	1878.8	20.4	110.4
13P99-176	395	5591	2.8	18.9617	2.8	0.3957	3.5	0.0544	2.0	0.57	341.6	6.6	338.5	10.0	317.5	64.7	341.6	6.6	NA
13P99-177	301	5876	2.0	18.6428	1.9	0.4804	2.7	0.0649	1.9	0.70	405.7	7.5	398.3	8.9	356.0	43.3	405.7	7.5	114.0
13P99-178	244	6562	1.3	19.0095	1.3	0.3208	2.2	0.0442	1.7	0.78	279.0	4.7	282.5	5.4	311.8	30.7	279.0	4.7	NA
13P99-179	161	12742	0.6	13.0838	1.0	1.8742	1.9	0.1778	1.6	0.84	1055.2	15.9	1072.0	12.8	1106.4	20.7	1055.2	15.9	95.4
13P99-180	400	45748	6.3	8.7763	0.8	5.3794	1.8	0.3424	1.6	0.89	1898.2	26.6	1881.6	15.5	1863.2	14.7	1863.2	14.7	101.9
13P99-181	300	56139	2.0	12.6686	1.0	2.0637	2.0	0.1896	1.7	0.86	1119.3	17.5	1136.8	13.7	1170.5	20.5	1119.3	17.5	95.6
13P99-182	121	91157	2.2	8.6184	1.0	5.3207	2.3	0.3326	2.1	0.91	1850.9	33.7	1872.2	19.7	1895.9	17.1	1895.9	17.1	97.6
13P99-183	678	27870	3.0	14.7207	0.9	1.1581	3.8	0.1236	3.7	0.97	751.5	26.3	781.1	20.8	866.5	18.5	751.5	26.3	86.7
13P99-184	251	9982	1.5	17.9740	1.3	0.5328	2.2	0.0695	1.8	0.82	432.9	7.7	433.7	7.9	437.8	28.2	432.9	7.7	98.9
13P99-185	170	54605	11.4	14.5805	1.2	1.2831	2.2	0.1357	1.9	0.84	820.2	14.4	838.2	12.8	886.3	25.4	820.2	14.4	92.5
13P99-186	113	4048	1.1	18.8895	2.0	0.3749	2.8	0.0514	2.0	0.71	322.8	6.3	323.3	7.9	326.2	45.4	322.8	6.3	NA

13P99-187	128	4785	1.2	19.1821	1.9	0.3578	2.7	0.0498	1.9	0.72	313.2	5.9	310.6	7.2	291.2	42.4	313.2	5.9	NA
13P99-188	54	5368	1.6	18.2804	3.9	0.4202	4.5	0.0557	2.4	0.52	349.5	8.0	356.2	13.6	400.1	86.5	349.5	8.0	NA
13P99-189	1	178	0.0	6.3918	17.5	2.1787	22.3	0.1010	13.8	0.62	620.3	81.5	1174.3	156.2	2417.6	299.5	2417.6	299.5	25.7
13P99-190	261	7588	2.5	19.2704	1.5	0.3187	2.2	0.0445	1.6	0.74	281.0	4.5	280.9	5.5	280.7	34.6	281.0	4.5	NA
13P99-191	173	6484	1.4	18.1180	1.7	0.5368	2.4	0.0705	1.6	0.69	439.4	6.9	436.3	8.4	420.1	38.2	439.4	6.9	104.6
13P99-192	57	7282	1.5	18.0720	3.0	0.3766	3.7	0.0494	2.2	0.59	310.6	6.7	324.5	10.4	425.7	67.8	310.6	6.7	NA
13P99-193	39	4075	4.1	17.2869	2.5	0.6474	3.6	0.0812	2.5	0.70	503.1	12.2	506.9	14.3	524.0	55.9	503.1	12.2	96.0
13P99-194	629	36058	5.8	14.4324	0.9	1.3593	4.4	0.1423	4.3	0.98	857.6	34.6	871.6	25.8	907.3	18.5	857.6	34.6	94.5
13P99-195	251	9974	1.2	18.1180	1.1	0.5312	2.0	0.0698	1.6	0.83	435.0	6.9	432.6	7.0	420.1	24.7	435.0	6.9	103.5
13P99-196	435	20768	3.4	14.0786	0.9	1.6118	2.1	0.1646	1.9	0.91	982.2	17.2	974.8	13.1	958.2	18.1	982.2	17.2	102.5
13P99-197	120	7543	1.9	14.0481	1.4	1.5772	2.2	0.1607	1.7	0.77	960.7	15.2	961.3	13.8	962.7	29.0	960.7	15.2	99.8
13P99-198	191	27502	2.4	8.6961	0.9	5.4518	1.8	0.3438	1.5	0.86	1905.1	25.4	1893.0	15.4	1879.8	16.8	1879.8	16.8	101.3
13P99-199	83	5350	1.7	8.9110	0.9	4.8629	1.8	0.3143	1.6	0.86	1761.8	24.0	1795.9	15.3	1835.7	17.1	1835.7	17.1	96.0
13P99-200	317	40402	3.0	8.8451	1.0	5.3120	2.3	0.3408	2.1	0.90	1890.4	34.2	1870.8	19.8	1849.1	18.3	1849.1	18.3	102.2
13P99-201	190	9264	1.4	14.3686	1.9	1.4570	2.7	0.1518	2.0	0.72	911.2	16.6	912.8	16.2	916.5	38.3	911.2	16.6	99.4
13P99-202	292	5410	0.9	19.4799	2.1	0.2889	2.8	0.0408	1.7	0.63	257.9	4.4	257.7	6.3	255.9	49.0	257.9	4.4	NA
13P99-203	155	13742	3.0	8.6772	1.0	5.0301	2.2	0.3166	2.0	0.89	1772.9	30.6	1824.4	18.8	1883.7	18.6	1883.7	18.6	94.1
13P99-204	805	10574	3.1	17.4618	1.2	0.4900	2.4	0.0621	2.1	0.87	388.1	8.0	404.9	8.1	501.9	26.5	388.1	8.0	NA
13P99-205	92	5396	0.7	19.0457	4.7	0.3808	5.2	0.0526	2.2	0.42	330.5	7.1	327.6	14.6	307.5	107.8	330.5	7.1	NA
13P99-206	250	6574	0.9	18.1294	1.4	0.5101	2.1	0.0671	1.5	0.75	418.5	6.3	418.5	7.1	418.7	30.3	418.5	6.3	100.0
13P99-207	292	49348	2.5	7.8897	0.8	6.6066	1.8	0.3780	1.6	0.89	2067.1	28.1	2060.2	15.7	2053.3	14.3	2053.3	14.3	100.7
13P99-208	424	28742	3.5	10.8633	0.9	3.2241	2.3	0.2540	2.1	0.92	1459.2	27.1	1463.0	17.6	1468.5	17.1	1468.5	17.1	99.4
13P99-209	132	21057	1.6	8.7391	1.0	4.7824	2.4	0.3031	2.2	0.91	1706.8	33.2	1781.8	20.4	1870.9	18.1	1870.9	18.1	91.2
13P99-210	711	17383	2.2	18.9851	1.1	0.3803	2.0	0.0524	1.7	0.85	329.0	5.5	327.2	5.6	314.7	24.3	329.0	5.5	NA
13P99-211	157	17323	1.4	9.3926	1.0	4.3971	2.0	0.2995	1.7	0.86	1689.0	25.6	1711.8	16.5	1739.8	18.4	1739.8	18.4	97.1
13P99-212	100	11625	0.9	7.2784	1.2	7.1883	2.4	0.3795	2.1	0.88	2073.7	37.5	2135.0	21.5	2194.6	20.1	2194.6	20.1	94.5
13P99-213	173	13096	1.9	8.6622	1.0	5.1644	2.1	0.3244	1.9	0.89	1811.4	29.6	1846.8	17.9	1886.8	17.3	1886.8	17.3	96.0
13P99-214	185	24226	1.3	8.6503	1.2	4.6422	2.2	0.2912	1.8	0.84	1647.7	26.5	1756.9	18.1	1889.3	20.9	1889.3	20.9	87.2
13P99-215	453	16678	1.2	19.2647	1.5	0.2883	2.5	0.0403	2.0	0.80	254.6	5.0	257.2	5.6	281.4	34.0	254.6	5.0	NA
13P99-216	103	5074	0.8	19.9206	2.8	0.2631	3.7	0.0380	2.4	0.65	240.5	5.7	237.2	7.9	204.2	65.3	240.5	5.7	NA
13P99-217	257	13211	0.8	19.4750	2.0	0.2729	2.7	0.0385	1.9	0.70	243.8	4.6	245.0	5.9	256.5	45.0	243.8	4.6	NA
13P99-218	35	6949	1.5	6.8003	1.2	8.1984	2.7	0.4044	2.4	0.89	2189.0	44.6	2253.2	24.4	2311.9	21.1	2311.9	21.1	94.7
13P99-219	127	6174	2.0	19.5177	2.5	0.2789	3.3	0.0395	2.1	0.65	249.6	5.2	249.8	7.2	251.5	56.9	249.6	5.2	NA
13P99-220	678	39005	3.7	17.4829	1.0	0.6072	2.2	0.0770	2.0	0.88	478.1	9.1	481.8	8.5	499.2	22.9	478.1	9.1	95.8
13P99-221	563	30717	3.0	14.1649	0.9	1.5292	2.7	0.1571	2.6	0.95	940.6	22.5	942.2	16.7	945.8	18.1	940.6	22.5	99.5

13P99-222	235	13903	3.2	17.9559	1.4	0.5036	2.5	0.0656	2.0	0.81	409.5	7.9	414.1	8.4	440.1	32.2	409.5	7.9	93.0
13P99-223	313	6446	2.8	17.5411	1.3	0.4996	2.9	0.0636	2.6	0.89	397.2	9.8	411.4	9.8	491.9	29.4	397.2	9.8	NA
13P99-224	60	8896	1.7	7.5447	1.1	7.0394	2.4	0.3852	2.1	0.89	2100.5	37.6	2116.4	21.0	2131.9	19.1	2131.9	19.1	98.5
13P99-225	735	86302	1.5	8.8751	0.8	5.0284	2.2	0.3237	2.1	0.93	1807.6	32.3	1824.1	18.6	1843.0	14.5	1843.0	14.5	98.1
13P99-226	342	17397	12.1	10.5165	0.9	3.5388	1.9	0.2699	1.7	0.88	1540.4	23.3	1535.9	15.4	1529.8	17.7	1529.8	17.7	100.7
13P99-227	444	13553	1.2	15.0272	0.8	1.2187	2.0	0.1328	1.9	0.92	803.9	14.2	809.2	11.4	823.6	17.1	803.9	14.2	97.6
13P99-228	625	38007	2.3	8.8555	1.1	1.3808	11.3	0.0887	11.3	1.00	547.7	59.1	880.8	66.7	1847.0	19.1	547.7	59.1	29.7
13P99-229	53	43302	0.9	5.9939	1.1	8.5487	3.1	0.3716	2.9	0.94	2037.0	50.1	2291.1	27.8	2526.1	18.0	2526.1	18.0	80.6
13P99-230	216	6649	1.0	19.0158	1.7	0.3168	2.4	0.0437	1.6	0.69	275.6	4.4	279.4	5.8	311.0	38.9	275.6	4.4	NA
13P99-231	381	7928	4.2	19.0915	1.5	0.3369	2.0	0.0466	1.4	0.70	293.9	4.1	294.8	5.2	302.0	33.2	293.9	4.1	NA
13P99-232	366	26777	5.2	8.2648	1.1	5.7179	2.2	0.3427	1.9	0.87	1899.9	31.1	1934.1	18.9	1970.9	19.3	1970.9	19.3	96.4
13P99-233	141	24579	2.6	7.2459	1.0	7.5901	2.3	0.3989	2.1	0.91	2163.9	38.3	2183.7	20.6	2202.4	16.6	2202.4	16.6	98.3
13P99-234	203	6904	1.7	19.1553	2.1	0.3124	2.9	0.0434	2.0	0.68	273.9	5.2	276.1	6.9	294.4	47.7	273.9	5.2	NA
13P99-235	153	5616	11.6	18.3019	1.9	0.4281	2.7	0.0568	1.9	0.71	356.3	6.7	361.9	8.3	397.5	43.0	356.3	6.7	NA
13P99-236	388	31082	14.7	8.8902	1.1	4.8802	2.6	0.3147	2.4	0.90	1763.6	36.5	1798.8	22.1	1839.9	20.3	1839.9	20.3	95.9
13P99-237	157	5938	2.1	17.9664	1.6	0.5385	2.4	0.0702	1.8	0.75	437.2	7.5	437.5	8.4	438.8	34.8	437.2	7.5	99.6
13P99-238	192	8111	1.6	17.5218	2.7	0.5238	3.2	0.0666	1.9	0.57	415.4	7.4	427.7	11.3	494.3	58.9	415.4	7.4	84.0
13P99-239	785	5544	0.9	20.0325	1.1	0.2523	1.9	0.0367	1.5	0.81	232.1	3.5	228.5	3.9	191.2	25.6	232.1	3.5	NA
13P99-240	209	16978	3.3	8.7234	0.8	5.1781	1.8	0.3276	1.6	0.89	1826.8	25.7	1849.0	15.5	1874.1	15.0	1874.1	15.0	97.5
13P99-241	227	18298	1.8	9.7522	1.0	2.9293	2.2	0.2072	2.0	0.89	1213.8	22.0	1389.5	17.0	1670.6	19.3	1670.6	19.3	72.7
13P99-242	536	67626	7.0	8.6300	0.9	5.2037	2.7	0.3257	2.6	0.94	1817.5	40.6	1853.2	23.1	1893.5	16.0	1893.5	16.0	96.0
13P99-243	437	59494	1.7	8.7549	0.8	4.6981	1.9	0.2983	1.8	0.92	1682.9	26.6	1766.9	16.3	1867.6	13.7	1867.6	13.7	90.1
13P99-244	121	32119	2.5	18.3946	2.3	0.3228	3.1	0.0431	2.0	0.66	271.8	5.4	284.1	7.6	386.1	51.8	271.8	5.4	NA
13P99-245	258	31484	2.1	13.5010	0.9	1.7481	1.9	0.1712	1.6	0.87	1018.6	15.4	1026.5	12.2	1043.3	19.2	1018.6	15.4	97.6
13P99-246	159	10666	0.7	15.3466	1.2	1.1121	2.2	0.1238	1.9	0.84	752.3	13.3	759.2	11.9	779.5	25.6	752.3	13.3	96.5
13P99-247	109	31288	1.2	6.0523	0.8	11.1079	1.8	0.4876	1.6	0.88	2560.2	33.0	2532.2	16.6	2509.8	14.3	2509.8	14.3	102.0
13P99-248	52	7256	1.3	8.9239	1.3	4.8728	2.4	0.3154	2.0	0.84	1767.1	30.7	1797.6	19.9	1833.0	23.3	1833.0	23.3	96.4
13P99-249	54	10905	2.3	6.0623	1.2	10.2765	2.2	0.4518	1.8	0.84	2403.4	36.4	2460.0	19.9	2507.1	19.6	2507.1	19.6	95.9
13P99-250	1539	12707	9.2	19.7005	0.9	0.2606	1.8	0.0372	1.6	0.87	235.6	3.6	235.1	3.8	229.9	20.9	235.6	3.6	NA
13P99-251	167	14820	5.3	8.0071	1.3	5.4198	2.3	0.3147	1.9	0.83	1764.0	30.0	1888.0	20.1	2027.2	23.2	2027.2	23.2	87.0
13P99-252	215	5669	3.3	19.6547	2.0	0.3244	2.6	0.0462	1.8	0.67	291.4	5.0	285.3	6.6	235.3	45.1	291.4	5.0	NA
13P99-253	293	38460	2.9	8.6856	0.8	5.1774	1.9	0.3261	1.7	0.90	1819.6	27.1	1848.9	16.1	1882.0	14.7	1882.0	14.7	96.7
13P99-254	284	28071	0.7	6.0238	0.8	10.9466	1.9	0.4782	1.8	0.92	2519.6	36.7	2518.6	17.8	2517.8	12.8	2517.8	12.8	100.1
13P99-255	348	38926	2.6	10.9500	1.2	1.9305	3.4	0.1533	3.2	0.93	919.5	27.4	1091.7	22.9	1453.4	23.4	919.5	27.4	63.3
13P99-256	735	11961	2.3	18.3571	0.9	0.4967	1.8	0.0661	1.6	0.87	412.8	6.2	409.5	6.0	390.7	19.4	412.8	6.2	105.7

13P99-257	113	11187	1.8	9.2964	0.9	4.5180	2.0	0.3046	1.8	0.88	1714.2	26.7	1734.3	16.7	1758.6	17.3	1758.6	17.3	97.5
13P99-258	194	6696	1.4	18.9541	1.8	0.3870	2.5	0.0532	1.7	0.69	334.1	5.7	332.2	7.1	318.4	41.3	334.1	5.7	NA
13P99-259	69	7502	1.2	6.3684	1.0	9.0582	2.5	0.4184	2.3	0.92	2253.1	42.9	2343.9	22.5	2423.9	16.6	2423.9	16.6	93.0
13P99-260	195	6615	2.8	18.0591	1.3	0.5486	2.0	0.0719	1.5	0.75	447.3	6.4	444.1	7.2	427.3	29.6	447.3	6.4	104.7
13P99-261	91	7756	2.0	6.2745	1.0	9.6287	2.6	0.4382	2.4	0.92	2342.5	47.1	2399.9	24.0	2449.0	17.5	2449.0	17.5	95.6
13P99-262	517	19963	0.7	15.1204	1.0	1.2413	2.1	0.1361	1.9	0.89	822.7	14.7	819.5	12.0	810.7	20.5	822.7	14.7	101.5
13P99-263	271	13723	2.1	17.9204	1.8	0.5346	2.5	0.0695	1.8	0.70	433.0	7.5	434.8	9.0	444.5	40.4	433.0	7.5	97.4
13P99-264	141	31838	1.0	6.2693	0.9	9.8594	1.7	0.4483	1.4	0.84	2387.7	28.9	2421.7	15.9	2450.4	15.8	2450.4	15.8	97.4
13P99-265	687	42323	5.2	8.7904	0.9	4.8533	3.4	0.3094	3.3	0.96	1737.8	49.8	1794.2	28.6	1860.3	16.3	1860.3	16.3	93.4
13P99-266	130	5011	0.7	19.9410	2.7	0.2792	3.5	0.0404	2.2	0.63	255.2	5.5	250.1	7.7	201.8	62.6	255.2	5.5	NA
13P99-267	680	18812	6.9	18.7221	1.0	0.3539	2.2	0.0481	1.9	0.88	302.6	5.7	307.7	5.7	346.4	22.8	302.6	5.7	NA
13P99-268	193	25241	1.1	7.0192	1.9	9.2706	2.4	0.4719	1.4	0.60	2492.1	29.8	2365.1	22.0	2257.4	33.2	2257.4	33.2	110.4
13P99-269	357	16411	1.7	14.1480	0.9	1.5104	1.7	0.1550	1.5	0.86	928.8	12.7	934.6	10.4	948.2	17.7	928.8	12.7	98.0
13P99-270	841	53290	3.8	5.9757	0.9	10.8513	2.3	0.4703	2.1	0.92	2484.9	42.9	2510.5	21.0	2531.2	15.0	2531.2	15.0	98.2
13P99-271	499	12545	3.0	19.4483	1.8	0.3291	2.4	0.0464	1.5	0.63	292.5	4.3	288.9	5.9	259.6	42.2	292.5	4.3	NA
13P99-272	135	5877	1.3	14.6921	1.8	1.1169	2.6	0.1190	1.9	0.73	724.9	13.2	761.5	14.1	870.5	37.4	724.9	13.2	83.3
13P99-273	491	5977	141.7	18.4664	1.3	0.5147	2.3	0.0689	2.0	0.84	429.7	8.2	421.6	8.1	377.4	28.4	429.7	8.2	113.9
13P99-274	182	20081	1.5	14.1149	1.1	1.4548	2.1	0.1489	1.8	0.85	895.0	15.0	911.9	12.8	953.0	23.1	895.0	15.0	93.9
13P99-275	105	12092	1.3	17.4949	2.0	0.5545	3.0	0.0704	2.2	0.75	438.3	9.5	448.0	10.8	497.7	43.5	438.3	9.5	88.1
13P99-276	62	9657	0.6	8.5963	1.1	5.3881	2.3	0.3359	2.0	0.88	1867.1	32.4	1883.0	19.6	1900.6	19.9	1900.6	19.9	98.2
13P99-277	212	5562	1.3	19.4366	1.6	0.3364	2.7	0.0474	2.2	0.80	298.7	6.4	294.4	6.9	261.0	37.0	298.7	6.4	NA
13P99-278	66	5130	0.4	19.3289	2.9	0.3334	3.7	0.0467	2.3	0.63	294.4	6.7	292.1	9.4	273.7	65.8	294.4	6.7	NA
13P99-279	1186	13539	2.7	18.2549	0.8	0.4996	1.9	0.0661	1.7	0.90	412.9	6.7	411.4	6.3	403.2	18.1	412.9	6.7	102.4
13P99-280	69	2215	1.4	20.2920	2.5	0.3468	3.3	0.0510	2.2	0.68	320.9	7.0	302.3	8.7	161.2	57.5	320.9	7.0	NA
13P99-281	399	9572	2.1	14.5274	1.0	1.3670	1.9	0.1440	1.6	0.85	867.4	13.0	874.9	11.0	893.8	20.5	867.4	13.0	97.0
13P99-282	87	2326	1.2	19.7944	2.6	0.3796	3.3	0.0545	2.1	0.63	342.1	7.0	326.7	9.3	218.9	59.8	342.1	7.0	NA
13P99-283	465	5401	2.2	20.0741	1.4	0.2716	2.2	0.0395	1.8	0.79	250.0	4.4	244.0	4.9	186.4	32.0	250.0	4.4	NA
13P99-284	1162	69073	53.7	10.7919	0.8	3.1672	2.1	0.2479	2.0	0.92	1427.6	25.3	1449.2	16.5	1481.0	15.8	1481.0	15.8	96.4
13P99-285	174	6514	1.2	18.0629	3.3	0.5255	3.7	0.0688	1.8	0.47	429.2	7.3	428.8	13.1	426.9	73.8	429.2	7.3	100.5
13P99-286	1209	33691	3.1	18.2236	1.0	0.4740	1.8	0.0627	1.5	0.84	391.7	5.8	394.0	6.0	407.1	22.1	391.7	5.8	NA
13P99-287	480	32245	4.2	14.4059	1.0	1.4122	2.1	0.1475	1.8	0.87	887.2	15.0	894.1	12.4	911.1	21.1	887.2	15.0	97.4
13P99-288	328	21300	1.0	13.9093	1.0	1.7008	2.0	0.1716	1.7	0.87	1020.8	16.5	1008.8	12.8	983.0	19.7	1020.8	16.5	103.8
13P99-289	182	15073	2.3	8.6371	0.7	5.3070	1.8	0.3324	1.6	0.91	1850.2	25.8	1870.0	15.0	1892.0	13.2	1892.0	13.2	97.8
13P99-290	242	7301	0.9	18.7156	2.0	0.3662	2.9	0.0497	2.1	0.72	312.7	6.5	316.8	8.0	347.1	46.0	312.7	6.5	NA
13P99-291	116	5360	1.8	18.5684	3.8	0.3731	4.3	0.0502	2.1	0.49	316.0	6.5	321.9	11.9	365.0	85.1	316.0	6.5	NA

13P99-292	300	7260	2.0	18.5102	1.3	0.5153	2.2	0.0692	1.8	0.79	431.2	7.3	422.0	7.6	372.0	30.2	431.2	7.3	115.9
13P99-293	145	19439	2.1	6.2709	0.8	8.9594	1.9	0.4075	1.7	0.90	2203.4	32.5	2333.9	17.6	2450.0	14.1	2450.0	14.1	89.9
13P99-294	392	15841	1.7	16.3242	1.2	0.7543	2.5	0.0893	2.2	0.88	551.4	11.7	570.7	11.1	648.4	26.2	551.4	11.7	85.0
13P99-295	165	32968	1.5	7.7542	0.7	6.6367	1.8	0.3732	1.7	0.92	2044.6	29.4	2064.2	16.2	2083.8	13.0	2083.8	13.0	98.1
13P99-296	206	7102	1.5	19.5555	2.3	0.3420	2.9	0.0485	1.8	0.61	305.4	5.3	298.7	7.6	247.0	53.6	305.4	5.3	NA
13P99-297	100	9162	0.7	5.8562	0.9	11.3443	1.9	0.4818	1.6	0.87	2535.2	34.3	2551.9	17.6	2565.1	15.8	2565.1	15.8	98.8
13P99-298	134	23994	1.6	8.8624	0.9	5.0387	1.7	0.3239	1.5	0.86	1808.6	23.7	1825.9	14.8	1845.6	16.1	1845.6	16.1	98.0
13P99-299	123	9051	1.5	13.4971	1.9	1.7206	2.6	0.1684	1.7	0.67	1003.5	15.9	1016.3	16.4	1043.9	38.5	1003.5	15.9	96.1
13P99-300	503	6598	1.0	8.3339	1.3	5.2834	2.2	0.3193	1.8	0.81	1786.5	27.6	1866.2	18.6	1956.1	22.7	1956.1	22.7	91.3
13P99-301	132	17569	6.0	6.1585	1.1	9.7273	3.4	0.4345	3.3	0.94	2325.9	63.5	2409.3	31.7	2480.6	19.1	2480.6	19.1	93.8
13P99-302	162	6315	1.3	17.9231	1.5	0.5535	2.2	0.0720	1.6	0.72	447.9	6.8	447.3	7.9	444.2	33.6	447.9	6.8	100.8
13P99-303	246	14978	0.8	7.7866	0.8	6.4864	1.9	0.3663	1.7	0.91	2012.0	30.0	2044.1	16.7	2076.5	13.5	2076.5	13.5	96.9
13P99-304	324	6085	1.0	20.0129	2.5	0.2721	3.0	0.0395	1.6	0.54	249.7	4.0	244.3	6.5	193.5	58.9	249.7	4.0	NA
13P99-305	823	10061	3.1	19.3433	1.0	0.3046	2.0	0.0427	1.7	0.87	269.7	4.6	270.0	4.8	272.0	22.9	269.7	4.6	NA
13P99-306	75	8600	2.6	8.5449	1.0	5.4431	2.4	0.3373	2.2	0.91	1873.8	35.0	1891.7	20.3	1911.3	17.7	1911.3	17.7	98.0
13P99-307	705	21569	3.1	17.9156	1.1	0.5300	2.1	0.0689	1.8	0.86	429.3	7.5	431.8	7.4	445.1	24.3	429.3	7.5	96.5
13P99-308	163	5440	3.0	18.1942	3.3	0.4933	3.7	0.0651	1.8	0.48	406.5	7.1	407.2	12.6	410.7	73.5	406.5	7.1	99.0
13P99-309	459	116622	1.2	7.5236	0.8	7.2461	2.3	0.3954	2.2	0.94	2147.8	39.9	2142.2	20.7	2136.8	13.3	2136.8	13.3	100.5
13P99-310	207	8424	1.1	19.0490	1.8	0.2897	2.5	0.0400	1.7	0.69	253.0	4.3	258.3	5.7	307.1	41.1	253.0	4.3	NA
13P99-311	327	23537	1.3	16.6575	1.0	0.7835	1.8	0.0947	1.6	0.85	583.0	8.8	587.5	8.2	604.8	20.7	583.0	8.8	96.4
13P99-312	234	132140	3.0	8.6783	0.8	5.3592	2.0	0.3373	1.8	0.91	1873.7	29.6	1878.4	17.1	1883.5	14.9	1883.5	14.9	99.5
13P99-313	725	73110	3.3	8.0613	0.8	6.3156	2.2	0.3692	2.0	0.93	2025.9	34.8	2020.6	18.9	2015.3	14.0	2015.3	14.0	100.5
13P99-314	213	9673	1.6	18.9197	2.0	0.3600	2.9	0.0494	2.2	0.75	310.8	6.7	312.2	7.9	322.6	44.4	310.8	6.7	NA
13P99-315	214	8043	2.3	19.4624	2.2	0.3240	2.9	0.0457	1.8	0.63	288.3	5.1	285.0	7.1	258.0	51.0	288.3	5.1	NA
13P99-316	165	24771	1.6	18.1642	1.7	0.4884	2.5	0.0643	1.8	0.73	401.9	7.1	403.8	8.3	414.4	37.7	401.9	7.1	97.0
13P99-317	311	16062	3.1	19.0656	1.7	0.3445	2.4	0.0476	1.7	0.72	300.0	5.0	300.5	6.2	305.1	38.0	300.0	5.0	NA
13P99-318	131	5497	1.1	19.2711	4.5	0.3806	4.9	0.0532	2.0	0.41	334.1	6.5	327.5	13.8	280.6	103.4	334.1	6.5	NA
13P99-319	505	16447	2.2	18.3299	1.5	0.5040	2.5	0.0670	1.9	0.79	418.1	7.8	414.4	8.3	394.0	33.9	418.1	7.8	106.1
13P99-320	273	31708	3.5	8.4931	0.8	5.7882	1.9	0.3565	1.8	0.91	1965.8	30.0	1944.6	16.8	1922.2	14.3	1922.2	14.3	102.3
13P99-321	810	27773	10.8	9.0189	0.8	4.9213	4.9	0.3219	4.8	0.99	1799.0	76.0	1805.9	41.4	1813.8	14.0	1813.8	14.0	99.2
13P99-322	256	7144	1.6	15.5836	1.0	1.2080	2.1	0.1365	1.8	0.87	825.0	13.9	804.3	11.5	747.2	21.5	825.0	13.9	110.4
13P99-323	538	8787	2.0	18.2244	2.0	0.5490	2.5	0.0726	1.5	0.62	451.6	6.7	444.3	9.0	407.0	44.0	451.6	6.7	111.0
13P99-324	139	6963	2.0	19.4228	2.0	0.2547	4.7	0.0359	4.3	0.91	227.2	9.6	230.4	9.7	262.6	45.1	227.2	9.6	NA
13P99-325	787	26943	1.4	6.4622	0.8	8.0934	2.4	0.3793	2.3	0.94	2073.1	40.6	2241.5	21.9	2399.0	13.5	2399.0	13.5	86.4
13P99-326	460	47283	5.8	8.7960	0.7	5.2666	1.7	0.3360	1.6	0.92	1867.3	25.1	1863.5	14.4	1859.2	12.3	1859.2	12.3	100.4

13P99-327	74	15147	1.9	11.2820	1.3	2.8810	2.1	0.2357	1.7	0.80	1364.5	21.1	1377.0	16.1	1396.3	24.5	1364.5	21.1	97.7
13P99-328	788	23273	2.7	17.9011	1.1	0.5456	2.1	0.0708	1.8	0.86	441.2	7.7	442.1	7.6	446.9	24.4	441.2	7.7	98.7
13P99-329	407	29336	2.1	15.4045	1.1	1.2444	2.2	0.1390	1.9	0.86	839.2	15.1	820.9	12.6	771.6	24.2	839.2	15.1	108.8
13P99-330	78	9618	0.7	10.1575	1.1	3.8306	2.1	0.2822	1.8	0.86	1602.4	25.6	1599.2	16.8	1594.9	19.7	1594.9	19.7	100.5
13P99-331	126	11337	1.1	10.6498	0.9	3.3558	1.8	0.2592	1.6	0.87	1485.7	20.9	1494.1	14.1	1506.1	16.8	1506.1	16.8	98.7
13P99-332	220	9068	2.5	17.3681	1.3	0.6126	1.9	0.0772	1.4	0.73	479.2	6.5	485.2	7.4	513.7	28.7	479.2	6.5	93.3
13P99-333	191	5382	1.2	18.4717	1.6	0.5099	2.4	0.0683	1.7	0.73	425.9	7.1	418.3	8.1	376.7	36.4	425.9	7.1	113.1
~~13P99-334~~	~~698~~	~~14667~~	~~3.2~~	~~17.8749~~	~~0.9~~	~~0.5199~~	~~2.2~~	~~0.0674~~	~~2.0~~	~~0.91~~	~~420.4~~	~~8.1~~	~~425.1~~	~~7.6~~	~~450.1~~	20.1	420.4	8.1	93.4
13P99-335	420	31456	3.8	5.3989	0.8	12.9320	2.0	0.5064	1.8	0.92	2641.1	39.0	2674.7	18.5	2700.2	13.0	2700.2	13.0	97.8
~~13P99-336~~	~~379~~	~~22839~~	~~1.6~~	~~8.6859~~	~~0.8~~	~~5.3701~~	~~1.8~~	~~0.3383~~	~~1.6~~	~~0.91~~	~~1878.5~~	~~26.7~~	~~1880.1~~	~~15.5~~	~~1881.9~~	13.7	1881.9	13.7	99.8
13P99-337	406	148451	2.5	8.7637	0.8	5.2755	1.8	0.3353	1.6	0.89	1864.1	26.0	1864.9	15.4	1865.8	14.9	1865.8	14.9	99.9
13P99-338	697	38729	3.4	8.7484	0.7	5.0129	2.9	0.3181	2.8	0.97	1780.3	44.2	1821.5	24.7	1869.0	12.2	1869.0	12.2	95.3
13P99-339	291	23660	1.4	8.7641	0.9	5.3869	2.3	0.3424	2.1	0.92	1898.2	34.9	1882.8	19.7	1865.7	16.0	1865.7	16.0	101.7
13P99-340	1079	27798	13.0	14.3554	1.0	1.4344	2.0	0.1493	1.7	0.87	897.3	14.5	903.4	11.9	918.4	20.0	897.3	14.5	97.7
13P99-341	407	16079	2.4	17.9367	1.4	0.5232	2.1	0.0681	1.5	0.73	424.5	6.3	427.3	7.3	442.5	31.8	424.5	6.3	95.9
13P99-342	387	31913	1.4	19.1231	1.4	0.2931	2.2	0.0407	1.7	0.78	256.9	4.4	261.0	5.1	298.2	31.9	256.9	4.4	NA
13P99-343	395	6992	4.9	19.2967	2.1	0.4082	2.9	0.0571	2.0	0.69	358.1	7.0	347.5	8.6	277.6	48.2	358.1	7.0	NA
13P99-344	104	8703	1.7	18.2234	3.1	0.2763	3.7	0.0365	2.1	0.56	231.2	4.7	247.8	8.2	407.1	69.1	231.2	4.7	NA
13P99-345	378	6533	1.3	19.3556	1.5	0.3142	2.3	0.0441	1.8	0.78	278.2	5.0	277.4	5.7	270.6	33.7	278.2	5.0	NA
13P99-346	274	55100	1.6	17.4684	1.4	0.5345	2.3	0.0677	1.9	0.81	422.4	7.8	434.8	8.3	501.1	30.1	422.4	7.8	84.3
13P99-347	1430	50004	1.9	5.7970	0.8	11.7957	1.6	0.4959	1.4	0.87	2596.3	29.6	2588.3	14.8	2582.1	12.8	2582.1	12.8	100.6
13P99-348	72	5250	1.9	18.5459	3.1	0.2758	3.9	0.0371	2.4	0.61	234.8	5.4	247.3	8.5	367.7	68.9	234.8	5.4	NA
13P99-349	78	48780	1.4	13.6146	1.4	1.5503	2.4	0.1531	1.9	0.80	918.2	16.5	950.6	14.9	1026.4	29.2	918.2	16.5	89.5
13P99-350	275	9913	2.6	18.2654	1.4	0.4909	2.4	0.0650	1.9	0.80	406.1	7.4	405.5	7.9	401.9	32.0	406.1	7.4	101.0
13P99-351	307	6059	1.1	17.9811	1.2	0.5625	2.0	0.0734	1.6	0.80	456.3	7.0	453.1	7.2	437.0	26.2	456.3	7.0	104.4
13P99-352	241	6096	0.9	18.1259	1.4	0.5200	2.4	0.0684	2.0	0.82	426.2	8.2	425.1	8.4	419.1	30.9	426.2	8.2	101.7
13P99-353	337	5924	2.8	19.4213	3.9	0.3414	4.3	0.0481	1.8	0.43	302.8	5.4	298.3	11.0	262.8	88.6	302.8	5.4	NA
13P99-354	964	18874	2.1	8.6022	0.8	3.7499	2.0	0.2340	1.8	0.91	1355.2	22.5	1582.1	16.2	1899.3	15.2	1899.3	15.2	71.4
13P99-355	180	7003	1.0	19.0675	2.5	0.3544	3.1	0.0490	1.9	0.60	308.5	5.6	308.0	8.3	304.9	56.9	308.5	5.6	NA
13P99-356	401	27640	1.8	13.8432	0.8	1.6903	1.9	0.1697	1.7	0.90	1010.5	15.7	1004.9	12.0	992.6	17.0	1010.5	15.7	101.8
13P99-357	272	31479	3.3	8.7014	1.0	5.2845	1.6	0.3335	1.3	0.79	1855.3	20.2	1866.4	13.6	1878.7	17.6	1878.7	17.6	98.8
13P99-358	726	26391	3.9	18.8802	1.2	0.3393	2.0	0.0465	1.6	0.80	292.7	4.6	296.6	5.2	327.3	27.1	292.7	4.6	NA
~~13P99-359~~	~~109~~	~~9586~~	~~0.8~~	~~14.8617~~	~~1.4~~	~~1.2502~~	~~2.2~~	~~0.1348~~	~~1.7~~	~~0.77~~	~~815.0~~	~~13.2~~	~~823.5~~	~~12.6~~	~~846.7~~	29.8	815.0	13.2	96.3
13P99-360	124	18850	1.8	7.6842	0.9	6.5867	1.8	0.3671	1.6	0.87	2015.7	27.0	2057.6	15.9	2099.8	15.7	2099.8	15.7	96.0
13P99-361	222	37886	4.5	6.6391	0.9	7.7277	2.4	0.3721	2.2	0.92	2039.3	38.0	2199.8	21.2	2353.0	15.5	2353.0	15.5	86.7

13P99-362	534	40702	3.9	8.7389	0.8	5.4358	2.1	0.3445	1.9	0.93	1908.4	32.1	1890.5	17.9	1870.9	13.8	1870.9	13.8	102.0
13P99-363	1048	15996	2.5	19.6006	1.3	0.2714	2.1	0.0386	1.6	0.77	244.0	3.9	243.8	4.5	241.7	30.6	244.0	3.9	NA
13P99-364	119	128638	1.1	17.5281	2.8	0.4538	3.4	0.0577	2.0	0.58	361.5	7.1	379.9	10.9	493.5	61.7	361.5	7.1	NA
13P99-365	215	5644	1.1	19.6539	3.2	0.2453	3.8	0.0350	1.9	0.51	221.5	4.2	222.7	7.5	235.4	74.4	221.5	4.2	NA
13P99-366	350	16461	0.9	18.9235	1.3	0.3305	2.0	0.0454	1.5	0.75	286.0	4.2	290.0	5.0	322.1	29.7	286.0	4.2	NA
13P99-367	228	25076	2.4	7.7345	0.8	6.6797	1.9	0.3747	1.7	0.89	2051.5	29.6	2069.9	16.6	2088.3	14.8	2088.3	14.8	98.2
13P99-368	466	5992	1.3	20.2843	1.9	0.2679	2.5	0.0394	1.7	0.68	249.2	4.2	241.0	5.4	162.1	43.3	249.2	4.2	NA
13P99-369	95	7448	2.3	14.6139	1.3	1.4009	2.3	0.1485	1.9	0.82	892.5	15.9	889.3	13.8	881.5	27.8	892.5	15.9	101.2
13P99-370	298	26219	1.5	8.0049	1.0	5.8093	2.1	0.3373	1.8	0.87	1873.5	29.1	1947.8	17.9	2027.7	18.3	2027.7	18.3	92.4
13P99-371	459	25009	1.5	17.7337	1.2	0.5060	2.2	0.0651	1.9	0.85	406.4	7.5	415.8	7.6	467.8	26.1	406.4	7.5	86.9
13P99-372	148	8624	0.7	10.1462	1.1	3.7648	2.0	0.2770	1.7	0.84	1576.4	23.1	1585.3	15.8	1597.0	19.8	1597.0	19.8	98.7
13P99-373	218	6838	2.5	17.9985	3.1	0.5207	3.7	0.0680	2.0	0.54	423.9	8.1	425.6	12.8	434.8	68.9	423.9	8.1	97.5
13P99-374	79	24744	1.3	5.9880	0.8	10.8250	1.9	0.4701	1.7	0.90	2484.1	34.4	2508.2	17.2	2527.8	13.6	2527.8	13.6	98.3
13P99-375	231	7367	1.8	18.6852	1.5	0.3776	2.1	0.0512	1.6	0.73	321.7	4.9	325.3	5.9	350.8	32.9	321.7	4.9	NA
13P99-376	640	31488	11.3	7.7223	0.8	4.7194	2.1	0.2643	1.9	0.92	1511.9	25.5	1770.7	17.3	2091.1	14.4	2091.1	14.4	72.3
13P99-377	441	40541	1.0	17.6591	1.0	0.5763	1.9	0.0738	1.6	0.84	459.1	7.1	462.1	7.1	477.1	23.2	459.1	7.1	96.2
13P99-378	330	38605	2.3	13.9269	0.8	1.5987	2.1	0.1615	2.0	0.93	965.0	17.6	969.7	13.1	980.4	15.4	965.0	17.6	98.4
13P99-379	397	23529	2.5	18.7074	1.1	0.3582	1.9	0.0486	1.5	0.81	305.9	4.6	310.9	5.1	348.1	25.3	305.9	4.6	NA
13P99-380	222	8785	1.3	13.7821	1.2	1.6201	2.2	0.1619	1.8	0.83	967.5	16.6	978.0	14.0	1001.6	25.3	967.5	16.6	96.6
13P99-381	256	6749	3.7	19.6314	1.7	0.3296	2.5	0.0469	1.9	0.74	295.6	5.4	289.2	6.3	238.0	38.6	295.6	5.4	NA
13P99-382	316	18879	1.7	9.5468	0.9	4.3116	1.7	0.2985	1.5	0.87	1684.0	22.3	1695.6	14.3	1709.9	15.9	1709.9	15.9	98.5
13P99-383	30	22180	1.4	9.4343	1.4	4.1489	2.3	0.2839	1.8	0.80	1610.9	26.0	1664.0	18.6	1731.6	25.1	1731.6	25.1	93.0
13P99-384	121	3419	1.3	19.6330	2.9	0.3362	3.6	0.0479	2.2	0.61	301.4	6.6	294.3	9.3	237.9	66.6	301.4	6.6	NA
13P99-385	419	39059	7.3	8.9198	0.9	5.1754	2.0	0.3348	1.8	0.90	1861.6	29.4	1848.6	17.2	1833.9	16.0	1833.9	16.0	101.5
13P99-386	863	27948	6.5	11.0641	0.8	2.7060	4.7	0.2171	4.6	0.98	1266.8	53.4	1330.1	34.9	1433.6	15.7	1266.8	53.4	88.4
13P99-387	667	20362	4.5	8.8558	0.8	5.2164	3.0	0.3350	2.8	0.96	1862.8	46.0	1855.3	25.3	1846.9	15.0	1846.9	15.0	100.9
13P99-388	525	8170	2.0	19.6149	2.8	0.2789	3.4	0.0397	2.0	0.59	250.8	4.9	249.8	7.5	240.0	63.4	250.8	4.9	NA
13P99-389	294	14844	1.5	19.0020	1.5	0.2965	2.4	0.0409	1.8	0.77	258.2	4.7	263.7	5.6	312.7	34.9	258.2	4.7	NA
13P99-390	103	7882	3.4	7.8916	0.9	6.3117	2.0	0.3613	1.7	0.90	1988.1	29.9	2020.1	17.1	2052.9	15.4	2052.9	15.4	96.8
13P99-391	127	7892	1.9	17.4632	1.5	0.5319	2.5	0.0674	2.0	0.80	420.3	8.3	433.1	8.9	501.7	33.4	420.3	8.3	83.8
13P99-392	257	24402	1.7	8.7621	0.9	5.2300	1.9	0.3324	1.7	0.89	1849.8	27.6	1857.5	16.4	1866.1	15.7	1866.1	15.7	99.1
13P99-393	180	23697	2.7	8.3432	0.9	5.5084	1.7	0.3333	1.5	0.86	1854.4	23.8	1901.9	14.7	1954.1	15.5	1954.1	15.5	94.9
13P99-394	58	2840	1.6	19.6167	3.3	0.2932	4.0	0.0417	2.2	0.56	263.5	5.8	261.1	9.2	239.8	76.7	263.5	5.8	NA
13P99-394	434	27885	4.1	12.9418	0.9	1.9258	2.4	0.1808	2.2	0.92	1071.1	21.6	1090.1	15.9	1128.2	18.9	1071.1	21.6	94.9
13P99-395	348	6213	5.0	19.0875	3.8	0.3924	4.3	0.0543	2.0	0.46	341.0	6.5	336.1	12.3	302.5	87.4	341.0	6.5	NA

13P99-395	426	28260	1.4	17.6473	1.2	0.5514	2.2	0.0706	1.9	0.83	439.6	7.9	445.9	8.1	478.5	27.4	439.6	7.9	91.9
13P99-396	354	5551	1.1	19.5451	1.4	0.3347	2.4	0.0474	1.9	0.81	298.8	5.6	293.1	6.0	248.2	31.5	298.8	5.6	NA
13P99-396	338	6907	1.6	17.7828	3.0	0.5962	3.5	0.0769	1.8	0.51	477.5	8.1	474.8	13.1	461.6	66.1	477.5	8.1	103.5
13P99-397	398	6248	1.4	19.5571	1.5	0.3172	2.1	0.0450	1.5	0.72	283.7	4.3	279.8	5.2	246.8	34.3	283.7	4.3	NA
13P99-397	113	8740	4.8	14.3706	1.3	1.4574	2.4	0.1519	2.1	0.84	911.6	17.5	912.9	14.7	916.2	27.1	911.6	17.5	99.5
13P99-398	93	2586	1.8	20.9856	2.5	0.2731	3.3	0.0416	2.0	0.62	262.5	5.2	245.1	7.1	82.0	60.5	262.5	5.2	NA
13P99-399	260	6654	2.2	19.1415	1.6	0.2809	2.7	0.0390	2.2	0.80	246.6	5.3	251.4	6.0	296.0	37.0	246.6	5.3	NA
13P99-400	144	6092	1.6	17.9196	1.6	0.5574	2.4	0.0724	1.9	0.77	450.9	8.1	449.8	8.8	444.6	34.7	450.9	8.1	101.4
13P99-401	145	65238	1.6	5.3938	0.8	12.6402	2.0	0.4945	1.8	0.91	2590.0	38.2	2653.2	18.5	2701.8	13.4	2701.8	13.4	95.9
13P99-402	359	31557	4.4	8.3255	1.0	5.4895	2.5	0.3315	2.2	0.91	1845.5	36.0	1899.0	21.1	1957.9	18.0	1957.9	18.0	94.3
13P99-403	222	15729	0.8	15.0069	1.1	1.1900	2.0	0.1295	1.7	0.83	785.1	12.4	796.0	11.1	826.4	23.5	785.1	12.4	95.0
13P99-404	118	5888	2.4	19.1754	2.6	0.2960	3.5	0.0412	2.5	0.69	260.0	6.3	263.3	8.2	292.0	58.2	260.0	6.3	NA
13P99-405	24	2568	1.6	17.0614	3.1	0.7357	3.7	0.0910	2.0	0.55	561.7	10.8	559.9	15.7	552.7	66.9	561.7	10.8	101.6
13P99-406	507	9783	2.1	18.1100	1.1	0.5375	2.0	0.0706	1.7	0.84	439.7	7.3	436.8	7.2	421.0	24.3	439.7	7.3	104.4
13P99-407	143	5381	1.3	19.8197	2.1	0.2922	2.8	0.0420	1.8	0.64	265.3	4.7	260.3	6.5	216.0	49.7	265.3	4.7	NA
13P99-408	164	5417	2.3	18.2447	2.0	0.5189	2.8	0.0687	2.0	0.72	428.1	8.4	424.4	9.7	404.5	43.8	428.1	8.4	105.8
13P99-409	575	24378	5.4	17.7739	1.0	0.5718	2.1	0.0737	1.8	0.88	458.4	8.1	459.2	7.7	462.8	22.0	458.4	8.1	99.1
13P99-410	334	11991	2.7	14.4083	0.8	1.4543	1.9	0.1520	1.7	0.89	912.0	14.3	911.6	11.3	910.8	17.3	912.0	14.3	100.1
13P99-411	171	23659	1.8	6.7220	0.9	8.7444	2.0	0.4263	1.8	0.90	2289.1	33.8	2311.7	17.8	2331.8	14.8	2331.8	14.8	98.2
13P99-412	491	21830	0.9	14.1460	0.9	1.4867	1.9	0.1525	1.7	0.89	915.2	14.1	925.0	11.3	948.5	17.6	915.2	14.1	96.5
13P99-413	308	7061	2.5	18.3395	1.2	0.4695	2.0	0.0624	1.5	0.79	390.5	5.9	390.8	6.4	392.9	27.1	390.5	5.9	NA
13P99-414	162	17759	1.5	6.1287	0.9	9.5541	3.7	0.4247	3.6	0.97	2281.6	69.7	2392.8	34.4	2488.7	15.0	2488.7	15.0	91.7
13P99-415	214	43220	1.1	9.5035	1.1	4.2090	1.9	0.2901	1.6	0.83	1642.1	23.2	1675.8	15.8	1718.2	19.7	1718.2	19.7	95.6
13P99-416	731	9403	1.6	19.1866	1.1	0.3215	2.2	0.0447	1.8	0.85	282.1	5.1	283.0	5.3	290.6	25.9	282.1	5.1	NA
13P99-417	205	8381	0.8	14.4418	1.1	1.4766	2.0	0.1547	1.7	0.83	927.1	14.4	920.9	12.1	906.0	22.9	927.1	14.4	102.3
13P99-418	126	17524	2.3	8.2917	0.9	5.8009	1.9	0.3489	1.6	0.87	1929.1	26.9	1946.5	16.0	1965.1	16.2	1965.1	16.2	98.2
13P99-419	1788	101202	7.2	6.0331	0.7	9.1645	2.1	0.4010	1.9	0.94	2173.7	35.9	2354.6	19.0	2515.2	12.1	2515.2	12.1	86.4
13P99-420	326	8998	1.7	18.0302	2.3	0.5206	2.8	0.0681	1.6	0.56	424.5	6.4	425.5	9.6	430.9	51.1	424.5	6.4	98.5
13P99-421	157	7449	1.4	17.9160	2.0	0.5414	2.7	0.0704	1.9	0.68	438.3	7.9	439.4	9.8	445.0	44.8	438.3	7.9	98.5
~~13P99-422~~	~~615~~	~~48782~~	~~4.8~~	~~8.7825~~	~~0.8~~	~~5.3408~~	~~3.6~~	~~0.3402~~	~~3.5~~	~~0.97~~	~~1887.6~~	~~57.9~~	~~1875.4~~	~~31.1~~	~~1862.0~~	14.8	1862.0	14.8	101.4
13P99-423	215	5286	1.9	19.3703	2.0	0.3174	2.8	0.0446	2.1	0.73	281.2	5.7	279.9	6.9	268.8	44.8	281.2	5.7	NA
13P99-424	291	9111	2.4	19.0761	2.6	0.3006	3.3	0.0416	2.0	0.62	262.7	5.2	266.9	7.7	303.8	59.2	262.7	5.2	NA
13P99-425	78	9265	0.8	6.3066	1.1	9.4099	2.2	0.4304	1.9	0.87	2307.6	36.4	2378.8	19.9	2440.4	18.4	2440.4	18.4	94.6
13P99-426	255	17500	1.5	14.4123	1.1	1.4622	1.8	0.1528	1.4	0.78	916.9	12.2	914.9	11.0	910.2	23.5	916.9	12.2	100.7
13P99-427	412	17125	1.6	13.8469	1.2	1.6433	2.2	0.1650	1.8	0.83	984.7	16.5	987.0	13.7	992.1	24.6	984.7	16.5	99.3

13P99-428	426	9686	0.8	19.1719	1.9	0.3201	2.6	0.0445	1.8	0.68	280.7	4.9	282.0	6.4	292.4	43.5	280.7	4.9	NA
13P99-429	510	18732	6.7	14.5863	1.1	1.3394	2.4	0.1417	2.1	0.89	854.2	17.1	863.0	14.0	885.4	23.0	854.2	17.1	96.5
13P99-430	180	18136	3.4	8.7435	0.8	5.4560	1.9	0.3460	1.7	0.91	1915.4	28.5	1893.7	16.2	1870.0	14.1	1870.0	14.1	102.4
13P99-431	410	27590	1.1	5.9113	0.9	10.0577	2.6	0.4312	2.4	0.93	2311.1	46.2	2440.1	23.6	2549.4	15.5	2549.4	15.5	90.7
13P99-432	516	12329	1.5	16.8609	0.9	0.7335	2.1	0.0897	1.9	0.90	553.8	9.9	558.6	8.9	578.5	20.0	553.8	9.9	95.7
13P99-433	368	6273	1.9	18.7225	2.2	0.4178	2.9	0.0567	1.9	0.64	355.7	6.4	354.5	8.6	346.4	50.1	355.7	6.4	NA
13P99-434	56	5247	2.0	9.0143	1.2	4.8092	2.3	0.3144	2.0	0.84	1762.4	30.3	1786.5	19.6	1814.8	22.7	1814.8	22.7	97.1
13P99-435	229	26035	0.7	8.7933	0.7	5.1675	2.0	0.3296	1.9	0.94	1836.2	30.2	1847.3	17.2	1859.7	12.7	1859.7	12.7	98.7
13P99-436	340	29076	2.0	13.7301	1.1	1.6795	2.1	0.1672	1.8	0.86	996.9	16.7	1000.8	13.4	1009.3	21.7	996.9	16.7	98.8
13P99-437	129	22833	1.7	6.0198	1.1	10.4341	2.2	0.4556	1.9	0.87	2419.9	38.5	2474.1	20.3	2518.9	18.1	2518.9	18.1	96.1
13P99-438	354	26162	2.6	9.0865	0.9	4.6695	1.9	0.3077	1.7	0.89	1729.5	26.0	1761.8	16.2	1800.3	16.3	1800.3	16.3	96.1
13P99-439	1275	61928	6.2	6.4613	0.8	8.9883	2.0	0.4212	1.8	0.91	2265.9	34.8	2336.8	18.3	2399.3	14.3	2399.3	14.3	94.4

* indicates radiogenic Pb (corrected for common Pb).

Initial Pb composition interpreted from Stacey and Kramers (1975), with uncertainties of 1.0 for $^{206}Pb/^{204}Pb$ and 0.3 for $^{207}Pb/^{204}Pb$.

All errors are reported at the 2-sigma level.

Discordance is calculated from comparison of $^{206}Pb^{*}/^{238}U$ and $^{206}Pb^{*}/^{207}Pb^{*}$ ages.

U concentration, U/Th, and $^{206}Pb/^{204}Pb$ have uncertainties of ~25%.

LA-ICP-MS analyses conducted at the University of Houston

DV 7-09-15_4 38.092° N; 73.996° E

				Isotope ratios							Apparent Ages (Ma)									
				^{207}Pb	±	^{207}Pb	±	^{206}Pb	±		^{206}Pb	±	^{207}Pb	±	^{207}Pb	±		±	% discordance Pb^{206}/U^{238}-Pb^{207}/Pb^{206}	% discordance Pb^{206}/U^{238}-Pb^{207}/U^{325}
Analysis #	U (ppm)	Th (ppm)	U/Th	^{206}Pb	(2%SD)	^{235}U	(2%SD)	^{238}U	(2%SD)	error corr.	^{238}U	(2SD)	^{235}U	(2SD)	^{206}Pb	(2SD)	Best Age	(2SD)		
DV 7/09/15_4-117	422	358	1.2	0.0497	6.6	0.2108	8.8	0.0307	5.9	0.67	195.1	11.4	194.2	15.6	180.0	153.2	195.1	11.4	-8.4	-0.4
DV 7/09/15_4-191	966	592	1.6	0.0504	6.4	0.2517	9.0	0.0362	6.3	0.71	229.0	14.2	228.0	18.4	213.9	147.9	229.0	14.2	-7.0	-0.5
DV 7/09/15_4-63	657	387	1.7	0.0511	9.6	0.2552	13.6	0.0362	9.6	0.71	229.1	21.6	230.8	28.0	247.3	221.3	229.1	21.6	7.3	0.7
DV 7/09/15_4-167	1150	590	1.9	0.0511	9.2	0.2548	13.2	0.0362	9.5	0.72	229.1	21.3	230.5	27.2	243.5	211.4	229.1	21.3	5.9	0.6
DV 7/09/15_4-23	856	1603	0.5	0.0577	5.0	0.2918	6.8	0.0366	4.7	0.69	231.7	10.8	259.9	15.6	520.2	108.7	231.7	10.8	55.5	10.9
DV 7/09/15_4-97	719	314	2.3	0.0511	5.2	0.2622	7.1	0.0372	4.9	0.68	235.5	11.3	236.4	15.0	243.3	119.3	235.5	11.3	3.2	0.4
DV 7/09/15_4-119	471	502	0.9	0.0520	7.4	0.2684	10.3	0.0374	7.2	0.70	236.7	16.8	241.4	22.2	284.1	169.6	236.7	16.8	16.7	2.0
DV 7/09/15_4-49	739	349	2.1	0.0527	4.8	0.2724	6.3	0.0375	4.2	0.66	237.2	9.8	244.6	13.8	314.1	108.5	237.2	9.8	24.5	3.0
DV 7/09/15_4-13	452	260	1.7	0.0526	5.4	0.2749	7.1	0.0379	4.6	0.65	239.5	10.9	246.6	15.5	311.0	122.6	239.5	10.9	23.0	2.9
DV 7/09/15_4-17	169	129	1.3	0.0624	10.0	0.3295	12.2	0.0383	7.2	0.58	242.1	17.0	289.2	30.8	686.5	212.3	242.1	17.0	64.7	16.3
DV 7/09/15_4-79	245	189	1.3	0.0504	11.2	0.2674	12.8	0.0385	6.2	0.48	243.2	14.8	240.6	27.4	214.6	259.4	243.2	14.8	-13.4	-1.1
DV 7/09/15_4-56	982	495	2.0	0.0521	5.4	0.2790	7.4	0.0388	5.1	0.69	245.4	12.4	249.9	16.5	291.3	123.1	245.4	12.4	15.8	1.8
DV 7/09/15_4-166	516	522	1.0	0.0523	7.7	0.2805	10.7	0.0389	7.4	0.70	246.1	17.9	251.0	23.8	296.5	175.4	246.1	17.9	17.0	2.0
DV 7/09/15_4-59	287	181	1.6	0.0554	5.8	0.2990	7.4	0.0391	4.6	0.61	247.5	11.1	265.6	17.3	427.3	130.0	247.5	11.1	42.1	6.8
DV 7/09/15_4-64	1872	790	2.4	0.0553	5.1	0.3034	7.2	0.0398	5.2	0.71	251.3	12.7	269.1	17.1	425.9	113.4	251.3	12.7	41.0	6.6
DV 7/09/15_4-149	372	440	0.8	0.0557	8.3	0.3082	10.2	0.0401	5.9	0.58	253.3	14.7	272.8	24.5	440.4	185.5	253.3	14.7	42.5	7.1
DV 7/09/15_4-67	1027	658	1.6	0.0553	6.4	0.3060	9.0	0.0402	6.4	0.70	253.8	15.9	271.1	21.5	422.4	143.6	253.8	15.9	39.9	6.4
DV 7/09/15_4-104	347	205	1.7	0.0549	10.0	0.3049	14.0	0.0402	9.9	0.70	254.1	24.6	270.2	33.2	409.6	222.7	254.1	24.6	38.0	6.0
DV 7/09/15_4-53	853	533	1.6	0.0573	5.6	0.3208	7.6	0.0405	5.2	0.68	256.2	13.0	282.5	18.6	505.0	122.3	256.2	13.0	49.3	9.3
DV 7/09/15_4-170	537	460	1.2	0.0525	7.1	0.2950	9.8	0.0407	6.8	0.69	257.2	17.1	262.5	22.6	308.8	160.8	257.2	17.1	16.7	2.0
DV 7/09/15_4-12	67	75	0.9	0.0459	17.2	0.2635	18.3	0.0416	6.3	0.34	262.5	16.1	237.5	38.8	0.0	415.0	262.5	16.1	-13071972.2	-10.5
DV 7/09/15_4-46	191	134	1.4	0.0510	7.7	0.2923	9.7	0.0416	5.9	0.61	262.5	15.2	260.3	22.3	239.1	178.0	262.5	15.2	-9.8	-0.8
DV 7/09/15_4-182	200	123	1.6	0.0541	8.0	0.3177	10.4	0.0425	6.7	0.65	268.4	17.6	280.1	25.5	377.1	179.2	268.4	17.6	28.8	4.2
DV 7/09/15_4-83	314	312	1.0	0.0556	6.9	0.3296	9.0	0.0430	5.7	0.64	271.4	15.2	289.3	22.6	435.5	154.4	271.4	15.2	37.7	6.2
DV 7/09/15_4-138	753	527	1.4	0.0536	6.0	0.3283	8.2	0.0444	5.6	0.68	279.9	15.4	288.2	20.7	352.2	135.7	279.9	15.4	20.5	2.9
DV 7/09/15_4-176	123	86	1.4	0.0519	11.9	0.3204	15.0	0.0448	9.1	0.61	282.4	25.1	282.2	36.9	279.5	271.9	282.4	25.1	-1.0	-0.1
DV 7/09/15_4-113	1426	539	2.6	0.0577	7.0	0.3583	10.1	0.0449	7.3	0.72	283.4	20.2	310.9	27.1	519.8	154.1	283.4	20.2	45.5	8.9
DV 7/09/15_4-198	338	285	1.2	0.0515	8.7	0.3309	12.0	0.0465	8.3	0.69	293.1	23.7	290.2	30.3	263.9	200.3	293.1	23.7	-11.1	-1.0
DV 7/09/15_4-19	465	381	1.2	0.0534	6.1	0.3432	8.5	0.0466	6.0	0.70	293.4	17.2	299.6	22.0	344.9	136.9	293.4	17.2	14.9	2.1
DV 7/09/15_4-39	268	292	0.9	0.0530	6.2	0.3442	8.2	0.0470	5.3	0.65	296.3	15.5	300.3	21.2	329.8	140.4	296.3	15.5	10.2	1.3

DV 7/09/15_4-111	356	437	0.8	0.0532	7.1	0.3569	9.1	0.0486	5.8	0.63	305.8	17.3	309.9	24.4	337.7	160.0	305.8	17.3	9.5	1.3
DV 7/09/15_4-100	520	319	1.6	0.0537	6.0	0.3711	8.3	0.0501	5.7	0.69	315.0	17.6	320.4	22.8	358.3	135.7	315.0	17.6	12.1	1.7
DV 7/09/15_4-54	1063	401	2.7	0.0529	6.2	0.3662	9.0	0.0502	6.5	0.72	315.5	20.0	316.8	24.4	325.8	140.8	315.5	20.0	3.2	0.4
DV 7/09/15_4-21	274	230	1.2	0.0535	6.3	0.3749	8.1	0.0508	5.2	0.63	319.4	16.1	323.3	22.5	348.0	142.5	319.4	16.1	8.2	1.2
DV 7/09/15_4-52	339	180	1.9	0.0627	7.3	0.4443	9.3	0.0514	5.8	0.62	322.8	18.2	373.3	29.1	698.7	155.8	322.8	18.2	53.8	13.5
DV 7/09/15_4-188	1049	1058	1.0	0.0525	5.5	0.3991	7.7	0.0551	5.4	0.70	345.8	18.2	341.0	22.5	306.0	125.3	345.8	18.2	-13.0	-1.4
DV 7/09/15_4-58	777	643	1.2	0.0669	8.2	0.5196	11.8	0.0563	8.5	0.72	352.9	29.2	424.9	41.0	836.0	170.5	352.9	29.2	57.8	16.9
DV 7/09/15_4-139	170	105	1.6	0.0564	8.2	0.4584	10.9	0.0589	7.3	0.67	368.7	26.1	383.2	35.0	467.8	181.0	368.7	26.1	21.2	3.8
DV 7/09/15_4-40	327	251	1.3	0.0598	7.6	0.5161	10.2	0.0625	6.9	0.67	390.8	26.1	422.6	35.3	597.9	163.6	390.8	26.1	34.6	7.5
DV 7/09/15_4-25	214	215	1.0	0.0557	6.2	0.4912	8.3	0.0638	5.6	0.67	398.9	21.7	405.7	27.9	441.6	138.2	398.9	21.7	9.7	1.7
DV 7/09/15_4-122	112	70	1.6	0.0556	9.9	0.5031	12.5	0.0655	7.7	0.61	409.0	30.4	413.8	42.4	436.1	219.4	409.0	30.4	6.2	1.2
DV 7/09/15_4-148	486	331	1.5	0.0559	7.2	0.5084	10.1	0.0658	7.0	0.70	411.0	27.9	417.4	34.4	450.2	160.4	411.0	27.9	8.7	1.5
DV 7/09/15_4-165	159	213	0.7	0.0560	9.5	0.5182	13.0	0.0671	8.8	0.68	418.6	35.8	424.0	45.0	452.4	211.4	418.6	35.8	7.5	1.3
DV 7/09/15_4-41	520	356	1.5	0.0567	6.1	0.5248	8.8	0.0671	6.3	0.71	418.6	25.4	428.3	30.6	479.1	135.8	418.6	25.4	12.6	2.3
DV 7/09/15_4-3	580	259	2.2	0.0564	6.9	0.5235	9.8	0.0672	7.0	0.71	419.5	28.5	427.5	34.2	468.0	152.3	419.5	28.5	10.4	1.9
DV 7/09/15_4-88	396	78	5.1	0.0550	5.4	0.5109	7.5	0.0673	5.2	0.69	419.9	21.3	419.1	25.7	413.4	120.3	419.9	21.3	-1.6	-0.2
DV 7/09/15_4-96	816	352	2.3	0.0562	7.4	0.5239	10.5	0.0676	7.5	0.71	421.7	30.6	427.7	36.7	459.2	164.2	421.7	30.6	8.2	1.4
DV 7/09/15_4-121	279	752	0.4	0.0594	8.1	0.5553	11.6	0.0676	8.3	0.71	421.9	33.8	448.5	41.9	583.1	175.7	421.9	33.8	27.6	5.9
DV 7/09/15_4-161	423	149	2.8	0.0555	8.3	0.5201	11.8	0.0679	8.4	0.71	423.6	34.3	425.2	41.0	432.8	185.2	423.6	34.3	2.1	0.4
DV 7/09/15_4-158	346	247	1.4	0.0579	6.6	0.5442	9.1	0.0681	6.2	0.68	425.0	25.5	441.2	32.5	525.4	145.5	425.0	25.5	19.1	3.7
DV 7/09/15_4-68	278	349	0.8	0.0608	5.1	0.5733	6.7	0.0684	4.3	0.64	426.3	17.7	460.1	24.6	632.2	110.5	426.3	17.7	32.6	7.4
DV 7/09/15_4-28	219	110	2.0	0.0546	6.1	0.5214	8.2	0.0691	5.5	0.66	430.9	22.7	426.1	28.4	397.2	136.8	430.9	22.7	-8.5	-1.1
DV 7/09/15_4-76	318	392	0.8	0.0577	5.1	0.5514	7.0	0.0692	4.8	0.68	431.6	20.0	445.9	25.3	519.9	112.9	431.6	20.0	17.0	3.2
DV 7/09/15_4-140	307	94	3.3	0.0559	6.3	0.5353	8.5	0.0694	5.7	0.68	432.3	24.0	435.4	30.1	447.7	139.4	432.3	24.0	3.4	0.7
DV 7/09/15_4-9	295	154	1.9	0.0579	6.0	0.5545	8.2	0.0694	5.6	0.68	432.4	23.3	447.9	29.7	525.5	132.1	432.4	23.3	17.7	3.5
DV 7/09/15_4-177	524	657	0.8	0.0548	5.8	0.5251	7.9	0.0695	5.4	0.69	433.0	22.5	428.6	27.6	403.7	128.9	433.0	22.5	-7.3	-1.0
DV 7/09/15_4-141	225	204	1.1	0.0565	7.6	0.5423	10.4	0.0695	7.2	0.69	433.3	30.2	439.9	37.3	471.7	167.2	433.3	30.2	8.2	1.5
DV 7/09/15_4-37	233	102	2.3	0.0570	7.3	0.5492	10.0	0.0698	6.9	0.68	435.1	28.8	444.5	35.9	490.9	160.6	435.1	28.8	11.4	2.1
DV 7/09/15_4-66	311	201	1.6	0.0577	9.5	0.5602	13.2	0.0704	9.2	0.69	438.5	38.8	451.7	48.1	518.6	208.8	438.5	38.8	15.5	2.9
DV 7/09/15_4-114	249	179	1.4	0.0571	6.7	0.5602	9.2	0.0710	6.3	0.68	442.1	27.0	451.6	33.7	497.3	148.7	442.1	27.0	11.1	2.1
DV 7/09/15_4-87	1458	660	2.2	0.0547	5.2	0.5360	7.6	0.0711	5.5	0.72	442.6	23.7	435.8	27.0	398.9	117.5	442.6	23.7	-11.0	-1.6
DV 7/09/15_4-77	154	95	1.6	0.0561	6.8	0.5530	9.1	0.0715	6.0	0.66	445.0	26.0	447.0	32.7	456.9	150.1	445.0	26.0	2.6	0.5
DV 7/09/15_4-32	302	193	1.6	0.0983	18.7	0.9785	20.4	0.0721	8.2	0.40	448.7	35.6	692.9	102.9	1592.8	349.7	448.7	35.6	71.8	35.2
DV 7/09/15_4-101	298	78	3.8	0.0562	7.6	0.5607	10.3	0.0722	7.1	0.68	449.6	30.7	452.0	37.7	461.8	167.4	449.6	30.7	2.6	0.5
DV 7/09/15_4-137	136	72	1.9	0.0603	9.2	0.6082	12.2	0.0730	8.1	0.66	454.4	35.5	482.5	47.0	614.4	198.3	454.4	35.5	26.0	5.8

DV 7/09/15_4-11	473	107	4.4	0.0727	16.4	0.7453	19.0	0.0742	9.7	0.51	461.4	43.0	565.5	82.6	1006.8	332.7	461.4	43.0	54.2	18.4
DV 7/09/15_4-20	503	507	1.0	0.0558	5.1	0.5752	7.2	0.0747	5.1	0.70	464.5	22.7	461.4	26.6	442.9	113.7	464.5	22.7	-4.9	-0.7
DV 7/09/15_4-133	166	253	0.7	0.0498	11.8	0.5156	13.2	0.0749	5.9	0.45	465.5	26.6	422.2	45.6	187.3	274.4	465.5	26.6	-148.5	-10.3
DV 7/09/15_4-183	236	143	1.7	0.0602	6.8	0.6240	9.5	0.0751	6.6	0.70	466.8	29.9	492.3	37.2	611.0	147.4	466.8	29.9	23.6	5.2
DV 7/09/15_4-38	135	276	0.5	0.0629	7.6	0.7232	9.8	0.0833	6.2	0.63	515.9	30.8	552.5	41.6	704.4	160.9	515.9	30.8	26.8	6.6
DV 7/09/15_4-152	52	91	0.6	0.0556	20.9	0.6852	22.1	0.0894	7.1	0.32	551.7	37.4	529.9	91.4	434.8	465.7	551.7	37.4	-26.9	-4.1
DV 7/09/15_4-50	508	131	3.9	0.0630	7.9	0.9592	11.2	0.1104	8.1	0.71	675.1	51.6	682.9	55.9	707.2	167.3	675.1	51.6	4.5	1.1
DV 7/09/15_4-142	123	156	0.8	0.0672	8.0	1.1186	10.1	0.1205	6.2	0.61	733.7	43.0	762.3	54.2	843.9	166.0	733.7	43.0	13.1	3.8
DV 7/09/15_4-15	139	88	1.6	0.0627	5.1	1.0493	6.7	0.1213	4.5	0.65	737.9	31.1	728.5	35.0	696.6	108.6	737.9	31.1	-5.9	-1.3
DV 7/09/15_4-45	92	42	2.2	0.0659	5.4	1.1780	7.0	0.1295	4.5	0.64	785.2	33.5	790.4	38.6	803.2	113.2	785.2	33.5	2.2	0.7
DV 7/09/15_4-155	140	144	1.0	0.0667	7.3	1.2134	9.3	0.1319	5.8	0.62	798.8	43.4	806.8	52.0	827.1	152.9	798.8	43.4	3.4	1.0
DV 7/09/15_4-62	489	159	3.1	0.0710	4.2	1.3154	7.2	0.1344	5.9	0.81	813.0	45.0	852.5	41.7	956.0	86.2	813.0	45.0	15.0	4.6
DV 7/09/15_4-193	420	166	2.5	0.0669	8.0	1.2893	11.0	0.1397	7.5	0.69	842.7	59.5	841.0	63.1	833.6	167.4	842.7	59.5	-1.1	-0.2
DV 7/09/15_4-120	151	95	1.6	0.0741	6.1	1.4459	8.2	0.1413	5.5	0.67	852.1	43.6	908.2	49.1	1043.6	123.0	852.1	43.6	18.4	6.2
DV 7/09/15_4-81	215	99	2.2	0.0718	5.5	1.4224	7.7	0.1436	5.4	0.70	864.9	43.9	898.4	46.1	980.9	112.6	864.9	43.9	11.8	3.7
DV 7/09/15_4-109	964	246	3.9	0.0690	4.8	1.4127	7.0	0.1482	5.1	0.73	890.8	42.3	894.3	41.5	900.2	99.1	890.8	42.3	1.0	0.4
DV 7/09/15_4-135	380	86	4.4	0.0688	9.1	1.4569	13.1	0.1533	9.5	0.72	919.7	81.2	912.7	79.1	892.3	187.5	892.3	187.5	-3.1	-0.8
DV 7/09/15_4-181	822	264	3.1	0.0709	6.1	1.6039	8.9	0.1640	6.4	0.73	978.8	58.2	971.8	55.6	954.3	125.2	954.3	125.2	-2.6	-0.7
DV 7/09/15_4-169	312	102	3.0	0.0713	6.1	1.5185	8.5	0.1545	5.9	0.70	926.0	51.2	937.9	52.1	965.2	124.0	965.2	124.0	4.1	1.3
DV 7/09/15_4-199	149	142	1.0	0.0718	8.5	1.6891	12.1	0.1704	8.7	0.72	1014.2	81.9	1004.4	77.6	980.5	172.7	980.5	172.7	-3.4	-1.0
DV 7/09/15_4-171	209	133	1.6	0.0721	6.2	1.5277	8.7	0.1536	6.1	0.71	920.9	52.7	941.6	53.7	989.4	126.0	989.4	126.0	6.9	2.2
DV 7/09/15_4-92	807	348	2.3	0.0763	5.2	2.0058	7.5	0.1906	5.5	0.72	1124.5	56.6	1117.5	51.2	1102.7	104.4	1102.7	104.4	-2.0	-0.6
DV 7/09/15_4-2	93	61	1.5	0.0802	6.3	2.1524	8.9	0.1945	6.3	0.70	1145.5	65.6	1165.8	61.6	1201.4	124.8	1201.4	124.8	4.7	1.7
DV 7/09/15_4-118	42	21	2.0	0.0828	7.0	2.1398	9.3	0.1872	6.2	0.66	1106.2	62.7	1161.8	64.6	1263.6	136.8	1263.6	136.8	12.5	4.8
DV 7/09/15_4-185	705	379	1.9	0.0849	5.1	2.8096	7.4	0.2399	5.3	0.72	1386.2	66.4	1358.1	55.5	1312.3	99.1	1312.3	99.1	-5.6	-2.1
DV 7/09/15_4-43	145	195	0.7	0.1010	6.2	3.7052	9.2	0.2658	6.8	0.73	1519.3	91.9	1572.5	73.7	1643.1	115.8	1643.1	115.8	7.5	3.4
DV 7/09/15_4-179	399	593	0.7	0.1012	5.2	3.9409	7.5	0.2824	5.3	0.72	1603.3	75.6	1622.1	60.6	1645.6	96.6	1645.6	96.6	2.6	1.2
DV 7/09/15_4-60	257	128	2.0	0.1060	5.4	4.7475	7.8	0.3248	5.6	0.72	1812.9	89.1	1775.7	65.4	1731.3	99.1	1731.3	99.1	-4.7	-2.1
DV 7/09/15_4-31	75	34	2.2	0.1062	4.8	4.3639	6.7	0.2976	4.7	0.70	1679.6	69.7	1705.5	55.2	1735.5	87.5	1735.5	87.5	3.2	1.5
DV 7/09/15_4-72	59	16	3.6	0.1070	6.0	4.4151	8.5	0.2993	6.0	0.70	1687.6	89.1	1715.2	70.2	1748.4	110.0	1748.4	110.0	3.5	1.6
DV 7/09/15_4-108	469	355	1.3	0.1073	4.8	4.2034	7.0	0.2838	5.2	0.74	1610.4	74.3	1674.7	57.8	1753.9	87.0	1753.9	87.0	8.2	3.8
DV 7/09/15_4-123	47	209	0.2	0.1073	8.1	4.6134	11.4	0.3112	8.0	0.70	1746.6	122.5	1751.7	95.3	1753.9	148.3	1753.9	148.3	0.4	0.3
DV 7/09/15_4-197	117	145	0.8	0.1083	6.3	5.0803	8.8	0.3398	6.1	0.70	1885.8	100.4	1832.8	74.5	1770.5	114.7	1770.5	114.7	-6.5	-2.9
DV 7/09/15_4-130	41	37	1.1	0.1088	6.5	4.5931	9.0	0.3056	6.2	0.69	1719.2	94.2	1748.0	75.3	1778.6	118.9	1778.6	118.9	3.3	1.6
DV 7/09/15_4-150	671	236	2.8	0.1097	6.8	4.0093	10.2	0.2648	7.7	0.75	1514.2	103.5	1636.1	83.2	1794.4	122.9	1794.4	122.9	15.6	7.4

DV 7/09/15_4-94	1342	882	1.5	0.1108	5.6	3.8790	8.4	0.2539	6.3	0.75	1458.4	81.8	1609.3	67.5	1811.8	101.1	1811.8	101.1	19.5	9.4
DV 7/09/15_4-69	689	192	3.6	0.1112	4.7	4.8155	7.0	0.3139	5.2	0.74	1760.0	79.6	1787.6	58.5	1819.5	85.1	1819.5	85.1	3.3	1.5
DV 7/09/15_4-75	580	163	3.6	0.1112	4.8	5.0239	7.1	0.3275	5.2	0.73	1826.2	82.8	1823.4	59.9	1819.6	87.3	1819.6	87.3	-0.4	-0.2
DV 7/09/15_4-99	1118	364	3.1	0.1113	4.5	4.7152	6.5	0.3070	4.8	0.72	1725.9	72.0	1769.9	54.8	1821.1	82.0	1821.1	82.0	5.2	2.5
DV 7/09/15_4-35	253	130	1.9	0.1122	4.6	4.5320	6.3	0.2925	4.4	0.69	1654.2	64.0	1736.9	52.5	1836.1	82.8	1836.1	82.8	9.9	4.8
DV 7/09/15_4-84	581	127	4.6	0.1123	5.5	5.4575	8.0	0.3525	5.8	0.72	1946.4	98.2	1893.9	68.9	1836.3	100.2	1836.3	100.2	-6.0	-2.8
DV 7/09/15_4-82	317	285	1.1	0.1123	4.9	4.9722	6.9	0.3211	5.0	0.71	1795.1	77.7	1814.6	58.7	1836.6	88.6	1836.6	88.6	2.3	1.1
DV 7/09/15_4-85	554	205	2.7	0.1123	4.7	5.1507	6.8	0.3326	4.9	0.72	1850.9	79.4	1844.5	58.0	1836.6	85.8	1836.6	85.8	-0.8	-0.3
DV 7/09/15_4-90	858	132	6.5	0.1124	4.8	5.2177	6.9	0.3364	5.0	0.72	1869.3	81.8	1855.5	58.9	1839.2	86.1	1839.2	86.1	-1.6	-0.7
DV 7/09/15_4-153	739	206	3.6	0.1127	9.9	5.0066	14.3	0.3220	10.4	0.72	1799.5	162.6	1820.4	121.8	1842.9	179.1	1842.9	179.1	2.4	1.1
DV 7/09/15_4-126	320	64	5.0	0.1127	8.5	5.1261	12.3	0.3293	8.9	0.72	1834.9	142.1	1840.4	104.7	1842.9	153.3	1842.9	153.3	0.4	0.3
DV 7/09/15_4-78	769	240	3.2	0.1127	4.7	5.0707	6.9	0.3261	5.2	0.74	1819.4	82.1	1831.2	59.0	1844.2	84.5	1844.2	84.5	1.3	0.6
DV 7/09/15_4-5	309	159	1.9	0.1128	7.7	5.0621	11.5	0.3250	8.5	0.74	1814.0	134.6	1829.8	97.4	1845.4	139.1	1845.4	139.1	1.7	0.9
DV 7/09/15_4-24	775	386	2.0	0.1129	4.6	5.2219	6.7	0.3351	4.9	0.73	1863.0	79.2	1856.2	56.8	1846.3	82.6	1846.3	82.6	-0.9	-0.4
DV 7/09/15_4-145	288	363	0.8	0.1129	8.7	4.1651	12.5	0.2672	9.0	0.72	1526.5	122.4	1667.2	103.0	1846.7	157.7	1846.7	157.7	17.3	8.4
DV 7/09/15_4-174	280	82	3.4	0.1130	6.3	5.1344	9.0	0.3294	6.4	0.71	1835.5	102.5	1841.8	76.9	1848.2	114.5	1848.2	114.5	0.7	0.3
DV 7/09/15_4-26	342	113	3.0	0.1132	7.5	5.2904	10.9	0.3385	8.0	0.73	1879.3	130.8	1867.3	93.7	1851.7	135.1	1851.7	135.1	-1.5	-0.6
DV 7/09/15_4-93	322	189	1.7	0.1133	4.8	5.1722	7.1	0.3310	5.2	0.73	1843.4	83.0	1848.0	60.1	1852.3	87.5	1852.3	87.5	0.5	0.3
DV 7/09/15_4-95	1079	543	2.0	0.1134	5.5	5.2641	8.0	0.3366	5.9	0.73	1870.2	95.2	1863.1	68.6	1854.0	99.8	1854.0	99.8	-0.9	-0.4
DV 7/09/15_4-70	512	128	4.0	0.1135	4.1	5.1430	6.0	0.3285	4.4	0.73	1831.3	70.7	1843.2	51.2	1856.2	74.4	1856.2	74.4	1.3	0.6
DV 7/09/15_4-159	1502	746	2.0	0.1136	6.8	4.8368	9.9	0.3086	7.2	0.73	1733.7	109.3	1791.3	83.5	1858.0	122.9	1858.0	122.9	6.7	3.2
DV 7/09/15_4-8	745	34	21.9	0.1137	4.8	5.2768	6.9	0.3361	5.0	0.72	1868.1	81.0	1865.1	58.8	1859.3	86.4	1859.3	86.4	-0.5	-0.2
DV 7/09/15_4-74	327	97	3.4	0.1138	5.8	5.2331	8.4	0.3333	6.1	0.72	1854.4	99.1	1858.0	72.2	1861.6	105.2	1861.6	105.2	0.4	0.2
DV 7/09/15_4-102	132	131	1.0	0.1139	6.8	5.2573	9.7	0.3343	7.0	0.72	1859.2	112.3	1862.0	82.8	1863.1	122.0	1863.1	122.0	0.2	0.1
DV 7/09/15_4-86	276	153	1.8	0.1140	4.4	5.1751	6.4	0.3291	4.7	0.72	1833.8	75.1	1848.5	54.9	1864.4	80.3	1864.4	80.3	1.6	0.8
DV 7/09/15_4-127	495	96	5.2	0.1141	6.0	5.2372	8.7	0.3321	6.3	0.72	1848.5	101.3	1858.7	74.5	1866.2	109.2	1866.2	109.2	0.9	0.5
DV 7/09/15_4-112	399	50	7.9	0.1142	7.1	5.3250	10.2	0.3377	7.4	0.72	1875.8	121.2	1872.9	87.8	1867.0	127.4	1867.0	127.4	-0.5	-0.2
DV 7/09/15_4-163	971	580	1.7	0.1144	7.6	5.2327	11.1	0.3316	8.0	0.72	1846.2	128.5	1858.0	94.5	1870.4	137.5	1870.4	137.5	1.3	0.6
DV 7/09/15_4-175	986	358	2.8	0.1145	9.0	4.9881	12.8	0.3159	9.2	0.72	1769.6	142.1	1817.3	109.0	1871.6	161.4	1871.6	161.4	5.5	2.6
DV 7/09/15_4-65	65	87	0.7	0.1153	5.6	5.0656	8.0	0.3186	5.7	0.71	1782.9	89.1	1830.4	67.9	1884.1	101.2	1884.1	101.2	5.4	2.6
DV 7/09/15_4-42	311	161	1.9	0.1153	5.1	5.2504	7.5	0.3300	5.6	0.73	1838.3	88.8	1860.8	64.4	1884.6	92.5	1884.6	92.5	2.5	1.2
DV 7/09/15_4-129	406	391	1.0	0.1154	5.6	5.2254	8.1	0.3278	5.8	0.72	1827.7	92.5	1856.8	69.1	1885.6	101.6	1885.6	101.6	3.1	1.6
DV 7/09/15_4-124	775	35	22.2	0.1159	9.8	5.3727	14.3	0.3354	10.4	0.73	1864.6	168.6	1880.5	122.7	1894.5	175.7	1894.5	175.7	1.6	0.8
DV 7/09/15_4-168	665	428	1.6	0.1160	8.7	5.4539	12.9	0.3409	9.5	0.74	1890.8	156.0	1893.4	110.9	1895.6	155.7	1895.6	155.7	0.3	0.1
DV 7/09/15_4-14	876	223	3.9	0.1162	6.1	5.3838	9.0	0.3354	6.7	0.73	1864.7	107.9	1882.3	77.5	1899.1	110.3	1899.1	110.3	1.8	0.9

DV 7/09/15_4-6	82	71	1.2	0.1167	5.0	5.5793	7.1	0.3463	5.1	0.71	1917.0	84.9	1912.9	61.4	1906.1	89.6	1906.1	89.6	-0.6	-0.2
DV 7/09/15_4-55	574	83	6.9	0.1169	8.0	5.4983	11.6	0.3408	8.4	0.72	1890.6	137.4	1900.3	99.7	1910.0	143.4	1910.0	143.4	1.0	0.5
DV 7/09/15_4-132	851	8	111.9	0.1189	8.6	5.7539	12.4	0.3503	9.0	0.72	1936.0	150.2	1939.5	108.1	1939.8	154.2	1939.8	154.2	0.2	0.2
DV 7/09/15_4-22	555	124	4.5	0.1196	7.1	5.8059	10.1	0.3516	7.2	0.71	1942.2	119.9	1947.3	87.3	1950.3	126.9	1950.3	126.9	0.4	0.3
DV 7/09/15_4-154	577	185	3.1	0.1211	7.2	4.8861	10.6	0.2924	7.7	0.73	1653.3	113.0	1799.9	89.6	1972.7	129.2	1972.7	129.2	16.2	8.1
DV 7/09/15_4-44	326	176	1.8	0.1214	4.5	5.6806	6.8	0.3390	5.1	0.74	1881.7	82.8	1928.4	58.6	1977.6	81.0	1977.6	81.0	4.8	2.4
DV 7/09/15_4-157	528	146	3.6	0.1228	6.6	5.9455	9.5	0.3509	6.9	0.72	1938.8	115.2	1967.9	83.1	1997.5	117.4	1997.5	117.4	2.9	1.5
DV 7/09/15_4-29	22	1	17.3	0.1232	7.3	6.7298	10.5	0.3958	7.6	0.72	2149.6	138.2	2076.5	92.8	2002.6	129.2	2002.6	129.2	-7.3	-3.5
DV 7/09/15_4-48	180	81	2.2	0.1240	4.8	5.6551	7.0	0.3305	5.1	0.72	1840.6	80.9	1924.5	60.1	2014.9	85.6	2014.9	85.6	8.6	4.4
DV 7/09/15_4-131	449	272	1.7	0.1259	5.4	6.8069	7.7	0.3914	5.5	0.71	2129.2	100.3	2086.6	68.7	2041.3	96.0	2041.3	96.0	-4.3	-2.0
DV 7/09/15_4-7	54	36	1.5	0.1301	6.0	7.0893	8.6	0.3948	6.1	0.71	2144.9	111.5	2122.7	76.3	2098.9	105.8	2098.9	105.8	-2.2	-1.0
DV 7/09/15_4-107	493	594	0.8	0.1462	5.1	8.8049	7.2	0.4363	5.1	0.70	2334.0	100.1	2318.0	65.8	2301.8	87.9	2301.8	87.9	-1.4	-0.7
DV 7/09/15_4-61	83	96	0.9	0.1533	4.3	9.3559	6.1	0.4424	4.4	0.72	2361.2	87.6	2373.5	56.3	2383.4	72.8	2383.4	72.8	0.9	0.5
DV 7/09/15_4-200	262	70	3.7	0.1546	5.2	9.2952	7.4	0.4356	5.4	0.72	2330.8	105.9	2367.5	68.3	2397.1	87.7	2397.1	87.7	2.8	1.6
DV 7/09/15_4-30	177	187	0.9	0.1574	5.4	9.6011	7.7	0.4420	5.5	0.71	2359.4	109.1	2397.3	71.1	2427.6	92.2	2427.6	92.2	2.8	1.6
DV 7/09/15_4-160	869	603	1.4	0.1580	8.3	8.9823	11.8	0.4122	8.3	0.71	2224.8	156.0	2336.2	107.8	2434.0	141.2	2434.0	141.2	8.6	4.8
DV 7/09/15_4-134	246	127	1.9	0.1591	5.6	10.8852	7.7	0.4954	5.4	0.69	2594.1	114.4	2513.4	72.0	2445.6	94.4	2445.6	94.4	-6.1	-3.2
DV 7/09/15_4-186	74	77	1.0	0.1613	8.2	10.8299	11.8	0.4866	8.4	0.72	2555.9	178.3	2508.6	109.9	2468.9	138.1	2468.9	138.1	-3.5	-1.9
DV 7/09/15_4-192	59	41	1.4	0.1617	5.9	10.4100	8.6	0.4664	6.2	0.72	2467.6	126.7	2471.9	79.6	2473.2	99.9	2473.2	99.9	0.2	0.2
DV 7/09/15_4-51	237	189	1.3	0.1639	4.7	10.3903	7.0	0.4596	5.2	0.74	2437.8	106.1	2470.2	64.9	2495.9	79.0	2495.9	79.0	2.3	1.3
DV 7/09/15_4-164	290	241	1.2	0.1647	6.4	10.3365	9.2	0.4551	6.6	0.72	2417.9	132.9	2465.4	85.1	2504.1	107.3	2504.1	107.3	3.4	1.9
DV 7/09/15_4-10	225	235	1.0	0.1648	4.3	10.5813	6.0	0.4650	4.3	0.71	2461.6	88.7	2487.1	56.1	2505.5	71.7	2505.5	71.7	1.8	1.0
DV 7/09/15_4-189	166	196	0.9	0.1689	6.9	11.5238	9.9	0.4941	7.1	0.72	2588.6	150.7	2566.5	92.5	2547.2	115.0	2547.2	115.0	-1.6	-0.9
DV 7/09/15_4-144	605	103	5.9	0.1750	6.9	11.0273	10.0	0.4564	7.2	0.72	2423.7	145.5	2525.4	92.9	2605.9	114.5	2605.9	114.5	7.0	4.0
DV 7/09/15_4-116	409	89	4.6	0.1755	6.2	12.2864	8.9	0.5070	6.5	0.72	2643.7	140.1	2626.5	84.1	2610.6	103.1	2610.6	103.1	-1.3	-0.7
DV 7/09/15_4-18	59	28	2.1	0.1798	9.6	13.1808	13.9	0.5310	10.1	0.72	2745.5	225.4	2692.7	131.7	2651.0	158.5	2651.0	158.5	-3.6	-2.0
DV 7/09/15_4-173	100	66	1.5	0.1805	7.1	12.0301	10.1	0.4832	7.2	0.71	2541.0	151.3	2606.8	95.1	2657.6	117.4	2657.6	117.4	4.4	2.5
DV 7/09/15_4-136	876	205	4.3	0.1852	7.7	13.3557	11.0	0.5221	7.8	0.71	2707.9	172.0	2705.1	103.8	2700.0	127.4	2700.0	127.4	-0.3	-0.1
DV 7/09/15_4-195	668	8	85.2	0.1899	6.9	13.6072	9.7	0.5189	6.8	0.70	2694.7	149.6	2722.8	92.0	2741.3	113.8	2741.3	113.8	1.7	1.0
DV 7/09/15_4-4	312	138	2.3	0.1911	5.5	12.5455	8.0	0.4755	5.8	0.72	2507.6	120.4	2646.1	75.2	2751.7	90.9	2751.7	90.9	8.9	5.2
DV 7/09/15_4-156	495	282	1.8	0.2297	9.7	17.1628	13.2	0.5415	8.9	0.68	2789.7	202.7	2944.0	127.2	3050.0	155.2	3050.0	155.2	8.5	5.2
Data Rejected From Population Analyses																				
DV 7/09/15_4-47	137	191	0.7	0.0539	13.5	0.2826	17.6	0.0380	11.4	0.64	240.5	26.8	252.7	39.5	365.8	304.2	240.5	26.8	34.2	4.8
DV 7/09/15_4-184	347	284	1.2	0.0509	11.9	0.2676	17.2	0.0381	12.4	0.72	241.0	29.3	240.7	36.9	236.4	275.0	241.0	29.3	-1.9	-0.1
DV 7/09/15_4-194	209	144	1.5	0.0503	15.9	0.2807	22.4	0.0404	15.8	0.71	255.6	39.7	251.2	49.9	207.3	368.3	255.6	39.7	-23.3	-1.7

DV 7/09/15_4-80	92	105	0.9	0.0962	16.5	0.5430	17.9	0.0409	7.0	0.39	258.6	17.8	440.4	64.0	1551.8	309.0	258.6	17.8	83.3	41.3
DV 7/09/15_4-16	174	121	1.4	0.0497	15.5	0.2818	20.3	0.0411	13.1	0.64	259.3	33.2	252.1	45.3	181.4	361.4	259.3	33.2	-43.0	-2.9
DV 7/09/15_4-98	127	111	1.1	0.0766	11.3	0.4348	12.9	0.0411	6.2	0.48	259.9	15.9	366.6	39.6	1111.1	225.1	259.9	15.9	76.6	29.1
DV 7/09/15_4-105	528	408	1.3	0.0514	11.2	0.3041	15.5	0.0429	10.7	0.69	270.6	28.2	269.6	36.6	258.0	257.8	270.6	28.2	-4.9	-0.4
DV 7/09/15_4-91	442	285	1.6	0.0575	11.2	0.4088	16.0	0.0516	11.4	0.71	324.2	36.0	348.0	47.1	509.0	246.6	324.2	36.0	36.3	6.8
DV 7/09/15_4-151	321	80	4.0	0.0584	12.7	0.5205	18.4	0.0646	13.3	0.73	403.4	52.2	425.5	64.0	545.1	276.5	403.4	52.2	26.0	5.2
DV 7/09/15_4-106	617	313	2.0	0.0564	12.8	0.5587	18.4	0.0717	13.3	0.72	446.7	57.5	450.7	67.2	468.7	282.7	446.7	57.5	4.7	0.9
DV 7/09/15_4-36	9	2	3.8	0.3072	12.0	3.6124	15.0	0.0852	9.0	0.60	527.1	45.7	1552.3	120.0	3506.9	185.8	527.1	45.7	85.0	66.0
DV 7/09/15_4-89	224	632	0.4	0.0718	10.2	1.0076	15.2	0.1017	11.3	0.74	624.6	67.3	707.7	77.8	980.1	208.5	624.6	67.3	36.3	11.7
DV 7/09/15_4-57	269	378	0.7	0.0751	5.5	1.2499	7.3	0.1206	4.9	0.66	734.0	33.9	823.3	41.3	1071.9	110.2	734.0	33.9	31.5	10.8
DV 7/09/15_4-73	102	144	0.7	0.0760	5.4	1.4291	7.3	0.1363	5.0	0.68	823.5	38.5	901.2	43.7	1096.2	108.1	823.5	38.5	24.9	8.6
DV 7/09/15_4-115	303	118	2.6	0.1139	7.6	2.1762	13.7	0.1383	11.4	0.83	835.3	89.5	1173.4	95.7	1862.5	137.2	835.3	89.5	55.2	28.8
DV 7/09/15_4-146	619	121	5.1	0.0852	7.0	1.7831	9.3	0.1515	6.2	0.67	909.6	52.6	1039.3	60.7	1320.6	134.7	1320.6	134.7	31.1	12.5
DV 7/09/15_4-34	470	307	1.5	0.0862	5.6	2.0597	8.2	0.1731	6.1	0.73	1028.9	57.9	1135.5	56.4	1343.3	108.2	1343.3	108.2	23.4	9.4
DV 7/09/15_4-125	279	107	2.6	0.0904	6.6	2.0915	9.9	0.1674	7.3	0.74	997.7	67.6	1146.0	67.8	1434.6	126.2	1434.6	126.2	30.5	12.9
DV 7/09/15_4-33	161	119	1.4	0.0917	5.8	2.2832	10.1	0.1803	8.3	0.82	1068.7	81.3	1207.1	71.2	1461.9	109.9	1461.9	109.9	26.9	11.5
DV 7/09/15_4-147	213	208	1.0	0.1020	7.4	2.9933	10.0	0.2126	6.8	0.68	1242.5	76.9	1405.9	76.6	1660.8	136.8	1660.8	136.8	25.2	11.6
DV 7/09/15_4-196	194	92	2.1	0.1074	10.9	4.7509	16.0	0.3205	11.7	0.73	1792.1	183.6	1776.3	135.2	1755.0	199.7	1755.0	199.7	-2.1	-0.9
DV 7/09/15_4-27	420	80	5.3	0.1140	10.3	5.2139	15.0	0.3313	10.9	0.72	1844.7	174.6	1854.9	128.4	1864.1	186.5	1864.1	186.5	1.0	0.5
DV 7/09/15_4-110	868	111	7.8	0.1151	10.1	4.9337	14.9	0.3105	11.0	0.74	1743.2	167.3	1808.0	126.1	1881.2	181.2	1881.2	181.2	7.3	3.6
DV 7/09/15_4-71	236	63	3.8	0.1169	5.8	3.8636	8.1	0.2397	5.7	0.70	1385.1	71.6	1606.1	65.7	1909.0	104.0	1909.0	104.0	27.4	13.8
DV 7/09/15_4-190	359	60	6.0	0.1190	13.1	6.0607	19.2	0.3688	14.0	0.73	2023.8	243.7	1984.6	168.6	1941.9	233.5	1941.9	233.5	-4.2	-2.0
DV 7/09/15_4-172	838	406	2.1	0.1200	10.9	5.8373	15.0	0.3528	10.3	0.69	1947.8	172.6	1952.0	130.3	1955.7	193.9	1955.7	193.9	0.4	0.2
DV 7/09/15_4-1	13	0	91.6	0.1210	7.7	7.2164	10.9	0.4320	7.8	0.71	2314.6	150.9	2138.5	97.5	1971.3	137.0	1971.3	137.0	-17.4	-8.2
DV 7/09/15_4-143	74	186	0.4	0.1257	10.7	5.8410	15.4	0.3366	11.1	0.72	1870.1	179.6	1952.5	133.9	2038.5	188.6	2038.5	188.6	8.3	4.2
DV 7/09/15_4-180	543	100	5.4	0.1257	10.4	6.5281	15.8	0.3763	11.8	0.75	2059.0	208.5	2049.7	139.6	2039.3	183.8	2039.3	183.8	-1.0	-0.5
DV 7/09/15_4-128	319	287	1.1	0.1413	10.2	7.7837	15.3	0.3986	11.4	0.74	2162.6	208.7	2206.3	138.2	2243.5	176.7	2243.5	176.7	3.6	2.0
DV 7/09/15_4-187	243	366	0.7	0.1598	11.0	10.0538	16.1	0.4557	11.7	0.73	2420.5	235.9	2439.7	149.5	2454.0	186.3	2454.0	186.3	1.4	0.8
DV 7/09/15_4-103	400	263	1.5	0.1615	11.9	10.3251	17.2	0.4631	12.5	0.72	2453.0	255.5	2464.4	161.0	2471.8	200.5	2471.8	200.5	0.8	0.5
DV 7/09/15_4-178	137.45	102.321	1.3	0.1662	10.9	11.1830	15.8	0.4877	11.4	0.72	2560.7	241.9	2538.5	148.5	2519.9	183.2	2519.9	183.2	-1.6	-0.9
DV 7/09/15_4-162	503.16	208.724	2.4	0.1860	5.6	10.2177	8.0	0.3982	5.7	0.71	2160.7	105.0	2454.7	74.4	2707.3	92.8	2707.3	92.8	20.2	12.0

DV 7-12-15_4 38.119° N; 73.829° E

				Isotope ratios							Apparent Ages (Ma)									
				^{207}Pb	±	^{207}Pb	±	^{206}Pb	±		^{206}Pb	±	^{207}Pb	±	^{207}Pb	±		±	% discordance Pb^{206}/U^{238}-Pb^{207}/Pb^{206}	% discordance Pb^{206}/U^{238}-Pb^{207}/U^{325}
Analysis #	U (ppm)	Th (ppm)	U/Th	^{206}Pb	(2%SD)	^{235}U	(2%SD)	^{238}U	(2%SD)	error corr.	^{238}U	(2SD)	^{235}U	(2SD)	^{206}Pb	(2SD)	Best Age	(2SD)		
DV 7/12/15_4-88	139	122	1.1	0.0704	11.1	0.3431	13.1	0.0353	7.1	0.54	223.7	15.5	299.5	34.1	940.6	227.1	223.7	15.5	76.2	25.3
DV 7/12/15_4-155	197	98	2.0	0.0521	9.0	0.2661	11.8	0.0370	7.6	0.64	234.1	17.4	239.5	25.1	290.5	206.3	234.1	17.4	19.4	2.3
DV 7/12/15_4-48	233	156	1.5	0.0564	8.6	0.2884	12.4	0.0370	9.0	0.72	234.5	20.7	257.3	28.2	468.5	190.3	234.5	20.7	50.0	8.9
DV 7/12/15_4-99	470	570	0.8	0.0566	5.7	0.2900	7.4	0.0371	4.8	0.64	235.0	11.0	258.6	16.8	476.1	125.0	235.0	11.0	50.6	9.1
DV 7/12/15_4-165	374	322	1.2	0.0529	6.2	0.2741	8.3	0.0376	5.5	0.66	237.7	12.8	245.9	18.1	323.4	141.5	237.7	12.8	26.5	3.4
DV 7/12/15_4-74	433	374	1.2	0.0576	9.0	0.3007	12.5	0.0378	8.8	0.70	239.3	20.6	267.0	29.5	515.9	197.4	239.3	20.6	53.6	10.4
DV 7/12/15_4-158	734	643	1.1	0.0538	8.4	0.2850	11.5	0.0384	8.0	0.69	242.6	19.0	254.6	26.0	363.9	188.6	242.6	19.0	33.3	4.7
DV 7/12/15_4-10	173	119	1.4	0.0561	8.1	0.2990	10.1	0.0386	6.1	0.60	244.2	14.6	265.6	23.6	457.1	178.8	244.2	14.6	46.6	8.1
DV 7/12/15_4-45	223	92	2.4	0.0520	8.3	0.2800	10.8	0.0390	6.9	0.64	246.7	16.7	250.7	23.9	285.6	189.6	246.7	16.7	13.6	1.6
DV 7/12/15_4-166	174	110	1.6	0.0533	8.8	0.2905	10.5	0.0395	5.8	0.55	249.8	14.2	258.9	23.9	340.3	198.2	249.8	14.2	26.6	3.5
DV 7/12/15_4-169	559	391	1.4	0.0636	11.9	0.3476	15.4	0.0396	9.7	0.63	250.4	23.9	302.9	40.3	728.5	253.0	250.4	23.9	65.6	17.4
DV 7/12/15_4-200	68	59	1.2	0.0552	13.0	0.3064	14.7	0.0402	6.9	0.47	254.3	17.3	271.4	35.1	419.8	290.2	254.3	17.3	39.4	6.3
DV 7/12/15_4-35	537	395	1.4	0.0538	4.9	0.3055	6.5	0.0412	4.3	0.66	260.1	10.9	270.7	15.3	360.8	109.9	260.1	10.9	27.9	3.9
DV 7/12/15_4-183	406	40	10.2	0.0565	7.8	0.3214	10.3	0.0412	6.8	0.66	260.4	17.4	283.0	25.5	470.8	172.1	260.4	17.4	44.7	8.0
DV 7/12/15_4-83	695	438	1.6	0.0496	10.8	0.2858	12.1	0.0418	5.3	0.44	263.9	13.8	255.2	27.2	174.5	252.9	263.9	13.8	-51.2	-3.4
DV 7/12/15_4-133	208	113	1.9	0.0524	7.7	0.3029	9.8	0.0419	6.1	0.62	264.6	15.9	268.7	23.1	301.8	174.4	264.6	15.9	12.3	1.5
DV 7/12/15_4-151	206	136	1.5	0.0503	7.8	0.2946	9.8	0.0425	6.0	0.60	268.1	15.7	262.2	22.7	206.6	181.5	268.1	15.7	-29.8	-2.3
DV 7/12/15_4-160	396	180	2.2	0.0517	6.8	0.3136	9.4	0.0439	6.4	0.68	277.0	17.4	276.9	22.7	273.7	156.6	277.0	17.4	-1.2	0.0
DV 7/12/15_4-53	503	283	1.8	0.0529	4.8	0.3241	6.5	0.0444	4.5	0.68	280.1	12.2	285.1	16.1	324.0	108.4	280.1	12.2	13.6	1.8
DV 7/12/15_4-11	352	166	2.1	0.0542	5.6	0.3374	7.4	0.0451	4.9	0.65	284.5	13.6	295.2	18.9	378.5	125.5	284.5	13.6	24.8	3.6
DV 7/12/15_4-140	249	241	1.0	0.0528	5.9	0.3407	7.6	0.0467	5.0	0.64	294.3	14.3	297.7	19.7	321.8	132.9	294.3	14.3	8.5	1.1
DV 7/12/15_4-70	376	262	1.4	0.0511	6.6	0.3398	8.8	0.0482	5.9	0.66	303.7	17.4	297.0	22.6	243.4	151.8	303.7	17.4	-24.8	-2.2
DV 7/12/15_4-134	305	243	1.3	0.0538	6.2	0.3757	7.9	0.0506	4.9	0.62	318.2	15.2	323.9	21.8	361.8	139.7	318.2	15.2	12.1	1.7
DV 7/12/15_4-79	408	213	1.9	0.0554	7.4	0.3896	9.9	0.0510	6.6	0.66	320.6	20.6	334.0	28.1	427.5	164.3	320.6	20.6	25.0	4.0
DV 7/12/15_4-62	367	276	1.3	0.0561	6.3	0.3951	8.5	0.0510	5.8	0.67	320.8	18.0	338.1	24.5	457.1	140.4	320.8	18.0	29.8	5.1
DV 7/12/15_4-139	84	81	1.0	0.0496	17.6	0.3497	18.5	0.0510	5.9	0.31	320.9	18.3	304.5	48.8	177.3	409.9	320.9	18.3	-81.0	-5.4
DV 7/12/15_4-161	391	337	1.2	0.0519	5.6	0.3804	7.2	0.0531	4.6	0.63	333.3	14.9	327.4	20.2	282.6	128.0	333.3	14.9	-18.0	-1.8
DV 7/12/15_4-50	323	271	1.2	0.0539	5.6	0.4076	7.1	0.0548	4.4	0.62	343.7	14.9	347.2	20.9	367.9	125.6	343.7	14.9	6.6	1.0
DV 7/12/15_4-142	445	428	1.0	0.0534	5.4	0.4044	7.4	0.0549	5.1	0.68	344.3	17.2	344.9	21.8	346.1	122.8	344.3	17.2	0.5	0.2
DV 7/12/15_4-107	716	143	5.0	0.0533	9.6	0.4196	13.7	0.0570	9.7	0.71	357.4	33.9	355.8	41.0	342.5	217.2	357.4	33.9	-4.4	-0.5
DV 7/12/15_4-124	608	114	5.3	0.0555	6.2	0.4383	8.6	0.0572	6.1	0.70	358.3	21.2	369.0	26.7	434.2	137.2	358.3	21.2	17.5	2.9

DV 7/12/15_4-46	319	146	2.2	0.0547	4.9	0.4378	6.4	0.0580	4.2	0.64	363.1	14.8	368.7	19.9	401.7	110.2	363.1	14.8	9.6	1.5
DV 7/12/15_4-9	894	430	2.1	0.0554	6.6	0.4447	9.3	0.0581	6.7	0.71	364.2	23.7	373.6	29.2	430.3	146.2	364.2	23.7	15.4	2.5
DV 7/12/15_4-137	358	238	1.5	0.0543	7.2	0.4389	10.1	0.0585	7.2	0.71	366.6	25.5	369.5	31.4	384.8	161.1	366.6	25.5	4.7	0.8
DV 7/12/15_4-108	106	93	1.1	0.0479	17.2	0.4019	18.1	0.0607	5.7	0.32	380.1	21.2	343.1	52.7	96.6	406.4	380.1	21.2	-293.6	-10.8
DV 7/12/15_4-154	520	523	1.0	0.0600	8.1	0.5037	11.2	0.0608	7.8	0.69	380.6	28.8	414.2	38.1	603.8	174.5	380.6	28.8	37.0	8.1
DV 7/12/15_4-51	281	204	1.4	0.0562	4.8	0.4798	6.2	0.0618	4.0	0.64	386.7	14.9	397.9	20.3	461.1	105.3	386.7	14.9	16.1	2.8
DV 7/12/15_4-159	1117	302	3.7	0.0541	5.1	0.4676	7.1	0.0626	5.0	0.70	391.4	18.9	389.5	23.0	375.9	114.6	391.4	18.9	-4.1	-0.5
DV 7/12/15_4-20	494	324	1.5	0.0558	5.8	0.4890	8.1	0.0636	5.7	0.70	397.2	21.8	404.2	26.9	442.5	128.5	397.2	21.8	10.2	1.7
DV 7/12/15_4-37	173	101	1.7	0.0626	6.6	0.5518	8.5	0.0638	5.3	0.62	398.8	20.6	446.2	30.6	696.3	141.1	398.8	20.6	42.7	10.6
DV 7/12/15_4-65	626	283	2.2	0.0538	6.3	0.4831	8.8	0.0650	6.2	0.70	406.3	24.3	400.2	29.1	363.7	141.9	406.3	24.3	-11.7	-1.5
DV 7/12/15_4-199	311	126	2.5	0.0588	9.3	0.5396	13.1	0.0665	9.2	0.70	414.9	36.8	438.2	46.5	560.2	203.3	414.9	36.8	25.9	5.3
DV 7/12/15_4-28	80	92	0.9	0.0526	10.8	0.4899	12.1	0.0675	5.5	0.45	421.3	22.3	404.9	40.5	309.5	246.7	421.3	22.3	-36.1	-4.1
DV 7/12/15_4-24	529	123	4.3	0.0727	7.4	0.6794	11.3	0.0677	8.6	0.76	422.2	35.2	526.4	46.5	1006.5	149.4	422.2	35.2	58.1	19.8
DV 7/12/15_4-90	351	122	2.9	0.0547	6.1	0.5195	7.8	0.0689	4.9	0.63	429.4	20.6	424.8	27.1	398.6	135.8	429.4	20.6	-7.7	-1.1
DV 7/12/15_4-98	174	108	1.6	0.0573	7.9	0.5465	10.5	0.0691	6.9	0.66	430.5	28.9	442.7	37.8	504.9	174.8	430.5	28.9	14.7	2.8
DV 7/12/15_4-86	175	191	0.9	0.0597	9.0	0.5706	11.5	0.0692	7.1	0.61	431.6	29.5	458.4	42.3	593.7	196.0	431.6	29.5	27.3	5.9
DV 7/12/15_4-109	771	488	1.6	0.0552	9.0	0.5294	12.7	0.0695	9.0	0.71	432.9	37.7	431.4	44.6	420.6	199.9	432.9	37.7	-2.9	-0.4
DV 7/12/15_4-179	880	482	1.8	0.0565	5.2	0.5416	7.5	0.0695	5.3	0.71	433.0	22.4	439.5	26.6	471.8	116.0	433.0	22.4	8.2	1.5
DV 7/12/15_4-126	874	451	1.9	0.0614	6.2	0.5929	9.1	0.0700	6.6	0.73	436.1	27.9	472.7	34.2	652.1	133.3	436.1	27.9	33.1	7.8
DV 7/12/15_4-103	755	393	1.9	0.0552	6.0	0.5342	8.4	0.0701	5.9	0.70	436.5	24.7	434.6	29.6	422.0	134.3	436.5	24.7	-3.5	-0.4
DV 7/12/15_4-163	993	451	2.2	0.0558	8.9	0.5421	12.6	0.0703	8.9	0.71	438.1	37.9	439.8	44.9	446.0	197.0	438.1	37.9	1.8	0.4
DV 7/12/15_4-186	810	948	0.9	0.0559	6.0	0.5429	8.4	0.0704	6.0	0.70	438.4	25.3	440.4	30.1	447.8	133.2	438.4	25.3	2.1	0.4
DV 7/12/15_4-193	359	117	3.1	0.0589	6.9	0.5743	9.1	0.0706	6.0	0.66	439.9	25.5	460.8	33.7	564.1	149.3	439.9	25.5	22.0	4.5
DV 7/12/15_4-52	604	355	1.7	0.0558	4.3	0.5453	5.7	0.0708	3.9	0.67	440.9	16.6	441.9	20.5	444.9	94.8	440.9	16.6	0.9	0.2
DV 7/12/15_4-64	877	249	3.5	0.0564	5.9	0.5511	8.4	0.0708	6.0	0.71	441.2	25.6	445.7	30.2	467.5	129.9	441.2	25.6	5.6	1.0
DV 7/12/15_4-180	140	72	2.0	0.0572	6.8	0.5621	8.9	0.0712	5.8	0.65	443.2	24.8	452.9	32.5	500.7	149.5	443.2	24.8	11.5	2.1
DV 7/12/15_4-55	1432	1542	0.9	0.0570	5.3	0.5617	7.6	0.0714	5.5	0.72	444.7	23.8	452.6	27.8	491.2	116.1	444.7	23.8	9.5	1.8
DV 7/12/15_4-106	521	367	1.4	0.0559	5.8	0.5537	7.9	0.0717	5.3	0.67	446.4	22.9	447.4	28.4	450.3	129.1	446.4	22.9	0.9	0.2
DV 7/12/15_4-168	407	207	2.0	0.0555	6.8	0.5492	9.6	0.0717	6.9	0.71	446.4	29.6	444.5	34.7	432.3	151.9	446.4	29.6	-3.3	-0.4
DV 7/12/15_4-145	300	236	1.3	0.0547	6.8	0.5425	8.8	0.0719	5.6	0.63	447.6	24.0	440.0	31.3	398.7	152.4	447.6	24.0	-12.3	-1.7
DV 7/12/15_4-81	441	258	1.7	0.0576	9.1	0.5765	11.7	0.0726	7.3	0.62	451.7	31.8	462.2	43.3	513.4	200.4	451.7	31.8	12.0	2.3
DV 7/12/15_4-76	186	113	1.6	0.0609	7.0	0.6238	8.9	0.0742	5.5	0.61	461.6	24.3	492.2	34.5	636.3	150.6	461.6	24.3	27.5	6.2
DV 7/12/15_4-170	683	238	2.9	0.0582	8.3	0.6030	12.0	0.0751	8.8	0.73	466.6	39.4	479.2	46.0	537.6	180.9	466.6	39.4	13.2	2.6
DV 7/12/15_4-112	862	520	1.7	0.0567	5.1	0.6349	7.2	0.0811	5.1	0.70	502.6	24.6	499.2	28.4	480.7	113.5	502.6	24.6	-4.6	-0.7

DV 7/12/15_4-102	219	134	1.6	0.0592	8.6	0.6658	12.1	0.0815	8.5	0.70	504.8	41.2	518.1	49.0	575.2	186.8	504.8	41.2	12.2	2.6
DV 7/12/15_4-104	617	124	5.0	0.0563	5.8	0.6489	8.4	0.0835	6.0	0.72	517.1	30.0	507.8	33.4	463.9	128.6	517.1	30.0	-11.5	-1.8
DV 7/12/15_4-138	388	411	0.9	0.0577	6.1	0.6659	8.4	0.0836	5.7	0.68	517.6	28.5	518.2	34.0	518.3	134.3	517.6	28.5	0.1	0.1
DV 7/12/15_4-75	336	193	1.7	0.0609	8.0	0.7232	11.4	0.0860	8.1	0.71	531.9	41.3	552.6	48.6	637.4	173.1	531.9	41.3	16.5	3.7
DV 7/12/15_4-122	357	338	1.1	0.0575	5.3	0.6902	7.4	0.0870	5.2	0.70	537.7	26.7	532.9	30.7	509.5	116.8	537.7	26.7	-5.6	-0.9
DV 7/12/15_4-182	148	89	1.7	0.0611	8.8	0.7681	12.1	0.0910	8.4	0.69	561.5	45.2	578.6	53.5	643.9	188.1	561.5	45.2	12.8	3.0
DV 7/12/15_4-5	167	104	1.6	0.0637	6.2	0.9627	8.5	0.1095	5.8	0.68	670.0	37.1	684.7	42.1	731.5	130.7	670.0	37.1	8.4	2.1
DV 7/12/15_4-29	150	74	2.0	0.0665	9.7	1.1063	13.6	0.1205	9.6	0.70	733.2	66.2	756.4	72.7	823.5	202.7	733.2	66.2	11.0	3.1
DV 7/12/15_4-117	237	230	1.0	0.0649	6.0	1.0794	8.4	0.1205	6.0	0.71	733.4	41.5	743.3	44.5	770.9	125.7	733.4	41.5	4.9	1.3
DV 7/12/15_4-19	138	318	0.4	0.0661	9.3	1.1078	13.1	0.1215	9.3	0.70	739.3	64.7	757.1	70.1	808.0	194.8	739.3	64.7	8.5	2.3
DV 7/12/15_4-147	321	457	0.7	0.0659	4.9	1.1197	6.9	0.1231	4.9	0.70	748.6	34.3	762.8	36.9	803.1	102.9	748.6	34.3	6.8	1.9
DV 7/12/15_4-94	153	120	1.3	0.0668	8.8	1.1422	12.0	0.1239	8.2	0.68	753.1	58.3	773.5	65.0	831.4	182.8	753.1	58.3	9.4	2.6
DV 7/12/15_4-119	127	171	0.7	0.0662	6.1	1.1728	8.0	0.1284	5.2	0.64	778.6	38.0	788.0	43.9	811.8	128.0	778.6	38.0	4.1	1.2
DV 7/12/15_4-174	53	33	1.6	0.0666	8.8	1.1895	11.7	0.1294	7.6	0.65	784.4	56.3	795.7	64.4	825.8	184.4	784.4	56.3	5.0	1.4
DV 7/12/15_4-127	357	99	3.6	0.0711	7.0	1.2818	9.2	0.1305	6.0	0.65	790.7	44.7	837.6	52.6	961.6	143.4	790.7	44.7	17.8	5.6
DV 7/12/15_4-2	572	770	0.7	0.0651	5.0	1.2160	7.3	0.1354	5.4	0.73	818.4	41.2	807.9	40.8	777.4	105.9	818.4	41.2	-5.3	-1.3
DV 7/12/15_4-87	852	231	3.7	0.0706	5.3	1.3483	7.3	0.1384	5.1	0.69	835.4	39.8	866.8	42.5	946.5	107.7	835.4	39.8	11.7	3.6
DV 7/12/15_4-188	626	175	3.6	0.0700	5.8	1.3482	8.0	0.1396	5.5	0.69	842.3	43.8	866.8	46.5	927.5	118.2	842.3	43.8	9.2	2.8
DV 7/12/15_4-67	201	146	1.4	0.0699	6.1	1.3894	8.6	0.1441	6.1	0.70	867.7	49.6	884.4	51.0	925.0	125.8	867.7	49.6	6.2	1.9
DV 7/12/15_4-148	604	94	6.4	0.0716	6.8	1.4300	9.5	0.1447	6.6	0.70	870.9	54.1	901.5	56.9	975.7	139.5	870.9	54.1	10.7	3.4
DV 7/12/15_4-57	199	104	1.9	0.0710	5.4	1.4735	7.6	0.1503	5.4	0.70	902.8	45.3	919.6	46.0	958.1	110.9	958.1	110.9	5.8	1.8
DV 7/12/15_4-6	218	131	1.7	0.0739	5.1	1.6583	7.2	0.1627	5.1	0.70	971.8	45.6	992.7	45.5	1037.6	103.9	1037.6	103.9	6.3	2.1
DV 7/12/15_4-43	546	188	2.9	0.0770	7.4	1.9677	10.6	0.1851	7.7	0.72	1095.0	77.4	1104.5	71.7	1121.2	146.9	1121.2	146.9	2.3	0.9
DV 7/12/15_4-136	150	167	0.9	0.0774	5.9	2.0801	8.3	0.1946	5.8	0.70	1146.4	60.9	1142.3	56.7	1132.0	117.6	1132.0	117.6	-1.3	-0.4
DV 7/12/15_4-30	836	101	8.3	0.0945	5.9	3.4465	8.5	0.2642	6.1	0.72	1511.2	82.3	1515.1	67.0	1518.5	112.1	1518.5	112.1	0.5	0.3
DV 7/12/15_4-71	237	46	5.2	0.0969	7.9	3.7712	11.5	0.2820	8.4	0.73	1601.5	118.5	1586.6	92.4	1565.7	148.1	1565.7	148.1	-2.3	-0.9
DV 7/12/15_4-44	99	111	0.9	0.1050	4.6	4.1887	6.5	0.2891	4.6	0.71	1637.0	66.8	1671.8	53.2	1713.9	84.4	1713.9	84.4	4.5	2.1
DV 7/12/15_4-125	328	294	1.1	0.1075	5.6	4.6870	8.0	0.3160	5.7	0.71	1770.0	87.7	1764.9	66.8	1756.6	103.1	1756.6	103.1	-0.8	-0.3
DV 7/12/15_4-152	289	288	1.0	0.1087	5.8	4.6670	8.2	0.3109	5.8	0.71	1745.3	88.8	1761.3	68.5	1778.4	105.8	1778.4	105.8	1.9	0.9
DV 7/12/15_4-14	606	501	1.2	0.1102	4.6	4.4365	6.6	0.2918	4.7	0.71	1650.7	68.7	1719.2	54.4	1801.9	83.9	1801.9	83.9	8.4	4.0
DV 7/12/15_4-123	432	217	2.0	0.1105	6.6	4.8147	9.8	0.3156	7.3	0.74	1768.3	112.9	1787.5	82.9	1807.6	120.4	1807.6	120.4	2.2	1.1
DV 7/12/15_4-54	248	24	10.4	0.1108	5.4	5.0377	7.9	0.3293	5.7	0.72	1835.2	91.4	1825.7	66.7	1813.2	98.7	1813.2	98.7	-1.2	-0.5
DV 7/12/15_4-128	490	248	2.0	0.1118	6.9	5.0390	9.9	0.3265	7.2	0.72	1821.3	114.6	1825.9	84.4	1828.8	124.3	1828.8	124.3	0.4	0.3
DV 7/12/15_4-143	65	54	1.2	0.1121	6.1	4.9469	8.6	0.3199	6.1	0.71	1789.0	95.1	1810.3	72.5	1833.1	109.9	1833.1	109.9	2.4	1.2
DV 7/12/15_4-85	267	139	1.9	0.1128	7.0	5.3134	9.9	0.3416	7.1	0.71	1894.1	116.6	1871.0	85.0	1844.2	125.9	1844.2	125.9	-2.7	-1.2

DV 7/12/15_4-192	177	100	1.8	0.1128	7.6	5.2095	10.9	0.3346	7.8	0.71	1860.7	126.0	1854.2	92.8	1845.1	137.4	1845.1	137.4	-0.8	-0.4
DV 7/12/15_4-175	271	73	3.7	0.1128	6.4	5.3410	9.2	0.3431	6.6	0.72	1901.5	109.5	1875.5	78.7	1845.2	115.0	1845.2	115.0	-3.0	-1.4
DV 7/12/15_4-189	312	156	2.0	0.1131	6.3	5.1086	9.0	0.3272	6.5	0.72	1824.7	102.9	1837.5	76.5	1850.1	113.4	1850.1	113.4	1.4	0.7
DV 7/12/15_4-93	757	231	3.3	0.1136	6.4	5.1826	9.2	0.3306	6.6	0.72	1841.5	105.4	1849.8	78.1	1857.6	115.3	1857.6	115.3	0.9	0.4
DV 7/12/15_4-198	607	177	3.4	0.1136	8.5	5.4863	12.1	0.3499	8.7	0.71	1933.9	145.0	1898.5	104.4	1858.3	153.1	1858.3	153.1	-4.1	-1.9
DV 7/12/15_4-110	341	57	5.9	0.1136	5.4	5.5258	7.7	0.3523	5.5	0.72	1945.5	93.0	1904.6	66.2	1858.3	97.0	1858.3	97.0	-4.7	-2.1
DV 7/12/15_4-129	554	287	1.9	0.1137	4.6	5.4702	6.6	0.3484	4.8	0.72	1927.0	79.7	1895.9	56.5	1859.7	82.3	1859.7	82.3	-3.6	-1.6
DV 7/12/15_4-173	328	138	2.4	0.1139	5.3	5.2449	7.8	0.3336	5.7	0.73	1855.8	92.3	1859.9	66.7	1863.0	96.5	1863.0	96.5	0.4	0.2
DV 7/12/15_4-105	516	158	3.3	0.1141	6.0	4.2103	8.3	0.2674	5.8	0.69	1527.6	78.6	1676.0	68.3	1865.4	108.3	1865.4	108.3	18.1	8.9
DV 7/12/15_4-95	609	318	1.9	0.1143	5.5	5.2523	7.9	0.3331	5.7	0.72	1853.2	91.1	1861.1	67.1	1868.5	99.0	1868.5	99.0	0.8	0.4
DV 7/12/15_4-194	432	311	1.4	0.1143	7.5	5.0966	10.5	0.3231	7.4	0.70	1804.8	116.3	1835.5	89.4	1868.9	135.1	1868.9	135.1	3.4	1.7
DV 7/12/15_4-92	519	139	3.7	0.1145	9.2	5.2421	13.1	0.3317	9.4	0.71	1846.8	150.6	1859.5	112.4	1872.3	166.1	1872.3	166.1	1.4	0.7
DV 7/12/15_4-176	447	238	1.9	0.1146	6.7	5.3066	9.6	0.3355	6.9	0.72	1865.1	112.3	1869.9	82.3	1873.8	120.7	1873.8	120.7	0.5	0.3
DV 7/12/15_4-59	497	293	1.7	0.1148	5.0	4.7142	6.9	0.2975	4.8	0.69	1679.1	70.8	1769.8	57.6	1876.9	89.9	1876.9	89.9	10.5	5.1
DV 7/12/15_4-187	498	113	4.4	0.1150	5.8	4.6671	8.2	0.2941	5.8	0.71	1662.1	85.6	1761.4	68.6	1879.1	104.0	1879.1	104.0	11.5	5.6
DV 7/12/15_4-42	697	152	4.6	0.1150	6.4	5.0990	9.3	0.3212	6.7	0.72	1795.5	105.4	1835.9	78.7	1880.1	115.1	1880.1	115.1	4.5	2.2
DV 7/12/15_4-34	336	56	5.9	0.1150	6.6	5.1584	9.5	0.3249	6.9	0.72	1813.8	108.6	1845.8	81.1	1880.2	119.0	1880.2	119.0	3.5	1.7
DV 7/12/15_4-195	782	275	2.8	0.1150	5.1	5.0540	7.3	0.3184	5.3	0.72	1781.9	82.4	1828.4	62.2	1880.2	92.1	1880.2	92.1	5.2	2.5
DV 7/12/15_4-25	1046	219	4.8	0.1151	4.8	5.4691	6.9	0.3444	5.0	0.72	1907.8	82.3	1895.8	59.4	1880.8	87.0	1880.8	87.0	-1.4	-0.6
DV 7/12/15_4-18	883	616	1.4	0.1151	5.9	5.0510	8.5	0.3179	6.2	0.72	1779.6	96.5	1827.9	72.5	1881.7	106.3	1881.7	106.3	5.4	2.6
DV 7/12/15_4-60	317	154	2.1	0.1167	8.0	5.4368	11.5	0.3375	8.2	0.71	1874.4	133.8	1890.7	98.6	1907.0	144.1	1907.0	144.1	1.7	0.9
DV 7/12/15_4-135	533	169	3.2	0.1169	9.2	5.5500	13.3	0.3439	9.6	0.72	1905.4	158.7	1908.4	114.7	1909.4	164.7	1909.4	164.7	0.2	0.2
DV 7/12/15_4-22	477	64	7.4	0.1174	7.6	5.5443	11.1	0.3421	8.1	0.73	1896.9	133.5	1907.5	95.8	1917.3	136.3	1917.3	136.3	1.1	0.6
DV 7/12/15_4-3	21	1	21.0	0.1178	8.2	5.8047	10.9	0.3572	7.2	0.66	1968.7	122.7	1947.1	94.8	1922.7	146.9	1922.7	146.9	-2.4	-1.1
DV 7/12/15_4-172	135	88	1.5	0.1198	5.1	5.5919	7.3	0.3381	5.3	0.72	1877.6	85.8	1914.8	63.1	1953.9	91.4	1953.9	91.4	3.9	1.9
DV 7/12/15_4-40	211	102	2.1	0.1201	4.5	5.6464	6.5	0.3405	4.8	0.72	1889.3	77.9	1923.2	56.4	1958.1	80.7	1958.1	80.7	3.5	1.8
DV 7/12/15_4-12	994	470	2.1	0.1223	9.4	6.1130	13.3	0.3622	9.5	0.71	1992.8	163.1	1992.1	117.0	1989.8	167.0	1989.8	167.0	-0.1	0.0
DV 7/12/15_4-116	301	173	1.7	0.1227	5.3	5.9226	7.4	0.3497	5.2	0.70	1933.2	86.8	1964.6	64.2	1995.6	93.7	1995.6	93.7	3.1	1.6
DV 7/12/15_4-114	630	49	12.9	0.1237	6.0	5.9491	8.7	0.3484	6.3	0.72	1926.9	105.2	1968.4	75.6	2010.2	106.3	2010.2	106.3	4.1	2.1
DV 7/12/15_4-4	40	87	0.5	0.1253	6.0	5.8503	8.4	0.3384	5.9	0.70	1878.7	96.9	1953.9	73.1	2033.0	106.0	2033.0	106.0	7.6	3.8
DV 7/12/15_4-17	260	110	2.4	0.1316	5.2	6.9224	7.6	0.3811	5.6	0.73	2081.6	99.7	2101.5	67.6	2119.5	91.1	2119.5	91.1	1.8	0.9
DV 7/12/15_4-77	478	291	1.6	0.1321	7.0	7.1151	10.0	0.3904	7.1	0.71	2124.9	127.9	2125.9	88.8	2125.9	123.2	2125.9	123.2	0.0	0.0
DV 7/12/15_4-197	626	101	6.2	0.1340	9.6	6.9968	12.5	0.3782	8.0	0.64	2068.0	140.9	2111.0	111.1	2151.6	167.5	2151.6	167.5	3.9	2.0
DV 7/12/15_4-58	198	89	2.2	0.1353	4.7	7.2440	6.8	0.3879	5.0	0.73	2113.2	90.5	2141.9	61.1	2168.0	82.0	2168.0	82.0	2.5	1.3
DV 7/12/15_4-68	132	84	1.6	0.1481	5.3	7.3735	7.6	0.3608	5.5	0.72	1986.2	93.9	2157.8	68.3	2324.1	91.4	2324.1	91.4	14.5	8.0

DV 7/12/15_4-111	740	450	1.6	0.1511	7.5	9.0442	10.8	0.4335	7.7	0.72	2321.6	151.0	2342.5	99.0	2358.7	128.9	2358.7	128.9	1.6	0.9
DV 7/12/15_4-132	12	1	16.8	0.1522	8.0	9.0797	11.0	0.4322	7.6	0.69	2315.7	148.2	2346.1	101.0	2370.4	136.0	2370.4	136.0	2.3	1.3
DV 7/12/15_4-171	238	180	1.3	0.1535	8.1	8.8179	12.4	0.4163	9.4	0.76	2243.8	178.4	2319.3	113.8	2385.0	138.6	2385.0	138.6	5.9	3.3
DV 7/12/15_4-153	463	131	3.5	0.1568	9.9	9.0468	14.3	0.4181	10.3	0.72	2251.9	196.7	2342.7	131.5	2420.9	168.0	2420.9	168.0	7.0	3.9
DV 7/12/15_4-149	241	148	1.6	0.1572	9.5	9.7367	13.4	0.4490	9.5	0.71	2390.8	189.3	2410.2	124.0	2425.3	161.0	2425.3	161.0	1.4	0.8
DV 7/12/15_4-33	1565	1164	1.3	0.1593	7.0	8.0427	11.1	0.3658	8.6	0.77	2009.6	148.9	2235.8	100.7	2448.2	119.1	2448.2	119.1	17.9	10.1
DV 7/12/15_4-89	431	119	3.6	0.1604	8.4	10.8650	11.9	0.4911	8.5	0.71	2575.3	179.7	2511.6	111.4	2459.4	142.6	2459.4	142.6	-4.7	-2.5
DV 7/12/15_4-27	581	413	1.4	0.1616	5.7	8.4849	8.5	0.3805	6.2	0.73	2078.5	110.8	2284.3	77.0	2472.2	97.0	2472.2	97.0	15.9	9.0
DV 7/12/15_4-32	780	220	3.5	0.1635	5.2	8.6570	7.5	0.3836	5.5	0.72	2093.1	97.7	2302.6	68.8	2492.2	88.3	2492.2	88.3	16.0	9.1
DV 7/12/15_4-196	112	57	2.0	0.1638	5.2	10.2336	7.4	0.4527	5.3	0.71	2407.4	107.2	2456.1	68.8	2495.1	87.6	2495.1	87.6	3.5	2.0
DV 7/12/15_4-56	66	74	0.9	0.1642	4.3	10.4012	6.0	0.4591	4.2	0.69	2435.6	85.3	2471.2	55.3	2499.0	72.4	2499.0	72.4	2.5	1.4
DV 7/12/15_4-21	41	142	0.3	0.1659	5.8	8.5198	8.5	0.3721	6.2	0.73	2039.1	109.3	2288.0	77.7	2516.8	98.2	2516.8	98.2	19.0	10.9
DV 7/12/15_4-16	230	155	1.5	0.1663	4.5	10.9405	6.5	0.4766	4.8	0.72	2512.4	99.5	2518.1	60.8	2521.2	75.6	2521.2	75.6	0.3	0.2
DV 7/12/15_4-190	611	231	2.6	0.1665	5.9	11.1810	8.6	0.4864	6.3	0.73	2555.2	132.2	2538.3	80.1	2523.1	99.0	2523.1	99.0	-1.3	-0.7
DV 7/12/15_4-150	405	1137	0.4	0.1666	5.8	11.1524	8.3	0.4850	5.9	0.71	2549.2	124.8	2535.9	77.4	2524.2	97.7	2524.2	97.7	-1.0	-0.5
DV 7/12/15_4-31	166	188	0.9	0.1677	5.1	10.1084	7.1	0.4368	5.0	0.70	2336.3	98.4	2444.7	66.1	2534.5	86.0	2534.5	86.0	7.8	4.4
DV 7/12/15_4-26	181	150	1.2	0.1693	5.3	11.2031	7.6	0.4795	5.4	0.71	2525.2	113.7	2540.2	70.7	2550.4	88.9	2550.4	88.9	1.0	0.6
DV 7/12/15_4-115	177	79	2.2	0.1858	5.5	13.1974	7.8	0.5145	5.6	0.72	2675.8	123.4	2693.9	73.9	2705.5	90.0	2705.5	90.0	1.1	0.7
DV 7/12/15_4-36	570	293	1.9	0.2076	5.1	15.5093	7.5	0.5413	5.6	0.74	2788.8	126.3	2847.1	72.0	2886.8	82.9	2886.8	82.9	3.4	2.0
DV 7/12/15_4-96	132	23	5.7	0.2466	8.7	20.4658	12.7	0.6015	9.3	0.73	3036.0	225.5	3113.6	123.9	3162.8	138.2	3162.8	138.2	4.0	2.5
DV 7/12/15_4-72	235	81	2.9	0.2724	5.8	24.5268	8.7	0.6526	6.6	0.75	3238.4	166.9	3289.6	85.3	3319.9	90.6	3319.9	90.6	2.5	1.6
Data Rejected From Population Analyses																				
DV 7/12/15_4-1	373	54	6.9	0.0542	21.3	0.4235	30.1	0.0566	21.3	0.71	355.0	73.5	358.5	91.1	379.7	478.5	355.0	73.5	6.5	1.0
DV 7/12/15_4-38	66	0	200.4	0.0767	7.6	1.2941	10.0	0.1223	6.5	0.65	743.6	45.8	843.1	57.1	1112.9	150.8	743.6	45.8	33.2	11.8
DV 7/12/15_4-23	722	253	2.9	0.0825	6.3	1.7944	8.8	0.1576	6.1	0.69	943.2	53.7	1043.4	57.3	1257.9	123.6	1257.9	123.6	25.0	9.6
DV 7/12/15_4-39	76	23	3.2	0.1053	10.5	4.0651	15.0	0.2796	10.8	0.72	1589.4	151.7	1647.3	123.0	1720.1	192.7	1720.1	192.7	7.6	3.5
DV 7/12/15_4-13	52	1	48.6	0.1183	7.7	6.7640	11.4	0.4144	8.3	0.73	2234.8	157.6	2081.0	100.8	1930.5	138.7	1930.5	138.7	-15.8	-7.4
DV 7/12/15_4-49	32	2E-02	2E+03	0.1243	6.7	7.2355	9.1	0.4218	6.2	0.68	2268.7	118.2	2140.9	81.3	2018.6	118.7	2018.6	118.7	-12.4	-6.0
DV 7/12/15_4-7	116	101	1.1	0.5800	11.0	12.9816	14.0	0.1622	8.7	0.62	969.0	78.1	2678.3	133.0	4458.7	160.9	4458.7	160.9	78.3	63.8
DV 7/12/15_4-47	1	1	0.9	0.6225	25.2	20.5366	31.9	0.2390	19.6	0.61	1381.7	244.1	3117.0	319.1	4561.3	365.2	4561.3	365.2	69.7	55.7
DV 7/12/15_4-41	30	288	0.1	0.7813	6.8	74.0318	9.7	0.6865	7.0	0.72	3369.1	184.0	4384.3	97.6	4888.1	96.8	4888.1	96.8	31.1	23.2
DV 7/12/15_4-15	1	2	0.3	0.9094	140.7	2117.8	176.6	16.8750	106.8	0.60	18587.6	65535.0	7776.4	65535.0	5103.5	2004.7	5103.5	2004.7	-264.2	-139.0
DV 7/12/15_4-82	678	159	4.3	0.0563	10.3	0.4049	14.7	0.0521	10.6	0.72	327.4	33.7	345.2	43.0	465.6	227.1	327.4	33.7	29.7	5.2
DV 7/12/15_4-113	497	163	3.0	0.0553	10.1	0.5352	14.6	0.0701	10.5	0.72	436.9	44.5	435.3	51.7	423.8	225.9	436.9	44.5	-3.1	-0.4
DV 7/12/15_4-131	768	238	3.2	0.0572	11.7	0.5762	16.8	0.0729	12.0	0.71	453.7	52.5	462.0	62.3	501.0	258.3	453.7	52.5	9.4	1.8

DV 7/12/15_4-130	671	1007	0.7	0.1265	11.0	1.9761	16.8	0.1132	12.7	0.76	691.0	83.3	1107.4	113.6	2049.8	193.7	691.0	83.3	66.3	37.6
DV 7/12/15_4-63	1292	21	62.3	0.0649	12.4	1.1817	17.6	0.1319	12.6	0.71	798.7	94.3	792.1	97.2	772.0	260.4	798.7	94.3	-3.5	-0.8
DV 7/12/15_4-69	427	285	1.5	0.0788	15.1	1.4676	22.9	0.1349	17.2	0.75	816.0	131.8	917.1	139.0	1167.7	299.0	816.0	131.8	30.1	11.0
DV 7/12/15_4-73	178	147	1.2	0.0713	12.5	1.5927	17.8	0.1619	12.7	0.71	967.6	113.8	967.3	111.2	965.6	254.5	965.6	254.5	-0.2	0.0
DV 7/12/15_4-97	824	235	3.5	0.1120	10.3	5.1673	14.4	0.3345	10.1	0.70	1860.0	164.0	1847.2	123.3	1831.3	186.0	1831.3	186.0	-1.6	-0.7
DV 7/12/15_4-66	146	68	2.1	0.1125	10.7	4.9722	15.3	0.3204	11.0	0.72	1791.7	172.0	1814.6	130.3	1839.7	193.9	1839.7	193.9	2.6	1.3
DV 7/12/15_4-118	587	230	2.6	0.1185	4.8	4.3334	7.6	0.2649	5.9	0.78	1515.1	80.0	1699.7	62.8	1933.4	85.9	1933.4	85.9	21.6	10.9
DV 7/12/15_4-144	653	230	2.8	0.1201	6.9	2.7274	17.5	0.1646	16.1	0.92	982.1	146.8	1335.9	130.8	1957.4	123.1	1957.4	123.1	49.8	26.5
DV 7/12/15_4-78	127	154	0.8	0.1246	11.6	5.4434	14.3	0.3166	8.3	0.58	1773.0	129.3	1891.7	122.8	2023.5	205.0	2023.5	205.0	12.4	6.3
DV 7/12/15_4-146	817	39	20.8	0.1434	4.9	6.2800	6.9	0.3174	4.9	0.70	1776.9	75.8	2015.7	60.7	2268.5	85.2	2268.5	85.2	21.7	11.8
DV 7/12/15_4-121	96	110	0.9	0.1695	12.7	11.0720	18.1	0.4730	12.9	0.71	2496.9	267.7	2529.2	169.9	2553.1	211.8	2553.1	211.8	2.2	1.3
DV 7/12/15_4-141	932	158	5.9	0.1924	5.6	8.3385	8.8	0.3141	6.8	0.77	1760.6	105.3	2268.5	80.2	2762.5	92.3	2762.5	92.3	36.3	22.4
DV 7/12/15_4-101	6	0.01	844.5	0.1960	12.4	13.8877	15.1	0.5134	8.7	0.57	2671.0	190.3	2742.1	144.3	2793.2	202.9	2793.2	202.9	4.4	2.6
DV 7/12/15_4-61	3	0.24	12.0	0.3305	23.7	13.7006	27.4	0.3005	13.9	0.51	1693.6	207.4	2729.2	265.5	3619.2	362.6	3619.2	362.6	53.2	37.9
DV 7/12/15_4-100	2	0.01	250.9	0.5359	22.8	13.7964	29.7	0.1866	19.1	0.64	1102.7	193.7	2735.8	289.1	4343.1	334.2	4343.1	334.2	74.6	59.7
DV 7/12/15_4-84	4	2	1.6	0.5902	18.0	28.1255	22.1	0.3454	12.8	0.58	1912.5	212.6	3423.5	220.5	4484.1	262.5	4484.1	262.5	57.3	44.1
DV 7/12/15_4-120	0.02	0.01	2.5	0.6915	135.2	12744.5	194.0	133.4913	139.1	0.72	31597.1	65535.0	9598.4	65535.0	4713.3	1949.4	4713.3	1949.4	-570.4	-229.2
DV 7/12/15_4-80	0.09	0.14	0.7	0.8605	112.2	6388.2	167.6	53.8071	124.6	0.74	25810.3	65535.0	8897.2	65535.0	5025.4	1602.0	5025.4	1602.0	-413.6	-190.1
DV 7/12/15_4-91	0.15	0.06	2.5	0.9299	107.7	6040.7	140.6	47.0782	90.3	0.64	24965.9	8994.0	8840.4	65535.0	5135.0	1534.2	5135.0	1534.2	-386.2	-182.4
DV 7/12/15_4-181	166	118	1.4	0.0931	20.4	0.5299	22.4	0.0412	9.3	0.42	260.4	23.8	431.7	78.9	1490.7	385.3	260.4	23.8	82.5	39.7
DV 7/12/15_4-157	118	70	1.7	0.0510	12.6	0.3452	17.0	0.0491	11.4	0.67	308.8	34.4	301.1	44.3	239.6	290.4	308.8	34.4	-28.9	-2.5
DV 7/12/15_4-162	238	157	1.5	0.0548	10.8	0.5018	15.0	0.0663	10.4	0.69	414.0	41.7	412.9	50.9	404.8	241.5	414.0	41.7	-2.3	-0.2
DV 7/12/15_4-191	392	333	1.2	0.0556	12.7	0.5398	18.0	0.0704	12.8	0.71	438.3	54.2	438.3	64.3	436.1	283.3	438.3	54.2	-0.5	0.0
DV 7/12/15_4-178	14	0.4	31.5	0.3203	17.1	4.8653	20.0	0.1101	10.4	0.52	673.3	66.4	1796.3	170.0	3571.1	263.0	673.3	66.4	81.1	62.5
DV 7/12/15_4-185	197	61	3.2	0.0765	6.9	1.5044	9.4	0.1424	6.4	0.68	858.4	51.3	932.2	57.2	1108.5	137.8	858.4	51.3	22.6	7.9
DV 7/12/15_4-167	400	61	6.6	0.0930	5.5	2.5879	7.4	0.2015	5.0	0.67	1183.6	54.2	1297.2	54.5	1488.7	104.3	1488.7	104.3	20.5	8.8
DV 7/12/15_4-164	640	233	2.7	0.1063	7.4	3.2488	11.6	0.2214	9.0	0.77	1289.3	105.2	1468.9	90.5	1737.1	135.2	1737.1	135.2	25.8	12.2
DV 7/12/15_4-177	46	30	1.5	0.1137	10.3	4.8158	15.0	0.3070	11.0	0.73	1726.0	166.7	1787.7	127.2	1858.9	185.7	1858.9	185.7	7.1	3.4
DV 7/12/15_4-184	279	100	2.8	0.1190	12.7	5.6805	19.1	0.3457	14.2	0.75	1914.1	236.1	1928.4	166.3	1941.6	227.4	1941.6	227.4	1.4	0.7
DV 7/12/15_4-156	50	0.004	12607	0.1209	8.3	6.7650	11.4	0.4055	7.8	0.69	2194.2	145.9	2081.2	101.0	1969.1	147.4	1969.1	147.4	-11.4	-5.4

DV 7-25-15_2 37.774° N; 73.722° E

				Isotope ratios							Apparent Ages (Ma)									
				^{207}Pb	±	^{207}Pb	±	^{206}Pb	±		^{206}Pb	±	^{207}Pb	±	^{207}Pb	±		±	% discordance Pb^{206}/U^{238}-Pb^{207}/Pb^{206}	% discordance Pb^{206}/U^{238}-Pb^{207}/U^{325}
Analysis #	U (ppm)	Th (ppm)	U/Th	^{206}Pb	(2%SD)	^{235}U	(2%SD)	^{238}U	(2%SD)	error corr.	^{238}U	(2SD)	^{235}U	(2SD)	^{206}Pb	(2SD)	Best Age	(2SD)		
DV 7/25/15_2-147	1834	950	1.9	0.0539	7.1	0.2511	10.3	0.0338	7.5	0.72	214.0	15.7	227.5	21.0	366.8	160.2	214.0	15.7	41.7	5.9
DV 7/25/15_2-141	1246	833	1.5	0.0537	6.7	0.2519	8.9	0.0340	6.0	0.67	215.5	12.7	228.1	18.2	358.3	150.2	215.5	12.7	39.9	5.5
DV 7/25/15_2-166	1135	937	1.2	0.0520	7.0	0.2473	9.3	0.0345	6.1	0.65	218.4	13.1	224.4	18.7	286.6	161.0	218.4	13.1	23.8	2.7
DV 7/25/15_2-63	1572	685	2.3	0.0521	8.7	0.2501	12.0	0.0348	8.3	0.69	220.6	18.0	226.7	24.5	287.7	199.8	220.6	18.0	23.3	2.7
DV 7/25/15_2-148	2357	2183	1.1	0.0596	9.9	0.2984	12.9	0.0363	8.3	0.64	229.6	18.8	265.2	30.2	590.8	214.8	229.6	18.8	61.1	13.4
DV 7/25/15_2-108	1733	1106	1.6	0.0512	7.5	0.2577	10.6	0.0365	7.5	0.71	231.0	17.0	232.8	22.0	249.4	172.4	231.0	17.0	7.4	0.8
DV 7/25/15_2-142	2020	1881	1.1	0.0510	5.5	0.2586	7.6	0.0367	5.3	0.69	232.5	12.1	233.5	15.9	242.0	126.7	232.5	12.1	3.9	0.5
DV 7/25/15_2-170	2053	1619	1.3	0.0507	7.8	0.2589	11.0	0.0370	7.8	0.71	234.1	17.9	233.8	22.9	229.4	179.3	234.1	17.9	-2.0	-0.1
DV 7/25/15_2-105	6842	129	53.0	0.0505	6.1	0.2583	9.0	0.0370	6.6	0.73	234.5	15.2	233.3	18.7	219.7	140.9	234.5	15.2	-6.7	-0.5
DV 7/25/15_2-136	1451	672	2.2	0.0429	41.5	0.2199	41.8	0.0371	5.3	0.13	234.8	12.3	201.8	76.7	251.8	58.9	234.8	12.3	9.7	-16.4
DV 7/25/15_2-13	1897	935	2.0	0.0513	7.3	0.2630	10.3	0.0371	7.3	0.71	235.1	16.9	237.1	21.8	255.6	167.6	235.1	16.9	8.0	0.8
DV 7/25/15_2-194	860	540	1.6	0.0514	7.1	0.2635	9.7	0.0371	6.7	0.68	235.1	15.4	237.5	20.6	257.9	162.7	235.1	15.4	8.8	1.0
DV 7/25/15_2-174	1057	1021	1.0	0.0515	12.1	0.2665	13.3	0.0375	5.7	0.42	237.2	13.3	239.9	28.5	264.8	277.3	237.2	13.3	10.4	1.1
DV 7/25/15_2-197	2356	1031	2.3	0.0501	7.3	0.2622	9.3	0.0379	5.8	0.62	239.8	13.6	236.4	19.6	199.6	169.0	239.8	13.6	-20.1	-1.4
DV 7/25/15_2-199	507	754	0.7	0.0520	11.3	0.2770	14.8	0.0386	9.7	0.65	244.1	23.2	248.3	32.7	285.3	257.5	244.1	23.2	14.5	1.7
DV 7/25/15_2-51	1083	389	2.8	0.0526	11.2	0.2799	13.0	0.0386	6.5	0.50	244.1	15.6	250.6	28.8	309.6	255.3	244.1	15.6	21.1	2.6
DV 7/25/15_2-200	1146	1327	0.9	0.0513	5.9	0.2738	8.2	0.0387	5.7	0.69	244.7	13.6	245.7	17.9	253.0	136.7	244.7	13.6	3.3	0.4
DV 7/25/15_2-133	961	553	1.7	0.0526	5.9	0.2814	7.6	0.0388	4.9	0.64	245.4	11.8	251.8	17.1	309.8	134.3	245.4	11.8	20.8	2.5
DV 7/25/15_2-39	1612	656	2.5	0.0536	8.9	0.2917	12.4	0.0395	8.6	0.70	249.5	21.2	259.9	28.4	353.9	200.7	249.5	21.2	29.5	4.0
DV 7/25/15_2-37	1416	937	1.5	0.0684	10.7	0.3743	12.9	0.0397	7.2	0.55	250.8	17.7	322.9	35.7	881.3	222.0	250.8	17.7	71.5	22.3
DV 7/25/15_2-113	1559	690	2.3	0.0555	8.0	0.3054	11.9	0.0399	8.9	0.74	252.1	22.0	270.6	28.4	432.1	178.1	252.1	22.0	41.7	6.8
DV 7/25/15_2-120	498	517	1.0	0.0532	7.6	0.2940	9.5	0.0401	5.8	0.61	253.2	14.5	261.7	22.0	336.3	171.7	253.2	14.5	24.7	3.3
DV 7/25/15_2-9	324	223	1.5	0.0515	11.7	0.2916	13.6	0.0411	6.9	0.51	259.6	17.5	259.8	31.1	261.3	268.0	259.6	17.5	0.7	0.1
DV 7/25/15_2-181	1990	861	2.3	0.0503	6.2	0.2853	8.9	0.0411	6.4	0.72	259.6	16.3	254.8	20.0	209.5	143.8	259.6	16.3	-23.9	-1.9
DV 7/25/15_2-47	1900	1037	1.8	0.0522	6.5	0.2975	9.2	0.0413	6.5	0.70	261.1	16.7	264.4	21.4	293.9	149.2	261.1	16.7	11.2	1.2
DV 7/25/15_2-7	1612	1862	0.9	0.0517	7.3	0.2956	9.7	0.0415	6.3	0.66	261.9	16.3	263.0	22.5	271.4	167.5	261.9	16.3	3.5	0.4
DV 7/25/15_2-12	542	264	2.1	0.0516	8.8	0.2992	10.4	0.0421	5.5	0.53	265.6	14.3	265.8	24.3	266.4	202.0	265.6	14.3	0.3	0.1
DV 7/25/15_2-115	227	413	0.6	0.0543	12.6	0.3173	14.7	0.0424	7.7	0.52	267.5	20.1	279.9	36.0	382.6	282.3	267.5	20.1	30.1	4.4
DV 7/25/15_2-31	2541	1671	1.5	0.0520	6.6	0.3130	9.4	0.0436	6.7	0.71	275.1	18.0	276.5	22.7	286.5	151.5	275.1	18.0	4.0	0.5
DV 7/25/15_2-177	384	338	1.1	0.0539	10.6	0.3278	13.9	0.0441	9.0	0.64	278.2	24.4	287.9	34.8	366.2	239.0	278.2	24.4	24.0	3.4
DV 7/25/15_2-157	1342	777	1.7	0.0512	7.8	0.3129	11.1	0.0443	7.8	0.70	279.3	21.4	276.4	26.7	249.7	180.5	279.3	21.4	-11.8	-1.1

DV 7/25/15_2-46	2031	337	6.0	0.0518	8.7	0.3162	12.5	0.0443	9.0	0.72	279.4	24.7	279.0	30.5	275.7	199.0	279.4	24.7	-1.3	-0.2
DV 7/25/15_2-139	1774	2031	0.9	0.0519	8.7	0.3181	12.1	0.0444	8.5	0.70	280.2	23.2	280.4	29.7	280.2	199.1	280.2	23.2	0.0	0.1
DV 7/25/15_2-76	886	380	2.3	0.0528	16.7	0.3249	17.9	0.0446	6.6	0.36	281.3	18.1	285.7	44.7	319.6	379.5	281.3	18.1	12.0	1.5
DV 7/25/15_2-144	573	234	2.4	0.0542	6.8	0.3346	8.6	0.0447	5.4	0.62	281.8	14.8	293.0	21.9	381.3	151.9	281.8	14.8	26.1	3.8
DV 7/25/15_2-86	1577	717	2.2	0.0493	12.1	0.3081	13.4	0.0453	6.0	0.44	285.5	16.7	272.7	32.2	162.6	282.4	285.5	16.7	-75.6	-4.7
DV 7/25/15_2-50	6991	1448	4.8	0.0528	8.3	0.3310	12.2	0.0455	8.9	0.73	286.6	25.0	290.3	30.7	320.2	188.5	286.6	25.0	10.5	1.3
DV 7/25/15_2-121	812	798	1.0	0.0512	7.5	0.3232	10.1	0.0458	6.8	0.67	288.5	19.3	284.4	25.1	248.4	172.5	288.5	19.3	-16.1	-1.4
DV 7/25/15_2-150	381	169	2.2	0.0516	11.6	0.3273	14.7	0.0460	9.1	0.61	289.7	25.7	287.5	36.9	267.1	266.9	289.7	25.7	-8.5	-0.8
DV 7/25/15_2-135	1156	1530	0.8	0.0538	5.5	0.3419	7.5	0.0460	5.1	0.68	289.9	14.6	298.6	19.5	364.6	124.7	289.9	14.6	20.5	2.9
DV 7/25/15_2-1	243	105	2.3	0.0651	11.1	0.4167	12.8	0.0464	6.3	0.50	292.6	17.9	353.7	38.2	776.1	233.6	292.6	17.9	62.3	17.3
DV 7/25/15_2-23	3247	1977	1.6	0.0530	6.4	0.3449	9.4	0.0472	6.9	0.73	297.1	20.0	300.8	24.5	327.4	146.1	297.1	20.0	9.2	1.2
DV 7/25/15_2-81	2250	894	2.5	0.0558	9.7	0.3641	11.4	0.0472	6.1	0.53	297.5	17.8	315.2	31.0	446.4	215.1	297.5	17.8	33.3	5.6
DV 7/25/15_2-187	257	214	1.2	0.0528	14.2	0.3498	16.9	0.0480	9.0	0.54	302.0	26.7	304.5	44.4	321.7	323.4	302.0	26.7	6.1	0.8
DV 7/25/15_2-179	636	288	2.2	0.0536	8.3	0.3711	11.8	0.0502	8.3	0.70	315.6	25.6	320.5	32.3	354.8	188.5	315.6	25.6	11.1	1.5
DV 7/25/15_2-183	4225	3895	1.1	0.0529	7.6	0.3686	11.1	0.0505	8.1	0.73	317.4	25.2	318.6	30.4	325.5	173.1	317.4	25.2	2.5	0.4
DV 7/25/15_2-18	858	502	1.7	0.0514	9.1	0.3709	12.8	0.0523	9.0	0.70	328.4	28.9	320.3	35.1	260.6	208.4	328.4	28.9	-26.0	-2.5
DV 7/25/15_2-101	2182	2077	1.1	0.0522	9.5	0.3960	13.3	0.0550	9.3	0.70	345.1	31.2	338.8	38.3	293.0	217.7	345.1	31.2	-17.8	-1.9
DV 7/25/15_2-25	808	224	3.6	0.0543	8.7	0.4196	11.3	0.0560	7.3	0.64	351.4	25.0	355.8	34.1	382.1	195.6	351.4	25.0	8.0	1.2
DV 7/25/15_2-164	262	148	1.8	0.0561	9.4	0.4402	11.7	0.0569	6.9	0.59	356.5	24.0	370.4	36.2	456.9	208.5	356.5	24.0	22.0	3.8
DV 7/25/15_2-196	3181	983	3.2	0.0540	8.7	0.4421	12.5	0.0593	9.0	0.72	371.5	32.3	371.7	38.8	370.2	195.8	371.5	32.3	-0.3	0.1
DV 7/25/15_2-110	746	288	2.6	0.0558	6.6	0.4641	8.9	0.0603	6.1	0.68	377.3	22.4	387.1	28.8	444.1	145.6	377.3	22.4	15.0	2.5
DV 7/25/15_2-107	3386	1273	2.7	0.0558	6.4	0.4736	9.2	0.0615	6.6	0.71	384.8	24.7	393.7	30.0	444.2	143.0	384.8	24.7	13.4	2.3
DV 7/25/15_2-176	396	137	2.9	0.0531	11.8	0.4512	15.2	0.0616	9.6	0.63	385.1	35.9	378.1	47.9	334.4	266.9	385.1	35.9	-15.2	-1.8
DV 7/25/15_2-38	1105	790	1.4	0.0546	6.4	0.4709	9.0	0.0625	6.4	0.70	390.7	24.3	391.8	29.3	397.3	143.2	390.7	24.3	1.6	0.3
DV 7/25/15_2-88	297	242	1.2	0.0525	9.8	0.4548	11.8	0.0628	6.6	0.55	392.5	25.0	380.6	37.4	307.2	223.4	392.5	25.0	-27.8	-3.1
DV 7/25/15_2-188	413	292	1.4	0.0546	7.1	0.4794	9.3	0.0636	6.1	0.65	397.6	23.5	397.7	30.6	395.9	158.1	397.6	23.5	-0.4	0.0
DV 7/25/15_2-65	1039	743	1.4	0.0564	6.4	0.5011	8.7	0.0644	6.0	0.69	402.2	23.5	412.4	29.7	467.8	141.0	402.2	23.5	14.0	2.5
DV 7/25/15_2-114	673	336	2.0	0.0564	6.3	0.5015	8.8	0.0644	6.1	0.69	402.2	23.7	412.7	29.7	469.7	140.3	402.2	23.7	14.4	2.5
DV 7/25/15_2-85	9443	3108	3.0	0.0571	6.8	0.5107	10.0	0.0648	7.4	0.74	404.5	29.0	418.9	34.3	497.1	149.1	404.5	29.0	18.6	3.4
DV 7/25/15_2-84	999	675	1.5	0.0549	6.0	0.4930	8.2	0.0651	5.7	0.69	406.7	22.6	407.0	27.7	406.8	134.1	406.7	22.6	0.0	0.1
DV 7/25/15_2-6	7140	5166	1.4	0.0565	6.5	0.5103	9.2	0.0655	6.4	0.70	409.2	25.3	418.7	31.4	470.9	144.5	409.2	25.3	13.1	2.3
DV 7/25/15_2-89	1329	452	2.9	0.0547	5.2	0.4962	7.2	0.0657	5.0	0.69	410.5	20.0	409.1	24.2	399.7	116.4	410.5	20.0	-2.7	-0.3
DV 7/25/15_2-102	1602	636	2.5	0.0548	5.9	0.5014	8.4	0.0663	6.1	0.72	414.0	24.5	412.7	28.6	402.8	131.2	414.0	24.5	-2.8	-0.3
DV 7/25/15_2-8	2546	485	5.2	0.0554	6.1	0.5110	8.3	0.0669	5.6	0.68	417.2	22.7	419.1	28.6	429.0	136.0	417.2	22.7	2.7	0.5
DV 7/25/15_2-140	938	1277	0.7	0.0579	8.3	0.5359	12.2	0.0670	9.0	0.73	418.3	36.3	435.7	43.2	526.5	182.0	418.3	36.3	20.6	4.0

DV 7/25/15_2-172	2018	1112	1.8	0.0573	7.0	0.5329	10.0	0.0675	7.1	0.71	420.8	29.0	433.7	35.2	501.6	154.5	420.8	29.0	16.1	3.0
DV 7/25/15_2-154	3312	2212	1.5	0.0769	12.1	0.7170	13.8	0.0676	6.6	0.48	421.5	27.0	548.9	58.5	1118.4	241.7	421.5	27.0	62.3	23.2
DV 7/25/15_2-55	1859	306	6.1	0.0561	6.5	0.5244	9.1	0.0677	6.4	0.70	422.6	26.3	428.1	31.8	455.3	143.8	422.6	26.3	7.2	1.3
DV 7/25/15_2-70	1209	553	2.2	0.0573	6.6	0.5396	9.4	0.0682	6.8	0.72	425.6	27.9	438.2	33.5	502.6	144.5	425.6	27.9	15.3	2.9
DV 7/25/15_2-68	527	2583	0.2	0.0662	14.8	0.6332	16.6	0.0693	7.5	0.45	432.2	31.4	498.1	65.5	811.2	310.5	432.2	31.4	46.7	13.2
DV 7/25/15_2-29	5136	3789	1.4	0.0541	6.2	0.5177	9.2	0.0694	6.8	0.74	432.4	28.5	423.6	31.8	374.1	139.3	432.4	28.5	-15.6	-2.1
DV 7/25/15_2-87	1471	889	1.7	0.0557	8.4	0.5406	12.1	0.0703	8.7	0.72	438.0	36.9	438.8	43.0	441.1	186.4	438.0	36.9	0.7	0.2
DV 7/25/15_2-36	994	345	2.9	0.0530	8.3	0.5169	11.6	0.0706	8.2	0.70	440.1	34.9	423.1	40.3	330.5	188.6	440.1	34.9	-33.2	-4.0
DV 7/25/15_2-78	6246	2496	2.5	0.0557	6.6	0.5458	9.6	0.0710	7.0	0.73	441.9	29.9	442.3	34.3	442.0	145.7	441.9	29.9	0.0	0.1
DV 7/25/15_2-83	1773	1685	1.1	0.0537	8.4	0.5261	12.1	0.0710	8.7	0.72	442.1	37.0	429.2	42.2	358.5	189.7	442.1	37.0	-23.3	-3.0
DV 7/25/15_2-193	1320	898	1.5	0.0551	6.8	0.5443	9.7	0.0716	6.9	0.71	445.6	29.7	441.2	34.6	415.7	152.1	445.6	29.7	-7.2	-1.0
DV 7/25/15_2-34	4253	2468	1.7	0.0555	5.6	0.5490	8.2	0.0717	6.0	0.73	446.4	26.0	444.3	29.5	432.4	125.6	446.4	26.0	-3.2	-0.5
DV 7/25/15_2-165	1620	858	1.9	0.0565	6.0	0.5605	8.5	0.0719	6.1	0.71	447.8	26.4	451.9	31.0	471.2	132.2	447.8	26.4	5.0	0.9
DV 7/25/15_2-48	759	531	1.4	0.0756	14.8	0.7519	17.6	0.0722	9.5	0.54	449.2	41.1	569.3	76.8	1083.7	297.7	449.2	41.1	58.5	21.1
DV 7/25/15_2-54	1847	2310	0.8	0.0561	6.0	0.5622	8.5	0.0727	6.0	0.71	452.1	26.3	453.0	31.0	454.8	132.7	452.1	26.3	0.6	0.2
DV 7/25/15_2-32	3048	1392	2.2	0.0566	9.1	0.5677	13.3	0.0727	9.7	0.73	452.7	42.6	456.5	49.0	474.5	201.7	452.7	42.6	4.6	0.8
DV 7/25/15_2-56	886	395	2.2	0.0592	7.5	0.5981	10.8	0.0732	7.8	0.72	455.3	34.2	476.0	41.0	574.1	162.4	455.3	34.2	20.7	4.3
DV 7/25/15_2-185	790	366	2.2	0.0554	7.3	0.5698	10.5	0.0745	7.5	0.72	463.4	33.7	457.9	38.6	427.9	163.1	463.4	33.7	-8.3	-1.2
DV 7/25/15_2-26	3875	621	6.2	0.0586	5.0	0.6453	7.3	0.0797	5.4	0.73	494.4	25.8	505.6	29.2	554.1	108.9	494.4	25.8	10.8	2.2
DV 7/25/15_2-95	1030	623	1.7	0.0563	9.2	0.6362	13.1	0.0820	9.4	0.71	507.8	45.7	500.0	51.6	462.9	202.9	507.8	45.7	-9.7	-1.6
DV 7/25/15_2-146	361	585	0.6	0.0559	9.2	0.6401	12.0	0.0830	7.6	0.63	513.8	37.6	502.4	47.4	448.4	205.5	513.8	37.6	-14.6	-2.3
DV 7/25/15_2-123	727	729	1.0	0.0522	20.4	0.6167	22.3	0.0857	8.8	0.40	529.8	44.9	487.8	86.5	292.4	466.8	529.8	44.9	-81.2	-8.6
DV 7/25/15_2-79	659	204	3.2	0.0624	10.9	0.8213	13.2	0.0953	7.5	0.56	586.8	41.9	608.8	60.5	689.5	232.7	586.8	41.9	14.9	3.6
DV 7/25/15_2-5	1042	781	1.3	0.0594	8.9	0.8008	12.6	0.0978	8.9	0.71	601.3	51.0	597.3	56.8	581.6	192.3	601.3	51.0	-3.4	-0.7
DV 7/25/15_2-149	2319	333	7.0	0.0643	8.1	0.9258	13.4	0.1043	10.7	0.80	639.3	65.4	665.4	65.7	752.8	171.4	639.3	65.4	15.1	3.9
DV 7/25/15_2-10	921	583	1.6	0.0621	6.5	0.8980	9.0	0.1049	6.2	0.69	643.1	38.1	650.7	43.5	676.3	139.8	643.1	38.1	4.9	1.2
DV 7/25/15_2-100	2147	828	2.6	0.0652	4.8	1.0528	7.0	0.1170	5.1	0.72	713.3	34.2	730.3	36.2	781.0	101.8	713.3	34.2	8.7	2.3
DV 7/25/15_2-116	346	569	0.6	0.0624	8.9	1.0632	11.3	0.1235	7.0	0.62	750.8	49.5	735.4	59.0	686.9	189.1	750.8	49.5	-9.3	-2.1
DV 7/25/15_2-182	552	723	0.8	0.0697	7.8	1.2201	10.1	0.1269	6.5	0.64	770.4	47.4	809.8	56.6	918.2	159.8	770.4	47.4	16.1	4.9
DV 7/25/15_2-190	517	342	1.5	0.0645	6.8	1.1416	10.0	0.1282	7.3	0.73	777.7	53.3	773.2	53.9	757.9	143.9	777.7	53.3	-2.6	-0.6
DV 7/25/15_2-92	481	558	0.9	0.0641	5.5	1.1518	7.8	0.1303	5.6	0.71	789.7	41.3	778.1	42.3	743.5	116.5	789.7	41.3	-6.2	-1.5
DV 7/25/15_2-24	1150	989	1.2	0.0659	6.3	1.2351	9.1	0.1358	6.6	0.72	820.9	51.0	816.7	51.3	802.8	132.7	820.9	51.0	-2.3	-0.5
DV 7/25/15_2-91	1082	358	3.0	0.0663	5.6	1.2566	8.1	0.1374	6.0	0.73	829.8	46.5	826.4	45.9	815.7	116.3	829.8	46.5	-1.7	-0.4
DV 7/25/15_2-119	442	220	2.0	0.0651	6.5	1.2562	9.2	0.1398	6.5	0.70	843.4	51.2	826.2	51.9	778.0	137.1	843.4	51.2	-8.4	-2.1
DV 7/25/15_2-71	2578	941	2.7	0.0700	5.0	1.3955	7.2	0.1444	5.2	0.72	869.4	42.4	887.0	42.4	929.2	102.1	869.4	42.4	6.4	2.0

DV 7/25/15_2-73	3143	878	3.6	0.0679	5.2	1.3669	7.6	0.1458	5.5	0.73	877.5	45.5	874.8	44.3	866.1	107.4	877.5	45.5	-1.3	-0.3
DV 7/25/15_2-49	1042	187	5.6	0.0703	7.3	1.4369	10.6	0.1482	7.8	0.73	891.0	64.5	904.4	63.5	937.7	149.3	891.0	64.5	5.0	1.5
DV 7/25/15_2-74	900	242	3.7	0.0690	6.0	1.4823	8.5	0.1556	6.1	0.71	932.3	53.2	923.2	51.7	899.4	122.9	899.4	122.9	-3.7	-1.0
DV 7/25/15_2-80	845	437	1.9	0.0693	5.6	1.4687	7.6	0.1535	5.2	0.68	920.4	44.9	917.6	46.1	909.0	115.4	909.0	115.4	-1.3	-0.3
DV 7/25/15_2-42	3375	1481	2.3	0.0698	6.5	1.4702	9.6	0.1529	7.1	0.73	917.0	60.3	918.2	57.9	921.2	134.4	921.2	134.4	0.5	0.1
DV 7/25/15_2-11	1494	223	6.7	0.0703	5.9	1.4715	8.3	0.1518	5.9	0.71	910.9	49.8	918.7	50.4	936.7	121.1	936.7	121.1	2.8	0.9
DV 7/25/15_2-134	229	87	2.6	0.0705	7.9	1.6148	11.1	0.1660	7.8	0.70	990.2	71.2	976.0	69.6	942.2	162.5	942.2	162.5	-5.1	-1.5
DV 7/25/15_2-97	4147	2108	2.0	0.0716	6.5	1.5961	9.4	0.1615	6.8	0.72	965.4	60.9	968.7	58.7	974.8	133.4	974.8	133.4	1.0	0.3
DV 7/25/15_2-2	4394	1546	2.8	0.0718	6.0	1.5690	8.1	0.1584	5.3	0.66	948.0	46.6	958.0	50.1	980.6	123.0	980.6	123.0	3.3	1.1
DV 7/25/15_2-195	1995	602	3.3	0.0720	6.5	1.5997	9.6	0.1609	7.1	0.73	961.6	63.0	970.1	60.0	986.7	133.2	986.7	133.2	2.6	0.9
DV 7/25/15_2-161	666	463	1.4	0.0728	7.4	1.6942	10.7	0.1687	7.8	0.72	1004.8	72.4	1006.4	68.6	1008.6	150.2	1008.6	150.2	0.4	0.2
DV 7/25/15_2-171	2313	1417	1.6	0.0733	7.1	1.5643	10.3	0.1547	7.5	0.72	927.4	64.5	956.2	63.8	1022.0	143.9	1022.0	143.9	9.3	3.0
DV 7/25/15_2-69	697	475	1.5	0.0750	7.4	1.9761	10.8	0.1909	7.9	0.73	1126.5	81.3	1107.4	72.9	1067.9	149.0	1067.9	149.0	-5.5	-1.7
DV 7/25/15_2-192	706	526	1.3	0.0754	6.8	1.6244	10.0	0.1561	7.3	0.73	934.9	63.3	979.7	62.7	1078.9	137.3	1078.9	137.3	13.3	4.6
DV 7/25/15_2-53	1060	425	2.5	0.0759	6.3	2.0150	8.8	0.1923	6.2	0.70	1133.9	64.9	1120.6	60.0	1092.7	125.7	1092.7	125.7	-3.8	-1.2
DV 7/25/15_2-168	762	528	1.4	0.0768	6.0	1.8705	8.9	0.1765	6.5	0.73	1047.9	63.3	1070.7	58.7	1116.4	120.2	1116.4	120.2	6.1	2.1
DV 7/25/15_2-143	900	279	3.2	0.0782	9.0	1.8493	14.4	0.1714	11.3	0.78	1019.8	106.2	1063.2	95.4	1151.4	179.7	1151.4	179.7	11.4	4.1
DV 7/25/15_2-118	1566	38	40.8	0.0847	7.1	2.6445	10.2	0.2262	7.4	0.72	1314.4	87.7	1313.1	75.7	1309.1	138.5	1309.1	138.5	-0.4	-0.1
DV 7/25/15_2-106	977	702	1.4	0.0892	5.8	2.8681	8.5	0.2329	6.2	0.73	1349.6	75.8	1373.6	64.1	1409.0	111.7	1409.0	111.7	4.2	1.7
DV 7/25/15_2-167	2889	2487	1.2	0.0897	7.4	2.6501	10.8	0.2142	7.9	0.73	1251.1	90.3	1314.7	79.9	1418.9	141.0	1418.9	141.0	11.8	4.8
DV 7/25/15_2-59	381	218	1.7	0.0910	6.6	3.0481	9.4	0.2425	6.7	0.71	1399.7	84.3	1419.7	71.8	1447.5	125.3	1447.5	125.3	3.3	1.4
DV 7/25/15_2-126	1481	181	8.2	0.0996	5.9	4.3415	8.9	0.3158	6.7	0.75	1769.4	104.0	1701.3	73.7	1616.5	109.6	1616.5	109.6	-9.5	-4.0
DV 7/25/15_2-186	528	353	1.5	0.1004	6.0	3.8954	8.8	0.2811	6.5	0.74	1596.7	92.6	1612.7	71.4	1632.0	110.6	1632.0	110.6	2.2	1.0
DV 7/25/15_2-90	1527	731	2.1	0.1015	8.1	3.8265	12.7	0.2733	9.8	0.77	1557.7	135.2	1598.3	102.4	1651.0	150.7	1651.0	150.7	5.7	2.5
DV 7/25/15_2-4	2425	2329	1.0	0.1031	6.1	3.4982	8.2	0.2460	5.4	0.67	1417.8	69.0	1526.8	64.9	1680.8	113.0	1680.8	113.0	15.6	7.1
DV 7/25/15_2-99	180	159	1.1	0.1060	6.3	4.0287	9.0	0.2754	6.4	0.71	1568.1	88.8	1640.0	73.0	1732.0	116.3	1732.0	116.3	9.5	4.4
DV 7/25/15_2-111	1783	223	8.0	0.1079	4.9	4.4593	7.1	0.2996	5.1	0.72	1689.2	76.5	1723.4	58.7	1763.6	89.3	1763.6	89.3	4.2	2.0
DV 7/25/15_2-45	286	191	1.5	0.1090	7.3	4.5331	10.6	0.3016	7.8	0.73	1699.1	116.1	1737.1	88.4	1783.3	132.7	1783.3	132.7	4.7	2.2
DV 7/25/15_2-40	2606	181	14.4	0.1103	6.4	4.6117	9.3	0.3031	6.9	0.73	1706.6	102.8	1751.4	78.1	1805.0	116.7	1805.0	116.7	5.4	2.6
DV 7/25/15_2-20	160	161	1.0	0.1115	6.5	5.2500	9.4	0.3410	6.7	0.72	1891.7	110.3	1860.8	80.1	1824.8	118.6	1824.8	118.6	-3.7	-1.7
DV 7/25/15_2-19	1436	140	10.3	0.1116	7.9	4.7790	11.4	0.3103	8.3	0.73	1742.2	126.9	1781.2	96.4	1825.6	143.0	1825.6	143.0	4.6	2.2
DV 7/25/15_2-33	3214	371	8.7	0.1123	9.9	5.3424	14.3	0.3449	10.4	0.72	1910.3	172.6	1875.7	123.3	1836.3	179.1	1836.3	179.1	-4.0	-1.8
DV 7/25/15_2-180	1122	514	2.2	0.1130	5.9	5.4019	8.8	0.3464	6.6	0.74	1917.3	109.1	1885.1	75.9	1848.7	107.4	1848.7	107.4	-3.7	-1.7
DV 7/25/15_2-98	764	349	2.2	0.1132	6.9	5.2538	10.0	0.3365	7.3	0.72	1869.6	117.7	1861.4	85.5	1850.9	125.4	1850.9	125.4	-1.0	-0.4
DV 7/25/15_2-151	633	232	2.7	0.1134	9.4	5.5331	13.7	0.3537	10.0	0.73	1952.1	167.7	1905.8	118.0	1854.2	169.4	1854.2	169.4	-5.3	-2.4

DV 7/25/15_2-178	805	231	3.5	0.1144	5.8	5.3450	8.5	0.3388	6.2	0.73	1880.7	101.7	1876.1	72.5	1869.9	103.8	1869.9	103.8	-0.6	-0.2
DV 7/25/15_2-22	1155	329	3.5	0.1153	8.2	5.5008	11.7	0.3457	8.3	0.71	1913.9	137.5	1900.7	100.6	1884.5	148.2	1884.5	148.2	-1.6	-0.7
DV 7/25/15_2-64	764	208	3.7	0.1155	5.6	4.6918	8.1	0.2943	5.8	0.72	1662.8	85.7	1765.8	67.6	1887.7	100.7	1887.7	100.7	11.9	5.8
DV 7/25/15_2-14	949	471	2.0	0.1197	5.3	5.6045	7.6	0.3394	5.5	0.72	1883.7	89.2	1916.8	65.7	1951.8	95.0	1951.8	95.0	3.5	1.7
DV 7/25/15_2-162	1372	833	1.6	0.1230	5.2	6.2377	7.7	0.3675	5.7	0.74	2017.6	99.2	2009.8	67.3	2000.6	91.8	2000.6	91.8	-0.9	-0.4
DV 7/25/15_2-112	3479	2375	1.5	0.1312	9.2	6.5384	13.0	0.3610	9.3	0.71	1986.9	158.6	2051.1	115.2	2114.6	160.8	2114.6	160.8	6.0	3.1
DV 7/25/15_2-129	6481	677	9.6	0.1566	4.6	9.8664	6.7	0.4565	4.9	0.73	2424.2	99.3	2422.4	61.8	2419.2	77.9	2419.2	77.9	-0.2	-0.1
DV 7/25/15_2-75	649	224	2.9	0.1579	6.2	8.7684	10.2	0.4023	8.2	0.80	2179.7	150.9	2314.2	93.4	2433.5	105.1	2433.5	105.1	10.4	5.8
DV 7/25/15_2-191	593	633	0.9	0.1599	8.9	8.5927	12.4	0.3893	8.7	0.70	2119.5	157.5	2295.8	113.6	2454.5	150.5	2454.5	150.5	13.6	7.7
DV 7/25/15_2-117	1693	989	1.7	0.1616	6.4	10.3682	9.5	0.4647	7.1	0.74	2460.4	144.4	2468.2	88.1	2473.0	107.6	2473.0	107.6	0.5	0.3
DV 7/25/15_2-160	643	368	1.7	0.1630	6.8	11.2575	10.1	0.5006	7.4	0.73	2616.4	159.9	2544.7	94.3	2486.8	115.4	2486.8	115.4	-5.2	-2.8
DV 7/25/15_2-27	1349	844	1.6	0.1658	6.2	10.8136	9.1	0.4725	6.7	0.73	2494.5	138.7	2507.2	84.9	2515.8	104.3	2515.8	104.3	0.8	0.5
DV 7/25/15_2-44	298	177	1.7	0.1662	7.7	11.3519	11.1	0.4956	8.0	0.72	2594.7	171.2	2552.5	103.8	2519.2	129.6	2519.2	129.6	-3.0	-1.7
DV 7/25/15_2-153	231	298	0.8	0.1690	6.0	11.4298	8.7	0.4901	6.4	0.73	2571.2	135.1	2558.9	81.5	2547.7	100.3	2547.7	100.3	-0.9	-0.5
DV 7/25/15_2-131	3363	1379	2.4	0.1708	7.1	9.7669	12.3	0.4143	10.1	0.82	2234.4	190.0	2413.0	113.6	2565.8	118.4	2565.8	118.4	12.9	7.4
DV 7/25/15_2-77	519	303	1.7	0.1820	5.2	12.5079	7.4	0.4978	5.4	0.71	2604.5	114.7	2643.3	69.9	2671.6	86.1	2671.6	86.1	2.5	1.5
DV 7/25/15_2-21	949	425	2.2	0.1951	7.9	12.7770	11.3	0.4746	8.0	0.71	2503.6	166.7	2663.4	106.5	2785.3	129.9	2785.3	129.9	10.1	6.0
DV 7/25/15_2-93	197	87	2.3	0.2487	7.8	21.3296	11.8	0.6216	8.9	0.75	3116.2	219.2	3153.7	114.7	3176.5	123.7	3176.5	123.7	1.9	1.2
DV 7/25/15_2-189	403	317	1.3	0.2519	9.7	22.2989	14.4	0.6412	10.6	0.74	3193.8	267.6	3196.8	140.5	3197.0	153.4	3197.0	153.4	0.1	0.1
Data Rejected From Population Analyses																				
DV 7/25/15_2-43	800	762	1.0	0.0497	11.0	0.2612	15.0	0.0381	10.2	0.68	241.1	24.2	235.6	31.5	181.2	256.4	241.1	24.2	-33.1	-2.3
DV 7/25/15_2-60	1115	1025	1.1	0.0925	12.8	0.5790	14.9	0.0453	7.7	0.52	285.8	21.6	463.8	55.7	1478.3	242.7	285.8	21.6	80.7	38.4
DV 7/25/15_2-72	870	483	1.8	0.0525	10.9	0.3351	15.2	0.0462	10.7	0.70	291.4	30.5	293.5	38.8	307.7	247.2	291.4	30.5	5.3	0.7
DV 7/25/15_2-109	4539	1092	4.2	0.0532	10.2	0.3733	14.8	0.0508	10.7	0.72	319.5	33.5	322.1	40.9	338.6	232.0	319.5	33.5	5.6	0.8
DV 7/25/15_2-155	3810	1773	2.1	0.0527	9.3	0.3706	13.7	0.0510	10.0	0.73	320.7	31.4	320.1	37.5	314.0	211.0	320.7	31.4	-2.1	-0.2
DV 7/25/15_2-173	1980	804	2.5	0.0562	11.3	0.5199	16.3	0.0671	11.8	0.72	418.8	47.7	425.1	56.7	458.5	250.7	418.8	47.7	8.7	1.5
DV 7/25/15_2-159	842	844	1.0	0.0629	9.2	0.5932	14.3	0.0683	10.9	0.76	426.0	45.0	472.9	54.1	705.7	196.7	426.0	45.0	39.6	9.9
DV 7/25/15_2-184	835	1171	0.7	0.0475	37.1	0.4492	38.6	0.0686	10.7	0.28	427.6	44.1	376.7	121.9	72.4	881.1	427.6	44.1	-490.5	-13.5
DV 7/25/15_2-16	1062	444	2.4	0.0599	12.3	0.5742	17.7	0.0695	12.7	0.72	433.3	53.3	460.7	65.6	598.4	266.6	433.3	53.3	27.6	6.0
DV 7/25/15_2-17	540	202	2.7	0.0570	12.9	0.5481	17.6	0.0697	12.0	0.68	434.2	50.5	443.7	63.4	491.9	283.5	434.2	50.5	11.7	2.2
DV 7/25/15_2-152	207	174	1.2	0.0511	23.7	0.4948	26.8	0.0702	12.4	0.46	437.5	52.5	408.2	90.1	243.4	546.3	437.5	52.5	-79.7	-7.2
DV 7/25/15_2-137	1358	155	8.7	0.0585	21.3	0.6587	31.7	0.0816	23.5	0.74	505.7	114.3	513.8	128.4	547.9	464.1	505.7	114.3	7.7	1.6
DV 7/25/15_2-175	1350	660	2.0	0.0626	7.8	0.7630	12.7	0.0883	10.0	0.79	545.4	52.4	575.7	55.8	696.1	166.6	545.4	52.4	21.7	5.3
DV 7/25/15_2-61	671	103	6.5	0.0657	7.4	0.9210	10.1	0.1015	6.9	0.68	623.1	40.8	662.9	49.1	798.1	155.5	623.1	40.8	21.9	6.0
DV 7/25/15_2-138	2833	1233	2.3	0.0668	7.7	0.9562	12.6	0.1038	10.0	0.79	636.5	60.9	681.4	62.9	830.6	161.0	636.5	60.9	23.4	6.6

DV 7/25/15_2-125	638	1104	0.6	0.0576	8.5	0.8329	12.2	0.1047	8.7	0.72	641.8	53.3	615.2	56.1	516.2	186.1	641.8	53.3	-24.3	-4.3
DV 7/25/15_2-58	108	437	0.2	0.0673	13.2	1.1111	17.1	0.1197	10.9	0.64	728.6	75.3	758.7	91.7	845.7	273.9	728.6	75.3	13.8	4.0
DV 7/25/15_2-41	913	844	1.1	0.0679	16.1	1.1221	21.5	0.1198	14.3	0.66	729.5	98.4	764.0	116.0	866.1	334.4	729.5	98.4	15.8	4.5
DV 7/25/15_2-3	722	592	1.2	0.0717	8.1	1.2301	11.7	0.1243	8.4	0.72	755.4	60.0	814.4	65.7	978.5	165.4	755.4	60.0	22.8	7.2
DV 7/25/15_2-156	848	117	7.3	0.0627	8.4	1.0972	12.2	0.1268	8.9	0.72	769.5	64.3	752.0	65.0	698.8	179.9	769.5	64.3	-10.1	-2.3
DV 7/25/15_2-15	1302	929	1.4	0.0651	14.3	1.1467	20.7	0.1277	14.9	0.72	774.6	108.9	775.7	112.5	777.3	300.3	774.6	108.9	0.4	0.1
DV 7/25/15_2-57	3037	1806	1.7	0.1041	30.3	1.8544	31.9	0.1291	10.0	0.31	782.5	73.9	1065.0	213.7	1698.0	558.7	782.5	73.9	53.9	26.5
DV 7/25/15_2-124	1118	1092	1.0	0.0661	6.6	1.5081	9.5	0.1654	6.9	0.73	986.6	63.4	933.7	58.2	808.6	137.1	808.6	137.1	-22.0	-5.7
DV 7/25/15_2-128	247	320	0.8	0.0675	7.8	1.5055	11.1	0.1616	7.9	0.71	965.5	70.5	932.6	67.7	853.6	162.5	853.6	162.5	-13.1	-3.5
DV 7/25/15_2-163	565	164	3.4	0.0680	12.4	1.3706	18.2	0.1462	13.3	0.73	879.6	109.3	876.4	107.0	867.3	257.1	879.6	109.3	-1.4	-0.4
DV 7/25/15_2-130	1791	250	7.2	0.0688	6.5	1.6347	9.3	0.1721	6.6	0.71	1023.7	62.8	983.7	58.6	893.4	134.8	893.4	134.8	-14.6	-4.1
DV 7/25/15_2-127	1332	699	1.9	0.0697	5.5	1.6479	8.2	0.1712	6.1	0.74	1018.8	57.1	988.7	51.7	920.5	113.3	920.5	113.3	-10.7	-3.0
DV 7/25/15_2-103	1107	422	2.6	0.0797	16.5	1.8150	18.1	0.1649	7.5	0.41	983.9	68.6	1050.9	119.2	1190.6	325.7	1190.6	325.7	17.4	6.4
DV 7/25/15_2-62	2497	292	8.5	0.0815	6.7	1.7964	11.1	0.1596	8.9	0.80	954.5	78.7	1044.1	72.4	1234.3	130.9	1234.3	130.9	22.7	8.6
DV 7/25/15_2-94	480	325	1.5	0.0849	10.7	2.4395	13.8	0.2083	8.9	0.64	1219.7	98.6	1254.3	100.0	1313.0	206.7	1313.0	206.7	7.1	2.8
DV 7/25/15_2-52	533	373	1.4	0.0935	11.8	3.2996	16.8	0.2556	12.0	0.71	1467.1	156.9	1480.9	131.4	1498.9	222.8	1498.9	222.8	2.1	0.9
DV 7/25/15_2-30	2717	229	11.9	0.1043	6.9	2.3765	12.0	0.1651	9.9	0.82	985.2	90.5	1235.6	86.1	1701.7	126.2	1701.7	126.2	42.1	20.3
DV 7/25/15_2-104	489	115	4.3	0.1118	11.1	4.7956	16.1	0.3108	11.7	0.72	1744.8	178.4	1784.1	136.1	1828.6	201.6	1828.6	201.6	4.6	2.2
DV 7/25/15_2-132	459	479	1.0	0.1122	10.7	5.0496	15.4	0.3260	11.1	0.72	1818.9	176.0	1827.7	131.2	1836.0	193.5	1836.0	193.5	0.9	0.5
DV 7/25/15_2-66	1418	654	2.2	0.1132	6.2	3.2564	8.8	0.2083	6.2	0.71	1219.9	69.1	1470.7	68.1	1852.0	112.0	1852.0	112.0	34.1	17.1
DV 7/25/15_2-35	2401	867	2.8	0.1135	5.0	3.7547	7.7	0.2398	5.9	0.76	1385.7	73.4	1583.1	61.7	1856.1	90.6	1856.1	90.6	25.3	12.5
DV 7/25/15_2-28	910	219	4.2	0.1178	21.2	5.2705	29.8	0.3243	20.9	0.70	1810.5	329.8	1864.1	259.4	1922.5	380.3	1922.5	380.3	5.8	2.9
DV 7/25/15_2-169	487	190	2.6	0.1235	14.2	6.3640	21.4	0.3735	16.0	0.75	2045.8	280.8	2027.3	189.6	2007.6	251.2	2007.6	251.2	-1.9	-0.9
DV 7/25/15_2-145	804	265	3.0	0.1243	14.1	5.9365	20.4	0.3460	14.8	0.72	1915.5	245.4	1966.6	179.4	2019.0	250.2	2019.0	250.2	5.1	2.6
DV 7/25/15_2-198	1199	433	2.8	0.1309	5.6	5.2088	10.5	0.2881	8.9	0.85	1632.3	128.9	1854.0	90.0	2110.5	98.7	2110.5	98.7	22.7	12.0
DV 7/25/15_2-82	3661	4520	0.8	0.1310	17.8	4.2916	23.8	0.2374	15.8	0.66	1373.1	194.8	1691.8	198.1	2111.4	312.2	2111.4	312.2	35.0	18.8
DV 7/25/15_2-96	1335	333	4.0	0.1500	4.8	5.8809	7.3	0.2841	5.6	0.75	1612.1	79.6	1958.4	63.6	2346.1	82.3	2346.1	82.3	31.3	17.7
DV 7/25/15_2-158	306	143	2.1	0.1633	12.4	11.2757	17.4	0.5004	12.2	0.70	2615.6	261.8	2546.2	163.2	2490.2	208.8	2490.2	208.8	-5.0	-2.7
DV 7/25/15_2-67	661	202	3.3	0.2275	12.4	17.3456	16.3	0.5524	10.7	0.65	2835.2	244.5	2954.1	158.0	3034.4	198.5	3034.4	198.5	6.6	4.0

DV 8-08-16_3 37.930° N; 73.993° E

				Isotope ratios							Apparent Ages (Ma)									
				^{207}Pb	±	^{207}Pb	±	^{206}Pb	±		^{206}Pb	±	^{207}Pb	±	^{207}Pb	±		±	% discordance Pb^{206}/U^{238}-Pb^{207}/Pb^{206}	% discordance Pb^{206}/U^{238}-Pb^{207}/U^{325}
Analysis #	U (ppm)	Th (ppm)	U/Th	^{206}Pb	(2%SD)	^{235}U	(2%SD)	^{238}U	(2%SD)	error corr.	^{238}U	(2SD)	^{235}U	(2SD)	^{206}Pb	(2SD)	Best Age	(2SD)		
DV 8/08/16_3-36	383	317	1.2	0.0519	6.6	0.2547	9.0	0.0356	6.2	0.68	225.3	13.6	230.3	18.6	279.8	152.1	225.3	13.6	19.5	2.2
DV 8/08/16_3-39	277	210	1.3	0.0514	6.6	0.2524	8.8	0.0356	5.9	0.67	225.4	13.1	228.5	18.0	258.4	150.7	225.4	13.1	12.8	1.4
DV 8/08/16_3-40	319	267	1.2	0.0513	7.0	0.2550	9.7	0.0360	6.8	0.69	228.2	15.2	230.7	20.1	254.0	161.1	228.2	15.2	10.2	1.1
DV 8/08/16_3-14	223	128	1.7	0.0490	10.1	0.2445	12.4	0.0361	7.2	0.58	228.9	16.2	222.1	24.7	148.4	235.7	228.9	16.2	-54.2	-3.0
DV 8/08/16_3-127	364	207	1.8	0.0517	7.6	0.2587	10.5	0.0362	7.3	0.69	229.4	16.4	233.6	21.9	273.7	174.0	229.4	16.4	16.2	1.8
DV 8/08/16_3-200	337	266	1.3	0.0513	9.2	0.2740	12.2	0.0387	8.0	0.65	244.6	19.2	245.8	26.7	256.0	212.0	244.6	19.2	4.4	0.5
DV 8/08/16_3-182	380	215	1.8	0.0487	11.8	0.2610	13.6	0.0389	6.8	0.50	245.7	16.5	235.5	28.7	132.4	278.0	245.7	16.5	-85.6	-4.3
DV 8/08/16_3-34	242	113	2.1	0.0533	7.7	0.2887	10.5	0.0392	7.2	0.68	247.9	17.6	257.5	23.9	343.5	173.3	247.9	17.6	27.8	3.7
DV 8/08/16_3-76	598	421	1.4	0.0520	6.3	0.2830	8.8	0.0395	6.2	0.70	249.5	15.3	253.0	19.8	283.3	144.4	249.5	15.3	11.9	1.4
DV 8/08/16_3-15	559	416	1.3	0.0513	6.0	0.2793	8.6	0.0395	6.1	0.71	249.6	15.0	250.1	19.0	252.2	139.0	249.6	15.0	1.0	0.2
DV 8/08/16_3-1	322	142	2.3	0.0524	7.1	0.2899	9.8	0.0401	6.8	0.69	253.4	17.0	258.5	22.5	302.0	161.7	253.4	17.0	16.1	2.0
DV 8/08/16_3-113	537	265	2.0	0.0518	6.8	0.2888	9.6	0.0404	6.7	0.71	255.3	16.9	257.6	21.7	275.5	155.0	255.3	16.9	7.3	0.9
DV 8/08/16_3-142	273	282	1.0	0.0535	7.5	0.3009	10.1	0.0408	6.8	0.67	257.7	17.1	267.1	23.7	348.7	169.5	257.7	17.1	26.1	3.5
DV 8/08/16_3-138	698	711	1.0	0.0517	8.4	0.3003	11.9	0.0421	8.5	0.71	265.6	22.1	266.6	27.9	273.4	191.4	265.6	22.1	2.9	0.4
DV 8/08/16_3-70	134	70	1.9	0.0545	9.2	0.3165	12.3	0.0421	8.2	0.66	265.6	21.3	279.2	30.0	392.2	206.9	265.6	21.3	32.3	4.9
DV 8/08/16_3-148	727	335	2.2	0.0532	9.3	0.3325	13.3	0.0452	9.5	0.71	285.3	26.5	291.5	33.7	339.1	211.5	285.3	26.5	15.9	2.1
DV 8/08/16_3-12	245	200	1.2	0.0524	6.6	0.3307	9.1	0.0457	6.3	0.69	288.3	17.7	290.1	23.0	302.0	151.5	288.3	17.7	4.6	0.6
DV 8/08/16_3-125	336	179	1.9	0.0536	7.0	0.3474	9.6	0.0470	6.6	0.69	296.1	19.1	302.8	25.1	352.4	157.2	296.1	19.1	16.0	2.2
DV 8/08/16_3-179	212	139	1.5	0.0425	18.8	0.2842	20.1	0.0485	6.9	0.34	305.2	20.6	254.0	45.1	0.0	454.3	305.2	20.6	-15201091.9	-20.2
DV 8/08/16_3-71	157	68	2.3	0.0590	10.4	0.3991	12.6	0.0490	7.2	0.57	308.3	21.6	341.0	36.5	568.1	226.2	308.3	21.6	45.7	9.6
DV 8/08/16_3-135	199	182	1.1	0.0514	7.0	0.3522	9.1	0.0496	5.9	0.65	312.2	18.1	306.4	24.2	260.4	160.3	312.2	18.1	-19.9	-1.9
DV 8/08/16_3-66	101	56	1.8	0.0518	10.2	0.3739	12.0	0.0523	6.4	0.53	328.4	20.6	322.5	33.2	277.9	232.6	328.4	20.6	-18.2	-1.8
DV 8/08/16_3-61	107	54	2.0	0.0575	10.3	0.4192	13.3	0.0528	8.6	0.64	331.7	27.7	355.4	40.0	511.5	225.4	331.7	27.7	35.2	6.7
DV 8/08/16_3-143	228	94	2.4	0.0543	9.1	0.4024	12.4	0.0537	8.5	0.68	337.3	28.0	343.4	36.3	382.1	204.8	337.3	28.0	11.7	1.8
DV 8/08/16_3-118	299	167	1.8	0.0543	6.9	0.4624	9.7	0.0617	6.7	0.70	386.0	25.2	385.9	31.1	381.9	155.7	386.0	25.2	-1.1	0.0
DV 8/08/16_3-141	402	82	4.9	0.0587	10.6	0.5185	13.5	0.0640	8.4	0.62	399.8	32.4	424.2	46.8	556.5	231.5	399.8	32.4	28.2	5.7
DV 8/08/16_3-102	105	61	1.7	0.0529	16.2	0.4715	17.3	0.0645	6.3	0.36	403.0	24.6	392.2	56.5	326.3	366.9	403.0	24.6	-23.5	-2.7
DV 8/08/16_3-33	89	43	2.1	0.0569	8.2	0.5083	10.5	0.0647	6.6	0.62	404.2	25.7	417.3	35.9	488.1	181.1	404.2	25.7	17.2	3.1
DV 8/08/16_3-192	1006	32	31.0	0.0552	7.4	0.4988	10.4	0.0655	7.4	0.71	408.8	29.4	410.9	35.3	421.0	164.5	408.8	29.4	2.9	0.5
DV 8/08/16_3-42	803	413	1.9	0.0643	5.7	0.5842	8.0	0.0658	5.7	0.70	411.0	22.5	467.2	29.9	751.4	120.0	411.0	22.5	45.3	12.0
DV 8/08/16_3-93	128	70	1.8	0.0553	8.0	0.5139	11.0	0.0673	7.5	0.69	419.8	30.7	421.1	37.8	425.2	178.3	419.8	30.7	1.3	0.3

DV 8/08/16_3-52	143	92	1.5	0.0558	6.8	0.5300	9.3	0.0688	6.5	0.69	428.9	26.8	431.8	32.8	444.8	150.9	428.9	26.8	3.6	0.7
DV 8/08/16_3-149	302	162	1.9	0.0566	6.7	0.5401	9.5	0.0691	6.9	0.72	430.6	28.5	438.5	34.0	477.7	147.4	430.6	28.5	9.9	1.8
DV 8/08/16_3-101	112	44	2.6	0.0586	11.3	0.5769	13.2	0.0713	6.7	0.51	444.2	28.9	462.5	49.0	551.6	247.3	444.2	28.9	19.5	4.0
DV 8/08/16_3-157	197	103	1.9	0.0554	6.8	0.5460	9.3	0.0714	6.3	0.68	444.6	27.1	442.4	33.2	428.5	151.3	444.6	27.1	-3.8	-0.5
DV 8/08/16_3-155	168	99	1.7	0.0548	7.6	0.5422	10.3	0.0717	6.9	0.67	446.4	29.8	439.8	36.6	403.3	170.4	446.4	29.8	-10.7	-1.5
DV 8/08/16_3-199	246	215	1.1	0.0547	6.6	0.5416	8.7	0.0717	5.7	0.65	446.6	24.7	439.5	31.1	400.4	147.7	446.6	24.7	-11.5	-1.6
DV 8/08/16_3-105	50	34	1.5	0.0530	11.3	0.5374	13.6	0.0735	7.5	0.55	457.2	33.1	436.7	48.3	327.0	257.6	457.2	33.1	-39.8	-4.7
DV 8/08/16_3-175	66	24	2.7	0.0586	12.5	0.6053	14.3	0.0749	6.9	0.48	465.5	31.0	480.6	54.8	551.0	273.8	465.5	31.0	15.5	3.1
DV 8/08/16_3-35	69	119	0.6	0.0546	9.5	0.5734	11.8	0.0760	7.1	0.59	472.3	32.3	460.2	43.8	397.8	213.2	472.3	32.3	-18.7	-2.6
DV 8/08/16_3-38	219	59	3.7	0.0627	7.6	0.6700	10.3	0.0774	7.0	0.67	480.6	32.2	520.7	42.0	698.5	162.4	480.6	32.2	31.2	7.7
DV 8/08/16_3-136	60	125	0.5	0.0602	9.3	0.6443	12.0	0.0776	7.7	0.63	481.6	35.5	505.0	48.0	609.9	201.6	481.6	35.5	21.0	4.6
DV 8/08/16_3-116	60	137	0.4	0.0564	9.2	0.6114	11.5	0.0785	6.9	0.60	486.9	32.4	484.5	44.4	469.4	204.1	486.9	32.4	-3.7	-0.5
DV 8/08/16_3-81	865	208	4.2	0.0584	7.0	0.6459	10.0	0.0801	7.2	0.72	496.7	34.6	506.0	39.9	545.7	152.4	496.7	34.6	9.0	1.8
DV 8/08/16_3-188	242	191	1.3	0.0582	7.9	0.6471	10.7	0.0805	7.2	0.68	499.2	34.8	506.7	42.6	538.4	172.0	499.2	34.8	7.3	1.5
DV 8/08/16_3-21	114	77	1.5	0.0568	6.7	0.6366	9.2	0.0812	6.3	0.69	503.1	30.6	500.2	36.2	484.8	147.0	503.1	30.6	-3.8	-0.6
DV 8/08/16_3-117	364	161	2.3	0.0585	7.6	0.6662	10.7	0.0824	7.5	0.70	510.5	36.9	518.4	43.5	550.1	166.3	510.5	36.9	7.2	1.5
DV 8/08/16_3-85	111	88	1.3	0.0625	8.1	0.7128	10.5	0.0827	6.6	0.63	512.1	32.6	546.4	44.2	689.7	173.3	512.1	32.6	25.7	6.3
DV 8/08/16_3-44	196	97	2.0	0.0587	6.5	0.6902	9.2	0.0852	6.5	0.70	527.2	33.0	532.9	38.1	555.1	142.1	527.2	33.0	5.0	1.1
DV 8/08/16_3-86	73	110	0.7	0.0548	9.5	0.6518	11.9	0.0861	7.3	0.61	532.6	37.1	509.6	47.7	405.0	211.7	532.6	37.1	-31.5	-4.5
DV 8/08/16_3-140	103	97	1.1	0.0612	7.2	0.7271	10.0	0.0861	6.9	0.69	532.6	35.3	554.9	42.6	645.2	154.8	532.6	35.3	17.5	4.0
DV 8/08/16_3-124	382	352	1.1	0.0615	6.5	0.7351	9.4	0.0866	6.7	0.72	535.3	34.5	559.5	40.4	655.8	140.0	535.3	34.5	18.4	4.3
DV 8/08/16_3-41	387	131	3.0	0.0594	6.7	0.7140	9.7	0.0870	7.0	0.72	537.9	36.4	547.1	40.9	583.2	144.6	537.9	36.4	7.8	1.7
DV 8/08/16_3-191	148	126	1.2	0.0583	8.7	0.7168	11.5	0.0890	7.5	0.65	549.8	39.7	548.8	48.9	542.6	191.0	549.8	39.7	-1.3	-0.2
DV 8/08/16_3-154	110	81	1.3	0.0595	6.5	0.7498	8.7	0.0913	5.9	0.67	563.5	31.9	568.1	38.0	584.6	140.2	563.5	31.9	3.6	0.8
DV 8/08/16_3-163	856	334	2.6	0.0593	5.7	0.7506	8.2	0.0917	5.9	0.72	565.6	32.1	568.6	35.8	578.2	124.7	565.6	32.1	2.2	0.5
DV 8/08/16_3-156	445	397	1.1	0.0598	5.6	0.7570	8.0	0.0917	5.7	0.71	565.7	30.8	572.3	34.9	596.4	122.1	565.7	30.8	5.1	1.2
DV 8/08/16_3-173	222	189	1.2	0.0612	8.5	0.7847	11.5	0.0930	7.8	0.67	573.1	42.7	588.2	51.5	644.6	183.3	573.1	42.7	11.1	2.6
DV 8/08/16_3-64	89	138	0.6	0.0600	6.9	0.7708	9.2	0.0931	6.2	0.66	574.1	33.9	580.2	40.8	602.1	149.4	574.1	33.9	4.7	1.1
DV 8/08/16_3-197	200	439	0.5	0.0652	7.6	0.8561	10.1	0.0951	6.7	0.66	585.8	37.6	628.0	47.3	781.1	159.0	585.8	37.6	25.0	6.7
DV 8/08/16_3-6	212	64	3.3	0.0593	6.5	0.8025	9.2	0.0981	6.5	0.71	603.0	37.6	598.2	41.6	577.6	141.0	603.0	37.6	-4.4	-0.8
DV 8/08/16_3-180	352	265	1.3	0.0608	6.4	0.8333	8.8	0.0994	6.2	0.69	610.7	35.9	615.4	40.8	630.5	137.3	610.7	35.9	3.1	0.8
DV 8/08/16_3-184	488	309	1.6	0.0607	8.2	0.8369	11.9	0.0999	8.6	0.72	614.1	50.5	617.4	55.1	627.6	177.3	614.1	50.5	2.2	0.5
DV 8/08/16_3-168	751	389	1.9	0.0608	6.4	0.8503	9.2	0.1013	6.5	0.71	621.9	38.7	624.8	42.7	633.1	138.8	621.9	38.7	1.8	0.5
DV 8/08/16_3-8	148	66	2.2	0.0610	6.9	0.8916	10.0	0.1059	7.2	0.72	648.7	44.3	647.2	47.7	639.4	148.7	648.7	44.3	-1.5	-0.2
DV 8/08/16_3-80	72	47	1.5	0.0604	8.2	0.8953	11.2	0.1074	7.6	0.68	657.9	47.6	649.2	53.5	616.7	176.6	657.9	47.6	-6.7	-1.3

DV 8/08/16_3-57	110	131	0.8	0.0653	7.4	1.0363	10.2	0.1150	7.1	0.69	701.7	47.1	722.1	52.8	783.7	155.7	701.7	47.1	10.5	2.8
DV 8/08/16_3-151	1130	401	2.8	0.0662	6.8	1.0788	9.8	0.1181	7.2	0.73	719.6	48.9	743.1	51.9	812.1	141.3	719.6	48.9	11.4	3.2
DV 8/08/16_3-193	1025	234	4.4	0.0633	6.1	1.0785	8.7	0.1235	6.3	0.71	750.5	44.5	742.9	46.1	718.2	130.0	750.5	44.5	-4.5	-1.0
DV 8/08/16_3-75	613	265	2.3	0.0663	7.5	1.1520	10.9	0.1259	7.9	0.72	764.7	57.0	778.2	59.1	814.7	156.8	764.7	57.0	6.1	1.7
DV 8/08/16_3-56	318	112	2.8	0.0653	7.0	1.1346	10.2	0.1259	7.4	0.72	764.7	53.2	770.0	54.9	783.1	148.0	764.7	53.2	2.3	0.7
DV 8/08/16_3-50	103	61	1.7	0.0658	7.8	1.1511	10.9	0.1268	7.7	0.70	769.3	56.1	777.8	59.6	799.9	163.2	769.3	56.1	3.8	1.1
DV 8/08/16_3-17	67	12	5.8	0.0660	7.7	1.1895	9.8	0.1306	6.0	0.61	791.1	44.9	795.7	53.9	806.3	161.4	791.1	44.9	1.9	0.6
DV 8/08/16_3-131	165	144	1.1	0.0680	7.2	1.2499	10.1	0.1332	7.2	0.71	806.0	54.5	823.4	57.3	868.4	148.7	806.0	54.5	7.2	2.1
DV 8/08/16_3-50	364	115	3.2	0.0698	5.9	1.3951	8.7	0.1447	6.4	0.73	871.4	51.9	886.9	51.2	923.4	121.7	871.4	51.9	5.6	1.7
DV 8/08/16_3-31	30	11	2.7	0.0718	8.6	1.4386	11.6	0.1452	7.8	0.67	873.9	64.1	905.1	69.8	980.0	176.0	873.9	64.1	10.8	3.5
DV 8/08/16_3-128	713	499	1.4	0.0700	6.0	1.4318	8.7	0.1483	6.4	0.73	891.4	53.1	902.3	52.2	927.1	123.0	891.4	53.1	3.9	1.2
DV 8/08/16_3-16	353	109	3.2	0.0715	6.0	1.4692	8.7	0.1488	6.4	0.73	894.3	53.5	917.8	52.8	972.2	121.6	894.3	53.5	8.0	2.6
DV 8/08/16_3-189	224	152	1.5	0.0690	6.8	1.4811	9.4	0.1555	6.6	0.70	931.5	57.2	922.7	57.2	899.8	139.6	899.8	139.6	-3.5	-1.0
DV 8/08/16_3-48	158	40	4.0	0.0706	7.4	1.4889	10.6	0.1529	7.6	0.72	917.0	65.3	925.8	64.4	944.9	151.3	944.9	151.3	3.0	1.0
DV 8/08/16_3-96	213	179	1.2	0.0709	8.5	1.6106	12.4	0.1645	9.0	0.73	981.8	81.9	974.3	77.6	955.0	173.8	955.0	173.8	-2.8	-0.8
DV 8/08/16_3-67	401	505	0.8	0.0716	6.3	1.5612	9.0	0.1580	6.6	0.72	945.7	57.8	954.9	56.0	974.2	127.6	974.2	127.6	2.9	1.0
DV 8/08/16_3-73	293	258	1.1	0.0719	6.2	1.5719	8.9	0.1583	6.4	0.71	947.5	56.2	959.2	55.1	983.8	126.5	983.8	126.5	3.7	1.2
DV 8/08/16_3-51	250	111	2.3	0.0720	8.6	1.6719	12.4	0.1683	9.0	0.72	1002.7	83.2	997.9	79.1	985.3	175.9	985.3	175.9	-1.8	-0.5
DV 8/08/16_3-195	395	163	2.4	0.0722	8.4	1.7510	12.1	0.1756	8.6	0.71	1043.1	83.1	1027.5	78.0	992.7	171.5	992.7	171.5	-5.1	-1.5
DV 8/08/16_3-97	175	95	1.8	0.0734	6.7	1.6699	9.4	0.1648	6.6	0.70	983.4	59.8	997.2	59.6	1024.9	136.3	1024.9	136.3	4.0	1.4
DV 8/08/16_3-198	73	51	1.4	0.0736	9.4	1.7443	11.6	0.1718	6.8	0.59	1022.3	64.6	1025.0	75.1	1029.2	190.5	1029.2	190.5	0.7	0.3
DV 8/08/16_3-178	377	126	3.0	0.0738	5.9	1.8334	8.3	0.1801	5.9	0.71	1067.4	58.4	1057.5	54.7	1035.1	118.5	1035.1	118.5	-3.1	-0.9
DV 8/08/16_3-159	201	288	0.7	0.0739	8.5	1.7750	12.2	0.1741	8.8	0.72	1034.5	84.5	1036.3	79.6	1038.1	171.4	1038.1	171.4	0.3	0.2
DV 8/08/16_3-49	121	59	2.1	0.0745	6.8	1.9902	9.6	0.1936	6.8	0.71	1140.8	71.2	1112.2	64.8	1054.5	136.4	1054.5	136.4	-8.2	-2.6
DV 8/08/16_3-174	34	30	1.1	0.0755	8.0	1.9189	9.9	0.1840	5.9	0.60	1089.0	59.6	1087.7	66.4	1083.1	160.1	1083.1	160.1	-0.5	-0.1
DV 8/08/16_3-153	436	114	3.8	0.0756	6.2	1.9465	8.9	0.1865	6.5	0.72	1102.6	65.8	1097.2	60.1	1084.5	124.1	1084.5	124.1	-1.7	-0.5
DV 8/08/16_3-18	105	33	3.2	0.0758	6.6	1.8416	9.4	0.1760	6.7	0.71	1044.9	64.9	1060.4	61.8	1090.3	131.4	1090.3	131.4	4.2	1.5
DV 8/08/16_3-152	258	185	1.4	0.0759	7.0	2.1058	10.1	0.2011	7.3	0.72	1181.2	79.2	1150.7	69.7	1091.6	139.8	1091.6	139.8	-8.2	-2.7
DV 8/08/16_3-130	119	129	0.9	0.0770	6.2	1.9809	8.8	0.1864	6.3	0.71	1101.9	63.9	1109.0	59.8	1121.2	124.4	1121.2	124.4	1.7	0.6
DV 8/08/16_3-87	233	148	1.6	0.0771	6.5	2.0150	9.3	0.1894	6.7	0.72	1118.2	68.4	1120.6	62.9	1122.8	128.9	1122.8	128.9	0.4	0.2
DV 8/08/16_3-120	398	59	6.7	0.0772	7.1	1.8206	10.3	0.1708	7.5	0.73	1016.5	70.6	1052.9	67.8	1126.0	141.2	1126.0	141.2	9.7	3.5
DV 8/08/16_3-171	638	282	2.3	0.0775	6.7	1.9093	9.7	0.1786	7.1	0.73	1059.3	69.4	1084.3	65.0	1133.0	133.3	1133.0	133.3	6.5	2.3
DV 8/08/16_3-77	102	172	0.6	0.0792	6.7	2.2006	9.5	0.2013	6.7	0.71	1182.5	72.6	1181.2	66.1	1176.6	132.5	1176.6	132.5	-0.5	-0.1
DV 8/08/16_3-28	41	54	0.7	0.0792	7.1	1.9794	9.8	0.1810	6.9	0.70	1072.3	68.1	1108.5	66.5	1178.2	139.7	1178.2	139.7	9.0	3.3
DV 8/08/16_3-89	73	87	0.8	0.0794	7.5	2.1406	10.0	0.1953	6.7	0.66	1149.9	70.3	1162.0	69.6	1182.3	148.8	1182.3	148.8	2.7	1.0

DV 8/08/16_3-185	419	390	1.1	0.0802	6.2	2.0303	8.8	0.1835	6.3	0.71	1086.0	63.2	1125.7	60.0	1201.3	121.3	1201.3	121.3	9.6	3.5
DV 8/08/16_3-119	53	41	1.3	0.0813	7.0	2.0144	9.7	0.1793	6.7	0.69	1063.4	65.3	1120.4	65.6	1229.5	137.0	1229.5	137.0	13.5	5.1
DV 8/08/16_3-62	54	87	0.6	0.0816	6.5	2.1752	8.7	0.1930	5.8	0.67	1137.7	60.7	1173.2	60.2	1237.1	126.6	1237.1	126.6	8.0	3.0
DV 8/08/16_3-176	195	76	2.6	0.0818	7.6	2.4906	10.9	0.2206	7.8	0.71	1284.8	91.0	1269.3	79.1	1241.1	149.5	1241.1	149.5	-3.5	-1.2
DV 8/08/16_3-110	311	164	1.9	0.0836	6.8	2.7525	9.9	0.2385	7.2	0.73	1378.7	89.1	1342.8	73.6	1283.0	132.1	1283.0	132.1	-7.5	-2.7
DV 8/08/16_3-122	522	274	1.9	0.0843	6.2	2.3164	8.9	0.1990	6.3	0.72	1170.2	67.9	1217.3	63.2	1298.6	120.8	1298.6	120.8	9.9	3.9
DV 8/08/16_3-25	573	250	2.3	0.0900	6.0	2.8176	8.8	0.2268	6.6	0.74	1317.9	78.1	1360.2	66.3	1425.2	114.0	1425.2	114.0	7.5	3.1
DV 8/08/16_3-183	279	181	1.5	0.0917	6.4	3.0362	8.9	0.2399	6.3	0.70	1386.1	78.7	1416.8	68.3	1461.4	120.8	1461.4	120.8	5.2	2.2
DV 8/08/16_3-7	250	189	1.3	0.0940	6.3	3.2489	9.3	0.2504	6.9	0.73	1440.5	88.8	1468.9	72.7	1507.9	119.9	1507.9	119.9	4.5	1.9
DV 8/08/16_3-104	64	35	1.8	0.0967	6.9	3.9766	9.6	0.2978	6.7	0.70	1680.5	99.4	1629.4	78.2	1561.5	129.4	1561.5	129.4	-7.6	-3.1
DV 8/08/16_3-10	81	67	1.2	0.1005	6.6	3.6433	9.6	0.2626	7.0	0.73	1503.2	93.9	1559.0	76.5	1633.3	122.1	1633.3	122.1	8.0	3.6
DV 8/08/16_3-5	293	60	4.9	0.1020	5.3	4.0507	8.2	0.2878	6.2	0.76	1630.3	90.0	1644.4	66.9	1660.3	99.0	1660.3	99.0	1.8	0.9
DV 8/08/16_3-3	100	55	1.8	0.1041	5.4	4.6068	7.9	0.3205	5.7	0.72	1792.3	89.5	1750.5	65.8	1698.7	100.2	1698.7	100.2	-5.5	-2.4
DV 8/08/16_3-65	140	57	2.5	0.1058	5.6	4.4974	7.9	0.3080	5.7	0.72	1731.0	87.2	1730.5	66.1	1727.9	102.0	1727.9	102.0	-0.2	0.0
DV 8/08/16_3-181	716	246	2.9	0.1105	5.9	5.0141	8.4	0.3288	6.1	0.72	1832.4	96.7	1821.7	71.3	1807.7	106.6	1807.7	106.6	-1.4	-0.6
DV 8/08/16_3-37	197	76	2.6	0.1110	6.1	4.2619	8.9	0.2782	6.5	0.73	1582.2	91.2	1686.0	72.9	1815.8	110.2	1815.8	110.2	12.9	6.2
DV 8/08/16_3-129	109	96	1.1	0.1110	6.4	4.6495	9.4	0.3034	6.9	0.73	1708.0	103.5	1758.2	78.9	1816.7	117.1	1816.7	117.1	6.0	2.9
DV 8/08/16_3-187	171	116	1.5	0.1117	8.1	4.9610	11.7	0.3217	8.5	0.72	1798.0	133.1	1812.7	99.3	1828.0	147.0	1828.0	147.0	1.6	0.8
DV 8/08/16_3-92	393	58	6.8	0.1124	9.5	4.3579	13.8	0.2808	10.0	0.73	1595.6	141.6	1704.4	114.2	1838.6	171.5	1838.6	171.5	13.2	6.4
DV 8/08/16_3-55	117	69	1.7	0.1125	7.0	5.0414	10.2	0.3247	7.4	0.72	1812.5	117.0	1826.3	86.6	1840.2	127.7	1840.2	127.7	1.5	0.8
DV 8/08/16_3-69	149	93	1.6	0.1126	6.7	4.7108	9.4	0.3030	6.7	0.71	1706.3	100.8	1769.2	79.1	1842.3	120.4	1842.3	120.4	7.4	3.6
DV 8/08/16_3-186	959	192	5.0	0.1129	6.6	5.1338	9.5	0.3295	6.9	0.72	1836.0	109.6	1841.7	80.7	1846.5	119.0	1846.5	119.0	0.6	0.3
DV 8/08/16_3-98	192	183	1.1	0.1129	7.8	5.3344	11.3	0.3422	8.2	0.72	1897.1	134.8	1874.4	97.2	1847.0	141.8	1847.0	141.8	-2.7	-1.2
DV 8/08/16_3-167	653	324	2.0	0.1130	5.9	5.1488	8.5	0.3303	6.2	0.72	1839.6	98.8	1844.2	72.3	1847.5	105.9	1847.5	105.9	0.4	0.2
DV 8/08/16_3-30	337	170	2.0	0.1135	8.3	4.8234	12.1	0.3079	8.8	0.72	1730.2	133.4	1789.0	102.1	1856.3	150.7	1856.3	150.7	6.8	3.3
DV 8/08/16_3-194	405	70	5.8	0.1138	6.7	5.2292	9.6	0.3329	6.9	0.72	1852.2	111.6	1857.4	81.9	1861.6	120.3	1861.6	120.3	0.5	0.3
DV 8/08/16_3-22	405	107	3.8	0.1139	6.3	4.6924	9.2	0.2986	6.8	0.73	1684.3	100.5	1765.9	77.1	1861.8	113.0	1861.8	113.0	9.5	4.6
DV 8/08/16_3-170	559	518	1.1	0.1143	5.8	5.2854	8.4	0.3350	6.1	0.72	1862.4	99.0	1866.5	72.1	1869.3	105.2	1869.3	105.2	0.4	0.2
DV 8/08/16_3-24	526	230	2.3	0.1144	6.0	4.8084	8.9	0.3045	6.6	0.74	1713.6	99.7	1786.4	74.9	1870.5	107.8	1870.5	107.8	8.4	4.1
DV 8/08/16_3-54	428	198	2.2	0.1144	8.7	5.2175	12.6	0.3303	9.1	0.72	1839.9	146.5	1855.5	107.5	1871.1	156.3	1871.1	156.3	1.7	0.8
DV 8/08/16_3-162	635	13	48.0	0.1147	6.5	5.4914	9.3	0.3469	6.8	0.72	1920.0	112.2	1899.3	80.5	1874.8	117.1	1874.8	117.1	-2.4	-1.1
DV 8/08/16_3-139	355	94	3.8	0.1154	6.0	5.1918	8.7	0.3261	6.4	0.73	1819.3	101.1	1851.3	74.3	1885.6	107.5	1885.6	107.5	3.5	1.7
DV 8/08/16_3-177	480	74	6.5	0.1159	6.1	5.3125	8.8	0.3321	6.3	0.72	1848.3	101.5	1870.9	75.1	1894.2	110.2	1894.2	110.2	2.4	1.2
DV 8/08/16_3-132	93	38	2.5	0.1165	5.9	5.0644	8.3	0.3149	6.0	0.71	1764.5	91.9	1830.2	70.7	1903.9	105.1	1903.9	105.1	7.3	3.6
DV 8/08/16_3-112	111	87	1.3	0.1166	7.0	5.6030	10.1	0.3480	7.3	0.72	1924.8	121.3	1916.6	87.1	1904.9	125.3	1904.9	125.3	-1.0	-0.4

DV 8/08/16_3-9	183	77	2.4	0.1169	9.5	5.0153	13.8	0.3108	10.0	0.73	1744.7	153.0	1821.9	117.1	1909.2	170.3	1909.2	170.3	8.6	4.2
DV 8/08/16_3-90	949	62	15.3	0.1187	8.4	5.0614	11.9	0.3088	8.5	0.71	1734.8	128.7	1829.7	101.2	1937.3	150.1	1937.3	150.1	10.5	5.2
DV 8/08/16_3-166	254	352	0.7	0.1199	7.6	5.5879	10.9	0.3376	7.8	0.72	1875.2	127.3	1914.2	94.0	1954.9	135.7	1954.9	135.7	4.1	2.0
DV 8/08/16_3-94	75	38	2.0	0.1211	6.5	6.1078	8.9	0.3654	6.2	0.69	2007.8	107.4	1991.4	78.2	1972.1	115.0	1972.1	115.0	-1.8	-0.8
DV 8/08/16_3-32	174	80	2.2	0.1218	6.0	5.8050	8.8	0.3454	6.4	0.73	1912.7	106.5	1947.2	76.0	1982.1	106.8	1982.1	106.8	3.5	1.8
DV 8/08/16_3-100	101	55	1.8	0.1237	7.2	6.1922	10.4	0.3625	7.5	0.72	1994.1	129.0	2003.3	91.0	2010.6	127.5	2010.6	127.5	0.8	0.5
DV 8/08/16_3-169	238	145	1.6	0.1238	8.3	6.4813	12.0	0.3792	8.6	0.72	2072.4	152.4	2043.4	105.6	2012.4	148.0	2012.4	148.0	-3.0	-1.4
DV 8/08/16_3-146	203	88	2.3	0.1245	5.7	6.0988	8.2	0.3549	5.9	0.72	1957.9	100.4	1990.1	72.0	2021.8	101.9	2021.8	101.9	3.2	1.6
DV 8/08/16_3-79	177	95	1.9	0.1246	7.4	5.8750	10.4	0.3416	7.3	0.70	1894.3	120.5	1957.6	90.4	2023.1	131.1	2023.1	131.1	6.4	3.2
DV 8/08/16_3-109	54	33	1.6	0.1351	6.5	8.0487	9.2	0.4314	6.5	0.71	2312.0	127.2	2236.5	83.7	2165.5	113.9	2165.5	113.9	-6.8	-3.4
DV 8/08/16_3-74	715	332	2.2	0.1377	8.7	7.4706	12.5	0.3930	9.0	0.72	2136.9	163.3	2169.5	112.2	2198.5	151.2	2198.5	151.2	2.8	1.5
DV 8/08/16_3-27	814	785	1.0	0.1378	8.7	6.8725	12.8	0.3614	9.5	0.74	1988.9	162.1	2095.1	114.2	2199.2	150.9	2199.2	150.9	9.6	5.1
DV 8/08/16_3-99	339	101	3.3	0.1401	6.1	7.7494	8.8	0.4008	6.4	0.72	2172.8	117.6	2202.4	79.6	2227.8	106.5	2227.8	106.5	2.5	1.3
DV 8/08/16_3-196	852	286	3.0	0.1530	6.1	8.5127	8.9	0.4033	6.5	0.73	2184.2	119.7	2287.3	80.6	2379.2	103.9	2379.2	103.9	8.2	4.5
DV 8/08/16_3-103	120	113	1.1	0.1548	7.2	9.4093	10.4	0.4402	7.4	0.71	2351.6	146.1	2378.7	95.4	2399.6	123.3	2399.6	123.3	2.0	1.1
DV 8/08/16_3-72	52	47	1.1	0.1596	6.5	9.8798	9.5	0.4486	7.0	0.73	2389.1	139.4	2423.6	88.1	2450.9	110.5	2450.9	110.5	2.5	1.4
DV 8/08/16_3-164	453	317	1.4	0.1598	6.1	9.9535	8.9	0.4513	6.6	0.73	2401.2	132.2	2430.5	82.7	2453.3	102.8	2453.3	102.8	2.1	1.2
DV 8/08/16_3-172	282	133	2.1	0.1601	5.9	10.0332	8.5	0.4542	6.2	0.72	2413.7	124.0	2437.8	78.8	2456.3	100.1	2456.3	100.1	1.7	1.0
DV 8/08/16_3-11	385	198	1.9	0.1622	5.6	9.6319	8.1	0.4302	5.9	0.73	2306.6	114.9	2400.2	74.9	2478.6	94.4	2478.6	94.4	6.9	3.9
DV 8/08/16_3-59	180	193	0.9	0.1631	7.3	10.1961	10.5	0.4529	7.6	0.72	2408.2	153.7	2452.7	97.8	2488.1	123.1	2488.1	123.1	3.2	1.8
DV 8/08/16_3-106	222	123	1.8	0.1634	8.3	10.9810	12.0	0.4867	8.6	0.72	2556.6	182.4	2521.5	111.8	2491.0	139.5	2491.0	139.5	-2.6	-1.4
DV 8/08/16_3-158	111	62	1.8	0.1639	7.6	10.2392	11.0	0.4526	8.0	0.72	2406.7	160.6	2456.6	102.5	2496.5	128.7	2496.5	128.7	3.6	2.0
DV 8/08/16_3-26	150	107	1.4	0.1645	5.2	9.7816	7.6	0.4307	5.7	0.74	2309.1	110.2	2414.4	70.6	2502.6	87.2	2502.6	87.2	7.7	4.4
DV 8/08/16_3-20	68	50	1.4	0.1648	5.0	10.2257	7.3	0.4494	5.3	0.72	2392.7	106.1	2455.4	67.5	2505.9	84.8	2505.9	84.8	4.5	2.6
DV 8/08/16_3-133	11	9	1.1	0.1649	6.6	10.2699	9.1	0.4512	6.3	0.69	2400.6	126.1	2459.4	84.6	2506.7	111.8	2506.7	111.8	4.2	2.4
DV 8/08/16_3-43	43	53	0.8	0.1659	6.2	10.9379	9.0	0.4776	6.6	0.72	2516.7	136.6	2517.9	83.8	2517.1	104.4	2517.1	104.4	0.0	0.0
DV 8/08/16_3-107	130	51	2.6	0.1661	7.3	11.8821	10.5	0.5181	7.5	0.72	2691.2	165.8	2595.2	98.8	2518.6	123.4	2518.6	123.4	-6.9	-3.7
DV 8/08/16_3-82	35	24	1.4	0.1666	8.0	10.8254	11.3	0.4706	8.0	0.71	2486.4	166.0	2508.2	105.5	2524.1	133.9	2524.1	133.9	1.5	0.9
DV 8/08/16_3-95	254	132	1.9	0.1727	6.7	11.9846	9.5	0.5027	6.8	0.71	2625.2	146.7	2603.2	89.5	2584.0	111.9	2584.0	111.9	-1.6	-0.8
DV 8/08/16_3-53	222	367	0.6	0.1742	6.0	11.0472	8.7	0.4595	6.4	0.73	2437.3	129.7	2527.1	81.3	2598.4	99.7	2598.4	99.7	6.2	3.6
DV 8/08/16_3-144	152	66	2.3	0.1818	6.5	12.4648	9.4	0.4968	6.8	0.72	2600.1	144.8	2640.1	88.2	2669.2	107.5	2669.2	107.5	2.6	1.5
DV 8/08/16_3-123	387	29	13.4	0.1833	7.1	10.6911	10.3	0.4222	7.4	0.72	2270.4	141.7	2496.7	95.8	2683.3	117.8	2683.3	117.8	15.4	9.1
DV 8/08/16_3-19	127	87	1.5	0.1866	5.4	11.7882	8.1	0.4576	6.0	0.74	2429.0	121.7	2587.7	75.7	2712.6	89.7	2712.6	89.7	10.5	6.1
DV 8/08/16_3-91	463	228	2.0	0.1934	6.8	13.2906	10.3	0.4979	7.8	0.75	2604.7	167.2	2700.5	97.6	2771.0	110.9	2771.0	110.9	6.0	3.5
DV 8/08/16_3-58	83	51	1.6	0.1987	6.3	14.1048	9.3	0.5142	6.8	0.73	2674.5	149.2	2756.8	87.9	2815.9	103.1	2815.9	103.1	5.0	3.0

DV 8/08/16_3-68	35	14	2.6	0.2079	5.9	15.4849	8.6	0.5396	6.2	0.72	2782.0	140.3	2845.6	81.7	2889.2	96.3	2889.2	96.3	3.7	2.2
DV 8/08/16_3-29	174	63	2.8	0.2356	5.6	18.4515	8.3	0.5674	6.1	0.73	2897.2	142.9	3013.6	79.9	3090.4	89.8	3090.4	89.8	6.3	3.9
DV 8/08/16_3-145	576	112	5.2	0.2357	5.9	16.9822	8.6	0.5221	6.2	0.72	2708.1	138.1	2933.8	82.4	3090.9	94.5	3090.9	94.5	12.4	7.7
DV 8/08/16_3-126	73	45	1.6	0.2390	6.1	16.8871	8.5	0.5120	6.1	0.70	2665.0	132.2	2928.4	82.1	3113.3	96.6	3113.3	96.6	14.4	9.0
DV 8/08/16_3-23	156	91	1.7	0.2593	5.5	18.4473	8.1	0.5154	6.1	0.74	2679.5	133.6	3013.4	78.6	3242.6	86.0	3242.6	86.0	17.4	11.1
Data Rejected From Population Analyses																				
DV 8/08/16_3-137	93	71	1.3	0.0524	12.4	0.3005	16.1	0.0415	10.3	0.64	262.3	26.5	266.8	37.8	304.3	282.1	262.3	26.5	13.8	1.7
DV 8/08/16_3-161	535	212	2.5	0.0506	10.6	0.3140	14.9	0.0449	10.5	0.70	283.4	29.2	277.3	36.2	223.7	245.0	283.4	29.2	-26.7	-2.2
DV 8/08/16_3-121	253	184	1.4	0.0521	11.6	0.3639	16.1	0.0506	11.2	0.70	318.1	34.9	315.1	43.8	288.8	264.5	318.1	34.9	-10.2	-1.0
DV 8/08/16_3-63	467	154	3.0	0.0557	11.9	0.4483	17.3	0.0583	12.5	0.72	365.4	44.5	376.1	54.3	440.4	264.4	365.4	44.5	17.0	2.9
DV 8/08/16_3-84	203	80	2.5	0.0538	12.3	0.4932	16.2	0.0664	10.5	0.65	414.2	42.3	407.1	54.3	364.6	277.3	414.2	42.3	-13.6	-1.7
DV 8/08/16_3-160	729	269	2.7	0.0584	11.0	0.7877	15.6	0.0977	11.1	0.71	601.1	63.6	589.9	69.9	544.5	240.3	601.1	63.6	-10.4	-1.9
DV 8/08/16_3-108	280	64	4.4	0.0585	7.0	0.8234	9.9	0.1020	7.0	0.71	625.9	42.0	609.9	45.5	547.9	152.7	625.9	42.0	-14.2	-2.6
DV 8/08/16_3-147	223	79	2.8	0.0664	19.4	0.9760	20.5	0.1065	6.7	0.32	652.1	41.3	691.6	103.3	819.9	405.7	652.1	41.3	20.5	5.7
DV 8/08/16_3-45	1299	898	1.4	0.0857	10.4	1.2702	14.7	0.1074	10.4	0.71	657.5	65.0	832.5	83.8	1331.7	201.8	657.5	65.0	50.6	21.0
DV 8/08/16_3-115	42	51	0.8	0.0704	8.2	1.0846	10.4	0.1115	6.5	0.62	681.6	41.9	745.9	55.2	940.8	167.7	681.6	41.9	27.6	8.6
DV 8/08/16_3-88	97	26	3.7	0.0701	13.9	1.2416	19.4	0.1284	13.6	0.70	778.6	99.4	819.6	109.6	930.3	285.6	778.6	99.4	16.3	5.0
DV 8/08/16_3-47	597	126	4.7	0.0708	10.2	1.2898	14.5	0.1321	10.3	0.71	799.7	77.2	841.2	82.9	950.4	209.5	799.7	77.2	15.9	4.9
DV 8/08/16_3-83	219	322	0.7	0.0643	7.6	1.2448	10.1	0.1402	6.8	0.67	845.8	54.0	821.1	57.2	752.1	159.4	845.8	54.0	-12.5	-3.0
DV 8/08/16_3-4	507	358	1.4	0.0739	11.0	1.5819	16.3	0.1550	12.0	0.74	928.8	103.5	963.1	101.4	1039.8	222.2	1039.8	222.2	10.7	3.6
DV 8/08/16_3-111	225	168	1.3	0.0775	11.8	2.1477	16.9	0.2007	12.1	0.72	1179.0	130.6	1164.3	117.9	1134.0	235.7	1134.0	235.7	-4.0	-1.3
DV 8/08/16_3-114	16	0	2414.4	0.1056	11.4	2.7705	14.4	0.1900	8.8	0.61	1121.6	90.9	1347.6	108.0	1724.3	209.3	1724.3	209.3	35.0	16.8
DV 8/08/16_3-13	498	67	7.4	0.1129	10.0	4.8412	14.6	0.3105	10.7	0.73	1743.2	162.9	1792.1	123.7	1847.4	181.5	1847.4	181.5	5.6	2.7
DV 8/08/16_3-150	74	127	0.6	0.1163	10.4	5.4513	15.1	0.3397	11.0	0.73	1885.1	179.7	1893.0	130.4	1899.7	186.9	1899.7	186.9	0.8	0.4
DV 8/08/16_3-134	280	300	0.9	0.1480	6.9	6.7368	10.0	0.3298	7.3	0.73	1837.4	117.3	2077.5	89.0	2323.0	118.1	2323.0	118.1	20.9	11.6
DV 8/08/16_3-165	333	195	1.7	0.1519	6.9	5.2362	9.7	0.2497	6.9	0.71	1436.9	88.8	1858.5	83.2	2367.8	117.8	2367.8	117.8	39.3	22.7
DV 8/08/16_3-190	497	216	2.3	0.1566	12.5	9.0828	17.7	0.4202	12.6	0.71	2261.4	239.8	2346.4	163.6	2419.5	212.5	2419.5	212.5	6.5	3.6
DV 8/08/16_3-46	73	25	3.0	0.1956	6.6	10.7542	9.4	0.3982	6.8	0.72	2161.0	124.4	2502.1	87.4	2790.2	107.2	2790.2	107.2	22.6	13.6
DV 8/08/16_3-2	85	72	1.2	0.1978	11.8	14.5284	16.2	0.5321	11.1	0.69	2750.1	249.3	2784.9	155.3	2808.1	193.1	2808.1	193.1	2.1	1.2

DV 7-25-15-1 38.121° N; 73.915° E

				Isotope ratios							Apparent Ages (Ma)									
				^{207}Pb	±	^{207}Pb	±	^{206}Pb	±		^{206}Pb	±	^{207}Pb	±	^{207}Pb	±		±	% discordance Pb^{206}/U^{238}-Pb^{207}/Pb^{206}	% discordance Pb^{206}/U^{238}-Pb^{207}/U^{325}
Analysis #	U (ppm)	Th (ppm)	U/Th	^{206}Pb	(2%SD)	^{235}U	(2%SD)	^{238}U	(2%SD)	error corr.	^{238}U	(2SD)	^{235}U	(2SD)	^{206}Pb	(2SD)	Best Age	(2SD)		
DV 7/25/15_1-90	406	174	2.3	0.0515	8.9	0.2459	12.3	0.0346	8.5	0.69	219.3	18.3	223.3	24.6	264.0	204.8	219.3	18.3	16.9	1.8
DV 7/25/15_1-129	397	207	1.9	0.0536	6.9	0.2638	9.6	0.0357	6.6	0.69	226.3	14.8	237.7	20.3	353.7	156.1	226.3	14.8	36.0	4.8
DV 7/25/15_1-82	772	439	1.8	0.0533	5.6	0.2678	7.6	0.0365	5.2	0.68	230.8	11.8	241.0	16.4	339.8	127.0	230.8	11.8	32.1	4.2
DV 7/25/15_1-102	362	261	1.4	0.0571	18.5	0.2886	19.2	0.0367	5.4	0.28	232.1	12.2	257.4	43.8	493.6	407.9	232.1	12.2	53.0	9.9
DV 7/25/15_1-84	236	121	2.0	0.0567	10.9	0.2873	12.9	0.0368	6.9	0.54	232.7	15.9	256.5	29.2	478.6	239.9	232.7	15.9	51.4	9.3
DV 7/25/15_1-59	441	353	1.2	0.0518	6.1	0.2628	8.1	0.0368	5.3	0.65	232.8	12.1	236.9	17.1	277.5	140.8	232.8	12.1	16.1	1.7
DV 7/25/15_1-24	728	313	2.3	0.0506	6.8	0.2574	9.6	0.0368	6.8	0.70	233.2	15.5	232.6	19.9	224.6	157.7	233.2	15.5	-3.8	-0.3
DV 7/25/15_1-9	278	188	1.5	0.0490	9.8	0.2504	11.1	0.0370	5.3	0.47	234.2	12.1	226.9	22.5	148.5	229.0	234.2	12.1	-57.7	-3.2
DV 7/25/15_1-43	204	116	1.8	0.0548	12.1	0.2806	13.6	0.0371	6.1	0.45	235.0	14.2	251.2	30.2	403.8	270.7	235.0	14.2	41.8	6.4
DV 7/25/15_1-139	650	302	2.2	0.0499	6.6	0.2564	8.8	0.0373	5.8	0.65	235.8	13.4	231.7	18.2	192.3	154.3	235.8	13.4	-22.6	-1.8
DV 7/25/15_1-23	437	396	1.1	0.0509	6.8	0.2674	9.2	0.0381	6.2	0.67	240.8	14.7	240.6	19.8	237.4	157.7	240.8	14.7	-1.4	-0.1
DV 7/25/15_1-54	294	194	1.5	0.0499	8.9	0.2624	11.0	0.0381	6.4	0.58	241.3	15.1	236.6	23.1	189.8	207.8	241.3	15.1	-27.1	-2.0
DV 7/25/15_1-35	1025	448	2.3	0.0508	9.0	0.2720	12.8	0.0388	9.1	0.71	245.5	22.0	244.3	27.9	230.9	208.7	245.5	22.0	-6.3	-0.5
DV 7/25/15_1-34	426	188	2.3	0.0514	6.7	0.2847	9.3	0.0401	6.5	0.69	253.7	16.2	254.4	21.0	259.8	154.9	253.7	16.2	2.3	0.3
DV 7/25/15_1-28	187	121	1.5	0.0494	14.3	0.2778	15.9	0.0407	6.8	0.43	257.3	17.2	248.9	35.0	169.0	334.3	257.3	17.2	-52.2	-3.4
DV 7/25/15_1-142	121	87	1.4	0.0663	10.8	0.3729	12.3	0.0408	5.8	0.47	258.0	14.6	321.8	33.8	815.5	226.3	258.0	14.6	68.4	19.8
DV 7/25/15_1-48	428	282	1.5	0.0542	9.1	0.3059	12.6	0.0409	8.8	0.70	258.3	22.4	271.0	30.1	381.1	203.4	258.3	22.4	32.2	4.7
DV 7/25/15_1-79	100	66	1.5	0.0583	17.5	0.3319	19.0	0.0413	7.4	0.39	260.6	19.0	291.0	48.2	541.9	383.1	260.6	19.0	51.9	10.5
DV 7/25/15_1-80	2178	821	2.7	0.0515	7.9	0.2948	11.6	0.0415	8.4	0.73	262.3	21.7	262.3	26.7	261.5	182.2	262.3	21.7	-0.3	0.0
DV 7/25/15_1-5	112	61	1.8	0.0645	17.9	0.3853	18.9	0.0433	6.0	0.31	273.2	16.0	330.9	53.3	756.8	378.0	273.2	16.0	63.9	17.4
DV 7/25/15_1-19	89	58	1.5	0.0509	11.3	0.3049	12.8	0.0434	5.9	0.46	274.1	15.9	270.2	30.3	234.5	261.7	274.1	15.9	-16.9	-1.5
DV 7/25/15_1-119	3496	1598	2.2	0.0520	6.2	0.3190	8.7	0.0445	6.2	0.70	280.5	17.0	281.2	21.5	287.1	142.3	280.5	17.0	2.3	0.2
DV 7/25/15_1-29	295	175	1.7	0.0525	10.1	0.3225	13.5	0.0445	8.9	0.66	280.8	24.5	283.9	33.4	307.4	230.5	280.8	24.5	8.6	1.1
DV 7/25/15_1-66	326	191	1.7	0.0531	7.6	0.3298	10.2	0.0451	6.9	0.67	284.2	19.1	289.4	25.8	331.1	172.6	284.2	19.1	14.2	1.8
DV 7/25/15_1-124	492	172	2.9	0.0515	8.8	0.3210	12.1	0.0452	8.3	0.68	285.2	23.1	282.7	29.8	263.2	202.6	285.2	23.1	-8.4	-0.9
DV 7/25/15_1-27	611	349	1.8	0.0529	7.5	0.3323	10.1	0.0456	6.9	0.68	287.3	19.4	291.3	25.7	322.4	169.4	287.3	19.4	10.9	1.4
DV 7/25/15_1-72	185	234	0.8	0.0567	7.9	0.3618	9.7	0.0462	5.5	0.57	291.3	15.8	313.5	26.1	481.0	175.5	291.3	15.8	39.4	7.1
DV 7/25/15_1-108	565	288	2.0	0.0533	7.2	0.3400	9.2	0.0463	5.8	0.63	291.5	16.6	297.2	23.7	341.2	162.7	291.5	16.6	14.6	1.9
DV 7/25/15_1-51	1043	171	6.1	0.0520	6.6	0.3371	9.3	0.0470	6.6	0.71	295.9	19.0	295.0	23.8	287.1	150.4	295.9	19.0	-3.1	-0.3
DV 7/25/15_1-56	595	197	3.0	0.0507	5.4	0.3421	7.3	0.0489	5.0	0.68	308.0	15.1	298.7	19.0	226.4	123.7	308.0	15.1	-36.0	-3.1
DV 7/25/15_1-67	360	296	1.2	0.0531	8.4	0.3631	11.5	0.0496	7.8	0.68	312.1	23.8	314.5	31.0	332.0	190.4	312.1	23.8	6.0	0.8

DV 7/25/15_1-100	132	33	4.0	0.0545	8.9	0.3736	10.2	0.0497	5.1	0.49	312.5	15.5	322.3	28.2	389.9	200.5	312.5	15.5	19.8	3.0
DV 7/25/15_1-60	367	172	2.1	0.0525	6.1	0.3634	8.1	0.0502	5.4	0.66	315.8	16.6	314.7	21.9	306.0	138.3	315.8	16.6	-3.2	-0.3
DV 7/25/15_1-132	252	218	1.2	0.0594	6.4	0.4109	8.3	0.0502	5.3	0.63	315.9	16.3	349.5	24.6	581.2	139.5	315.9	16.3	45.6	9.6
DV 7/25/15_1-53	185	107	1.7	0.0504	12.1	0.3515	13.3	0.0506	5.7	0.42	318.0	17.6	305.8	35.2	213.2	280.0	318.0	17.6	-49.2	-4.0
DV 7/25/15_1-143	103	138	0.7	0.0471	11.6	0.3286	13.6	0.0506	7.1	0.52	318.3	22.0	288.5	34.1	55.9	275.9	318.3	22.0	-469.6	-10.3
DV 7/25/15_1-16	383	328	1.2	0.0559	8.1	0.3920	10.6	0.0508	6.9	0.64	319.2	21.4	335.8	30.3	450.4	179.9	319.2	21.4	29.1	4.9
DV 7/25/15_1-92	359	298	1.2	0.0511	7.0	0.3774	9.2	0.0535	6.0	0.65	336.2	19.8	325.1	25.6	245.1	160.6	336.2	19.8	-37.2	-3.4
DV 7/25/15_1-18	188	152	1.2	0.0517	10.5	0.3821	14.2	0.0536	9.5	0.67	336.5	31.1	328.6	39.8	270.7	241.1	336.5	31.1	-24.3	-2.4
DV 7/25/15_1-106	240	90	2.7	0.0746	7.7	0.5809	9.0	0.0564	4.7	0.51	353.8	16.2	465.0	33.7	1058.9	155.9	353.8	16.2	66.6	23.9
DV 7/25/15_1-150	174	143	1.2	0.0556	6.7	0.4474	8.5	0.0584	5.3	0.62	365.8	18.7	375.5	26.7	437.4	149.0	365.8	18.7	16.4	2.6
DV 7/25/15_1-26	133	72	1.9	0.0565	7.3	0.4725	9.3	0.0607	5.7	0.61	379.7	21.2	392.9	30.3	470.1	162.2	379.7	21.2	19.2	3.4
DV 7/25/15_1-52	792	152	5.2	0.0555	6.3	0.4690	8.9	0.0613	6.3	0.71	383.4	23.5	390.5	29.0	432.0	141.0	383.4	23.5	11.2	1.8
DV 7/25/15_1-146	99	55	1.8	0.0589	8.2	0.5049	10.1	0.0622	5.8	0.58	388.9	22.1	415.0	34.3	565.0	178.4	388.9	22.1	31.2	6.3
DV 7/25/15_1-64	291	155	1.9	0.0572	6.7	0.4974	8.9	0.0630	5.9	0.66	394.1	22.5	409.9	30.1	499.3	148.5	394.1	22.5	21.1	3.9
DV 7/25/15_1-13	1805	725	2.5	0.0585	5.1	0.5129	7.2	0.0635	5.1	0.71	396.7	19.8	420.4	24.9	550.2	111.8	396.7	19.8	27.9	5.6
DV 7/25/15_1-21	314	169	1.9	0.0564	6.9	0.4976	9.6	0.0639	6.8	0.70	399.4	26.3	410.1	32.5	469.0	151.9	399.4	26.3	14.8	2.6
DV 7/25/15_1-134	113	104	1.1	0.0519	10.9	0.4659	12.5	0.0652	6.2	0.49	407.0	24.4	388.4	40.5	280.9	249.7	407.0	24.4	-44.9	-4.8
DV 7/25/15_1-135	163	94	1.7	0.0544	10.6	0.4973	13.1	0.0663	7.8	0.59	414.1	31.1	409.9	44.4	388.3	238.4	414.1	31.1	-6.6	-1.0
DV 7/25/15_1-49	204	70	2.9	0.0534	7.2	0.4912	9.5	0.0667	6.2	0.65	416.0	24.8	405.7	31.7	347.3	163.4	416.0	24.8	-19.8	-2.5
DV 7/25/15_1-44	929	435	2.1	0.0560	5.5	0.5160	7.7	0.0668	5.4	0.70	417.0	21.8	422.5	26.6	451.6	122.3	417.0	21.8	7.7	1.3
DV 7/25/15_1-46	225	95	2.4	0.0565	10.9	0.5247	14.6	0.0673	9.7	0.66	420.1	39.6	428.3	51.1	471.9	241.6	420.1	39.6	11.0	1.9
DV 7/25/15_1-8	430	340	1.3	0.0515	9.0	0.4816	10.4	0.0678	5.3	0.50	422.9	21.6	399.2	34.4	261.3	207.2	422.9	21.6	-61.8	-5.9
DV 7/25/15_1-58	321	132	2.4	0.0542	6.8	0.5097	9.5	0.0682	6.5	0.69	425.1	26.9	418.3	32.4	380.2	153.9	425.1	26.9	-11.8	-1.6
DV 7/25/15_1-117	434	286	1.5	0.0592	7.5	0.5623	10.3	0.0689	7.1	0.69	429.7	29.7	453.0	37.7	573.6	162.7	429.7	29.7	25.1	5.2
DV 7/25/15_1-101	283	150	1.9	0.0537	7.5	0.5178	9.9	0.0698	6.6	0.66	435.1	27.8	423.7	34.4	359.6	168.7	435.1	27.8	-21.0	-2.7
DV 7/25/15_1-128	207	138	1.5	0.0574	6.2	0.5563	8.1	0.0704	5.3	0.65	438.3	22.3	449.1	29.5	506.6	136.1	438.3	22.3	13.5	2.4
DV 7/25/15_1-38	496	490	1.0	0.0570	6.2	0.5537	8.4	0.0704	5.8	0.68	438.5	24.5	447.4	30.5	492.4	135.9	438.5	24.5	11.0	2.0
DV 7/25/15_1-69	474	145	3.3	0.0556	6.2	0.5630	8.5	0.0734	5.8	0.68	456.7	25.8	453.4	31.2	436.3	138.2	456.7	25.8	-4.7	-0.7
DV 7/25/15_1-74	894	481	1.9	0.0570	4.9	0.5801	6.8	0.0738	4.7	0.69	459.1	21.0	464.5	25.3	489.9	107.7	459.1	21.0	6.3	1.2
DV 7/25/15_1-95	1022	255	4.0	0.0552	7.8	0.5635	10.9	0.0739	7.7	0.70	459.6	34.1	453.8	39.9	419.5	173.7	459.6	34.1	-9.6	-1.3
DV 7/25/15_1-68	232	189	1.2	0.0589	6.7	0.6011	9.2	0.0740	6.3	0.68	459.9	28.0	477.9	35.2	564.7	146.9	459.9	28.0	18.6	3.8
DV 7/25/15_1-65	107	56	1.9	0.0564	7.2	0.5878	9.3	0.0755	5.9	0.63	469.4	26.7	469.5	35.0	468.9	160.0	469.4	26.7	-0.1	0.0
DV 7/25/15_1-110	316	125	2.5	0.0580	5.6	0.6198	7.3	0.0775	4.8	0.64	481.3	22.2	489.7	28.5	528.7	123.2	481.3	22.2	9.0	1.7
DV 7/25/15_1-50	366	309	1.2	0.0585	5.9	0.6350	8.2	0.0787	5.7	0.70	488.6	26.8	499.2	32.2	547.1	128.2	488.6	26.8	10.7	2.1
DV 7/25/15_1-149	251	156	1.6	0.0784	19.7	0.8932	22.0	0.0827	9.7	0.44	512.3	47.9	648.1	105.8	1156.5	391.5	512.3	47.9	55.7	20.9

DV 7/25/15_1-47	457	158	2.9	0.0728	5.4	0.8688	8.4	0.0865	6.4	0.76	534.9	32.9	634.9	39.6	1008.7	109.6	534.9	32.9	47.0	15.8
DV 7/25/15_1-122	349	96	3.6	0.0588	6.3	0.7173	8.3	0.0886	5.5	0.66	547.0	28.8	549.1	35.3	558.9	136.7	547.0	28.8	2.1	0.4
DV 7/25/15_1-76	307	62	4.9	0.0740	6.0	0.9370	8.7	0.0918	6.3	0.72	566.1	34.2	671.3	42.8	1041.3	121.3	566.1	34.2	45.6	15.7
DV 7/25/15_1-87	402	32	12.4	0.0600	7.4	0.8112	10.5	0.0981	7.5	0.71	603.1	42.9	603.1	47.8	601.9	160.4	603.1	42.9	-0.2	0.0
DV 7/25/15_1-10	482	295	1.6	0.0605	6.2	0.8302	8.5	0.0994	5.9	0.68	610.7	34.1	613.7	39.2	622.3	134.1	610.7	34.1	1.9	0.5
DV 7/25/15_1-118	187	37	5.1	0.0607	7.0	0.8413	9.2	0.1005	6.0	0.65	617.4	35.4	619.9	42.6	629.2	150.1	617.4	35.4	1.9	0.4
DV 7/25/15_1-130	149	112	1.3	0.0618	7.1	0.8705	9.7	0.1022	6.7	0.69	627.4	40.0	635.8	46.1	667.5	151.9	627.4	40.0	6.0	1.3
DV 7/25/15_1-7	104	98	1.1	0.0693	6.3	1.1667	8.5	0.1220	5.7	0.67	741.9	40.1	785.1	46.3	907.4	129.4	741.9	40.1	18.2	5.5
DV 7/25/15_1-57	203	123	1.6	0.0641	6.1	1.1259	8.5	0.1273	5.9	0.69	772.4	43.2	765.8	45.9	745.9	129.9	772.4	43.2	-3.6	-0.9
DV 7/25/15_1-39	443	63	7.0	0.0690	8.5	1.2238	12.7	0.1286	9.5	0.74	779.7	69.8	811.5	71.3	899.0	175.5	779.7	69.8	13.3	3.9
DV 7/25/15_1-85	502	239	2.1	0.0669	7.5	1.1969	10.8	0.1297	7.8	0.72	786.1	57.4	799.2	59.6	834.5	155.8	786.1	57.4	5.8	1.6
DV 7/25/15_1-17	423	339	1.2	0.0655	5.7	1.2380	8.1	0.1369	5.8	0.71	826.9	44.7	818.0	45.6	792.0	120.5	826.9	44.7	-4.4	-1.1
DV 7/25/15_1-75	183	119	1.5	0.0669	7.6	1.2649	10.4	0.1370	7.2	0.69	827.4	55.7	830.1	59.2	836.2	158.0	827.4	55.7	1.0	0.3
DV 7/25/15_1-89	163	82	2.0	0.0704	9.7	1.3361	14.0	0.1376	10.0	0.72	831.2	78.1	861.6	81.2	939.1	199.8	831.2	78.1	11.5	3.5
DV 7/25/15_1-36	163	103	1.6	0.0722	7.0	1.6064	9.9	0.1614	7.0	0.70	964.3	62.3	972.7	61.8	990.8	142.6	990.8	142.6	2.7	0.9
DV 7/25/15_1-30	120	47	2.5	0.0748	7.2	1.7854	10.1	0.1731	7.1	0.70	1028.9	68.0	1040.2	66.0	1062.7	144.8	1062.7	144.8	3.2	1.1
DV 7/25/15_1-86	542	84	6.5	0.0757	7.2	1.8472	10.3	0.1769	7.4	0.72	1049.8	71.8	1062.4	68.0	1087.1	144.0	1087.1	144.0	3.4	1.2
DV 7/25/15_1-120	51	46	1.1	0.0853	7.8	2.3592	10.2	0.2005	6.6	0.64	1178.2	70.6	1230.3	72.8	1323.4	151.5	1323.4	151.5	11.0	4.2
DV 7/25/15_1-61	135	70	1.9	0.1036	8.1	3.9913	11.9	0.2793	8.7	0.73	1588.1	122.6	1632.4	97.0	1689.6	150.0	1689.6	150.0	6.0	2.7
DV 7/25/15_1-93	140	104	1.4	0.1058	5.9	4.1719	8.6	0.2858	6.3	0.72	1620.4	89.6	1668.5	70.5	1728.2	108.7	1728.2	108.7	6.2	2.9
DV 7/25/15_1-144	151	105	1.4	0.1059	5.5	4.4229	7.7	0.3031	5.5	0.71	1706.6	82.2	1716.6	64.2	1730.6	100.8	1730.6	100.8	1.4	0.6
DV 7/25/15_1-112	163	76	2.1	0.1103	9.4	5.1202	13.4	0.3367	9.5	0.71	1870.7	155.0	1839.5	114.0	1804.2	170.6	1804.2	170.6	-3.7	-1.7
DV 7/25/15_1-96	84	56	1.5	0.1107	6.9	4.7762	9.6	0.3123	6.8	0.69	1752.1	103.9	1780.7	81.1	1810.9	126.1	1810.9	126.1	3.2	1.6
DV 7/25/15_1-78	26	18	1.4	0.1111	6.5	4.6395	8.7	0.3027	5.8	0.67	1704.9	87.0	1756.4	72.6	1817.3	117.4	1817.3	117.4	6.2	2.9
DV 7/25/15_1-97	340	89	3.8	0.1117	5.4	4.9690	7.3	0.3221	5.0	0.67	1799.9	78.1	1814.1	61.8	1826.9	98.7	1826.9	98.7	1.5	0.8
DV 7/25/15_1-42	750	42	17.7	0.1119	5.1	5.1199	7.4	0.3317	5.4	0.73	1846.6	87.3	1839.4	63.3	1830.6	92.7	1830.6	92.7	-0.9	-0.4
DV 7/25/15_1-115	199	304	0.7	0.1125	6.7	4.8911	9.3	0.3153	6.6	0.70	1766.8	101.7	1800.7	78.8	1840.4	120.5	1840.4	120.5	4.0	1.9
DV 7/25/15_1-40	491	251	2.0	0.1126	5.9	4.3183	8.2	0.2780	5.7	0.69	1581.3	79.9	1696.9	67.6	1842.0	106.7	1842.0	106.7	14.2	6.8
DV 7/25/15_1-4	373	230	1.6	0.1127	5.1	4.7901	7.3	0.3080	5.2	0.71	1730.7	78.4	1783.2	61.0	1842.8	92.9	1842.8	92.9	6.1	2.9
DV 7/25/15_1-71	40	46	0.9	0.1127	6.6	5.2978	9.2	0.3408	6.4	0.70	1890.7	105.6	1868.5	79.0	1843.2	120.1	1843.2	120.1	-2.6	-1.2
DV 7/25/15_1-37	192	93	2.1	0.1130	5.5	5.1193	8.0	0.3285	5.8	0.72	1831.1	92.7	1839.3	68.2	1847.8	100.3	1847.8	100.3	0.9	0.4
DV 7/25/15_1-63	279	69	4.0	0.1131	7.1	4.9892	10.3	0.3199	7.4	0.72	1789.1	116.2	1817.5	87.2	1849.7	128.7	1849.7	128.7	3.3	1.6
DV 7/25/15_1-20	426	121	3.5	0.1132	8.2	5.0941	11.6	0.3262	8.2	0.71	1820.1	130.7	1835.1	98.9	1850.8	148.3	1850.8	148.3	1.7	0.8
DV 7/25/15_1-116	675	105	6.4	0.1132	5.5	5.0787	7.7	0.3255	5.3	0.69	1816.6	84.7	1832.6	65.0	1850.9	99.7	1850.9	99.7	1.9	0.9
DV 7/25/15_1-1	394	30	12.9	0.1136	6.3	4.5594	8.9	0.2906	6.3	0.71	1644.6	91.5	1741.9	74.2	1858.2	113.9	1858.2	113.9	11.5	5.6

DV 7/25/15_1-136	265	39	6.7	0.1138	6.1	5.2816	8.6	0.3371	6.1	0.70	1872.5	98.7	1865.9	73.6	1860.2	110.5	1860.2	110.5	-0.7	-0.4
DV 7/25/15_1-11	251	79	3.2	0.1141	5.6	4.9607	7.9	0.3151	5.6	0.71	1765.7	86.1	1812.7	66.5	1865.2	100.5	1865.2	100.5	5.3	2.6
DV 7/25/15_1-145	223	128	1.7	0.1142	5.4	5.0829	7.7	0.3232	5.5	0.71	1805.1	86.9	1833.3	65.6	1867.0	97.9	1867.0	97.9	3.3	1.5
DV 7/25/15_1-14	416	221	1.9	0.1146	5.5	5.1261	7.8	0.3240	5.6	0.71	1809.2	87.9	1840.4	66.6	1874.2	99.6	1874.2	99.6	3.5	1.7
DV 7/25/15_1-127	274	74	3.7	0.1148	6.0	4.9527	8.4	0.3130	6.0	0.71	1755.6	91.7	1811.3	71.3	1877.2	107.6	1877.2	107.6	6.5	3.1
DV 7/25/15_1-99	416	71	5.8	0.1167	7.9	5.5039	11.3	0.3415	8.1	0.71	1894.0	133.2	1901.2	97.1	1905.9	141.6	1905.9	141.6	0.6	0.4
DV 7/25/15_1-22	775	163	4.7	0.1177	6.9	5.5292	9.8	0.3405	7.0	0.71	1889.2	114.1	1905.1	84.2	1921.3	123.3	1921.3	123.3	1.7	0.8
DV 7/25/15_1-12	507	42	12.1	0.1181	5.6	5.4707	7.8	0.3356	5.5	0.70	1865.4	88.8	1896.0	67.2	1928.0	100.4	1928.0	100.4	3.2	1.6
DV 7/25/15_1-140	453	406	1.1	0.1223	5.0	5.9509	7.1	0.3531	5.0	0.71	1949.4	84.8	1968.7	61.8	1990.7	89.3	1990.7	89.3	2.1	1.0
DV 7/25/15_1-133	157	72	2.2	0.1240	5.6	6.0365	7.9	0.3535	5.6	0.71	1951.4	95.1	1981.1	69.2	2013.9	99.3	2013.9	99.3	3.1	1.5
DV 7/25/15_1-111	48	54	0.9	0.1247	7.0	6.6378	10.2	0.3861	7.4	0.72	2104.8	132.6	2064.4	90.0	2024.1	124.6	2024.1	124.6	-4.0	-2.0
DV 7/25/15_1-126	291	595	0.5	0.1251	4.8	5.9626	6.7	0.3459	4.7	0.69	1915.0	77.3	1970.4	58.3	2030.2	85.5	2030.2	85.5	5.7	2.8
DV 7/25/15_1-147	420	205	2.0	0.1349	8.4	6.0383	13.7	0.3248	10.8	0.79	1813.1	171.3	1981.4	120.0	2163.3	146.9	2163.3	146.9	16.2	8.5
DV 7/25/15_1-6	335	168	2.0	0.1443	7.7	7.0152	12.3	0.3522	9.6	0.78	1945.1	161.0	2113.4	109.5	2279.3	132.3	2279.3	132.3	14.7	8.0
DV 7/25/15_1-98	522	285	1.8	0.1452	7.9	7.6600	11.2	0.3819	8.0	0.71	2085.2	142.6	2191.9	100.9	2290.2	135.8	2290.2	135.8	9.0	4.9
DV 7/25/15_1-55	99	65	1.5	0.1579	7.4	9.5938	10.5	0.4405	7.5	0.71	2352.7	148.1	2396.6	96.9	2433.6	124.7	2433.6	124.7	3.3	1.8
DV 7/25/15_1-73	34	40	0.9	0.1596	7.0	10.9825	9.5	0.4989	6.5	0.68	2609.1	140.1	2521.7	88.9	2451.2	117.8	2451.2	117.8	-6.4	-3.5
DV 7/25/15_1-107	254	205	1.2	0.1628	5.6	11.3371	7.6	0.5049	5.2	0.68	2634.7	113.4	2551.3	71.2	2484.8	94.1	2484.8	94.1	-6.0	-3.3
DV 7/25/15_1-2	68	34	2.0	0.1632	6.0	10.9652	8.6	0.4867	6.2	0.71	2556.3	129.8	2520.2	79.8	2488.9	100.8	2488.9	100.8	-2.7	-1.4
DV 7/25/15_1-138	218	50	4.4	0.1638	5.1	10.1280	7.2	0.4489	5.1	0.71	2390.6	102.4	2446.5	66.7	2494.9	85.5	2494.9	85.5	4.2	2.3
DV 7/25/15_1-141	81	137	0.6	0.1659	5.5	11.0685	7.8	0.4843	5.6	0.72	2545.9	118.3	2528.9	73.1	2516.8	92.1	2516.8	92.1	-1.2	-0.7
DV 7/25/15_1-77	132	90	1.5	0.1726	6.3	9.7611	9.2	0.4099	6.6	0.72	2214.4	124.1	2412.5	84.5	2583.3	106.0	2583.3	106.0	14.3	8.2
DV 7/25/15_1-32	171	62	2.8	0.1800	5.8	12.2668	8.2	0.4940	5.9	0.71	2587.8	125.1	2625.0	77.2	2653.0	95.5	2653.0	95.5	2.5	1.4
DV 7/25/15_1-70	758	102	7.4	0.2030	7.2	13.5958	10.7	0.4857	7.9	0.74	2552.1	166.8	2722.0	101.3	2850.2	116.9	2850.2	116.9	10.5	6.2
Data Rejected From Population Analyses																				
DV 7/25/15_1-81	302	238	1.3	0.0525	11.1	0.2884	15.3	0.0398	10.6	0.69	251.8	26.1	257.3	34.9	305.9	253.5	251.8	26.1	17.7	2.1
DV 7/25/15_1-148	765	378	2.0	0.0553	10.1	0.3038	15.1	0.0399	11.2	0.74	252.1	27.7	269.4	35.7	424.1	225.6	252.1	27.7	40.6	6.4
DV 7/25/15_1-123	74	96	0.8	0.0852	16.4	0.5695	17.8	0.0485	6.9	0.39	305.2	20.6	457.7	65.5	1321.2	317.1	305.2	20.6	76.9	33.3
DV 7/25/15_1-83	183	179	1.0	0.0550	11.5	0.3809	16.0	0.0502	11.0	0.69	315.7	34.0	327.7	44.7	412.6	257.9	315.7	34.0	23.5	3.7
DV 7/25/15_1-25	382	329	1.2	0.0553	10.8	0.4074	15.1	0.0534	10.5	0.69	335.5	34.3	347.0	44.3	423.5	241.7	335.5	34.3	20.8	3.3
DV 7/25/15_1-91	914	345	2.7	0.0551	10.4	0.4884	14.6	0.0642	10.3	0.70	401.4	39.9	403.8	48.6	415.8	231.6	401.4	39.9	3.5	0.6
DV 7/25/15_1-113	235	171	1.4	0.0549	12.3	0.5377	17.0	0.0711	11.8	0.69	442.5	50.3	436.9	60.5	407.5	275.9	442.5	50.3	-8.6	-1.3
DV 7/25/15_1-121	294	157	1.9	0.0517	14.6	0.5093	18.3	0.0715	11.0	0.60	445.2	47.4	418.0	62.7	271.5	334.7	445.2	47.4	-64.0	-6.5
DV 7/25/15_1-125	630	256	2.5	0.0581	10.3	0.5972	14.7	0.0746	10.4	0.71	463.7	46.7	475.5	55.7	533.9	225.9	463.7	46.7	13.1	2.5
DV 7/25/15_1-15	359	59	6.0	0.0651	11.6	1.1700	16.3	0.1303	11.5	0.71	789.3	85.6	786.7	89.6	777.1	243.2	789.3	85.6	-1.6	-0.3

DV 7/25/15_1-33	141	142	1.0	0.0714	12.6	1.5815	17.9	0.1605	12.7	0.71	959.3	113.3	963.0	111.8	970.3	257.6	970.3	257.6	1.1	0.4
DV 7/25/15_1-109	175	47	3.7	0.0953	6.5	2.0281	8.9	0.1542	6.2	0.69	924.6	53.1	1125.0	60.7	1534.8	122.1	1534.8	122.1	39.8	17.8
DV 7/25/15_1-105	484	289	1.7	0.1012	5.2	2.1755	9.9	0.1559	8.5	0.85	933.8	73.6	1173.2	69.1	1645.6	96.9	1645.6	96.9	43.3	20.4
DV 7/25/15_1-104	521	99	5.2	0.1145	13.4	5.2204	19.5	0.3303	14.2	0.73	1840.0	227.2	1855.9	167.8	1872.6	242.1	1872.6	242.1	1.7	0.9
DV 7/25/15_1-31	325	124	2.6	0.1151	10.1	4.5533	14.7	0.2867	10.6	0.72	1625.0	152.7	1740.8	122.9	1881.8	182.8	1881.8	182.8	13.6	6.6
DV 7/25/15_1-131	25	28	0.9	0.1192	10.5	5.6821	14.6	0.3459	10.2	0.70	1915.0	168.2	1928.7	126.4	1944.8	187.0	1944.8	187.0	1.5	0.7
DV 7/25/15_1-41	956	26	37.2	0.1208	13.8	5.2253	21.1	0.3137	16.0	0.76	1758.6	245.8	1856.7	181.7	1967.8	246.0	1967.8	246.0	10.6	5.3
DV 7/25/15_1-114	136	98	1.4	0.1230	12.7	6.0667	18.0	0.3577	12.8	0.71	1971.2	216.8	1985.5	157.9	2000.4	225.2	2000.4	225.2	1.5	0.7
DV 7/25/15_1-137	1054	195	5.4	0.1268	14.2	4.5570	15.2	0.2609	5.6	0.37	1494.4	74.6	1741.5	127.6	2054.1	250.5	2054.1	250.5	27.3	14.2
DV 7/25/15_1-45	480	175	2.7	0.1272	14.9	3.8131	18.3	0.2173	10.7	0.58	1267.3	122.6	1595.5	148.4	2060.3	263.1	2060.3	263.1	38.5	20.6
DV 7/25/15_1-3	114	63	1.8	0.1514	12.0	8.6613	16.5	0.4144	11.4	0.69	2235.2	215.5	2303.0	151.6	2361.5	204.7	2361.5	204.7	5.4	2.9
DV 7/25/15_1-62	1094	1632	0.7	0.1554	14.0	8.5551	18.9	0.3993	12.8	0.67	2165.7	235.3	2291.8	173.8	2405.7	237.5	2405.7	237.5	10.0	5.5
DV 7/25/15_1-103	65	26	2.5	0.2044	11.0	15.8123	15.7	0.5605	11.1	0.71	2868.9	258.2	2865.5	150.6	2862.0	179.4	2862.0	179.4	-0.2	-0.1
DV 7/25/15_1-88	86	512	0.2	0.7655	7.9	61.4093	11.7	0.5814	8.7	0.74	2954.7	205.4	4197.3	117.7	4858.8	113.9	4858.8	113.9	39.2	29.6

DV 8-08-16_1 38.121° N; 73.915° E

				Isotope ratios							Apparent Ages (Ma)									
				^{207}Pb	±	^{207}Pb	±	^{206}Pb	±		^{206}Pb	±	^{207}Pb	±	^{207}Pb	±		±	% discordance Pb^{206}/U^{238}-Pb^{207}/Pb^{206}	% discordance Pb^{206}/U^{238}-Pb^{207}/U^{325}
Analysis #	U (ppm)	Th (ppm)	U/Th	^{206}Pb	(2%SD)	^{235}U	(2%SD)	^{238}U	(2%SD)	error corr.	^{238}U	(2SD)	^{235}U	(2SD)	^{206}Pb	(2SD)	Best Age	(2SD)		
DV 8/08/16_1-66	173	103	1.7	0.0531	9.3	0.2605	12.2	0.035556	7.9	0.64	225.2	17.5	235.0	25.6	332.1	211.8	225.2	17.5	32.2	4.2
DV 8/08/16_1-4	98	91	1.1	0.0551	10.7	0.2772	12.7	0.036417	6.8	0.53	230.6	15.3	248.4	27.9	418.1	239.3	230.6	15.3	44.8	7.2
DV 8/08/16_1-133	257	186	1.4	0.0459	10.7	0.2317	12.6	0.036556	6.8	0.54	231.5	15.4	211.6	24.1	204	84.0	231.5	15.4	-12.9	-9.4
DV 8/08/16_1-43	499	374	1.3	0.0597	6.0	0.3043	7.7	0.036944	4.9	0.63	233.9	11.3	269.8	18.2	592.7	129.2	233.9	11.3	60.5	13.3
DV 8/08/16_1-40	109	170	0.6	0.0555	8.8	0.2881	10.2	0.037654	5.3	0.51	238.3	12.3	257.1	23.2	430.6	196.0	238.3	12.3	44.7	7.3
DV 8/08/16_1-13	1065	922	1.2	0.0493	4.8	0.2583	6.6	0.037968	4.6	0.68	240.2	10.8	233.3	13.8	161.6	112.6	240.2	10.8	-48.7	-3.0
DV 8/08/16_1-50	397	259	1.5	0.051	6.7	0.2679	9.0	0.038058	6.1	0.67	240.8	14.3	241.0	19.3	241.7	153.8	240.8	14.3	0.4	0.1
DV 8/08/16_1-5	59	98	0.6	0.0474	17.5	0.2524	20.0	0.038608	9.9	0.49	244.2	23.6	228.5	41.0	67.0	415.6	244.2	23.6	-264.7	-6.9
DV 8/08/16_1-12	195	175	1.1	0.0515	6.7	0.2758	8.2	0.038781	4.8	0.58	245.3	11.5	247.3	18.0	264.5	153.0	245.3	11.5	7.3	0.8
DV 8/08/16_1-57	660	276	2.4	0.0519	5.1	0.2804	7.1	0.039193	5.0	0.70	247.8	12.1	251.0	15.8	279.0	116.8	247.8	12.1	11.2	1.3
DV 8/08/16_1-51	676	321	2.1	0.0529	5.9	0.287	8.2	0.039323	5.8	0.70	248.6	14.1	256.2	18.6	323.9	133.4	248.6	14.1	23.2	2.9
DV 8/08/16_1-155	229	91	2.5	0.0513	6.2	0.2825	7.8	0.039914	4.8	0.61	252.3	11.9	252.7	17.5	255.6	141.8	252.3	11.9	1.3	0.1
DV 8/08/16_1-185	128	127	1.0	0.0578	10.0	0.3225	12.4	0.04046	7.4	0.59	255.7	18.4	283.8	30.6	522.3	218.7	255.7	18.4	51.0	9.9
DV 8/08/16_1-11	102	57	1.8	0.0508	9.9	0.2841	11.4	0.040527	5.8	0.50	256.1	14.5	253.9	25.7	230.9	228.5	256.1	14.5	-10.9	-0.9
DV 8/08/16_1-140	140	106	1.3	0.0457	14.5	0.2596	16.8	0.041152	8.4	0.50	260.0	21.4	234.4	35.1	236.6	108.0	260.0	21.4	-10.4	-10.9
DV 8/08/16_1-118	342	225	1.5	0.0521	7.6	0.2958	10.4	0.041154	7.1	0.68	260.0	18.2	263.1	24.1	288.3	173.9	260.0	18.2	9.8	1.2
DV 8/08/16_1-178	436	191	2.3	0.052	6.1	0.296	8.4	0.041333	5.7	0.68	261.1	14.7	263.3	19.4	283.2	140.5	261.1	14.7	7.8	0.8
DV 8/08/16_1-75	198	244	0.8	0.0509	12.1	0.2925	13.2	0.041603	5.4	0.41	262.8	14.0	260.6	30.4	238.3	278.4	262.8	14.0	-10.2	-0.8
DV 8/08/16_1-90	656	495	1.3	0.0522	5.6	0.3	7.8	0.041628	5.5	0.70	262.9	14.2	266.4	18.3	293.8	126.8	262.9	14.2	10.5	1.3
DV 8/08/16_1-147	871	592	1.5	0.051	7.5	0.2958	10.8	0.042026	7.7	0.71	265.4	20.0	263.1	25.0	241.5	173.9	265.4	20.0	-9.9	-0.9
DV 8/08/16_1-189	1745	928	1.9	0.0511	4.9	0.297	6.8	0.042144	4.7	0.69	266.1	12.4	264.1	15.7	245.6	112.1	266.1	12.4	-8.3	-0.8
DV 8/08/16_1-65	165	118	1.4	0.0564	10.3	0.3284	13.7	0.042216	9.1	0.66	266.6	23.8	288.3	34.5	466.7	228.3	266.6	23.8	42.9	7.6
DV 8/08/16_1-184	471	261	1.8	0.0514	5.5	0.3	7.7	0.042346	5.4	0.70	267.4	14.3	266.4	18.2	257.7	127.5	267.4	14.3	-3.7	-0.4
DV 8/08/16_1-6	563	48	11.8	0.0513	5.6	0.3022	7.5	0.042669	5.0	0.66	269.4	13.3	268.1	17.8	254.8	129.6	269.4	13.3	-5.7	-0.5
DV 8/08/16_1-93	218	162	1.3	0.0522	8.3	0.3085	11.0	0.042803	7.3	0.66	270.2	19.3	273.0	26.5	294.1	189.9	270.2	19.3	8.1	1.0
DV 8/08/16_1-105	235	93	2.5	0.0504	6.5	0.3001	8.8	0.043084	6.0	0.67	271.9	15.9	266.5	20.7	215.4	151.6	271.9	15.9	-26.2	-2.0
DV 8/08/16_1-115	134	137	1.0	0.0545	8.7	0.3257	11.2	0.043271	7.0	0.63	273.1	18.7	286.2	27.9	392.2	195.5	273.1	18.7	30.4	4.6
DV 8/08/16_1-96	939	377	2.5	0.052	6.2	0.315	8.7	0.043867	6.2	0.70	276.8	16.7	278.1	21.2	286.0	141.6	276.8	16.7	3.2	0.5
DV 8/08/16_1-134	276	119	2.3	0.0518	6.8	0.3191	9.1	0.044627	6.1	0.67	281.4	16.9	281.2	22.4	277.4	155.3	281.4	16.9	-1.5	-0.1
DV 8/08/16_1-68	70	45	1.5	0.0555	10.1	0.3504	11.4	0.045786	5.4	0.47	288.6	15.2	305.1	30.1	430.8	224.4	288.6	15.2	33.0	5.4
DV 8/08/16_1-145	553	205	2.7	0.0514	5.6	0.3251	7.3	0.045865	4.8	0.64	289.1	13.5	285.8	18.3	257.6	129.2	289.1	13.5	-12.2	-1.2

DV 8/08/16_1-9	308	105	2.9	0.0496	6.1	0.323	7.7	0.047189	4.7	0.61	297.2	13.8	284.2	19.1	175.3	143.1	297.2	13.8	-69.6	-4.6
DV 8/08/16_1-22	228	105	2.2	0.0527	6.0	0.3441	7.7	0.047289	4.9	0.63	297.9	14.1	300.3	19.9	316.7	135.9	297.9	14.1	5.9	0.8
DV 8/08/16_1-128	432	175	2.5	0.0535	5.0	0.3499	6.5	0.047366	4.3	0.65	298.3	12.5	304.6	17.2	350.6	112.2	298.3	12.5	14.9	2.1
DV 8/08/16_1-36	356	188	1.9	0.0541	6.7	0.3569	9.1	0.047845	6.2	0.68	301.3	18.3	309.9	24.3	373.4	150.1	301.3	18.3	19.3	2.8
DV 8/08/16_1-41	31	15	2.1	0.0486	20.0	0.3212	21.4	0.047904	7.6	0.35	301.6	22.3	282.9	52.8	128.7	470.4	301.6	22.3	-134.5	-6.6
DV 8/08/16_1-107	188	144	1.3	0.0514	6.7	0.3412	8.7	0.04804	5.7	0.65	302.5	16.8	298.1	22.6	260.7	152.7	302.5	16.8	-16.0	-1.5
DV 8/08/16_1-169	218	84	2.6	0.0503	7.1	0.3356	8.7	0.048357	5.2	0.59	304.4	15.4	293.8	22.3	210.5	163.8	304.4	15.4	-44.6	-3.6
DV 8/08/16_1-170	387	105	3.7	0.0542	7.0	0.3625	9.6	0.048526	6.6	0.68	305.5	19.7	314.1	25.9	379.0	157.3	305.5	19.7	19.4	2.7
DV 8/08/16_1-69	707	71	10.0	0.0529	7.7	0.3551	11.1	0.048589	7.9	0.72	305.9	23.7	308.5	29.4	326.5	175.2	305.9	23.7	6.3	0.9
DV 8/08/16_1-119	969	281	3.4	0.0518	8.3	0.3482	11.7	0.048716	8.4	0.71	306.6	25.0	303.4	30.8	275.6	189.8	306.6	25.0	-11.3	-1.1
DV 8/08/16_1-34	111	80	1.4	0.0429	31.9	0.2897	32.5	0.048986	6.4	0.20	308.3	19.3	258.4	74.4	299.2	120.3	308.3	19.3	-2.3	-19.3
DV 8/08/16_1-187	428	91	4.7	0.0526	6.8	0.357	9.4	0.049186	6.6	0.70	309.5	19.9	310.0	25.1	313.2	153.8	309.5	19.9	1.2	0.1
DV 8/08/16_1-146	394	338	1.2	0.0529	5.3	0.3603	7.1	0.049326	4.7	0.66	310.4	14.3	312.4	19.1	326.6	121.3	310.4	14.3	5.0	0.7
DV 8/08/16_1-14	237	113	2.1	0.0511	6.5	0.3484	8.5	0.049425	5.5	0.64	311.0	16.6	303.5	22.2	244.0	148.9	311.0	16.6	-27.4	-2.5
DV 8/08/16_1-111	351	167	2.1	0.0533	6.3	0.3637	8.8	0.049452	6.2	0.70	311.2	18.9	315.0	23.8	340.3	141.8	311.2	18.9	8.6	1.2
DV 8/08/16_1-47	255	160	1.6	0.0559	7.6	0.3837	10.3	0.049769	7.0	0.67	313.1	21.4	329.8	29.1	447.6	169.6	313.1	21.4	30.1	5.1
DV 8/08/16_1-32	200	124	1.6	0.053	9.5	0.3715	13.3	0.050806	9.3	0.70	319.5	29.0	320.8	36.6	328.3	216.5	319.5	29.0	2.7	0.4
DV 8/08/16_1-193	225	188	1.2	0.0532	5.5	0.3754	7.1	0.051145	4.5	0.63	321.5	14.2	323.7	19.7	337.1	125.0	321.5	14.2	4.6	0.7
DV 8/08/16_1-200	493	112	4.4	0.0531	6.8	0.3764	9.7	0.051315	7.0	0.71	322.6	22.0	324.4	27.1	333.5	155.1	322.6	22.0	3.3	0.5
DV 8/08/16_1-110	1627	994	1.6	0.0529	7.0	0.3821	10.2	0.052273	7.4	0.72	328.5	23.6	328.6	28.5	326.5	159.4	328.5	23.6	-0.6	0.0
DV 8/08/16_1-7	468	177	2.6	0.0526	5.3	0.3926	7.0	0.054043	4.6	0.65	339.3	15.1	336.3	20.0	313.0	121.2	339.3	15.1	-8.4	-0.9
DV 8/08/16_1-98	107	76	1.4	0.0511	8.4	0.3892	9.9	0.055111	5.1	0.52	345.8	17.3	333.8	28.1	247.2	194.4	345.8	17.3	-39.9	-3.6
DV 8/08/16_1-126	128	102	1.2	0.0536	7.4	0.4298	9.2	0.058097	5.4	0.59	364.0	19.3	363.0	28.0	354.1	167.5	364.0	19.3	-2.8	-0.3
DV 8/08/16_1-88	133	139	1.0	0.0588	7.0	0.4826	8.5	0.059494	5.0	0.58	372.5	17.9	399.9	28.3	558.1	152.3	372.5	17.9	33.2	6.8
DV 8/08/16_1-153	227	153	1.5	0.0554	5.9	0.4553	8.1	0.059577	5.5	0.68	373.1	20.0	381.0	25.7	428.7	132.5	373.1	20.0	13.0	2.1
DV 8/08/16_1-162	326	134	2.4	0.0545	5.9	0.4554	8.2	0.060637	5.7	0.70	379.5	21.1	381.1	25.9	390.7	131.3	379.5	21.1	2.9	0.4
DV 8/08/16_1-149	377	316	1.2	0.0552	5.2	0.4719	7.2	0.061989	4.9	0.69	387.7	18.6	392.5	23.3	419.7	116.2	387.7	18.6	7.6	1.2
DV 8/08/16_1-138	212	113	1.9	0.0556	5.4	0.4765	7.2	0.062063	4.8	0.66	388.2	18.1	395.7	23.6	437.9	120.0	388.2	18.1	11.4	1.9
DV 8/08/16_1-159	480	101	4.7	0.0541	7.3	0.4635	10.5	0.062123	7.5	0.72	388.5	28.4	386.7	33.7	375.6	164.6	388.5	28.4	-3.4	-0.5
DV 8/08/16_1-160	70	19	3.6	0.0593	9.4	0.5115	12.1	0.062605	7.6	0.63	391.5	28.8	419.5	41.6	576.5	205.0	391.5	28.8	32.1	6.7
DV 8/08/16_1-59	438	145	3.0	0.0552	9.4	0.4816	13.5	0.06328	9.8	0.72	395.5	37.5	399.2	44.7	418.5	209.8	395.5	37.5	5.5	0.9
DV 8/08/16_1-121	93	44	2.1	0.0564	7.3	0.4929	8.8	0.063299	5.0	0.56	395.7	19.0	406.9	29.5	468.6	161.6	395.7	19.0	15.6	2.8
DV 8/08/16_1-156	62	24	2.6	0.0492	21.8	0.4335	22.5	0.063941	5.4	0.24	399.5	20.7	365.7	69.1	155.7	511.2	399.5	20.7	-156.6	-9.3
DV 8/08/16_1-63	691	471	1.5	0.0559	9.1	0.4932	13.0	0.063972	9.3	0.71	399.7	36.0	407.1	43.6	447.1	202.5	399.7	36.0	10.6	1.8
DV 8/08/16_1-168	135	140	1.0	0.0544	9.8	0.4821	13.1	0.064259	8.7	0.66	401.5	33.9	399.5	43.3	388.5	219.7	401.5	33.9	-3.3	-0.5

DV 8/08/16_1-23	152	55	2.8	0.0548	6.1	0.4926	8.0	0.065179	5.1	0.64	407.0	20.3	406.7	26.7	402.3	136.8	407.0	20.3	-1.2	-0.1
DV 8/08/16_1-191	283	166	1.7	0.0543	5.1	0.4915	6.9	0.065549	4.6	0.67	409.3	18.4	405.9	23.0	385.3	115.3	409.3	18.4	-6.2	-0.8
DV 8/08/16_1-21	127	68	1.9	0.0572	6.5	0.5186	8.1	0.065736	4.9	0.60	410.4	19.5	424.2	28.2	497.8	144.0	410.4	19.5	17.6	3.3
DV 8/08/16_1-30	368	220	1.7	0.056	5.2	0.5172	7.0	0.066902	4.7	0.66	417.5	18.9	423.3	24.2	453.3	116.3	417.5	18.9	7.9	1.4
DV 8/08/16_1-154	196	148	1.3	0.0554	6.5	0.5146	9.0	0.067312	6.2	0.69	419.9	25.3	421.5	31.1	429.6	146.0	419.9	25.3	2.2	0.4
DV 8/08/16_1-157	65	31	2.1	0.0532	8.3	0.4943	11.0	0.067371	7.3	0.66	420.3	29.7	407.8	37.0	337.4	187.2	420.3	29.7	-24.6	-3.1
DV 8/08/16_1-58	465	64	7.3	0.0562	5.1	0.5238	7.0	0.067557	4.9	0.69	421.4	20.0	427.7	24.5	459.6	112.2	421.4	20.0	8.3	1.5
DV 8/08/16_1-167	227	85	2.7	0.0559	6.5	0.5219	9.2	0.067699	6.4	0.70	422.3	26.4	426.4	31.9	449.0	145.4	422.3	26.4	5.9	1.0
DV 8/08/16_1-86	587	278	2.1	0.056	6.8	0.5245	9.7	0.067833	7.0	0.72	423.1	28.6	428.1	34.0	452.6	151.0	423.1	28.6	6.5	1.2
DV 8/08/16_1-79	178	142	1.3	0.055	10.5	0.5147	14.1	0.067838	9.4	0.67	423.1	38.6	421.6	48.6	410.6	234.2	423.1	38.6	-3.0	-0.4
DV 8/08/16_1-158	191	103	1.9	0.0569	5.9	0.5376	7.9	0.068475	5.3	0.66	427.0	21.7	436.9	27.9	489.1	129.9	427.0	21.7	12.7	2.3
DV 8/08/16_1-52	101	37	2.7	0.0584	8.5	0.5533	10.6	0.06866	6.3	0.59	428.1	26.2	447.1	38.3	544.7	186.3	428.1	26.2	21.4	4.3
DV 8/08/16_1-3	504	281	1.8	0.0558	5.4	0.5456	7.6	0.070772	5.3	0.70	440.8	22.8	442.1	27.2	446.4	121.0	440.8	22.8	1.2	0.3
DV 8/08/16_1-91	139	65	2.1	0.0555	8.3	0.5432	11.4	0.070826	7.8	0.69	441.1	33.3	440.5	40.6	434.4	184.1	441.1	33.3	-1.6	-0.1
DV 8/08/16_1-85	567	252	2.2	0.0681	7.4	0.667	8.5	0.070945	4.3	0.50	441.8	18.4	518.9	34.6	871.5	152.7	441.8	18.4	49.3	14.8
DV 8/08/16_1-101	472	255	1.9	0.0554	5.4	0.5548	7.6	0.072537	5.4	0.71	451.4	23.6	448.1	27.5	428.1	119.7	451.4	23.6	-5.4	-0.7
DV 8/08/16_1-196	725	196	3.7	0.0555	4.8	0.5618	6.6	0.073392	4.6	0.69	456.6	20.4	452.7	24.1	430.7	106.0	456.6	20.4	-6.0	-0.9
DV 8/08/16_1-83	399	338	1.2	0.057	7.2	0.5777	10.3	0.073422	7.4	0.72	456.7	32.8	463.0	38.4	491.3	158.6	456.7	32.8	7.0	1.3
DV 8/08/16_1-125	211	236	0.9	0.0541	6.4	0.562	8.0	0.07528	4.8	0.59	467.9	21.4	452.9	29.1	374.6	144.5	467.9	21.4	-24.9	-3.3
DV 8/08/16_1-181	244	84	2.9	0.056	7.9	0.59	11.1	0.07645	7.8	0.70	474.9	35.9	470.8	41.9	451.4	175.6	474.9	35.9	-5.2	-0.9
DV 8/08/16_1-39	774	220	3.5	0.0567	7.3	0.6023	10.4	0.076966	7.4	0.71	478.0	34.3	478.7	39.9	480.4	162.3	478.0	34.3	0.5	0.1
DV 8/08/16_1-82	162	73	2.2	0.0557	7.1	0.5995	9.1	0.077945	5.8	0.63	483.8	27.0	476.9	34.7	440.8	157.0	483.8	27.0	-9.8	-1.5
DV 8/08/16_1-144	280	168	1.7	0.0555	7.7	0.5998	11.3	0.078368	8.3	0.73	486.4	38.9	477.1	43.0	431.5	170.8	486.4	38.9	-12.7	-1.9
DV 8/08/16_1-108	516	208	2.5	0.0568	4.8	0.6193	6.7	0.078958	4.7	0.69	489.9	22.1	489.4	26.1	483.9	106.7	489.9	22.1	-1.3	-0.1
DV 8/08/16_1-100	137	143	1.0	0.0563	6.3	0.6151	8.3	0.079094	5.4	0.65	490.7	25.6	486.8	32.0	465.3	139.0	490.7	25.6	-5.5	-0.8
DV 8/08/16_1-199	516	486	1.1	0.0573	5.7	0.6489	8.2	0.081986	5.9	0.71	508.0	28.7	507.8	32.6	503.8	125.9	508.0	28.7	-0.8	0.0
DV 8/08/16_1-180	324	484	0.7	0.0574	6.4	0.6551	8.9	0.082818	6.3	0.70	512.9	31.1	511.6	35.9	506.1	140.0	512.9	31.1	-1.3	-0.3
DV 8/08/16_1-24	125	78	1.6	0.0546	8.5	0.6247	10.0	0.082855	5.2	0.52	513.1	25.8	492.8	38.9	397.2	190.7	513.1	25.8	-29.2	-4.1
DV 8/08/16_1-97	507	218	2.3	0.0582	8.9	0.6778	12.6	0.084401	8.9	0.71	522.3	44.7	525.4	51.6	535.9	194.5	522.3	44.7	2.5	0.6
DV 8/08/16_1-198	294	120	2.4	0.0569	6.0	0.6765	8.3	0.086167	5.8	0.69	532.8	29.8	524.7	34.2	486.4	132.3	532.8	29.8	-9.5	-1.6
DV 8/08/16_1-18	127	458	0.3	0.0607	5.8	0.7767	7.7	0.092698	5.1	0.65	571.5	27.7	583.6	34.1	628.9	125.1	571.5	27.7	9.1	2.1
DV 8/08/16_1-151	203	96	2.1	0.0599	4.8	0.7735	6.5	0.093657	4.4	0.67	577.1	24.3	581.8	28.8	599.3	104.4	577.1	24.3	3.7	0.8
DV 8/08/16_1-130	465	304	1.5	0.059	5.3	0.7653	7.5	0.094057	5.3	0.71	579.5	29.5	577.1	33.0	565.3	115.5	579.5	29.5	-2.5	-0.4
DV 8/08/16_1-166	520	111	4.7	0.0615	8.1	0.8032	12.6	0.094752	9.6	0.76	583.6	53.6	598.7	56.8	656.4	173.9	583.6	53.6	11.1	2.5
DV 8/08/16_1-76	351	350	1.0	0.0606	7.4	0.8264	10.6	0.098789	7.6	0.72	607.3	44.0	611.6	48.5	625.3	158.5	607.3	44.0	2.9	0.7

DV 8/08/16_1-1	97	21	4.7	0.0597	8.2	0.8164	9.9	0.099106	5.6	0.56	609.2	32.3	606.1	45.1	591.9	177.5	609.2	32.3	-2.9	-0.5
DV 8/08/16_1-192	116	39	3.0	0.0624	6.1	0.8567	8.4	0.099528	5.8	0.68	611.6	33.7	628.3	39.3	687.1	130.6	611.6	33.7	11.0	2.7
DV 8/08/16_1-54	424	119	3.6	0.0629	8.6	0.8774	16.8	0.101032	14.4	0.86	620.5	85.3	639.6	79.8	706.1	183.6	620.5	85.3	12.1	3.0
DV 8/08/16_1-122	200	349	0.6	0.0596	6.0	0.8359	8.5	0.101625	6.0	0.70	623.9	35.6	616.9	39.1	588.5	130.2	623.9	35.6	-6.0	-1.1
DV 8/08/16_1-48	627	253	2.5	0.0614	5.4	0.863	7.8	0.101876	5.7	0.72	625.4	33.7	631.8	36.8	653.2	116.7	625.4	33.7	4.3	1.0
DV 8/08/16_1-81	463	122	3.8	0.0692	7.1	1.1524	9.9	0.120573	6.9	0.69	733.9	47.9	778.4	54.0	905.8	147.1	733.9	47.9	19.0	5.7
DV 8/08/16_1-37	281	215	1.3	0.0659	7.8	1.1044	10.9	0.121377	7.7	0.70	738.5	53.7	755.5	58.4	804.5	163.6	738.5	53.7	8.2	2.2
DV 8/08/16_1-17	80	127	0.6	0.064	7.4	1.0995	9.8	0.124394	6.5	0.66	755.8	46.5	753.1	52.2	742.9	155.7	755.8	46.5	-1.7	-0.4
DV 8/08/16_1-148	380	45	8.4	0.066	6.7	1.1715	9.0	0.128616	6.0	0.67	780.0	44.4	787.3	49.4	807.3	140.3	780.0	44.4	3.4	0.9
DV 8/08/16_1-120	199	196	1.0	0.0667	6.8	1.1925	9.8	0.129548	7.1	0.72	785.3	52.2	797.1	54.1	827.7	141.9	785.3	52.2	5.1	1.5
DV 8/08/16_1-25	91	82	1.1	0.0694	6.0	1.2535	7.9	0.130824	5.3	0.66	792.6	39.2	825.0	44.8	911.4	123.2	792.6	39.2	13.0	3.9
DV 8/08/16_1-29	323	415	0.8	0.0702	6.9	1.3093	9.9	0.135105	7.2	0.72	816.9	55.0	849.8	57.3	934.9	142.1	816.9	55.0	12.6	3.9
DV 8/08/16_1-163	658	225	2.9	0.0675	6.7	1.2595	9.5	0.135337	6.8	0.71	818.2	52.6	827.7	54.1	853.1	138.6	818.2	52.6	4.1	1.1
DV 8/08/16_1-171	291	41	7.0	0.0695	7.2	1.3455	10.7	0.140363	8.0	0.74	846.7	63.2	865.6	62.4	914.7	147.7	846.7	63.2	7.4	2.2
DV 8/08/16_1-179	375	64	5.9	0.0685	5.5	1.4278	7.9	0.151289	5.7	0.72	908.2	48.3	900.6	47.1	882.5	113.2	882.5	113.2	-2.9	-0.8
DV 8/08/16_1-89	282	181	1.6	0.0703	4.9	1.4309	6.9	0.147474	5.0	0.71	886.8	41.1	901.9	41.4	936.5	99.7	886.8	41.1	5.3	1.7
DV 8/08/16_1-20	120	155	0.8	0.0692	6.4	1.4915	8.5	0.156196	5.7	0.67	935.6	49.9	926.9	52.0	904.3	131.5	904.3	131.5	-3.5	-0.9
DV 8/08/16_1-80	276	34	8.0	0.0697	8.8	1.4425	12.8	0.149934	9.2	0.72	900.6	77.6	906.8	76.7	919.5	181.6	919.5	181.6	2.1	0.7
DV 8/08/16_1-56	225	104	2.2	0.0699	6.0	1.4973	8.4	0.155322	6.0	0.71	930.7	51.8	929.3	51.4	924.2	122.8	924.2	122.8	-0.7	-0.2
DV 8/08/16_1-142	150	77	2.0	0.0706	6.9	1.5198	9.8	0.156011	7.0	0.71	934.6	60.9	938.4	60.2	946.0	141.5	946.0	141.5	1.2	0.4
DV 8/08/16_1-143	59	29	2.0	0.0713	5.7	1.5322	7.7	0.155718	5.2	0.67	932.9	44.9	943.4	47.3	966.5	117.0	966.5	117.0	3.5	1.1
DV 8/08/16_1-102	140	89	1.6	0.0716	6.2	1.6261	8.3	0.164408	5.6	0.67	981.2	51.0	980.3	52.2	975.4	125.4	975.4	125.4	-0.6	-0.1
DV 8/08/16_1-26	113	161	0.7	0.0727	6.6	1.5604	9.2	0.155609	6.5	0.70	932.3	56.2	954.6	56.9	1004.5	133.0	1004.5	133.0	7.2	2.3
DV 8/08/16_1-117	435	200	2.2	0.076	4.7	1.7719	6.7	0.168817	4.9	0.72	1005.6	45.4	1035.2	43.7	1095.7	93.5	1095.7	93.5	8.2	2.9
DV 8/08/16_1-64	1051	230	4.6	0.0778	4.3	2.0202	6.1	0.188039	4.4	0.71	1110.7	45.0	1122.3	41.6	1143.0	85.3	1143.0	85.3	2.8	1.0
DV 8/08/16_1-84	397	204	1.9	0.0783	9.5	1.8929	14.3	0.175201	10.7	0.75	1040.7	102.7	1078.6	95.4	1153.5	189.5	1153.5	189.5	9.8	3.5
DV 8/08/16_1-67	125	56	2.2	0.08	6.1	2.3017	8.8	0.208408	6.5	0.73	1220.3	71.9	1212.8	62.7	1197.6	119.6	1197.6	119.6	-1.9	-0.6
DV 8/08/16_1-165	606	72	8.4	0.0904	5.3	2.9616	7.5	0.237707	5.3	0.71	1374.8	65.9	1397.8	56.7	1433.3	100.5	1433.3	100.5	4.1	1.6
DV 8/08/16_1-61	220	112	2.0	0.0908	6.2	3.0943	8.9	0.246948	6.5	0.72	1422.7	82.5	1431.3	68.5	1442.4	117.5	1442.4	117.5	1.4	0.6
DV 8/08/16_1-103	855	86	9.9	0.0921	4.3	2.8809	6.1	0.226556	4.4	0.72	1316.4	52.9	1376.9	46.3	1469.3	81.3	1469.3	81.3	10.4	4.4
DV 8/08/16_1-175	464	110	4.2	0.093	6.1	2.7862	8.9	0.217237	6.6	0.73	1267.3	76.0	1351.8	67.0	1488.6	114.9	1488.6	114.9	14.9	6.3
DV 8/08/16_1-72	236	158	1.5	0.0969	4.8	3.5174	6.9	0.262925	5.0	0.72	1504.8	66.6	1531.1	54.4	1565.7	90.0	1565.7	90.0	3.9	1.7
DV 8/08/16_1-116	515	778	0.7	0.0979	4.3	3.6675	6.2	0.271205	4.4	0.72	1546.9	61.2	1564.3	49.2	1585.4	80.5	1585.4	80.5	2.4	1.1
DV 8/08/16_1-197	98	38	2.6	0.1011	7.2	3.1873	10.9	0.228467	8.2	0.75	1326.5	98.8	1454.1	84.7	1643.6	133.9	1643.6	133.9	19.3	8.8
DV 8/08/16_1-190	60	24	2.5	0.1043	5.0	4.562	6.8	0.317198	4.7	0.68	1776.0	73.4	1742.4	57.0	1701.6	91.8	1701.6	91.8	-4.4	-1.9

DV 8/08/16_1-42	172	105	1.6	0.1047	5.2	4.3459	7.4	0.300913	5.3	0.71	1695.8	78.7	1702.1	60.9	1708.5	95.4	1708.5	95.4	0.7	0.4
DV 8/08/16_1-38	76	73	1.0	0.1059	5.2	4.3007	7.4	0.294384	5.3	0.71	1663.4	78.0	1693.5	61.2	1729.5	95.7	1729.5	95.7	3.8	1.8
DV 8/08/16_1-33	160	72	2.2	0.1077	4.9	4.4235	7.0	0.297636	5.0	0.71	1679.6	73.9	1716.8	57.9	1760.9	90.0	1760.9	90.0	4.6	2.2
DV 8/08/16_1-8	778	62	12.6	0.1087	8.4	4.6284	12.1	0.308364	8.7	0.72	1732.7	132.2	1754.4	101.2	1778.3	153.5	1778.3	153.5	2.6	1.2
DV 8/08/16_1-94	37	19	1.9	0.1092	6.0	4.6829	8.3	0.310722	5.7	0.68	1744.3	86.5	1764.2	69.2	1785.4	110.2	1785.4	110.2	2.3	1.1
DV 8/08/16_1-77	25	17	1.5	0.1096	5.7	4.3134	7.7	0.285107	5.2	0.67	1617.0	74.8	1695.9	63.7	1792.8	104.0	1792.8	104.0	9.8	4.7
DV 8/08/16_1-132	223	227	1.0	0.1112	5.1	4.932	7.3	0.321325	5.3	0.72	1796.2	83.0	1807.8	62.0	1819.3	92.7	1819.3	92.7	1.3	0.6
DV 8/08/16_1-123	498	38	13.1	0.1113	6.6	4.7084	9.2	0.3065	6.4	0.70	1723.5	97.0	1768.7	77.0	1820.4	119.7	1820.4	119.7	5.3	2.6
DV 8/08/16_1-161	521	62	8.3	0.1115	4.9	4.7397	7.0	0.308314	5.1	0.72	1732.4	77.0	1774.3	58.9	1823.9	88.6	1823.9	88.6	5.0	2.4
DV 8/08/16_1-124	177	74	2.4	0.1116	6.1	5.0707	8.8	0.329193	6.4	0.72	1834.5	101.5	1831.2	75.0	1825.4	111.4	1825.4	111.4	-0.5	-0.2
DV 8/08/16_1-19	161	77	2.1	0.1119	6.0	5.1565	8.4	0.334015	6.0	0.71	1857.8	96.7	1845.5	71.7	1829.7	107.9	1829.7	107.9	-1.5	-0.7
DV 8/08/16_1-55	660	167	4.0	0.112	5.3	4.8355	7.5	0.312963	5.4	0.71	1755.3	82.7	1791.1	63.4	1831.7	96.0	1831.7	96.0	4.2	2.0
DV 8/08/16_1-95	1116	486	2.3	0.1125	5.2	5.0865	7.6	0.327536	5.5	0.72	1826.4	87.3	1833.8	64.3	1839.8	94.9	1839.8	94.9	0.7	0.4
DV 8/08/16_1-104	332	126	2.6	0.1126	4.9	4.1241	6.8	0.265285	4.8	0.70	1516.8	65.1	1659.1	55.9	1841.6	88.2	1841.6	88.2	17.6	8.6
DV 8/08/16_1-129	292	81	3.6	0.1126	4.8	5.1507	6.9	0.331255	5.0	0.72	1844.5	79.9	1844.5	58.7	1842.6	87.1	1842.6	87.1	-0.1	0.0
DV 8/08/16_1-194	260	90	2.9	0.1131	7.5	4.8835	10.6	0.312859	7.5	0.71	1754.8	115.5	1799.4	89.4	1849.9	135.2	1849.9	135.2	5.1	2.5
DV 8/08/16_1-109	960	454	2.1	0.1132	5.0	5.3422	7.2	0.341756	5.2	0.72	1895.1	85.0	1875.6	61.5	1851.6	90.5	1851.6	90.5	-2.4	-1.0
DV 8/08/16_1-106	277	57	4.8	0.1132	5.4	5.4418	7.9	0.348099	5.8	0.73	1925.5	95.9	1891.5	67.8	1851.7	98.0	1851.7	98.0	-4.0	-1.8
DV 8/08/16_1-15	169	52	3.2	0.1133	6.7	5.3344	9.8	0.341015	7.2	0.73	1891.5	117.9	1874.4	83.8	1853.5	120.4	1853.5	120.4	-2.1	-0.9
DV 8/08/16_1-87	276	74	3.7	0.1137	4.5	5.294	6.5	0.337232	4.8	0.73	1873.3	77.3	1867.9	55.6	1859.5	80.8	1859.5	80.8	-0.7	-0.3
DV 8/08/16_1-127	282	91	3.1	0.1137	5.2	5.2124	7.4	0.332026	5.4	0.72	1848.2	86.0	1854.7	63.2	1859.8	93.2	1859.8	93.2	0.6	0.3
DV 8/08/16_1-70	466	227	2.1	0.1138	4.6	5.2304	6.5	0.333004	4.7	0.71	1852.9	75.8	1857.6	55.8	1861.0	82.8	1861.0	82.8	0.4	0.3
DV 8/08/16_1-164	447	136	3.3	0.1139	6.3	5.141	9.1	0.327286	6.7	0.73	1825.2	106.0	1842.9	77.9	1863.0	113.6	1863.0	113.6	2.0	1.0
DV 8/08/16_1-131	995	778	1.3	0.1142	4.5	5.2596	6.4	0.333771	4.6	0.71	1856.6	74.2	1862.3	54.8	1866.9	81.4	1866.9	81.4	0.5	0.3
DV 8/08/16_1-173	840	90	9.4	0.1153	7.5	4.6011	10.3	0.289539	7.1	0.69	1639.2	103.1	1749.5	86.2	1884.2	134.7	1884.2	134.7	13.0	6.3
DV 8/08/16_1-46	161	62	2.6	0.1161	5.1	5.0467	7.3	0.314975	5.3	0.72	1765.1	81.7	1827.2	61.9	1897.4	91.1	1897.4	91.1	7.0	3.4
DV 8/08/16_1-27	411	52	7.9	0.1174	5.6	5.5241	8.0	0.340941	5.8	0.72	1891.2	95.8	1904.4	69.3	1917.1	99.9	1917.1	99.9	1.3	0.7
DV 8/08/16_1-139	262	215	1.2	0.1195	6.4	5.121	8.9	0.31068	6.2	0.70	1744.1	95.5	1839.6	75.9	1948.0	114.3	1948.0	114.3	10.5	5.2
DV 8/08/16_1-177	454	141	3.2	0.1227	9.4	5.6478	13.9	0.333876	10.3	0.74	1857.1	166.1	1923.4	120.5	1996.0	166.5	1996.0	166.5	7.0	3.4
DV 8/08/16_1-174	338	122	2.8	0.1236	5.9	5.8918	8.4	0.345834	6.0	0.71	1914.7	100.1	1960.0	73.3	2008.6	105.1	2008.6	105.1	4.7	2.3
DV 8/08/16_1-49	137	75	1.8	0.1274	5.8	6.5044	8.2	0.369953	5.9	0.71	2029.2	102.5	2046.5	72.7	2062.8	102.6	2062.8	102.6	1.6	0.8
DV 8/08/16_1-195	850	179	4.7	0.1292	4.3	5.9217	6.2	0.332182	4.5	0.72	1848.9	72.7	1964.4	53.7	2086.6	74.9	2086.6	74.9	11.4	5.9
DV 8/08/16_1-113	443	153	2.9	0.13	6.0	6.9334	8.9	0.386149	6.5	0.73	2104.9	117.1	2102.9	78.8	2098.6	106.0	2098.6	106.0	-0.3	-0.1
DV 8/08/16_1-112	153	115	1.3	0.136	5.4	7.3639	7.9	0.392202	5.8	0.73	2133.0	105.1	2156.6	70.5	2176.7	93.4	2176.7	93.4	2.0	1.1
DV 8/08/16_1-35	451	155	2.9	0.1369	5.4	6.8436	7.6	0.362218	5.4	0.71	1992.7	93.0	2091.4	67.6	2188.6	93.7	2188.6	93.7	9.0	4.7

DV 8/08/16_1-114	628	278	2.3	0.14	4.6	6.75	6.5	0.349247	4.7	0.71	1931.0	77.8	2079.2	57.9	2227.0	80.0	2227.0	80.0	13.3	7.1
DV 8/08/16_1-136	306	234	1.3	0.1436	7.8	7.8818	11.0	0.397657	7.9	0.71	2158.2	144.2	2217.6	99.8	2271.4	134.0	2271.4	134.0	5.0	2.7
DV 8/08/16_1-92	356	294	1.2	0.147	4.2	8.5836	6.1	0.422857	4.4	0.72	2273.4	84.6	2294.8	55.4	2311.6	72.6	2311.6	72.6	1.7	0.9
DV 8/08/16_1-176	134	312	0.4	0.152	8.0	7.4632	10.5	0.356168	6.9	0.66	1964.0	117.5	2168.6	94.7	2368.6	135.9	2368.6	135.9	17.1	9.4
DV 8/08/16_1-152	75	72	1.0	0.1568	5.2	9.6547	7.4	0.44649	5.3	0.71	2379.6	105.7	2402.4	68.1	2421.3	87.9	2421.3	87.9	1.7	0.9
DV 8/08/16_1-183	1514	596	2.5	0.1589	5.1	9.4839	7.4	0.432923	5.4	0.73	2318.9	105.7	2386.0	68.1	2443.9	86.1	2443.9	86.1	5.1	2.8
DV 8/08/16_1-141	593	297	2.0	0.1638	4.9	10.374	7.0	0.459001	5.1	0.72	2435.1	104.1	2468.7	65.3	2495.3	81.9	2495.3	81.9	2.4	1.4
DV 8/08/16_1-188	133	89	1.5	0.1642	4.9	10.895	7.1	0.481262	5.2	0.72	2532.8	108.8	2514.2	66.2	2499.1	82.4	2499.1	82.4	-1.3	-0.7
DV 8/08/16_1-2	217	314	0.7	0.168	9.3	10.166	13.1	0.438422	9.2	0.70	2343.6	181.7	2450.0	121.8	2537.6	156.3	2537.6	156.3	7.6	4.3
DV 8/08/16_1-99	66	74	0.9	0.1706	6.4	11.449	9.1	0.485969	6.6	0.72	2553.2	138.9	2560.4	85.5	2563.8	106.3	2563.8	106.3	0.4	0.3
DV 8/08/16_1-186	101	82	1.2	0.1841	4.8	12.525	7.0	0.493485	5.1	0.72	2585.7	109.0	2644.6	65.9	2690.0	79.7	2690.0	79.7	3.9	2.2
DV 8/08/16_1-78	440	168	2.6	0.1958	6.4	12.32	9.2	0.455779	6.6	0.72	2420.9	133.7	2629.1	86.7	2791.8	105.2	2791.8	105.2	13.3	7.9
Data Rejected From Population Analyses																				
DV 8/08/16_1-53	288	283	1.0	0.0523	15.9	0.2966	22.8	0.041104	16.3	0.71	259.7	41.5	263.7	53.0	298.4	363.7	259.7	41.5	13.0	1.5
DV 8/08/16_1-31	144	41	3.5	0.0554	13.8	0.3399	18.6	0.044452	12.4	0.67	280.4	34.1	297.1	47.9	428.7	308.1	280.4	34.1	34.6	5.6
DV 8/08/16_1-71	157	101	1.6	0.0583	12.2	0.3584	16.2	0.044523	10.6	0.65	280.8	29.0	311.1	43.3	542.2	267.4	280.8	29.0	48.2	9.7
DV 8/08/16_1-74	279	65	4.3	0.0537	10.0	0.4052	14.6	0.05469	10.6	0.73	343.3	35.5	345.4	42.8	357.8	226.7	343.3	35.5	4.1	0.6
DV 8/08/16_1-60	534	194	2.7	0.0566	11.8	0.5609	17.1	0.071795	12.3	0.72	447.0	53.2	452.1	62.4	476.5	261.7	447.0	53.2	6.2	1.1
DV 8/08/16_1-16	668	80	8.4	0.0664	7.6	0.8968	9.7	0.097896	6.1	0.62	602.1	34.8	650.0	46.7	818.0	159.3	602.1	34.8	26.4	7.4
DV 8/08/16_1-44	59	19	3.0	0.068	10.5	1.3559	11.9	0.144449	5.5	0.46	869.8	44.9	870.1	69.4	869.4	217.8	869.8	44.9	0.0	0.0
DV 8/08/16_1-28	95	62	1.5	0.0725	17.0	1.4491	24.4	0.144819	17.6	0.72	871.9	143.2	909.5	147.7	1000.2	344.6	871.9	143.2	12.8	4.1
DV 8/08/16_1-135	105	68	1.5	0.0722	10.0	1.6663	14.1	0.167248	9.9	0.70	996.9	91.3	995.8	89.5	991.4	204.1	991.4	204.1	-0.6	-0.1
DV 8/08/16_1-73	214	189	1.1	0.1068	10.1	4.0464	14.1	0.274615	10.0	0.70	1564.2	138.3	1643.6	115.6	1744.7	184.1	1744.7	184.1	10.3	4.8
DV 8/08/16_1-10	309	123	2.5	0.1117	11.0	5.1827	15.7	0.336147	11.2	0.71	1868.1	181.7	1849.8	134.0	1827.1	198.6	1827.1	198.6	-2.2	-1.0
DV 8/08/16_1-45	385	59	6.6	0.1119	5.5	3.8585	7.5	0.249816	5.2	0.69	1437.5	66.9	1605.0	60.6	1831.2	99.0	1831.2	99.0	21.5	10.4
DV 8/08/16_1-137	1487	185	8.1	0.1169	12.0	5.472	17.5	0.33931	12.8	0.73	1883.3	208.6	1896.2	151.7	1908.8	216.2	1908.8	216.2	1.3	0.7
DV 8/08/16_1-182	731	704	1.0	0.1316	15.0	7.0969	21.2	0.391225	15.0	0.71	2128.5	272.3	2123.7	191.1	2119.1	263.2	2119.1	263.2	-0.4	-0.2
DV 8/08/16_1-172	180	70	2.6	0.161	10.1	9.8308	14.1	0.442866	9.9	0.70	2363.5	195.0	2419.0	130.4	2466.5	170.1	2466.5	170.1	4.2	2.3
DV 8/08/16_1-62	67	17	4.0	0.1817	27.1	13.56	38.9	0.540804	28.0	0.72	2786.8	634.5	2719.5	385.3	2668.4	448.0	2668.4	448.0	-4.4	-2.5
DV 8/08/16_1-150	288	152	1.9	0.2712	11.3	21.292	13.8	0.56911	8.0	0.58	2904.2	187.4	3152.0	135.1	3313.1	177.3	3313.1	177.3	12.3	7.9

B. Appendix 2: U-Pb Zircon Analysis

LA-ICP-MS analyses conducted at the University of Arizona Laserchron Center

15_006	38.688	73.349																	
	U	206Pb	U/Th	206Pb*	±	207Pb*	±	206Pb*	±	error	206Pb*	±	207Pb*	±	206Pb*	±	Best age	±	Conc
	(ppm)	204Pb		207Pb*	(%)	235U*	(%)	238U	(%)	corr.	238U*	(Ma)	235U	(Ma)	207Pb*	(Ma)	(Ma)	(Ma)	(%)
Chapman15-006C July5-Spot 28	189	14900	2.2	18.8038	1.6	0.2437	3.9	0.0332	3.5	0.91	210.8	7.3	221.5	7.7	336.5	37.2	210.8	7.3	NA
Chapman15-006C July5-Spot 21	312	12187	1.0	19.3691	1.4	0.2796	2.8	0.0393	2.5	0.87	248.3	6.0	250.3	6.3	269.0	32.6	248.3	6.0	NA
Chapman15-006C July5-Spot 57	248	7177	1.7	16.8483	3.1	0.3298	4.8	0.0403	3.7	0.76	254.7	9.2	289.4	12.2	580.1	67.8	254.7	9.2	NA
Chapman15-006C July5-Spot 72	159	805548	2.0	18.4804	1.6	0.3046	4.1	0.0408	3.8	0.92	257.9	9.6	269.9	9.8	375.7	36.2	257.9	9.6	NA
Chapman15-006C July5-Spot 41	430	6767	2.8	19.9277	1.2	0.2850	3.0	0.0412	2.7	0.91	260.2	7.0	254.6	6.8	203.4	29.0	260.2	7.0	NA
Chapman15-006C July5-Spot 29	146	6282	0.9	20.0910	1.3	0.2841	2.9	0.0414	2.5	0.89	261.5	6.5	253.9	6.4	184.4	30.3	261.5	6.5	NA
Chapman15-006C July5-Spot 74	77	6225	0.6	19.3639	2.1	0.2970	5.5	0.0417	5.0	0.92	263.4	13.0	264.0	12.7	269.6	49.2	263.4	13.0	NA
Chapman15-006C July5-Spot 1	78	1791	1.4	22.0808	2.0	0.2632	4.5	0.0422	4.0	0.90	266.2	10.5	237.3	9.5	40.1	48.6	266.2	10.5	NA
Chapman15-006C July5-Spot 11	129	3391	2.6	20.5002	4.6	0.2863	5.7	0.0426	3.4	0.59	268.7	8.8	255.6	12.9	137.3	108.6	268.7	8.8	NA
Chapman15-006C July5-Spot 24	218	34107	2.1	18.5556	1.2	0.3252	2.7	0.0438	2.5	0.90	276.1	6.7	285.9	6.8	366.5	26.2	276.1	6.7	NA
Chapman15-006C July5-Spot 56	470	236164	3.5	18.3996	1.4	0.3516	3.1	0.0469	2.8	0.90	295.6	8.0	305.9	8.1	385.5	30.5	295.6	8.0	NA
Chapman15-006C July5-Spot 38	68	34766	1.0	17.4463	2.1	0.3717	5.9	0.0470	5.5	0.93	296.3	15.9	320.9	16.2	503.8	46.0	296.3	15.9	NA
Chapman15-006C July5-Spot 80	75	1453	2.8	17.3461	5.1	0.3778	5.9	0.0475	3.0	0.51	299.3	8.7	325.4	16.4	516.5	111.2	299.3	8.7	NA
Chapman15-006C July5-Spot 79	135	3712	3.0	19.6672	4.1	0.3366	5.4	0.0480	3.5	0.65	302.3	10.4	294.6	13.9	233.9	95.8	302.3	10.4	NA
Chapman15-006C July5-Spot 13	193	226242	3.8	18.5355	1.2	0.3597	4.0	0.0484	3.8	0.95	304.4	11.3	312.0	10.7	369.0	27.3	304.4	11.3	NA
Chapman15-006C July5-Spot 2	328	39642	1.0	18.6323	1.2	0.3773	3.4	0.0510	3.2	0.93	320.6	10.0	325.0	9.5	357.2	27.7	320.6	10.0	NA
Chapman15-006C July5-Spot 59	302	14337	1.3	18.7254	1.6	0.3970	3.6	0.0539	3.3	0.90	338.5	10.7	339.5	10.5	346.0	36.1	338.5	10.7	NA
Chapman15-006C July5-Spot 27	373	31868	1.8	18.8680	1.2	0.3950	3.8	0.0540	3.6	0.95	339.3	11.9	338.0	11.0	328.8	27.8	339.3	11.9	NA
Chapman15-006C July5-Spot 58	178	20859	2.2	19.0768	1.3	0.3925	3.6	0.0543	3.4	0.93	340.9	11.3	336.2	10.4	303.8	29.5	340.9	11.3	NA
Chapman15-006C July5-Spot 19	52	9077	1.8	18.2138	2.7	0.4224	5.5	0.0558	4.8	0.87	350.1	16.4	357.8	16.6	408.3	60.3	350.1	16.4	NA
Chapman15-006C July5-Spot 47	368	11668	1.7	18.6180	0.9	0.4252	2.6	0.0574	2.4	0.93	359.9	8.4	359.8	7.8	358.9	20.6	359.9	8.4	NA
Chapman15-006C July5-Spot 40	185	21684	1.6	18.2034	1.4	0.4366	3.1	0.0576	2.8	0.89	361.3	9.7	367.9	9.6	409.5	31.9	361.3	9.7	NA
Chapman15-006C July5-Spot 26	212	14798	1.8	18.4966	1.2	0.4367	3.4	0.0586	3.2	0.94	367.0	11.5	368.0	10.6	373.7	26.5	367.0	11.5	NA

Chapman15-006C July5-Spot 44	177	7800	0.8	18.4686	1.4	0.4635	3.1	0.0621	2.8	0.89	388.3	10.4	386.7	9.9	377.1	30.9	388.3	10.4	NA
Chapman15-006C July5-Spot 3	358	12171	1.4	18.2472	1.0	0.4753	3.1	0.0629	2.9	0.95	393.3	11.3	394.8	10.2	404.2	22.2	393.3	11.3	NA
Chapman15-006C July5-Spot 70	247	12060	2.0	18.6527	1.4	0.4674	4.0	0.0632	3.8	0.94	395.2	14.5	389.4	13.0	354.8	31.3	395.2	14.5	NA
Chapman15-006C July5-Spot 69	76	19296	1.9	18.1707	2.0	0.4799	5.3	0.0632	4.9	0.93	395.3	18.9	398.0	17.5	413.6	43.9	395.3	18.9	NA
Chapman15-006C July5-Spot 82	119	3061	2.1	18.8151	1.1	0.4649	3.5	0.0634	3.4	0.95	396.5	13.0	387.7	11.4	335.2	23.8	396.5	13.0	NA
Chapman15-006C July5-Spot 73	63	26279	2.0	17.0633	2.2	0.5173	6.4	0.0640	6.1	0.94	400.0	23.5	423.3	22.3	552.5	47.2	400.0	23.5	NA
Chapman15-006C July5-Spot 43	252	48503	2.9	18.1235	1.2	0.5042	4.0	0.0663	3.8	0.95	413.6	15.2	414.5	13.5	419.4	26.5	413.6	15.2	98.6
Chapman15-006C July5-Spot 90	219	19305	1.5	17.9080	1.2	0.5106	3.0	0.0663	2.8	0.92	414.0	11.2	418.9	10.4	446.0	26.3	414.0	11.2	92.8
Chapman15-006C July5-Spot 81	178	13670	2.0	18.2561	1.2	0.5011	3.7	0.0663	3.5	0.94	414.1	14.0	412.4	12.6	403.1	27.5	414.1	14.0	102.7
Chapman15-006C July5-Spot 37	340	42751	1.4	17.8275	1.0	0.5139	3.6	0.0664	3.5	0.96	414.7	14.0	421.0	12.5	456.1	22.6	414.7	14.0	90.9
Chapman15-006C July5-Spot 89	261	14181	1.2	18.0523	1.2	0.5110	3.1	0.0669	2.9	0.93	417.5	11.7	419.1	10.7	428.2	26.0	417.5	11.7	97.5
Chapman15-006C July5-Spot 25	298	472898	1.4	17.7820	0.9	0.5352	2.7	0.0690	2.6	0.95	430.3	10.7	435.3	9.6	461.7	19.5	430.3	10.7	93.2
Chapman15-006C July5-Spot 51	204	22803	2.0	17.1857	1.4	0.5599	5.1	0.0698	5.0	0.96	434.9	20.8	451.4	18.8	536.9	30.3	434.9	20.8	81.0
Chapman15-006C July5-Spot 77	233	25974	2.8	17.7475	1.3	0.5508	3.3	0.0709	3.0	0.92	441.6	13.0	445.5	11.9	466.0	27.8	441.6	13.0	94.8
Chapman15-006C July5-Spot 65	197	209396	1.6	17.3687	1.2	0.5676	3.7	0.0715	3.5	0.94	445.2	15.2	456.4	13.7	513.6	27.0	445.2	15.2	86.7
Chapman15-006C July5-Spot 86	376	13620	1.8	17.8060	1.0	0.5574	2.9	0.0720	2.7	0.94	448.1	11.7	449.8	10.4	458.7	21.3	448.1	11.7	97.7
Chapman15-006C July5-Spot 66	146	13464	1.5	17.8030	1.4	0.5577	3.5	0.0720	3.2	0.92	448.3	13.8	450.0	12.6	459.1	30.3	448.3	13.8	97.6
Chapman15-006C July5-Spot 92	227	22860	2.4	17.7289	1.0	0.5661	2.9	0.0728	2.8	0.94	453.0	12.1	455.5	10.8	468.3	22.6	453.0	12.1	96.7
Chapman15-006C July5-Spot 9	352	14724	3.1	17.8889	1.2	0.5626	3.6	0.0730	3.4	0.94	454.2	14.8	453.2	13.1	448.4	26.9	454.2	14.8	101.3
Chapman15-006C July5-Spot 83	185	22428	1.7	17.4065	1.1	0.6381	3.2	0.0806	3.0	0.94	499.5	14.3	501.1	12.5	508.8	23.7	499.5	14.3	98.2
Chapman15-006C July5-Spot 18	106	6334	3.2	17.5785	1.1	0.6457	3.9	0.0823	3.7	0.96	509.9	18.3	505.8	15.6	487.2	25.0	509.9	18.3	104.7
Chapman15-006C July5-Spot 64	377	1057704	2.9	16.3345	1.2	0.7311	4.2	0.0866	4.1	0.96	535.4	20.9	557.2	18.2	647.0	24.9	535.4	20.9	82.8
Chapman15-006C July5-Spot 71	45	5590	2.3	16.6902	1.7	0.7912	5.4	0.0958	5.1	0.95	589.6	28.5	591.8	24.0	600.5	37.9	589.6	28.5	98.2
Chapman15-006C July5-Spot 6	200	27965	2.2	16.5519	1.0	0.8580	3.4	0.1030	3.2	0.96	631.9	19.5	629.0	15.8	618.5	20.9	631.9	19.5	102.2
Chapman15-006C July5-Spot 33	146	18605	2.5	16.1293	0.9	0.9423	2.5	0.1102	2.4	0.94	674.1	15.1	674.1	12.4	674.1	18.2	674.1	15.1	100.0
Chapman15-006C July5-Spot 62	246	39874	7.5	15.8652	1.1	0.9608	3.4	0.1106	3.3	0.94	675.9	20.9	683.7	17.2	709.3	24.2	675.9	20.9	95.3
Chapman15-006C July5-Spot 42	364	86614	4.1	15.9835	1.1	0.9604	3.6	0.1113	3.5	0.96	680.5	22.4	683.5	18.1	693.5	22.7	680.5	22.4	98.1
Chapman15-006C July5-Spot 53	61	10899	2.1	15.5507	1.6	1.0498	4.6	0.1184	4.3	0.93	721.3	29.0	728.8	23.7	751.7	34.2	721.3	29.0	96.0
Chapman15-006C July5-Spot 76	72	10190	1.7	15.5780	1.2	1.0794	4.2	0.1220	4.0	0.95	741.8	27.9	743.4	22.0	748.0	26.1	741.8	27.9	99.2
Chapman15-006C July5-Spot 60	66	12111	1.8	15.0920	1.2	1.1317	3.5	0.1239	3.3	0.94	752.8	23.3	768.6	18.9	814.6	25.9	752.8	23.3	92.4

Chapman15-006C July5-Spot 61	97	42833	2.1	15.3731	1.1	1.1371	4.1	0.1268	4.0	0.97	769.5	28.8	771.1	22.2	775.9	22.4	769.5	28.8	99.2
Chapman15-006C July5-Spot 96	190	68804	3.1	15.0979	1.2	1.1870	3.7	0.1300	3.5	0.95	787.7	26.1	794.6	20.5	813.8	25.4	787.7	26.1	96.8
Chapman15-006C July5-Spot 63	227	51843	2.6	14.7835	1.5	1.2404	3.4	0.1330	3.0	0.90	805.0	22.9	819.1	18.9	857.6	30.7	805.0	22.9	93.9
Chapman15-006C July5-Spot 22	219	46702	0.9	14.1899	0.9	1.4342	3.6	0.1476	3.5	0.97	887.5	29.2	903.3	21.7	942.2	18.1	942.2	18.1	94.2
Chapman15-006C July5-Spot 4	238	58551	2.7	13.8319	0.9	1.5857	3.2	0.1591	3.1	0.96	951.6	27.3	964.6	20.0	994.3	17.4	994.3	17.4	95.7
Chapman15-006C July5-Spot 46	237	122192	5.7	13.8049	0.9	1.6554	2.4	0.1657	2.2	0.93	988.6	20.5	991.6	15.3	998.2	18.4	998.2	18.4	99.0
Chapman15-006C July5-Spot 31	98	19246	2.1	11.7384	0.6	2.6726	3.4	0.2275	3.4	0.98	1321.5	40.1	1320.9	25.2	1319.9	12.3	1319.9	12.3	100.1
Chapman15-006C July5-Spot 32	114	72207	2.1	11.7350	0.8	2.7007	2.6	0.2299	2.5	0.95	1333.7	30.2	1328.7	19.5	1320.4	15.2	1320.4	15.2	101.0
Chapman15-006C July5-Spot 12	373	66402	1.5	11.0279	1.0	3.0661	3.5	0.2452	3.3	0.96	1413.8	42.3	1424.3	26.7	1439.9	19.2	1439.9	19.2	98.2
Chapman15-006C July5-Spot 67	194	57926	2.8	10.4616	1.0	3.5744	3.0	0.2712	2.9	0.94	1546.9	39.4	1543.9	24.1	1539.7	18.8	1539.7	18.8	100.5
Chapman15-006C July5-Spot 50	76	18712	2.4	9.5564	0.9	4.5826	4.4	0.3176	4.3	0.98	1778.1	66.2	1746.1	36.3	1708.0	16.3	1708.0	16.3	104.1
Chapman15-006C July5-Spot 16	146	47193	0.9	9.3856	0.9	4.3322	3.3	0.2949	3.2	0.96	1666.0	46.7	1699.5	27.4	1741.1	17.4	1741.1	17.4	95.7
Chapman15-006C July5-Spot 36	53	16350	1.4	9.1457	1.1	5.0112	6.2	0.3324	6.1	0.98	1850.0	98.3	1821.2	52.6	1788.4	20.4	1788.4	20.4	103.4
Chapman15-006C July5-Spot 17	56	699293	0.5	9.0662	1.1	4.8319	5.4	0.3177	5.3	0.98	1778.6	82.7	1790.5	45.7	1804.3	19.7	1804.3	19.7	98.6
Chapman15-006C July5-Spot 35	28	17660	8.2	8.9756	1.1	5.0093	8.1	0.3261	8.0	0.99	1819.4	126.7	1820.9	68.4	1822.6	19.3	1822.6	19.3	99.8
Chapman15-006C July5-Spot 68	209	42590	3.0	8.9385	1.0	5.1478	3.7	0.3337	3.6	0.97	1856.4	58.3	1844.0	31.8	1830.1	17.6	1830.1	17.6	101.4
Chapman15-006C July5-Spot 88	30	17403	0.8	8.9227	1.2	4.9867	6.0	0.3227	5.8	0.98	1802.9	91.8	1817.1	50.4	1833.3	21.3	1833.3	21.3	98.3
Chapman15-006C July5-Spot 75	33	25916	0.6	8.8397	1.4	4.9847	5.6	0.3196	5.5	0.97	1787.7	85.3	1816.7	47.7	1850.2	24.7	1850.2	24.7	96.6
Chapman15-006C July5-Spot 15	430	91323	1.5	8.4960	0.7	5.0890	3.0	0.3136	2.9	0.97	1758.3	44.2	1834.3	25.2	1921.6	13.2	1921.6	13.2	91.5
Chapman15-006C July5-Spot 14	368	50052	2.0	8.4430	1.0	5.2013	2.9	0.3185	2.7	0.94	1782.4	41.8	1852.8	24.3	1932.8	17.2	1932.8	17.2	92.2
Chapman15-006C July5-Spot 95B	84	12796	0.7	8.3315	0.9	5.9590	3.2	0.3601	3.1	0.96	1982.5	53.0	1969.9	28.2	1956.6	16.6	1956.6	16.6	101.3
Chapman15-006C July5-Spot 95A	75	80930	0.7	8.1882	1.0	5.9556	4.1	0.3537	4.0	0.97	1952.1	66.7	1969.4	35.6	1987.5	18.1	1987.5	18.1	98.2
Chapman15-006C July5-Spot 84	66	31198	1.6	8.0098	0.8	6.6597	4.1	0.3869	4.0	0.98	2108.3	72.6	2067.3	36.4	2026.6	14.5	2026.6	14.5	104.0
Chapman15-006C July5-Spot 34	111	53631	1.3	7.7266	1.2	6.8604	4.1	0.3844	3.9	0.95	2097.0	69.6	2093.5	36.2	2090.1	21.9	2090.1	21.9	100.3
Chapman15-006C July5-Spot 7	157	270509	1.2	7.0077	0.9	8.3231	3.7	0.4230	3.6	0.97	2274.2	68.2	2266.8	33.4	2260.2	16.2	2260.2	16.2	100.6
Chapman15-006C July5-Spot 94	91	175169	4.9	7.0050	0.8	8.0559	3.9	0.4093	3.8	0.98	2211.6	71.4	2237.3	35.2	2260.9	13.7	2260.9	13.7	97.8
Chapman15-006C July5-Spot 87	151	61528	0.6	6.3139	1.0	10.0599	3.4	0.4607	3.2	0.95	2442.5	66.0	2440.3	31.5	2438.4	17.6	2438.4	17.6	100.2
Chapman15-006C July5-Spot 52	210	180091	1.7	6.2411	1.1	10.1849	3.6	0.4610	3.4	0.95	2444.0	68.9	2451.7	33.1	2458.1	19.3	2458.1	19.3	99.4
Chapman15-006C July5-Spot 85	152	93934	1.0	6.1640	0.8	10.2253	3.5	0.4571	3.4	0.97	2426.9	68.1	2455.4	32.1	2479.0	13.6	2479.0	13.6	97.9
Chapman15-006C July5-Spot 10	23	181102	1.1	6.1545	0.9	10.7677	6.0	0.4806	5.9	0.99	2530.0	123.5	2503.3	55.5	2481.6	14.4	2481.6	14.4	102.0

Chapman15-006C July5-Spot 5	62	57103	1.5	6.1391	1.0	10.6217	3.5	0.4729	3.4	0.96	2496.4	69.4	2490.6	32.4	2485.9	16.4	2485.9	16.4	100.4
Chapman15-006C July5-Spot 55	46	54920	1.8	6.0819	1.6	10.3345	5.7	0.4559	5.5	0.96	2421.2	110.4	2465.2	52.8	2501.6	27.0	2501.6	27.0	96.8
Chapman15-006C July5-Spot 39	47	125048	1.8	6.0732	1.1	11.3369	6.5	0.4994	6.4	0.99	2611.0	136.9	2551.2	60.4	2504.1	18.4	2504.1	18.4	104.3
Chapman15-006C July5-Spot 8	90	15058	1.2	6.0152	0.9	10.5975	4.0	0.4623	3.9	0.98	2449.9	80.3	2488.5	37.4	2520.2	14.4	2520.2	14.4	97.2
Chapman15-006C July5-Spot 20	94	66438	0.8	6.0008	1.1	10.7693	3.8	0.4687	3.6	0.95	2477.9	74.2	2503.4	35.1	2524.2	18.9	2524.2	18.9	98.2
Chapman15-006C July5-Spot 54	41	46028	2.0	5.9722	1.6	10.9907	5.2	0.4761	5.0	0.96	2510.1	104.2	2522.3	48.9	2532.2	26.0	2532.2	26.0	99.1

15_020 38.587 74.123

						Isotope ratios						Apparent ages (Ma)							
15_020	U (ppm)	206Pb 204Pb	U/Th	206Pb* 207Pb*	± (%)	207Pb* 235U*	± (%)	206Pb* 238U	± (%)	error corr.	206Pb* 238U*	± (Ma)	207Pb* 235U	± (Ma)	206Pb* 207Pb*	± (Ma)	Best age (Ma)	± (Ma)	Conc (%)
Chapman 15-020A-Spot 24	333	7650	3.0	19.9548	1.1	0.2153	3.4	0.0312	3.2	0.94	197.8	6.2	198.0	6.0	200.2	26.3	197.8	6.2	NA
Chapman 15-020A-Spot 39	192	5362	2.8	20.2844	1.6	0.2225	3.2	0.0327	2.7	0.86	207.6	5.6	204.0	5.8	162.1	37.1	207.6	5.6	NA
Chapman 15-020A-Spot 47	188	1965808	2.3	19.4847	1.0	0.2339	2.6	0.0331	2.4	0.93	209.6	5.0	213.4	5.0	255.3	22.3	209.6	5.0	NA
Chapman 15-020A-Spot 25	135	4687	3.3	20.4365	2.0	0.2230	3.7	0.0331	3.2	0.85	209.6	6.5	204.4	6.9	144.6	46.9	209.6	6.5	NA
Chapman 15-020A-Spot 45	101	4349	2.0	20.6614	2.4	0.2221	4.2	0.0333	3.5	0.82	211.1	7.3	203.7	7.8	118.8	56.7	211.1	7.3	NA
Chapman 15-020A-Spot 21	201	4547	3.0	20.5079	1.6	0.2242	3.5	0.0333	3.1	0.89	211.5	6.5	205.4	6.5	136.4	37.3	211.5	6.5	NA
Chapman 15-020A-Spot 37	191	7196	2.7	20.5902	1.9	0.2236	3.9	0.0334	3.4	0.87	211.8	7.0	204.9	7.2	127.0	44.7	211.8	7.0	NA
Chapman 15-020A-Spot 46	186	13123	2.1	19.6896	1.3	0.2368	3.0	0.0338	2.8	0.91	214.4	5.8	215.8	5.9	231.2	29.6	214.4	5.8	NA
Chapman 15-020A-Spot 20	200	6566	2.7	20.1063	1.5	0.2328	3.9	0.0339	3.6	0.93	215.2	7.6	212.5	7.4	182.6	33.9	215.2	7.6	NA
Chapman 15-020A-Spot 3	262	6392	2.9	20.4254	1.2	0.2299	2.7	0.0341	2.4	0.89	215.9	5.0	210.2	5.1	145.9	28.9	215.9	5.0	NA
Chapman 15-020A-Spot 101	181	5417	3.4	20.2393	1.5	0.2332	2.6	0.0342	2.2	0.82	217.0	4.6	212.8	5.1	167.3	34.9	217.0	4.6	NA
Chapman 15-020A-Spot 76	340	14458	2.2	19.9002	1.1	0.2384	2.5	0.0344	2.2	0.90	218.1	4.8	217.1	4.9	206.6	25.4	218.1	4.8	NA
Chapman 15-020A-Spot 26	138	12453	3.4	20.1208	1.5	0.2360	3.6	0.0344	3.2	0.91	218.3	7.0	215.2	6.9	181.0	33.9	218.3	7.0	NA
Chapman 15-020A-Spot 14	198	4313	3.4	20.5484	1.4	0.2322	2.8	0.0346	2.4	0.87	219.3	5.2	212.0	5.4	131.7	32.6	219.3	5.2	NA
Chapman 15-020A-Spot 100	237	11024	1.8	19.3134	1.4	0.2478	2.9	0.0347	2.5	0.87	220.0	5.5	224.8	5.8	275.6	32.3	220.0	5.5	NA
Chapman 15-020A-Spot 1	337	48595	2.5	19.2353	1.0	0.2493	2.5	0.0348	2.3	0.91	220.4	5.0	226.0	5.1	284.9	23.4	220.4	5.0	NA
Chapman 15-020A-Spot 61	116	8000	2.2	20.3266	1.4	0.2360	2.9	0.0348	2.6	0.88	220.4	5.6	215.1	5.6	157.2	31.8	220.4	5.6	NA
Chapman 15-020A-Spot 77	205	76466	3.2	19.1733	1.0	0.2502	2.8	0.0348	2.7	0.94	220.5	5.8	226.8	5.8	292.3	23.0	220.5	5.8	NA
Chapman 15-020A-Spot 104	122	5969	1.5	20.0327	2.4	0.2396	4.4	0.0348	3.7	0.84	220.6	8.1	218.1	8.7	191.2	55.0	220.6	8.1	NA
Chapman 15-020A-Spot 15	121	3130	2.9	20.9018	2.1	0.2298	4.2	0.0348	3.6	0.86	220.7	7.8	210.0	7.9	91.5	50.4	220.7	7.8	NA
Chapman 15-020A-Spot 13	106	3933	2.5	21.1106	1.8	0.2278	4.4	0.0349	4.0	0.91	221.0	8.7	208.4	8.2	67.9	42.7	221.0	8.7	NA
Chapman 15-020A-Spot 93	112	18000	1.9	19.4959	2.0	0.2474	4.1	0.0350	3.6	0.87	221.7	7.8	224.5	8.3	254.0	47.0	221.7	7.8	NA
Chapman 15-020A-Spot 49	152	12599	3.9	19.2543	1.7	0.2512	3.8	0.0351	3.4	0.90	222.2	7.5	227.5	7.8	282.6	38.9	222.2	7.5	NA
Chapman 15-020A-Spot 92	115	22134	1.9	19.5808	1.9	0.2473	4.6	0.0351	4.2	0.91	222.5	9.2	224.4	9.3	244.0	43.5	222.5	9.2	NA

Chapman 15-020A-Spot 73	258	7357	3.6	20.5533	1.3	0.2365	2.5	0.0353	2.2	0.85	223.3	4.8	215.5	4.9	131.2	31.2	223.3	4.8	NA
Chapman 15-020A-Spot 90	188	16104	1.6	19.6502	1.2	0.2476	3.4	0.0353	3.1	0.93	223.6	6.9	224.6	6.8	235.9	27.8	223.6	6.9	NA
Chapman 15-020A-Spot 89	199	34759	2.2	19.8143	1.1	0.2457	2.7	0.0353	2.5	0.92	223.7	5.5	223.1	5.5	216.6	25.3	223.7	5.5	NA
Chapman 15-020A-Spot 6	138	10543	2.0	19.9325	1.8	0.2447	3.9	0.0354	3.5	0.89	224.1	7.7	222.3	7.8	202.8	41.0	224.1	7.7	NA
Chapman 15-020A-Spot 2	319	139175	2.7	19.2644	0.9	0.2533	2.5	0.0354	2.3	0.93	224.2	5.1	229.3	5.1	281.4	20.6	224.2	5.1	NA
Chapman 15-020A-Spot 95	315	29282	2.0	19.6707	1.3	0.2484	3.2	0.0354	2.9	0.91	224.5	6.5	225.3	6.5	233.5	30.3	224.5	6.5	NA
Chapman 15-020A-Spot 99	229	8730	1.7	19.8669	1.9	0.2495	4.1	0.0360	3.7	0.89	227.7	8.2	226.2	8.4	210.5	43.8	227.7	8.2	NA
Chapman 15-020A-Spot 60	97	2058	1.9	22.4288	4.0	0.2235	4.7	0.0364	2.6	0.55	230.2	5.9	204.8	8.8	78.2	96.8	230.2	5.9	NA
Chapman 15-020A-Spot 17	378	10807	2.6	19.4741	1.3	0.2578	2.7	0.0364	2.3	0.86	230.6	5.2	232.9	5.5	256.6	30.9	230.6	5.2	NA
Chapman 15-020A-Spot 29	43	1571	2.9	25.7138	3.8	0.2039	5.1	0.0380	3.4	0.67	240.6	8.1	188.4	8.8	424.2	99.9	240.6	8.1	NA
Chapman 15-020A-Spot 4	82	5792	4.6	7.8312	14.5	0.6761	17.4	0.0384	9.7	0.56	242.9	23.1	524.4	71.5	2066.5	256.7	242.9	23.1	NA
Chapman 15-020A-Spot 79	166	11230	2.0	19.2253	1.5	0.2812	2.7	0.0392	2.3	0.84	248.0	5.6	251.6	6.1	286.1	33.4	248.0	5.6	NA
Chapman 15-020A-Spot 43	226	35390	2.2	19.0832	1.0	0.2870	2.1	0.0397	1.9	0.88	251.1	4.6	256.2	4.8	303.0	23.1	251.1	4.6	NA
Chapman 15-020A-Spot 83	337	40253	2.1	19.0301	0.8	0.2969	2.3	0.0410	2.1	0.94	258.9	5.4	264.0	5.3	309.3	18.2	258.9	5.4	NA
Chapman 15-020A-Spot 66	241	16100	2.8	19.0123	0.9	0.2976	2.8	0.0410	2.7	0.95	259.3	6.8	264.5	6.6	311.5	20.9	259.3	6.8	NA
Chapman 15-020A-Spot 87	53	1607	1.2	23.1330	2.2	0.2453	4.7	0.0412	4.2	0.89	260.0	10.6	222.8	9.4	154.4	53.7	260.0	10.6	NA
Chapman 15-020A-Spot 86	62	8371	1.1	20.0980	2.2	0.2863	5.9	0.0417	5.5	0.93	263.5	14.2	255.6	13.4	183.6	52.0	263.5	14.2	NA
Chapman 15-020A-Spot 42	143	6218	2.1	20.3402	1.9	0.2830	3.7	0.0417	3.2	0.86	263.6	8.2	253.0	8.2	155.6	43.3	263.6	8.2	NA
Chapman 15-020A-Spot 10	286	97203	1.2	18.6067	1.0	0.3183	2.9	0.0430	2.7	0.94	271.1	7.1	280.6	7.0	360.3	23.0	271.1	7.1	NA
Chapman 15-020A-Spot 11	151	6409	1.5	19.5832	1.7	0.3064	3.6	0.0435	3.2	0.88	274.6	8.5	271.4	8.6	243.7	38.9	274.6	8.5	NA
Chapman 15-020A-Spot 64	232	34596	3.1	19.0062	1.4	0.3179	4.1	0.0438	3.8	0.94	276.5	10.3	280.3	10.0	312.2	32.4	276.5	10.3	NA
Chapman 15-020A-Spot 41	279	77117	2.0	18.8858	1.0	0.3472	2.5	0.0476	2.3	0.92	299.5	6.7	302.6	6.5	326.7	22.3	299.5	6.7	NA
Chapman 15-020A-Spot 51	264	20196	1.7	18.3059	1.5	0.3617	3.2	0.0480	2.9	0.89	302.3	8.5	313.5	8.7	397.0	32.7	302.3	8.5	NA
Chapman 15-020A-Spot 67	323	17952	2.0	19.1433	1.1	0.3491	3.0	0.0485	2.8	0.93	305.1	8.4	304.0	8.0	295.8	24.9	305.1	8.4	NA
Chapman 15-020A-Spot 38	151	21149	2.9	19.1128	1.3	0.3536	3.5	0.0490	3.2	0.93	308.5	9.8	307.4	9.3	299.4	30.1	308.5	9.8	NA
Chapman 15-020A-Spot 23	241	13359	1.2	19.3226	1.1	0.3532	2.7	0.0495	2.5	0.91	311.4	7.6	307.1	7.3	274.5	25.9	311.4	7.6	NA
Chapman 15-020A-Spot 7	132	16362	2.4	18.6642	1.7	0.3681	4.0	0.0498	3.6	0.90	313.5	11.0	318.3	10.9	353.4	38.3	313.5	11.0	NA
Chapman 15-020A-Spot 82	183	29208	1.0	18.4222	1.2	0.3759	3.0	0.0502	2.8	0.91	315.9	8.5	324.0	8.4	382.8	28.0	315.9	8.5	NA
Chapman 15-020A-Spot 81	179	20323	0.9	18.6601	1.1	0.3728	2.5	0.0505	2.2	0.90	317.3	6.9	321.7	6.8	353.9	24.2	317.3	6.9	NA
Chapman 15-020A-Spot 33	135	15740	1.5	18.8995	1.2	0.3702	2.9	0.0507	2.6	0.92	319.1	8.2	319.8	7.9	325.0	26.2	319.1	8.2	NA

Chapman 15-020A-Spot 94	213	79642	2.2	18.4542	1.4	0.3809	3.0	0.0510	2.7	0.89	320.6	8.4	327.7	8.4	378.9	30.8	320.6	8.4	NA
Chapman 15-020A-Spot 80	183	12292	0.9	19.0736	1.4	0.3689	3.2	0.0510	2.9	0.90	320.9	9.0	318.9	8.8	304.1	32.6	320.9	9.0	NA
Chapman 15-020A-Spot 88	44	2195	0.5	20.9731	2.2	0.3478	5.7	0.0529	5.3	0.92	332.3	17.2	303.0	15.1	83.4	52.4	332.3	17.2	NA
Chapman 15-020A-Spot 98	114	9043	2.6	18.6551	1.3	0.4506	2.8	0.0610	2.5	0.88	381.5	9.1	377.7	8.8	354.5	30.3	381.5	9.1	NA
Chapman 15-020A-Spot 28	174	17492	2.1	18.2114	1.2	0.4903	3.6	0.0648	3.4	0.94	404.5	13.3	405.1	12.0	408.6	26.4	404.5	13.3	99.0
Chapman 15-020A-Spot 68	142	577990	2.7	18.2799	1.5	0.4989	5.0	0.0661	4.8	0.95	412.9	19.3	411.0	17.0	400.2	33.6	412.9	19.3	103.2
Chapman 15-020A-Spot 18	138	33009	1.4	17.6295	1.2	0.5343	3.1	0.0683	2.8	0.92	426.0	11.5	434.6	10.8	480.8	26.8	426.0	11.5	88.6
Chapman 15-020A-Spot 65	123	39053	2.4	17.9221	1.2	0.5329	3.3	0.0693	3.1	0.94	431.7	12.8	433.7	11.5	444.3	25.6	431.7	12.8	97.2
Chapman 15-020A-Spot 34	93	13187	2.3	18.1752	1.3	0.5266	3.6	0.0694	3.4	0.93	432.7	14.0	429.6	12.6	413.0	29.1	432.7	14.0	104.8
Chapman 15-020A-Spot 71	149	9366	1.7	18.1381	1.1	0.5315	2.4	0.0699	2.1	0.89	435.7	8.9	432.8	8.3	417.6	24.1	435.7	8.9	104.3
Chapman 15-020A-Spot 58	178	13253	0.7	18.1129	0.9	0.5348	2.7	0.0703	2.5	0.94	437.7	10.6	435.0	9.4	420.7	20.1	437.7	10.6	104.0
Chapman 15-020A-Spot 72	196	10305	2.3	17.9812	1.0	0.5467	3.0	0.0713	2.8	0.94	443.9	12.1	442.8	10.8	437.0	23.0	443.9	12.1	101.6
Chapman 15-020A-Spot 48	43	10289	1.8	17.7212	1.6	0.5616	4.7	0.0722	4.5	0.94	449.3	19.3	452.6	17.3	469.3	35.8	449.3	19.3	95.7
Chapman 15-020A-Spot 62	147	24789	1.6	17.6066	0.9	0.5738	3.0	0.0733	2.8	0.95	455.9	12.5	460.5	11.0	483.7	19.8	455.9	12.5	94.2
Chapman 15-020A-Spot 50	156	13029	2.2	17.4779	0.9	0.6306	2.8	0.0799	2.7	0.95	495.7	12.8	496.4	11.2	499.9	20.0	495.7	12.8	99.2
Chapman 15-020A-Spot 32	87	39501	2.2	17.5339	1.3	0.6308	3.2	0.0802	2.9	0.91	497.4	13.9	496.6	12.5	492.8	29.0	497.4	13.9	100.9
Chapman 15-020A-Spot 59	206	48265	1.6	17.1558	0.9	0.7278	2.7	0.0906	2.6	0.94	558.9	13.8	555.3	11.7	540.7	19.8	558.9	13.8	103.4
Chapman 15-020A-Spot 22	106	22654	1.4	16.3805	1.1	0.8220	3.3	0.0977	3.1	0.94	600.6	17.6	609.1	14.9	640.9	23.7	600.6	17.6	93.7
Chapman 15-020A-Spot 9	51	1836642	4.5	14.4899	1.5	1.3204	5.1	0.1388	4.8	0.95	837.7	38.1	854.7	29.4	899.1	31.3	837.7	38.1	93.2
Chapman 15-020A-Spot 36	92	13222	2.4	14.5034	1.9	1.4421	5.4	0.1517	5.0	0.94	910.5	42.8	906.6	32.3	897.2	39.3	897.2	39.3	101.5
Chapman 15-020A-Spot 75	147	32224	5.1	13.9712	0.8	1.6024	2.8	0.1624	2.7	0.96	969.9	23.9	971.2	17.3	973.9	16.4	973.9	16.4	99.6
Chapman 15-020A-Spot 44	135	84141	1.4	12.8572	0.6	2.0481	3.0	0.1910	2.9	0.98	1126.7	30.2	1131.6	20.4	1141.2	12.6	1141.2	12.6	98.7
Chapman 15-020A-Spot 27	111	391964	1.8	10.1146	0.9	3.7520	3.2	0.2752	3.0	0.96	1567.4	42.1	1582.5	25.4	1602.8	17.4	1602.8	17.4	97.8
Chapman 15-020A-Spot 84	117	75584	2.4	8.9138	0.7	5.2638	3.4	0.3403	3.4	0.98	1888.1	55.1	1863.0	29.4	1835.1	13.3	1835.1	13.3	102.9
Chapman 15-020A-Spot 30	84	28613	1.0	8.7847	0.9	5.0289	3.1	0.3204	3.0	0.96	1791.7	47.0	1824.2	26.6	1861.5	16.7	1861.5	16.7	96.3
Chapman 15-020A-Spot 63	292	448631	1.5	8.3317	1.7	5.7204	4.8	0.3457	4.5	0.94	1913.9	74.7	1934.5	41.6	1956.6	30.1	1956.6	30.1	97.8
Chapman 15-020A-Spot 5	209	1602480	11.5	6.2349	0.9	10.3875	2.5	0.4697	2.4	0.94	2482.3	48.6	2469.9	23.3	2459.7	14.7	2459.7	14.7	100.9
Chapman 15-020A-Spot 31	36	97750	0.7	6.1494	1.0	11.0332	3.4	0.4921	3.2	0.96	2579.7	68.2	2525.9	31.2	2483.0	16.5	2483.0	16.5	103.9
Chapman 15-020A-Spot 12	121	87049	1.6	6.0840	1.1	10.0266	3.8	0.4424	3.6	0.95	2361.5	70.7	2437.2	34.7	2501.1	19.3	2501.1	19.3	94.4

* indicates radiogenic Pb (corrected for common Pb).
Initial Pb composition interpreted from Stacey and Kramers (1975), with uncertainties of 1.0 for $^{206}Pb/^{204}Pb$ and 0.3 for $^{207}Pb/^{204}Pb$.

All errors are reported at the 2-sigma level.

Discordance is calculated from comparison of $^{206}Pb^{*}/^{238}U$ and $^{206}Pb^{*}/^{207}Pb^{*}$ ages.

U concentration, U/Th, and $^{206}Pb/^{204}Pb$ have uncertainties of ~25%.

Decay constants: 235U=9.8485×10-10. 238U=1.55125×10-10. 238U/235U=137.88.

Isotope ratios are corrected for Pb/U fractionation by comparison with standard zircon with an age of 564 ± 4 Ma (2-sigma).

LA-ICP-MS analyses conducted at the University of Houston

DV_7-5-15_f1	38.688	73.369																		
	Isotope ratios									Apparent Ages (Ma)										
	$^{207}Pb/^{206}Pb$	± (2%SD)	$^{207}Pb/^{235}U$	± (2%SD)	$^{206}Pb/^{238}U$	± (2%SD)	error corr.	$^{206}Pb/^{238}Th$	± (2SD)	$^{206}Pb/^{238}U$	± (2SD)	$^{207}Pb/^{235}U$	± (2SD)	$^{207}Pb/^{206}Pb$	± (2SD)	$^{208}Pb/^{232}Th$	± (2SD)	% discordance Pb^{206}/U^{238}-Pb^{207}/Pb^{206}	% discordance Pb^{206}/U^{238}-Pb^{207}/U^{325}	Best Age	± (2SD)
DV_7-5-15_F1_6	0.050	10.93	0.176	15.16	0.025	10.52	0.69	0.008	13.1	160.46	16.7	164.2	22.99	216.6	252.96	168.4	21.97	25.9	2.3	160.5	16.7
DV_7-5-15_F1_153	0.051	6.55	0.224	8.94	0.032	6.14	0.68	0.010	10.7	202.84	12.3	205.2	16.62	230.7	151.17	203.3	21.56	12.1	1.2	202.8	12.3
DV_7-5-15_F1_214	0.061	9.40	0.284	10.93	0.034	5.68	0.51	0.011	9.7	212.66	11.9	254.1	24.57	654.2	201.63	226.9	21.82	67.5	16.3	212.7	11.9
DV_7-5-15_F1_29	0.052	8.25	0.273	11.15	0.038	7.52	0.67	0.012	11.6	240.38	17.7	244.8	24.25	284.5	188.73	238.9	27.46	15.5	1.8	240.4	17.7
DV_7-5-15_F1_105	0.053	6.65	0.278	8.93	0.038	5.98	0.67	0.012	9.2	240.44	14.1	249.1	19.74	329.8	150.87	248.0	22.79	27.1	3.5	240.4	14.1
DV_7-5-15_F1_48	0.054	11.03	0.287	15.54	0.039	10.96	0.70	0.012	13.6	245.28	26.4	256.3	35.21	355.8	249.10	242.7	32.78	31.1	4.3	245.3	26.4
DV_7-5-15_F1_156	0.051	7.02	0.273	9.33	0.039	6.19	0.66	0.013	9.2	245.64	14.9	245.3	20.33	239.9	161.88	264.3	24.07	-2.4	-0.2	245.6	14.9
DV_7-5-15_F1_146	0.053	12.64	0.292	17.46	0.040	12.06	0.69	0.012	16.0	250.71	29.7	260.4	40.13	347.1	285.95	246.0	39.22	27.8	3.7	250.7	29.7
DV_7-5-15_F1_71	0.074	9.05	0.408	12.11	0.040	8.06	0.66	0.017	16.1	253.65	20.1	347.3	35.65	1031.4	182.97	344.3	55.03	75.4	27.0	253.7	20.1
DV_7-5-15_F1_116	0.058	9.52	0.319	11.64	0.040	6.72	0.58	0.014	14.9	253.80	16.7	281.3	28.61	514.7	209.08	274.0	40.72	50.7	9.8	253.8	16.7
DV_7-5-15_F1_183	0.054	8.44	0.298	10.96	0.040	7.07	0.64	0.014	8.9	253.80	17.6	265.0	25.57	363.2	190.25	271.4	23.91	30.1	4.2	253.8	17.6
DV_7-5-15_F1_9	0.053	9.39	0.296	12.94	0.040	8.92	0.69	0.013	11.2	255.04	22.3	263.2	30.01	334.6	212.80	257.4	28.72	23.8	3.1	255.0	22.3
DV_7-5-15_F1_93	0.053	11.44	0.294	15.02	0.040	9.74	0.65	0.012	12.5	255.42	24.4	261.9	34.70	318.4	260.10	235.3	29.22	19.8	2.5	255.4	24.4
DV_7-5-15_F1_164	0.054	9.98	0.301	13.99	0.041	9.84	0.70	0.014	13.4	256.48	24.8	267.3	32.90	361.2	225.23	286.1	38.04	29.0	4.0	256.5	24.8
DV_7-5-15_F1_151	0.056	18.22	0.316	20.11	0.041	8.55	0.42	0.012	8.4	257.08	21.5	278.6	49.05	461.8	403.87	246.8	20.58	44.3	7.7	257.1	21.5
DV_7-5-15_F1_185	0.062	9.53	0.350	13.38	0.041	9.45	0.70	0.013	13.6	257.51	23.9	305.0	35.27	684.8	203.33	265.1	35.81	62.4	15.6	257.5	23.9
DV_7-5-15_F1_136	0.052	10.57	0.294	15.05	0.041	10.73	0.71	0.014	11.0	257.69	27.1	261.9	34.76	298.4	241.20	289.0	31.52	13.6	1.6	257.7	27.1
DV_7-5-15_F1_252	0.051	12.04	0.285	16.28	0.041	10.93	0.67	0.013	14.8	258.35	27.7	254.9	36.71	221.0	278.55	265.1	39.02	-16.9	-1.4	258.3	27.7
DV_7-5-15_F1_145	0.052	10.40	0.294	13.17	0.041	8.10	0.61	0.013	11.3	260.44	20.7	261.3	30.35	267.5	238.65	268.4	30.25	2.6	0.3	260.4	20.7
DV_7-5-15_F1_103	0.051	10.73	0.292	14.01	0.042	9.02	0.64	0.013	11.6	262.90	23.2	259.8	32.13	229.4	247.82	261.5	30.21	-14.6	-1.2	262.9	23.2
DV_7-5-15_F1_96	0.045	28.59	0.259	29.81	0.042	8.45	0.28	0.013	15.7	263.00	21.8	233.8	62.32	0.0	689.14	258.4	40.35	-13097399.1	-12.5	263.0	21.8
DV_7-5-15_F1_135	0.050	15.02	0.287	17.90	0.042	9.76	0.54	0.013	12.3	263.55	25.2	256.1	40.53	186.3	349.55	267.7	32.84	-41.5	-2.9	263.6	25.2
DV_7-5-15_F1_37	0.052	8.73	0.300	11.75	0.042	7.89	0.67	0.013	10.2	265.19	20.5	266.7	27.56	277.0	199.88	259.7	26.39	4.3	0.5	265.2	20.5

DV_7-5-15_F1_216	0.052	9.43	0.304	13.18	0.042	9.27	0.70	0.014	9.7	265.22	24.1	269.6	31.22	305.8	214.78	288.9	27.95	13.3	1.6	265.2	24.1
DV_7-5-15_F1_117	0.052	7.54	0.301	10.26	0.042	6.98	0.68	0.014	11.2	265.41	18.2	267.4	24.13	282.9	172.40	280.8	31.32	6.2	0.7	265.4	18.2
DV_7-5-15_F1_114	0.054	9.43	0.317	13.03	0.042	9.01	0.69	0.014	10.8	266.36	23.5	279.7	31.88	391.1	211.55	285.5	30.67	31.9	4.8	266.4	23.5
DV_7-5-15_F1_224	0.053	9.85	0.312	13.13	0.042	8.74	0.66	0.014	12.5	267.31	22.9	275.5	31.69	343.8	222.85	278.2	34.52	22.3	3.0	267.3	22.9
DV_7-5-15_F1_1	0.050	6.95	0.294	9.49	0.042	6.48	0.68	0.013	10.1	268.00	17.0	261.5	21.88	201.8	161.37	263.2	26.52	-32.8	-2.5	268.0	17.0
DV_7-5-15_F1_229	0.049	13.32	0.287	14.43	0.042	5.64	0.39	0.013	13.7	268.22	14.8	256.1	32.68	144.3	312.40	257.0	35.06	-85.9	-4.7	268.2	14.8
DV_7-5-15_F1_41	0.054	9.99	0.318	13.79	0.043	9.52	0.69	0.014	12.2	271.46	25.3	280.5	33.81	354.3	225.63	283.9	34.33	23.4	3.2	271.5	25.3
DV_7-5-15_F1_42	0.051	14.96	0.304	21.01	0.043	14.77	0.70	0.013	20.0	271.57	39.3	269.8	49.82	251.6	344.03	268.9	53.37	-7.9	-0.7	271.6	39.3
DV_7-5-15_F1_227	0.056	6.93	0.334	8.89	0.043	5.65	0.63	0.015	8.5	272.04	15.0	292.5	22.60	457.5	153.77	309.8	26.21	40.5	7.0	272.0	15.0
DV_7-5-15_F1_19	0.055	8.64	0.325	10.77	0.043	6.45	0.60	0.013	31.4	272.12	17.2	285.9	26.84	397.8	193.72	260.5	81.50	31.6	4.8	272.1	17.2
DV_7-5-15_F1_134	0.053	9.85	0.319	13.03	0.043	8.54	0.65	0.014	12.6	273.38	22.9	281.4	32.03	346.7	222.88	283.5	35.43	21.2	2.8	273.4	22.9
DV_7-5-15_F1_141	0.047	10.93	0.278	13.04	0.043	7.14	0.55	0.014	13.6	273.51	19.1	249.3	28.83	24.8	262.30	272.7	36.75	-1000.9	-9.7	273.5	19.1
DV_7-5-15_F1_34	0.054	8.40	0.326	11.01	0.043	7.14	0.65	0.013	13.5	273.83	19.1	286.6	27.49	389.8	188.46	271.0	36.34	29.8	4.5	273.8	19.1
DV_7-5-15_F1_228	0.061	6.81	0.369	8.98	0.044	5.92	0.65	0.013	8.5	275.71	16.0	319.0	24.58	646.3	146.25	264.7	22.46	57.3	13.6	275.7	16.0
DV_7-5-15_F1_140	0.053	7.91	0.320	9.98	0.044	6.12	0.61	0.014	11.6	276.12	16.6	281.8	24.56	327.7	179.43	280.4	32.39	15.7	2.0	276.1	16.6
DV_7-5-15_F1_219	0.056	13.34	0.341	19.20	0.044	13.85	0.72	0.015	15.5	276.75	37.5	297.6	49.57	462.4	295.70	305.1	47.11	40.2	7.0	276.8	37.5
DV_7-5-15_F1_57	0.053	12.81	0.324	17.75	0.044	12.29	0.69	0.014	18.1	277.11	33.3	285.1	44.15	349.1	289.70	276.2	49.65	20.6	2.8	277.1	33.3
DV_7-5-15_F1_250	0.052	10.61	0.318	14.00	0.044	9.11	0.65	0.014	12.6	277.60	24.8	280.3	34.31	300.8	241.95	271.6	33.98	7.7	1.0	277.6	24.8
DV_7-5-15_F1_88	0.054	11.65	0.332	16.55	0.044	11.75	0.71	0.014	16.6	280.31	32.2	291.2	41.91	377.0	262.11	277.6	45.92	25.7	3.7	280.3	32.2
DV_7-5-15_F1_15	0.053	7.98	0.323	10.54	0.045	6.92	0.65	0.013	11.5	281.51	19.1	284.6	26.17	307.4	181.69	270.4	30.86	8.4	1.1	281.5	19.1
DV_7-5-15_F1_102	0.064	38.74	0.396	39.22	0.045	6.13	0.16	0.014	9.6	282.45	17.0	338.9	113.46	744.7	818.83	289.7	27.51	62.1	16.6	282.4	17.0
DV_7-5-15_F1_248	0.050	9.55	0.311	12.67	0.045	8.32	0.66	0.015	11.0	282.64	23.0	275.2	30.55	209.8	221.33	294.4	32.08	-34.7	-2.7	282.6	23.0
DV_7-5-15_F1_32	0.058	7.82	0.359	9.90	0.045	6.09	0.61	0.015	9.8	283.81	16.9	311.4	26.55	520.7	171.69	291.3	28.49	45.5	8.8	283.8	16.9
DV_7-5-15_F1_128	0.052	6.87	0.322	8.79	0.045	5.50	0.62	0.014	9.8	284.27	15.3	283.7	21.75	276.8	157.39	274.9	26.87	-2.7	-0.2	284.3	15.3
DV_7-5-15_F1_179	0.052	6.46	0.326	9.07	0.045	6.43	0.70	0.014	8.9	284.33	17.9	286.8	22.66	305.6	147.26	286.3	25.20	7.0	0.9	284.3	17.9
DV_7-5-15_F1_149	0.052	7.24	0.322	9.76	0.045	6.59	0.67	0.015	9.2	284.63	18.3	283.7	24.17	274.5	165.87	293.1	26.69	-3.7	-0.3	284.6	18.3
DV_7-5-15_F1_242	0.053	8.91	0.333	10.96	0.045	6.40	0.58	0.014	9.6	286.27	17.9	291.5	27.79	331.1	202.10	287.7	27.48	13.6	1.8	286.3	17.9
DV_7-5-15_F1_89	0.054	8.28	0.338	11.47	0.045	7.94	0.69	0.014	11.4	286.39	22.2	295.6	29.42	366.8	186.67	274.4	30.98	21.9	3.1	286.4	22.2
DV_7-5-15_F1_24	0.061	8.65	0.386	10.82	0.045	6.51	0.60	0.016	9.9	286.82	18.3	331.1	30.57	653.1	185.67	312.1	30.78	56.1	13.4	286.8	18.3
DV_7-5-15_F1_68	0.062	12.34	0.393	15.56	0.046	9.49	0.61	0.017	13.5	288.22	26.8	336.5	44.61	682.8	263.51	343.8	46.00	57.8	14.3	288.2	26.8

DV_7-5-15_F1_207	0.052	10.37	0.328	14.20	0.046	9.76	0.68	0.014	9.4	288.43	27.5	288.1	35.63	283.7	237.13	290.9	27.20	-1.7	-0.1	288.4	27.5
DV_7-5-15_F1_180	0.054	8.09	0.342	10.47	0.046	6.72	0.64	0.014	12.1	290.21	19.1	298.8	27.11	364.9	182.29	288.6	34.82	20.5	2.9	290.2	19.1
DV_7-5-15_F1_65	0.052	7.32	0.330	10.02	0.046	6.86	0.68	0.013	11.1	290.45	19.5	289.3	25.24	277.5	167.65	267.4	29.55	-4.7	-0.4	290.4	19.5
DV_7-5-15_F1_249	0.051	9.64	0.327	11.92	0.047	7.00	0.59	0.016	11.5	293.22	20.1	287.2	29.84	236.6	222.46	311.8	35.53	-23.9	-2.1	293.2	20.1
DV_7-5-15_F1_144	0.056	8.08	0.365	10.55	0.047	6.82	0.64	0.016	11.7	296.53	19.8	315.6	28.63	457.1	179.27	316.0	36.72	35.1	6.0	296.5	19.8
DV_7-5-15_F1_181	0.050	8.77	0.327	10.56	0.048	5.97	0.56	0.015	8.5	300.68	17.5	287.6	26.46	181.1	204.32	293.3	24.78	-66.0	-4.5	300.7	17.5
DV_7-5-15_F1_33	0.073	14.27	0.480	20.44	0.048	14.65	0.72	0.019	17.6	302.08	43.2	398.3	67.45	1000.9	289.83	386.7	67.53	69.8	24.2	302.1	43.2
DV_7-5-15_F1_231	0.058	10.19	0.383	13.71	0.048	9.21	0.67	0.017	12.0	302.12	27.2	329.0	38.54	521.6	223.63	331.0	39.56	42.1	8.2	302.1	27.2
DV_7-5-15_F1_246	0.054	8.58	0.357	11.40	0.048	7.51	0.66	0.015	8.6	303.59	22.3	310.1	30.49	357.2	193.68	308.6	26.36	15.0	2.1	303.6	22.3
DV_7-5-15_F1_73	0.054	10.06	0.363	13.04	0.048	8.31	0.64	0.015	13.6	304.01	24.7	314.4	35.28	390.1	225.85	293.3	39.70	22.1	3.3	304.0	24.7
DV_7-5-15_F1_21	0.055	10.50	0.369	14.90	0.048	10.59	0.71	0.016	12.9	304.61	31.5	318.7	40.79	420.9	234.48	315.3	40.30	27.6	4.4	304.6	31.5
DV_7-5-15_F1_193	0.053	8.61	0.357	12.41	0.048	9.00	0.72	0.020	17.6	304.70	26.8	310.1	33.17	348.6	194.60	402.3	70.24	12.6	1.7	304.7	26.8
DV_7-5-15_F1_70	0.054	9.34	0.361	13.05	0.048	9.12	0.70	0.015	12.5	304.75	27.1	313.1	35.16	373.1	210.31	305.6	37.84	18.3	2.7	304.7	27.1
DV_7-5-15_F1_209	0.057	7.61	0.378	10.09	0.048	6.71	0.66	0.015	9.1	305.29	20.0	325.7	28.11	472.6	168.25	309.1	28.01	35.4	6.3	305.3	20.0
DV_7-5-15_F1_192	0.058	6.88	0.395	8.81	0.049	5.60	0.62	0.016	10.6	308.75	16.9	338.1	25.33	543.3	150.37	324.5	34.04	43.2	8.7	308.8	16.9
DV_7-5-15_F1_54	0.057	20.59	0.397	21.72	0.051	6.96	0.32	0.017	14.7	318.29	21.6	339.5	62.77	485.2	454.51	341.6	49.98	34.4	6.3	318.3	21.6
DV_7-5-15_F1_63	0.052	10.64	0.367	14.54	0.051	9.92	0.68	0.019	13.8	319.48	30.9	317.1	39.62	297.5	242.66	379.8	51.90	-7.4	-0.7	319.5	30.9
DV_7-5-15_F1_221	0.053	12.89	0.374	15.78	0.051	9.16	0.58	0.016	11.1	321.47	28.7	322.8	43.67	330.0	292.47	315.3	34.82	2.6	0.4	321.5	28.7
DV_7-5-15_F1_110	0.056	8.41	0.397	11.33	0.051	7.60	0.67	0.016	12.4	322.57	23.9	339.3	32.67	453.5	186.59	328.4	40.44	28.9	4.9	322.6	23.9
DV_7-5-15_F1_247	0.067	12.16	0.484	18.10	0.052	13.41	0.74	0.019	17.9	329.24	43.0	400.5	59.99	833.6	253.39	381.9	67.71	60.5	17.8	329.2	43.0
DV_7-5-15_F1_175	0.057	6.02	0.416	7.87	0.053	5.16	0.64	0.016	9.3	330.04	16.6	353.1	23.47	505.6	132.39	326.1	30.03	34.7	6.5	330.0	16.6
DV_7-5-15_F1_121	0.066	8.01	0.490	11.34	0.053	8.04	0.71	0.014	13.1	335.31	26.3	404.8	37.87	821.6	167.35	287.1	37.50	59.2	17.2	335.3	26.3
DV_7-5-15_F1_138	0.057	13.97	0.427	20.12	0.055	14.50	0.72	0.018	18.1	343.28	48.5	361.1	61.22	475.1	308.93	351.5	63.31	27.8	4.9	343.3	48.5
DV_7-5-15_F1_203	0.053	9.22	0.405	12.66	0.055	8.74	0.69	0.018	13.4	345.14	29.4	345.4	37.08	345.5	208.55	353.5	46.92	0.1	0.1	345.1	29.4
DV_7-5-15_F1_217	0.053	8.16	0.409	10.85	0.056	7.23	0.66	0.017	9.1	348.26	24.5	348.1	31.99	344.9	184.63	339.6	30.54	-1.0	0.0	348.3	24.5
DV_7-5-15_F1_172	0.062	13.24	0.474	18.88	0.056	13.48	0.71	0.019	14.1	349.06	45.8	394.3	61.75	667.2	283.51	388.2	54.35	47.7	11.5	349.1	45.8
DV_7-5-15_F1_11	0.057	10.13	0.440	13.61	0.056	9.10	0.67	0.016	13.8	350.53	31.1	370.3	42.25	494.0	223.34	315.1	43.22	29.0	5.3	350.5	31.1
DV_7-5-15_F1_222	0.054	6.28	0.420	8.32	0.056	5.54	0.66	0.020	9.3	352.04	19.0	356.3	25.00	382.2	141.12	401.2	36.80	7.9	1.2	352.0	19.0
DV_7-5-15_F1_125	0.067	9.12	0.518	12.59	0.056	8.69	0.69	0.023	10.0	353.47	29.9	423.7	43.63	824.9	190.42	457.0	45.36	57.1	16.6	353.5	29.9
DV_7-5-15_F1_236	0.076	12.83	0.593	17.74	0.057	12.28	0.69	0.015	9.6	354.78	42.4	472.8	67.16	1093.7	256.82	307.4	29.42	67.6	25.0	354.8	42.4

DV_7-5-15_F1_165	0.055	6.92	0.428	9.28	0.057	6.24	0.67	0.019	9.3	355.62	21.6	361.7	28.23	399.2	155.13	371.6	34.28	10.9	1.7	355.6	21.6
DV_7-5-15_F1_184	0.056	9.71	0.441	12.07	0.057	7.24	0.59	0.018	9.2	355.76	25.1	370.8	37.51	464.3	215.05	362.9	33.24	23.4	4.1	355.8	25.1
DV_7-5-15_F1_39	0.055	9.74	0.434	11.77	0.057	6.63	0.56	0.019	11.3	358.68	23.1	366.2	36.20	411.3	217.85	389.7	43.57	12.8	2.0	358.7	23.1
DV_7-5-15_F1_239	0.053	6.16	0.421	8.38	0.057	5.71	0.68	0.019	8.6	359.98	20.0	356.9	25.22	334.7	139.65	372.1	31.81	-7.5	-0.9	360.0	20.0
DV_7-5-15_F1_74	0.073	10.19	0.586	13.92	0.058	9.49	0.68	0.018	16.8	362.31	33.4	468.3	52.25	1026.1	206.17	364.1	60.60	64.7	22.6	362.3	33.4
DV_7-5-15_F1_109	0.054	9.88	0.432	13.80	0.058	9.64	0.70	0.018	10.2	365.41	34.3	364.3	42.28	355.4	223.22	357.0	36.22	-2.8	-0.3	365.4	34.3
DV_7-5-15_F1_223	0.056	10.06	0.453	14.34	0.058	10.27	0.71	0.019	8.9	365.68	36.5	379.5	45.43	462.3	222.87	386.9	34.26	20.9	3.6	365.7	36.5
DV_7-5-15_F1_169	0.055	7.10	0.444	9.67	0.059	6.63	0.68	0.018	10.9	367.56	23.7	373.0	30.19	405.5	158.86	366.2	39.45	9.4	1.5	367.6	23.7
DV_7-5-15_F1_241	0.053	8.26	0.440	9.65	0.060	5.02	0.52	0.019	8.7	378.10	18.4	369.9	29.94	316.8	187.83	389.0	33.49	-19.4	-2.2	378.1	18.4
DV_7-5-15_F1_211	0.064	10.70	0.538	13.49	0.061	8.29	0.61	0.024	18.6	379.45	30.5	436.9	47.93	750.0	225.95	469.6	86.72	49.4	13.1	379.4	30.5
DV_7-5-15_F1_170	0.056	9.21	0.474	11.86	0.061	7.54	0.63	0.020	9.4	380.55	27.8	393.7	38.74	470.2	203.80	390.9	36.29	19.1	3.3	380.5	27.8
DV_7-5-15_F1_17	0.055	11.08	0.468	16.72	0.061	12.53	0.75	0.019	17.6	383.84	46.7	390.1	54.20	425.0	247.16	382.9	66.72	9.7	1.6	383.8	46.7
DV_7-5-15_F1_26	0.064	13.01	0.547	18.55	0.062	13.23	0.71	0.019	17.3	387.61	49.8	443.4	66.72	741.8	275.13	383.3	65.93	47.8	12.6	387.6	49.8
DV_7-5-15_F1_173	0.057	13.65	0.491	18.46	0.062	12.46	0.67	0.019	16.5	389.44	47.1	405.6	61.79	496.8	300.79	386.5	63.24	21.6	4.0	389.4	47.1
DV_7-5-15_F1_166	0.067	9.33	0.573	13.26	0.062	9.46	0.71	0.028	13.4	390.00	35.8	459.7	49.07	823.2	194.82	564.9	74.63	52.6	15.2	390.0	35.8
DV_7-5-15_F1_7	0.059	9.57	0.517	13.66	0.063	9.77	0.71	0.021	15.7	394.93	37.4	423.0	47.31	576.8	208.04	423.2	65.80	31.5	6.6	394.9	37.4
DV_7-5-15_F1_47	0.054	8.19	0.476	11.06	0.063	7.45	0.67	0.020	10.3	395.20	28.6	395.0	36.21	391.3	183.81	391.0	39.75	-1.0	-0.1	395.2	28.6
DV_7-5-15_F1_118	0.055	6.19	0.481	8.56	0.064	5.93	0.69	0.020	8.9	397.97	22.9	399.1	28.26	403.8	138.57	402.0	35.32	1.4	0.3	398.0	22.9
DV_7-5-15_F1_251	0.059	8.38	0.524	11.48	0.064	7.82	0.68	0.024	15.3	399.02	30.3	427.7	40.11	583.1	181.94	477.4	72.10	31.6	6.7	399.0	30.3
DV_7-5-15_F1_81	0.054	7.09	0.476	9.23	0.064	5.93	0.64	0.020	10.0	399.83	23.0	395.1	30.23	365.5	159.74	405.6	40.23	-9.4	-1.2	399.8	23.0
DV_7-5-15_F1_83	0.063	10.46	0.563	14.28	0.065	9.72	0.68	0.019	15.1	404.26	38.1	453.6	52.27	709.8	222.41	385.1	57.68	43.0	10.9	404.3	38.1
DV_7-5-15_F1_40	0.059	6.28	0.531	8.81	0.065	6.20	0.70	0.015	21.8	404.29	24.3	432.8	31.04	585.1	136.23	291.5	63.31	30.9	6.6	404.3	24.3
DV_7-5-15_F1_2	0.057	11.39	0.517	15.92	0.065	11.13	0.70	0.020	13.0	407.12	43.9	423.1	55.12	508.9	250.36	400.0	51.42	20.0	3.8	407.1	43.9
DV_7-5-15_F1_25	0.068	11.41	0.613	15.23	0.065	10.11	0.66	0.023	14.3	408.17	40.0	485.4	58.84	866.3	236.50	466.8	66.20	52.9	15.9	408.2	40.0
DV_7-5-15_F1_87	0.056	7.98	0.507	10.72	0.065	7.17	0.67	0.020	12.3	408.43	28.4	416.5	36.64	459.0	176.95	390.7	47.56	11.0	1.9	408.4	28.4
DV_7-5-15_F1_188	0.058	9.17	0.524	10.55	0.066	5.32	0.49	0.020	9.6	409.18	21.1	428.1	36.87	529.5	200.87	408.7	38.92	22.7	4.4	409.2	21.1
DV_7-5-15_F1_79	0.059	10.55	0.531	14.31	0.066	9.67	0.68	0.016	16.4	410.54	38.5	432.6	50.45	549.7	230.38	316.5	51.63	25.3	5.1	410.5	38.5
DV_7-5-15_F1_115	0.057	7.43	0.514	9.91	0.066	6.56	0.66	0.022	11.1	410.81	26.1	421.4	34.18	478.2	164.32	446.2	48.84	14.1	2.5	410.8	26.1
DV_7-5-15_F1_55	0.065	11.19	0.594	14.18	0.066	8.73	0.61	0.019	18.9	412.26	34.9	473.3	53.72	779.1	235.33	375.9	70.67	47.1	12.9	412.3	34.9
DV_7-5-15_F1_178	0.054	10.74	0.496	15.25	0.066	10.87	0.71	0.021	13.6	412.64	43.4	408.9	51.38	386.1	241.21	421.0	56.67	-6.9	-0.9	412.6	43.4

DV_7-5-15_F1_50	0.057	7.55	0.526	9.53	0.067	5.84	0.61	0.021	10.7	417.17	23.6	429.1	33.38	491.3	166.56	428.1	45.28	15.1	2.8	417.2	23.6
DV_7-5-15_F1_45	0.063	7.16	0.579	9.72	0.067	6.60	0.68	0.023	11.5	417.84	26.7	463.5	36.18	694.3	152.54	461.3	52.72	39.8	9.9	417.8	26.7
DV_7-5-15_F1_243	0.060	13.84	0.553	19.93	0.067	14.35	0.72	0.022	13.8	419.02	58.2	447.3	72.23	593.0	299.91	443.2	60.53	29.3	6.3	419.0	58.2
DV_7-5-15_F1_204	0.057	9.33	0.529	12.81	0.068	8.85	0.69	0.022	16.1	421.36	36.1	431.3	45.06	482.6	206.08	433.0	69.24	12.7	2.3	421.4	36.1
DV_7-5-15_F1_245	0.056	5.90	0.521	8.27	0.068	5.80	0.70	0.022	8.1	421.86	23.7	425.7	28.77	444.1	131.12	449.5	36.10	5.0	0.9	421.9	23.7
DV_7-5-15_F1_163	0.063	6.39	0.590	8.52	0.068	5.71	0.66	0.024	8.0	422.42	23.3	471.0	32.13	713.3	135.79	485.2	38.48	40.8	10.3	422.4	23.3
DV_7-5-15_F1_80	0.057	6.63	0.535	8.71	0.068	5.66	0.65	0.021	13.8	422.55	23.2	435.4	30.84	501.8	145.89	425.9	58.33	15.8	3.0	422.6	23.2
DV_7-5-15_F1_14	0.058	6.77	0.540	9.45	0.068	6.62	0.70	0.020	11.4	424.36	27.2	438.6	33.67	512.1	148.75	408.7	46.08	17.1	3.3	424.4	27.2
DV_7-5-15_F1_36	0.055	7.60	0.521	10.49	0.068	7.26	0.69	0.022	13.0	424.83	29.9	425.5	36.50	427.0	169.38	431.8	55.42	0.5	0.2	424.8	29.9
DV_7-5-15_F1_139	0.058	9.54	0.546	13.65	0.068	9.78	0.72	0.023	10.2	425.14	40.2	442.3	48.97	530.6	208.94	461.1	46.42	19.9	3.9	425.1	40.2
DV_7-5-15_F1_126	0.057	9.83	0.534	13.62	0.068	9.44	0.69	0.022	16.0	425.32	38.9	434.5	48.17	481.5	217.13	435.0	68.95	11.7	2.1	425.3	38.9
DV_7-5-15_F1_10	0.058	7.00	0.545	8.97	0.068	5.63	0.62	0.021	9.8	426.08	23.2	441.7	32.13	521.7	153.65	424.0	41.30	18.3	3.5	426.1	23.2
DV_7-5-15_F1_220	0.057	7.85	0.536	11.03	0.068	7.81	0.70	0.021	9.0	426.62	32.3	435.8	39.09	482.7	173.29	424.3	37.87	11.6	2.1	426.6	32.3
DV_7-5-15_F1_143	0.055	6.94	0.525	9.34	0.069	6.29	0.67	0.023	8.6	428.00	26.0	428.6	32.66	429.9	154.59	457.8	38.99	0.4	0.1	428.0	26.0
DV_7-5-15_F1_208	0.065	11.83	0.616	15.66	0.069	10.32	0.66	0.026	17.0	429.35	42.9	487.2	60.66	767.2	249.07	512.4	86.24	44.0	11.9	429.4	42.9
DV_7-5-15_F1_91	0.055	12.56	0.520	18.04	0.069	12.95	0.72	0.021	9.3	430.53	53.9	425.3	62.76	395.1	281.69	412.3	38.09	-9.0	-1.2	430.5	53.9
DV_7-5-15_F1_67	0.057	11.18	0.543	14.66	0.069	9.49	0.65	0.021	12.7	430.60	39.5	440.4	52.44	489.5	246.69	420.3	52.91	12.0	2.2	430.6	39.5
DV_7-5-15_F1_52	0.062	7.52	0.588	10.24	0.069	6.97	0.68	0.022	9.7	430.73	29.0	469.5	38.50	661.2	161.14	448.0	42.85	34.9	8.3	430.7	29.0
DV_7-5-15_F1_92	0.054	7.09	0.518	9.27	0.069	5.98	0.64	0.021	9.0	432.72	25.0	423.9	32.12	374.1	159.57	412.0	36.80	-15.7	-2.1	432.7	25.0
DV_7-5-15_F1_237	0.057	7.98	0.551	11.27	0.070	7.99	0.71	0.021	12.3	433.33	33.5	445.6	40.67	507.1	175.49	428.9	52.35	14.5	2.7	433.3	33.5
DV_7-5-15_F1_58	0.055	9.79	0.532	13.69	0.070	9.58	0.70	0.020	17.1	433.82	40.2	433.1	48.30	426.7	218.31	409.8	69.67	-1.7	-0.2	433.8	40.2
DV_7-5-15_F1_201	0.054	8.23	0.519	11.06	0.070	7.47	0.67	0.023	11.5	434.10	31.4	424.7	38.42	372.2	185.27	451.7	51.65	-16.6	-2.2	434.1	31.4
DV_7-5-15_F1_131	0.057	8.41	0.552	11.69	0.070	8.14	0.69	0.023	12.6	434.93	34.2	446.6	42.26	505.4	185.12	464.3	57.87	14.0	2.6	434.9	34.2
DV_7-5-15_F1_202	0.054	6.75	0.522	8.49	0.070	5.26	0.61	0.022	7.8	436.13	22.2	426.3	29.57	371.4	152.02	435.0	33.73	-17.4	-2.3	436.1	22.2
DV_7-5-15_F1_20	0.061	15.28	0.593	20.51	0.070	13.70	0.67	0.023	11.6	437.26	57.9	473.1	77.71	648.4	328.04	454.7	52.33	32.6	7.6	437.3	57.9
DV_7-5-15_F1_95	0.053	8.28	0.511	10.26	0.070	6.07	0.59	0.022	10.9	437.63	25.7	419.3	35.25	317.2	188.17	436.9	47.38	-38.0	-4.4	437.6	25.7
DV_7-5-15_F1_194	0.056	6.02	0.543	7.88	0.071	5.20	0.65	0.022	8.7	440.33	22.1	440.6	28.18	439.8	133.83	448.8	38.47	-0.1	0.0	440.3	22.1
DV_7-5-15_F1_189	0.057	6.35	0.552	8.68	0.071	6.00	0.68	0.022	7.8	440.69	25.6	446.2	31.35	473.0	140.52	443.0	34.09	6.8	1.2	440.7	25.6
DV_7-5-15_F1_234	0.060	9.02	0.582	11.01	0.071	6.37	0.57	0.022	9.2	441.12	27.2	465.7	41.16	586.8	195.72	443.0	40.54	24.8	5.3	441.1	27.2
DV_7-5-15_F1_99	0.070	8.86	0.685	12.29	0.071	8.52	0.69	0.031	16.5	443.12	36.5	529.7	50.76	920.6	182.22	610.1	99.19	51.9	16.3	443.1	36.5

DV_7-5-15_F1_244	0.058	6.28	0.573	8.84	0.071	6.23	0.70	0.024	8.3	443.46	26.7	459.8	32.70	539.8	137.34	476.3	39.26	17.9	3.5	443.5	26.7
DV_7-5-15_F1_30	0.056	9.35	0.550	12.41	0.071	8.17	0.66	0.024	11.6	443.84	35.0	445.0	44.73	448.9	207.75	478.5	55.00	1.1	0.3	443.8	35.0
DV_7-5-15_F1_31	0.056	10.80	0.554	15.45	0.071	11.06	0.72	0.022	14.3	444.98	47.6	447.3	55.94	457.0	239.49	443.3	62.70	2.6	0.5	445.0	47.6
DV_7-5-15_F1_186	0.058	8.41	0.578	11.33	0.072	7.66	0.67	0.023	7.8	446.01	33.0	462.9	42.14	545.8	183.66	459.8	35.28	18.3	3.6	446.0	33.0
DV_7-5-15_F1_199	0.059	8.97	0.589	11.50	0.073	7.28	0.63	0.022	10.1	452.14	31.8	470.0	43.31	556.2	195.59	434.6	43.32	18.7	3.8	452.1	31.8
DV_7-5-15_F1_210	0.055	5.10	0.561	6.73	0.074	4.52	0.65	0.023	7.6	457.62	20.0	452.1	24.57	422.0	113.88	456.2	34.38	-8.4	-1.2	457.6	20.0
DV_7-5-15_F1_187	0.054	10.21	0.551	11.82	0.074	6.06	0.50	0.023	9.7	458.83	26.8	445.9	42.70	377.7	229.58	456.5	43.68	-21.5	-2.9	458.8	26.8
DV_7-5-15_F1_195	0.064	9.29	0.664	11.56	0.075	6.97	0.60	0.023	9.0	465.16	31.3	516.8	46.87	750.5	196.11	468.9	41.92	38.0	10.0	465.2	31.3
DV_7-5-15_F1_137	0.063	11.32	0.656	15.29	0.075	10.29	0.67	0.034	16.3	467.46	46.4	511.9	61.54	714.1	240.45	668.1	107.69	34.5	8.7	467.5	46.4
DV_7-5-15_F1_56	0.060	6.20	0.764	8.66	0.092	6.07	0.70	0.037	11.8	570.01	33.1	576.5	38.12	599.6	134.23	729.2	85.04	4.9	1.1	570.0	33.1
DV_7-5-15_F1_176	0.061	10.25	0.830	13.81	0.098	9.30	0.67	0.031	14.0	605.01	53.7	613.9	63.69	645.0	220.29	608.7	84.19	6.2	1.4	605.0	53.7
DV_7-5-15_F1_191	0.061	5.73	0.853	7.49	0.102	4.94	0.64	0.031	7.3	624.60	29.4	626.1	35.02	629.8	123.49	613.5	44.00	0.8	0.2	624.6	29.4
DV_7-5-15_F1_213	0.062	13.94	0.879	20.09	0.103	14.51	0.72	0.031	18.8	631.12	87.2	640.2	95.70	670.4	298.28	624.9	116.05	5.9	1.4	631.1	87.2
DV_7-5-15_F1_159	0.064	9.82	0.933	11.30	0.106	5.65	0.49	0.030	9.3	652.00	35.1	669.2	55.43	726.0	208.15	605.4	55.56	10.2	2.6	652.0	35.1
DV_7-5-15_F1_161	0.064	8.34	0.965	11.82	0.110	8.43	0.71	0.037	9.3	670.27	53.7	685.8	59.03	735.6	176.52	725.8	66.09	8.9	2.3	670.3	53.7
DV_7-5-15_F1_155	0.065	8.30	1.057	11.45	0.118	7.93	0.69	0.037	9.8	719.39	54.0	732.3	59.83	770.6	174.66	742.3	71.67	6.6	1.8	719.4	54.0
DV_7-5-15_F1_84	0.066	6.29	1.143	8.42	0.125	5.60	0.66	0.040	8.9	761.27	40.2	773.8	45.62	807.9	131.70	793.4	69.66	5.8	1.6	761.3	40.2
DV_7-5-15_F1_158	0.067	5.94	1.179	7.75	0.127	5.05	0.64	0.040	7.8	772.90	36.8	790.8	42.61	840.1	123.66	796.1	60.79	8.0	2.3	772.9	36.8
DV_7-5-15_F1_198	0.067	9.44	1.211	12.71	0.132	8.58	0.67	0.044	12.8	797.01	64.3	805.7	70.82	828.2	197.02	866.0	108.99	3.8	1.1	797.0	64.3
DV_7-5-15_F1_157	0.067	6.52	1.239	8.97	0.134	6.21	0.69	0.042	11.4	812.11	47.4	818.4	50.45	833.9	135.97	835.2	93.75	2.6	0.8	812.1	47.4
DV_7-5-15_F1_22	0.066	12.40	1.239	17.44	0.135	12.27	0.70	0.040	18.4	817.21	94.2	818.5	98.29	819.8	259.00	794.1	143.65	0.3	0.2	817.2	94.2
DV_7-5-15_F1_43	0.071	9.83	1.326	11.73	0.135	6.42	0.55	0.042	12.0	817.94	49.3	857.2	67.98	958.0	200.95	823.8	96.93	14.6	4.6	817.9	49.3
DV_7-5-15_F1_200	0.069	10.96	1.469	15.52	0.155	11.04	0.71	0.043	9.4	927.06	95.4	917.9	94.05	894.0	226.34	853.6	78.74	-3.7	-1.0	927.1	95.4
DV_7-5-15_F1_94	0.069	12.57	1.566	18.25	0.165	13.24	0.73	0.049	18.1	984.43	120.9	957.0	113.59	892.5	259.52	970.5	172.68	-10.3	-2.9	984.4	120.9
DV_7-5-15_F1_106	0.071	7.66	1.635	10.97	0.168	7.86	0.72	0.049	10.5	999.29	72.7	983.7	69.22	947.4	156.92	960.0	98.98	-5.5	-1.6	999.3	72.7
DV_7-5-15_F1_27	0.084	7.54	2.149	12.64	0.185	10.17	0.80	0.066	10.0	1093.59	102.3	1164.8	87.83	1297.6	146.53	1285.2	125.42	15.7	6.1	1093.6	102.3
DV_7-5-15_F1_132	0.098	14.10	3.362	19.97	0.249	14.16	0.71	0.079	18.8	1433.56	182.0	1495.6	157.53	1583.1	263.64	1533.0	279.70	9.4	4.1	1583.1	263.6
DV_7-5-15_F1_154	0.105	10.45	3.546	14.88	0.245	10.63	0.71	0.089	13.2	1412.59	134.8	1537.6	118.43	1712.6	192.26	1730.3	219.33	17.5	8.1	1712.6	192.3
DV_7-5-15_F1_77	0.108	9.63	4.633	12.76	0.311	8.38	0.66	0.090	12.5	1744.19	128.1	1755.3	107.00	1766.7	176.01	1742.7	210.10	1.3	0.6	1766.7	176.0
DV_7-5-15_F1_38	0.109	8.03	4.705	11.26	0.313	7.91	0.70	0.093	11.7	1756.92	121.6	1768.1	94.53	1779.4	146.54	1789.6	201.16	1.3	0.6	1779.4	146.5

Rejected data

DV_7-5-15_F1_233	0.105	11.68	0.356	16.59	0.025	11.81	0.71	0.009	18.7	156.45	18.3	309.0	44.23	1712.4	214.84	171.8	31.96	90.9	49.4	156.5	18.3
DV_7-5-15_F1_133	0.117	8.87	0.428	12.86	0.026	9.33	0.72	0.010	13.7	167.97	15.5	361.7	39.14	1918.4	159.05	197.6	27.05	91.2	53.6	168.0	15.5
DV_7-5-15_F1_171	0.135	11.12	0.537	13.14	0.029	7.06	0.53	0.016	12.5	183.42	12.8	436.6	46.66	2162.9	193.88	315.0	38.97	91.5	58.0	183.4	12.8
DV_7-5-15_F1_3	0.080	6.92	0.339	9.14	0.031	5.99	0.65	0.013	9.7	194.21	11.5	296.2	23.48	1202.7	136.44	260.7	25.23	83.9	34.4	194.2	11.5
DV_7-5-15_F1_8	0.052	14.53	0.252	21.15	0.035	15.38	0.73	0.012	15.0	224.61	34.0	228.4	43.29	265.6	333.34	239.7	35.66	15.4	1.7	224.6	34.0
DV_7-5-15_F1_35	0.097	14.28	0.496	20.16	0.037	14.24	0.71	0.018	16.4	234.96	32.9	409.3	68.00	1564.9	267.66	355.0	57.76	85.0	42.6	235.0	32.9
DV_7-5-15_F1_230	0.077	6.09	0.416	7.90	0.039	5.11	0.64	0.013	9.2	247.46	12.4	353.2	23.58	1122.1	121.52	264.0	24.21	77.9	29.9	247.5	12.4
DV_7-5-15_F1_226	0.054	14.59	0.322	21.07	0.043	15.23	0.72	0.015	17.2	270.73	40.4	283.1	52.09	384.1	327.69	307.1	52.52	29.5	4.4	270.7	40.4
DV_7-5-15_F1_218	0.055	15.74	0.324	22.16	0.043	15.63	0.70	0.014	16.9	271.22	41.5	284.7	55.06	394.8	352.97	281.2	47.36	31.3	4.7	271.2	41.5
DV_7-5-15_F1_152	0.055	17.07	0.341	22.93	0.045	15.32	0.67	0.016	14.9	283.23	42.5	298.2	59.31	415.4	381.45	315.3	46.62	31.8	5.0	283.2	42.5
DV_7-5-15_F1_215	0.143	297.84	0.892	302.13	0.045	50.71	0.17	0.016	270.7	285.61	141.7	647.7	65535.00	2260.8	5140.36	329.7	329.66	87.4	55.9	285.6	141.7
DV_7-5-15_F1_13	0.120	25.60	0.786	27.24	0.047	9.34	0.34	0.021	18.7	297.51	27.2	588.6	122.29	1963.6	456.80	424.5	78.85	84.8	49.5	297.5	27.2
DV_7-5-15_F1_205	0.081	19.72	0.527	30.17	0.047	22.86	0.76	0.017	25.3	297.71	66.5	429.8	106.09	1216.4	387.77	340.3	85.51	75.5	30.7	297.7	66.5
DV_7-5-15_F1_76	0.063	15.17	0.415	22.23	0.048	16.25	0.73	0.016	18.8	299.32	47.5	352.3	66.25	715.9	322.20	320.9	59.85	58.2	15.0	299.3	47.5
DV_7-5-15_F1_61	0.114	11.30	0.750	14.18	0.048	8.59	0.60	0.018	14.0	299.39	25.1	568.5	61.82	1870.0	203.81	367.1	50.96	84.0	47.3	299.4	25.1
DV_7-5-15_F1_100	0.091	12.02	0.609	19.05	0.048	14.79	0.78	0.019	22.7	304.71	44.0	483.0	73.35	1450.4	228.77	374.7	84.56	79.0	36.9	304.7	44.0
DV_7-5-15_F1_86	0.188	21.56	1.285	26.67	0.050	15.70	0.59	0.030	20.7	311.69	47.8	839.2	153.45	2724.5	355.08	594.5	121.77	88.6	62.9	311.7	47.8
DV_7-5-15_F1_62	0.092	8.34	0.644	12.20	0.050	8.92	0.73	0.020	11.1	317.18	27.6	504.7	48.55	1477.5	158.15	398.5	43.79	78.5	37.2	317.2	27.6
DV_7-5-15_F1_119	0.230	7.36	1.997	9.89	0.063	6.62	0.67	0.037	9.1	392.56	25.2	1114.5	67.00	3055.4	117.79	740.6	66.42	87.2	64.8	392.6	25.2
DV_7-5-15_F1_162	0.056	15.20	0.494	21.93	0.063	15.83	0.72	0.020	15.5	396.57	60.9	407.3	73.71	467.2	336.49	405.7	62.49	15.1	2.6	396.6	60.9
DV_7-5-15_F1_196	0.333	13.05	2.917	15.62	0.063	8.65	0.55	0.035	11.5	396.65	33.3	1386.3	118.63	3631.3	199.76	698.2	79.38	89.1	71.4	396.7	33.3
DV_7-5-15_F1_240	0.161	9.64	1.466	14.56	0.066	10.93	0.75	0.044	13.2	412.11	43.6	916.5	88.10	2465.2	162.87	876.5	113.39	83.3	55.0	412.1	43.6
DV_7-5-15_F1_142	0.056	15.56	0.517	22.56	0.067	16.36	0.72	0.021	18.7	418.83	66.3	423.0	78.21	443.9	345.82	417.2	77.46	5.6	1.0	418.8	66.3
DV_7-5-15_F1_104	0.055	22.38	0.515	32.14	0.067	23.07	0.72	0.022	20.3	420.62	93.9	421.9	111.40	426.7	499.11	436.3	87.86	1.4	0.3	420.6	93.9
DV_7-5-15_F1_75	0.084	8.63	0.814	12.17	0.070	8.59	0.71	0.033	12.0	436.94	36.3	604.8	55.50	1295.0	167.76	656.2	77.67	66.3	27.7	436.9	36.3
DV_7-5-15_F1_98	0.057	16.86	0.554	24.09	0.070	17.21	0.71	0.022	20.9	437.65	72.8	447.7	87.43	497.5	371.42	443.9	91.80	12.0	2.2	437.6	72.8
DV_7-5-15_F1_108	0.443	6.91	4.299	9.40	0.070	6.38	0.68	0.157	8.8	438.31	27.0	1693.1	77.58	4061.0	102.98	2941.4	242.38	89.2	74.1	438.3	27.0
DV_7-5-15_F1_64	0.242	17.74	2.485	19.51	0.074	8.14	0.42	0.028	12.5	462.66	36.4	1267.7	142.20	3132.9	281.98	566.6	70.23	85.2	63.5	462.7	36.4

DV_7-5-15_F1_182	0.210	8.17	2.284	12.34	0.079	9.31	0.75	0.039	11.7	488.99	43.8	1207.3	87.39	2905.6	132.40	782.5	90.33	83.2	59.5	489.0	43.8
DV_7-5-15_F1_206	0.271	6.00	3.043	8.72	0.081	6.41	0.73	0.564	11.7	503.61	31.1	1418.4	66.71	3313.8	94.06	9036.1	868.45	84.8	64.5	503.6	31.1
DV_7-5-15_F1_53	0.353	10.73	4.007	13.41	0.082	8.07	0.60	0.249	12.9	508.96	39.5	1635.6	109.40	3721.6	163.24	4494.2	528.25	86.3	68.9	509.0	39.5
DV_7-5-15_F1_232	0.481	7.55	5.653	12.20	0.085	9.62	0.79	0.199	11.4	526.55	48.7	1924.3	105.64	4184.8	111.59	3665.2	386.32	87.4	72.6	526.5	48.7
DV_7-5-15_F1_225	0.090	7.60	1.101	10.06	0.088	6.67	0.66	0.026	13.5	546.06	34.9	753.8	53.60	1430.6	145.01	514.4	68.63	61.8	27.6	546.1	34.9
DV_7-5-15_F1_160	0.232	8.04	2.851	11.39	0.089	8.11	0.71	0.046	9.6	549.86	42.8	1369.2	85.83	3066.4	128.52	910.4	85.50	82.1	59.8	549.9	42.8
DV_7-5-15_F1_112	0.481	6.86	6.242	9.25	0.094	6.22	0.67	0.037	8.5	579.65	34.5	2010.3	81.14	4183.2	101.51	731.5	61.05	86.1	71.2	579.6	34.5
DV_7-5-15_F1_111	0.359	33.01	4.710	46.25	0.095	32.40	0.70	0.075	9.9	585.77	181.5	1768.9	408.00	3744.7	501.54	1465.1	140.84	84.4	66.9	585.8	181.5
DV_7-5-15_F1_72	0.528	9.02	7.087	13.12	0.097	9.53	0.73	0.234	10.5	598.62	54.5	2122.4	117.27	4320.4	132.40	4254.6	407.89	86.1	71.8	598.6	54.5
DV_7-5-15_F1_120	0.077	8.23	1.066	12.59	0.101	9.54	0.76	0.037	9.6	619.55	56.4	736.7	66.07	1109.8	164.47	731.1	68.93	44.2	15.9	619.5	56.4
DV_7-5-15_F1_78	0.453	7.62	6.307	10.42	0.101	7.12	0.68	0.248	10.1	620.07	42.1	2019.5	91.58	4093.8	113.20	4471.0	408.00	84.9	69.3	620.1	42.1
DV_7-5-15_F1_197	0.080	7.57	1.137	11.73	0.103	9.02	0.76	0.023	16.0	634.05	54.5	771.1	63.45	1190.2	149.44	451.7	71.51	46.7	17.8	634.0	54.5
DV_7-5-15_F1_46	0.084	18.91	1.205	21.92	0.104	11.09	0.51	0.057	25.6	639.04	67.5	803.1	122.22	1287.8	368.16	1113.4	279.05	50.4	20.4	639.0	67.5
DV_7-5-15_F1_85	0.064	20.32	0.968	26.45	0.109	16.94	0.64	0.029	19.9	665.68	107.1	687.4	132.85	757.2	428.63	573.6	113.09	12.1	3.2	665.7	107.1
DV_7-5-15_F1_5	0.456	8.31	6.973	11.24	0.111	7.59	0.67	0.801	10.8	677.50	48.8	2108.0	100.16	4104.6	123.46	11891.2	993.81	83.5	67.9	677.5	48.8
DV_7-5-15_F1_148	0.074	16.14	1.126	23.49	0.111	17.09	0.73	0.035	15.1	677.79	109.9	766.0	127.01	1031.1	326.23	686.9	102.02	34.3	11.5	677.8	109.9
DV_7-5-15_F1_82	0.069	8.09	1.068	10.65	0.112	6.95	0.65	0.033	10.1	682.29	45.0	737.8	55.93	908.1	166.61	658.3	65.26	24.9	7.5	682.3	45.0
DV_7-5-15_F1_147	0.387	7.59	6.188	10.46	0.116	7.23	0.69	0.045	8.7	706.54	48.4	2002.7	91.69	3859.9	114.51	885.8	75.85	81.7	64.7	706.5	48.4
DV_7-5-15_F1_4	0.073	5.85	1.242	8.37	0.124	6.02	0.72	0.037	9.9	753.78	42.8	819.9	47.14	1001.8	118.71	743.5	72.57	24.8	8.1	753.8	42.8
DV_7-5-15_F1_97	0.571	8.08	9.809	12.67	0.125	9.77	0.77	0.101	11.5	756.41	69.7	2417.0	117.28	4435.5	117.74	1938.8	213.03	82.9	68.7	756.4	69.7
DV_7-5-15_F1_44	0.434	7.36	7.561	10.10	0.126	6.95	0.69	0.061	10.7	766.45	50.2	2180.3	90.85	4030.9	109.78	1200.9	124.64	81.0	64.8	766.5	50.2
DV_7-5-15_F1_124	0.475	20.78	8.295	28.55	0.126	19.59	0.69	0.585	20.6	767.47	141.7	2263.8	264.55	4166.9	307.61	9309.3	1599.22	81.6	66.1	767.5	141.7
DV_7-5-15_F1_59	0.473	8.90	8.307	12.51	0.127	8.80	0.70	1.170	11.6	771.86	64.0	2265.1	113.83	4159.7	131.77	15657.5	1307.69	81.4	65.9	771.9	64.0
DV_7-5-15_F1_66	0.594	6.64	10.603	9.24	0.129	6.44	0.69	0.253	9.6	784.30	47.5	2489.0	85.92	4492.8	96.64	4552.6	394.11	82.5	68.5	784.3	47.5
DV_7-5-15_F1_174	0.128	19.80	2.412	27.16	0.137	18.62	0.68	0.047	18.2	827.40	144.6	1246.2	197.42	2065.8	349.03	936.7	167.29	59.9	33.6	827.4	144.6
DV_7-5-15_F1_123	0.598	9.05	11.761	12.41	0.143	8.50	0.68	0.088	10.4	858.93	68.4	2585.5	116.65	4503.1	131.64	1696.9	169.28	80.9	66.8	858.9	68.4
DV_7-5-15_F1_212	0.617	9.40	12.168	15.22	0.143	12.02	0.79	0.081	11.2	861.02	96.9	2617.5	143.78	4548.6	136.47	1582.9	170.52	81.1	67.1	861.0	96.9
DV_7-5-15_F1_28	0.528	8.51	10.463	11.80	0.144	8.19	0.69	0.106	10.4	864.57	66.3	2476.6	109.78	4321.7	124.88	2030.5	201.76	80.0	65.1	864.6	66.3
DV_7-5-15_F1_60	0.077	9.43	1.539	16.39	0.145	13.41	0.82	0.044	18.1	874.79	109.7	946.0	101.19	1113.4	188.26	870.3	154.35	21.4	7.5	874.8	109.7
DV_7-5-15_F1_107	0.087	17.52	1.896	21.09	0.159	11.75	0.56	0.094	27.9	949.65	103.8	1079.6	141.12	1350.5	338.12	1808.6	487.77	29.7	12.0	949.6	103.8

DV_7-5-15_F1_167	0.682	10.24	16.263	14.07	0.173	9.70	0.69	2.558	13.3	1027.51	92.1	2892.4	135.42	4693.4	147.75	25650.7	2032.07	78.1	64.5	1027.5	92.1
DV_7-5-15_F1_90	0.702	8.63	16.811	19.29	0.174	17.25	0.89	0.061	13.6	1031.47	164.5	2924.1	186.94	4734.7	124.35	1203.5	159.87	78.2	64.7	1031.5	164.5
DV_7-5-15_F1_49	0.675	12.07	16.396	18.34	0.176	13.81	0.75	0.073	17.2	1044.97	133.3	2900.2	177.27	4678.3	174.35	1431.5	238.65	77.7	64.0	1045.0	133.3
DV_7-5-15_F1_16	0.387	9.43	9.552	15.53	0.179	12.36	0.79	0.110	12.9	1060.98	120.9	2392.6	143.74	3858.7	142.29	2105.3	260.30	72.5	55.7	1061.0	120.9
DV_7-5-15_F1_130	0.581	10.04	14.489	12.72	0.181	7.83	0.61	0.084	9.1	1070.34	77.2	2782.3	121.40	4462.0	146.27	1637.1	143.66	76.0	61.5	1070.3	77.2
DV_7-5-15_F1_18	0.554	10.63	13.906	13.90	0.182	8.98	0.64	0.100	12.6	1077.33	89.1	2743.3	132.42	4391.5	155.39	1929.3	232.91	75.5	60.7	1077.3	89.1
DV_7-5-15_F1_113	0.615	8.79	15.966	13.55	0.188	10.33	0.76	1.801	28.5	1110.55	105.4	2874.8	130.23	4544.8	127.60	20819.0	4094.17	75.6	61.4	1110.6	105.4
DV_7-5-15_F1_168	0.658	26.60	17.578	37.24	0.194	26.08	0.70	0.172	27.4	1141.32	272.9	2966.9	373.76	4641.0	384.56	3203.9	829.62	75.4	61.5	1141.3	272.9
DV_7-5-15_F1_190	0.101	21.89	3.376	28.58	0.243	18.41	0.64	0.060	11.7	1402.09	232.1	1498.9	227.63	1637.0	406.54	1180.7	134.09	14.4	6.5	1637.0	406.5
DV_7-5-15_F1_177	0.145	19.30	7.338	28.88	0.367	21.51	0.74	0.112	13.1	2016.20	372.8	2153.5	263.89	2285.7	332.14	2140.5	267.54	11.8	6.4	2285.7	332.1
DV_7-5-15_F1_127	0.152	7.67	6.463	11.21	0.309	8.20	0.73	0.133	12.0	1736.44	124.8	2040.8	98.91	2363.0	130.93	2522.0	287.07	26.5	14.9	2363.0	130.9
DV_7-5-15_F1_23	0.170	13.15	8.290	19.62	0.354	14.57	0.74	0.115	10.7	1954.14	245.7	2263.2	179.59	2553.8	220.09	2202.8	224.61	23.5	13.7	2553.8	220.1
DV_7-5-15_F1_238	0.581	8.52	21.532	11.56	0.268	7.85	0.68	0.144	9.2	1532.35	107.0	3162.8	112.62	4462.1	124.03	2713.6	234.18	65.7	51.6	4462.1	124.0
DV_7-5-15_F1_69	0.604	10.17	18.399	14.50	0.221	10.34	0.71	0.239	11.9	1286.37	120.6	3010.8	140.50	4516.6	147.82	4339.0	471.13	71.5	57.3	4516.6	147.8
DV_7-5-15_F1_129	0.659	7.43	19.257	10.39	0.212	7.28	0.70	0.716	10.7	1237.69	82.0	3054.8	100.58	4644.5	107.45	10917.2	923.83	73.4	59.5	4644.5	107.5
DV_7-5-15_F1_101	0.666	94.77	297.798	120.49	3.241	74.41	0.62	0.209	67.0	9313.83	4161.2	5787.4	65535.00	4658.6	1369.37	3838.2	2488.94	-99.9	-60.9	4658.6	1369.4
DV_7-5-15_F1_150	0.689	34.85	40.070	48.14	0.421	33.22	0.69	0.206	35.8	2265.99	636.7	3772.4	517.49	4708.8	502.69	3794.1	1276.30	51.9	39.9	4708.8	502.7
DV_7-5-15_F1_235	0.710	7.95	30.376	11.16	0.310	7.86	0.70	0.174	10.0	1739.74	119.9	3499.1	110.09	4751.9	114.55	3244.0	300.45	63.4	50.3	4751.9	114.5
DV_7-5-15_F1_122	0.711	8.14	39.429	12.77	0.402	9.85	0.77	0.191	9.2	2178.09	182.1	3756.5	127.13	4752.8	117.28	3533.2	301.61	54.2	42.0	4752.8	117.3
DV_7-5-15_F1_51	0.753	7.61	23.467	11.17	0.226	8.19	0.73	0.076	11.1	1312.33	97.3	3246.5	109.20	4835.3	109.31	1483.5	159.39	72.9	59.6	4835.3	109.3
DV_7-5-15_F1_12	0.876	65.83	936106.108	111.69	7745.939	90.23	0.81	1958.438	68.6	57727.98	9564.2	13961.0	65535.00	5050.0	939.44	153217.0	23393.45	-1043.1	-313.5	5050.0	939.4

DV 7/7/15_2	38.699	73.44																			
	Isotope ratios											Apparent Ages (Ma)									
	$^{207}Pb/^{206}Pb$	± (2%SD)	$^{207}Pb/^{235}U$	± (2%SD)	$^{206}Pb/^{238}U$	± (2%SD)	error corr.	$^{206}Pb/^{238}Th$	± (2SD)	$^{206}Pb/^{238}U$	± (2SD)	$^{207}Pb/^{235}U$	± (2SD)	$^{207}Pb/^{206}Pb$	± (2SD)	$^{208}Pb/^{232}Th$	± (2SD)	% discordance Pb^{206}/U^{238}-Pb^{207}/Pb^{206}	% discordance Pb^{206}/U^{238}-Pb^{207}/U^{325}	Best Age	± (2SD)
DV 7/7/15_2-23	0.054	4.92	0.209	6.79	0.028	4.75	0.689	0.009	8.66	175.98	8.25	192.96	11.93	352.25	111.22	172.80	14.91	50.04073164	8.80	175.98	8.25
DV 7/7/15_2-128	0.053	5.82	0.231	7.72	0.032	5.16	0.657	0.008	8.71	200.26	10.18	211.43	14.74	322.92	132.27	155.75	13.52	37.98515875	5.28	200.26	10.18
DV 7/7/15_2-116	0.043	9.89	0.190	13.68	0.032	9.50	0.691	0.007	13.00	203.75	19.04	176.66	22.18	0.00	238.41	143.20	18.56	-10146709.4	-15.33	203.75	19.04
DV 7/7/15_2-8	0.044	5.75	0.207	7.55	0.033	4.98	0.648	0.008	8.29	206.70	10.14	190.67	13.12	0.00	138.59	162.35	13.41	-10293734.1	-8.41	206.70	10.14
DV 7/7/15_2-125	0.043	7.30	0.195	9.24	0.033	5.75	0.613	0.007	9.38	207.35	11.73	181.09	15.32	0.00	175.88	142.50	13.33	-10326112	-14.50	207.35	11.73
DV 7/7/15_2-132	0.044	7.33	0.200	9.45	0.033	6.04	0.631	0.007	10.08	209.09	12.42	184.95	15.98	0.00	176.64	147.01	14.76	-10413002.7	-13.05	209.09	12.42
DV 7/7/15_2-16	0.046	6.52	0.220	8.74	0.033	5.90	0.667	0.009	10.64	211.05	12.25	201.62	15.99	22.57	156.37	181.64	19.24	-835.13285	-4.68	211.05	12.25
DV 7/7/15_2-131	0.043	7.20	0.197	9.84	0.033	6.77	0.682	0.007	9.91	211.09	14.06	182.17	16.40	0.00	173.51	140.72	13.90	-10512533	-15.88	211.09	14.06
DV 7/7/15_2-118	0.045	6.74	0.208	9.28	0.034	6.46	0.688	0.007	10.40	212.46	13.50	191.59	16.21	0.00	162.38	149.31	15.48	-10580583.2	-10.90	212.46	13.50
DV 7/7/15_2-50	0.055	9.21	0.257	12.91	0.034	9.07	0.701	0.011	15.08	214.31	19.12	232.40	26.83	410.20	205.90	222.43	33.38	47.75593365	7.79	214.31	19.12
DV 7/7/15_2-105	0.044	6.67	0.205	9.00	0.034	6.12	0.672	0.008	8.87	214.80	12.93	188.94	15.51	0.00	160.70	154.49	13.66	-10697158.6	-13.69	214.80	12.93
DV 7/7/15_2-114	0.043	6.68	0.201	8.54	0.034	5.39	0.622	0.007	9.56	215.40	11.43	185.99	14.51	0.00	161.11	149.17	14.21	-10727211	-15.82	215.40	11.43
DV 7/7/15_2-152	0.042	6.30	0.200	8.73	0.034	6.11	0.693	0.007	9.61	215.49	12.95	185.19	14.78	0.00	151.81	143.47	13.74	-10731712.3	-16.36	215.49	12.95
DV 7/7/15_2-185	0.041	10.74	0.195	13.02	0.034	7.39	0.565	0.007	11.11	215.92	15.69	180.64	21.55	0.00	258.91	138.34	15.32	-10752954.1	-19.53	215.92	15.69
DV 7/7/15_2-51	0.054	6.73	0.253	8.52	0.034	5.26	0.613	0.011	9.20	216.96	11.22	229.33	17.50	352.05	152.13	219.23	20.07	38.37245332	5.39	216.96	11.22
DV 7/7/15_2-104	0.047	5.42	0.223	7.06	0.034	4.63	0.641	0.008	9.18	217.23	9.88	204.70	13.10	50.26	129.50	160.72	14.71	-332.195529	-6.12	217.23	9.88
DV 7/7/15_2-150	0.041	7.28	0.195	10.30	0.034	7.34	0.707	0.007	11.61	217.43	15.69	180.71	17.05	0.00	175.59	146.93	17.01	-10828003.8	-20.32	217.43	15.69
DV 7/7/15_2-96	0.055	6.06	0.260	8.07	0.034	5.40	0.660	0.010	8.99	217.58	11.55	234.50	16.89	406.07	135.61	192.12	17.20	46.41780084	7.22	217.58	11.55
DV 7/7/15_2-98	0.048	6.41	0.226	9.32	0.034	6.83	0.726	0.009	9.67	217.71	14.61	207.28	17.48	88.14	151.96	175.24	16.87	-147.004183	-5.03	217.71	14.61
DV 7/7/15_2-79	0.048	7.90	0.226	10.30	0.034	6.66	0.642	0.010	10.58	218.22	14.30	207.17	19.30	87.01	187.28	194.33	20.47	-150.787819	-5.33	218.22	14.30
DV 7/7/15_2-111	0.062	6.09	0.294	8.29	0.034	5.70	0.678	0.009	9.94	218.23	12.24	261.91	19.13	661.09	130.47	186.12	18.42	66.98975627	16.68	218.23	12.24

DV 7/7/15_2-143	0.044	13.88	0.209	15.35	0.034	6.63	0.428	0.009	11.93	218.28	14.23	192.64	26.94	0.00	334.50	177.85	21.14	-10870493.8	-13.31	218.28	14.23
DV 7/7/15_2-70	0.054	7.36	0.257	11.57	0.034	8.96	0.771	0.009	10.35	218.36	19.23	232.59	24.05	385.65	165.35	179.37	18.49	43.37855882	6.12	218.36	19.23
DV 7/7/15_2-184	0.045	7.70	0.217	10.71	0.035	7.47	0.695	0.007	10.98	219.08	16.09	199.73	19.41	0.00	185.49	146.74	16.06	-10910313.8	-9.69	219.08	16.09
DV 7/7/15_2-200	0.039	6.40	0.186	8.95	0.035	6.26	0.699	0.007	9.46	219.61	13.51	172.87	14.22	0.00	154.32	131.59	12.42	-10936631	-27.04	219.61	13.51
DV 7/7/15_2-198	0.048	8.20	0.231	11.04	0.035	7.39	0.669	0.008	10.87	219.93	15.98	211.04	21.03	102.97	193.90	161.67	17.51	-113.580245	-4.21	219.93	15.98
DV 7/7/15_2-124	0.042	7.39	0.203	9.67	0.035	6.32	0.646	0.008	10.03	220.00	13.67	187.98	16.60	0.00	178.02	155.23	15.52	-10956151.5	-17.04	220.00	13.67
DV 7/7/15_2-87	0.046	7.00	0.218	8.73	0.035	5.29	0.598	0.009	9.72	220.39	11.46	200.38	15.88	0.00	168.83	178.72	17.31	-10975452.6	-9.98	220.39	11.46
DV 7/7/15_2-100	0.045	8.11	0.219	10.10	0.035	6.08	0.596	0.009	9.44	220.80	13.21	200.83	18.41	0.00	195.58	187.99	17.68	-10995809.1	-9.94	220.80	13.21
DV 7/7/15_2-95	0.045	6.50	0.217	8.60	0.035	5.70	0.655	0.009	8.71	221.73	12.43	199.26	15.56	0.00	156.68	183.06	15.88	-11042293.2	-11.28	221.73	12.43
DV 7/7/15_2-170	0.039	9.32	0.190	11.82	0.035	7.31	0.615	0.007	11.47	221.79	15.94	176.72	19.18	0.00	224.60	141.55	16.18	-11045459.5	-25.51	221.79	15.94
DV 7/7/15_2-167	0.041	6.50	0.202	8.57	0.035	5.64	0.652	0.007	9.35	223.62	12.40	186.62	14.62	0.00	156.70	144.66	13.49	-11136384.6	-19.83	223.62	12.40
DV 7/7/15_2-81	0.048	8.60	0.235	12.64	0.035	9.31	0.733	0.009	9.65	224.25	20.51	214.03	24.41	105.66	203.30	181.90	17.48	-112.243067	-4.78	224.25	20.51
DV 7/7/15_2-74	0.047	7.55	0.232	9.99	0.036	6.61	0.656	0.009	10.40	225.77	14.66	211.77	19.11	64.33	179.67	190.56	19.73	-250.934815	-6.61	225.77	14.66
DV 7/7/15_2-73	0.047	7.94	0.230	10.06	0.036	6.22	0.614	0.009	10.23	226.01	13.82	210.32	19.11	43.82	189.83	185.56	18.91	-415.821185	-7.46	226.01	13.82
DV 7/7/15_2-69	0.048	7.57	0.235	9.96	0.036	6.52	0.650	0.010	10.08	226.02	14.49	214.17	19.23	93.07	179.25	196.60	19.72	-142.847942	-5.54	226.02	14.49
DV 7/7/15_2-25	0.054	15.90	0.287	17.04	0.037	6.19	0.360	0.011	12.90	236.81	14.39	256.54	38.66	389.92	356.95	220.34	28.30	39.26838926	7.69	236.81	14.39
DV 7/7/15_2-182	0.042	5.86	0.223	8.20	0.038	5.76	0.699	0.008	9.07	239.09	13.53	204.01	15.15	0.00	141.28	154.01	13.92	-11906965.8	-17.20	239.09	13.53
DV 7/7/15_2-43	0.051	8.89	0.267	10.97	0.038	6.47	0.586	0.012	12.27	240.72	15.29	240.53	23.51	218.62	205.80	239.06	29.17	-10.1125777	-0.08	240.72	15.29
DV 7/7/15_2-49	0.051	5.34	0.275	7.50	0.039	5.31	0.703	0.013	10.01	243.75	12.70	246.49	16.42	260.96	122.59	259.94	25.87	6.592732232	1.11	243.75	12.70
DV 7/7/15_2-21	0.049	13.60	0.272	15.93	0.039	8.35	0.521	0.010	11.09	246.02	20.15	244.13	34.58	166.60	317.69	203.75	22.49	-47.6710291	-0.78	246.02	20.15
DV 7/7/15_2-129	0.052	7.54	0.283	10.81	0.039	7.80	0.716	0.006	13.31	246.44	18.85	252.79	24.19	297.21	172.12	120.63	16.02	17.0830146	2.51	246.44	18.85
DV 7/7/15_2-76	0.056	9.59	0.304	12.74	0.040	8.43	0.658	0.011	11.65	250.79	20.73	269.22	30.13	437.42	213.37	222.76	25.82	42.6664461	6.85	250.79	20.73
DV 7/7/15_2-183	0.045	8.79	0.245	11.63	0.040	7.65	0.655	0.009	9.39	250.81	18.81	222.76	23.27	0.00	211.78	172.47	16.13	-12490203.1	-12.59	250.81	18.81
DV 7/7/15_2-120	0.045	13.16	0.249	14.28	0.040	5.62	0.388	0.009	10.57	251.92	13.90	225.61	28.90	0.00	317.30	175.09	18.43	-12545945.9	-11.66	251.92	13.90

DV 7/7/15_2-168	0.040	7.18	0.222	9.13	0.040	5.69	0.618	0.008	9.15	252.62	14.09	203.48	16.84	0.00	173.09	163.43	14.89	-12580590.2	-24.15	252.62	14.09
DV 7/7/15_2-45	0.051	17.21	0.284	18.07	0.040	5.56	0.305	0.011	14.87	253.91	13.85	253.95	40.63	236.68	396.98	224.21	33.19	-7.28284933	0.02	253.91	13.85
DV 7/7/15_2-92	0.054	7.50	0.301	9.82	0.040	6.40	0.645	0.014	13.39	255.22	16.01	267.17	23.07	372.51	168.89	282.31	37.57	31.48710331	4.47	255.22	16.01
DV 7/7/15_2-177	0.040	9.94	0.222	13.27	0.040	8.82	0.663	0.008	11.19	255.51	22.11	203.62	24.49	0.00	239.58	164.13	18.29	-12724298.5	-25.48	255.51	22.11
DV 7/7/15_2-175	0.040	7.83	0.222	9.97	0.040	6.22	0.620	0.008	9.33	255.83	15.61	203.64	18.40	0.00	188.62	168.09	15.62	-12740656	-25.63	255.83	15.61
DV 7/7/15_2-18	0.047	6.13	0.280	8.48	0.042	5.94	0.692	0.011	9.25	264.39	15.39	250.88	18.86	59.37	146.03	218.73	20.13	-345.318072	-5.38	264.39	15.39
DV 7/7/15_2-3	0.046	18.26	0.279	19.58	0.042	7.12	0.360	0.010	20.41	266.56	18.58	249.63	43.35	2.44	440.05	205.12	41.70	-10834.4474	-6.79	266.56	18.58
DV 7/7/15_2-130	0.043	6.76	0.252	8.94	0.042	5.93	0.655	0.009	8.47	267.13	15.52	227.88	18.25	0.00	162.83	179.38	15.13	-13303295.9	-17.23	267.13	15.52
DV 7/7/15_2-68	0.045	10.45	0.264	12.92	0.043	7.64	0.588	0.011	11.61	268.32	20.09	237.76	27.39	0.00	251.78	228.20	26.37	-13362299.1	-12.85	268.32	20.09
DV 7/7/15_2-88	0.048	14.21	0.284	15.75	0.043	6.84	0.431	0.011	13.01	272.73	18.26	254.00	35.40	85.11	337.11	225.71	29.22	-220.452948	-7.37	272.73	18.26
DV 7/7/15_2-144	0.043	7.00	0.265	9.99	0.044	7.19	0.714	0.009	11.55	280.22	19.72	238.62	21.25	0.00	168.70	188.47	21.68	-13955300.1	-17.44	280.22	19.72
DV 7/7/15_2-171	0.042	8.82	0.264	11.31	0.045	7.11	0.625	0.009	9.93	284.58	19.78	238.20	24.01	0.00	212.71	178.38	17.64	-14172131.6	-19.47	284.58	19.78
DV 7/7/15_2-109	0.048	9.90	0.303	11.40	0.045	5.73	0.496	0.011	9.39	284.83	15.98	268.44	26.90	114.61	233.58	213.75	19.98	-148.515578	-6.10	284.83	15.98
DV 7/7/15_2-85	0.049	8.66	0.305	11.25	0.045	7.23	0.638	0.012	9.99	286.20	20.24	270.53	26.71	138.36	203.33	240.77	23.92	-106.851566	-5.79	286.20	20.24
DV 7/7/15_2-97	0.048	8.69	0.298	10.74	0.045	6.37	0.588	0.011	9.83	286.67	17.86	265.19	25.06	77.54	206.40	226.38	22.15	-269.705688	-8.10	286.67	17.86
DV 7/7/15_2-179	0.040	7.29	0.255	9.36	0.046	5.91	0.628	0.009	9.49	287.88	16.65	230.25	19.29	0.00	175.71	179.71	16.98	-14336374.6	-25.03	287.88	16.65
DV 7/7/15_2-9	0.044	8.90	0.291	11.40	0.046	7.19	0.625	0.011	12.98	292.32	20.56	259.50	26.12	0.00	214.53	226.08	29.20	-14557803.1	-12.65	292.32	20.56
DV 7/7/15_2-60	0.053	5.87	0.345	7.52	0.047	4.73	0.626	0.015	8.79	296.27	13.70	300.75	19.58	341.96	132.80	304.71	26.59	13.36109752	1.49	296.27	13.70
DV 7/7/15_2-7	0.050	9.44	0.338	11.43	0.047	6.52	0.564	0.011	11.15	298.32	19.00	295.95	29.35	194.73	219.40	224.77	24.93	-53.1981032	-0.80	298.32	19.00
DV 7/7/15_2-140	0.044	11.51	0.295	13.56	0.048	7.23	0.529	0.010	11.27	302.93	21.40	262.49	31.38	0.00	277.45	204.76	22.97	-15085861	-15.40	302.93	21.40
DV 7/7/15_2-107	0.045	7.18	0.303	8.82	0.049	5.21	0.580	0.011	9.36	308.41	15.68	268.44	20.80	0.00	173.12	226.90	21.13	-15359046	-14.89	308.41	15.68
DV 7/7/15_2-181	0.040	15.38	0.275	16.63	0.050	6.35	0.380	0.011	15.54	312.67	19.38	246.98	36.48	0.00	370.83	219.91	34.03	-15571244	-26.60	312.67	19.38
DV 7/7/15_2-137	0.046	8.98	0.320	11.09	0.050	6.57	0.586	0.011	10.10	314.41	20.16	281.60	27.28	0.97	216.50	223.96	22.50	-32269.153	-11.65	314.41	20.16
DV 7/7/15_2-53	0.072	6.30	0.506	8.92	0.051	6.35	0.708	0.011	9.44	321.38	19.90	415.92	30.46	977.59	128.40	220.23	20.69	67.12515593	22.73	321.38	19.90

DV 7/7/15_2-108	0.062	9.53	0.442	10.75	0.052	5.06	0.462	0.014	9.58	324.08	16.00	371.85	33.48	669.55	203.95	274.96	26.17	51.59723595	12.85	324.08	16.00
DV 7/7/15_2-123	0.053	11.72	0.405	14.06	0.055	7.83	0.553	0.009	12.63	343.28	26.18	345.46	41.20	345.70	265.14	183.98	23.14	0.699558213	0.63	343.28	26.18
DV 7/7/15_2-30	0.051	6.68	0.441	8.76	0.061	5.74	0.648	0.017	8.98	383.93	21.38	371.01	27.24	246.67	153.69	341.56	30.42	-55.6485038	-3.48	383.93	21.38
DV 7/7/15_2-40	0.059	10.39	0.530	11.62	0.064	5.26	0.448	0.019	10.44	399.34	20.35	431.52	40.87	581.21	225.62	374.42	38.77	31.29048048	7.46	399.34	20.35
DV 7/7/15_2-27	0.051	4.72	0.473	6.53	0.066	4.59	0.691	0.018	8.13	410.58	18.24	393.33	21.29	243.19	108.80	355.34	28.64	-68.834635	-4.39	410.58	18.24
DV 7/7/15_2-13	0.055	5.52	0.517	7.94	0.066	5.78	0.719	0.021	9.27	411.49	23.05	423.30	27.50	419.17	123.33	420.77	38.63	1.83253103	2.79	411.49	23.05
DV 7/7/15_2-11	0.048	5.00	0.456	6.99	0.066	4.97	0.699	0.017	8.79	412.59	19.87	381.42	22.23	120.94	117.90	336.80	29.38	-241.143821	-8.17	412.59	19.87
DV 7/7/15_2-24	0.058	17.07	0.543	18.62	0.067	7.49	0.400	-80.374	1407.08	416.30	30.21	440.42	66.62	517.38	374.66	0.00	0.00	19.53710159	5.48	416.30	30.21
DV 7/7/15_2-26	0.052	6.41	0.494	9.81	0.067	7.47	0.757	0.018	10.60	416.35	30.11	407.46	32.92	306.80	146.01	353.70	37.21	-35.7058721	-2.18	416.35	30.11
DV 7/7/15_2-119	0.047	7.24	0.441	9.81	0.068	6.69	0.675	0.013	11.87	423.07	27.41	371.06	30.50	43.13	172.99	265.39	31.32	-880.866372	-14.02	423.07	27.41
DV 7/7/15_2-165	0.043	6.96	0.417	9.36	0.069	6.30	0.668	0.014	9.77	432.83	26.39	353.99	27.99	0.00	167.86	271.60	26.38	-21555208	-22.27	432.83	26.39
DV 7/7/15_2-57	0.056	4.97	0.549	6.79	0.071	4.66	0.682	0.022	8.99	441.15	19.87	444.46	24.45	462.32	110.13	446.49	39.75	4.579507589	0.75	441.15	19.87
DV 7/7/15_2-32	0.052	5.51	0.521	7.46	0.071	5.09	0.674	0.019	8.47	441.39	21.71	425.55	25.92	301.81	125.53	384.36	32.28	-46.2487865	-3.72	441.39	21.71
DV 7/7/15_2-17	0.050	11.94	0.507	13.01	0.071	5.25	0.397	0.020	11.71	442.62	22.45	416.68	44.50	208.98	276.83	392.35	45.56	-111.805782	-6.23	442.62	22.45
DV 7/7/15_2-122	0.049	6.96	0.484	8.60	0.072	5.14	0.587	0.017	9.62	446.25	22.14	400.84	28.49	131.86	163.73	330.93	31.60	-238.430814	-11.33	446.25	22.14
DV 7/7/15_2-196	0.045	7.89	0.446	9.92	0.072	6.02	0.606	0.014	10.62	448.90	26.12	374.82	31.11	0.00	190.28	283.07	29.87	-22355359.7	-19.76	448.90	26.12
DV 7/7/15_2-66	0.053	9.15	0.523	11.58	0.072	7.15	0.614	0.020	15.02	449.57	31.05	427.37	40.43	317.22	207.91	408.86	60.88	-41.7204706	-5.19	449.57	31.05
DV 7/7/15_2-71	0.054	10.36	0.540	14.76	0.073	10.56	0.713	0.020	15.44	455.76	46.45	438.18	52.59	352.83	233.95	398.66	61.05	-29.1732378	-4.01	455.76	46.45
DV 7/7/15_2-91	0.050	9.64	0.501	11.15	0.073	5.67	0.502	0.019	8.96	456.09	24.97	412.22	37.80	172.81	225.02	376.71	33.46	-163.924729	-10.64	456.09	24.97
DV 7/7/15_2-22	0.055	12.85	0.566	17.51	0.073	11.93	0.680	0.014	13.38	456.31	52.56	455.23	64.32	395.21	288.02	285.88	38.03	-15.459253	-0.24	456.31	52.56
DV 7/7/15_2-110	0.047	10.51	0.488	14.36	0.074	9.83	0.681	0.018	15.67	461.36	43.78	403.38	47.85	70.03	250.06	351.75	54.72	-558.786564	-14.37	461.36	43.78
DV 7/7/15_2-75	0.057	7.23	0.590	9.10	0.076	5.59	0.607	0.020	10.91	470.62	25.35	470.84	34.29	476.83	159.76	402.55	43.54	1.302254921	0.05	470.62	25.35
DV 7/7/15_2-82	0.052	12.05	0.545	13.31	0.076	5.72	0.425	0.020	9.86	470.85	25.96	441.75	47.72	295.13	275.06	406.79	39.76	-59.5404049	-6.59	470.85	25.96
DV 7/7/15_2-37	0.054	5.08	0.575	6.75	0.076	4.50	0.658	0.022	9.15	471.94	20.48	461.18	25.01	376.46	114.34	448.77	40.64	-25.3620029	-2.33	471.94	20.48
DV 7/7/15_2-121	0.048	10.12	0.503	11.58	0.076	5.71	0.486	0.017	13.18	474.04	26.10	414.05	39.41	77.04	240.52	345.62	45.20	-515.277173	-14.49	474.04	26.10

DV 7/7/15_2-159	0.047	6.11	0.522	8.27	0.079	5.64	0.674	0.016	9.25	492.39	26.74	426.34	28.81	67.11	145.39	325.52	29.90	-633.679228	-15.49	492.39	26.74
DV 7/7/15_2-166	0.045	7.93	0.501	10.77	0.080	7.33	0.677	0.016	9.64	496.55	35.04	412.47	36.54	0.00	191.19	313.40	30.02	-24728305	-20.38	496.55	35.04
DV 7/7/15_2-197	0.043	8.62	0.485	11.33	0.081	7.36	0.649	0.016	10.71	500.07	35.43	401.66	37.60	0.00	207.71	321.19	34.14	-24903891.5	-24.50	500.07	35.43
DV 7/7/15_2-93	0.049	10.01	0.562	11.59	0.082	5.90	0.504	0.019	39.99	510.37	28.97	452.83	42.37	169.24	233.84	388.46	154.45	-201.570197	-12.71	510.37	28.97
DV 7/7/15_2-48	0.058	5.60	0.672	7.35	0.083	4.81	0.648	0.025	8.98	515.35	23.81	521.99	30.00	537.78	122.42	500.71	44.46	4.170742168	1.27	515.35	23.81
DV 7/7/15_2-86	0.056	10.36	0.656	12.72	0.085	7.42	0.580	0.022	11.12	525.90	37.48	511.91	51.18	451.02	230.11	433.09	47.71	-16.6020113	-2.73	525.90	37.48
DV 7/7/15_2-28	0.054	5.59	0.658	7.19	0.087	4.59	0.628	0.022	14.94	535.54	23.60	513.64	28.98	371.53	125.91	432.55	64.05	-44.1440349	-4.26	535.54	23.60
DV 7/7/15_2-176	0.047	5.98	0.612	8.08	0.094	5.49	0.673	0.018	11.31	580.52	30.47	484.93	31.18	40.70	142.96	358.49	40.21	-1326.38005	-19.71	580.52	30.47
DV 7/7/15_2-54	0.062	6.47	0.926	8.84	0.108	6.05	0.682	0.034	9.81	662.77	38.13	665.68	43.21	673.03	138.42	672.97	65.02	1.525032857	0.44	662.77	38.13
DV 7/7/15_2-55	0.062	5.38	0.980	7.82	0.114	5.70	0.726	0.038	8.88	696.41	37.63	693.73	39.33	683.57	114.90	749.13	65.40	-1.87949475	-0.39	696.41	37.63
DV 7/7/15_2-42	0.062	5.61	1.057	7.53	0.123	5.08	0.668	0.036	8.29	747.14	35.82	732.19	39.33	667.04	120.10	707.61	57.71	-12.0080391	-2.04	747.14	35.82
DV 7/7/15_2-41	0.064	8.89	1.105	11.65	0.124	7.56	0.646	0.035	10.23	755.58	53.91	755.71	62.15	734.13	188.15	700.38	70.53	-2.92237918	0.02	755.58	53.91
DV 7/7/15_2-35	0.067	8.20	1.224	10.21	0.131	6.14	0.597	0.038	8.89	794.23	45.90	811.68	57.15	828.49	171.00	746.93	65.32	4.135245789	2.15	794.23	45.90
DV 7/7/15_2-59	0.073	5.42	1.464	7.50	0.145	5.20	0.691	0.032	9.77	872.46	42.45	915.77	45.27	1024.51	109.75	630.02	60.69	14.84119342	4.73	872.46	42.45
DV 7/7/15_2-44	0.071	6.86	1.478	9.00	0.150	5.86	0.647	0.046	9.32	903.27	49.36	921.23	54.52	947.79	140.50	901.71	82.32	4.696699603	1.95	903.27	49.36
DV 7/7/15_2-34	0.070	9.05	1.532	11.26	0.157	6.75	0.595	0.043	12.45	938.40	58.91	943.17	69.30	921.48	186.13	859.35	104.98	-1.83585001	0.51	938.40	58.91
DV 7/7/15_2-56	0.071	6.91	1.608	9.97	0.164	7.20	0.721	0.051	9.44	981.61	65.61	973.50	62.49	954.86	141.30	996.66	92.05	-2.8022962	-0.83	981.61	65.61
DV 7/7/15_2-62	0.077	7.38	1.844	10.52	0.175	7.50	0.712	0.044	9.32	1042.34	72.19	1061.42	69.34	1110.33	147.46	868.88	79.39	6.123443577	1.80	1042.34	72.19
DV 7/7/15_2-33	0.074	6.45	1.831	8.68	0.176	5.86	0.669	0.052	10.71	1046.71	56.63	1056.64	57.07	1043.90	130.20	1023.10	107.08	-0.26919467	0.94	1046.71	56.63
DV 7/7/15_2-63	0.077	7.18	1.908	10.82	0.183	8.09	0.748	0.062	11.53	1083.29	80.67	1083.80	72.17	1113.29	143.27	1221.89	137.12	2.694728387	0.05	1083.29	80.67
DV 7/7/15_2-90	0.071	6.08	1.814	8.78	0.184	6.39	0.721	0.036	8.77	1088.85	64.06	1050.35	57.52	971.19	124.04	723.26	62.40	-12.1151916	-3.67	1088.85	64.06
DV 7/7/15_2-64	0.076	7.22	2.159	10.37	0.206	7.48	0.718	0.052	9.07	1205.14	82.24	1167.83	72.08	1106.64	144.36	1021.58	90.58	-8.9001231	-3.19	1106.64	144.36
DV 7/7/15_2-52	0.082	7.78	2.263	11.12	0.201	7.96	0.714	0.060	11.34	1179.69	85.82	1200.93	78.44	1235.07	152.59	1171.91	129.53	4.483873137	1.77	1179.69	85.82
DV 7/7/15_2-58	0.079	4.87	2.198	7.01	0.202	5.08	0.720	0.061	8.60	1186.40	55.04	1180.47	48.99	1171.21	96.33	1206.17	100.93	-1.296852	-0.50	1186.40	55.04
DV 7/7/15_2-72	0.082	6.49	2.718	9.54	0.241	7.03	0.733	0.060	8.69	1389.69	87.94	1333.41	70.90	1249.12	127.04	1172.25	99.26	-11.2543241	-4.22	1249.12	127.04

DV 7/7/15_2-29	0.088	4.57	3.423	6.31	0.276	4.43	0.689	0.066	8.46	1571.99	61.79	1509.61	49.64	1385.06	87.82	1295.73	106.44	-13.4962414	-4.13	1385.06	87.82
DV 7/7/15_2-89	0.090	9.91	3.440	14.04	0.276	9.98	0.708	0.068	14.31	1572.66	139.26	1513.56	110.87	1432.05	189.14	1339.00	186.30	-9.81813577	-3.90	1432.05	189.14
DV 7/7/15_2-126	0.094	4.80	3.909	6.81	0.301	4.92	0.709	0.060	8.27	1694.40	73.39	1615.52	55.14	1501.97	90.77	1186.80	95.55	-12.8112794	-4.88	1501.97	90.77
DV 7/7/15_2-6	0.114	5.53	5.908	7.93	0.362	5.77	0.717	0.081	8.86	1992.58	98.89	1962.48	68.98	1865.54	99.76	1579.70	135.02	-6.80971511	-1.53	1865.54	99.76
DV 7/7/15_2-84	0.119	5.38	5.579	7.56	0.340	5.39	0.704	0.075	8.44	1888.79	88.27	1912.86	65.23	1940.29	96.18	1460.53	119.32	2.654236419	1.26	1940.29	96.18
DV 7/7/15_2-133	0.130	6.55	7.714	9.27	0.427	6.63	0.708	0.085	17.09	2290.08	127.86	2198.25	83.54	2101.93	114.97	1648.31	272.30	-8.95140076	-4.18	2101.93	114.97
DV 7/7/15_2-61	0.140	4.88	6.918	6.96	0.361	4.99	0.714	0.121	8.24	1987.84	85.36	2101.02	61.84	2221.17	84.47	2317.03	181.23	10.5048177	5.39	2221.17	84.47
DV 7/7/15_2-31	0.146	4.24	8.556	6.12	0.417	4.49	0.721	0.103	8.14	2247.87	85.19	2291.91	55.73	2301.20	72.90	1981.64	154.21	2.317408655	1.92	2301.20	72.90
DV 7/7/15_2-46	0.150	5.47	8.832	7.56	0.424	5.26	0.690	0.121	9.03	2278.07	101.00	2320.82	69.08	2346.47	93.56	2307.60	197.93	2.915202573	1.84	2346.47	93.56
DV 7/7/15_2-80	0.177	4.77	11.105	7.33	0.455	5.62	0.759	0.055	10.03	2417.88	113.39	2531.99	68.36	2627.14	79.33	1080.43	105.80	7.965613083	4.51	2627.14	79.33
DV 7/7/15_2-77	0.753	7.96	135.469	11.48	1.308	8.31	0.721	0.666	9.67	5391.31	303.81	4991.72	116.17	4834.82	114.28	10319.30	796.92	-11.5099306	-8.00	4834.82	114.28

Rejected data

DV 7/7/15_2-5	0.078	6.00	0.373	7.48	0.033	4.57	0.597	0.013	8.50	211.81	9.52	322.04	20.65	1149.47	119.25	262.49	22.19	81.57356899	34.23	211.81	9.52
DV 7/7/15_2-180	0.051	16.91	0.622	23.62	0.089	16.51	0.698	0.017	17.18	548.03	86.73	491.13	92.23	220.21	391.20	349.04	59.55	-148.863009	-11.59	548.03	86.73
DV 7/7/15_2-194	0.046	8.39	0.653	11.82	0.102	8.34	0.705	0.019	10.44	624.74	49.69	510.20	47.46	13.95	201.65	385.56	39.92	-4378.73313	-22.45	624.74	49.69
DV 7/7/15_2-158	0.355	6.34	5.025	8.82	0.102	6.19	0.696	0.307	9.41	626.51	36.98	1823.60	74.83	3727.17	96.38	5414.77	452.05	83.19066156	65.64	626.51	36.98
DV 7/7/15_2-199	0.045	6.32	0.631	8.36	0.102	5.49	0.655	0.019	9.67	626.54	32.78	496.91	32.88	0.00	152.29	385.32	36.95	-31202056.7	-26.09	626.54	32.78
DV 7/7/15_2-147	0.050	9.32	0.721	10.91	0.104	5.75	0.520	0.023	10.27	638.90	34.96	551.26	46.45	187.80	216.87	457.38	46.51	-240.19791	-15.90	638.90	34.96
DV 7/7/15_2-195	0.123	31.77	1.775	34.28	0.104	12.88	0.376	0.606	57.83	638.94	78.36	1036.48	226.35	2000.56	564.49	9571.55	4973.43	68.06176647	38.35	638.94	78.36
DV 7/7/15_2-2	0.082	32.64	1.236	35.00	0.105	12.69	0.361	5.979	254.55	641.48	77.47	817.25	199.00	1256.49	638.15	39269.08	39269.08	48.94711876	21.51	641.48	77.47
DV 7/7/15_2-141	0.054	24.96	0.781	27.19	0.105	10.82	0.396	0.024	17.76	643.76	66.28	586.23	121.67	353.82	563.84	487.24	85.67	-81.9465569	-9.81	643.76	66.28
DV 7/7/15_2-127	0.054	7.80	0.787	10.28	0.105	6.76	0.652	0.018	9.05	646.21	41.59	589.58	45.99	362.53	175.80	350.95	31.52	-78.250837	-9.61	646.21	41.59
DV 7/7/15_2-112	0.052	6.91	0.785	9.30	0.109	6.30	0.669	0.023	10.63	666.99	39.91	588.26	41.55	281.68	158.13	468.15	49.26	-136.785372	-13.38	666.99	39.91
DV 7/7/15_2-1	0.056	6.22	0.932	8.35	0.115	5.66	0.668	0.028	8.74	704.60	37.80	668.94	40.95	464.48	137.78	559.90	48.31	-51.6974469	-5.33	704.60	37.80
DV 7/7/15_2-78	0.072	26.93	1.165	28.56	0.118	9.55	0.333	45.288	351.01	718.65	64.92	784.48	157.33	980.25	548.60	77511.55	77511.55	26.68672329	8.39	718.65	64.92

DV 7/7/15_2-163	0.053	6.40	0.900	9.40	0.123	6.94	0.733	0.023	10.24	748.30	49.02	651.73	45.26	315.26	145.45	465.47	47.16	-137.360085	-14.82	748.30	49.02
DV 7/7/15_2-20	0.060	9.29	1.052	12.67	0.124	8.66	0.680	0.030	12.12	751.85	61.46	729.96	66.04	604.79	200.92	602.06	72.01	-24.3162755	-3.00	751.85	61.46
DV 7/7/15_2-47	0.061	10.08	1.069	12.94	0.125	8.14	0.627	0.036	12.13	760.66	58.40	738.02	67.99	655.70	216.30	708.80	84.67	-16.0068723	-3.07	760.66	58.40
DV 7/7/15_2-4	0.056	4.93	1.043	7.04	0.129	5.12	0.714	0.032	8.08	782.38	37.70	725.45	36.51	470.96	109.08	629.76	50.18	-66.1242328	-7.85	782.38	37.70
DV 7/7/15_2-14	0.059	6.09	1.100	8.29	0.131	5.70	0.679	0.032	8.97	791.92	42.47	753.39	44.10	574.67	132.35	643.57	56.93	-37.8058662	-5.11	791.92	42.47
DV 7/7/15_2-145	0.055	5.61	1.055	7.84	0.138	5.55	0.699	0.028	9.06	831.00	43.29	731.54	40.89	422.39	125.17	562.17	50.29	-96.7350866	-13.60	831.00	43.29
DV 7/7/15_2-169	0.285	28.27	5.511	33.14	0.139	17.30	0.522	1.480	31.99	840.45	136.32	1902.34	292.63	3391.69	440.63	18356.13	4281.88	75.22033519	55.82	840.45	136.32
DV 7/7/15_2-106	0.056	12.96	1.112	14.34	0.143	6.22	0.429	0.033	19.73	864.26	50.33	758.91	76.81	447.79	287.88	652.51	127.11	-93.00592	-13.88	864.26	50.33
DV 7/7/15_2-190	0.053	5.98	1.085	8.52	0.147	6.10	0.713	0.028	9.01	884.67	50.43	745.90	45.06	337.67	135.36	553.12	49.24	-161.99429	-18.60	884.67	50.43
DV 7/7/15_2-135	0.057	9.26	1.188	13.32	0.151	9.62	0.719	0.032	9.20	906.78	81.38	794.90	73.56	477.96	204.73	634.64	57.57	-89.717739	-14.07	906.78	81.38
DV 7/7/15_2-172	0.538	7.60	11.883	10.12	0.159	6.72	0.660	0.116	10.18	952.49	59.46	2595.22	95.01	4348.62	111.37	2212.29	214.42	78.09667937	63.30	952.49	59.46
DV 7/7/15_2-113	0.060	11.18	1.358	15.71	0.162	11.07	0.702	0.036	18.88	967.57	99.49	870.86	92.11	619.55	241.34	720.78	134.16	-56.1735155	-11.11	967.57	99.49
DV 7/7/15_2-146	0.059	5.44	1.333	7.36	0.163	5.05	0.674	0.033	8.52	971.19	45.50	860.24	42.74	569.17	118.30	665.49	55.84	-70.6329264	-12.90	971.19	45.50
DV 7/7/15_2-94	0.609	8.33	14.245	11.97	0.170	8.65	0.719	0.124	10.07	1009.48	80.79	2766.14	114.04	4529.85	120.90	2365.13	226.06	77.71496753	63.51	1009.48	80.79
DV 7/7/15_2-189	0.507	10.01	12.106	13.37	0.172	8.88	0.663	0.167	11.26	1025.27	84.15	2612.67	126.00	4260.61	147.37	3123.31	328.53	75.93617803	60.76	1025.27	84.15
DV 7/7/15_2-153	0.524	9.27	12.581	12.76	0.173	8.81	0.687	0.137	10.97	1029.04	83.77	2648.84	120.58	4309.08	136.14	2589.32	268.34	76.11913907	61.15	1029.04	83.77
DV 7/7/15_2-162	0.517	9.84	12.558	13.81	0.175	9.72	0.702	0.105	11.20	1038.92	93.30	2647.09	130.59	4291.53	144.68	2017.25	216.26	75.79129825	60.75	1038.92	93.30
DV 7/7/15_2-148	0.074	5.43	2.551	7.51	0.248	5.27	0.691	0.052	20.72	1427.08	67.45	1286.60	54.86	1045.25	109.57	1020.53	207.28	-36.5299092	-10.92	1045.25	109.57
DV 7/7/15_2-134	0.533	8.45	13.584	11.71	0.183	8.16	0.692	0.129	9.52	1085.95	81.53	2721.16	111.19	4336.21	123.96	2448.84	220.67	74.95633075	60.09	1085.95	81.53
DV 7/7/15_2-178	0.521	8.08	13.349	10.75	0.185	7.13	0.660	0.204	10.19	1093.57	71.70	2704.68	101.89	4300.56	118.62	3750.44	351.73	74.57152011	59.57	1093.57	71.70
DV 7/7/15_2-174	0.524	8.96	13.438	12.01	0.185	8.03	0.666	0.108	9.96	1093.70	80.74	2710.92	113.98	4309.84	131.58	2067.84	196.82	74.62327841	59.66	1093.70	80.74
DV 7/7/15_2-117	0.066	4.94	1.729	7.19	0.189	5.31	0.726	0.038	8.29	1117.10	54.45	1019.22	46.29	801.88	103.57	760.63	61.96	-39.310817	-9.60	1117.10	54.45
DV 7/7/15_2-102	0.594	10.91	15.642	14.85	0.190	10.12	0.678	0.155	11.44	1121.02	104.11	2855.21	142.62	4493.99	158.66	2920.51	313.64	75.05506641	60.74	1121.02	104.11
DV 7/7/15_2-67	0.072	11.43	1.878	16.41	0.191	11.80	0.718	0.048	13.11	1124.35	121.78	1073.26	109.14	977.65	232.97	944.15	121.26	-15.0054659	-4.76	1124.35	121.78
DV 7/7/15_2-188	0.503	8.77	13.346	11.83	0.192	7.95	0.671	0.099	10.17	1129.52	82.42	2704.42	112.19	4249.22	129.27	1915.50	186.65	73.41822643	58.23	1129.52	82.42
DV 7/7/15_2-149	0.077	6.84	2.993	9.93	0.279	7.25	0.725	0.052	8.68	1585.18	101.89	1405.93	75.69	1129.99	136.21	1023.28	86.79	-40.2831915	-12.75	1129.99	136.21

DV 7/7/15_2-161	0.587	8.28	15.979	11.36	0.196	7.82	0.684	0.076	9.78	1154.79	82.63	2875.53	108.97	4475.67	120.57	1475.42	139.70	74.1986017	59.84	1154.79	82.63
DV 7/7/15_2-83	0.078	7.69	2.628	12.54	0.243	9.94	0.790	0.065	8.44	1404.62	125.44	1308.54	92.48	1156.19	152.64	1272.31	104.35	-21.4864852	-7.34	1156.19	152.64
DV 7/7/15_2-115	0.580	9.83	16.254	13.44	0.202	9.21	0.682	0.162	11.24	1186.10	99.82	2891.85	129.22	4458.89	143.14	3036.92	319.59	73.39930266	58.98	1186.10	99.82
DV 7/7/15_2-101	0.592	7.88	16.613	10.96	0.203	7.67	0.695	0.143	9.44	1189.57	83.31	2912.74	105.30	4487.29	114.67	2698.94	239.84	73.4903007	59.16	1189.57	83.31
DV 7/7/15_2-139	0.081	8.02	2.908	11.37	0.260	8.11	0.709	0.051	11.48	1487.52	107.70	1383.97	86.09	1214.33	157.79	998.43	112.13	-22.4974069	-7.48	1214.33	157.79
DV 7/7/15_2-103	0.144	6.12	10.253	9.05	0.514	6.74	0.737	0.097	11.61	2675.14	147.55	2457.86	83.93	2273.77	105.42	1864.08	207.79	-17.6519852	-8.84	2273.77	105.42
DV 7/7/15_2-36	0.179	9.93	15.996	13.68	0.639	9.43	0.687	0.375	29.49	3187.03	237.33	2876.56	131.44	2641.73	164.90	6440.98	1695.77	-20.641832	-10.79	2641.73	164.90
DV 7/7/15_2-187	0.464	17.39	19.471	20.98	0.303	11.74	0.559	0.144	19.18	1704.86	175.92	3065.45	205.33	4130.55	258.05	2710.59	492.39	58.72545929	44.38	4130.55	258.05
DV 7/7/15_2-156	0.512	15.22	14.660	21.33	0.206	14.97	0.701	0.255	13.86	1208.92	165.01	2793.45	205.47	4276.03	223.91	4584.22	576.58	71.72799705	56.72	4276.03	223.91
DV 7/7/15_2-186	0.521	10.49	16.752	14.37	0.232	9.83	0.683	0.111	10.30	1344.15	119.26	2920.76	138.50	4302.29	154.11	2134.01	209.70	68.75722067	53.98	4302.29	154.11
DV 7/7/15_2-192	0.529	9.52	18.367	12.71	0.250	8.43	0.662	0.144	10.89	1440.87	108.88	3009.17	123.01	4325.17	139.72	2719.92	279.08	66.68639413	52.12	4325.17	139.72
DV 7/7/15_2-193	0.534	8.70	23.156	11.93	0.313	8.17	0.684	0.162	10.56	1754.98	125.56	3233.54	116.60	4338.66	127.53	3037.03	300.05	59.55017868	45.73	4338.66	127.53
DV 7/7/15_2-164	0.538	9.47	15.363	13.02	0.206	8.97	0.687	0.168	10.95	1205.45	98.68	2838.04	124.76	4349.85	138.73	3136.35	320.63	72.28750826	57.53	4349.85	138.73
DV 7/7/15_2-191	0.553	8.11	21.199	11.09	0.277	7.58	0.682	0.158	10.47	1574.31	105.85	3147.73	107.95	4389.59	118.59	2971.81	291.47	64.13528654	49.99	4389.59	118.59
DV 7/7/15_2-155	0.554	10.11	18.958	13.66	0.247	9.22	0.672	0.154	10.80	1421.42	117.64	3039.70	132.48	4390.59	147.82	2901.26	294.03	67.62583086	53.24	4390.59	147.82
DV 7/7/15_2-151	0.554	8.51	16.054	11.31	0.209	7.50	0.659	0.111	9.96	1221.73	83.53	2880.02	108.52	4392.14	124.35	2133.98	202.74	72.18379555	57.58	4392.14	124.35
DV 7/7/15_2-160	0.566	9.30	20.561	12.47	0.262	8.35	0.666	0.104	10.41	1497.71	111.59	3118.11	121.30	4423.96	135.71	2001.79	199.39	66.14539968	51.97	4423.96	135.71
DV 7/7/15_2-154	0.578	9.91	20.124	13.60	0.251	9.35	0.685	0.164	10.81	1442.80	120.86	3097.33	132.26	4453.36	144.37	3064.26	309.72	67.60206429	53.42	4453.36	144.37
DV 7/7/15_2-138	0.584	8.43	20.033	11.35	0.247	7.66	0.669	0.141	9.86	1424.15	97.85	3092.93	110.22	4467.98	122.79	2658.48	247.25	68.12534315	53.95	4467.98	122.79
DV 7/7/15_2-10	0.593	7.43	17.993	10.61	0.213	7.63	0.714	0.146	9.58	1243.34	86.33	2989.34	102.44	4490.62	108.15	2762.74	248.88	72.31247305	58.41	4490.62	108.15
DV 7/7/15_2-136	0.595	8.48	23.380	11.70	0.283	8.11	0.689	0.146	10.37	1605.84	115.35	3242.88	114.41	4496.82	123.34	2760.96	269.40	64.28950905	50.48	4496.82	123.34
DV 7/7/15_2-142	0.600	105.29	4483.119	128.73	53.854	74.06	0.575	123.393	79.16	25815.77	5947.14	8537.64	65535.00	4507.11	1530.49	97492.67	31088.52	-472.779051	-202.38	4507.11	1530.49
DV 7/7/15_2-173	0.609	8.05	54.791	11.09	0.649	7.66	0.688	0.384	9.90	3223.79	194.47	4083.47	111.01	4528.81	116.85	6574.98	563.50	28.81601892	21.05	4528.81	116.85
DV 7/7/15_2-19	0.636	9.61	19.055	13.58	0.211	9.64	0.707	0.124	11.15	1236.44	108.51	3044.62	131.78	4591.94	139.19	2363.04	250.23	73.07366128	59.39	4591.94	139.19
DV 7/7/15_2-15	0.636	9.62	19.158	13.26	0.212	9.17	0.688	0.139	10.77	1238.76	103.39	3049.81	128.67	4593.56	139.39	2627.74	267.10	73.03271745	59.38	4593.56	139.39
DV 7/7/15_2-157	0.655	161.04	2607.496	196.22	28.691	112.10	0.571	1757.632	391.72	21858.70	65535.00	7987.54	65535.00	4634.29	2329.13	151031.66	151031.66	-371.672907	-173.66	4634.29	2329.13
DV 7/7/15_2-12	0.656	8.68	23.565	11.76	0.253	8.00	0.675	0.126	9.89	1451.65	103.93	3250.55	115.08	4636.43	125.53	2405.65	225.57	68.69044054	55.34	4636.43	125.53
DV 7/7/15_2-99	0.665	9.08	32.535	12.39	0.354	8.48	0.680	0.206	10.28	1955.58	143.05	3566.63	122.69	4657.22	131.27	3793.85	358.74	58.00977829	45.17	4657.22	131.27

DV 7/7/15_2-65	0.666	8.62	34.074	11.60	0.372	7.80	0.669	3.939	10.96	2040.17	136.41	3612.18	114.91	4659.40	124.58	32280.66	1847.85	56.21379262	43.52	4659.40	124.58
DV 7/7/15_2-38	0.694	9.76	27.493	14.00	0.283	10.06	0.717	0.253	11.21	1608.37	143.24	3401.19	138.00	4718.78	140.75	4566.13	463.36	65.91553137	52.71	4718.78	140.75
DV 7/7/15_2-39	0.720	144.08	682.351	176.42	6.787	101.81	0.577	16.071	96.68	13231.32	9086.09	6627.41	65535.00	4770.62	2073.69	57349.44	48715.02	-177.350486	-99.65	4770.62	2073.69

DV 7/7/15_4 38.689 73.44

	Isotope ratios											Apparent Ages (Ma)									
	^{207}Pb	±	^{207}Pb	±	^{206}Pb	±		^{206}Pb	±	^{206}Pb	±	^{207}Pb	±	^{207}Pb	±	^{208}Pb	±	% discordance Pb^{206}/U^{238}-Pb^{207}/Pb^{206}	% discordance Pb^{206}/U^{238}-Pb^{207}/U^{325}		±
	^{206}Pb	(2%SD)	^{235}U	(2%SD)	^{238}U	(2%SD)	error corr.	^{238}Th	(2SD)	^{238}U	(2SD)	^{235}U	(2SD)	^{206}Pb	(2SD)	^{232}Th	(2SD)			Best Age	(2SD)
DV 7/7/15_4-144	0.063	4.72	0.209	7.13	0.024	5.38	0.750	0.008	6.72	153.13	8.14	192.39	12.50	705.53	100.39	158.50	10.61	78.30	20.41	153.13	8.14
DV 7/7/15_4-69	0.063	6.45	0.212	9.79	0.024	7.40	0.753	0.006	7.95	154.95	11.33	195.51	17.42	715.75	136.91	126.85	10.05	78.35	20.75	154.95	11.33
DV 7/7/15_4-146	0.062	5.23	0.219	7.78	0.026	5.79	0.741	0.008	6.90	162.74	9.30	201.36	14.21	680.99	111.62	162.09	11.14	76.10	19.18	162.74	9.30
DV 7/7/15_4-98	0.061	4.36	0.216	6.56	0.026	4.94	0.747	0.009	5.94	164.23	8.01	198.46	11.83	625.52	94.00	186.18	11.01	73.75	17.25	164.23	8.01
DV 7/7/15_4-107	0.057	6.20	0.207	9.16	0.026	6.77	0.736	0.007	7.98	167.71	11.21	190.80	15.93	486.16	136.83	148.43	11.80	65.50	12.10	167.71	11.21
DV 7/7/15_4-24	0.060	7.45	0.247	10.74	0.030	7.76	0.720	0.011	8.48	189.23	14.47	223.99	21.59	605.51	161.13	217.54	18.36	68.75	15.52	189.23	14.47
DV 7/7/15_4-23	0.051	5.54	0.215	8.00	0.030	5.80	0.721	0.010	6.54	192.68	11.00	197.97	14.38	260.12	127.26	204.34	13.29	25.93	2.67	192.68	11.00
DV 7/7/15_4-130	0.054	6.56	0.227	8.98	0.030	6.15	0.682	0.009	13.55	192.94	11.70	207.35	16.84	374.06	147.67	180.72	24.39	48.42	6.95	192.94	11.70
DV 7/7/15_4-22	0.054	5.53	0.228	7.68	0.031	5.36	0.694	0.010	6.68	194.76	10.29	208.58	14.48	366.36	124.64	193.27	12.86	46.84	6.63	194.76	10.29
DV 7/7/15_4-68	0.052	8.09	0.226	12.04	0.031	8.94	0.741	0.010	6.81	197.79	17.41	206.67	22.52	306.32	184.20	207.42	14.06	35.43	4.29	197.79	17.41
DV 7/7/15_4-63	0.051	5.74	0.220	8.64	0.031	6.49	0.748	0.011	8.66	197.98	12.65	202.09	15.84	247.48	132.03	212.20	18.29	20.00	2.03	197.98	12.65
DV 7/7/15_4-104	0.055	4.81	0.236	7.23	0.031	5.43	0.747	0.011	6.80	199.06	10.64	215.21	14.01	394.99	107.81	212.73	14.40	49.60	7.51	199.06	10.64
DV 7/7/15_4-124	0.051	5.71	0.222	8.21	0.031	5.92	0.718	0.011	6.58	199.06	11.61	203.28	15.12	252.11	131.44	213.62	13.98	21.04	2.08	199.06	11.61
DV 7/7/15_4-25	0.052	5.23	0.226	7.81	0.031	5.84	0.743	0.010	6.66	199.12	11.44	206.48	14.60	289.90	119.48	210.75	13.97	31.32	3.57	199.12	11.44
DV 7/7/15_4-119	0.055	4.70	0.240	6.98	0.032	5.20	0.740	0.012	5.66	200.96	10.29	218.10	13.71	406.78	105.13	231.70	13.03	50.60	7.86	200.96	10.29
DV 7/7/15_4-100	0.054	8.26	0.234	12.06	0.032	8.81	0.729	0.011	6.33	200.99	17.44	213.87	23.26	355.92	186.43	221.14	13.93	43.53	6.02	200.99	17.44
DV 7/7/15_4-129	0.051	6.97	0.225	10.35	0.032	7.67	0.739	0.011	10.17	201.42	15.22	205.79	19.28	255.70	160.20	212.71	21.54	21.23	2.12	201.42	15.22
DV 7/7/15_4-142	0.051	7.16	0.223	10.88	0.032	8.21	0.753	0.011	12.45	201.88	16.32	204.25	20.13	231.00	165.32	223.44	27.68	12.61	1.16	201.88	16.32
DV 7/7/15_4-135	0.052	4.72	0.228	6.94	0.032	5.12	0.733	0.010	7.14	201.93	10.18	208.72	13.10	285.67	107.95	209.60	14.88	29.31	3.26	201.93	10.18
DV 7/7/15_4-110	0.054	4.77	0.235	7.01	0.032	5.17	0.732	0.011	9.41	202.08	10.29	214.59	13.56	353.42	107.83	215.10	20.15	42.82	5.83	202.08	10.29
DV 7/7/15_4-72	0.052	5.03	0.228	7.71	0.032	5.87	0.758	0.011	5.14	202.15	11.68	208.76	14.54	281.14	115.10	220.38	11.26	28.10	3.16	202.15	11.68
DV 7/7/15_4-105	0.051	7.92	0.223	11.45	0.032	8.30	0.723	0.012	7.46	202.91	16.57	204.82	21.24	225.97	182.95	234.31	17.39	10.20	0.93	202.91	16.57
DV 7/7/15_4-131	0.051	7.58	0.226	11.29	0.032	8.39	0.741	0.011	8.84	203.08	16.77	207.00	21.14	251.38	174.33	216.24	19.02	19.21	1.89	203.08	16.77
DV 7/7/15_4-106	0.051	5.40	0.227	8.14	0.032	6.12	0.748	0.011	6.57	203.12	12.24	207.34	15.27	254.71	124.18	223.69	14.62	20.25	2.03	203.12	12.24
DV 7/7/15_4-40	0.052	5.91	0.230	8.99	0.032	6.80	0.753	0.010	6.46	204.36	13.68	210.52	17.10	278.09	135.35	201.18	12.93	26.51	2.93	204.36	13.68

DV 7/7/15_4-26	0.053	5.74	0.233	8.18	0.032	5.86	0.712	0.011	6.73	204.40	11.78	212.97	15.72	307.34	130.81	218.20	14.60	33.49	4.02	204.40	11.78
DV 7/7/15_4-58	0.052	4.80	0.231	7.27	0.032	5.49	0.751	0.011	8.75	204.87	11.08	211.06	13.86	278.04	109.88	214.74	18.69	26.32	2.93	204.87	11.08
DV 7/7/15_4-123	0.050	5.48	0.224	7.68	0.032	5.41	0.700	0.011	6.61	205.01	10.91	205.09	14.26	205.63	127.16	212.71	13.98	0.30	0.04	205.01	10.91
DV 7/7/15_4-38	0.051	6.26	0.229	9.32	0.032	6.93	0.741	0.010	6.94	205.22	14.00	209.43	17.64	255.10	143.92	206.89	14.30	19.55	2.01	205.22	14.00
DV 7/7/15_4-36	0.057	5.89	0.255	8.06	0.032	5.54	0.683	0.011	7.62	205.38	11.19	230.62	16.63	494.64	129.76	220.26	16.69	58.48	10.94	205.38	11.19
DV 7/7/15_4-27	0.059	5.73	0.266	8.50	0.032	6.32	0.739	0.013	7.24	205.60	12.78	239.46	18.14	584.74	124.29	254.84	18.34	64.84	14.14	205.60	12.78
DV 7/7/15_4-139	0.051	6.51	0.228	8.81	0.032	5.97	0.675	0.010	7.62	205.76	12.10	208.14	16.59	234.58	150.15	208.06	15.77	12.29	1.14	205.76	12.10
DV 7/7/15_4-117	0.052	6.56	0.234	9.38	0.032	6.73	0.715	0.011	9.99	205.82	13.63	213.50	18.05	298.51	149.58	213.53	21.22	31.05	3.60	205.82	13.63
DV 7/7/15_4-136	0.062	7.55	0.280	10.88	0.032	7.86	0.720	0.012	7.22	206.05	15.94	250.33	24.14	688.36	160.99	243.95	17.50	70.07	17.69	206.05	15.94
DV 7/7/15_4-60	0.051	6.95	0.232	9.62	0.033	6.68	0.691	0.011	8.10	207.17	13.61	211.85	18.39	261.52	159.56	226.35	18.25	20.78	2.21	207.17	13.61
DV 7/7/15_4-51	0.053	6.26	0.240	9.72	0.033	7.45	0.765	0.010	6.70	207.78	15.24	218.35	19.10	331.34	142.07	209.67	13.98	37.29	4.84	207.78	15.24
DV 7/7/15_4-128	0.052	5.20	0.234	7.14	0.033	4.93	0.685	0.011	6.14	207.86	10.09	213.26	13.74	272.89	119.22	216.29	13.21	23.83	2.53	207.86	10.09
DV 7/7/15_4-145	0.052	5.62	0.236	7.98	0.033	5.70	0.710	0.011	6.89	207.98	11.66	215.53	15.51	298.05	128.22	211.42	14.50	30.22	3.50	207.98	11.66
DV 7/7/15_4-28	0.051	6.50	0.229	10.04	0.033	7.68	0.762	0.010	6.15	208.13	15.73	209.31	19.00	221.06	150.36	204.99	12.54	5.85	0.56	208.13	15.73
DV 7/7/15_4-134	0.050	5.12	0.227	7.24	0.033	5.15	0.707	0.011	6.26	208.37	10.57	207.60	13.59	198.36	118.88	212.64	13.24	-5.04	-0.37	208.37	10.57
DV 7/7/15_4-115	0.052	5.11	0.235	7.00	0.033	4.83	0.684	0.011	5.77	208.48	9.91	214.12	13.52	276.06	116.95	218.10	12.52	24.48	2.64	208.48	9.91
DV 7/7/15_4-93	0.050	5.72	0.228	8.35	0.033	6.11	0.729	0.011	6.85	208.64	12.55	208.40	15.73	203.28	132.65	217.10	14.79	-2.63	-0.11	208.64	12.55
DV 7/7/15_4-97	0.053	4.95	0.242	7.26	0.033	5.34	0.731	0.012	5.68	208.72	10.97	220.31	14.38	343.75	111.99	239.88	13.56	39.28	5.26	208.72	10.97
DV 7/7/15_4-109	0.052	7.83	0.237	10.94	0.033	7.66	0.698	0.011	10.99	209.35	15.79	216.13	21.30	289.84	178.88	221.34	24.21	27.77	3.14	209.35	15.79
DV 7/7/15_4-94	0.052	5.74	0.236	7.62	0.033	5.05	0.658	0.011	6.00	209.80	10.42	215.12	14.77	271.39	131.52	221.84	13.24	22.70	2.47	209.80	10.42
DV 7/7/15_4-37	0.051	7.38	0.235	10.12	0.033	6.95	0.684	0.010	7.89	209.87	14.35	214.00	19.53	257.78	169.67	205.39	16.13	18.58	1.93	209.87	14.35
DV 7/7/15_4-7	0.054	6.69	0.246	9.69	0.033	7.03	0.724	0.011	7.70	210.20	14.54	223.05	19.41	359.79	150.96	224.61	17.20	41.58	5.76	210.20	14.54
DV 7/7/15_4-82	0.052	4.69	0.236	7.37	0.033	5.71	0.771	0.011	5.17	210.35	11.81	215.05	14.28	264.13	107.72	215.91	11.11	20.36	2.19	210.35	11.81
DV 7/7/15_4-57	0.051	6.45	0.235	9.19	0.033	6.57	0.713	0.011	7.87	210.67	13.63	214.09	17.74	249.13	148.40	223.09	17.47	15.44	1.60	210.67	13.63
DV 7/7/15_4-84	0.051	5.46	0.236	7.46	0.033	5.11	0.681	0.011	6.11	210.89	10.61	215.03	14.45	257.96	125.39	222.05	13.51	18.25	1.93	210.89	10.61
DV 7/7/15_4-132	0.051	5.19	0.237	7.46	0.033	5.38	0.718	0.011	7.83	211.44	11.20	215.59	14.48	260.63	119.25	223.89	17.45	18.87	1.92	211.44	11.20
DV 7/7/15_4-34	0.055	7.73	0.254	10.83	0.033	7.61	0.700	0.010	9.06	211.70	15.85	229.53	22.26	414.56	172.79	209.75	18.92	48.93	7.77	211.70	15.85
DV 7/7/15_4-33	0.052	5.88	0.240	8.11	0.033	5.62	0.689	0.010	6.38	211.96	11.72	218.53	15.94	288.11	134.27	198.20	12.59	26.43	3.01	211.96	11.72
DV 7/7/15_4-149	0.055	5.16	0.253	6.78	0.033	4.43	0.649	0.010	6.62	212.02	9.25	229.16	13.91	407.98	115.46	197.95	13.05	48.03	7.48	212.02	9.25
DV 7/7/15_4-32	0.051	5.35	0.234	7.95	0.033	5.91	0.740	0.011	11.10	212.08	12.33	213.86	15.33	231.78	123.54	217.94	24.08	8.50	0.83	212.08	12.33

DV 7/7/15_4-121	0.049	5.83	0.228	8.16	0.034	5.74	0.700	0.011	6.27	212.65	12.01	208.58	15.39	162.30	136.28	222.70	13.90	-31.03	-1.95	212.65	12.01
DV 7/7/15_4-78	0.051	5.46	0.238	7.62	0.034	5.35	0.698	0.011	6.03	212.86	11.20	216.75	14.87	256.37	125.45	220.98	13.26	16.97	1.79	212.86	11.20
DV 7/7/15_4-74	0.052	6.13	0.242	8.72	0.034	6.24	0.712	0.011	6.25	213.05	13.07	220.40	17.29	296.88	139.79	229.13	14.24	28.24	3.34	213.05	13.07
DV 7/7/15_4-85	0.050	6.85	0.234	9.54	0.034	6.67	0.696	0.011	6.22	213.07	13.98	213.37	18.37	214.05	158.70	227.24	14.06	0.46	0.14	213.07	13.98
DV 7/7/15_4-150	0.057	6.09	0.264	8.72	0.034	6.27	0.716	0.011	8.63	213.11	13.15	237.96	18.50	490.07	134.23	225.70	19.39	56.51	10.44	213.11	13.15
DV 7/7/15_4-42	0.051	5.67	0.236	8.59	0.034	6.48	0.751	0.010	6.50	213.40	13.59	215.05	16.65	230.73	131.04	208.07	13.46	7.51	0.76	213.40	13.59
DV 7/7/15_4-39	0.052	7.69	0.241	11.37	0.034	8.40	0.737	0.010	8.41	213.57	17.64	219.45	22.45	281.13	175.99	207.46	17.38	24.03	2.68	213.57	17.64
DV 7/7/15_4-99	0.052	5.95	0.242	8.43	0.034	6.01	0.709	0.011	6.45	213.67	12.62	220.44	16.71	291.10	135.79	228.73	14.68	26.60	3.07	213.67	12.62
DV 7/7/15_4-41	0.051	6.35	0.239	9.01	0.034	6.42	0.710	0.010	9.27	213.82	13.50	217.27	17.62	252.50	145.96	207.30	19.13	15.32	1.59	213.82	13.50
DV 7/7/15_4-95	0.052	8.75	0.242	13.27	0.034	10.00	0.752	0.011	8.95	214.10	21.05	219.71	26.23	277.88	200.40	225.79	20.11	22.95	2.55	214.10	21.05
DV 7/7/15_4-87	0.053	7.24	0.248	10.45	0.034	7.55	0.721	0.011	6.27	214.10	15.90	224.58	21.05	333.33	164.15	230.27	14.37	35.77	4.67	214.10	15.90
DV 7/7/15_4-46	0.050	6.55	0.234	9.44	0.034	6.83	0.720	0.011	7.82	214.14	14.38	213.51	18.17	204.11	151.89	217.59	16.92	-4.91	-0.29	214.14	14.38
DV 7/7/15_4-53	0.055	5.70	0.257	7.79	0.034	5.34	0.682	0.011	6.55	214.19	11.25	231.91	16.15	412.99	127.35	230.03	15.00	48.14	7.64	214.19	11.25
DV 7/7/15_4-8	0.053	6.33	0.246	9.01	0.034	6.44	0.712	0.010	6.96	214.31	13.57	222.93	18.05	313.99	143.99	208.12	14.41	31.75	3.87	214.31	13.57
DV 7/7/15_4-17	0.053	7.49	0.245	10.61	0.034	7.54	0.708	0.011	7.75	214.42	15.90	222.76	21.23	310.99	170.46	223.93	17.27	31.05	3.74	214.42	15.90
DV 7/7/15_4-73	0.060	8.27	0.280	10.25	0.034	6.08	0.590	0.012	7.55	214.55	12.83	250.37	22.74	598.28	179.13	246.46	18.50	64.14	14.30	214.55	12.83
DV 7/7/15_4-9	0.050	8.13	0.236	11.47	0.034	8.10	0.705	0.011	7.77	214.74	17.11	214.81	22.20	214.67	188.31	226.64	17.52	-0.03	0.03	214.74	17.11
DV 7/7/15_4-62	0.053	6.75	0.249	9.53	0.034	6.74	0.705	0.012	8.01	214.85	14.25	225.58	19.27	336.18	153.02	245.19	19.54	36.09	4.75	214.85	14.25
DV 7/7/15_4-3	0.053	7.31	0.248	9.81	0.034	6.55	0.667	0.011	7.65	214.94	13.86	225.25	19.83	332.90	165.81	224.70	17.10	35.43	4.58	214.94	13.86
DV 7/7/15_4-79	0.051	7.86	0.237	11.95	0.034	9.01	0.753	0.011	6.07	214.97	19.06	216.09	23.26	225.55	181.76	225.84	13.63	4.69	0.52	214.97	19.06
DV 7/7/15_4-50	0.051	6.12	0.237	8.75	0.034	6.28	0.715	0.010	7.91	214.98	13.28	215.65	17.01	220.44	141.65	209.72	16.51	2.48	0.31	214.98	13.28
DV 7/7/15_4-52	0.053	5.79	0.247	8.02	0.034	5.59	0.693	0.011	6.48	215.15	11.83	223.88	16.12	314.07	131.62	220.78	14.22	31.50	3.90	215.15	11.83
DV 7/7/15_4-31	0.060	6.29	0.283	8.73	0.034	6.09	0.694	0.012	7.39	215.18	12.88	253.31	19.58	621.41	135.72	242.98	17.86	65.37	15.05	215.18	12.88
DV 7/7/15_4-89	0.051	7.30	0.240	10.26	0.034	7.24	0.703	0.011	9.01	215.49	15.33	218.56	20.17	249.16	167.90	223.08	20.00	13.52	1.40	215.49	15.33
DV 7/7/15_4-83	0.051	5.42	0.240	8.14	0.034	6.10	0.746	0.011	7.21	215.53	12.93	218.73	16.01	250.70	124.64	211.13	15.14	14.03	1.47	215.53	12.93
DV 7/7/15_4-14	0.053	7.01	0.250	9.83	0.034	6.92	0.701	0.010	8.88	215.76	14.68	226.38	19.96	337.42	158.87	197.67	17.47	36.05	4.69	215.76	14.68
DV 7/7/15_4-66	0.056	6.68	0.265	9.03	0.034	6.10	0.673	0.012	6.79	215.77	12.95	238.71	19.21	468.17	147.87	244.63	16.52	53.91	9.61	215.77	12.95
DV 7/7/15_4-43	0.070	55.28	0.330	55.57	0.034	5.71	0.102	0.010	5.91	215.94	12.12	289.36	140.81	932.14	1134.49	206.26	12.14	76.83	25.37	215.94	12.12
DV 7/7/15_4-11	0.053	6.39	0.251	8.87	0.034	6.18	0.694	0.010	6.97	216.91	13.18	227.50	18.08	337.70	144.71	208.13	14.43	35.77	4.66	216.91	13.18
DV 7/7/15_4-20	0.052	7.46	0.243	10.53	0.034	7.46	0.706	0.010	9.05	217.00	15.93	221.18	20.94	265.03	171.10	207.37	18.68	18.12	1.89	217.00	15.93

DV 7/7/15_4-21	0.051	5.50	0.241	7.84	0.034	5.63	0.714	0.012	6.26	217.28	12.03	219.21	15.47	238.65	126.72	240.52	14.98	8.96	0.88	217.28	12.03
DV 7/7/15_4-47	0.050	5.41	0.239	7.75	0.034	5.58	0.716	0.011	5.96	217.57	11.93	217.42	15.16	213.22	125.33	211.50	12.53	-2.04	-0.07	217.57	11.93
DV 7/7/15_4-29	0.051	6.35	0.242	8.99	0.034	6.39	0.707	0.010	6.45	217.79	13.67	220.10	17.78	243.29	146.35	210.30	13.50	10.48	1.05	217.79	13.67
DV 7/7/15_4-5	0.052	7.92	0.247	11.04	0.034	7.70	0.696	0.011	7.93	218.10	16.51	224.05	22.19	285.84	181.09	227.36	17.93	23.70	2.66	218.10	16.51
DV 7/7/15_4-92	0.051	6.37	0.244	9.29	0.035	6.79	0.728	0.012	7.62	218.69	14.59	221.98	18.53	254.49	146.55	233.50	17.70	14.06	1.48	218.69	14.59
DV 7/7/15_4-147	0.054	6.10	0.258	7.66	0.035	4.66	0.604	0.013	7.43	219.14	10.04	233.08	15.95	375.19	137.35	252.09	18.63	41.59	5.98	219.14	10.04
DV 7/7/15_4-81	0.050	6.66	0.240	9.89	0.035	7.33	0.739	0.011	8.84	219.34	15.81	218.50	19.44	206.77	154.42	226.41	19.91	-6.08	-0.38	219.34	15.81
DV 7/7/15_4-12	0.052	7.50	0.250	10.13	0.035	6.83	0.672	0.011	8.30	220.73	14.83	226.52	20.56	286.35	171.36	217.63	17.97	22.92	2.56	220.73	14.83
DV 7/7/15_4-45	0.050	5.60	0.243	8.05	0.035	5.81	0.718	0.011	6.61	220.74	12.61	220.66	15.96	217.47	129.66	220.59	14.50	-1.50	-0.03	220.74	12.61
DV 7/7/15_4-15	0.055	6.77	0.266	9.38	0.035	6.52	0.692	0.012	7.88	221.50	14.20	239.27	20.00	416.78	151.19	247.69	19.40	46.85	7.43	221.50	14.20
DV 7/7/15_4-18	0.052	7.95	0.252	11.43	0.035	8.24	0.719	0.011	9.08	221.62	17.95	227.87	23.34	292.03	181.46	220.73	19.94	24.11	2.74	221.62	17.95
DV 7/7/15_4-120	0.054	10.84	0.263	12.24	0.035	5.72	0.465	0.016	12.46	222.64	12.52	237.09	25.90	382.21	243.69	312.38	38.65	41.75	6.09	222.64	12.52
DV 7/7/15_4-2	0.050	6.55	0.245	9.02	0.035	6.21	0.687	0.011	7.84	223.09	13.62	222.33	18.01	212.72	151.72	219.37	17.12	-4.87	-0.34	223.09	13.62
DV 7/7/15_4-1	0.059	6.45	0.295	9.10	0.036	6.43	0.705	0.011	7.31	230.25	14.54	262.74	21.07	561.74	140.55	230.80	16.77	59.01	12.37	230.25	14.54
DV 7/7/15_4-90	0.052	7.32	0.265	11.68	0.037	9.11	0.779	0.012	8.74	233.98	20.94	238.72	24.84	283.03	167.47	242.71	21.09	17.33	1.98	233.98	20.94
DV 7/7/15_4-76	0.052	5.28	0.266	7.70	0.037	5.63	0.727	0.013	8.35	235.11	12.99	239.67	16.43	281.85	120.89	255.59	21.21	16.58	1.90	235.11	12.99
DV 7/7/15_4-56	0.052	9.70	0.280	11.24	0.039	5.72	0.506	0.013	10.27	247.14	13.87	251.00	25.01	284.57	221.77	253.14	25.84	13.15	1.54	247.14	13.87
DV 7/7/15_4-111	0.055	4.56	0.299	6.63	0.039	4.84	0.725	0.014	6.37	247.57	11.76	265.27	15.47	423.96	101.81	286.79	18.14	41.60	6.67	247.57	11.76
DV 7/7/15_4-44	0.058	13.36	0.317	15.90	0.039	8.63	0.542	0.011	6.02	249.59	21.13	279.45	38.85	535.27	292.50	229.66	13.76	53.37	10.69	249.59	21.13
DV 7/7/15_4-30	0.056	8.46	0.307	10.44	0.040	6.16	0.587	0.012	6.81	252.02	15.23	271.95	24.92	445.63	187.91	250.80	16.99	43.45	7.33	252.02	15.23
DV 7/7/15_4-138	0.053	10.05	0.306	13.61	0.041	9.20	0.675	0.014	12.37	261.96	23.62	270.80	32.37	347.27	227.29	276.14	33.95	24.56	3.26	261.96	23.62
DV 7/7/15_4-102	0.053	4.52	0.306	6.75	0.042	5.05	0.743	0.015	8.21	263.81	13.06	271.09	16.07	333.56	102.49	308.75	25.16	20.91	2.69	263.81	13.06
DV 7/7/15_4-71	0.056	7.15	0.323	10.25	0.042	7.36	0.716	0.015	9.12	265.73	19.16	284.31	25.42	437.31	159.24	295.87	26.82	39.24	6.54	265.73	19.16
DV 7/7/15_4-64	0.054	5.13	0.313	8.00	0.042	6.17	0.767	0.014	5.89	266.40	16.09	276.48	19.37	359.90	115.82	279.22	16.34	25.98	3.65	266.40	16.09
DV 7/7/15_4-13	0.065	9.16	0.376	11.15	0.042	6.38	0.570	0.014	8.67	266.71	16.67	324.21	30.95	760.14	193.16	285.36	24.57	64.91	17.73	266.71	16.67
DV 7/7/15_4-55	0.053	5.95	0.325	8.84	0.045	6.56	0.739	0.014	6.13	280.97	18.04	285.70	22.01	321.88	135.21	290.34	17.69	12.71	1.65	280.97	18.04
DV 7/7/15_4-35	0.055	5.32	0.347	8.68	0.046	6.89	0.790	0.018	13.41	287.04	19.34	302.27	22.71	419.79	118.79	366.22	48.71	31.62	5.04	287.04	19.34
DV 7/7/15_4-91	0.054	6.64	0.348	9.23	0.047	6.44	0.695	0.015	6.94	294.37	18.53	303.10	24.19	368.39	149.53	301.32	20.77	20.09	2.88	294.37	18.53
DV 7/7/15_4-101	0.056	4.20	0.362	6.15	0.047	4.54	0.731	0.013	5.26	297.70	13.20	313.62	16.60	432.76	93.50	267.54	14.00	31.21	5.08	297.70	13.20
DV 7/7/15_4-48	0.052	5.15	0.345	7.40	0.048	5.34	0.718	0.014	6.60	300.58	15.68	300.71	19.25	299.20	117.49	290.31	19.03	-0.46	0.04	300.58	15.68

DV 7/7/15_4-10	0.053	7.01	0.350	10.04	0.048	7.21	0.716	0.014	6.92	302.40	21.30	304.82	26.46	322.57	159.26	282.58	19.44	6.25	0.79	302.40	21.30
DV 7/7/15_4-75	0.054	7.45	0.359	11.06	0.048	8.19	0.739	0.016	12.79	304.56	24.38	311.35	29.66	359.73	168.02	319.04	40.54	15.34	2.18	304.56	24.38
DV 7/7/15_4-143	0.055	5.71	0.375	7.37	0.050	4.70	0.633	0.016	6.46	313.12	14.37	323.04	20.41	394.50	128.00	324.65	20.80	20.63	3.07	313.12	14.37
DV 7/7/15_4-67	0.057	7.11	0.394	9.61	0.050	6.49	0.672	0.017	9.42	314.02	19.89	337.16	27.58	497.29	156.75	348.31	32.54	36.85	6.86	314.02	19.89
DV 7/7/15_4-125	0.059	7.49	0.412	11.23	0.050	8.39	0.746	0.015	10.21	316.16	25.90	350.28	33.28	582.71	162.52	297.33	30.17	45.74	9.74	316.16	25.90
DV 7/7/15_4-96	0.058	6.67	0.404	9.38	0.051	6.62	0.703	0.018	7.85	320.41	20.70	344.88	27.43	510.90	146.54	365.98	28.49	37.28	7.09	320.41	20.70
DV 7/7/15_4-113	0.055	9.27	0.449	12.92	0.059	9.02	0.696	0.019	9.57	370.26	32.44	376.52	40.66	414.60	207.14	388.11	36.82	10.69	1.66	370.26	32.44
DV 7/7/15_4-70	0.055	4.95	0.451	7.06	0.060	5.07	0.713	0.020	5.87	374.92	18.47	378.27	22.31	396.02	111.02	391.22	22.77	5.33	0.88	374.92	18.47
DV 7/7/15_4-148	0.058	7.22	0.498	10.01	0.063	6.96	0.693	0.020	15.96	391.75	26.47	410.21	33.80	514.62	158.49	391.92	62.03	23.88	4.50	391.75	26.47
DV 7/7/15_4-65	0.055	7.19	0.481	9.81	0.063	6.71	0.681	0.021	8.15	394.89	25.69	398.63	32.37	417.60	160.54	413.94	33.43	5.44	0.94	394.89	25.69
DV 7/7/15_4-140	0.057	4.28	0.499	6.23	0.063	4.57	0.727	0.018	6.09	396.23	17.55	411.03	21.07	494.47	94.38	370.16	22.35	19.87	3.60	396.23	17.55
DV 7/7/15_4-122	0.057	5.64	0.498	8.24	0.064	6.04	0.729	0.022	6.76	397.98	23.31	410.20	27.83	479.12	124.73	430.75	28.85	16.94	2.98	397.98	23.31
DV 7/7/15_4-4	0.056	7.24	0.493	10.17	0.064	7.15	0.702	0.020	8.41	401.78	27.86	406.73	34.09	433.68	161.26	404.20	33.67	7.36	1.22	401.78	27.86
DV 7/7/15_4-141	0.055	5.53	0.515	7.50	0.067	5.10	0.675	0.020	11.94	420.62	20.75	422.13	25.91	429.71	123.30	409.81	48.48	2.12	0.36	420.62	20.75
DV 7/7/15_4-54	0.058	5.64	0.553	8.15	0.069	5.91	0.722	0.023	7.47	429.27	24.55	446.63	29.45	534.55	123.39	469.00	34.68	19.70	3.89	429.27	24.55
DV 7/7/15_4-108	0.054	6.03	0.534	8.57	0.071	6.12	0.710	0.023	5.73	442.66	26.18	434.24	30.30	389.08	135.44	455.19	25.79	-13.77	-1.94	442.66	26.18
DV 7/7/15_4-127	0.063	4.24	0.780	6.07	0.089	4.39	0.716	0.019	11.82	550.37	23.14	585.27	27.01	722.67	89.88	388.11	45.48	23.84	5.96	550.37	23.14
DV 7/7/15_4-61	0.062	6.80	0.863	9.24	0.100	6.28	0.677	0.034	8.31	615.96	36.87	631.72	43.48	685.92	145.19	680.33	55.69	10.20	2.49	615.96	36.87
DV 7/7/15_4-59	0.065	5.46	0.997	7.98	0.112	5.85	0.729	0.036	5.67	684.25	37.96	702.37	40.48	758.26	115.23	713.25	39.76	9.76	2.58	684.25	37.96
DV 7/7/15_4-114	0.067	4.66	1.167	6.95	0.127	5.19	0.742	0.042	6.08	771.61	37.74	785.15	38.00	823.23	97.23	830.23	49.55	6.27	1.72	771.61	37.74
DV 7/7/15_4-49	0.084	5.35	2.484	8.13	0.215	6.16	0.753	0.063	5.73	1257.31	70.32	1267.33	58.95	1282.26	104.24	1237.30	68.84	1.95	0.79	1282.26	104.24
DV 7/7/15_4-126	0.114	4.07	4.759	6.08	0.303	4.56	0.743	0.094	5.29	1706.68	68.36	1777.76	51.06	1861.91	73.41	1816.94	92.06	8.34	4.00	1861.91	73.41
DV 7/7/15_4-77	0.120	4.82	5.718	7.36	0.347	5.59	0.755	0.105	5.45	1918.27	92.69	1934.02	63.66	1948.77	86.18	2018.97	105.08	1.56	0.81	1948.77	86.18

Rejected data

DV 7/7/15_4-116	0.080	5.90	0.217	8.53	0.020	6.19	0.723	0.004	13.00	126.16	7.73	199.38	15.44	1187.09	116.43	71.99	9.35	89.37	36.72	126.16	7.73
DV 7/7/15_4-86	0.066	4.91	0.208	7.40	0.023	5.57	0.748	0.006	7.66	145.48	8.01	192.13	12.95	810.13	102.76	123.59	9.43	82.04	24.28	145.48	8.01
DV 7/7/15_4-118	0.064	10.04	0.220	15.16	0.025	11.38	0.749	0.007	26.23	159.79	17.96	202.30	27.81	731.64	212.61	133.29	34.87	78.16	21.02	159.79	17.96
DV 7/7/15_4-133	0.056	9.74	0.208	14.84	0.027	11.20	0.754	0.007	29.63	173.16	19.14	192.22	25.99	432.75	217.01	144.11	42.60	59.99	9.92	173.16	19.14
DV 7/7/15_4-103	0.055	13.38	0.228	19.14	0.030	13.70	0.715	0.010	13.98	191.77	25.89	208.42	36.08	400.15	299.72	202.45	28.18	52.07	7.99	191.77	25.89

DV 7/7/15_4-80	0.051	10.82	0.237	16.01	0.034	11.81	0.737	0.011	7.38	212.60	24.71	215.72	31.13	247.14	249.20	225.38	16.55	13.98	1.45	212.60	24.71
DV 7/7/15_4-16	0.056	10.75	0.261	15.66	0.034	11.41	0.728	0.010	12.29	213.77	24.00	235.86	32.98	461.36	238.16	204.12	24.98	53.67	9.37	213.77	24.00
DV 7/7/15_4-137	0.074	10.79	0.359	13.60	0.035	8.30	0.609	0.014	12.84	222.38	18.15	311.53	36.51	1046.36	217.59	271.20	34.61	78.75	28.61	222.38	18.15
DV 7/7/15_4-112	0.061	12.22	0.360	18.25	0.042	13.56	0.742	0.016	11.44	268.30	35.64	312.20	49.08	653.84	262.27	330.60	37.54	58.97	14.06	268.30	35.64
DV 7/7/15_4-19	0.058	17.90	0.414	24.61	0.052	16.90	0.686	0.017	21.95	325.06	53.57	351.76	73.29	531.22	392.10	343.65	74.93	38.81	7.59	325.06	53.57
DV 7/7/15_4-88	0.062	15.37	0.590	19.07	0.069	11.30	0.592	0.024	12.33	432.41	47.26	471.12	72.01	661.93	329.42	481.51	58.77	34.67	8.22	432.41	47.26
DV 7/7/15_4-6	0.079	6.23	1.452	9.35	0.134	6.98	0.745	0.045	7.82	808.43	53.03	910.89	56.26	1167.24	123.44	882.90	67.69	30.74	11.25	808.43	53.03

LY725171 38.453 71.59

	Isotope ratios									Apparent Ages (Ma)									
	^{207}Pb	±	^{207}Pb	±	^{206}Pb	±		^{208}Pb	±	^{206}Pb	±	^{207}Pb	±	^{207}Pb	±	^{208}Pb	±		±
	^{206}Pb	(2%SD)	^{235}U	(2%SD)	^{238}U	(2%SD)	error corr.	^{238}Th	(2SD)	^{238}U	(2SD)	^{235}U	(2SD)	^{206}Pb	(2SD)	^{232}Th	(2SD)	Best Age	(2SD)
LY725171_147	0.051	3.11	0.233	2.99	0.033	2.08	0.290	0.011	13.23	211.52	4.32	212.50	5.73	223.36	71.80	218.52	28.77	211.52	-0.46
LY725171_118	0.056	3.77	0.266	3.77	0.034	1.79	0.237	0.012	3.01	211.00	3.85	239.12	8.04	450.97	83.80	243.23	7.27	211.00	-8.79
LY725171_187	0.050	5.56	0.241	5.91	0.035	3.15	0.375	0.012	14.49	219.66	6.81	219.48	11.66	217.54	128.62	245.82	35.43	219.66	0.08
LY725171_142	0.050	5.54	0.242	4.91	0.035	2.42	-0.028	0.011	11.12	221.32	5.27	220.10	9.73	207.05	128.48	223.14	24.69	221.32	0.56
LY725171_009	0.052	6.19	0.249	6.40	0.035	2.83	0.295	0.011	9.93	222.15	6.18	225.86	12.97	264.67	142.09	223.23	22.06	222.15	-1.64
LY725171_158	0.051	6.91	0.254	6.33	0.036	2.89	0.015	0.012	12.66	229.54	6.51	229.86	13.01	233.09	159.59	240.54	30.30	229.54	-0.14
LY725171_085	0.050	2.44	0.264	2.26	0.038	1.80	0.295	0.012	10.98	243.16	4.30	237.97	4.79	187.05	56.77	240.95	26.31	243.16	2.18
LY725171_086	0.051	3.33	0.283	3.00	0.040	1.79	0.102	0.013	10.10	252.56	4.44	252.81	6.71	255.14	76.61	265.73	26.68	252.56	-0.10
LY725171_006	0.053	3.92	0.294	4.31	0.040	2.13	0.419	0.012	9.12	252.89	5.29	262.02	9.95	344.51	88.80	250.68	22.73	252.89	-3.49
LY725171_065	0.051	2.57	0.282	3.06	0.040	2.16	0.562	0.013	17.85	254.68	5.40	252.34	6.84	230.66	59.39	255.06	45.30	254.68	0.93
LY725171_149	0.053	3.61	0.298	4.24	0.041	2.11	0.524	0.013	17.23	257.98	5.33	264.58	9.88	323.43	82.08	268.76	46.05	257.98	-2.49
LY725171_103	0.053	3.98	0.303	3.31	0.042	2.91	0.186	0.013	4.16	264.37	7.55	268.94	7.82	308.94	90.71	265.03	10.95	264.37	-1.70
LY725171_029	0.053	2.67	0.307	2.80	0.042	1.68	0.374	0.014	4.15	267.35	4.41	271.80	6.67	310.38	60.86	271.32	11.19	267.35	-1.64
LY725171_007	0.054	3.73	0.320	4.02	0.043	2.19	0.399	0.014	7.93	271.77	5.82	282.23	9.91	369.84	84.10	273.12	21.54	271.77	-3.71
LY725171_017	0.056	5.21	0.336	6.04	0.043	2.46	0.516	0.014	9.88	273.11	6.57	293.79	15.41	461.54	115.58	286.15	28.08	273.11	-7.04
LY725171_088	0.054	3.54	0.331	3.73	0.044	2.15	0.378	0.015	9.74	280.06	5.89	289.96	9.42	370.53	79.63	300.96	29.11	280.06	-3.41
LY725171_111	0.054	3.85	0.334	3.57	0.045	2.17	0.170	0.015	3.68	285.06	6.04	292.54	9.08	352.77	86.98	298.71	10.93	285.06	-2.56
LY725171_175	0.052	3.32	0.327	3.69	0.046	1.66	0.435	0.015	5.96	287.81	4.68	287.31	9.24	283.26	76.02	291.87	17.26	287.81	0.17
LY725171_087	0.057	2.85	0.360	3.11	0.046	2.03	0.447	0.015	9.61	290.91	5.77	312.39	8.36	475.94	63.04	293.75	28.04	290.91	-6.88
LY725171_091	0.056	4.99	0.362	5.15	0.047	2.22	0.286	0.015	9.75	294.71	6.40	313.75	13.89	457.76	110.66	307.90	29.81	294.71	-6.07
LY725171_199	0.052	2.67	0.334	2.98	0.047	2.81	0.575	0.016	19.36	295.12	8.10	292.43	7.58	271.06	61.29	315.05	60.61	295.12	0.92
LY725171_054	0.050	8.59	0.325	6.68	0.048	5.00	-0.064	0.016	5.27	299.84	14.65	285.98	16.64	174.14	200.50	318.36	16.64	299.84	4.85
LY725171_058	0.051	6.07	0.345	5.28	0.049	4.06	0.174	0.016	8.66	310.62	12.32	300.63	13.73	223.79	140.40	325.63	28.00	310.62	3.32
LY725171_186	0.052	4.63	0.359	5.20	0.050	2.71	0.459	0.017	13.91	313.86	8.29	311.33	13.95	292.43	105.74	331.56	45.81	313.86	0.81
LY725171_136	0.052	4.83	0.371	4.87	0.052	2.33	0.255	0.017	6.99	324.96	7.38	320.12	13.36	285.08	110.41	341.93	23.71	324.96	1.51

LY725171_120	0.052	3.31	0.372	3.44	0.052	2.52	0.420	0.017	3.58	325.51	7.99	321.09	9.48	289.15	75.53	337.84	12.00	325.51	1.38
LY725171_183	0.051	4.56	0.379	4.82	0.053	2.41	0.353	0.017	11.82	334.89	7.86	326.00	13.44	262.99	104.79	348.39	40.86	334.89	2.73
LY725171_013	0.056	5.16	0.428	6.10	0.055	2.87	0.537	0.018	8.58	347.52	9.71	361.49	18.56	452.11	114.66	361.70	30.80	347.52	-3.86
LY725171_076	0.055	3.37	0.436	4.01	0.058	2.29	0.544	0.018	5.38	362.24	8.07	367.31	12.36	399.43	75.43	367.22	19.59	362.24	-1.38
LY725171_188	0.056	3.06	0.451	4.73	0.059	3.30	0.765	0.020	13.88	367.61	11.80	377.63	14.92	439.59	68.19	395.59	54.44	367.61	-2.66
LY725171_003	0.056	4.78	0.467	4.56	0.061	2.47	0.180	0.017	8.44	380.56	9.13	389.26	14.74	441.26	106.28	344.70	28.87	380.56	-2.23
LY725171_089	0.057	1.79	0.508	2.34	0.064	1.72	0.650	0.020	12.01	401.75	6.72	416.93	8.00	501.77	39.36	404.18	48.13	401.75	-3.64
LY725171_127	0.053	3.03	0.487	2.96	0.066	1.84	0.271	0.020	5.62	412.85	7.36	402.59	9.84	344.09	68.60	409.25	22.76	412.85	2.55
LY725171_027	0.058	2.99	0.525	2.53	0.066	1.67	0.032	0.021	8.95	413.39	6.69	428.71	8.86	511.88	65.71	419.89	37.21	413.39	-3.57
LY725171_046	0.058	3.94	0.529	4.63	0.066	3.42	0.556	0.021	4.96	414.60	13.73	431.03	16.25	519.84	86.45	420.46	20.64	414.60	-3.81
LY725171_039	0.058	4.26	0.529	4.98	0.066	2.66	0.517	0.021	8.53	414.67	10.70	431.45	17.51	522.06	93.52	426.15	35.99	414.67	-3.89
LY725171_123	0.056	2.36	0.519	2.49	0.067	1.57	0.397	0.022	1.84	420.25	6.38	424.68	8.65	448.79	52.43	438.57	8.00	420.25	-1.04
LY725171_008	0.056	2.62	0.519	3.53	0.068	2.06	0.677	0.021	8.37	421.29	8.41	424.24	12.25	440.33	58.26	421.56	34.96	421.29	-0.70
LY725171_125	0.058	2.80	0.553	2.62	0.069	1.60	0.192	0.023	2.67	430.83	6.69	447.28	9.48	532.78	61.30	452.90	11.94	430.83	-3.68
LY725171_107	0.057	2.90	0.544	2.27	0.070	2.60	0.297	0.021	3.19	433.87	10.93	441.25	8.11	479.96	64.10	427.09	13.48	433.87	-1.67
LY725171_034	0.055	2.61	0.534	2.07	0.070	1.77	0.077	0.022	5.05	435.33	7.45	434.45	7.30	429.82	58.28	443.95	22.20	435.33	0.20
LY725171_132	0.059	2.67	0.577	2.83	0.070	1.60	0.382	0.023	6.27	438.60	6.76	462.61	10.53	583.62	57.95	462.38	28.66	438.60	-5.19
LY725171_124	0.056	1.92	0.545	2.01	0.071	1.23	0.373	0.022	4.83	439.50	5.22	441.84	7.19	454.09	42.67	436.77	20.88	439.50	-0.53
LY725171_189	0.053	4.30	0.544	6.59	0.074	3.67	0.794	0.024	17.35	462.89	16.38	441.26	23.58	329.96	97.44	474.61	81.54	462.89	4.90
LY725171_075	0.056	3.73	0.580	4.11	0.075	2.13	0.426	0.023	8.31	465.23	9.54	464.39	15.30	460.22	82.76	468.02	38.50	465.23	0.18
LY725171_004	0.061	5.38	0.633	7.24	0.075	2.42	0.838	0.025	9.85	468.32	10.93	497.68	28.50	635.07	115.84	494.96	48.22	468.32	-5.90
LY725171_015	0.057	5.71	0.597	6.87	0.076	2.96	0.575	0.023	6.27	471.41	13.47	475.49	26.08	495.20	125.74	463.56	28.76	471.41	-0.86
LY725171_096	0.064	3.45	0.732	3.56	0.083	2.68	0.415	0.028	5.79	511.50	13.18	557.48	15.26	749.96	72.96	561.48	32.07	511.50	-8.25
LY725171_010	0.061	5.56	0.716	6.61	0.085	2.69	0.563	0.029	11.64	524.80	13.58	548.43	28.01	647.84	119.35	570.99	65.66	524.80	-4.31
LY725171_036	0.059	2.40	0.743	3.04	0.091	1.97	0.612	0.029	6.11	561.96	10.59	563.88	13.14	571.62	52.30	583.01	35.16	561.96	-0.34
LY725171_163	0.057	3.05	0.723	3.11	0.093	2.00	0.350	0.030	19.42	571.41	10.94	552.48	13.26	475.18	67.54	594.55	114.09	571.41	3.43
LY725171_025	0.060	1.98	0.794	1.95	0.096	1.65	0.407	0.030	12.06	590.11	9.30	593.46	8.76	606.30	42.74	589.80	70.25	590.11	-0.56
LY725171_179	0.059	2.91	0.782	3.13	0.096	1.81	0.407	0.031	14.52	591.14	10.20	586.81	13.94	570.10	63.24	619.01	88.68	591.14	0.74
LY725171_117	0.062	2.44	0.825	2.64	0.096	2.03	0.475	0.029	2.70	592.97	11.48	611.02	12.10	678.53	52.24	585.42	15.56	592.97	-2.95
LY725171_176	0.061	3.34	0.810	3.29	0.096	2.20	0.313	0.032	10.80	593.76	12.48	602.32	14.95	634.70	71.79	642.42	68.42	593.76	-1.42

LY725171_048	0.061	2.41	0.828	3.56	0.098	3.14	0.748	0.031	4.96	603.90	18.13	612.53	16.36	644.56	51.76	607.96	29.73	603.90	-1.41
LY725171_078	0.061	3.56	0.820	4.04	0.098	2.02	0.474	0.031	5.69	604.05	11.65	608.22	18.47	623.79	76.70	609.23	34.17	604.05	-0.69
LY725171_066	0.060	2.16	0.826	2.41	0.099	2.04	0.539	0.030	12.93	609.38	11.84	611.65	11.09	620.08	46.64	603.42	77.04	609.38	-0.37
LY725171_018	0.061	5.25	0.838	6.37	0.100	2.57	0.599	0.032	9.45	614.83	15.07	618.31	29.50	631.08	113.09	645.98	60.15	614.83	-0.56
LY725171_165	0.061	3.27	0.857	3.24	0.101	2.25	0.334	0.035	26.42	622.89	13.34	628.66	15.16	649.47	70.12	688.42	179.63	622.89	-0.92
LY725171_115	0.060	2.96	0.839	3.00	0.102	1.92	0.338	0.032	2.11	627.14	11.49	618.77	13.88	588.28	64.26	630.19	13.11	627.14	1.35
LY725171_130	0.067	2.21	0.972	2.42	0.105	1.82	0.485	0.035	5.94	642.13	11.09	689.39	12.11	846.83	46.01	688.44	40.25	642.13	-6.86
LY725171_182	0.060	3.31	0.891	4.12	0.107	2.14	0.601	0.034	11.69	657.08	13.40	646.96	19.71	611.80	71.49	679.26	78.23	657.08	1.56
LY725171_097	0.062	2.83	0.914	3.00	0.108	2.60	0.496	0.035	5.99	658.24	16.24	659.14	14.55	662.23	60.65	687.22	40.50	658.24	-0.14
LY725171_079	0.062	3.49	0.921	3.12	0.108	2.59	0.264	0.034	6.98	659.27	16.24	663.09	15.18	676.10	74.57	679.41	46.71	659.27	-0.58
LY725171_106	0.060	2.99	0.902	2.23	0.110	2.56	0.225	0.033	3.28	670.82	16.30	652.95	10.73	591.65	64.83	655.95	21.18	670.82	2.74
LY725171_070	0.063	4.45	0.952	5.59	0.110	3.22	0.605	0.043	10.29	670.93	20.51	679.08	27.68	706.20	94.77	845.84	85.40	670.93	-1.20
LY725171_128	0.062	3.42	0.936	3.56	0.110	2.01	0.352	0.035	5.00	672.16	12.83	670.72	17.50	665.88	73.27	693.37	34.11	672.16	0.22
LY725171_178	0.061	4.59	0.954	4.43	0.114	2.54	0.220	0.041	10.59	694.03	16.72	680.11	21.95	634.29	98.91	805.55	83.83	694.03	2.05
LY725171_051	0.065	4.40	1.037	3.37	0.116	3.27	0.120	0.040	5.25	707.58	21.88	722.39	17.43	768.64	92.71	794.39	40.90	707.58	-2.05
LY725171_038	0.064	3.30	1.027	3.66	0.116	2.15	0.456	0.037	6.40	709.07	14.46	717.21	18.85	742.77	69.73	733.57	46.16	709.07	-1.14
LY725171_056	0.061	4.29	0.981	2.97	0.116	3.89	0.239	0.036	8.24	709.40	26.12	694.21	14.92	645.33	92.20	710.74	57.60	709.40	2.19
LY725171_073	0.063	4.45	1.010	4.71	0.117	2.84	0.389	0.038	6.20	710.96	19.15	708.77	24.01	701.80	94.76	756.75	46.11	710.96	0.31
LY725171_192	0.065	3.29	1.105	5.33	0.123	3.24	0.813	0.041	13.48	749.95	22.92	755.73	28.39	772.87	69.23	809.81	107.28	749.95	-0.76
LY725171_144	0.062	4.32	1.064	3.54	0.124	2.92	0.118	0.039	15.04	751.59	20.72	735.71	18.55	687.65	92.12	774.78	114.67	751.59	2.16
LY725171_148	0.072	2.44	1.227	2.40	0.124	1.94	0.387	0.036	13.04	752.76	13.78	812.78	13.45	980.90	49.63	722.83	92.81	752.76	-7.39
LY725171_139	0.067	3.73	1.149	3.89	0.124	2.20	0.352	0.040	8.35	756.10	15.70	776.95	21.10	837.36	77.71	783.55	64.26	756.10	-2.68
LY725171_152	0.066	3.50	1.165	3.22	0.128	1.56	0.055	0.040	12.11	778.40	11.43	784.52	17.62	801.97	73.39	798.53	95.00	778.40	-0.78
LY725171_145	0.069	3.03	1.218	2.66	0.129	2.14	0.216	0.041	14.95	779.82	15.72	808.94	14.82	889.93	62.61	806.58	118.59	779.82	-3.60
LY725171_143	0.064	3.46	1.131	2.86	0.129	2.11	0.054	0.040	10.76	779.84	15.48	768.18	15.40	734.42	73.22	793.41	83.88	779.84	1.52
LY725171_090	0.066	4.31	1.170	4.00	0.129	2.59	0.202	0.041	13.61	783.81	19.14	786.79	21.93	795.27	90.35	818.01	109.42	783.81	-0.38
LY725171_026	0.069	3.65	1.233	3.62	0.129	1.91	0.248	0.039	9.00	784.56	14.09	815.92	20.31	902.43	75.27	778.84	68.92	784.56	-3.84
LY725171_092	0.061	2.17	1.085	2.68	0.130	1.79	0.591	0.040	9.04	785.57	13.20	745.99	14.15	629.01	46.76	792.68	70.38	785.57	5.30
LY725171_137	0.066	4.14	1.184	3.91	0.130	2.61	0.241	0.041	7.26	790.63	19.43	793.30	21.51	800.81	86.78	806.21	57.42	790.63	-0.34
LY725171_164	0.063	2.64	1.156	3.18	0.134	1.89	0.557	0.043	26.32	808.09	14.37	780.02	17.30	700.54	56.26	850.13	220.34	808.09	3.60

LY725171_035	0.065	2.87	1.215	3.74	0.135	2.02	0.653	0.042	4.98	816.28	15.45	807.58	20.85	783.67	60.26	823.19	40.24	816.28	1.08
LY725171_033	0.068	2.77	1.259	2.25	0.135	1.97	0.146	0.043	6.23	817.56	15.16	827.33	12.75	853.69	57.55	856.81	52.36	817.56	-1.18
LY725171_126	0.065	2.52	1.212	2.27	0.135	1.72	0.227	0.041	4.78	818.33	13.20	806.14	12.62	772.63	52.94	821.12	38.50	818.33	1.51
LY725171_151	0.068	4.55	1.274	4.12	0.136	2.10	0.040	0.043	12.48	820.85	16.16	834.14	23.44	869.70	94.23	845.85	103.67	820.85	-1.59
LY725171_037	0.067	2.94	1.262	3.52	0.137	2.13	0.550	0.043	6.49	826.18	16.52	828.99	19.92	836.51	61.30	850.45	54.08	826.18	-0.34
LY725171_057	0.068	5.66	1.302	4.68	0.139	4.24	0.197	0.044	8.17	839.50	33.34	846.55	26.86	865.08	117.31	877.98	70.31	839.50	-0.83
LY725171_162	0.065	3.58	1.239	3.49	0.139	2.22	0.276	0.043	19.18	840.43	17.51	818.65	19.62	759.89	75.54	858.64	161.90	840.43	2.66
LY725171_080	0.071	1.85	1.359	2.12	0.139	2.27	0.648	0.045	5.87	840.84	17.87	871.45	12.42	950.06	37.80	894.96	51.46	840.84	-3.51
LY725171_198	0.066	1.44	1.295	1.89	0.141	2.07	0.740	0.043	14.51	851.40	16.52	843.32	10.83	822.12	30.03	850.19	121.16	851.40	0.96
LY725171_113	0.071	2.40	1.376	2.81	0.141	2.29	0.574	0.046	1.61	853.02	18.33	878.77	16.50	944.19	49.11	915.38	14.42	853.02	-2.93
LY725171_191	0.065	2.94	1.267	4.77	0.142	2.84	0.820	0.046	13.37	856.50	22.75	831.03	27.09	763.52	61.86	902.45	118.31	856.50	3.06
LY725171_068	0.075	2.96	1.487	2.94	0.145	1.84	0.303	0.054	13.39	870.86	15.00	925.08	17.87	1056.68	59.59	1064.47	139.31	870.86	-5.86
LY725171_082	0.066	2.51	1.330	2.47	0.145	2.16	0.417	0.044	7.86	875.50	17.66	859.00	14.33	816.63	52.51	874.23	67.33	875.50	1.92
LY725171_200	0.066	2.53	1.380	2.69	0.151	2.65	0.551	0.048	18.81	907.36	22.46	880.63	15.86	814.03	52.98	944.03	174.21	907.36	3.04
LY725171_167	0.068	2.65	1.466	2.73	0.156	2.22	0.443	0.051	20.81	934.47	19.27	916.34	16.49	872.95	54.80	995.91	203.23	934.47	1.98
LY725171_014	0.074	3.33	1.591	5.08	0.156	2.87	0.788	0.053	7.15	936.53	25.00	966.51	31.68	1035.33	67.21	1049.19	73.21	936.53	-3.10
LY725171_140	0.068	2.10	1.488	2.54	0.158	2.02	0.598	0.048	8.61	945.00	17.74	925.58	15.44	879.59	43.39	944.48	79.61	945.00	2.10
LY725171_077	0.070	3.47	1.548	3.91	0.160	2.39	0.478	0.050	4.99	954.27	21.24	949.67	24.12	939.02	71.21	981.05	47.86	954.27	0.48
LY725171_024	0.070	2.75	1.546	2.53	0.160	2.02	0.288	0.049	12.23	955.72	17.97	948.89	15.60	933.09	56.37	976.19	116.90	955.72	0.72
LY725171_155	0.069	2.94	1.526	1.92	0.160	1.70	-0.310	0.051	7.34	957.40	15.16	940.90	11.78	902.47	60.53	1006.90	72.26	957.40	1.75
LY725171_053	0.073	3.61	1.613	2.34	0.161	3.06	0.128	0.050	4.00	960.40	27.26	975.39	14.70	1009.31	73.12	985.95	38.50	960.40	-1.54
LY725171_141	0.069	3.34	1.533	2.67	0.161	2.03	0.009	0.049	10.78	961.40	18.17	943.67	16.39	902.52	68.86	972.07	102.52	961.40	1.88
LY725171_074	0.072	4.09	1.601	4.80	0.162	2.54	0.525	0.049	1.88	970.23	22.92	970.74	30.03	971.88	83.40	968.98	17.84	970.23	-0.05
LY725171_157	0.068	2.95	1.535	1.86	0.163	1.50	-0.532	0.049	12.22	970.72	13.50	944.35	11.46	883.35	60.95	972.53	116.32	970.72	2.79
LY725171_093	0.071	1.60	1.587	2.00	0.163	2.10	0.696	0.050	8.61	973.94	18.99	965.13	12.44	945.12	32.81	985.55	82.96	973.94	0.91
LY725171_095	0.072	3.01	1.631	3.09	0.165	2.73	0.468	0.052	8.12	986.07	24.93	982.16	19.43	973.41	61.47	1024.76	81.29	986.07	0.40
LY725171_011	0.071	3.44	1.632	4.84	0.166	2.41	0.746	0.050	7.42	989.17	22.07	982.69	30.47	968.22	70.19	991.41	71.89	989.17	0.66
LY725171_062	0.076	2.25	1.766	2.93	0.169	2.12	0.645	0.057	13.10	1004.57	19.67	1032.88	19.01	1093.32	45.09	1118.42	142.99	1004.57	8.83
LY725171_159	0.071	1.93	1.695	2.67	0.174	1.89	0.691	0.050	16.64	1034.78	18.10	1006.81	17.05	946.44	39.52	990.04	161.45	1034.78	-8.54
LY725171_002	0.075	1.62	1.861	2.27	0.179	2.00	0.719	0.055	8.13	1061.03	19.53	1067.19	14.97	1079.78	32.47	1079.00	85.58	1061.03	1.77

LY725171_160	0.079	3.07	2.147	3.13	0.197	2.11	0.368	0.061	16.77	1161.61	22.47	1164.14	21.71	1168.85	60.76	1191.26	194.95	1161.61	0.62
LY725171_169	0.085	4.09	2.575	3.76	0.220	2.99	0.282	0.069	6.48	1283.97	34.79	1293.63	27.51	1309.69	79.39	1348.24	84.70	1283.97	2.00
LY725171_101	0.094	2.62	3.223	2.37	0.249	2.88	0.516	0.086	4.09	1434.58	37.06	1462.63	18.36	1503.60	49.52	1672.13	65.69	1434.58	4.81
LY725171_063	0.096	1.37	3.626	2.63	0.274	2.22	0.853	0.078	13.15	1561.33	30.72	1555.25	20.91	1546.99	25.77	1526.55	194.33	1561.33	-0.92
LY725171_055	0.110	3.68	4.828	2.23	0.318	3.75	0.328	0.094	4.56	1778.31	58.31	1789.81	18.73	1803.25	66.96	1813.51	79.31	1778.31	1.40
LY725171_116	0.112	1.67	4.951	2.14	0.320	1.50	0.631	0.094	1.39	1787.56	23.40	1810.91	18.11	1837.89	30.24	1807.73	23.98	1787.56	2.82
LY725171_043	0.113	2.39	4.971	3.53	0.320	1.92	0.773	0.093	6.20	1787.89	29.98	1814.48	29.89	1845.15	43.17	1788.73	106.35	1787.89	3.20
LY725171_170	0.110	3.39	4.925	2.61	0.323	2.85	0.231	0.099	5.32	1805.58	44.85	1806.48	22.01	1807.52	61.60	1915.02	97.36	1805.58	0.11
LY725171_150	0.110	2.04	4.943	3.07	0.327	1.64	0.790	0.097	17.14	1821.52	25.99	1809.57	25.94	1795.83	37.15	1873.81	309.03	1821.52	-1.41
LY725171_060	0.110	1.01	4.982	2.70	0.328	1.97	0.954	0.099	7.56	1827.39	31.28	1816.28	22.87	1803.57	18.46	1912.43	138.37	1827.39	-1.30
LY725171_114	0.112	1.96	5.112	2.64	0.332	1.86	0.671	0.099	2.07	1848.14	29.81	1838.07	22.42	1826.70	35.51	1912.61	37.86	1848.14	-1.16
LY725171_041	0.112	2.39	5.157	3.67	0.334	1.89	0.814	0.098	6.04	1856.91	30.53	1845.51	31.20	1832.68	43.39	1886.14	109.02	1856.91	-1.31
LY725171_138	0.112	1.43	5.178	1.95	0.335	1.94	0.731	0.097	6.35	1863.46	31.32	1849.07	16.62	1832.93	25.85	1877.00	114.19	1863.46	-1.64
LY725171_083	0.113	1.73	5.219	2.00	0.336	2.17	0.661	0.098	7.90	1868.86	35.22	1855.79	17.08	1841.18	31.26	1887.65	142.97	1868.86	-1.48
LY725171_059	0.112	1.26	5.201	2.71	0.336	1.99	0.901	0.097	7.03	1868.92	32.21	1852.83	23.13	1834.82	22.88	1880.35	126.60	1868.92	-1.82
LY725171_105	0.112	2.59	5.204	2.04	0.337	2.61	0.401	0.099	3.84	1873.45	42.47	1853.24	17.39	1830.63	46.98	1901.24	69.80	1873.45	-2.29
LY725171_185	0.111	2.90	5.176	4.14	0.338	2.48	0.723	0.102	2.03	1874.90	40.30	1848.64	35.21	1819.21	52.69	1966.28	38.16	1874.90	-2.97
LY725171_104	0.113	4.22	5.265	1.71	0.339	3.99	0.079	0.099	3.92	1881.98	65.19	1863.19	14.61	1842.28	76.36	1908.46	71.44	1881.98	-2.11
LY725171_146	0.110	2.14	5.207	2.26	0.342	2.05	0.513	0.101	12.94	1896.31	33.74	1853.74	19.27	1806.31	38.86	1951.22	242.10	1896.31	-4.75
LY725171_156	0.114	2.93	5.362	2.24	0.342	1.73	-0.074	0.099	11.99	1896.36	28.41	1878.75	19.18	1859.33	52.94	1904.08	219.01	1896.36	-1.95
LY725171_069	0.115	1.40	5.446	2.38	0.342	2.07	0.812	0.097	7.48	1896.45	34.08	1892.15	20.42	1887.44	25.15	1865.89	133.82	1896.45	-0.47
LY725171_067	0.118	1.87	5.674	2.30	0.348	2.02	0.631	0.099	12.97	1922.85	33.57	1927.41	19.84	1932.33	33.49	1914.54	238.30	1922.85	0.49
LY725171_180	0.111	1.65	5.318	2.08	0.348	1.65	0.633	0.106	14.39	1925.58	27.42	1871.72	17.81	1812.44	29.89	2035.61	280.60	1925.58	-5.88
LY725171_084	0.114	1.41	5.477	2.21	0.349	1.92	0.775	0.098	11.17	1929.50	32.00	1897.06	18.97	1861.74	25.46	1891.56	202.68	1929.50	-3.51
LY725171_184	0.113	4.75	5.463	5.77	0.351	2.30	0.604	0.113	3.49	1937.95	38.48	1894.83	49.55	1847.91	85.87	2165.28	71.84	1937.95	-4.65
LY725171_168	0.111	2.14	5.401	2.60	0.352	2.48	0.647	0.101	20.38	1943.96	41.65	1885.03	22.26	1820.73	38.80	1950.95	382.58	1943.96	-6.34
LY725171_171	0.122	2.70	5.919	2.06	0.353	2.01	0.120	0.109	4.88	1946.94	33.84	1964.07	17.88	1982.18	48.09	2084.53	96.90	1946.94	1.81
LY725171_193	0.111	2.44	5.401	4.77	0.353	2.80	0.921	0.103	13.20	1946.99	47.09	1884.96	40.88	1817.30	44.36	1986.93	251.43	1946.99	-6.66
LY725171_131	0.113	0.98	5.515	1.98	0.355	1.61	0.869	0.101	5.67	1956.87	27.24	1902.95	16.98	1844.66	17.81	1939.78	105.15	1956.87	-5.73
LY725171_108	0.119	2.72	5.830	2.44	0.356	2.79	0.466	0.099	3.69	1965.27	47.23	1950.86	21.12	1935.59	48.62	1916.98	67.65	1965.27	-1.51

LY725171_102	0.126	2.70	6.247	3.21	0.360	3.19	0.643	0.125	3.62	1984.32	54.49	2011.08	28.11	2038.68	47.83	2372.94	81.29	1984.32	2.74
LY725171_016	0.138	3.79	6.976	5.10	0.366	2.26	0.728	0.103	8.87	2012.10	39.14	2108.36	45.34	2203.63	65.75	1974.75	167.50	2012.10	9.52
LY725171_045	0.126	2.08	6.429	3.31	0.371	3.17	0.795	0.108	5.24	2031.92	55.33	2036.28	29.11	2040.71	36.82	2077.31	103.66	2031.92	0.43
LY725171_197	0.123	1.49	6.396	2.08	0.378	2.16	0.754	0.107	14.54	2067.71	38.17	2031.71	18.30	1995.35	26.47	2054.55	286.15	2067.71	-3.50
LY725171_195	0.127	1.59	6.858	3.46	0.390	2.88	0.891	0.115	15.76	2124.42	52.13	2093.18	30.69	2062.60	27.99	2203.47	331.63	2124.42	-2.91
LY725171_005	0.129	1.68	7.006	3.22	0.393	2.47	0.859	0.108	9.35	2134.45	44.93	2112.15	28.62	2090.50	29.46	2072.44	184.98	2134.45	-2.06
LY725171_177	0.155	1.96	8.695	2.10	0.407	2.04	0.550	0.115	10.58	2200.43	38.00	2306.57	19.13	2401.94	33.41	2201.36	221.79	2200.43	9.16
LY725171_052	0.157	3.29	9.039	1.81	0.417	3.00	0.133	0.124	3.63	2247.76	56.99	2341.93	16.51	2425.00	55.84	2354.19	80.73	2247.76	7.89
LY725171_112	0.164	2.29	9.763	2.34	0.431	1.82	0.414	0.132	2.54	2309.37	35.27	2412.62	21.56	2500.93	38.61	2499.32	59.70	2309.37	8.29
LY725171_161	0.148	2.19	8.932	4.03	0.438	2.83	0.852	0.129	19.16	2342.81	55.51	2331.12	36.80	2320.90	37.62	2451.06	447.23	2342.81	-0.94
LY725171_064	0.148	1.64	9.007	2.04	0.443	2.04	0.678	0.128	17.86	2363.08	40.41	2338.72	18.65	2317.53	28.10	2441.87	415.01	2363.08	-1.93
LY725171_153	0.144	3.24	8.806	3.02	0.443	1.52	0.104	0.126	12.07	2366.00	30.08	2318.15	27.56	2276.27	55.77	2395.92	274.53	2366.00	-3.79
LY725171_194	0.145	1.65	9.096	2.50	0.454	2.10	0.755	0.135	15.65	2412.33	42.17	2347.72	22.85	2292.06	28.42	2563.87	380.44	2412.33	-4.99
LY725171_040	0.164	3.14	10.383	4.08	0.460	2.21	0.646	0.128	8.40	2440.59	44.89	2469.55	37.81	2493.47	52.95	2435.19	193.64	2440.59	2.17
LY725171_031	0.165	1.84	10.583	1.78	0.465	1.68	0.435	0.130	6.08	2461.94	34.42	2487.26	16.54	2508.00	31.00	2476.42	142.12	2461.94	1.87
LY725171_021	0.167	1.64	10.808	1.96	0.468	1.92	0.644	0.130	8.55	2476.85	39.52	2506.78	18.21	2531.11	27.47	2472.03	199.99	2476.85	2.19
LY725171_049	0.160	3.31	10.313	2.02	0.469	3.55	0.400	0.134	1.45	2477.41	73.12	2463.26	18.70	2451.60	56.02	2541.34	34.56	2477.41	-1.04
LY725171_174	0.156	1.93	10.273	2.01	0.476	1.75	0.483	0.137	5.52	2510.68	36.49	2459.65	18.58	2417.73	32.69	2601.16	135.20	2510.68	-3.70
LY725171_110	0.163	2.91	10.874	2.83	0.483	2.53	0.417	0.137	1.73	2538.37	53.18	2512.43	26.37	2491.53	49.03	2593.64	42.19	2538.37	-1.85
LY725171_134	0.168	1.54	11.190	2.04	0.484	1.78	0.681	0.144	2.28	2543.96	37.40	2539.07	18.97	2535.17	25.87	2711.90	57.96	2543.96	-0.35
LY725171_061	0.172	2.17	11.648	2.71	0.492	2.06	0.616	0.140	12.87	2579.08	43.86	2576.49	25.32	2574.46	36.23	2656.08	322.85	2579.08	-0.18
LY725171_081	0.176	1.79	12.109	1.95	0.498	2.21	0.634	0.141	7.78	2604.45	47.36	2612.90	18.25	2619.45	29.83	2667.54	195.26	2604.45	0.58
LY725171_094	0.232	1.33	19.873	1.75	0.622	2.25	0.807	0.163	7.19	3119.81	55.77	3085.18	16.92	3062.72	21.34	3046.49	204.27	3119.81	-1.83
LY725171_001	0.264	1.20	23.779	1.91	0.652	1.77	0.791	0.172	8.14	3236.39	45.08	3259.36	18.65	3273.52	18.84	3207.50	242.78	3236.39	1.15
~~LY725171_044~~	~~0.099~~	~~7.73~~	~~0.912~~	~~10.30~~	~~0.067~~	~~3.12~~	~~0.873~~	~~0.034~~	~~9.02~~	~~418.61~~	~~12.65~~	~~658.35~~	~~49.95~~	~~1598.50~~	~~144.23~~	~~678.55~~	~~60.29~~	~~418.61~~	~~-36.42~~
~~LY725171_071~~	~~0.104~~	~~3.17~~	~~1.768~~	~~3.36~~	~~0.123~~	~~2.49~~	~~0.444~~	~~0.147~~	~~5.92~~	~~747.05~~	~~17.60~~	~~1033.62~~	~~21.79~~	~~1702.63~~	~~58.45~~	~~2771.26~~	~~153.85~~	~~747.05~~	~~-27.73~~
~~LY725171_072~~	~~0.081~~	~~3.70~~	~~0.823~~	~~5.02~~	~~0.073~~	~~4.10~~	~~0.688~~	~~0.014~~	~~9.56~~	~~456.02~~	~~18.05~~	~~609.67~~	~~23.01~~	~~1231.61~~	~~72.64~~	~~287.34~~	~~27.31~~	~~456.02~~	~~-25.20~~
~~LY725171_050~~	~~0.074~~	~~7.71~~	~~0.534~~	~~10.33~~	~~0.052~~	~~4.37~~	~~0.734~~	~~0.028~~	~~13.97~~	~~327.57~~	~~13.96~~	~~434.37~~	~~36.51~~	~~1049.08~~	~~155.43~~	~~552.97~~	~~76.35~~	~~327.57~~	~~-24.59~~
~~LY725171_196~~	~~0.070~~	~~7.98~~	~~0.384~~	~~8.32~~	~~0.040~~	~~2.11~~	~~0.286~~	~~0.015~~	~~15.25~~	~~251.58~~	~~5.21~~	~~330.08~~	~~23.46~~	~~928.45~~	~~163.89~~	~~298.17~~	~~45.18~~	~~251.58~~	~~-23.78~~

LY725171_133	0.112	1.43	2.542	2.25	0.165	1.56	0.776	0.062	6.03	985.98	14.31	1284.25	16.41	1825.15	25.96	1214.54	71.23	985.98	-23.23
LY725171_119	0.072	1.54	0.550	2.46	0.056	2.37	0.798	0.010	2.45	349.68	8.05	444.88	8.87	972.79	31.36	207.86	5.06	349.68	-21.40
LY725171_012	0.084	5.37	1.192	6.87	0.103	2.46	0.723	0.044	8.21	631.74	14.78	797.10	37.94	1292.50	104.42	868.29	69.90	631.74	-20.75
LY725171_135	0.073	3.61	0.712	3.24	0.070	1.93	0.095	0.025	2.78	438.58	8.16	546.10	13.67	1024.37	72.95	492.86	13.52	438.58	-19.69
LY725171_109	0.065	5.42	0.416	4.78	0.046	2.49	-0.013	0.017	3.63	290.90	7.09	353.45	14.26	787.90	113.70	343.58	12.39	290.90	-17.70
LY725171_019	0.068	5.75	0.620	6.39	0.066	2.19	0.450	0.028	10.95	414.99	8.81	489.86	24.84	857.16	119.31	558.42	60.42	414.99	-15.28
LY725171_099	0.070	6.41	0.840	11.89	0.087	4.05	1.212	0.030	6.49	534.97	20.78	619.16	55.17	940.32	131.36	604.94	38.72	534.97	-13.60
LY725171_020	0.067	2.76	0.675	2.66	0.073	2.32	0.390	0.025	6.70	453.33	10.14	523.86	10.87	844.45	57.44	507.52	33.60	453.33	-13.46
LY725171_100	0.078	2.35	1.298	2.99	0.120	3.72	0.777	0.047	4.58	731.30	25.75	844.86	17.13	1156.26	46.58	930.57	41.65	731.30	-13.44
LY725171_121	0.071	1.63	0.877	3.12	0.090	2.40	0.859	0.029	4.39	556.00	12.79	639.28	14.82	945.85	33.30	568.65	24.65	556.00	-13.03
LY725171_181	0.069	3.41	1.645	4.13	0.172	2.08	0.567	0.053	11.61	1023.23	19.69	987.65	26.10	909.40	70.31	1041.89	118.26	1023.23	-11.13
LY725171_030	0.074	3.55	1.181	3.29	0.116	1.96	0.162	0.040	4.84	708.01	13.13	791.91	18.11	1036.03	71.65	792.20	37.61	708.01	-10.59
LY725171_122	0.080	1.56	2.048	2.62	0.185	2.23	0.804	0.064	1.91	1092.93	22.43	1131.76	17.90	1207.02	30.80	1255.33	23.31	1092.93	10.44
LY725171_129	0.123	2.11	5.466	2.81	0.323	2.10	0.668	0.102	6.38	1805.97	33.07	1895.34	24.16	1994.69	37.42	1954.35	119.22	1805.97	10.45
LY725171_028	0.110	1.95	4.266	1.94	0.281	1.57	0.397	0.084	9.08	1597.77	22.23	1686.76	15.94	1799.25	35.50	1622.40	142.01	1597.77	12.61
LY725171_172	0.139	2.88	6.854	2.39	0.357	2.33	0.256	0.043	11.28	1965.67	39.42	2092.77	21.17	2220.22	49.85	842.14	93.23	1965.67	12.95
LY725171_032	0.168	1.69	9.501	1.53	0.411	1.50	0.379	0.120	5.96	2220.72	28.19	2387.62	14.03	2533.26	28.31	2299.32	130.05	2220.72	14.07
LY725171_023	0.168	1.54	9.559	1.96	0.412	2.27	0.744	0.117	8.67	2224.97	42.70	2393.22	18.01	2539.70	25.84	2231.35	184.10	2224.97	14.15
LY725171_042	0.135	2.06	6.328	3.37	0.340	1.74	0.863	0.115	6.34	1884.97	28.46	2022.32	29.52	2165.58	35.92	2197.29	132.42	1884.97	14.89
LY725171_047	0.112	2.14	4.324	3.65	0.280	3.52	0.823	0.080	5.14	1590.82	49.62	1698.00	30.11	1832.97	38.76	1546.55	76.63	1590.82	15.22
LY725171_166	0.166	2.43	8.798	2.71	0.384	2.46	0.561	0.135	20.38	2096.81	44.01	2317.31	24.71	2517.72	40.85	2554.36	495.10	2096.81	20.07
LY725171_022	0.169	1.41	8.887	1.62	0.382	1.66	0.628	0.131	8.55	2086.88	29.54	2326.46	14.76	2543.89	23.66	2496.00	201.78	2086.88	21.90
LY725171_154	0.085	4.36	2.025	3.51	0.172	2.37	-0.066	0.059	7.60	1023.46	22.42	1123.94	23.85	1323.67	84.46	1160.68	85.92	1023.46	29.33
LY725171_098	0.163	1.87	7.371	2.21	0.328	2.71	0.731	0.086	5.56	1829.21	43.21	2157.52	19.76	2486.43	31.45	1667.67	89.16	1829.21	35.93
LY725171_190	0.100	3.20	2.467	8.01	0.180	5.64	0.949	0.089	17.24	1065.08	55.36	1262.29	57.92	1616.18	59.51	1715.80	285.64	1065.08	51.74
LY725171_173	0.198	2.66	6.313	2.77	0.232	2.30	0.461	0.049	7.38	1342.54	27.92	2020.22	24.26	2807.66	43.51	972.73	70.20	1342.54	109.13

C. Appendix 3: Muscovite $^{40}Ar/^{39}Ar$ Analysis

Analyses Conducted at USGS

Complete $^{40}Ar/^{39}Ar$ results

Sample: **15_006** J-value: 0.0076750 ± 0.0000046 (1σ) D/amu: 1.00995 ± 0.00081 (1σ)

Material: mica

File	Laser Power	^{40}Ar	^{40}Ar	± $1\sigma_{40}$	^{39}Ar	± $1\sigma_{39}$	^{38}Ar	± $1\sigma_{38}$	^{37}Ar	± $1\sigma_{37}$	^{36}Ar	± $1\sigma_{36}$	$\%^{40}Ar^*$	$^{40}Ar^*/^{39}Ar_K$	± 1σ	Age	± 2σ	K/Ca
	(%)	(moles)	(Volts)	(Volts)	(Volts)	(Volts)	(Volts)	(Volts)	(Volts)	(Volts)	(Volts)	(Volts)				(Ma)	(Ma)	
MAA7011-000	35	1.011E-15	0.171266	± 0.000187	0.009363	± 0.000042	0.000124	± 0.000015	0.000133	± 0.000067	0.000125	± 0.000004	78.20	14.305351	± 0.138343	190.69	± 3.50	30.2
MAA7012-000	35	1.016E-15	0.172100	± 0.000169	0.009580	± 0.000044	0.000116	± 0.000013	0.000022	± 0.000051	0.000060	± 0.000004	89.65	16.105549	± 0.137830	213.34	± 3.45	187.5
MAA7014-000	35	2.732E-15	0.462952	± 0.000275	0.031314	± 0.000069	0.000381	± 0.000025	0.000165	± 0.000056	0.000033	± 0.000004	97.87	14.469443	± 0.048218	192.77	± 1.22	81.6
MAA7015-000	35	4.376E-15	0.741393	± 0.000325	0.046248	± 0.000084	0.000565	± 0.000022	0.000130	± 0.000055	0.000024	± 0.000004	99.02	15.873577	± 0.037673	210.44	± 0.94	152.6
MAA7017-000	35	2.733E-15	0.463017	± 0.000251	0.037860	± 0.000093	0.000448	± 0.000017	0.000604	± 0.000067	0.000065	± 0.000004	95.84	11.720603	± 0.040534	157.67	± 1.04	27.0
MAA7018-000	35	1.850E-15	0.313442	± 0.000254	0.020937	± 0.000054	0.000270	± 0.000016	0.000086	± 0.000052	0.000048	± 0.000004	95.46	14.291534	± 0.064139	190.52	± 1.62	104.4
MAA7020-000	35	5.172E-15	0.876303	± 0.000410	0.060244	± 0.000132	0.000781	± 0.000026	0.000305	± 0.000057	0.000056	± 0.000004	98.09	14.267905	± 0.036430	190.22	± 0.92	85.0
MAA7021-000	35	1.451E-15	0.245793	± 0.000239	0.014134	± 0.000046	0.000187	± 0.000013	0.000088	± 0.000058	0.000034	± 0.000003	95.87	16.672234	± 0.090840	220.41	± 2.26	69.2
MAA7023-000	35	1.298E-15	0.219922	± 0.000220	0.015536	± 0.000041	0.000194	± 0.000017	0.000154	± 0.000053	0.000074	± 0.000004	89.97	12.735899	± 0.082368	170.71	± 2.11	43.3
MAA7024-000	35	3.914E-16	0.066319	± 0.000144	0.003609	± 0.000027	0.000051	± 0.000010	0.000150	± 0.000058	0.000069	± 0.000004	69.14	12.706459	± 0.336448	170.34	± 8.61	10.3
MAA7029-000	35	5.621E-16	0.095236	± 0.000131	0.004771	± 0.000029	0.000091	± 0.000010	0.000065	± 0.000063	0.000171	± 0.000004	46.44	9.269291	± 0.277117	125.80	± 7.27	31.6
MAA7032-000	35	1.396E-15	0.236469	± 0.000185	0.014478	± 0.000047	0.000185	± 0.000013	0.000446	± 0.000053	0.000020	± 0.000004	97.43	15.912697	± 0.093220	210.93	± 2.33	14.0
MAA7033-000	35	1.101E-15	0.186593	± 0.000240	0.011630	± 0.000040	0.000155	± 0.000013	0.000075	± 0.000054	0.000019	± 0.000004	96.95	15.555255	± 0.110397	206.44	± 2.77	66.6
MAA7035-000	35	9.325E-16	0.157991	± 0.000146	0.011763	± 0.000047	0.000162	± 0.000016	0.000029	± 0.000047	0.000015	± 0.000004	97.10	13.041961	± 0.104584	174.63	± 2.67	174.6
MAA7036-000	35	3.776E-15	0.639747	± 0.000258	0.045735	± 0.000097	0.000581	± 0.000018	0.000264	± 0.000054	0.000056	± 0.000004	97.39	13.622502	± 0.037656	182.03	± 0.96	74.6
MAA7038-000	35	6.090E-15	1.031815	± 0.000365	0.068724	± 0.000123	0.000848	± 0.000014	0.000247	± 0.000067	0.000129	± 0.000005	96.28	14.454635	± 0.032893	192.58	± 0.83	119.9
MAA7039-000	35	1.383E-15	0.234309	± 0.000220	0.014678	± 0.000046	0.000158	± 0.000013	0.000315	± 0.000052	0.000027	± 0.000004	96.51	15.406094	± 0.090961	204.57	± 2.29	20.0
MAA7041-000	35	4.778E-15	0.809511	± 0.000416	0.050141	± 0.000095	0.000591	± 0.000027	0.000171	± 0.000055	0.000054	± 0.000004	98.02	15.824869	± 0.038393	209.83	± 0.96	126.3
MAA7042-000	35	6.599E-16	0.111816	± 0.000157	0.008608	± 0.000039	0.000103	± 0.000020	0.000020	± 0.000044	0.000012	± 0.000004	96.89	12.585263	± 0.136435	168.78	± 3.50	180.7
MAA7045-000	35	6.864E-16	0.116296	± 0.000183	0.006922	± 0.000037	0.000123	± 0.000009	0.000141	± 0.000051	0.000086	± 0.000004	77.91	13.090787	± 0.179697	175.25	± 4.59	21.1
MAA7050-000	35	1.189E-15	0.201522	± 0.000192	0.012525	± 0.000050	0.000178	± 0.000014	0.000026	± 0.000044	0.000079	± 0.000004	88.26	14.200246	± 0.112059	189.36	± 2.84	204.9
MAA7053-000	35	6.291E-16	0.106595	± 0.000181	0.006041	± 0.000027	0.000070	± 0.000010	0.000080	± 0.000058	0.000039	± 0.000003	88.99	15.702673	± 0.185654	208.29	± 4.66	32.4
MAA7056-000	35	5.315E-16	0.090056	± 0.000162	0.008454	± 0.000034	0.000144	± 0.000011	0.000233	± 0.000055	0.000034	± 0.000004	88.60	9.438515	± 0.132747	128.02	± 3.48	15.6
MAA7057-000	35	4.353E-15	0.737548	± 0.000313	0.051873	± 0.000105	0.000610	± 0.000017	0.000213	± 0.000056	0.000063	± 0.000004	97.45	13.855322	± 0.036132	184.98	± 0.92	104.8

MAA7059-000	35	6.803E-16	0.115261	± 0.000194	0.009876	± 0.000035	0.000124	± 0.000011	0.000086	± 0.000052	0.000028	± 0.000004	92.65	10.812342	± 0.121363	145.93	± 3.15	49.5
MAA7060-000	35	6.842E-15	1.159328	± 0.000436	0.078153	± 0.000128	0.000961	± 0.000029	0.000866	± 0.000082	0.000093	± 0.000004	97.60	14.477509	± 0.028947	192.87	± 0.73	38.8
MAA7062-000	35	2.173E-15	0.368197	± 0.000266	0.026688	± 0.000069	0.000297	± 0.000017	0.000214	± 0.000065	0.000044	± 0.000004	96.47	13.309389	± 0.057564	178.04	± 1.47	53.7
MAA7063-000	35	4.543E-16	0.076966	± 0.000121	0.005299	± 0.000032	0.000088	± 0.000009	0.000230	± 0.000054	0.000085	± 0.000004	67.01	9.733174	± 0.230746	131.88	± 6.03	9.9
MAA7066-000	35	4.191E-16	0.071012	± 0.000155	0.003488	± 0.000026	0.000066	± 0.000013	0.000054	± 0.000051	0.000123	± 0.000004	48.08	9.788440	± 0.363286	132.60	± 9.49	27.6
MAA7068-000	35	2.322E-16	0.039339	± 0.000145	0.002346	± 0.000025	0.000055	± 0.000010	0.000068	± 0.000046	0.000053	± 0.000004	60.08	10.075067	± 0.483310	136.34	± 12.61	14.8
MAA7069-000	35	2.440E-15	0.413449	± 0.000240	0.024976	± 0.000060	0.000344	± 0.000011	0.000309	± 0.000054	0.000049	± 0.000004	96.45	15.966228	± 0.057739	211.60	± 1.45	34.8
MAA7071-000	35	1.128E-15	0.191091	± 0.000203	0.011358	± 0.000039	0.000133	± 0.000013	0.000208	± 0.000051	0.000029	± 0.000004	95.43	16.055329	± 0.116569	212.71	± 2.92	23.5
MAA7072-000	35	4.261E-16	0.072189	± 0.000157	0.005128	± 0.000030	0.000064	± 0.000009	0.000201	± 0.000075	0.000044	± 0.000004	81.91	11.531071	± 0.225261	155.23	± 5.81	11.0
MAA7074-000	35	1.098E-14	1.860322	± 0.000600	0.128304	± 0.000182	0.001573	± 0.000026	0.004979	± 0.000236	0.000103	± 0.000004	98.37	14.263411	± 0.022412	190.16	± 0.57	11.1
MAA7075-000	35	1.127E-15	0.190872	± 0.000211	0.016334	± 0.000050	0.000188	± 0.000011	0.000514	± 0.000088	0.000041	± 0.000004	93.56	10.933094	± 0.075521	147.49	± 1.96	13.7
MAA7077-000	35	2.777E-15	0.470537	± 0.000232	0.033744	± 0.000071	0.000409	± 0.000021	0.000347	± 0.000071	0.000033	± 0.000004	97.92	13.654018	± 0.045103	182.43	± 1.15	41.8
MAA7078-000	35	7.526E-15	1.275138	± 0.000387	0.087729	± 0.000139	0.001046	± 0.000029	0.001285	± 0.000090	0.000061	± 0.000004	98.58	14.329066	± 0.027055	190.99	± 0.68	29.4
MAA7080-000	35	6.520E-16	0.110476	± 0.000311	0.006042	± 0.000049	0.000096	± 0.000015	0.000003	± 0.000056	0.000168	± 0.000005	54.54	9.972533	± 0.274430	135.00	± 7.16	780.0
MAA7083-000	35	4.483E-16	0.075960	± 0.000142	0.002940	± 0.000029	0.000063	± 0.000015	0.000083	± 0.000061	0.000147	± 0.000004	42.12	10.882212	± 0.412185	146.83	± 10.69	15.3
MAA7084-000	35	1.193E-15	0.202156	± 0.000190	0.011634	± 0.000041	0.000135	± 0.000015	0.000015	± 0.000051	0.000020	± 0.000004	97.02	16.857776	± 0.116397	222.72	± 2.90	341.4
MAA7086-000	35	1.116E-15	0.189171	± 0.000193	0.010358	± 0.000044	0.000110	± 0.000016	0.000305	± 0.000068	0.000035	± 0.000004	94.43	17.246445	± 0.128705	227.55	± 3.19	14.6
MAA7089-000	35	2.918E-15	0.494414	± 0.000234	0.033924	± 0.000070	0.000449	± 0.000019	0.000326	± 0.000067	0.000133	± 0.000004	91.97	13.403657	± 0.048722	179.24	± 1.24	44.7
MAA7090-000	35	4.930E-15	0.835232	± 0.000340	0.059765	± 0.000115	0.000773	± 0.000020	0.000176	± 0.000058	0.000057	± 0.000004	97.98	13.692499	± 0.032276	182.92	± 0.82	145.9
MAA7092-000	35	7.752E-16	0.131338	± 0.000167	0.009724	± 0.000046	0.000130	± 0.000011	0.000119	± 0.000056	0.000015	± 0.000003	96.51	13.035921	± 0.123188	174.55	± 3.15	35.0
MAA7093-000	35	2.726E-16	0.046191	± 0.000133	0.002444	± 0.000023	0.000041	± 0.000009	0.000101	± 0.000048	0.000052	± 0.000004	66.64	12.596790	± 0.476336	168.93	± 12.20	10.4
MAA7095-000	35	3.145E-16	0.053287	± 0.000134	0.003073	± 0.000022	0.000049	± 0.000012	0.000241	± 0.000059	0.000071	± 0.000004	60.30	10.455482	± 0.362494	141.29	± 9.43	5.5
MAA7096-000	35	4.851E-16	0.082185	± 0.000150	0.004699	± 0.000032	0.000044	± 0.000011	0.000048	± 0.000050	0.000025	± 0.000004	91.02	15.919285	± 0.255399	211.01	± 6.39	42.1
MAA7098-000	35	4.012E-16	0.067985	± 0.000128	0.003761	± 0.000029	0.000056	± 0.000012	0.000023	± 0.000051	0.000027	± 0.000004	87.97	15.900240	± 0.319401	210.77	± 8.00	71.5

Sample: **15-020** J-value: 0.0076750 ± 0.0000046 (1σ) D/amu: 1.00936 ± 0.00091 (1σ)

Material: mica

File	Laser Power	^{40}Ar	^{40}Ar	± 1σ$_{40}$	^{39}Ar	± 1σ$_{39}$	^{38}Ar	± 1σ$_{38}$	^{37}Ar	± 1σ$_{37}$	^{36}Ar	± 1σ$_{36}$	%^{40}Ar*	$^{40}Ar^*/^{39}Ar_K$	± 1σ	Age	± 2σ	K/Ca
	(%)	(moles)	(Volts)	(Volts)	(Volts)	(Volts)	(Volts)	(Volts)	(Volts)	(Volts)	(Volts)	(Volts)				(Ma)	(Ma)	
MAA6865-000	35	2.537E-15	0.429839	± 0.000301	0.025275	± 0.000067	0.000286	± 0.000022	0.000155	± 0.000080	0.000067	± 0.000003	95.33	16.212854	± 0.057207	214.68	± 1.43	70.2
MAA6867-000	35	9.522E-16	0.161331	± 0.000224	0.008946	± 0.000041	0.000126	± 0.000017	0.000088	± 0.000070	0.000053	± 0.000003	90.27	16.279483	± 0.123990	215.51	± 3.10	43.6
MAA6868-000	35	7.069E-16	0.119781	± 0.000215	0.008431	± 0.000042	0.000117	± 0.000016	0.000464	± 0.000084	0.000127	± 0.000003	68.27	9.699657	± 0.119670	131.44	± 3.13	7.8
MAA6870-000	35	1.117E-14	1.893046	± 0.000807	0.130937	± 0.000220	0.001628	± 0.000046	0.002542	± 0.000137	0.000245	± 0.000007	96.14	13.899627	± 0.028836	185.55	± 0.73	22.2
MAA6871-000	35	1.557E-14	2.637836	± 0.000918	0.184807	± 0.000221	0.002289	± 0.000022	0.003363	± 0.000192	0.000323	± 0.000007	96.35	13.751933	± 0.020472	183.67	± 0.52	23.6
MAA6873-000	35	1.791E-15	0.303507	± 0.000306	0.024466	± 0.000060	0.000308	± 0.000015	0.000285	± 0.000063	0.000049	± 0.000005	95.22	11.812403	± 0.069710	158.86	± 1.80	36.9
MAA6874-000	35	5.758E-16	0.097560	± 0.000223	0.003996	± 0.000035	0.000094	± 0.000013	0.000187	± 0.000061	0.000209	± 0.000006	35.96	8.779755	± 0.454478	119.37	± 11.96	9.2
MAA6876-000	35	3.938E-16	0.066718	± 0.000214	0.003648	± 0.000033	0.000083	± 0.000010	0.000913	± 0.000074	0.000081	± 0.000005	64.04	11.713657	± 0.443309	157.58	± 11.43	1.7
MAA6877-000	35	1.837E-15	0.311182	± 0.000281	0.018469	± 0.000054	0.000214	± 0.000019	0.000058	± 0.000051	0.000048	± 0.000005	95.37	16.069011	± 0.094047	212.88	± 2.35	137.4
MAA6879-000	35	6.073E-16	0.102890	± 0.000219	0.006013	± 0.000040	0.000082	± 0.000012	0.000097	± 0.000043	0.000007	± 0.000005	98.07	16.782063	± 0.265342	221.78	± 6.60	26.6
MAA6880-000	35	1.048E-15	0.177506	± 0.000236	0.010071	± 0.000042	0.000124	± 0.000014	0.000025	± 0.000053	0.000016	± 0.000005	97.37	17.162318	± 0.161147	226.50	± 4.00	176.6
MAA6882-000	35	1.621E-14	2.746772	± 0.000771	0.199595	± 0.000256	0.002367	± 0.000029	0.001264	± 0.000088	0.000257	± 0.000006	97.21	13.377150	± 0.019501	178.90	± 0.50	67.9
MAA6883-000	35	4.476E-15	0.758436	± 0.000304	0.046598	± 0.000088	0.000552	± 0.000029	0.000093	± 0.000050	0.000078	± 0.000005	96.91	15.774041	± 0.044190	209.19	± 1.11	214.8
MAA6885-000	35	6.589E-15	1.116373	± 0.000449	0.079540	± 0.000147	0.000969	± 0.000028	0.002376	± 0.000145	0.000202	± 0.000006	94.60	13.278222	± 0.033093	177.64	± 0.84	14.4
MAA6886-000	35	2.424E-15	0.410709	± 0.000335	0.031980	± 0.000071	0.000430	± 0.000015	0.001243	± 0.000112	0.000045	± 0.000005	96.73	12.423515	± 0.054532	166.71	± 1.40	11.1
MAA6888-000	35	8.735E-16	0.147995	± 0.000255	0.007334	± 0.000042	0.000154	± 0.000013	0.000219	± 0.000057	0.000260	± 0.000005	47.50	9.585004	± 0.226739	129.94	± 5.93	14.4
MAA6889-000	35	3.200E-16	0.054211	± 0.000193	0.003441	± 0.000033	0.000069	± 0.000013	0.000064	± 0.000055	0.000051	± 0.000005	72.16	11.368540	± 0.449235	153.13	± 11.61	23.0
MAA6892-000	35	1.916E-15	0.324554	± 0.000300	0.019513	± 0.000055	0.000241	± 0.000013	0.000192	± 0.000058	0.000034	± 0.000005	96.89	16.115178	± 0.089159	213.46	± 2.23	43.7
MAA6895-000	35	2.064E-16	0.034966	± 0.000185	0.001949	± 0.000030	0.000016	± 0.000011	0.000051	± 0.000041	0.000010	± 0.000005	91.25	16.374602	± 0.797184	216.70	± 19.90	16.5
MAA6897-000	35	6.546E-15	1.109108	± 0.000514	0.071851	± 0.000122	0.000887	± 0.000024	0.000151	± 0.000047	0.000149	± 0.000005	95.98	14.816087	± 0.034063	197.14	± 0.86	205.1
MAA6898-000	35	1.423E-15	0.241099	± 0.000239	0.016294	± 0.000051	0.000203	± 0.000013	0.000026	± 0.000046	0.000008	± 0.000005	99.03	14.653562	± 0.101650	195.09	± 2.57	264.6
MAA6900-000	35	2.754E-15	0.466556	± 0.000273	0.034068	± 0.000090	0.000435	± 0.000028	0.000452	± 0.000077	0.000072	± 0.000005	95.41	13.066100	± 0.056836	174.93	± 1.45	32.4
MAA6901-000	35	2.787E-15	0.472183	± 0.000341	0.032524	± 0.000081	0.000403	± 0.000020	0.001672	± 0.000096	0.000074	± 0.000005	95.32	13.838376	± 0.059436	184.77	± 1.51	8.4
MAA6903-000	35	3.936E-15	0.666957	± 0.000323	0.046995	± 0.000088	0.000618	± 0.000018	0.001676	± 0.000101	0.000203	± 0.000006	90.92	12.904265	± 0.043543	172.87	± 1.11	12.1
MAA6904-000	35	4.697E-16	0.079585	± 0.000204	0.004561	± 0.000035	0.000083	± 0.000011	0.001162	± 0.000107	0.000138	± 0.000005	48.20	8.411521	± 0.348039	114.52	± 9.19	1.7
MAA6907-000	35	3.710E-16	0.062853	± 0.000191	0.003105	± 0.000030	0.000063	± 0.000014	0.000059	± 0.000064	0.000117	± 0.000005	44.42	8.991893	± 0.503469	122.16	± 13.23	22.6
MAA6910-000	35	3.107E-15	0.526422	± 0.000381	0.031922	± 0.000084	0.000351	± 0.000018	0.000084	± 0.000057	0.000040	± 0.000005	97.72	16.114972	± 0.067601	213.46	± 1.69	162.5
MAA6912-000	35	2.133E-15	0.361321	± 0.000265	0.020773	± 0.000053	0.000272	± 0.000026	0.000168	± 0.000059	0.000094	± 0.000005	92.27	16.049607	± 0.085337	212.64	± 2.13	53.1
MAA6913-000	35	6.526E-16	0.110574	± 0.000211	0.006668	± 0.000042	0.000088	± 0.000013	0.000007	± 0.000058	0.000026	± 0.000005	93.09	15.436940	± 0.241540	204.96	± 6.07	435.1
MAA6915-000	35	2.748E-15	0.465682	± 0.000259	0.029583	± 0.000064	0.000366	± 0.000025	0.000105	± 0.000058	0.000035	± 0.000005	97.77	15.391073	± 0.059719	204.38	± 1.50	121.1

MAA6916-000	35	6.199E-15	1.050252	± 0.000443	0.068308	± 0.000142	0.000837	± 0.000018	0.001513	± 0.000094	0.000026	± 0.000005	99.28	15.264833	± 0.039127	202.80	± 0.98	19.4
MAA6918-000	35	1.682E-15	0.284912	± 0.000242	0.021169	± 0.000061	0.000287	± 0.000015	0.000468	± 0.000064	0.000032	± 0.000005	96.62	13.003854	± 0.078390	174.14	± 2.00	19.4
MAA6919-000	35	2.099E-15	0.355607	± 0.000264	0.024909	± 0.000074	0.000325	± 0.000019	0.000261	± 0.000073	0.000034	± 0.000005	97.14	13.868577	± 0.072872	185.15	± 1.85	41.1
MAA6921-000	35	2.792E-15	0.473095	± 0.000298	0.033218	± 0.000081	0.000395	± 0.000019	0.000160	± 0.000060	0.000040	± 0.000005	97.49	13.884216	± 0.056079	185.35	± 1.42	89.4
MAA6922-000	35	1.614E-15	0.273497	± 0.000249	0.016703	± 0.000054	0.000187	± 0.000017	0.000085	± 0.000065	0.000071	± 0.000005	92.29	15.110651	± 0.104802	200.86	± 2.64	85.0
MAA6928-000	35	9.201E-16	0.155904	± 0.000228	0.008942	± 0.000043	0.000103	± 0.000012	0.000069	± 0.000050	0.000073	± 0.000005	86.07	15.005828	± 0.185852	199.54	± 4.68	56.0
MAA6930-000	35	5.561E-15	0.942285	± 0.000409	0.057242	± 0.000101	0.000652	± 0.000024	0.000195	± 0.000055	0.000058	± 0.000005	98.16	16.158991	± 0.039757	214.01	± 0.99	126.1
MAA6931-000	35	3.386E-16	0.057365	± 0.000193	0.003007	± 0.000032	0.000050	± 0.000012	0.000061	± 0.000057	0.000058	± 0.000005	69.83	13.319710	± 0.534894	178.17	± 13.64	21.4
MAA6933-000	35	2.565E-16	0.043459	± 0.000206	0.001680	± 0.000027	0.000029	± 0.000011	0.000225	± 0.000053	0.000068	± 0.000005	53.01	13.718104	± 0.970368	183.24	± 24.67	3.2
MAA6934-000	35	2.643E-15	0.447859	± 0.000328	0.033024	± 0.000079	0.000398	± 0.000017	0.000323	± 0.000061	0.000065	± 0.000005	95.64	12.970820	± 0.056573	173.72	± 1.45	44.0

The values in this table represent blank, discrimination, and decay (^{37}Ar and ^{39}Ar) corrected values.

Instrument: MAP 215-50

Standard: 28.201 Ma Fish Canyon sanidine (Kuiper et al., 2008)

Atmospheric argon ratios			
$^{40}Ar/^{36}Ar$	298.56	± 0.31	Lee et al. (2006)
$^{38}Ar/^{36}Ar$	0.1885	± 0.0003	Lee et al. (2006)

Decay constants		
λ_{40Ar}	$(0.580 \pm 0.014) \times 10^{-10}$ a^{-1}	Min et al. (2000)
$\lambda_{\beta-}$	$(4.884 \pm 0.099) \times 10^{-10}$ a^{-1}	Min et al. (2000)
^{39}Ar	$(2.58 \pm 0.03) \times 10^{-3}$ a^{-1}	Stoenner et al. (1965)
^{37}Ar	$(8.23 \pm 0.042) \times 10^{-4}$ h^{-1}	Stoenner et al. (1965)
^{36}Cl	$(2.303 \pm 0.046) \times 10^{-6}$ a^{-1}	

Interfering isotope production ratios	
$(^{40}Ar/^{39}Ar)_K$	$(5.4 \pm 1.4) \times 10^{-4}$
$(^{38}Ar/^{39}Ar)_K$	$(1.210 \pm 0.002) \times 10^{-2}$
$(^{39}Ar/^{37}Ar)_{Ca}$	$(6.95 \pm 0.09) \times 10^{-4}$
$(^{38}Ar/^{37}Ar)_{Ca}$	$(1.96 \pm 0.08) \times 10^{-5}$
$(^{36}Ar/^{37}Ar)_{Ca}$	$(2.65 \pm 0.022) \times 10^{-4}$

D. Appendix 4: Zircon Fission Track

Analyses Conducted at the University of Arizona

ICPMS FT Age Calculation			Sample Name							decay constant =	1.54993E-10
			15-006C							(per yr)	
Date	7-Jul-16										
Analyst	JBC		No. of Crystals	86							
			Degrees of Freedom	85							
Session Zeta and unc	2729	107									
Grain #	**N s**	**Area (microns^2)**	**U (ppm)**	**± 1 σ**	**Rho s (tracks/cm^2)**	**Age (Ma)**	**± 1 σ**		**U-Pb Age (Ma)**	**max tracks**	**NOTES**
47	19	100	264.9	34.4	1.900E+07	**97.13**	**25.89**	**25.89**	359.9	72	
12	39	196	268.3	34.9	1.990E+07	**100.40**	**21.08**	**21.08**	1439.9	622	
27	20	100	268.7	34.9	2.000E+07	**100.78**	**26.36**	**26.36**	339.3	69	
46	13	100	170.4	22.2	1.300E+07	**103.25**	**31.88**	**31.88**	998.2	135	
32	9	144	81.9	10.6	6.250E+06	**103.28**	**37.17**	**37.17**	1320.4	127	
3	40	196	257.9	33.5	2.041E+07	**107.08**	**22.32**	**22.32**	393.3	150	
38	4	100	49.1	6.4	4.000E+06	**110.26**	**57.13**	**57.13**	296.3	11	*not etched?*
4	14	100	171.4	22.3	1.400E+07	**110.48**	**33.12**	**33.12**	994.3	135	*dirty mount*
87	9	100	108.7	14.1	9.000E+06	**111.96**	**40.30**	**40.30**	2438.4	236	*lumpy grain*
58	11	100	127.9	16.6	1.100E+07	**116.31**	**38.46**	**38.46**	340.9	33	*faintly etched*
77	21	144	167.7	21.8	1.458E+07	**117.55**	**30.21**	**30.21**	441.6	81	
14	47	196	264.6	34.4	2.398E+07	**122.50**	**24.41**	**24.41**	1932.8	856	
21	40	196	224.6	29.2	2.041E+07	**122.82**	**25.60**	**25.60**	248.3	82	
42	24	100	261.8	34.0	2.400E+07	**123.89**	**30.37**	**30.37**	680.5	138	
18	7	100	76.0	9.9	7.000E+06	**124.40**	**49.96**	**49.96**	509.9	30	
64	36	144	271.5	35.3	2.500E+07	**124.46**	**26.76**	**26.76**	535.4	160	
29	14	144	104.9	13.6	9.722E+06	**125.21**	**37.54**	**37.54**	261.5	30	
9	24	100	253.5	33.0	2.400E+07	**127.91**	**31.36**	**31.36**	454.2	87	
89	35	196	188.2	24.5	1.786E+07	**128.18**	**27.79**	**27.79**	417.5	117	
16	10	100	105.2	13.7	1.000E+07	**128.40**	**44.19**	**44.19**	1741.1	154	
70	34	196	177.9	23.1	1.735E+07	**131.70**	**28.81**	**28.81**	395.2	104	
83	13	100	133.1	17.3	1.300E+07	**131.88**	**40.72**	**40.72**	499.5	51	
92	16	100	163.3	21.2	1.600E+07	**132.29**	**37.64**	**37.64**	453.0	56	

37	36	144	245.0	31.8	2.500E+07	**137.75**	**29.61**	**29.61**	414.7	111	
90	32	196	157.4	20.5	1.633E+07	**140.05**	**31.22**	**31.22**	414.0	97	
67	21	144	139.5	18.1	1.458E+07	**141.09**	**36.26**	**36.26**	1539.7	256	
54	8	256	29.4	3.8	3.125E+06	**143.53**	**54.36**	**54.36**	2532.2	171	
96	21	144	136.8	17.8	1.458E+07	**143.80**	**36.96**	**36.96**	787.7	121	
73	5	100	45.6	5.9	5.000E+06	**147.96**	**69.15**	**69.15**	400.0	14	
25	24	100	214.6	27.9	2.400E+07	**150.80**	**36.97**	**36.97**	430.3	70	
5	5	100	44.7	5.8	5.000E+06	**150.82**	**70.49**	**70.49**	2485.9	99	*not etched*
52	17	100	150.8	19.6	1.700E+07	**152.00**	**42.25**	**42.25**	2458.1	331	
41	35	100	309.8	40.3	3.500E+07	**152.32**	**33.03**	**33.03**	260.2	60	
86	31	100	270.9	35.2	3.100E+07	**154.31**	**34.74**	**34.74**	448.1	92	
59	26	100	217.1	28.2	2.600E+07	**161.41**	**38.50**	**38.50**	338.5	55	
69	13	196	54.6	7.1	6.633E+06	**163.52**	**50.50**	**50.50**	395.3	32	*not etched*
13	17	100	139.1	18.1	1.700E+07	**164.67**	**45.77**	**45.77**	304.4	32	
63	21	100	163.3	21.2	2.100E+07	**173.16**	**44.51**	**44.51**	805.0	103	
84	9	144	47.7	6.2	6.250E+06	**176.28**	**63.45**	**63.45**	2026.6	120	
62	24	100	176.9	23.0	2.400E+07	**182.54**	**44.75**	**44.75**	675.9	92	
44	25	144	127.4	16.6	1.736E+07	**183.30**	**44.31**	**44.31**	388.3	54	
65	28	144	142.0	18.5	1.944E+07	**184.21**	**42.87**	**42.87**	445.2	69	
40	27	144	132.9	17.3	1.875E+07	**189.68**	**44.68**	**44.68**	361.3	52	
68	43	196	150.1	19.5	2.194E+07	**196.42**	**40.11**	**40.11**	1830.1	456	
94	14	144	65.6	8.5	9.722E+06	**199.15**	**59.70**	**59.70**	2260.9	187	
79	21	144	97.1	12.6	1.458E+07	**201.77**	**51.86**	**51.86**	302.3	32	
56	51	100	338.4	44.0	5.100E+07	**202.45**	**39.49**	**39.49**	295.6	75	
8	25	256	64.7	8.4	9.766E+06	**202.85**	**49.04**	**49.04**	2520.2	374	
2	36	100	235.9	30.7	3.600E+07	**204.91**	**44.05**	**44.05**	320.6	57	
6	22	100	144.2	18.7	2.200E+07	**204.93**	**51.80**	**51.80**	631.9	70	
15	48	100	309.2	40.2	4.800E+07	**208.39**	**41.30**	**41.30**	1921.6	507	*spotty image*
7	45	256	112.9	14.7	1.758E+07	**209.06**	**42.16**	**42.16**	2260.2	573	
43	29	100	181.4	23.6	2.900E+07	**214.56**	**49.36**	**49.36**	413.6	57	
66	17	100	105.2	13.7	1.700E+07	**216.81**	**60.27**	**60.27**	448.3	36	
81	30	144	128.4	16.7	2.083E+07	**217.70**	**49.53**	**49.53**	414.1	58	
82	20	144	85.6	11.1	1.389E+07	**217.72**	**56.96**	**56.96**	396.5	37	
36	9	144	38.4	5.0	6.250E+06	**218.07**	**78.49**	**78.49**	1788.4	84	
26	25	100	152.6	19.8	2.500E+07	**219.70**	**53.11**	**53.11**	367.0	42	

28	44	196	135.8	17.7	2.245E+07	**221.73**	**44.99**	**44.99**	210.8	42	
61	12	100	69.9	9.1	1.200E+07	**230.20**	**73.44**	**73.44**	769.5	42	
76	9	100	52.0	6.8	9.000E+06	**231.99**	**83.50**	**83.50**	741.8	30	
57	31	100	178.4	23.2	3.100E+07	**232.80**	**52.42**	**52.42**	254.7	34	
22	29	100	157.5	20.5	2.900E+07	**246.46**	**56.70**	**56.70**	942.2	117	
85	29	144	109.3	14.2	2.014E+07	**246.62**	**56.73**	**56.73**	2479.0	349	
20	13	100	67.6	8.8	1.300E+07	**257.31**	**79.46**	**79.46**	2524.2	153	
50	11	100	54.8	7.1	1.100E+07	**268.46**	**88.77**	**88.77**	1708.0	78	
19	15	196	37.6	4.9	7.653E+06	**271.66**	**79.25**	**79.25**	350.1	19	
51	30	100	147.0	19.1	3.000E+07	**272.65**	**62.04**	**62.04**	434.9	48	
55	10	144	33.3	4.3	6.944E+06	**278.24**	**95.76**	**95.76**	2501.6	107	
33	32	144	105.2	13.7	2.222E+07	**281.92**	**62.84**	**62.84**	674.1	79	
74	12	100	55.6	7.2	1.200E+07	**288.13**	**91.92**	**91.92**	263.4	11	
60	23	225	47.3	6.1	1.022E+07	**288.59**	**71.81**	**71.81**	752.8	62	
24	36	100	157.2	20.4	3.600E+07	**305.14**	**65.60**	**65.60**	276.1	33	
95b	20	144	60.5	7.9	1.389E+07	**305.85**	**80.01**	**80.01**	1956.6	146	
11	43	196	93.2	12.1	2.194E+07	**313.52**	**64.02**	**64.02**	268.7	37	
72	39	144	114.2	14.8	2.708E+07	**315.84**	**66.31**	**66.31**	257.9	32	
34	19	100	79.9	10.4	1.900E+07	**316.49**	**84.37**	**84.37**	2090.1	145	
10	4	100	16.6	2.2	4.000E+06	**320.99**	**166.31**	**166.31**	2481.6	37	
35	7	144	20.0	2.6	4.861E+06	**322.76**	**129.62**	**129.62**	1822.6	45	
80	19	144	53.6	7.0	1.319E+07	**327.24**	**87.24**	**87.24**	299.3	17	
1	14	100	56.0	7.3	1.400E+07	**332.60**	**99.70**	**99.70**	266.2	11	*blurry image*
88	8	144	21.7	2.8	5.556E+06	**340.21**	**128.85**	**128.85**	1833.3	49	
31	36	196	70.6	9.2	1.837E+07	**345.54**	**74.28**	**74.28**	1319.9	149	
17	11	100	40.5	5.3	1.100E+07	**360.42**	**119.18**	**119.18**	1804.3	62	
53	12	100	43.6	5.7	1.200E+07	**365.25**	**116.52**	**116.52**	721.3	24	
39	10	100	33.9	4.4	1.000E+07	**389.90**	**134.18**	**134.18**	2504.1	76	
75	8	100	23.7	3.1	8.000E+06	**444.94**	**168.51**	**168.51**	1850.2	37	*blurry image, not etched*
71	11	100	32.3	4.2	1.100E+07	**448.54**	**148.32**	**148.32**	589.6	15	
95a	30	144	53.9	7.0	2.083E+07	**506.94**	**115.35**	**115.35**	1987.5	132	

ICPMS FT Age Calculation

Sample Name
15-20A

decay constant = 1.54993E-10
(per yr)

Date 10-Jul-16

Analyst	JBC		No. of Crystals	96						
			Degrees of Freedom	95						
Session Zeta and unc	2729	107								
Grain #	N s	Area (microns^2)	U (ppm)	± 1 σ	Rho s (tracks/cm^2)	Age (Ma)	± 1 σ	U-Pb Age (Ma)	max tracks	NOTES
Spot 66	17	100	207.4	27.0	1.700E+07	**110.87**	**30.82**	259.3	40	
Spot 33	14	144	116.3	15.1	9.722E+06	**113.06**	**33.89**	319.1	40	
Spot 39	20	144	165.6	21.5	1.389E+07	**113.44**	**29.68**	207.6	37	
Spot 10	21	100	246.0	32.0	2.100E+07	**115.46**	**29.67**	271.1	50	
Spot 27	16	196	95.4	12.4	8.163E+06	**115.73**	**32.93**	1602.8	249	
Spot 41	30	144	240.2	31.2	2.083E+07	**117.30**	**26.69**	299.5	78	
Spot 67	27	100	278.4	36.2	2.700E+07	**131.00**	**30.85**	305.1	64	
Spot 62	18	144	126.9	16.5	1.250E+07	**133.05**	**36.19**	455.9	63	*poor*
Spot 6	23	196	118.8	15.4	1.173E+07	**133.45**	**33.21**	224.1	39	
Spot 5	18	100	179.9	23.4	1.800E+07	**135.10**	**36.75**	2459.7	395	
Spot 11	13	100	129.9	16.9	1.300E+07	**135.16**	**41.74**	274.6	27	
Spot 44	23	196	116.1	15.1	1.173E+07	**136.44**	**33.95**	1141.2	208	
Spot 70	12	100	116.1	15.1	1.200E+07	**139.54**	**44.52**		0	
Spot 40	21	144	139.6	18.2	1.458E+07	**140.96**	**36.23**		0	
Spot 58	24	144	153.1	19.9	1.667E+07	**146.84**	**36.00**	437.7	73	
Spot 20	19	100	172.5	22.4	1.900E+07	**148.59**	**39.61**	215.2	28	
Spot 23	23	100	207.9	27.0	2.300E+07	**149.25**	**37.14**	311.4	49	
Spot 75	14	100	126.3	16.4	1.400E+07	**149.45**	**44.80**	973.9	97	
Spot 24	32	100	286.4	37.2	3.200E+07	**150.66**	**33.58**	197.8	42	
Spot 59	29	144	177.2	23.0	2.014E+07	**153.21**	**35.24**	558.9	109	
Spot 14	40	196	170.7	22.2	2.041E+07	**161.11**	**33.58**	219.3	55	
Spot 37	21	100	164.8	21.4	2.100E+07	**171.57**	**44.10**	211.8	26	
Spot 83	37	100	290.2	37.7	3.700E+07	**171.64**	**36.60**	258.9	56	
Spot 51	45	144	227.6	29.6	3.125E+07	**184.66**	**37.24**	302.3	74	
Spot 46	32	144	160.2	20.8	2.222E+07	**186.56**	**41.59**	214.4	37	
Spot 57	31	144	154.5	20.1	2.153E+07	**187.36**	**42.18**		0	
Spot 101	22	100	156.2	20.3	2.200E+07	**189.43**	**47.88**	216.984	25	
Spot 89	25	100	171.7	22.3	2.500E+07	**195.66**	**47.30**	223.7	29	
Spot 95	40	100	271.4	35.3	4.000E+07	**198.06**	**41.28**	224.5	45	
Spot 77	38	144	176.6	23.0	2.639E+07	**200.78**	**42.48**	220.5	42	
Spot 16	29	100	193.9	25.2	2.900E+07	**200.90**	**46.22**		0	

Spot 82	24	100	157.5	20.5	2.400E+07	**204.70**	**50.18**	315.9	37	
Spot 25	18	100	116.1	15.1	1.800E+07	**208.15**	**56.62**	209.6	18	
Spot 99	44	144	197.1	25.6	3.056E+07	**208.18**	**42.24**	227.703	48	
Spot 73	25	72	222.0	28.9	3.472E+07	**209.93**	**50.75**	223.3	27	
Spot 76	67	144	292.7	38.1	4.653E+07	**213.34**	**38.97**	218.1	69	
Spot 17	52	100	325.4	42.3	5.200E+07	**214.45**	**41.62**	230.6	56	
Spot 100	47	144	203.9	26.5	3.264E+07	**214.83**	**42.81**	219.968	48	
Spot 1	67	144	290.0	37.7	4.653E+07	**215.32**	**39.33**	220.4	69	
Spot 79	33	144	142.6	18.5	2.292E+07	**215.65**	**47.61**	248.0	38	
Spot 71	30	144	128.6	16.7	2.083E+07	**217.27**	**49.44**	435.7	61	
Spot 94	43	144	183.4	23.8	2.986E+07	**218.44**	**44.60**	320.6	64	
Spot 2	45	100	274.5	35.7	4.500E+07	**219.86**	**44.33**	224.2	46	
Spot 34	19	144	80.4	10.5	1.319E+07	**220.16**	**58.69**	432.7	38	
Spot 43	32	100	194.3	25.3	3.200E+07	**220.88**	**49.23**	251.1	36	
Spot 29	12	196	36.8	4.8	6.122E+06	**222.99**	**71.14**	240.6	13	*not etched*
Spot 90	27	100	162.1	21.1	2.700E+07	**223.37**	**52.61**	223.6	27	
Spot 47	27	100	161.9	21.1	2.700E+07	**223.58**	**52.66**	209.6	25	
Spot 32	18	144	74.8	9.7	1.250E+07	**224.23**	**60.99**	497.4	41	
Spot 49	22	100	130.9	17.0	2.200E+07	**225.41**	**56.98**	222.2	22	
Spot 92	24	144	99.1	12.9	1.667E+07	**225.46**	**55.27**	222.5	24	
Spot 13	30	196	91.0	11.8	1.531E+07	**225.54**	**51.32**	221.0	29	
Spot 26	20	100	118.7	15.4	2.000E+07	**225.96**	**59.11**	218.3	19	
Spot 98	24	144	98.2	12.8	1.667E+07	**227.54**	**55.78**	381.477	41	
Spot 80	39	144	157.2	20.4	2.708E+07	**230.85**	**48.47**	320.9	55	
Spot 45	15	100	86.9	11.3	1.500E+07	**231.46**	**67.52**	211.1	14	
Spot 21	30	100	173.0	22.5	3.000E+07	**232.44**	**52.89**	211.5	27	
Spot 93	24	144	96.1	12.5	1.667E+07	**232.49**	**57.00**	221.7	23	
Spot 3	57	144	225.2	29.3	3.958E+07	**235.48**	**44.67**	215.9	52	
Spot 78	31	100	174.0	22.6	3.100E+07	**238.60**	**53.72**		0	
Spot 104	27	144	104.8	13.6	1.875E+07	**239.55**	**56.42**	220.615	25	
Spot 50	24	100	134.1	17.4	2.400E+07	**239.67**	**58.76**	495.7	51	
Spot 61	18	100	100.1	13.0	1.800E+07	**240.75**	**65.49**	220.4	16	
Spot 15	27	144	104.2	13.6	1.875E+07	**240.88**	**56.73**	220.7	25	
Spot 103	32	144	123.3	16.0	2.222E+07	**241.38**	**53.80**		0	
Spot 72	31	100	169.1	22.0	3.100E+07	**245.48**	**55.27**	443.9	57	

Spot 64	37	100	200.1	26.0	3.700E+07	**247.47**	**52.77**	276.5	41	
Spot 96	12	100	64.7	8.4	1.200E+07	**248.06**	**79.13**		0	
Spot 28	28	100	150.2	19.5	2.800E+07	**249.42**	**58.04**	404.5	46	
Spot 18	45	196	118.7	15.4	2.296E+07	**258.59**	**52.14**	426.0	75	
Spot 19	22	100	113.3	14.7	2.200E+07	**259.75**	**65.66**		0	
Spot 22	18	100	91.6	11.9	1.800E+07	**262.76**	**71.47**	600.6	42	
Spot 85	22	100	111.2	14.5	2.200E+07	**264.53**	**66.86**		0	
Spot 81	44	144	154.2	20.1	3.056E+07	**264.81**	**53.73**	317.3	53	
Spot 84	29	144	100.4	13.1	2.014E+07	**267.93**	**61.64**	1835.1	225	
Spot 63	51	100	251.1	32.6	5.100E+07	**271.36**	**52.93**	1956.6	421	*poor*
Spot 42	36	144	122.7	16.0	2.500E+07	**272.10**	**58.49**	263.6	35	
Spot 60	17	100	83.4	10.8	1.700E+07	**272.42**	**75.72**	230.2	14	
Spot 38	27	100	129.7	16.9	2.700E+07	**277.88**	**65.45**	308.5	30	
Spot 12	22	100	104.5	13.6	2.200E+07	**281.02**	**71.03**	2501.1	234	
Spot 7	24	100	113.9	14.8	2.400E+07	**281.33**	**68.97**	313.5	27	
Spot 36	24	144	78.8	10.2	1.667E+07	**282.29**	**69.21**	897.2	80	
Spot 88	12	144	38.0	4.9	8.333E+06	**292.36**	**93.27**	332.3	14	
Spot 86	17	144	53.5	7.0	1.181E+07	**294.13**	**81.76**	263.5	15	
Spot 48	12	144	36.8	4.8	8.333E+06	**302.13**	**96.38**	449.3	18	*poor*
Spot 35	21	144	57.5	7.5	1.458E+07	**337.39**	**86.71**		0	
Spot 30	19	100	72.7	9.4	1.900E+07	**347.25**	**92.57**	1861.5	115	
Spot 31	12	144	30.8	4.0	8.333E+06	**359.18**	**114.58**	2483.0	98	
Spot 87	21	144	46.0	6.0	1.458E+07	**418.75**	**107.63**	260.0	13	
Spot 55	34	100	106.5	13.8	3.400E+07	**421.52**	**92.21**		0	
Spot 97	28	100	84.9	11.0	2.800E+07	**434.83**	**101.19**		0	
Spot 9	15	100	44.0	5.7	1.500E+07	**449.31**	**131.07**	837.7	29	
Spot 8	31	100	89.9	11.7	3.100E+07	**454.15**	**102.26**		0	
Spot 4	36	144	70.4	9.2	2.500E+07	**467.02**	**100.40**	242.9	18	
Spot 68	47	100	121.9	15.9	4.700E+07	**505.60**	**100.76**	412.9	38	
Spot 56	18	100	44.8	5.8	1.800E+07	**525.63**	**142.98**		0	
Spot 91	18	100	44.2	5.7	1.800E+07	**533.47**	**145.11**		0	